Uniwersytet Mikołaja Kopernika w Toruniu

Wydział Nauk Biologicznych i Weterynaryjnych

Szkoła Doktorska Nauk Ścisłych i Przyrodniczych
Academia Scientarum Thoruniesis

Joanna Trzcińska-Wencel

Nanocząstki srebra i tlenku cynku pochodzenia grzybowego: biosynteza, aktywność przeciwdrobnoustrojowa i stymulatory wzrostu kukurydzy

Rozprawa doktorska

Promotor:
prof. dr hab. Patrycja Golińska

Promotor pomocniczy:
dr Magdalena Wypij

Toruń, 2025

"Nauka jest najlepszym narzędziem, jakie mamy do odkrywania prawdy o świecie, ale musi być używana z odpowiedzialnością i troską o przyszłość ludzkości."

Carl Sagan

Podziękowania

Składam serdeczne podziękowania prof. dr hab. Patrycji Golińskiej za opiekę naukową, nieocenione wsparcie oraz cierpliwość.

Serdecznie dziękuję dr Magdalenie Wypij za pomoc w trakcie realizacji badań i okazaną życzliwość.

Dziękuję także mojemu Rodzeństwu i bliskim za nieustanną wiarę we mnie.

Z głębi serca, wyjątkowe podziękowania kieruję do mojego Męża, Twoja miłość, wiara, cierpliwość i wsparcie były dla mnie bezcennym źródłem siły.

Finansowanie

Badania przeprowadzone w ramach rozprawy doktorskiej zostały sfinansowane z grantów Grants4NCUStudents, Inicjatywa Doskonałości – Uczelnia Badawcza (IDUB), Uniwersytet Mikołaja Kopernika w Toruniu:

- *Search for the antifungal activity of biogenic nanoparticles against selected plant pathogens* (136/2022)
- *Silver nanoparticles as an alternative strategy against bacterial biofilm formation and antibiotic-resistant bacteria* (38/2021)
- *Biological nano-alternatives to conventional pesticides* (102/2021)

oraz grantu Preludium 21 z Narodowego Centrum Nauki:

- *Mycogenic metal nanoparticles for plant growth stimulation and increased plant production* (2022/45/N/NZ9/01483)

Spis treści

Wykaz skrótów

ABA – kwas abscysynowy (*ang.* abscisic acid)

AgNPs – nanocząstki srebra (*ang.* silver nanoparticles)

APX – peroksydaza askorbinianowa (*ang*. ascorbate peroxidase)

ASC – kwas askorbinowy (*ang*. ascorbic acid)

CAT – katalaza (*ang*. catalase)

CuNPs – nanocząstki miedzi (*ang.* copper nanoparticles)

DLS – dynamiczne rozpraszanie światła (*ang.* dynamic light scattering)

FDA – dwuoctan fluoresceiny (*ang.* fluorescein diacetate)

Fe_3O_4NPs – nanocząstki tlenku żelaza (*ang.* iron oxide nanoparticles)

FIC – ułamkowe stężenie hamujące (*ang.* fractional inhibitory concentration)

FTIR – spektroskopia w podczerwieni z transformacją Fouriera (*ang.* Fourier transformed infrared spectroscopy)

GA – gibereliny (*ang.* gibberellins)

HCA – hierarchiczna analiza skupień (*ang.* hierarchical cluster analysis)

IOR – Instytut Ochrony Roślin, Państwowy Instytut Badawczy

MAPK – kinazy aktywowane mitogenem (*ang.* mitogen-activated protein kinases)

MBC – minimalne stężenie bójcze (*ang*. minimal biocidal concentration)

MDA – dialdehyd malonowy (*ang*. malondialdehyde)

MFC – minimalne stężenie grzybobójcze (*ang.* minimal fungicidal concentration)

MgONPs – nanocząstki tlenku magnezu (*ang.* magnesium oxide nanoparticles)

MIC – minimalne stężenie hamujące (*ang*. minimal inhibitory concentration)

MNPs – nanocząstki metali (*ang.* metal nanoparticles)

MONPs – nanocząstki tlenków metali (*ang.* metal oxide nanoparticles)

NADH – dinukleotyd nikotynoamidoadeninowy (*ang.* nicotinamide adenine dinucleotide, hydrogen)

NMs – nanomateriały (*ang.* nanomaterials)

NPs – nanocząstki (*ang.* nanoparticles)

NTA – analiza śledzenia nanocząstek (*ang.* nanoparticle tracking analysis)

PCA – analiza głównych składowych (*ang.* principal component analysis)

POX – peroksydazy (*ang*. peroxidases)

PPO – oksydaza polifenolowa (*ang.* polyphenol oxidase)

RFT – reaktywne formy tlenu (*ang*. reactive oxygen species)

RPM – obroty na minutę (*ang.* revolutions per minute)

SOD – dysmutaza ponadtlenkowa (*ang*. superoxide dismutase)

TEM – transmisyjna mikroskopia elektronowa (*ang.* transmission electron microscopy)

XRD – proszkowa dyfrakcja promieniowania rentgenowskiego (*ang.* X-ray powder diffraction)

ZnONPs – nanocząstki tlenku cynku (*ang.* zinc oxide nanoparticles)

Streszczenie

Rolnictwo stanowi podstawę zapewnienia bezpieczeństwa żywnościowego na świecie, jednak nieustannie rosnąca populacja przyczynia się do zwiększenia zagrożenia związanego z niedożywieniem czy głodem. Jedną z najważniejszych roślin uprawnych na świecie i w Polsce jest kukurydza (*Zea mays*), której wzrost jest w znacznym stopniu ograniczany przez niekorzystne czynniki abiotyczne i biotyczne.

Głównym celem niniejszej pracy była biosynteza AgNPs i ZnONPs z wykorzystaniem szczepów grzybowych z rodzaju *Fusarium* oraz oznaczenie ich aktywności przeciwdrobnoustrojowej i stymulującej wzrost kukurydzy.

AgNPs i ZnONPs biosyntezowane z wykorzystaniem różnych szczepów grzybowych z rodzaju *Fusarium* wykazywały zróżnicowaną aktywność wobec bakterii i grzybów. Do dalszych badań wyselekcjonowano AgNPs 1 z *Fusarium culmorum* JTW1, które charakteryzowały się najsilniejszą aktywnością przeciwbakteryjną, AgNPs 2 z *Fusarium solani* IOR 825 o wysokiej aktywności wobec grzybów fitopatogennych oraz ZnONPs 1 z *F. solani* IOR 825 o wysokim potencjale do stymulacji wzrostu kukurydzy. Badane AgNPs oraz ZnONPs miały odmienne właściwości fizykochemiczne, takie jak rozmiar, kształt czy właściwości powierzchniowe, w zależności od szczepu grzybowego wykorzystanego do syntezy (AgNPs) lub warunków syntezy (ZnONPs).

AgNPs 1 hamowały wzrost i działały bójczo wobec szerokiego zestawu bakterii Gram-dodatnich i Gram-ujemnych, działały synergistycznie z antybiotykami, szczególnie streptomycyną wobec bakterii Gram-ujemnych, hamowały formowanie i aktywność hydrolityczną biofilmów bakteryjnych. AgNPs 1 i AgNPs 2 hamowały rozwój grzybni i wykazywały aktywność bójczą wobec zarodników fitopatogenów. AgNPs 2 w stężeniu ≥32 μg mL^{-1} efektywnie dezynfekowały powierzchnię ziarniaków kukurydzy i stymulowały produkcję suchej masy roślin. W organach roślin rozwijających się z ziarniaków traktowanych najniższym efektywnie dezynfekującym stężeniem AgNPs 2 obserwowano zmiany poziomu H_2O_2 i w aktywności enzymów przeciwutleniających oraz poziomu askorbinianu. Najwyższe stosowane stężenie AgNPs (512 μg mL^{-1}) promowało produkcję świeżej i suchej masy, jednak skutkowało obniżoną zawartością chlorofilu oraz podwyższonym poziomem MDA.

ZnONPs syntezowane dwiema metodami (ZnONPs 1 oraz ZnONPs 2) z wykorzystaniem *F. solani* IOR 825 wykazywały aktywność przeciwgrzybową, szczególnie wobec *Fusarium oxysporum* IOR 342 i *Phoma lingam*. Traktowanie ziarniaków kukurydzy ZnONPs 1 w stężeniach 32 i 128 μg mL^{-1} spowodowało największy wzrost masy

(szczególnie suchej) roślin. Najniższe badane stężenie ZnONPs (32 μg mL^{-1}) wywołało niewielkie zmiany w poziomie H_2O_2 i aktywności peroksydazy askorbinianowej w liściach i korzeniach. Wyższe testowane stężenia ZnONPs 1 obniżyły zawartość chlorofilu oraz zwiększyły poziom glutationu i MDA w liściach.

Wyselekcjonowane AgNPs 2 i ZnONPs 1 wytwarzane z wykorzystaniem *Fusarium solani* IOR 825, w niskich stężeniach, szczególnie 32 μg mL^{-1}, wykazują potencjał do bezpiecznego stosowania w rolnictwie. AgNPs 2 efektywnie hamują rozwój fitopatogenów, w tym na powierzchni ziarniaków kukurydzy. Zarówno AgNPs 2 i ZnONPs 1 stymulują wzrost kukurydzy bez powodowania stresu oksydacyjnego i wpływu na zawartość chlorofilu. Ponadto, biosynteza nanocząstek i procedura przedsiewnego traktowania ziarniaków roztworami nanocząstek są proste, opłacalne i przyjazne dla środowiska, dając im potencjał do zastosowania w praktyce.

Słowa kluczowe: nanocząstki mykogeniczne; aktywność przeciwdrobnoustrojowa; promotory wzrostu roślin; rolnictwo

Abstract

The worldwide food security highly depend on agriculture, however the increasing population contributes to the threat of malnutrition or hunger. Maize (*Zea mays*) is one of the most important crop plants in the world, including Poland, however its growth is significantly limited by adverse abiotic and biotic factors.

The main aim of the study was biosynthesis of AgNPs and ZnONPs using fungal strains of the genus *Fusarium* and evaluation of their antimicrobial and growth-stimulating activity in maize.

AgNPs and ZnONPs synthesized from broad set of fungal strains of the genus *Fusarium* showed different activities against bacteria and fungi. Among others, AgNPs 1 from *Fusarium culmorum* JTW1 with the strongest antibacterial activity, AgNPs 2 from *Fusarium solani* IOR 825 with high antifungal activity against phytopathogens, and ZnONPs 1 from *F. solani* IOR 825 with high potential to promote maize growth, were selected for further studies. The AgNPs and ZnONPs showed varied physicochemical properties, such as size, shape and surface properties, depending on the fungal strain used for synthesis (AgNPs) or synthesis conditions (ZnONPs).

AgNPs 1 showed inhibitory and biocidal activity against a broad spectrum of Gram-positive and Gram-negative bacteria, synergistic effect with antibiotics, especially streptomycin against Gram-negative bacteria, and inhibited the formation and hydrolytic activity of bacterial biofilms. AgNPs 1 and AgNPs 2 prevented the growth of mycelia and spore germination of fungal phytopathogens. AgNPs 2 at concentrations ≥32 μg mL^{-1} effectively disinfected the surface of maize grains and stimulated seedling dry mass production. In the organs of maize plantlets developed from grains treated with the lowest effectively disinfecting concentration of AgNPs 2, changes in H_2O_2 and ascorbate levels and antioxidant enzymes activity were observed. The highest AgNPs concentration (512 μg mL^{-1}) promoted production of fresh and dry mass of plants, but resulted in reduced chlorophyll content and increased MDA level.

ZnONPs synthesized by two methods (ZnONPs 1 and ZnONPs 2) using *F. solani* IOR 825 showed high antifungal activity, particularly against *Fusarium oxysporum* IOR 342 and *Phoma lingam.* The treatment of maize grains with ZnONPs 1 at the concentrations of 32 and 128 μg mL^{-1} resulted in the most effective increase in plant mass (especially dry mass). The lowest tested concentration of ZnONPs 1 (32 μg mL^{-1}) caused minor changes in H_2O_2 levels and ascorbate peroxidase activity in both leaves and roots. The application of ZnONPs

1 at higher concentrations reduced chlorophyll content and increased glutathione and MDA levels in the leaves.

Selected AgNPs 2 and ZnONPs 1 synthesized from *Fusarium solani* IOR 825, at low concentration of 32 μg mL^{-1}, show potential for safe use in agriculture. AgNPs 2 effectively inhibit the growth of phytopathogens, including these on the maize grain surface. Both AgNPs 2 and ZnONPs 1 stimulate plant growth without causing oxidative stress or affecting chlorophyll content. In addition, the biosynthesis of nanoparticles and the pre-sowing treatment of grains with nanoparticle solutions are simple, cost-effective and environmentally friendly, thereby having the potential for practical application.

Keywords: mycogenic nanoparticles; antimicrobial activity; plant growth promoters; agriculture

Wykaz publikacji wchodzących w skład rozprawy doktorskiej

	Publikacja	Punkty MNiSW	IF
P1	**Trzcińska-Wencel, J**., Wypij, M., & Golińska, P. (2023). Mycogenic synthesis of silver nanoparticles and its optimization. W: M. Rai & P. Golińska (Red.), *Mycosynthesis of Nanomaterials: Perspectives and Challenges* (s. 126-145). CRC Press, Taylor and Francis Group.	50	-
P2	**Trzcińska-Wencel,** J., Golińska, P., & Rai, M. (2024). Toxicity of nanomaterials to plants. W: M. Rai & G. D. Avila-Quezada (Red.), *Nanotechnology in Plant Health* (s. 369-389). CRC Press, Taylor and Francis Group.	50	-
P3	**Trzcińska-Wencel, J.,** Wypij, M., Rai, M., Golińska, P. (2023). Biogenic nanosilver bearing antimicrobial and antibiofilm activities and its potential for application in agriculture and industry. Frontiers in Microbiology, 14: 1125685.	100	4,02
P4	**Trzcińska-Wencel, J.,** Wypij, M., Terzyk, A. P., Rai, M., Golińska, P. (2023). Biofabrication of novel silver and zinc oxide nanoparticles from *Fusarium solani* IOR 825 and their potential application in agriculture as biocontrol agents of phytopathogens, and seed germination and seedling growth promoters. Frontiers in Chemistry, 11: 1235437.	100	3,58
P5	**Trzcińska-Wencel,** J. Mucha, N., Rai, M., Tyburski, J., Golińska, P. Pre-sowing treatment with bio-AgNPs as a grain sterilization technique triggers an organ specific and dose-dependent response of the antioxidant system of maize. Złożono w czasopiśmie (11.09.2024) w recenzji w Frontiers in Plant Sciences. ID manuskryptu: 1494741-R1	-	-
P6	**Trzcińska-Wencel, J**. Mucha, N., Nadrowska J., Gade, A. Rai, M., Tyburski, J., Golińska, P. ZnONPs biosynthesized from *Fusarium solani* IOR 825: unveiling their growth stimulating effects in maize (*Zea mays* L.). Złożono w czasopiśmie (10.01.2025) w recenzji w Scientific Reports. ID manuskryptu: SREP-25-00106	-	-
SUMA		300	7,6

I Wstęp

Współczesny świat zmaga się z szeregiem wyzwań, które nieustannie skłaniają ludzi, w tym szczególnie naukowców i wynalazców, do poszukiwania skutecznych rozwiązań. Na kierunek rozwoju świata wpływają zależności i powiązania między wszystkimi organizmami, od mikroorganizmów, przez rośliny i zwierzęta. Jednak, umiejętność myślenia zobowiązuje ludzi do podjęcia prób wykorzystania potencjału jaki drzemie w naturze przy równoczesnym uwzględnieniu i ograniczeniu negatywnych konsekwencji tych działań. Począwszy od ewolucji organizmów, poprzez kamienie milowe cywilizacji ludzkiej, w tym pierwsze narzędzia, pismo, rolnictwo, tworzenie struktur organizacyjnych, przemysłu i rozwój zaawansowanych technologii zmieniały i rozwijały świat. Jednak, lista wyzwań dla ludzkości, w kontekście pojedynczych jednostek oraz całej populacji i ekosystemu, nieustannie rośnie. Naprawienie całego świata nie jest możliwe na raz i w pojedynkę, jednak połączone starania większych społeczności potrafią przyczynić się do zmian w dobrym kierunku (Stearns, 2008; Dakos i in., 2019). Wyjątkowy postęp związany z rozwojem nanotechnologii datowany na lata 90. XX w. był możliwy dzięki staraniom i zaangażowaniu licznych naukowców, m.in. Richarda Feynmana, Norio Taniguchi czy Erica Drexlera (Amin i in., 2024). Dotychczasowe osiągnięcia z zakresu nanotechnologii zrewolucjonizowały medycynę, elektronikę, przemysł i rolnictwo, a niniejsza praca jest cegiełką do dalszego rozwoju, jako że stanowi próbę zrozumienia jak nanocząstki srebra i tlenku cynku, z szerokim potencjałem do zastosowania w celu poprawy różnych obszarów życia ludzi, wpływają na mikroorganizmy i rośliny.

1.1. Nanotechnologia

Nanotechnologia zajmuje się opracowywaniem, wytwarzaniem i badaniem nanomateriałów (NMs), czyli jedno-, dwu- i trójwymiarowych struktur, których rozmiar mieści się w skali nano (1-100 nm przynajmniej w jednym wymiarze). Różnorodność nanomateriałów obejmuje nanocząstki nieorganiczne (metali i tlenków metali), nanomateriały węglowe (grafen, tlenek grafenu, fulereny i nanorurki węglowe), nanostruktury organiczne (liposomy i polimery) oraz szeroki zakres mieszanych materiałów (nanokompozyty). Nanomateriały, w tym nanocząstki metali, cechują niewielkie rozmiary, wysoki stosunek powierzchni do objętości i stabilność, co nadaje im właściwości magnetyczne, katalityczne, elektryczne, optyczne, czy wysoką reaktywność chemiczną, których nie posiadają odpowiadające im materiały w skali makro (Bhushan, 2017). Ze względu na swoje unikalne właściwości nanomateriały znajdują zastosowanie w medycynie,

elektronice, energetyce, budownictwie, ochronie środowiska, przemyśle spożywczym czy rolnictwie (Cheng i in., 2024; Singh A. i in., 2024).

1.2. Synteza nanocząstek

Do wytworzenia nanocząstek stosuje się głównie chemiczne oraz fizyczne metody syntezy, do których należą m.in. współstrącanie, metoda zol-żel, mikroemulsje czy ablacja laserowa. Procedury te są wydajne i umożliwiają uzyskanie jednorodnych produktów, jednak ich wadą jest konieczność przeprowadzenia dodatkowych procesów oczyszczania czy stabilizacji nanocząstek oraz stosowanie toksycznych odczynników chemicznych, wysokiej temperatury czy ciśnienia (Abid i in., 2022). Wymagania te generują nie tylko koszty, ale niosą ze sobą ryzyko dla organizmów i zanieczyszczenia środowiska (Borehalli Mayegowda i in., 2023). Uwzględniając powyższe, uwaga naukowców jest skierowana na opracowanie rozwiązań, które wyjdą naprzeciw tym wyzwaniom. W porównaniu z metodami fizycznymi i chemicznymi, biosynteza (zielona synteza) nanocząstek z wykorzystaniem materiału pochodzenia biologicznego jest procesem ograniczającym stosowanie toksycznych odczynników i energii oraz tanim. W procesie biosyntezy cząsteczki pełniące funkcję redukującą i opłaszczającą nanocząstki są pochodzenia naturalnego (np. ekstrakty roślinne, bakteryjne, grzybowe) (Zhu i in., 2021; Abdelgadir i in., 2024; Lavecchia i in., 2024; Waqif i in., 2024).

Grzyby pleśniowe ze względu na szybki wzrost na prostych podłożach, znaczną produkcję biomasy, wytwarzanie enzymów i metabolitów oraz zdolność adaptacji do nowych warunków środowiska, są wydajnym systemem w biosyntezie nanocząstek zarówno wewnątrzkomórkowej, jak i zewnątrzkomórkowej (Kamal Kumar i in., 2020). Dotychczasowe badania wskazują, że właściwości fizyko-chemiczne wytworzonych nanostruktur zależą od warunków procesu syntezy (np. stężenie prekursora, pH czy temperatura mieszaniny reakcyjnej), szczepu grzybowego, warunków jego hodowli, czy przygotowania ekstraktu grzybowego (Rai i in., 2021; Rai & Golinska, 2023; Herrera Pérez i in., 2024).

Dotychczasowy stan wiedzy na temat biologicznej syntezy AgNPs z wykorzystaniem grzybów strzępkowych opisano w publikacji pierwszej (**P1**) wchodzącej w skład niniejszej dysertacji. Doniesienia literaturowe wskazują, że do biosyntezy nanocząstek najczęściej wykorzystywano grzyby należące do rodzajów *Fusarium, Aspergillus, Trichoderma* oraz *Penicillium.* W badaniach tych nanocząstki pozyskiwano głównie na drodze syntezy zewnątrzkomórkowej, a uzyskane struktury miały przeważnie kształt kulisty i były

polidyspersyjne, chociaż monodysperyjne AgNPs wytworzono z wykorzystaniem ekstraktów z *Fusarium oxysporum* i *Penicillium chrysogenum* (**P1**). Główne parametry reakcji, które wpływają na wydajności biosyntezy i jakość wytworzonych AgNPs obejmują temperaturę, stężenie jonów metali, pH mieszaniny reakcyjnej, czas trwania reakcji. Są one kluczowe dla uzyskania AgNPs o pożądanych parametrach fizykochemicznych, które warunkują ich późniejsze zastosowanie (**P1**). Podobnie, biosyntezę ZnONPs z wykorzystaniem grzybów opisało wielu badaczy, którzy zastosowali ekstrakty m.in. z *Aspergillus fumigatus* (Gaber i in., 2024)*, Aspergillus niger* (Gao i in., 2019; Es-haghi i in., 2021), *Fusarium oxysporum* (Gupta & Chundawat, 2020), *Trichoderma* sp. (Kumar i in., 2024; Gallo i in., 2025) i wiele innych. W procesie biosyntezy ZnONPs jako źródło jonów cynku stosuje się różne prekursory, takie jak azotan cynku ($Zn(NO_3)_2$) (Rilda i in., 2024), octan cynku ($Zn(CH_3COO)_2$) (Mongy & Shalaby, 2024), chlorek cynku ($ZnCl_2$) (Essawy i in., 2024) czy siarczan cynku ($ZnSO_4$) (Ashour & Abd-Elhalim, 2024).

Mechanizm biologicznej syntezy nanocząstek metali (MNPs) nie został w pełni opisany. Jednak liczne doniesienia literaturowe wskazują na zaangażowanie w ten proces różnorodnych cząsteczek pochodzących z ekstraktów roślinnych i mikroorganizmów, w tym m.in. węglowodanów, enzymów i białek oraz flawonoidów, które redukują jony metali (M^+) do metalu (M^0) w wyniku reakcji utleniania-redukcji i pełnią rolę czynników ograniczających wzrost tworzonych nanocząstek (Ahmad i in., 2003; Alavi & Ashengroph, 2023). Zredukowane metale tworzą agregaty i formują jądra metaliczne (nukleacja) (Qamar & Ahmad, 2021). Schematyczne przedstawienie tego procesu znajduje się na Rycinie 1.

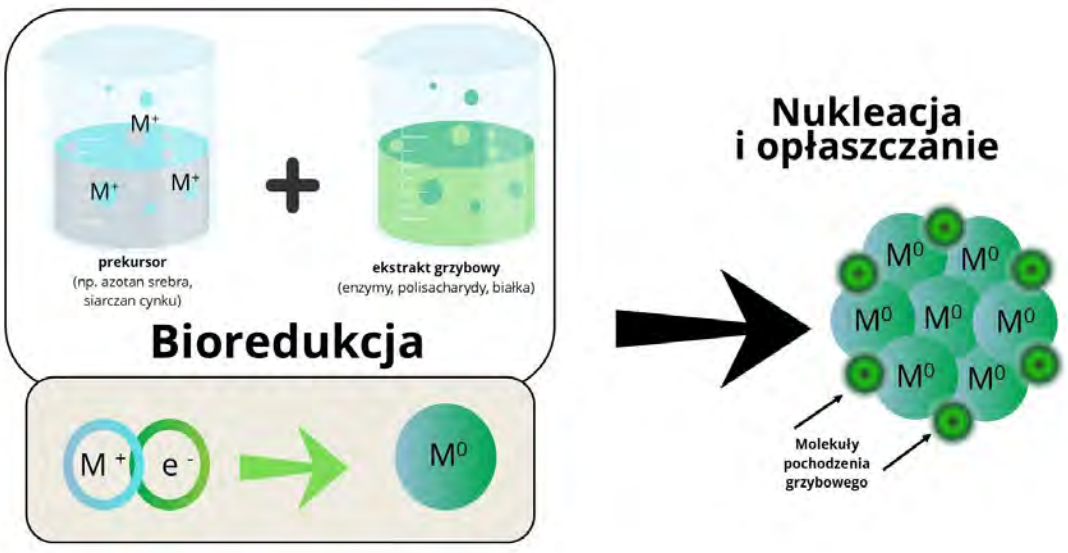

Rycina 1. Schemat przedstawiający proces biosyntezy nanocząstek metali (opracowane na podstawie Qamar & Ahmad (2021).

Zaproponowano kilka hipotetycznych mechanizmów syntezy nanocząstek metali przez grzyby. W przypadku biosyntezy AgNPs z wykorzystaniem *Fusarium oxysporum*, *Fusarium acuminatum* i *Aspergillus terreus* badacze wskazują na kluczową rolę reduktazy azotanowej i NADH w bioredukcji jonów srebra (Durán i in., 2005; Ingle i in., 2008; G. Li i in., 2012). Niedawne badania nad syntezą AgNPs z wykorzystaniem *Penicillium cyclopium* wykluczyły enzymatyczny charakter tego procesu, wskazując jednak na rolę polipeptydów i cukrów w redukcji jonów srebra i formowaniu AgNPs (Wanarska & Maliszewska, 2019). Natomiast badania Ma i współautorów (2019) wykazały udział białek, głównie aktyny w stabilizowaniu AgNPs wytworzonych z wykorzystaniem *Penicillium aculeatum* Su1 (Ma i in., 2019).

W biosyntezie ZnONPs, jednym z najczęściej proponowanych mechanizmów jest wytrącanie wodorotlenku cynku ($Zn(OH)_2$) w reakcji z NaOH i jego przekształcanie do ZnONPs w wyniku ogrzewania i/lub aktywności cząsteczek pochodzących z ekstraktów biologicznych. Natomiast drugi proponowany mechanizm obejmuje bezpośrednią redukcję jonów Zn^{2+} przez biomolekuły grzybowe do metalicznego cynku, a następnie jego reakcję z tlenem rozpuszczonym w roztworze prekursora, która prowadzi do powstania jąder ZnO (Gurgur i in., 2020; Mongy & Shalaby, 2024). Wśród cząsteczek pochodzenia naturalnego (grzybowego), zaangażowanych w ten proces wymienia się białka związane z metabolizmem i odpowiedzią na stres, w tym głównie oksydoreduktazy (Kadam i in., 2019; Gallo i in., 2025).

1.3. Produkcja roślinna – wyzwania i rozwiązania

Rolnictwo stanowi podstawę zapewnienia bezpieczeństwa żywnościowego w skali ogólnoświatowej, regionalnej, krajowej i lokalnej. Jedną z najważniejszych roślin uprawnych jest kukurydza (*Zea mays*), która obok pszenicy (*Triticum* spp.) i ryżu (*Oryza sativa*) jest najczęściej wykorzystywana do produkcji żywności i paszy (Rycina 2) (FAO, 2022).

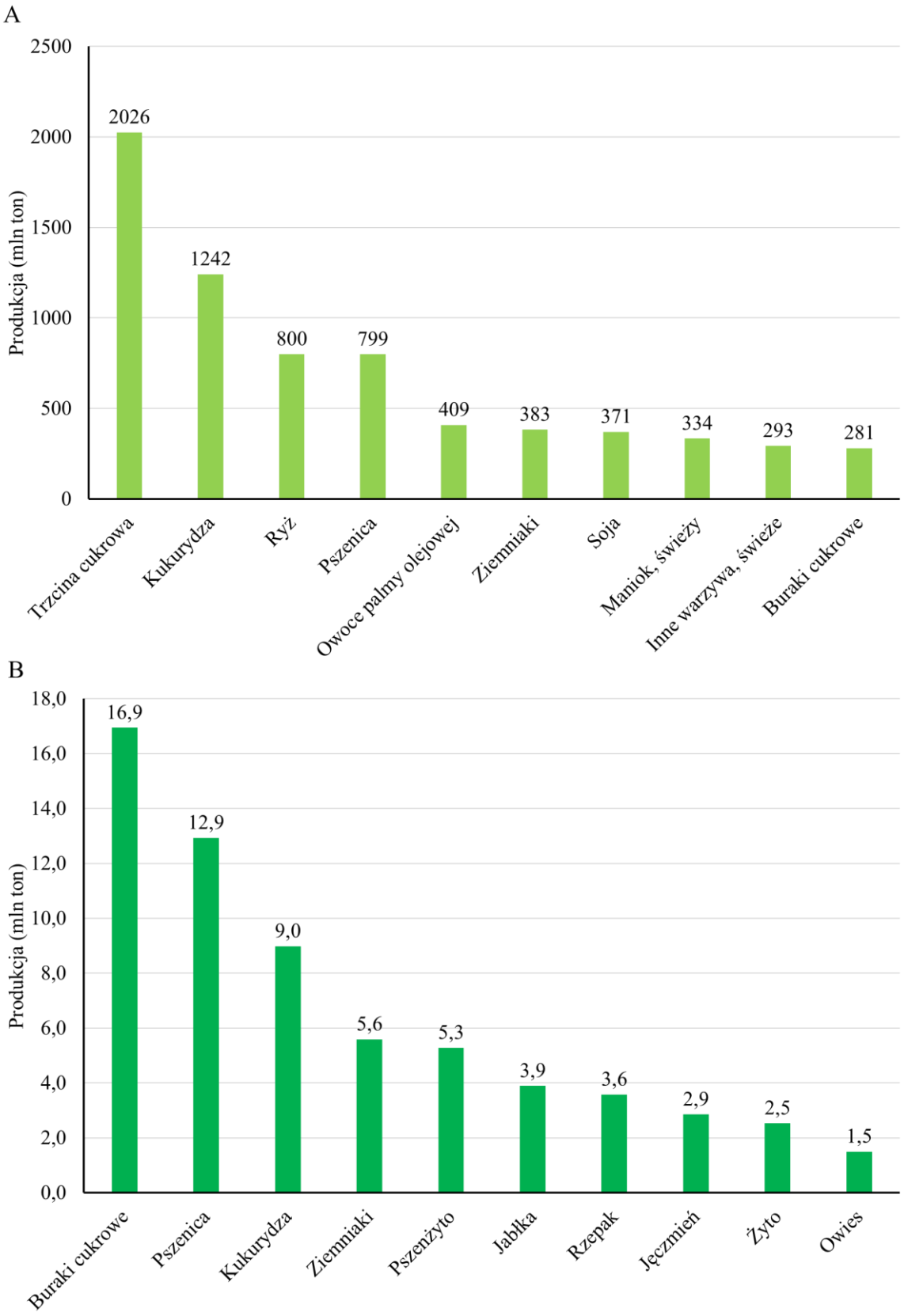

Rycina 2. Produkcja roślin uprawnych o najwyższych plonach w 2023 roku: A: światowa, B: Polska (opracowane na podstawie danych: FAOSTAT, 2025, https://www.fao.org/faostat/en/#data/QCL).

W latach 2013-2023 produkcja kukurydzy wzrosła o 225 mln ton w skali świata, z czego o blisko 5 mln ton w Polsce (Rycina 3). Produkty na bazie kukurydzy odgrywają kluczową rolę jako źródło składników odżywczych (węglowodanów, białek, tłuszczu, mikro- i makroelementów) oraz wielu innych, korzystnych dla zdrowia związków, takich jak witaminy (ryboflawina, tiamina, witamina C, E) lub ksantofile (luteina i zeaksantyna) (Rouf Shah i in., 2016).

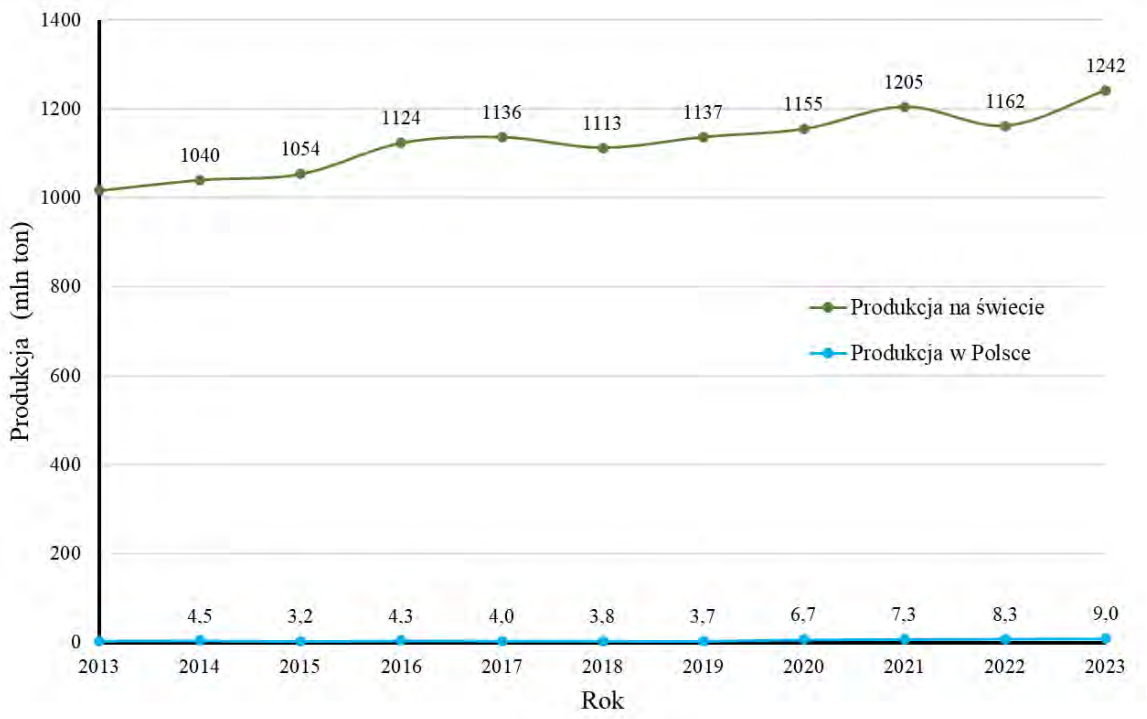

Rycina 3. Produkcja kukurydzy w latach 2013-2023 (opracowane na podstawie danych: FAOSTAT, 2025, https://www.fao.org/faostat/en/#data/QCL).

Jednakże, nieustannie rosnąca populacja ludzka przyczynia się do zwiększenia zagrożenia związanego z niedożywieniem czy głodem. Problemy te wynikają m.in. z niewystarczającej i nieefektywnej produkcji roślinnej związanej ze zmianami klimatycznymi, zanieczyszczeniami środowiska, utratą różnorodności genetycznej, czy opornością patogenów i szkodników na środki agrochemiczne (Khatri i in., 2024). Podobnie jak inne uprawy, kukurydza jest podatna na niekorzystne czynniki abiotyczne (dostępność wody i składników odżywczych lub czynniki klimatyczne) i biotyczne, które mogą w znacznym stopniu ograniczać jej wzrost. Te ostatnie są reprezentowane przez takie patogeny jak np. *Aspergillus flavus, Colletotrichum graminicola, Fusarium graminearum, Macrophomina phaseolina, Sclerophthora macrospora,* które poza hamowaniem wzrostu roślin, mogą powodować akumulację mykotoksyn w produktach przeznaczonych do

spożycia, co stanowi zagrożenie dla zdrowia ludzi i zwierząt (Miedaner & Juroszek, 2021; Martín i in., 2022; Akhtar & Kumar, 2024).

Obecnie, w celu zwiększenia roślinnej produkcji rolnej stosuje się i udoskonala dostępne praktyki agrotechniczne, takie jak precyzyjne metody nawożenia i nawadniania, stosowanie biostymulatorów, prowadzenie uprawy współrzędnej oraz innowacyjne techniki wykrywania i eliminacji szkodników czy chwastów (Begam i in., 2024; Burlakoti i in., 2024). Innym kluczowym aspektem jest kontrola rozwoju patogenów roślin uprawnych z wykorzystaniem środków biokontroli, chemicznych fungicydów, a także poprzez optymalizację warunków przechowywania zbiorów (Martín i in., 2022). Obiecującym sposobem na zwiększenie wydajności kiełkowania nasion oraz wzrostu roślin są techniki przedsiewnego traktowania nasion takie jak np. biokondycjonowanie, osmokondycjonowanie czy hydrokondycjonowanie. Techniki kondycjonowania nasion są uważane za zrównoważone pod względem wpływu na środowiskowo i opłacalne, dzięki czemu są bezpieczne i przystępne dla rolników (Zulfiqar, 2021).

1.4. Zastosowanie nanotechnologii w rolnictwie

W rolnictwie coraz częstsze zastosowanie znajdują rozwiązania nanotechnologiczne (Zain i in., 2024; Cao i in., 2025). Potencjał nanomateriałów do różnych zastosowań w rolnictwie, w tym do ochrony roślin (biosensory, kontrola chorób roślin), jak również aspekty związane z odpowiedzią roślin na działanie nanomateriałów wprowadzanych do środowiska w sposób celowy (np. zastosowania rolnicze, jak powyżej) lub niezamierzony (np. pozostałości przemysłowe) przedstawiono, w oparciu o dostępne doniesienia, w publikacji drugiej (**P2**) wchodzącej w skład niniejszej dysertacji. W monografii tej omówiono procesy pobierania i transportu nanomateriałów w roślinach, wpływ nanocząstek metali na wzrost i rozwój roślin, w tym na działanie systemu antyoksydacyjnego, procesy związane z adaptacją i detoksykacją, uwzględniając zmiany ekspresji genów, wpływ na biosyntezę białek oraz inne odpowiedzi roślin na poziomie komórkowym. Praca ta skupia się również na omówieniu podejść i technik wykorzystywanych do badania fitotoksyczności nanomateriałów, która zależy głównie od zastosowanego stężenia i właściwości fizykochemicznych nanomateriałów. W opracowaniu tym omówiono także wpływ nanomateriałów na ilość i jakość plonów oraz na słabo poznane zagadnienie związane z przekazywaniem nanomateriałów roślinom potomnym przez rośliny macierzyste.

1.4.1. Zwalczanie patogenów roślin uprawnych

Szczególnym problemem w rolnictwie są patogeny upraw, w tym grzybowe, które zmniejszają plony i jakość produkcji rolnej (Martín i in., 2022; Akhtar & Kumar, 2024). W zwalczaniu fitopatogenów grzybowych w uprawach przemysłowych, szeroko rozpowszechnione jest stosowanie pestycydów, środków chemicznych, takich jak kaptan, ditiokarbaminiany, tiabendazol (TBZ) czy imazalil (IMZ). Jednak ich powszechne stosowanie wiąże się z ryzykiem rozwoju oporności u grzybów czy negatywnego wpływu na inne organizmy i środowisko (Jaramillo-López i in., 2024; Kaur i in., 2024; Zhou i in., 2025). Rosnące zapotrzebowanie na produkcję żywności przyczynia się do ogólnoświatowego wzrostu wykorzystania pestycydów. W 2022 odnotowano 4% wzrost zużycia substancji czynnych w rolnictwie w stosunku do roku 2021 i 13% wzrost w ciągu dekady (FAO, 2024). Pomimo poznania patogenezy grzybów, zrozumienia występowania oporności na agrochemikalia oraz stosowania zmodyfikowanych preparatów, rozwój i ekspansja oporności u grzybów fitopatogennych jest nadal poważnym problemem, co wynika z dużych zdolności adaptacyjnych tych mikroorganizmów do zmian środowiskowych (Kretschmer i in., 2009; Li i in., 2017). Kreuje to pilną potrzebę opracowania zrównoważonej, ale i skutecznej metody kontroli patogenów roślin, tak aby zminimalizować straty plonów przy równoczesnym ograniczeniu negatywnego wpływu na środowisko (Faizan i in., 2024).

Nanotechnologia dostarcza różnego rodzaju nanomateriały czy nanokompozyty, których stosowanie prowadzi do precyzyjnego i efektywnego doprowadzania i uwalniania związków aktywnych, co ogranicza stosowanie konwencjonalnych preparatów, w tym pestycydów (Faizan i in., 2024; Zain i in., 2024). Spośród wielu rodzajów nanocząstek metali, najsilniejsze działanie przeciwdrobnoustrojowe wykazują nanocząstki na bazie srebra (Rodrigues i in., 2024), które od tysięcy lat znane jest z takiej aktywności (Kaiser i in., 2023). Wiele badań wskazuje, że bionanocząstki srebra wykazują silniejszą aktywność przeciwdrobnoustrojową i większą biokompatybilność w porównaniu do tych produkowanych na drodze syntezy chemicznej (Hamouda i in., 2019; Dowlath i in., 2021; Ghetas i in., 2022). Wynika to z naturalnego opłaszczenia bio-AgNPs cząsteczkami pochodzenia biologicznego, które odpowiadają za ich właściwości fizykochemiczne takie jak wielkość, stabilność, ładunek powierzchniowy (Ghetas i in., 2022; Herrera Pérez i in., 2024). Aktywność przeciwdrobnoustrojowa AgNPs zależy także od ich stężenia i rodzaju traktowanego mikroorganizmu (Kashyap i in., 2024). Szerokie spektrum aktywności przeciwdrobnoustrojowej AgNPs wynika z ich wielokierunkowego działania w komórce

mikroorganizmów i jest następstwem zewnątrz- i wewnątrz-komórkowej akumulacji nanocząstek oraz stopniowego uwalniania jonów srebra. Plejotropowy efekt działania nanocząstek srebra na komórki mikroorganizmów obejmuje oddziaływania elektrostatyczne z powierzchnią komórki, interakcje i uszkodzenia błony komórkowej, nadmierną produkcję reaktywnych form tlenu, zaburzanie funkcjonowania enzymów w łańcuchu oddechowym, zaburzanie i hamowanie szlaków metabolicznych poprzez inaktywację enzymów (np. wynikającą z wiązania z grupami -SH białek), uszkodzenia DNA czy hamowanie syntezy białek (Rodrigues i in., 2024).

1.4.2. Promowanie wzrostu roślin

Współczesne rolnictwo stoi w obliczu wielu wyzwań, takich jak nieprzewidywalne zmiany klimatu, zanieczyszczenie środowiska i znaczny wzrost popytu na żywność, które determinują potrzebę wprowadzania nowoczesnych i precyzyjnych rozwiązań w celu zwiększania produkcji roślinnej (Hickey i in., 2019). Biostymulacja jest definiowana jako interakcja między organizmami a czynnikami zewnętrznymi lub bodźcami, powodującymi zmiany w organizmie poprzez modyfikację procesów komórkowych i metabolicznych, z korzystnym wpływem na wzrost roślin (Jardin, 2015). Stymulacja wzrostu roślin, poprawa ich odporności na niekorzystne czynniki biotyczne lub abiotyczne, a w konsekwencji zwiększenie plonów jest możliwe przez stosowanie biostymulatorów, które obejmują mikroorganizmy i substancje (lub mieszaniny substancji), z wyłączeniem składników odżywczych, hormonów roślinnych lub pestycydów (Rouphael & Colla, 2020). Wśród biostymulatorów o charakterze substancji wyróżnia się kwasy humusowe i fulwowe, hydrolizaty białkowe, biopolimery i związki nieorganiczne (Jardin, 2015). Nanomateriały stosowane w rolnictwie dzielą się na nieorganiczne, głównie nanocząstki metali, tlenków metali i niemetali oraz organiczne takie jak micele, nanożele, czy struktury polimerowe (Mittal i in., 2020). Badania nad potencjałem nanocząstek metali do hamowania fitopatogenów i/lub szkodników koncentrują się głównie na nanocząstkach miedzi (CuNPs) lub AgNPs (Yan & Chen, 2019; Ibrahim i in., 2019; Noman i in., 2020a; Noman in., 2020b). Natomiast badania nad wykorzystaniem nanocząstek do stymulowania wzrostu roślin i zwiększania produkcji roślinnej obejmują głównie nanocząstki tlenków metali (MONPs), takich jak nanocząstki tlenku magnezu (MgONPs), tlenku cynku (ZnONPs), tlenków żelaza (Fe_3O_4NPs) (Alabdallah i in., 2021).

W ostatnich latach nanocząstki tlenku cynku (ZnONPs), ze względu na ich niezwykłe właściwości, stały się przedmiotem szeroko prowadzonych badań pod kątem aplikacji w

rolnictwie (Cao i in., 2025). Zastosowanie ZnONPs w uprawach rolnych wynika z istotnej roli cynku w procesach wzrostu i metabolizmie roślin (Kumar i in., 2021). Cynk odgrywa podwójną rolę, jako składnik strukturalny i katalityczny w roślinach, będąc niezbędnym w ekspresji genów, biosyntezie białek, aktywności enzymatycznej, transporcie jonów, metabolizmie komórkowym, proliferacji, produkcji hormonów wzrostu i chlorofilu (Kaur i in., 2024). Zn jest również zaangażowany w regulację fizjologicznych i molekularnych mechanizmów odpowiedzi roślin na różne stresy (Umair Hassan i in., 2020; Donia & Carbone, 2023). Co istotne, Zn w nadmiernych stężeniach jest toksyczny dla roślin i prowadzi do nieefektywnej produkcji biomasy związanej z niższą wydajnością fotosyntezy, hamowaniem wydłużania i podziału komórek oraz zaburzeniem integralności błon (Kaur i in., 2024). Aktywność biologiczna ZnONPs w dużym stopniu zależy od gatunku rośliny, stadium jej rozwoju i fazy wzrostu, warunków środowiskowych oraz właściwości fizykochemicznych nanocząstek, które jak wspomniano już wcześniej, zależą od metody i warunków procesu syntezy (Chen i in., 2018; Zafar i in., 2019; Shen i in., 2022; Li i in., 2023).

1.4.3. Ryzyko toksyczności nanocząstek i wyzwania

Rosnące zainteresowanie aplikacją nanomateriałów w rolnictwie wynika z ich unikalnej aktywności biologicznej wobec fitopatogenów, ale także z możliwości wykorzystania ich jako nawozów czy biostymulatorów. Pomimo wielu pozytywnych aspektów stosowania nanopreparatów w rolnictwie zaobserwowano, że NMs, zwłaszcza w wyższych dawkach, mogą powodować negatywne konsekwencje dla organizmów roślinnych. Aspekty związane z tym zagadnieniem zostały opisane w publikacji drugiej (**P2**)**.** Badania wykazały, że wpływ NMs na rośliny, o czym wspomniano powyżej, zależy od ich właściwości, ale także od gatunku rośliny i warunków środowiskowych. Natomiast w odpowiedzi na toksyczność NMs, rośliny intensyfikują syntezę biomolekuł związanych ze stresem i systemem antyoksydacyjnym (Cao i in., 2025). Wchłanianie i biotransformacja NMs przez rośliny są ograniczane przez naturalne bariery, takie jak kutikula lub śluz (Wang i in., 2023). Niemniej jednak, interakcje i wpływ nanomateriałów na rośliny nie są dokładnie poznanie, co wynika ze zróżnicowanych właściwości stosowanych nanostruktur, warunków środowiskowych i mechanizmów odpowiedzi roślin, a są kluczowe, zwłaszcza w zakresie wpływu na rozwój roślin i jakość plonów (Singh i in., 2022). Wyzwaniami związanymi z nanomateriałami są nieujednolicone systemy oceny ich wpływu na środowisko i organizmy, luki w regulacjach prawnych oraz obawy społeczeństwa, w tym ryzyko akumulacji

nanomateriałów w roślinach uprawnych i związane z tym zagrożenie dla zdrowia zwierząt i ludzi (El-Moneim i in., 2021).

II Cel pracy i hipotezy badawcze

Głównym celem niniejszej pracy była biosynteza AgNPs i ZnONPs z wykorzystaniem szczepów grzybowych z rodzaju *Fusarium* oraz oznaczenie ich aktywności przeciwdrobnoustrojowej i stymulującej wzrost kukurydzy.

Cele szczegółowe:

1) biosynteza nanocząstek srebra i tlenku cynku z wykorzystaniem szczepów grzybowych z rodzaju *Fusarium* w celu selekcji szczepów zdolnych do wydajnej syntezy,
2) ocena właściwości przeciwdrobnoustrojowych nanocząstek srebra i tlenku cynku w celu selekcji najaktywniejszych nanocząstek oraz ocena ich właściwości fizykochemicznych,
3) zbadanie wpływu wyselekcjonowanych nanocząstek na formowanie biofilmów bakteryjnych oraz kiełkowania zarodników i rozwoju grzybni fitopatogentów,
4) zoptymalizowanie warunków przedsiewnego traktowania ziarniaków kukurydzy na podstawie oceny wpływu na kiełkowanie, wzrost i kondycję roślin w celu:
    a) skutecznej dezynfekcji powierzchniowej ziarniaków z użyciem AgNPs,
    b) najwydajniejszej stymulacji wzrostu roślin pod wpływem ZnONPs,
    c) niepowodowania efektu toksyczności w roślinach po traktowaniu AgNPs lub ZnONPs.

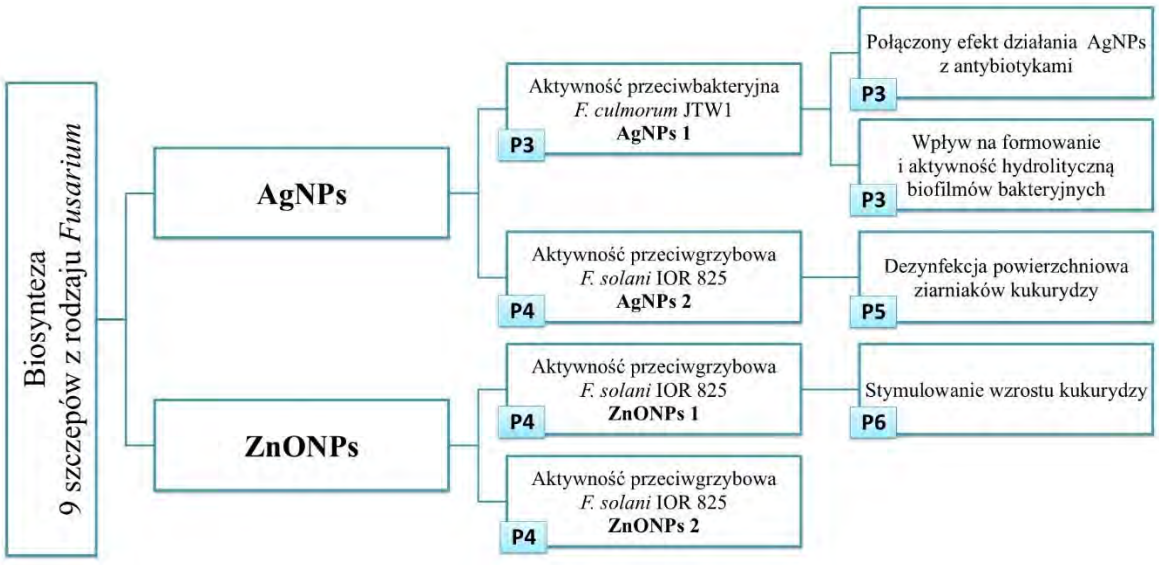

Rycina 4. Schemat przedstawiający przebieg realizacji zadań badawczych wykonanych w ramach niniejszej pracy.

Postawiłam następujące hipotezy badawcze:

Hipoteza główna:

Biologicznie syntezowane nanocząstki są skuteczne jako środki przeciwdrobnoustrojowe i stymulujące wzrost kukurydzy.

Hipotezy szczegółowe:

1) Grzyby z rodzaju *Fusarium* są wydajnym systemem do syntezy nanocząstek srebra i tlenku cynku.
2) Właściwości fizykochemiczne nanocząstek srebra i tlenku cynku zależą od szczepu grzybowego wykorzystanego do biosyntezy.
3) Aktywność biologiczna nanocząstek jest uwarunkowana ich właściwościami fizykochemicznymi i jest zależna od dawki.
4) Stymulacja wzrostu kukurydzy przez nanocząstki i ich fitotoksyczność zależą od dawki.
5) Mechanizmy odpowiedzi kukurydzy na nanocząstki srebra i tlenku cynku różnią się w poszczególnych organach.

III Materiał i metody

3.1. Badania wstępne

Do biosyntezy nanocząstek srebra i tlenku cynku wykorzystano dziewięć szczepów grzybów z rodzaju *Fusarium* pochodzących z kolekcji prof. dr hab. Patrycji Golińskiej, w Katedrze Mikrobiologii Uniwersytetu Mikołaja Kopernika. Szczepy grzybowe wykorzystane do optymalizacji syntezy nanocząstek (Tabela 1) przechowywano na skosach z pożywką PDA (*ang*. Potato Dextrose Agar, Becton Dickinson) w 4 ºC i w 70% glicerolu w – 80 ºC.

Tabela 1. Szczepy grzybowe wykorzystane do optymalizacji syntezy nanocząstek i ich pochodzenie.

Szczep	**Źródło izolacji**
Fusarium culmorum	wyizolowany z gleby leśnej
Fusarium culmorum JTW1 (DMS 114849)	wyizolowany z gleby
Fusarium graminearum A	wyizolowany z pszenicy ozimej
Fusarium graminearum D	wyizolowany z pszenicy ozimej
Fusarium oxysporum	wyizolowany z gleby leśnej
Fusarium oxysporum D	wyizolowany z pszenicy ozimej
Fusarium poae A	wyizolowany z pszenicy ozimej
Fusarium solani IOR 825	wyizolowany z pietruszki
Fusarium tricinctum A	wyizolowany z pszenicy ozimej

5.2. Zestawienie materiałów i metod wykorzystanych w badaniach

Szczegółowe opisy dotyczące badań nad właściwościami fizykochemicznymi i aktywnościami nanocząstek znajdują się w artykułach wchodzących w skład niniejszej pracy. W Tabeli 2 przedstawiono materiały i metody wykorzystane w badaniach wraz z odniesieniami do publikacji eksperymentalnych stanowiących podstawę niniejszej dysertacji.

Wszystkie nanocząstki pozyskane z wykorzystaniem wyżej wymienionych grzybów (Tabela 1) przebadano pod względem aktywności przeciwdrobnoustrojowej, wobec bakterii referencyjnych, fitopatogennych i przenoszonych przez żywność oraz grzybów patogennych dla roślin (dane częściowo opublikowane). Podstawą wyboru bionanocząstek srebra (AgNPs 1, AgNPs 2) oraz tlenku cynku (ZnONPs 1, ZnONPs 2) do dalszych badań była ich wysoka aktywność przeciwdrobnoustrojowa, szczególnie wobec patogenów roślin (**P3, P4**).

Tabela 2. Materiał i metody wykorzystane w badaniach.

MATERIAŁ BADAWCZY	**Publikacje**
Szczepy grzybowe wykorzystane do syntezy nanocząstek	P3-P6
Szczepy bakteryjne, grzybowe i grzybopodobne wykorzystane w badaniach aktywności przeciwdrobnoustrojowej	P3, P4
Ziarniaki kukurydzy wykorzystane do oceny wpływu nanocząstek na kiełkowanie i rozwój roślin	P4-P6
METODY	
Identyfikacja molekularna szczepu *Fusarium culmorum* JTW1	P3
Opis warunków hodowli grzybów oraz biosyntezy nanocząstek	
AgNPs 1	P3
AgNPs 2	P4, P5
ZnONPs 1	P4, P6
ZnONPs 2	P4
Metody wykorzystane do charakterystyki właściwości fizykochemicznych nanocząstek	
Dyfrakcja proszkowa promieniowania rentgenowskiego (XRD)	P3-P6
Transmisyjna mikroskopia elektronowa (TEM)	P3-P6
Spektroskopia w podczerwieni z transformacją Fouriera (FTIR)	P3-P6
Dynamiczne rozpraszanie światła (DLS)	P3-P6
Pomiar potencjału Zeta	P3-P6
Analiza śledzenia nanocząstek (NTA)	P3, P5, P6
Aktywność przeciwdrobnoustrojowa nanocząstek	
Wyznaczenie MIC, MBC i MFC metodą mikrorozcieńczeń	P3, P4
Wyznaczenie indeksu FIC (łączone działanie NPs z antybiotykami) metodą mikrorozcieńczeń	P3
Oznaczenie hamowania formowania biofilmu na podstawie barwienia fioletem krystalicznym i aktywności hydrolitycznej biofilmów z wykorzystaniem FDA	P3
Oznaczanie hamowania rozwoju grzybni fitopatogenów metodą dyfuzji w agarze	P3
Ocena hamowania rozwoju grzybni z wykorzystaniem techniki „poisoned food”	P4

Wpływ przedsiewnego traktowania ziarniaków z użyciem AgNPs oraz ZnONPs na kiełkowanie oraz wzrost u 7-dniowych siewek kukurydzy	
Ocena parametrów kiełkowania (procent kiełkowania, średni czas kiełkowania, wskaźnik szybkości kiełkowania)	P4
Ocena wzrostu (długość, świeża sucha masa) pędów i korzeni	P4
Wyznaczenie wskaźników wigoru siewek	P4
Wpływ przedsiewnego traktowania ziarniaków kukurydzy z użyciem AgNPs oraz ZnONPs na kiełkowanie oraz wzrost u 14-dniowych roślin (oddzielnie dla liści, łodyg, korzeni i skiełkowanego ziarniaka)	
Ocena parametrów kiełkowania (procent kiełkowania, średni czas kiełkowania, wskaźnik szybkości kiełkowania)	P5, P6
Ocena wzrostu (długość, świeża sucha masa)	P5, P6
Wyznaczenie wskaźników wigoru roślin	P5, P6
Oznaczenie poziomu zawartości chlorofilu w liściach	
Oznaczenie stężenia nadtlenku wodoru (H_2O_2)	P5, P6
Analiza peroksydacji lipidów przez oznaczenie poziomu dialdehydu malonowego (MDA)	P5, P6
Oznaczenie poziomu nieenzymatycznych przeciwutleniaczy (całkowity glutation (GSH+GGSG); askorbinian (ASC) i dehydroaskorbinian (DHA), współczynnik redoks askorbinianu)	P5, P6
Zbadanie aktywności enzymów antyoksydacyjnych, w tym peroksydazy (POX), peroksydazy askorobinianowej (APX), dysmutazy ponadtlenkowej (SOD), katalazy (CAT)	P5, P6
Oznaczenie akumulacji AgNPs	P5
Analiza statystyczna	
Jednoczynnikowa ANOVA, post-hoc test Tukey'a	P3-P6
Analiza głównych składowych (PCA)	P5, P6
Hierarchiczna analiza skupień (HCA)	P5, P6

IV Omówienie wyników badań

4.1. Biosynteza AgNPs i ZnONPs

Biosynteza jest przyjazną dla środowiska, niedrogą i prostą metodą, którą można wykorzystać do wydajnej produkcji AgNPs oraz ZnONPs, szczególnie z wykorzystaniem grzybów z rodzaju *Fusarium* (Rai i in., 2021). Potwierdziły to również badania wstępne do niniejszej pracy, w których zdolność do syntezy AgNPs i ZnONPs wykazywało odpowiednio 8 oraz 5 spośród 9 testowanych szczepów grzybowych (Tabela 3). Poza obserwacjami zmiany zabarwienia mieszaniny reakcyjnej z żółtej na ciemno brązową (AgNPs) lub strącania się białego osadu (ZnONPs) obecność nanocząstek potwierdzono za pomocą spektroskopii UV-vis, która wykazała charakterystyczne piki absorbancji w zakresie długości fali 420-434 nm dla AgNPs (Chan & Mat Don, 2013) oraz w zakresie długości fali 353-374 nm dla ZnONPs (Singh S. i in., 2024).

Tabela 3. Analiza UV-vis nanocząstek srebra (AgNPs) i tlenku cynku (wytwarzanych dwiema metodami: ZnONPs 1 oraz ZnONPs 2) z wykorzystaniem szczepów z rodzaju *Fusarium*, rosnących w optymalnym podłożu hodowlanym.

		Długości fali λ [nm]		
Szczep	**Podłoże**	**AgNPs**	**ZnONPs 1**	**ZnONPs 2**
Fusarium culmorum	PDB	-	355	374
Fusarium culmorum JTW1 (DMS 114849)	PDB	430	-	-
Fusarium graminearum A	PDB	421	353	-
Fusarium graminearum D	PDB	433	-	-
Fusarium oxysporum	PDB	432	355	-
Fusarium oxysporum D	PDB	434	-	358
Fusarium poae A	PDB	420	-	-
Fusarium solani IOR 825	SDB	420	358	356
Fusarium tricinctum	PDB	429	-	-

PDB; bulion glukozowo-ziemniaczany, SDB; bulion glukozowy wg. Sabourauda.

4.2. Właściwości fizyko-chemiczne i przeciwdrobnoustrojowe AgNPs

Wszystkie pozyskane w niniejszej pracy nanocząstki srebra wykazywały zróżnicowaną aktywność przeciwdrobnoustrojową i właściwości fizyko-chemiczne (dane częściowo opublikowane **P3**, **P4**), co wskazuje, że ich aktywność biologiczna może zależeć

od parametrów fizycznych i chemicznych nanocząstek, które są determinowane m. in. przez szczep grzybowy wykorzystany do syntezy, ale również od wrażliwości zbadanych szczepów wobec których testowano nanocząstki (**P1**). Porównując dwie wyselekcjonowane nanocząstki srebra, mianowicie AgNPs 1 wytwarzane za pomocą *F. culmorum* JTW1, wykazujące silną aktywność przeciwbakteryjną (**P3**) z AgNPs 2 pozyskanymi z *F. solani* IOR 825, które charakteryzowała wysoka aktywność przeciwgrzybowa (**P4**) wykazano, że analizowane NPs różniły się właściwościami fizyko-chemicznymi. Na podstawie wyników analiz z transmisyjnego mikroskopu elektronowego oraz wyników pomiaru średnicy hydrodynamicznej (DLS) wykazano, że AgNPs 1 miały większy rozmiar niż AgNPs 2. Ponadto, AgNPs 1 charakteryzowały się większą stabilnością (potencjał Zeta -38 mV), w porównaniu do AgNPs 2 (-17 mV) (**P3**, **P4**; Lavecchia i in., 2024). Wpływ właściwości fizyko-chemicznych, w tym głównie rozmiaru, kształtu i właściwości powierzchniowych, na aktywność przeciwdrobnoustrojową AgNPs został zbadany przez wielu autorów, którzy wykazali, że wraz ze spadkiem wielkości rośnie aktywność AgNPs wobec mikroorganizmów (Szerencsés i in., 2020). Jednak inni badacze wskazują na niewielki wpływ wielkości czy kształtu nanocząstek na ich aktywność biologiczną, którą wiążą z ładunkiem powierzchniowym NPs (Abbaszadegan i in., 2015; El Badawy i in., 2011). W niniejszej pracy, obydwa rodzaje AgNPs miały kształt kulisty i strukturę sześcienną, ściennie centrowaną (*ang.* face-centered cubic, fcc). Analiza FTIR nanocząstek wykazała obecność pików odpowiadających drganiom wiązań N-H (aminy pierwszorzędowe), C-H (związki aromatyczne), O-H (wiązanie wewnątrzcząsteczkowe), C= C (alkeny), C-H (aldehydy, alkany), C-N (aminy aromatyczne i alifatyczne), wskazując na obecność na ich powierzchni cząsteczek, m.in. o charakterze białkowym (**P3**, **P4)**. Jak pokazują badania, AgNPs opłaszczone związkami pochodzącymi z ekstraktów grzybowych, mogą być nierozpoznawanie przez mikroorganizmy i skutecznie omijać wykształcone przez nie mechanizmy oporności, co przyczynia się do zwiększonej aktywności przeciwdrobnoustrojowej AgNPs (Alavi & Ashengroph, 2023).

Na podkreślenie zasługuje fakt, że AgNPs 1 oprócz szerokiego spektrum działania wobec bakterii Gram-dodatnich i Gram-ujemnych, w niskich stężeniach, ograniczały formowanie i aktywność hydrolityczną biofilmów bakteryjnych (**P3**), które są strukturami charakteryzującymi się dużą opornością na środki przeciwbakteryjne i są przyczyną poważnych problemów w medycynie i przemyśle (Tripathi & Goshisht, 2022). W badaniach przeprowadzonych przez Hussain i in. (2019) opisano bio-AgNPs, które zaburzały quorum-sensing i ograniczały syntezę egzopolisacharydów, a tym samym formowanie biofilmów.

Ponadto, w innych badaniach wykazano, że AgNPs mogą hamować adhezję i ruchliwość komórek mikroorganizmów w wyniku wywoływanego stresu oksydacyjnego, zaburzania homeostazy żelaza oraz oddychania tlenowego i beztlenowego (Zhang i in., 2020). Co więcej, szczególnie interesujące w niniejszej pracy są wyniki badań łączonego działania AgNPs 1 i antybiotyków, zwłaszcza ze streptomycyną, w celu wzmocnienia działania przeciwbakteryjnego wobec bakterii Gram-ujemnych, takich jak *Escherichia coli*, *Klebsiella pneumoniae i Pseudomonas aeruginosa* (**P3**), należących do grupy ESKAPE, które wykazują oporność na wiele leków (Miller & Arias, 2024). Podobnie jak w niniejszej pracy, zwiększoną aktywność przeciwbakteryjną AgNPs w połączeniu ze streptomycyną opisali Shruthi i współautorzy (2019). Natomiast, inni badacze wykazali synergistyczne działanie AgNPs w połączeniu z kanamycyną, enoksacyną, neomycyną i tetracykliną wobec bakterii Gram-ujemnych (Fayaz i in., 2010; Deng i in., 2016), czego nie potwierdzono w badaniach przeprowadzonych w niniejszej pracy (**P3**), co może zależeć od wrażliwości badanych bakterii na testowane czynniki przeciwdrobnoustrojowe. Mechanizm zintegrowanego działania antybiotyków i AgNPs nie jest do końca poznany. Sugeruje się, że efekt synergistyczny może wynikać z tworzenia wiązań AgNPs-antybiotyk lub jednoczesnego, ale osobnego działania AgNPs i antybiotyku, co powoduje zmiany potencjału błony komórkowej i uszkodzenia ultrastrukturalne, a tym samym zwiększanie przepuszczalności błony komórkowej i przenikanie antybiotyków do komórki (Deng i in., 2016; Vazquez-Muñoz i in., 2019; Maniah i in., 2024). Chociaż AgNPs 1 wykazywały przede wszystkim silną aktywność przeciwbakteryjną, to hamowały także kiełkowanie zarodników i wzrost groźnych patogenów roślin, takich jak *Botrytis cinerea*, *Phoma lingam* i *Sclerotinia sclerotiorum* (**P3**).

Wyróżniającą aktywność wobec grzybowych patogenów roślin wykazywały AgNPs 2 syntezowane z wykorzystaniem *F. solani* IOR 825. Nanocząstki te w niskich stężeniach (16-64 $\mu g\ mL^{-1}$) działały bójczo wobec zarodników 15 z 22 testowanych szczepów grzybowych i grzybopodobnych (**P4**). Obserwowane różnice między wrażliwością szczepów grzybowych w odpowiedzi na AgNPs mogą wynikać z różnych mechanizmów oporności badanych grzybów (Ribeiro i in., 2023). Podobnie, jak w niniejszej pracy, hamowanie wzrostu grzybni i rozwoju zarodników *Sclerotinia sclerotiorum* przez bio-AgNPs wykazali Guilger i in. (2017) oraz Tomah i in. (2020). Działanie przeciwgrzybowe może być skutkiem wpływu AgNPs na zmianę przepuszczalności błony komórkowej czy akumulacji wewnątrzkomórkowej nanocząstek. Pod wpływem działania AgNPs obserwuje się również zmiany morfologiczne strzępek czy wakuolizację komórek grzybni (Li i in., 2022).

Natomiast zwiększone toksyczne działanie AgNPs na kiełkujące zarodniki grzybów w porównaniu ze strzępkami grzybni może wynikać z różnic w ich strukturze, np. ściany zarodników charakteryzuje mniejsza zawartość chityny niż w strzępkach grzybni (Brown i in., 2020). Ponadto, podczas procesu kiełkowania zarodników, disiarczkowe reduktazy i glukanazy rozluźniają ściany komórkowe tworząc wrażliwe miejsce na działanie substancji toksycznych, takich jak AgNPs (Matras i in., 2022).

4.3. Wpływ przedsiewnej dezynfekcji ziarniaków z wykorzystaniem bio-AgNPs na wzrost i kondycję kukurydzy

Kiełkowanie nasion i wczesny wzrost siewek są kluczowe dla późniejszych etapów rozwoju roślin, jednak zakażenia grzybowe są częstą przyczyną hamowania tych procesów (Magan i in., 2004; Rajjou i in., 2012; Akhtar & Kumar, 2024). W celu kontroli patogenów, zwiększenia wydajności kiełkowania i osiągnięcia lepszego wzrostu siewek stosowane są techniki przedsiewnego traktowania nasion, w tym roztworami nanocząstek (Abbasi Khalaki i in., 2021). Biologicznie syntezowane AgNPs wykazują potencjał do stosowania w rolnictwie jako środki przeciwdrobnoustrojowe i/lub stymulatory wzrostu roślin (Acharya i in., 2020; Sencan i in., 2024).

W niniejszej pracy, nanocząstki srebra z *F. solani* IOR 825 (AgNPs 2), z uwagi na silne działanie przeciwgrzybowe, zostały wyselekcjonowane do dalszych badań nad wpływem przedsiewnego traktowania ziarniaków kukurydzy w celu ich dezynfekcji powierzchniowej i ochrony przed patogenami. Efekt dezynfekujący powierzchnię ziarniaków uzyskano przy stężeniu AgNPs wynoszącym 32 µg mL^{-1} (**P4**). W badaniach Garcidueñas-Piña i in. (2023) wykazano, że bio-AgNPs w stężeniach 10 i 1000 µg mL^{-1} dezynfekowały powierzchnię nasion *Arabidopsis thaliana* i *Psidium guajava*, ze skutecznością w zakresie 89-95%.

Stężenie bioAgNPs wykorzystane do przedsiewnego traktowania nasion jest ważnym czynnikiem wpływającym na kiełkowanie i późniejszy wzrost i rozwój roślin (Prażak i in., 2020; Song i in., 2022; Garcidueñas-Piña i in., 2023; Pintos i in., 2024). Większość badań wskazuje, że niskie stężenia AgNPs wykorzystane do przedsiewnego traktowania nasion wpływają pozytywnie na wydajność kiełkowania, która wynika ze zwiększonego pobierania wody (Prażak i in., 2020; Soliman i in., 2020; Song i in., 2022; Pintos i in., 2024). Chociaż jak pokazują wyniki badań Garcidueñas-Piña i in. (2023) traktowanie nasion AgNPs w stężeniu 10 i 1000 µg mL^{-1} nie wpłynęło na wydajność kiełkowania rzodkiewnika, ale stężenie 1000 µg mL^{-1} zwiększyło wydajność kiełkowania gujawy. W niniejszej pracy nie

zaobserwowano wpływu AgNPs w badanych stężeniach (32-512 µg mL^{-1}) na parametry kiełkowania ziarniaków kukurydzy w porównaniu z kontrolą (**P4**, **P5**).

Analiza parametrów wzrostu 7-dniowych siewek kukurydzy rozwijających się z ziarniaków traktowanych AgNPs w zakresie stężeń 32-128 µg mL^{-1} nie wykazała negatywnego wpływu na produkcję biomasy. Natomiast przedsiewne traktowanie ziarniaków nanocząstkami w stężeniu 256 µg mL^{-1} wywołało niewielką redukcję świeżej biomasy (**P4**). W celu pełniejszego zrozumienia wpływu traktowania ziarniaków kukurydzy przez AgNPs na jej wzrost i kondycję zdecydowano o poszerzeniu prowadzonych badań. Parametry kiełkowania ziarniaków, wzrostu i stresu oksydacyjnego oraz komponentów systemu antyoksydacyjnego i zawartości chlorofilu oznaczono u 14-dniowych roślin rozwijających się z ziarniaków traktowanych trzema różnymi stężeniami (32, 128 i 512 µg mL^{-1}) AgNPs (**P5**). W niniejszych badaniach, parametry wzrostu roślin wskazują na zwiększenie suchej masy liści po traktowaniu ziarniaków kukurydzy niższymi stężeniami AgNPs (32 i 128 µg mL^{-1}), natomiast zastosowanie najwyższego stężenia nanocząstek (512 µg mL^{-1}) zwiększało długość oraz świeżą i suchą masę pędów. Warto podkreślić, nie wykryto znaczących zmian wskazujących na występowanie stresu oksydacyjnego w roślinach rozwijających się z ziarniaków traktowanych niższymi stężeniami AgNPs (32 i 128 µg mL^{-1}). Jednak zabieg ten miał wpływ na poziom H_2O_2 i zawartość/aktywność kilku składników systemu antyoksydacyjnego, które zmieniały się w sposób specyficzny dla danego organu i w zależności od zastosowanego stężenia AgNPs (**P5**). Badania innych autorów wykazały, że przedsiewne traktowanie nasion z użyciem AgNPs może aktywować ekspresję genów związanych z proliferacją komórek, metabolizmem i szlakami sygnalizacji hormonalnej (Gupta i in., 2018; Soliman i in., 2020), a także aktywować szlaki sygnalizacji stresu, takie jak transdukcja sygnału hormonów roślinnych, metabolizm glutationu, biosyntezy flawonoli, szlak sygnalizacji MAPK oraz interakcji roślina-patogen (Yan i in., 2023). Wywołanie tych zmian metabolicznych i transkrypcyjnych może wywoływać na długotrwałą „pamięć stresu", która jest kluczowa w ochronie roślin przed stresem abiotycznym i biotycznym (Yan i in., 2023).

W niniejszej pracy, w liściach kukurydzy rozwijającej się z ziarniaków traktowanych najwyższym testowanym stężeniem AgNPs zaobserwowano zwiększoną peroksydację lipidów i niższą zawartość chlorofilu. Mimo wyższej, aktywności peroksydazy i zwiększonej zawartości askorbinianu, RFT nie były skutecznie neutralizowane, w porównaniu do liści roślin rozwijających się z ziarniaków traktowanych niższymi stężeniami AgNPs (**P5**). Przy obniżonych poziomach chlorofilu nadmierny przepływ elektronów może

skutkować brakiem równowagi między miejscami donorowymi i akceptorowymi fotosystemu II. W konsekwencji, RTF generowane na skutek redukcji tlenu cząsteczkowego mogą powodować uszkodzenie komponentów fotosystemu prowadząc do hamowania fotosyntezy, tym samym zmniejszając jej wydajność (Bhattacharjee, 2019). Powyższe wyniki wskazują, że stosowanie AgNPs w zbyt wysokich stężeniach może wpływać toksycznie na rozwijające się rośliny, co jest zgodne z obserwacjami innych badaczy (Gupta i in., 2018; Salih i in., 2022; Karim i in., 2023; Koley i in., 2023). Jednak szczególnie interesujące jest to, że w poszczególnych organach kukurydzy rozwijającej się z ziarniaków traktowanych AgNPs 1 nie stwierdzono akumulacji jonów srebra (**P5**).

Uzyskane wyniki podkreślają konieczność precyzyjnego doboru warunków przedsiewnego traktowania nasion AgNPs, które w niskich stężeniach są skuteczne w kontroli patogenów na powierzchni ziarniaków zapobiegając infekcjom w trakcie kiełkowania, a w późniejszych etapach stymulują wzrost roślin. Jednak, AgNPs w zbyt wysokich dawkach mogą przyczynić się do nadmiernej produkcji RFT. Jeżeli nie są one skutecznie neutralizowane przez komórkowe systemy przeciwutleniające, mogą inicjować peroksydację lipidów w błonach biologicznych komórek roślin czy powodować degradację chlorofilu prowadząc do obniżenia zawartości tego barwnika.

4.4. Właściwości fizykochemiczne i aktywność przeciwdrobnoustrojowa ZnONPs wobec fitopatogenów

Badania właściwości przeciwdrobnoustrojowych pozyskanych w niniejszej pracy ZnONPs wykazały, że ich aktywność wobec bakterii patogennych dla roślin była porównywalna (dane częściowo opublikowane, **P4**), za wyjątkiem ZnONPs 1 i ZnONPs 2 pozyskanych z *F. solani* IOR 825, które charakteryzowały się silniejszymi właściwościami hamującymi wzrost (MIC) oraz bójczymi (MBC) wobec *Agrobacterium tumefaciens, Pseudomonas syringae* i *Xanthomonas campestris*. Żadna ze zbadanych nanocząstek ZnO nie hamowała wzrostu *Pectobacterium carotovorum* (**P4**).

W niniejszej pracy, badania przesiewowe aktywności przeciwgrzybowej ZnONPs potwierdziły, że nanocząstki syntezowane dwiema metodami (ZnONPs 1 oraz ZnONPs 2) z wykorzystaniem ekstraktów *F. solani* IOR 825, charakteryzowały się najsilniejszymi właściwościami hamującymi wzrost grzybów (dane częściowo opublikowane, **P4**). Nanocząstki ZnONPs 1 oraz ZnONPs 2 w stężeniu 1000 μg mL^{-1} hamowały wzrost 10 spośród 22 zbadanych grzybów fitopatogennych, w tym najsilniej *Fusarium oxysporum* IOR 342 oraz *Phoma lingam* IOR 2284 (odpowiednio na poziomie 100 i 60%). Zarówno ZnONPs

1, jak i ZnONPs 2 hamowały kiełkowanie (128-2048 µg mL^{-1}) i działały biobójczo (256-2048 µg mL^{-1}) wobec zarodników, odpowiednio 19 i 18 oraz 16 i 14 z 22 testowanych mikroorganizmów (**P4**), co może być dodatkowym atutem w aplikacjach rolniczych.

Dotychczas, aktywność przeciwgrzybową (hamowanie wzrostu grzybni i/lub kiełkowania zarodników) bio-ZnONPs wykazano wobec wielu fitopatogenów, takich jak *Alternaria alternata Alternaria brassicae*, *Aspergillus niger, Aspergillus terreus, Botrytis cinerea, Colletotrichum* sp., *Fusarium oxysporum*, *Fusarium solani, Macrophomina phaseolina, Penicillium expansum* i *Sclerospora graminicola* (Dhiman i in., 2021; González-Merino i in., 2021; Mohamed i in., 2021), jednak w niższych stężeniach niż w niniejszej pracy. Ze względu na silne właściwości utleniające, ZnONPs w reakcji z cząsteczkami wody lub anionami wodorotlenkowymi generują RFT. Stres oksydacyjny w komórkach mikroorganizmów prowadzi do zahamowania syntezy białek i replikacji DNA. Natomiast jony Zn^{2+} uwalniane z ZnONPs działają jako inhibitory enzymów poprzez utlenianie grup tiolowych lub powodują uszkodzenia błony cytoplazmatycznej (Mendes i in., 2022). Ponadto, zaproponowane przez autorów mechanizmy aktywności przeciwgrzybowej ZnONPs w komórkach *A. alternata* były związane z peroksydacją lipidów oraz uszkodzeniami błony komórkowej, prowadzącymi do wycieku białek i kwasów nukleinowych z komórek (Zhu i in., 2021). Autorzy sugerują, że stosowanie ZnONPs hamuje aktywność enzymów zaangażowanych w kiełkowanie zarodników i rozwój grzybni fitopatogenów, co ogranicza rozwój chorób grzybowych i zapobiega rozprzestrzenianiu się patogenów (González-Merino i in., 2021).

Interesujące jest to, że biosyntezowane ZnONPs są uważane za bardziej stabilne i biokompatybilne w porównaniu z chemicznymi, co wynika z obecności na ich powierzchni czynników ograniczających i stabilizujących pochodzenia naturalnego (Asif i in., 2021; Khalil & Alqahtany, 2020; Siddique i in., 2021). Porównując nanocząstki tlenku cynku syntezowane dwiema metodami (ZnONPs 1 oraz ZnONPs 2) z wykorzystaniem *F. solani* IOR 825 zaobserwowano, że ich rdzeń metaliczny był podobnej wielkości (średnia 120 i 175 nm; analiza TEM), jednak ich właściwości powierzchniowe były odmienne. Średnia wartość średnicy hydrodynamicznej tych nanostruktur wynosiła odpowiednio 261 i 1711 nm, a ich potencjał Zeta wynosił około -9 i -22 mV. Analiza FTIR wykazała podobny wzór grup funkcyjnych obecnych na ich powierzchni, za wyjątkiem dodatkowego wiązania C=C przypisanego do alkanów w widmie ZnONPs 2. Zarówno ZnONPs 1 jak i ZnONPs 2 wykazywały heksagonalną strukturę wurtzytu (**P4**). Odmienne właściwości fizyko-chemiczne ZnONPs 1 i ZnONPs 2 mogą wynikać z różnych warunków, w których

prowadzono proces biosyntezy, w tym różnego stężenia ekstraktu grzybowego, pH i temperatury. Wpływ stężenia ekstraktu z *Lactobacillus plantarum* TA4, pH i temperatury na wydajność oraz właściwości fizykochemiczne ZnONPs został opisany także w badaniach Mohd Yusof i in. (2022). Autorzy donoszą, że wydajność biosyntezy zwiększała się przy wyższym pH i stężeniu jonów cynku, podczas gdy rozmiar nanocząstek malał wraz ze spadkiem stężenia ekstraktu bakteryjnego w mieszaninie reakcyjnej.

Chociaż zbadane nanocząstki tlenku cynku wykazywały aktywność przeciwdrobnoustrojową, to nie była ona tak silna jak w przypadku bio-AgNPs. Jednakże głównym założeniem niniejszej pracy było zbadanie potencjału wyselekcjonowanych ZnONPs do stymulacji wzrostu kukurydzy.

4.5. Stymulujący efekt ZnONPs na wzrost kukurydzy

Kluczowa rola cynku dla wzrostu i rozwoju roślin a także ich odporności na stresy biotyczne lub abiotyczne wynika z jego udziału w szerokim zakresie procesów fizjologicznych (Camp, 1945; Umair Hassan i in., 2020). Cynk jest niezbędny dla roślin jako składnik zaangażowany w przemiany węglowodanów, fotosyntezę, biosyntezę białek, i oddychanie. Ponadto, pełni on rolę w zapewnianiu stabilności struktury i aktywności białek, co jest kluczowe w procesach transkrypcji oraz integralności i funkcjonalności błony komórkowej (Hacisalihoglu, 2020). Liczne badania podkreślają znaczącą rolę Zn w wydłużaniu komórek i syntezie tryptofanu, prekursora kwasu indolilo-3-octowego (Mašev & Kutáček, 1966; Sharifi, 2016; Sharma i in., 2021).

W niniejszych badaniach, nie odnotowano różnic w parametrach kiełkowania niezależnie od stężenia ZnONPs 1 i ZnONPs 2 (1-256 μg mL^{-1}) zastosowanego do przedsiewnego traktowania ziarniaków kukurydzy. Badania El-Badri i in. (2021) wykazały, że stymulacja kiełkowania nasion po traktowaniu ZnONPs była związana ze wzrostem aktywności metabolicznej i modulowaniem ekspresji genów kodujących białka zaangażowane w syntezę niektórych fitohormonów, mianowicie kwasu abscysynowego (ABA) i giberelin (GA). Natomiast ZnONPs w zakresie stężeń 16-256 μg mL^{-1} stymulowały wzrost siewek kukurydzy w porównaniu z kontrolą (**P4**). W 7-dniowych siewkach rozwijających się z ziarniaków traktowanych ZnONPs 1 odnotowano największy wzrost długości siewek oraz ich masy, szczególnie suchej (o 30,7%) po zastosowaniu stężenia 32 μg mL^{-1}. W przypadku ZnONPs 2 największy wzrost tych parametrów zanotowano po zastosowaniu stężenia 128 μg mL^{-1} (**P4**). W konsekwencji ZnONPs 1, które poprawiły

wzrost roślin już w znacznie niższych stężeniu, wykorzystano do dalszych badań przedstawionych w publikacji **P6**.

W niniejszej pracy oceniano wzrost 14-dniowych roślin rozwijających się z ziarniaków przedsiewnie traktowanych różnymi stężeniami (32, 128 i 512 μg mL^{-1}) ZnONPs, oraz wpływ takiego traktowania na poziom H_2O_2, zmiany w peroksydacji lipidów, aktywność enzymów antyoksydacyjnych i zawartość nieenzymatycznych przeciwutleniaczy w poszczególnych organach, a także poziom chlorofilu (**P6**).

Wzrost kukurydzy był stymulowany (świeża i sucha masa liści, łodyg i korzeni) na podobnym poziomie po traktowaniu ziarników ZnONPs w stężeniu 32 i 128 μg mL^{-1}. Przy czym odpowiedź systemu antyoksydacyjnego, produkcja chlorofilu i wytwarzanie nadtlenku wodoru w roślinach rozwijających się z ziarniaków zaprawianych najniższym testowanym stężeniem ZnONPs były najbardziej zbliżone do roślin kontrolnych (**P6**). Zarówno RFT, jak i działanie systemu antyoksydacyjnego odgrywają kluczową rolę w odpowiedzi roślin na różne stresy, ale co równie ważne, są zaangażowane w procesy wzrostu i rozwoju roślin pełniąc rolę regulatorową i sygnałową (Choudhary i in., 2020; Voothuluru i in., 2020). Z niniejszych badań wynika, że poprawa wzrostu kukurydzy w wyniku traktowania ziarniaków ZnONPs może być związana z utrzymaniem aktywności enzymów o właściwościach przeciwutleniających na poziomie, który umożliwia zachowanie równowagi oksydoredukcyjnej, w tym kontrolę stężenia H_2O_2 w tkankach, co zaobserwowano w liściach i korzeniach. Ponadto, wykazano, że traktowanie ziarniaków kukurydzy ZnONPs w stężeniu 512 μg mL^{-1} wywołało stres oksydacyjny, zwłaszcza w liściach, na co wskazuje jednoczesny wzrost zawartości H_2O_2, glutationu i MDA, oraz niewielka, ale istotna redukcja zawartości chlorofilu (**P6**).

Dotychczas, wykazano że stosowanie biosyntezowanych ZnONPs do zaprawiania nasion stymulowało wzrost m.in. *Vigna radiata* (fasola mung), *Cajanus cajan* (nikla indyjska), *Solanum lycopersicum* L. (pomidor), *Capsicum annuum* L. (papryka czerwona) (Rani i in., 2020; Sharma i in., 2022). Jednakże, wyniki niniejszej pracy, jak i te przedstawione przez innych autorów wyraźnie podkreślają znaczenie optymalizacji stężenia bio-ZnONPs zastosowanego w procesie przedsiewnego zaprawiania nasion w celu stymulacji kiełkowania i wzrostu roślin (Ashwini i in., 2024; Caser i in., 2024; Ramzan i in., 2024; D. Sharma i in., 2021; Singh N. i in., 2024).

Jednoczesna stymulacja wzrostu i brak fitotoksyczności ZnONPs 1 w stężeniu 32 μg mL^{-1} wskazuje na ich potencjał do wykorzystania w promowaniu wzrostu kukurydzy. Jednak do pełnego wykorzystania potencjału bio-nanocząstek tlenku cynku w ochronie i

promowaniu wzrostu roślin niezbędne są dalsze badania prowadzące do kompletnego poznania mechanizmów interakcji pomiędzy nanomateriałami i roślinami (Kang i in., 2024) i ich wpływu na środowisko (Ali i in., 2018).

V Publikacje wchodzące w skład rozprawy doktorskiej

Chapter 7

Mycogenic Synthesis of Silver Nanoparticles and its Optimization

Joanna Trzcińska-Wencel, Magdalena Wypij and *Patrycja Golińska**

Introduction

Today, over 1.5 million species of fungi are believed to thrive and survive in various habitats on Earth. However, only 70,000 species have been well identified. Fungi being predominately decomposer organisms secrete many enzymes extracellularly to break-down compounds of great complexity into simpler forms and use diverse energy sources (Blackwell 2011; Adebayo et al. 2021). Therefore, their wide range and diversity makes them an important tool for synthesis, applications, and developing new products in nanotechnology, including silver nanoparticles (AgNPs) (Rai et al. 2009; Guilger-Casagrande and Lima 2019; Adebayo et al. 2021). Moreover, fungal-mediated synthesis of AgNPs offers various advantages over biosynthesis by bacteria, plants, or algae. In comparison to the other biological systems, it is believed that the fungi may have greater potential for NPs synthesis because they release a large number of metabolites, especially proteins, demonstrate bioaccumulation ability and high binding capacity, tolerance to metals, and intracellular uptake competencies for metals (Mandal et al. 2006; Narayanan and Sakthivel 2010; Alghuthaymi et al. 2015; Rauwel et al. 2015; Singh et al. 2016; Madakka et al. 2018). It is suggested that biomolecules such as peptides, proteins, or enzymes secreted by these microorganisms are responsible for the reduction of silver ions and induction of nanoparticle synthesis and encapsulation (Konappa et al. 2021). In the contaminated

Department of Microbiology, Faculty of Biological and Veterinary Sciences, Nicolaus Copernicus University, Lwowska 1, 87 100 Toruń, Poland.
* Corresponding author: golinska@umk.pl

environment, fungi as a biological system, attempt to reduce the number of silver ions to prevent silver toxicity and environmental pollution (Pandiarajan et al. 2011; Adebayo et al. 2021). Furthermore, the fungal growth is easy to perform, fast, and provides a huge amount of biomass used for nanoparticle synthesis that can take place intra- and/or extracellularly (Boroumand Moghaddam et al. 2015; Adebayo et al. 2021). In addition, fungal biomass does not require additional steps to extract the filtrate which is used for the biosynthesis of AgNPs (Gade et al. 2008). It should be also emphasized that the biosynthesis of silver nanoparticles is an eco-friendly process when compared to chemical synthesis that involves the use of reagents that are toxic and hazardous to health and the environment (Guilger-Casagrande and Lima 2019). Although mycosynthesis of AgNPs is important for process efficiency, the classical strategy for optimization of biosynthesis parameters through fixing all process parameters except one variable is time and labor-consuming as well as not consider the interactions between different bioprocess factors (Othman et al. 2017). Moreover, the genetic manipulation to overexpress specific enzymes in order to intensify synthesis is much more difficult among eukaryotes than prokaryotes (Rauwel et al. 2015).

Fungi as nanofactories—an overview

Many fungal strains have been reported as a biological system for the synthesis of AgNPs including *Fusarium oxysporum, Aspergillus niger, Alternaria alternata, Penicillium oxalicum, Fusarium solani, Trichoderma asperellum, Rhizopus stolonifer, Cladosporium cladosporioides, Candida albicans, Phoma* spp. and many others (Gade et al. 2008; Mukherjee et al. 2008; Abd El-Aziz et al. 2015; AbdelRahim et al. 2017; Hamzah et al. 2018; Feroze et al. 2019; Hulikere and Joshi 2019; Hikmet and Hussein 2021; Govindappa et al. 2022).

The biosynthesis of AgNPs is preliminarily confirmed by visual observation of the color change of the reaction mixture consisting of fungal extract and silver nitrate ($AgNO_3$) and then by measuring the absorbance of the AgNPs suspension using UV-Vis spectroscopy. Generally, UV-Vis spectra of AgNPs are monitored in the range of 200–700 nm and the presence of a maximum absorption peak around 380–450 nm is related to the AgNPs characteristic surface plasmon resonance (SPR) (Desai et al. 2012; Mistry et al. 2021). Basically, physico-chemical properties of the biosynthesized AgNPs including shape, size, size distribution, crystallinity, stability, and capping agents are investigated by using analytical techniques such as Transmission Electron Microscopy (TEM), High-Resolution TEM (HRTEM), Scanning Electron Microscopy (SEM), Field-Emission SEM (FESEM), Atomic Force Microscopy (AFM), Dynamic Light Scattering (DLS), X-ray diffraction (XRD), Zeta potential and Fourier Transform Infrared Spectroscopy (FTIR) (Verma et al. 2010; Mishra et al. 2011; Kumar et al. 2012; Costa Silva et al. 2017; Elamawi et al. 2018).

These physical and chemical properties, but also biological activity of biosynthesized AgNPs depend on the fungal strains used for the synthesis. Therefore, various fungal nanofactories that have the ability to synthesize AgNPs are described below and in Table 1. The majority of the studies have involved fungi

Table 1. An overview of fungi and yeasts used for intra- and extra-cellular synthesis of AgNPs with various shapes and sizes.

Fungi	Type of synthesis	A max	Morphology	Size [nm]	References
*Acremonium borodinens*e	extracellular	420	spherical		Lawrance et al. 2021
Alternaria alternata	extracellular	440	spherical	8–48	Govindappa et al. 2022
Aspergillus brunneoviolaceus	extracellular	411	spherical	0.7–15.2	Mistry et al. 2021
Aspergillus caespitosus	Exo-filtrates	410	spherical, hexagonal, irregular shapes	10–50	El-Bendary et al. 2021
Aspergillus caespitosus	Endo-filtrates	410	spherical, hexagonal, irregular shapes	3–100	El-Bendary et al. 2021
Aspergillus clavatus	extracellular	415	Spherical, hexagonal, polydispersed	10–25	Verma et al. 2010
Aspergillus fumigatus	extracellular	420	spherical, triangular	5–25	Bhainsa and D'souza 2006
Aspergillus niger	extracellular	420	spherical	20	Gade et al. 2008
Aspergillus oryzae NRRL447	exogenous proteins	410	spherical	15–109.6	Elshafei et al. 2021
Aspergillus terreus	extracellular	440	spherical, nearly spherical	1–20	Li et al. 2012
Aspergillus terreus BA6	extracellular	420	spherical	7–23	Lotfy et al. 2021
Candida albicans	extracellular	420	different morphologies	20–80	Rahimi et al. 2016
Candida albicans	extracellular	429	spherical	40.19	Hikmet and Hussein 2021
Candida glabrata	extracellular	460	spherical and oval	2–15	Jalal et al. 2018
Candida guilliermondii	extracellular	425	near spherical	10–20	Mishra et al. 2011
Cladosporium cladosporioides	extracellular	440	spherical	30–60	Hulikere and Joshi 2019
Cladosporium cladosporioides	extracellular	415	spherical, polydisperse	10–100	Balaji et al. 2009
Cladosporium halotolerans	extracellular	415	spherical	20	Ameen et al. 2021
Colletotrichum sp. ALF2-6	extracellular	420	spherical, near to spherical, triangular and hexagonal	5–60	Azmath et al. 2016
*Duddingtonia flagran*s	extracellular	413	quasispherical	10.3 ± 7.2	Costa Silva et al. 2017

Table 1 contd. ...

...Table 1 contd.

Fungi	Type of synthesis	A max	Morphology	Size [nm]	References
Fusarium acuminatum	Extracellular	420	spherical	5-40	Ingle et al. 2008
Fusarium equiseti	extracellular	300	spherical, with smooth surface	2–50	Haji Basheerudeen et al. 2021
Fusarium mangiferae	extracellular	416	spherical, oval	25–52	Hamzah et al. 2018
Fusarium oxysporum	extracellular	440	Spherical, needle-shaped, monodispersed	3.4–26.8	Ishida et al. 2014
Fusarium oxysporum	extracellular	413	spherical, monodispersed	40 ± 5.0	Salaheldin et al. 2016
Fusarium oxysporum	extracellular	413	highly variable, spherical, triangular, aggregated	5–15	Ahmad et al. 2003
Fusarium oxysporum	intracellular	430	spherical, aggregated	25–50	Korbekandi et al. 2013
Fusarium oxysporum-NFW16	extracellular	423	spherical, monodispersed	30–36.1	Ilahi et al. 2021
Fusarium semitectum	extracellular	420	spherical	10–60	Basavaraja et al. 2008
Fusarium solani	extracellular	415	spherical	5–30	Abd El-Aziz at al. 2015
Guignardia mangiferae	extracellular	417	spherical	5–30	Balakumaran et al. 2015
Penicillium brevicompactum WA 2315	extracellular	420	different morphologies	23–105	Shaligram et al. 2009
Penicillium chrysogenum	extracellular	400	spherical, monodispersed	48.2	Barabadi et al. 2021
Penicillium fellutanum	extracellular	430	spherical	5–25	Kathiresan et al. 2009
Penicillium oxalicum	extracellular		spherical	60–80	Feroze et al. 2019
Penicillium oxalicum GRS-1	extracellular	420	spherical, monodispersed	10–40	Rose et al. 2019
Penicillium radiatolobatum	extracellular	410	spherical, triangle, hexagonal, polydispersed	5.09–24.85	Naveen et al. 2021
Penicillium toxicarium	extracellular	396	spherical	48.03–73.04	Korcan et al. 2021
Phaenerochaete chrysosporium	extracellular	470	pyramidal	50–200	Vigneshwaran et al. 2006

Table 1 contd. ...

...Table 1 contd.

Fungi	Type of synthesis	A max	Morphology	Size [nm]	References
*Phoma glomerat*a	extracellular	440	spherical	60–80	Birla et al. 2009
*Rhizopus stolonife*r	extracellular	420	spherical	6.04	AbdelRahim et al. 2017
Saccharomyces cerevisiae	extracellular	410	spherical	> 70	Niknejad et al. 2015
Trichoderma asperellum	extracellular	410	spherical	13–18	Mukherjee et al. 2008
Trichoderma harzianum	extracellular	438	cubic	72	Konappa et al. 2021
Trichoderma longibrachiatum	extracellular	385	spherical, polydispersed	5–25	Elamawi et al. 2018
Trichoderma viride	extracellular		polydispersed, globular	1–50	Elgorban et al. 2016
Verticillium sp.	intracellular	450	spherical	25	Mukherjee et al. 2001

Key: A, absorbance

Fusarium spp., *Aspergillus* spp., *Trichoderma* spp., and *Penicillium* spp. Among the presented studies, extracellular synthesis predominated and the synthesized nanoparticles were mainly spherical in shape. However, pyramidal-shaped ones were synthesized from *Phaenerochaete chrysosporium* (Vigneshwaran et al. 2006) while highly heterogeneous nanoparticles were biofabricated using *Fusarium oxysporum* (Ahmad et al. 2003), *Penicillium brevicompactum* WA 2315 (Shaligram et al. 2009), *Penicillium radiatolobatum* (Naveen et al. 2021) and *Colletotrichum* sp. ALF2-6 (Azmath et al. 2016). In fact, the smallest nanoparticles were synthetized from *Candida glabrata* and *Aspergillus brunneoviolaceus* with sizes in the range 2–15 nm and 0.7–15.2 nm, respectively (Jalal et al. 2018; Mistry et al. 2021). Maximum absorbance peaks ranged at a wavelength from 300 nm (with NP size 2–50 nm) to 470 nm (with NP size 50–200 nm) which may be associated with the size distribution of the mycogenic nanoparticles (Vigneshwaran et al. 2006; Haji Basheerudeen et al. 2021).

Aspergillus spp.

Several studies investigated the use of biomass or cellular filtrate of *Aspergillus* species for the synthesis of AgNPs (Bhainsa and D'souza 2006; Gade et al. 2008; Verma et al. 2010; Yari et al. 2022). The ability to synthesize nanoparticles by *Aspergillus* spp. was demonstrated with absorbance maximum peaks in the 410–440 nm wavelength range and spherical or irregular shapes (Table 1). Therefore, Wang and coworkers (2021) synthesized polydispersed spherical silver nanoparticles with sizes between 1 and 24 nm using the culture supernatants of *Aspergillus sydowii* strain isolated from soil. TEM-based size distribution of bio-AgNPs showed that 38%

of the AgNPs were in size from 1 to 5 nm, 45% in a range of 5–10 nm, and 12% between 10 and 15 nm (Wang et al. 2021). El-Bendary and coworkers (2021) compared the biosynthesis of AgNPs carried out using the extracellular and intracellular filtrates of the *Aspergillus caespitosus*. Both exo- and endocellularly synthesized AgNPs showed an absorbance peak at 410 nm. Nanoparticles were spherical and hexagonal, had anisotropic crystalline structure, and ranged in size 10–50 nm and 3–100 nm, respectively. Moreover, UV–visible spectroscopy confirmed, that biosynthesized AgNPs (bioAgNPs) were stable for up to 5 months of storage at 4ºC (El-Bendary et al. 2021). Recently, Yari et al. (2022) synthetized spherical and agglomerated AgNPs with a size > 40 nm using mycelial extract of *Aspergillus terreus*. In addition, the small zeta potential value (+ 0.7 mV) of synthesized nanoparticles resulted in a high agglomeration propensity. Moreover, they proposed that the hydroxyl and amide I functional groups detected in the fungal extract from *A. terreus* may assist in forming and stabilizing biosynthesized nanoparticles.

Fusarium spp.

Many scientists used different fungi of the genus *Fusarium* to prepare AgNPs with different sizes and shapes depending upon species (Ishida et al. 2014; Korbekandi et al. 2013; Abd El-Aziz et al. 2015; Rai et al. 2021). *Fusarium* spp. are filamentous fungi that are widely distributed in soil, water and associated with plants (Nelson et al. 1994). *F. oxysporum* is the most frequently reported fungus for AgNPs synthesis (Durán et al. 2005; Salaheldin et al. 2016; Korbekandi et al. 2013; Ilahi et al. 2021; Allend et al. 2021). Ahmad et al. (2003) reported for the first time on the extracellular biosynthesis of AgNPs by a eukaryotic system, namely *Fusarium oxysporum.* Transmission electron microscopy (TEM) showed spherical, triangular, and small particles in the range of 5–15 nm and their aggregates in the size range 5–50 nm. In addition, the authors proposed that the NADH-dependent reductase released by the fungus may be responsible for the reduction of Ag^+ ions and the formation of silver nanoparticles (Ahmed et al. 2003). Furthermore, Anil Kumar et al. (2007) elucidated this mechanism by *in vitro* synthesis of AgNPs with nitrate reductase purified from *Fusarium oxysporum,* phytochelatin, and, α-NADPH as a cofactor. The enzymatic synthesis provided spherical nanoparticles in the size of 10–25 nm in diameter and stabilized by capping peptides. UV-visible spectroscopy showed an absorption peak at 413 nm. Surface plasmon resonance (SPR) absorption peak for silver nanoparticles was not observed in the absence of enzyme or phytochelatin or α-NADPH cofactor in the reaction mixture. This indicated that the reduction of Ag^+ ions involves enzymatic reduction of nitrate to nitrite. Moreover, the enzymatic process is simple and easy for downstream processing and may be suitable for mass-scale production (Anil Kumar et al. 2007). Ishida and coworkers (2014) also reported extracellular biosynthesis of AgNPs by using *F. oxysporum*, but these AgNPs were slightly different in morphology. They were in the size range 3.4–26.8, spherical and needle-shaped (Ishida et al. 2014). Otherwise, intracellular synthesis of AgNPs by *F. oxysporum* was reported by Korbekandi et al. (2013). However, intracellular synthesis required additional processing steps to release synthesized nanoparticles from cells and is less efficient compared to extracellular process

(Durán et al. 2005). Recently, marine endophytic fungi *Fusarium equiseti* isolated from seaweed were used for the synthesis of AgNPs. Analysis of morphological features of these AgNPs proved their small size (2–50 nm), spherical shape, and smooth surface (Haji Basheerudeen et al. 2021). Other reports provide mycosynthesis of silver nanoparticles by different *Fusarium* species, such as *F. acuminatum, F. mangiferae, F. semitectum, F. solani,* and *F. pallidoroseum* (Ingle et al. 2008; Haji Basheerudeen et al. 2021; Basavaraja et al. 2008; Abd El-Aziz et al. 2015; Shukla et al. 2021), as showed in Table 1.

Penicillium spp.

Various species of the genus *Penicillium* were capable of producing AgNPs with different sizes and morphologies in a green approach (Shaligram et al. 2009; Kathiresan et al. 2009; Rose et al. 2019; Korcan et al. 2021). Silver nanoparticles synthesized from *Penicillum* spp., showed a remarkable variety of shapes (Table 1), including spherical (Kathiresan et al. 2009; Feroze et al. 2019; Rose et al. 2019), hexagonal, and triangle ones (Naveen et al. 2021). Hence, AgNPs with sizes ranging from 5.09 to 24.85 nm were prepared from the endophytic fungus *Penicillium radiatolobatum*. The morphology of these NPs was highly variable, namely mostly spherical, but some triangles and hexagonal were also recorded (Naveen et al. 2021). Similar results were presented by Kathiresan et al. (2009). They proved an extracellular biosynthesis of spherical and small (5–25 nm) AgNPs by synthesized from *P. fellutanum* isolated from mangrove root soil. As mentioned previously, the size, shape, and dispersion of the biosynthesized nanoparticles vary depending on the fungal strains and methods used in the synthesis process. For example, spherical, but different sizes (60–80 nm and 10–40 nm) AgNPs from *Penicillium oxalicum* were obtained by Feroze et al. (2019) and Rose et al. (2019), respectively.

Trichoderma spp.

Several non-pathogenic, species of the *Trichoderma* were used for the extracellular biosynthesis of spherical AgNPs including *T. asperellum*, *T. longibrachiatum*, and *T. viride* (Mukherjee et al. 2008; Elgorban et al. 2016; Elamawi et al. 2018; Qu et al. 2021). UV-visible spectroscopy provided maximum absorption peaks for all silver nanoparticles synthesized from *Trichoderma* in the range from 385 nm for *T. longibrachiatum* (size 5–25 nm) to 438 nm for *T. harzanium* (size 72 nm) (Table 1). Size analysis of AgNPs from *T. viride* using TEM showed a formation of spherical and irregularly formed, polydispersed particles in a range 1–50 nm. TEM analysis proved also a thin layer of organic material on the surface of nanoparticles, which provided stability of AgNPs (Elgorban et al. 2016). Silver nanoparticles synthesized from *T. asperellum* were spherical in shape and size ranging from 13–18 nm (Mukherjee et al. 2008). Konappa and coworkers (2021) synthesized cubic, polydispersed AgNPs using *T. harzianum* cell filtrate. This cell filtrate was rich in the alkaloids, flavanones, steroids, and phospholipids that were believed to be the ones responsible for the reduction of ions and/or capping silver nanoparticles (Konappa et al. 2021). In addition, other *Trichoderma* strains namely,

T. atroviride, T. crissum, T. longibrachiatum, T. spirale, *T. virens*, *T. afroharzianum*, *T. hamatum*, *T. citrinoviride, T. koningiopsis* and *T. velutinum* were successfully used for the synthesis of spherical AgNPs in size ranged from 5 to 35 nm. However, the results confirmed that AgNPs were most efficiently synthesized by the species of *T. longibrachiatum* (155.2 ± 15.02 mg of AgNPs per 100 mL of filtrate) (Qu et al. 2021).

Yeasts

Recently, many researchers have focused on the synthesis of silver nanoparticles using yeasts, which are non-toxic, and exhibit bio-accumulative potential for the synthesis of nanoparticles with high efficiency and low cost. Moreover, yeasts adopt different mechanisms for the formation and stabilization of AgNPs that display differences in size and shape (Boroumand Moghaddam et al. 2015; Skalickova et al. 2017; Shu et al. 2020). Thus, the presence of silver ions in the culture medium triggers a stress response, including the production of biomolecules responsible for internal stress elimination such as phytochelatin synthase and glutathione. Bioreduction of silver ions into nanoparticles is enabled by the redox and nucleophilic properties of these molecules (Kowshik et al. 2003; Skalickova et al. 2017). In addition, Shu et al. (2020) studied the formation of nanoparticles in yeast cell-free extract and suggested that reducing agents such as amino acids, vitamins, and carbohydrates present in yeast extract were responsible for Ag^{+} ions reduction (Shu et al. 2020). Moreover, another study indicated a potential role of pigments in nanoparticle formation, specifically cell-associated melanin produced by *Yarrowia lipolytica*. Silver ions may be reduced to silver nanoparticles during the transition of quinone residues of melanin to alternate between the hydroxyl and quinone forms (Apte et al. 2013a; 2013b; Roy et al. 2019).

A number of studies have confirmed the ability of yeasts to the synthesis of AgNPs including *Candida guilliermondii, Candida utilis, Saccharomyces cerevisiae, Saccharomyces uvarum, Pichia kudriavzevii,* and marine yeast of *Candida* sp. VITDKGB (Mishra et al. 2011; Niknejad et al. 2015; Waghmare et al. 2015; Korbekandi et al. 2016; Dhabalia et al. 2020; Kumar et al. 2011; Ammar et al. 2021). Jalal et al. (2018) reported the synthesis of spherical and oval AgNPs by *C. glabrata.* The produced nanoparticles ranged in size from 2 to 15 nm and were smaller than those synthesized by other *Candida* species, especially those belonging to *C. albicans* (Table 1). Size distribution, shape, state of aggregation, and surrounding dielectric medium of nanoparticles affect the optical absorption spectrum of silver nanoparticles (Smitha et al. 2008). Ag NPs synthesized from *C. glabrata* showed a maximum absorbance peak at wavelength 460 nm. This SPR wavelength shifted towards a longer wavelength region indicating polydisperse and agglomerated nanoparticles (Vanaja et al. 2013; Jalal et al. 2018).

Other fungi

A number of scientists have developed a variety of fungi for the synthesis of metal nanoparticles. These include fungal extract from endophytic fungi, namely

Alternaria alternata isolated from *Dendrophthoe falcata* (Govindappa et al. 2022), *Colletotrichum* sp. ALF2-6 isolated from *Andrographis paniculata* (Azmath et al. 2016), *Guignardia mangiferae* isolated from the leaves of *Citrus* sp. (Balakumaran et al. 2015). *Verticillium* sp. isolated from the *Taxus* plant was employed for intracellular synthesis of AgNPs. Interestingly, a number of silver nanoparticles were observed in TEM micrographs associated with the cell wall of the *Verticillium* cells after the synthesis process. Obtained nanoparticles were spherical, with an average size of 25 nm ± 12 nm and fairly good monodispersity (Mukherjee et al. 2001).

Otherwise, spherical, monodispersed AgNPs with an average size of 9.46 ± 2.64 nm were synthesized by a mycelial aqueous extract of *Rhizopus stolonifer* isolated from tomato fruits (AbdelRahim et al. 2017). In addition, *Phoma glomerata* was studied for the rapid synthesis of spherical, small size (average size 19 nm), and very stable (zeta potential value of −30.7 mV) AgNPs in the presence of bright sunlight as an inducing agent. Furthermore, the authors suggested that photosensitizated aromatic molecules from fungal extract generate free electrons, which may be involved in the rapid synthesis of AgNPs under sunlight (Gade et al. 2014). Besides, some other fungi have been found for AgNPs synthesis, namely nematophagous fungus *Duddingtonia flagrans* (Costa Silva et al. 2017), white-rot fungus, *Phaenerochaete chrysosporium* (Vigneshwaran et al. 2006), soilborne pathogen *Rhizoctonia solani* isolated from *Rosmarinus officinalis* (Ashrafi et al. 2013) and many others (Table 1).

Influence of physico-chemical parameters on mycosynthesis of AgNPs

Control of biosynthesis conditions of nanoparticles is an important area of research in nanoscience (AbdelRahim et al. 2017). The optimization of these conditions is the preliminary investigation for their large-scale production and industrial applications (Nayak et al. 2011). According to Srikar and coauthors (2016), the major physical and chemical parameters that affect the synthesis of AgNPs include temperature, metal ion concentration, pH of the reaction mixture, duration of reaction, and agitation. It should be emphasized that these parameters affect both the quality and quantity of the synthesized silver nanoparticles, as well as, their properties for further applications (Das et al. 2020). Therefore, by adjusting synthesis conditions it is possible to manipulate the metabolism of fungi and subsequently biosynthesis of nanoparticles with the desired characteristics, such as specific size and morphology (Zielonka and Klimek-Ochab 2017). However, according to Birla et al. (2013), the physico-chemical conditions during the synthesis with the use of the fungus depends on the selected strain, its growth requirements, and metabolic activity. Table 2 shows selected studies on the synthesis of AgNPs using different fungal species and synthesis conditions.

Effect of temperature

Temperature is one of the key controlling factors affecting the formation of AgNPs and their properties (Figure 1) (Birla et al. 2013; Rose et al. 2019) that can also influence the reaction rate of the synthesis process (Phanjom and Ahmed 2017). For

Table 2. Optimization of the synthesis of silver nanoparticles by fungi.

Fungus	Type of parameters	Optimized conditions	Nanoparticle characteristics	References
Arthroderma fulvum	temperature, pH, concentration of $AgNO_3$ and time of reaction	55ºC; pH 10; 1.5 mM $AgNO_3$; 12 h	20.56 nm, spherical	Xue et al. 2016
Aspergillus fumigatus BTCB10	temperature, fungal culture age, substrate concentration and biomass weight, pH	25ºC; 7 days of culture; 7 g of biomass; 1 mM $AgNO_3$; pH 6	322.8 nm, spherical	Shahzad et al. 2019
Aspergillus niger NRC1731	pH, time incubation and concentration of $AgNO_3$	1.82 mM silver nitrate for 34 h at pH 7.0	3–20 nm, spherical	Elsayed et al. 2018
Aspergillus oryzae MTCC1846	temperature, pH and concentration of $AgNO_3$	90ºC; pH 10; 1 mM $AgNO_3$	4–9 nm, spherical	Phanjom and Ahmed 2017
Aspergillus sydowii	temperature, pH and $AgNO_3$ concentrations	50ºC; 8.0 pH; 1.5 mM $AgNO_3$	1–21 nm, spherical	Wang et al. 2021
Aspergillus terreus BA6	reaction pH, dextrose (g/l), peptone (g/l), and $AgNO_3$ concentration (mM)	pH 6.25; dextrose 27.5 (g/l); peptone 8.75 (g/l); and $AgNO_3$ 4.26 mM;	7–23 nm, –17.5 mV, spherical, well dispersed	Lotfy et al. 2021
Duddingtonia flagans	temperature and pH, culture medium	60ºC; pH 10; filtrate supplemented with chitin	30-409 nm, –28.6 mV, spherical	Costa Silva et al. 2017
Fusarium oxysporum	temperature and culture media	28ºC and modified medium for nitrate reductase	24 nm, spherical	Hamedi et al. 2017
Fusarium sp. 4F1, *Trichoderma* sp. TrS	pH and concentration of $AgNO_3$, time incubation	pH 9; 72 hrs of incubation period and 2 mM concentration of $AgNO_3$	spherical, monodispersed and stable	Pal and Hossain 2020
Penicillium oxalicum GRS-1	temperature, quantity of biomassa, concentration of $AgNO_3$ and pH	60ºC; 25 g of biomass; 1.5 mM $AgNO_3$, pH 7-8	10–40 nm, spherical	Rose et al. 2019
Rhizopus stolonifer	temperature and concentration of $AgNO_3$	40ºC; 10 mM $AgNO_3$	2.86 nm, spherical	AbdelRahim et al. 2017
Sclerotinia sclerotiorum MTCC 8785	culture media, quantity of biomass, concentration of $AgNO_3$, pH and temperature	potato dextrose broth; 10 g of biomass, 1 mM $AgNO_3$; pH 11; 80°C	10–15 nm, spherical	Saxena et al. 2016
Trichoderma longibrachiatum	temperature, quantity of biomass and agitation	28ºC; 10 g of biomass without agitation	24.43 nm, –19.7 mV, spherical	Elamawi et al. 2018

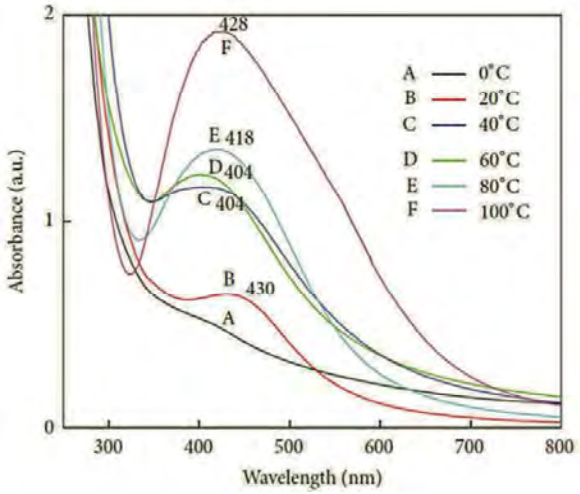

Figure 1. Effect of temperature on the size of SNPs from *Fusarium oxysporum*: UV-Vis spectral analysis shows reduction of SNPs. A: 0°C, B: 20°C, C: 40°C, D: 60°C, E: 80°C, and F: 100°C. Spectrum C and spectrum D have the blue shift which indicates the small size of synthesized SNPs. Spectrum F asymmetric spectra indicate the aggregation of particles at high temperatures (adapted and modified from Birla et al. 2013, an open-access article).

example, Hamedi et al. (2017) analyzed the efficiency of AgNPs synthesis at various temperatures, namely 23, 28, and 33°C using the cell-free filtrates of *Fusarium oxysporum* and found that AgNPs were most efficiently synthesized at 28°C. Similar observations were done by Elamawi and coauthors (2018). They recorded that AgNPs synthesis using *Trichoderma longibrachiatum* was effective at 28°C, while inhibited at 23 or 33°C. In turn, other scientists, such as Rose et al. (2019) and Costa Silva et al. (2017), reported a favorable effect of temperature increase on the production of silver nanoparticles. Rose and coauthors (2019) studied AgNPs synthesis using a fungal strain of *Penicillium oxalicum* GRS-1 and observed that the nanoparticles biosynthesized at 60°C showed the highest and narrower absorbance peak when analyzed by UV-Vis spectroscopy and were in the range of 10–40 nm. In contrast, those synthesized at 20, 30, 40 and 50°C showed broader absorbance peaks, which indicated the existence of nanoparticles with different sizes ranging from 10 to 100 nm. Similarly, Costa Silva et al. (2017), reported that optimum synthesis of AgNPs using *Duddingtonia flagans* filtrate was found to be at 60°C, while synthesis was inhibited at 30°C. AbdelRahim and coauthors (2017), synthesized AgNPs at 20, 40, and 60°C using *Rhizopus stolonifer* aqueous mycelial extract and found that obtained NPs were in the mean sizes of 25.89, 2.86, and 48.43 nm, respectively. These results clearly proved that temperature is a key factor in the manipulation of nanoparticle size. In contrast, Shahzad et al. (2019) demonstrated that AgNPs size increased from 332.8 nm to 1073.45 nm together with temperature increase from 25°C to 55°C, respectively when Dynamic light scattering (DLS) analyses were performed. The synthesis of nanoparticles at higher temperatures is probably carried out by transferring electrons from free amino acids present in fungal extracts to silver ions (Guilger-Casagrande and Lima 2019). However, very high temperatures

lead to denaturation of the proteins that cover the surface of nanoparticles. This denaturation alters the nucleation of Ag^+ ions, resulting in nanoparticle aggregation and size increase (Birla et al. 2013; Guilger-Casagrande and Lima 2019). Moreover, Phanjom and Ahmed (2017) demonstrated that the higher the temperature of the reaction mixture, the lowest the reaction time. The increase in temperature from 30 to 50, 70 and 90°C reduced reaction time from 6 h to 1 h, 45 min and 20 min, respectively. However, the synthesis of AgNPs at 10°C was completely inhibited.

Effect of pH

The pH value contributes greatly to increasing or decreasing the number of H^+ ions in the reaction mixture (Manosalva et al. 2019). It is well known that a lower pH value leads to an increase in the concentration of H^+ (Siddiqi et al. 2018). The pH does not directly affect the conformational changes of proteins and enzymes, but the change in the concentration of H^+ ions can shape and alter the electronegative properties of the substrate that can affect their binding with the enzymatic active site (Wei et al. 2015; Siddiqi et al. 2018). Therefore, pH is an essential factor affecting AgNPs production by biological systems. The effect of pH of the reaction solution on the efficiency of the synthesis of nanoparticles was evaluated by many authors (Xue et al. 2016; Shahzad et al. 2019; Pal and Hossain 2020; Lotfy et al. 2021). Much more effective synthesis of metal nanoparticles at alkaline pH is associated with greater competition between protons and metal ions for the formation of bonds with negatively charged regions (Sintubin et al. 2009). For example, Saxena et al. (2016) observed that the maximum production of AgNPs was attained at pH 11 when compared with lower pH values, namely 3, 5, 7, and 9. Recently, Wang et al. (2021) investigated the effect of pH on the synthesis of AgNPs using *Aspergillus sydowii* and noticed that the absorbance was increased when pH increased from 5 to 8. The optimal pH for synthesis was found to be 8.0. Similarly, the synthesis of nanoparticles employing *Penicillium oxalicum* GRS-1 was most efficient at pH 7 and 8, as reported by Rose et al. (2019). They also reported that there was no nanoparticle formation in the acidic range of pH. The absorbance peaks recorded in UV-Vis spectroscopy analyses of reaction mixtures became more symmetrical with an increase in pH values which can be explained by the presence of OH^- groups that play a crucial role in stabilizing of AgNPs. Undoubtedly, the prevention of aggregation and maintaining the stability and small size of AgNPs is possible thanks to the availability of such groups (Rose et al. 2019). Recently, Lotfy et al. (2021), showed the optimum synthesis of AgNPs using filtrate of *A. terreus* BA6 at pH 6.25, but the production of smaller AgNPs is more favorable at higher pH while Elsayed and coauthors (2018) observed that AgNPs obtained from *Aspergillus niger* NRC1731 presented greater monodispersion and stability at pH 7.

Effect of concentrations of $AgNO_3$

Similarly, as with other conditions, the concentration of precursor is one of the most important factors affecting the synthesis of silver nanoparticles (Figure 2) (Birla et al. 2013; Phanjom and Ahmed 2017). Silver nitrate is predominantly used as a

salt for the synthesis of AgNPs in biological systems (Guilger-Casagrande and Lima 2019; Srikar et al. 2016). Phanjom and Ahmed (2017) used different concentrations of an aqueous solution of $AgNO_3$ ranging from 1 to 10 mM for synthesis of AgNPs using fungal cell filtrate of *Aspergillus oryzae.* Authors suggested that the metal precursor concentrations at 1–8 mM resulted in a smaller nanoparticle size (in the range of 3–28 nm) and improved dispersion. While concentrations of $AgNO_3$ at 9–10 mM have an influence on large size of nanoparticles in the range of 14–105 nm. Other authors, analyzed the effect of different $AgNO_3$ concentrations (0.5, 1, 1.5, 2, and 2.5 mM) on silver nanoparticles production and showed that the optimal substrate concentration was found to be 1.5 mM (Rose et al. 2019; Wang et al. 2021). Similarly, Elsayed et al. (2018) used different concentrations of silver nitrate (0.5–2.5 mM) in the reaction mixture with filtrate of *Aspergillus niger* NRC1731 and showed that 1.82 mM silver nitrate is the optimal concentration for the AgNPs biosynthesis. Pal and Hossain (2020) reported that the most efficient biosynthesis of AgNPs from *Fusarium* 4F1 and *Trichoderma* TRS was achieved when 2 mM concentration of $AgNO_3$ was used, while the lower concentration of silver salt (1 mM) affected the decrease in the production of AgNPs. In other studies, the use of 10 mM (final concentration in the reaction mixture) of $AgNO_3$ for the synthesis of AgNPs resulted in the formation of smaller nanoparticles (2.86 ± 0.3 nm) than the use of 1 mM and 100 mM of metal ions (54.67 ± 4.1 and 14.23 ± 1.3 nm, respectively) that additionally exhibited irregular shape (AbdelRahim et al. 2017). It should be also emphasized that higher concentrations of $AgNO_3$ used for synthesis may lead to greater toxicity against microbial cells used for synthesis (Balakumaran et al. 2015).

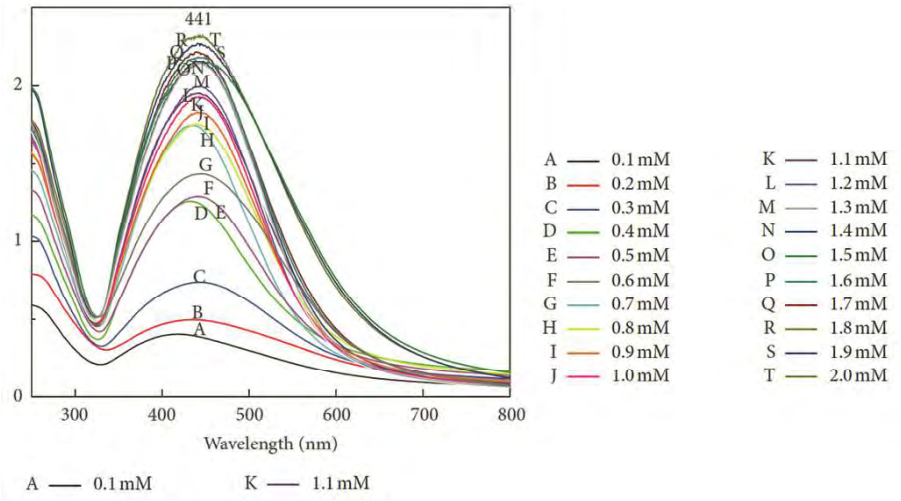

Figure 2. Effect of salt concentration on the synthesis of SNPs from *Fusarium oxysporum*. UV-Vis extinction spectra show maximum surface plasmon absorbance in 2 mM (T) concentration of SNPs. Synthesis of SNPs is proportional to the salt concentration (treatment of 1.5 mM $AgNO_3$ gives a maximum synthesis of SNPs as compared with 2mM $AgNO_3$) (adapted from Birla et al. 2013, an open-access article).

Effect of the culture medium and quantity of biomass

Fungi for the synthesis of nanoparticles require an appropriate culture medium and culture conditions for their growth. Moreover, a culture medium containing specific substrates may induce fungi for the synthesis of enzymes involved in the synthesis of AgNPs by reduction of silver ions (Guilger-Casagrande and Lima 2019). Lotfy and coauthors (2021) for efficient synthesis of silver nanoparticles by *Aspergillus terreus* BA6 used dextrose (27.5 g/L) and peptone (8.75 g/L) in the culture medium. The synthesis carried out at another ratio of the dextrose and peptone (20:10 g/L and 12.5:12.5 g/L, respectively) results in a decrease in biosynthesis efficiency. Saxena et al. (2016) analyzed a set of culture media like Potato dextrose broth (PDB), Sabouraud's dextrose (SDB), Protease production media (PP), Czapek Dox (CZAPEK), Richard medium (RM), and Glucose Yeast Extract Peptone (GYP) to grow fungal mycelia for enhanced extracellular synthesis of AgNPs from *Sclerotinia sclerotiorum.* Fungal biomass grown in PDB has shown enhanced AgNPs synthesis followed by SDB, RM, CZAPEK, PP, and GYP. Interestingly, in the case of synthesis of AgNPs from *Duddingyonia flagans*, the fungal biomass was transferred to pure water and to water containing insect carapaces as a source of chitin (substrate for fungal enzymes). The obtained fungal filtrate from biomass supplemented with chitin contained around three times more protein and showed higher nanoparticle production when compared with non-supplemented fungal filtrate (Costa Silva et al. 2017). Moreover, a significant effect of the amount of fungal biomass on the synthesis of nanoparticles was revealed in studies by Saxena et al. (2016) and Elamawi et al. (2018). Rose et al. (2019) reported that with an increase in biomass amount of

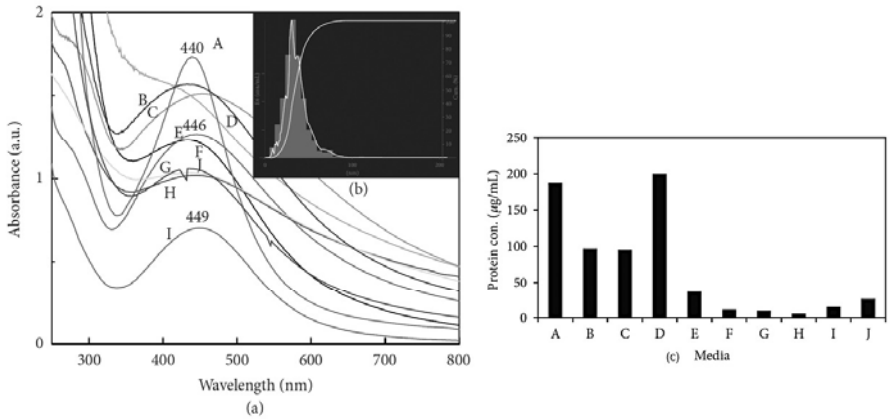

Figure 3. UV-Vis extinction spectroscopy (a) of SNPs synthesized by growing fungus *Fusarium oxysporum* on different culture media—A: MGYP broth, B: PDB, C: lipase production medium, D: protease production medium, E: sucrose peptone yeast broth, F: gluten glucose medium, G: Richard's medium, H: Czapek dox medium, I: glucose peptone yeast broth, and J: Sabouraud broth. Fungus grown in MGYP medium shows maximum synthesis with symmetry in the spectrum. Analysis of sizes distribution (b) of SNPs prepared from the fungus that grew on MGYP medium by NTA. Histogram of protein concentration (c) in different media: highest protein concentration is found in MGYP (A) and protease production medium (D) (adapted from Birla et al. 2013, an open-access article).

Penicillium oxalicum GRS-1 from 5 to 25 g, more symmetrical, sharp, and narrower absorbance peaks were obtained, indicating the small-sized and uniform distribution of Ag nanoparticles. In other studies, the greater production, smaller size, and better dispersion of the AgNPs was observed when a lower amount (7 g) of wet biomass of *Aspergillus fumigatus* BTCB10 was used for synthesis when compared to the use of 10 g of the biomass (Shahzad et al. 2019). The effect of different growth media on protein and AgNPs synthesis by *Fusarium oxysporum* is shown in Figure 3.

Conclusion and future perspectives

Fungi are considered as efficient producers of metal nanoparticles from the metal precursors due to their ability to secrete a broad range of reducing and stabilizing components (Narayanan et al. 2011). In addition, the physico-chemical parameters such as temperature, pH, precursor concentration, biomass amount, media for fungal growth, and culture conditions can be used to optimize the biosynthesis process (Manosalva et al. 2019). Optimization of physico-chemical conditions plays a crucial role not only in synthesis efficiency but also in nanoparticle properties such as morphology, bioactivity, and biocompatibility. In turn, these affect AgNPs suitability for use in a variety of therapies (de Oliveira et al. 2019). Silver nanoparticles due to their outstanding properties affect all spheres of human life, which has led nanotechnology to be widely used in various industries and biomedical applications (Seetharaman et al. 2021). Therefore, the synthesis of silver nanoparticles by using fungi may be carried out on large scale due to the low cost and simplicity of the process. Nevertheless, the toxicity concerns are a major challenge in the synthesis and safe application of AgNPs (Zhao et al. 2018).

Acknowledgement

J.T.W. acknowledges grant No. 2022/45/N/NZ9/01483 from National Science Centre, Poland, and also to NCU (No. 38/2021). MW thanks to NSC (No. 2016/23N/N/NZ9/00247) for financial assistance.

References

Abd El-Aziz, A.R.M., Al-Othman, M.R., Mahmoud, M.A., and Metwaly, H.A. 2015. Biosynthesis of silver nanoparticles using *Fusarium solani* and its impact on grain borne fungi. Dig. J. Nanomater. Biostructures 10: 655–662.

AbdelRahim, K., Mahmoud, S.Y., Ali, A.M., Almaary, K.S., Mustafa, A.E.Z.M., and Husseiny, S.M. 2017. Extracellular biosynthesis of silver nanoparticles using *Rhizopus stolonifer.* Saudi J. Biol. Sci. 24: 208–216.

Adebayo, E.A., Azeez, M.A., Alao, M.B., Oke, A.M., and Aina, D.A. 2021. Fungi as veritable tool in current advances in nanobiotechnology. Heliyon 7: e08480.

Ahmad, A., Mukherjee, P., Senapati, S., Mandal, D., Khan, M.I., Kumar, R., and Sastry, M. 2003. Extracellular biosynthesis of silver nanoparticles using the fungus *Fusarium oxysporum.* Colloids Surf. B: Biointerfaces 28*:* 313–318.

Alghuthaymi, M.A., Almoammar, H., Rai, M., Said-Galiev, E., and Abd-Elsalam, K.A. 2015. Myconanoparticles: synthesis and their role in phytopathogens management. Biotechnol. Biotechnol. Equip. 29: 221–236.

Allend, S.O., Garcia, M.O., da Cunha, K.F., de Albernaz, D.T.F., da Silva, M.E., Ishikame, R.Y., and Hartwig, D.D. 2021. Biogenic silver nanoparticle (Bio-AgNP) has an antibacterial effect against carbapenem-resistant *Acinetobacter baumannii* with synergism and additivity when combined with polymyxin B. J. Appl. Microbiol. 132: 1036–1047.

Ameen, F., Al-Homaidan, A.A., Al-Sabri, A., Almansob, A., and AlNAdhari, S. 2021. Anti-oxidant, anti-fungal and cytotoxic effects of silver nanoparticles synthesized using marine fungus *Cladosporium halotolerans*. Appl. Nanosci. 1–9.

Ammar, H.A., Abd El Aty, A.A., and El Awdan, S.A. 2021. Extracellular myco-synthesis of nano-silver using the fermentable yeasts *Pichia kudriavzevii* HA-NY2 and *Saccharomyces uvarum* HA-NY3, and their effective biomedical applications. Bioprocess Biosyst. Eng. 44*:* 841–854.

Anil Kumar, S., Abyaneh, M.K., Gosavi, S.W., Kulkarni, S.K., Pasricha, R., Ahmad, A., and Khan, M.I. 2007. Nitrate reductase-mediated synthesis of silver nanoparticles from $AgNO_3$. Biotechnol. Lett. 29: 439–445.

Apte, M., Girme, G., Bankar, A., RaviKumar, A., and Zinjarde, S. 2013a. 3, 4-dihydroxy-L-phenylalanine-derived melanin from *Yarrowia lipolytica* mediates the synthesis of silver and gold nanostructures. J. Nanobiotechnology 11: 1–9.

Apte, M., Sambre, D., Gaikawad, S., Joshi, S., Bankar, A., Kumar, A.R., and Zinjarde, S. 2013b. Psychrotrophic yeast *Yarrowia lipolytica* NCYC 789 mediates the synthesis of antimicrobial silver nanoparticles via cell-associated melanin. AMB Express 3: 1–8.

Ashrafi, S.J., Rastegar, M.F., Ashrafi, M., Yazdian, F., Pourrahim, R., and Suresh, A.K. 2013. Influence of external factors on the production and morphology of biogenic silver nanocrystallites. J. Nanosci. Nanotechnol. 13: 2295–2301.

Azmath, P., Baker, S., Rakshith, D., and Satish, S. 2016. Mycosynthesis of silver nanoparticles bearing antibacterial activity. Saudi Pharm. J. 24: 140–146.

Balaji, D.S., Basavaraja, S., Deshpande, R., Mahesh, D.B., Prabhakar, B.K., and Venkataraman, A. 2009. Extracellular biosynthesis of functionalized silver nanoparticles by strains of *Cladosporium cladosporioides* fungus. Colloid Surf. B: biointerfaces 68: 88–92.

Balakumaran, M.D., Ramachandran, R., and Kalaichelvan, P.T. 2015. Exploitation of endophytic fungus, *Guignardia mangiferae* for extracellular synthesis of silver nanoparticles and their *in vitro* biological activities. Microbiol. Res. 178: 9–17.

Barabadi, H., Mohammadzadeh, A., Vahidi, H., Rashedi, M., Saravanan, M., Talank, N., and Alizadeh, A. 2021. *Penicillium chrysogenum*-derived silver nanoparticles: exploration of their antibacterial and biofilm inhibitory activity against the standard and pathogenic *Acinetobacter baumannii* compared to tetracycline. J. Clust. Sci. 1–14.

Basavaraja, S., Balaji, S.D., Lagashetty, A., Rajasab, A.H., and Venkataraman, A. 2008. Extracellular biosynthesis of silver nanoparticles using the *fungus Fusarium semitectum*. Mater. Res. Bull. 43: 1164–1170.

Bhainsa, K.C., and D'souza, S.F. 2006. Extracellular biosynthesis of silver nanoparticles using the fungus *Aspergillus fumigatus*. Colloid Surf. B: biointerfaces 47: 160–164.

Birla, S.S., Tiwari, V.V., Gade, A.K., Ingle, A.P., Yadav, A.P., and Rai, M.K. 2009. Fabrication of silver nanoparticles by *Phoma glomerata* and its combined effect against *Escherichia coli, Pseudomonas aeruginosa* and *Staphylococcus aureus*. Lett. Appl. Microbiol. 48: 173–179.

Birla, S.S., Gaikwad, S.C., Gade, A.K., and Rai, M.K. 2013. Rapid synthesis of silver nanoparticles from *Fusarium oxysporum* by optimizing physicocultural conditions. Sci World J. 2013: 796018.

Blackwell, M. 2011. The Fungi: 1, 2, 3… 5.1 million species? Am. J. Bot. 98: 426–438.

Boroumand Moghaddam, A., Namvar, F., Moniri, M., Azizi, S., and Mohamad, R. 2015. Nanoparticles biosynthesized by fungi and yeast: a review of their preparation, properties, and medical applications. Molecules 20: 16540–16565.

Costa Silva, L.P., Oliveira, J.P., Keijok, W.J., Silva, A.R., Aguiar, A.R., Guimarães, M.C.C., Ferraz, C.M. Araújo, J.V., Tobias, F.L., and Braga, F.R. 2017. Extracellular biosynthesis of silver nanoparticles using the cell-free filtrate of nematophagus fungus *Duddingtonia flagans*. Int. J. Nanomed. 12: 6373–6381.

Das, C.A., Kumar, V.G., Dhas, T.S., Karthick, V., Govindaraju, K., Joselin, J.M., and Baalamurugan, J. 2020. Antibacterial activity of silver nanoparticles (biosynthesis): A short review on recent advances. Biocatal. Agric. Biotechnol. 27: 101593.

Desai, R., Mankad, V., Gupta, S.K., and Jha, P.K. 2012. Size distribution of silver nanoparticles: UV-visible spectroscopic assessment. Nanosci. Nanotechnol. Lett 4: 30–34.

Dhabalia, D., Ukkund, S.J., Syed, U.T., Uddin, W., and Kabir, M.A. 2020. Antifungal activity of biosynthesized silver nanoparticles from *Candida albicans* on the strain lacking the CNP41 gene. Mater. Res. Express 7: 125401.

Durán, N., Marcato, P.D., Alves, O.L., De Souza, G.I., and Esposito, E. 2005. Mechanistic aspects of biosynthesis of silver nanoparticles by several *Fusarium oxysporum* strains. J. Nanobiotechnology 3: 1–7.

Elamawi, R.M., Al-Harbi, R.E., and Hendi, A.A. 2018. Biosynthesis and characterization of silver nanoparticles using *Trichoderma longibrachiatum* and their effect on phytopathogenic fungi. Egypt. J. Biol. Pest. Control. 28*:* 1–11.

El-Bendary, M.A., Moharam, M.E., Hamed, S.R., Abo El-Ola, S.M., Khalil, S.K., Mounier, M.M., and Allam, M.A. 2021. Mycosynthesis of silver nanoparticles using *Aspergillus caespitosus*: Characterization, antimicrobial activities, cytotoxicity, and their performance as an antimicrobial agent for textile materials. Appl. Organomet. Chem. 35: e6338.

Elgorban, A.M., Al-Rahmah, A.N., Sayed, S.R., Hirad, A., Mostafa, A.A.F. and Bahkali, A.H. 2016. Antimicrobial activity and green synthesis of silver nanoparticles using *Trichoderma viride.* Biotechnol, Biotechnol. Equip. 30: 299–304.

Elsayed, M.A., Othman, A.M., Hassan, M.M., and Elshafei, A.M. 2018. Optimization of silver nanoparticles biosynthesis mediated by *Aspergillus niger* NRC1731 through application of statistical methods: enhancement and characterization. 3 Biotech 8: 1–10.

Elshafei, A.M., Othman, A.M., Elsayed, M.A., Al-Balakocy, N.G., and Hassan, M.M. 2021. Green synthesis of silver nanoparticles using *Aspergillus oryzae* NRRL447 exogenous proteins: Optimization via central composite design, characterization and biological applications. Environ. Nanotechnol. Monit. Manag. 16: 100553.

Feroze, N., Arshad, B., Younas, M., Afridi, M.I., Saqib, S., and Ayaz, A. 2019. Fungal mediated synthesis of silver nanoparticles and evaluation of antibacterial activity. Microsc. Res. Tech. 83: 72–80.

Gade, A.K., Bonde, P.P., Ingle, A.P., Marcato, P.D., Duran, N., and Rai, M.K. 2008. Exploitation of *Aspergillus niger* for synthesis of silver nanoparticles. J. Biobased. Mater. 2: 243–247.

Gade, A., Gaikwad, S., Duran, N., and Rai, M. 2014. Green synthesis of silver nanoparticles by *Phoma glomerata*. Micron 59: 52–59.

Govindappa, M., Manasa, D.J., Vridhi Vinaykiya, Bhoomika, V., Suryanshi Dutta, Ritu Pawar, and Vinay, B. 2022. Raghavendra Screening of Antibacterial and Antioxidant Activity of Biogenically Synthesized Silver Nanoparticles from *Alternaria alternata*, Endophytic Fungus of *Dendrophthoe falcata*-a Parasitic Plant. BioNanoSci.

Guilger-Casagrande, M., and Lima, R.D. 2019. Synthesis of silver nanoparticles mediated by fungi: a review. Front. Bioeng. Biotechnol. 7: 287.

Haji Basheerudeen, M.A., Mushtaq, S.A., Soundhararajan, R., Nachimuthu, S.K., and Srinivasan, H. 2021. Marine endophytic fungi mediated silver nanoparticles and their application in plant growth promotion in *Vigna radiata* L. Int. J. Nano. Dimens. 12: 1–10.

Hamedi, S., Ghaseminezhad, M., Shokrollahzadeh, S., and Shojaosadati, S.A. 2017. Controlled biosynthesis of silver nanoparticles using nitrate reductase enzyme induction of filamentous fungus and their antibacterial evaluation. Artif. Cells Nanomed. Biotechnol. 45: 1588–1596.

Hamzah, H.M., Salah, R.F., and Maroof, M.N. 2018. *Fusarium mangiferae* as new cell factories for producing silver nanoparticles. J. Microbiol Biotechnol. 28: 1654–1663.

Hikmet, R.A., and Hussein, N.N. 2021. Mycosynthesis of Silver Nanoparticles by Candida albicans Yeast and its Biological Applications. Arch. Razi Inst. 76: 857–869.

Hulikere, M.M., and Joshi, C.G. 2019. Characterization, antioxidant and antimicrobial activity of silver nanoparticles synthesized using marine endophytic fungus-*Cladosporium cladosporioides*. Process Biochem. 82: 199–204.

Ilahi, N., Haleem, A., Iqbal, S., Fatima, N., Sajjad, W., Sideeq, A., and Ahmed, S. 2021. Biosynthesis of silver nanoparticles using endophytic *Fusarium oxysporum* strain NFW16 and their *in vitro* antibacterial potential. *Microscopy research and technique*. https://doi.org/10.1002/jemt.24018.

Ingle, A., Gade, A., Pierrat, S., Sonnichsen, C., and Rai, M. 2008. Mycosynthesis of silver nanoparticles using the fungus *Fusarium acuminatum* and its activity against some human pathogenic bacteria. Curr. Nanosci. 4: 141–144.

Ishida, K., Cipriano, T.F., Rocha, G.M., Weissmüller, G., Gomes, F., Miranda, K., and Rozental, S. 2014. Silver nanoparticle production by the fungus *Fusarium oxysporum*: nanoparticle characterisation and analysis of antifungal activity against pathogenic yeasts. Memorias do Instituto Oswaldo Cruz 109: 220–228.

Jalal, M., Ansari, M.A., Alzohairy, M.A., Ali, S.G., Khan, H.M., Almatroudi, A., and Raees, K. 2018. Biosynthesis of silver nanoparticles from oropharyngeal *Candida glabrata* isolates and their antimicrobial activity against clinical strains of bacteria and fungi. Nanomaterials 8: 586.

Kathiresan, K., Manivannan, S., Nabeel, M.A., and Dhivya, B. 2009. Studies on silver nanoparticles synthesized by a marine fungus, *Penicillium fellutanum* isolated from coastal mangrove sediment. Colloids Surf. B. 71: 133–137.

Konappa, N., Udayashankar, A.C., Dhamodaran, N., Krishnamurthy, S., Jagannath, S., Uzma, F., and Jogaiah, S. 2021. Ameliorated antibacterial and antioxidant properties by *Trichoderma harzianum* mediated green synthesis of silver nanoparticles. Biomolecules 11: 535.

Korbekandi, H., Ashari, Z., Iravani, S., and Abbasi, S. 2013. Optimization of biological synthesis of silver nanoparticles using *Fusarium oxysporum*. Iran. J. Pharm. Res. 12: 289.

Korbekandi, H., Mohseni, S., Mardani Jouneghani, R., Pourhossein, M., and Iravani, S. 2016. Biosynthesis of silver nanoparticles using *Saccharomyces cerevisiae*. Artif. Cells. Nanomed. Biotechnol. 44: 235–239.

Korcan, S.E., Kahraman, T., Acikbas, Y., Liman, R., Ciğerci, İ.H., Konuk, M., and Ocak, İ. 2021. Cyto–genotoxicity, antibacterial, and antibiofilm properties of green synthesized silver nanoparticles using *Penicillium toxicarium*. Microsc. Res. Tech. 84: 2530–2543.

Kowshik, M., Ashtaputre, S., Kharrazi, S., Vogel, W., Urban, J., Kulkarni, S.K., and Paknikar, K.M. 2003. Extracellular synthesis of silver nanoparticles by a silver-tolerant yeast strain MKY3. Nanotechnology 14: 95.

Kumar, D., Karthik, L., Kumar, G., and Roa, K.B. 2011. Biosynthesis of silver nanoparticles from marine yeast and their antimicrobial activity against multidrug resistant pathogens. Pharmacologyonline 3: 1100–1111.

Kumar, R.R., Priyadharsani, K.P., and Thamaraiselvi, K. 2012. Mycogenic synthesis of silver nanoparticles by the Japanese environmental isolate *Aspergillus tamarii*. J. Nanopart. Res. 14: 1–7.

Lawrance, N., Benaltraja, V., Ramasamy, A., Devaraj, B., Subramani, T., and Parameswaran, R. 2021. Synthesis and characterization of silver nanoparticles using *Acremonium borodinense* and their anti-bacterial and hemolytic activity. Biocatal. Agric. Biotechnol. 102222.

Li, G., He, D., Qian, Y., Guan, B., Gao, S., Cui, Y., and Wang, L. 2012. Fungus-mediated green synthesis of silver nanoparticles using *Aspergillus terreus*. Int. J. Mol. Sci. 13: 466–476.

Lotfy, W.A., Alkersh, B.M., Sabry, S.A., and Ghozlan, H.A. 2021. Biosynthesis of silver nanoparticles by *Aspergillus terreus:* Characterization, optimization, and biological activities. Front. Bioeng. Biotechnol. 9: 633468.

Madakka, M., Jayaraju, N., and Rajesh, N. 2018. Mycosynthesis of silver nanoparticles and their characterization. MethodsX 5: 20–29.

Mandal, D., Bolander, M.E., Mukhopadhyay, D., Sarkar, G., and Mukherjee, P. 2006. The use of microorganisms for the formation of metal nanoparticles and their application. Appl. Microbiol. Biotechnol. 69: 485–492.

Manosalva, N., Tortella, G., Cristina Diez, M., Schalchli, H., Seabra, A.B., Durán, N., and Rubilar, O. 2019. Green synthesis of silver nanoparticles: effect of synthesis reaction parameters on antimicrobial activity. World J. Microbiol. Biotechnol. 35: 1–9.

Mishra, A., Tripathy, S.K., and Yun, S.I. 2011. Bio-synthesis of gold and silver nanoparticles from *Candida guilliermondii* and their antimicrobial effect against pathogenic bacteria. J. Nanosci. Nanotechnol. 11: 243–248.

Mistry, H., Thakor, R., Patil, C., Trivedi, J., and Bariya, H. 2021. Biogenically proficient synthesis and characterization of silver nanoparticles employing marine procured fungi *Aspergillus brunneoviolaceus* along with their antibacterial and antioxidative potency. Biotechnol. Lett. 43: 307–316.

Mukherjee, P., Ahmad, A., Mandal, D., Senapati, S., Sainkar, S.R., Khan, M.I., and Sastry, M. 2001. Fungus-mediated synthesis of silver nanoparticles and their immobilization in the mycelial matrix: a novel biological approach to nanoparticle synthesis. Nano lett. 1: 515–519.

Mukherjee, P., Roy, M., Mandal, B.P., Dey, G.K., Mukherjee, P.K., Ghatak, J., and Kale, S.P. 2008. Green synthesis of highly stabilized nanocrystalline silver particles by a non-pathogenic and agriculturally important fungus *T. asperellum*. Nanotechnology 19: 075103.

Narayanan, K.B., and Sakthivel, N. 2010. Biological synthesis of metal nanoparticles by microbes. Adv. Colloid Interface Sci. 156: 1–13.

Narayanan, K.B., and Sakthivel, N. 2011. Green synthesis of biogenic metal nanoparticles by terrestrial and aquatic phototrophic and heterotrophic eukaryotes and biocompatible agents. Adv. Colloid Interface Sci. 169: 59–79.

Naveen, K.V., Sathiyaseelan, A., Mariadoss, A.V.A., Xiaowen, H., Saravanakumar, K., and Wang, M.H. 2021. Fabrication of mycogenic silver nanoparticles using endophytic fungal extract and their characterization, antibacterial and cytotoxic activities. Inorg. Chem. Commun.128: 108575.

Nayak, R.R., Pradhan, N., Behera, D., Pradhan, K.M., Mishra, S., Sukla, L.B., and Mishra, B.K. 2011. Green synthesis of silver nanoparticle by *Penicillium purpurogenum* NPMF: the process and optimization. J. Nanopart. Res. 13: 3129–3137.

Nelson, P.E., Dignani, M.C., and Anaissie, E.J. 1994. Taxonomy, biology, and clinical aspects of *Fusarium* species. Clin. Microbiol. Rev. 7: 479–504.

Niknejad, F., Nabili, M., Ghazvini, R.D., and Moazeni, M. 2015. Green synthesis of silver nanoparticles: advantages of the yeast *Saccharomyces cerevisiae* model. Curr. Med. Mycol. 1: 17.

Othman, A.M., Elsayed, M.A., Elshafei, A.M., and Hassan, M.M. 2017. Application of response surface methodology to optimize the extracellular fungal mediated nanosilver green synthesis. J. Genet. Eng. Biotechnol. 15: 497–504.

Pal, S., and Hossain, K.S. 2020. Optimization of mycobiosynthesis of silver nanoparticles by using *Fusarium* 4F1 and *Trichoderma* TRS isolates. Bangladesh J. Bot. 49: 343–348.

Pandiarajan, G. Govindaraj, R., Makesh Kumar, B., and Ganesan, V. 2011. Biosynthesis of silver nanoparticles using silver nitrate through biotransformation. J. Ecobiotechnol. 2: 13.

Phanjom, P., and Ahmed, G. 2017. Effect of different physicochemical conditions on the synthesis of silver nanoparticles using fungal cell filtrate of *Aspergillus oryzae* (MTCC No. 1846) and their antibacterial effects. Adv. Nat. Sci. Nanosci. Nanotechnol. 8: 1–13.

Qu, M., Yao, W., Cui, X., Xia, R., Qin, L., and Liu, X. 2021. Biosynthesis of silver nanoparticles (AgNPs) employing *Trichoderma* strains to control empty-gut disease of oak silkworm (*Antheraea pernyi*). Mater. Today Commun. 28: 102619.

Rahimi, G., Alizadeh, F., and Khodavandi, A. 2016. Mycosynthesis of silver nanoparticles from *Candida albicans* and its antibacterial activity against *Escherichia coli* and *Staphylococcus aureus.* Trop. J. Pharm. Res. 15: 371–375.

Rai, M., Yadav, A., and Gade, A. 2009. Silver nanoparticles as a new generation of antimicrobials. Biotechnol. Adv. 27: 76–83.

Rai, M., Bonde, S., Golinska, P., Trzcińska-Wencel, J., Gade, A., Abd-Elsalam, K., and Ingle, A. 2021. *Fusarium* as a novel fungus for the synthesis of nanoparticles: mechanism and applications. J. Fungi 7: 139.

Rauwel, P., Küünal, S., Ferdov, S., and Rauwel, E. 2015. A review on the green synthesis of silver nanoparticles and their morphologies studied via TEM. Adv. Mater. Sci. Eng. 2015. https://doi.org/10.1155/2015/682749.

Rose, G.K., Soni, R., Rishi, P., and Soni, S.K. 2019. Optimization of the biological synthesis of silver nanoparticles using *Penicillium oxalicum* GRS-1 and their antimicrobial effects against common food-borne pathogens. Green Process. Synth. 8: 144–156.

Roy, S., Shankar, S., and Rhim, J.W. 2019. Melanin-mediated synthesis of silver nanoparticle and its use for the preparation of carrageenan-based antibacterial films. Food Hydrocoll. 88: 237–246.

Salaheldin, T.A., Husseiny, S.M., Al-Enizi, A.M., Elzatahry, A., and Cowley, A.H. 2016. Evaluation of the cytotoxic behavior of fungal extracellular synthesized Ag nanoparticles using confocal laser scanning microscope. Int. J. Mol. Sci. 17: 329.

Saxena, J., Sharma, P.K., Sharma, M.M., and Singh, A. 2016. Process optimization for green synthesis of silver nanoparticles by *Sclerotinia sclerotiorum* MTCC 8785 and evaluation of its antibacterial properties. Springerplus 5: 861.

Seetharaman, P.K., Chandrasekaran, R., Periakaruppan, R., Gnanasekar, S., Sivaperumal, S., Abd-Elsalam, K.A., and Kuca, K. 2021. Functional attributes of myco-synthesized silver nanoparticles from endophytic fungi: A new implication in biomedical applications. Biology 10: 473.

Shahzad, A., Saeed, H., Iqtedar, M., Hussain, S.Z., Kaleem, A., and Abdullah, R. 2019. Size-controlled production of silver nanoparticles by *Aspergillus fumigatus* BTCB10: likely antibacterial and cytotoxic effects. J. Nanomater. 2019: 5168698

Shaligram, N.S., Bule, M., Bhambure, R., Singhal, R.S., Singh, S.K., Szakacs, G., and Pandey, A. 2009. Biosynthesis of silver nanoparticles using aqueous extract from the compactin producing fungal strain. Process Biochem. 44: 939–943.

Shu, M., He, F., Li, Z., Zhu, X., Ma, Y., Zhou, Z., and Zeng, M. 2020. Biosynthesis and antibacterial activity of silver nanoparticles using yeast extract as reducing and capping agents. Nanoscale Res. Lett. 15: 1–9.

Shukla, G., Gaurav, S.S., Singh, A., and Rani, P. 2021. Synthesis of mycogenic silver nanoparticles by *Fusarium pallidoroseum* and evaluation of its larvicidal effect against white grubs (*Holotrichia* sp.). Mater. Today 49: 3517–3527.

Siddiqi, K.S., Husen, A., and Rao, R.A. 2018. A review on biosynthesis of silver nanoparticles and their biocidal properties. J. Nanobiotechnology 16: 1–28.

Singh, P., Kim, Y.J., Zhang, D., and Yang, D.C. 2016. Biological synthesis of nanoparticles from plants and microorganisms. Trends Biotechnol. 34: 588–599.

Sintubin, L., Windt, W.D., Dick, J., Mast, J., Ha, D.V.D., and Verstraete, W. 2009. Lactic acid bacteria as reducing and capping agent for the fast and efficient production of silver nanoparticles. Appl. Microbiol. Biotechnol. 84: 741–749.

Skalickova, S., Baron, M., and Sochor, J. 2017. Nanoparticles biosynthesized by yeast: a review of their application. Kvasny Prumysl 63: 290–292.

Smitha, S.L., Nissamudeen, K.M., Philip, D., and Gopchandran, K.G. 2008. Studies on surface plasmon resonance and photoluminescence of silver nanoparticles. Spectrochim. Acta A Mol. Biomol. Spectrosc. 71: 186–190.

Srikar, S.K., Giri, D.D., Pal, D.B., Mishra, P.K., and Upadhyay, S.N. 2016. Green synthesis of silver nanoparticles: a review. Green Sustain. Chem. 6: 34–56.

Vanaja, M., Gnanajobitha, G., Paulkumar, K., Rajeshkumar, S., Malarkodi, C., and Annadurai, G. 2013. Phytosynthesis of silver nanoparticles by *Cissus quadrangularis*: influence of physicochemical factors. J. Nanostructure Chem. 3: 1–8.

Verma, V.C., Kharwar, R.N., and Gange, A.C. 2010. Biosynthesis of antimicrobial silver nanoparticles by the endophytic fungus *Aspergillus clavatus*. Nanomedicine 5: 33–40.

Vigneshwaran, N., Kathe, A.A., Varadarajan, P.V., Nachane, R.P., and Balasubramanya, R.H. 2006. Biomimetics of silver nanoparticles by white rot fungus, *Phaenerochaete chrysosporium.* Colloids Surf. B 53*:* 55–59.

Waghmare, S.R., Mulla, M.N., Marathe, S.R., and Sonawane, K.D. 2015. Ecofriendly production of silver nanoparticles using *Candida utilis* and its mechanistic action against pathogenic microorganisms. 3 Biotech 5: 33–38.

Wang, D., Xue, B., Wang, L., Zhang, Y., Liu, L., and Zhou, Y. 2021. Fungus-mediated green synthesis of nano-silver using *Aspergillus sydowii* and its antifungal/antiproliferative activities. Sci. Rep. 11: 1–9.

Wei, L., Lu, J., Xu, H., Patel, A., Chen, Z.S., and Chen, G. 2015. Silver nanoparticles: synthesis, properties, and therapeutic applications. Drug Discov. Today 20: 595–601.

Xue, B., He, D., Gao, S., Wang, D., Yokoyama, K., and Wang, L. 2016. Biosynthesis of silver nanoparticles by the fungus *Arthroderma fulvum* and its antifungal activity against genera of *Candida*, *Aspergillus* and *Fusarium*. Int. J. Nanomed. 11: 1899–1906.

Yari, T., Vaghari, H., Adibpour, M., Jafarizadeh-Malmiri, H., and Berenjian, A. 2022. Potential application of *Aspergillus terreus*, as a biofactory, in extracellular fabrication of silver nanoparticles. Fuel 308: 122007.

Zhao, X., Zhou, L., Riaz Rajoka, M.S., Yan, L., Jiang, C., Shao, D., and Jin, M. 2018. Fungal silver nanoparticles: synthesis, application and challenges. Crit. Rev. Biotechnol. 38: 817–835.

Zielonka, A., and Klimek-Ochab, M. 2017. Fungal synthesis of size-defined nanoparticles. Advances in Natural Sciences: Nanoscience and Nanotechnology 8: 043001.

P2

Chapter 22

Toxicity of Nanomaterials to Plants

Joanna Trzcińska-Wencel,[1] *Patrycja Golińska*[1,*] and *Mahendra Rai*[1,2]

Introduction

As nanomaterial production and applications in industry, medicine, agriculture, and environment protection sectors continuously expand, nanomaterial residues are present in the environment and generate concerns regarding their potentially adverse impact on non-target organisms (Montes et al. 2017). The diversity of nanomaterials (NMs) includes inorganic nanoparticles (metal and metal oxide), carbon-based nanomaterials (graphene, graphene oxide, fullerenes, and carbon nanotubes), other organic nanostructures (liposomes and polymer-based) and a wide range of combinations (nanocomposites). The potential phytotoxicity of NMs in plants at different levels is shown in Figure 1. Their activity is associated with unique characteristics (extremely small size, high surface area to volume ratio, variety of shapes, coating agents, and many others) (Dhyani et al. 2022). Nevertheless, their toxic effect is determined by the exposure conditions and the nature of the plants. A number of techniques and methods are used for toxicity assessment and the fate of NMs in plant organisms. Identification of interactions at the cellular, subcellular, and molecular

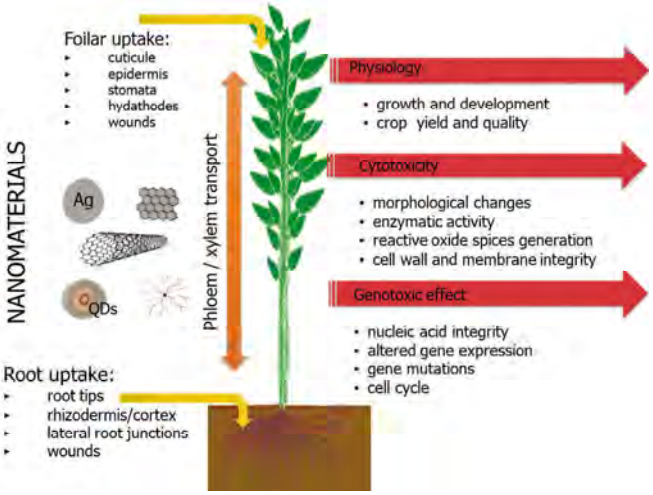

Figure 1. Uptake, transport, and potential toxic effect of various nanomaterials on plants.

[1] Faculty of Biological and Veterinary Sciences, Nicolaus Copernicus University, Toruń, Poland.
[2] Nanobiotechnology Research Lab., Department of Biotechnology, Sant Gadge Baba Amravati University, Amravati, India.
* Corresponding author: golinska@umk.pl

levels provides a particular understanding of toxicity to specific tissues and organisms, which facilitates the advancement of the safety of NM use (Barabadi et al. 2019). In some conditions, NMs negatively affect the life cycle of plants and alter seed germination, seedling growth, and organs and impair the efficiency of processes, such as photosynthesis, flowering, and yield (Ruttkay-Nedecky et al. 2017). However, the genomics and proteomics studies, combined with biochemical analyses, confirm a range of plant responses to the NMs, indicating substances and processes that mitigate NMs-induced stress (Fen et al. 2022).

Diversity of Nanomaterials Used for Plant Protection

Nanomaterials have found applications for monitoring and detecting plant diseases and also as plant protection products with antimicrobial, antifungal, and anti-insecticide properties. In addition, some of NMs in the form of nano-fertilizers or hydrogels, are used for improving soil quality and facilitating nutrient availability for plants (Dhyani et al. 2022).

Nanomaterials for Biosensing of Plant Pathogens

It is essential to detect plant pathogens before disease symptoms appear. To ensure proper prevention, diagnosis, and management of plant diseases and pests, different types of developments involving nanotechnology products, such as metal nanoparticles, carbon nanomaterials, hybrid nanocomposites, etc., are used (Babu et al. 2022). Nanoparticles (NPs) can be used for pathogen detection and as diagnostic tools to mark specific substances synthesized during plant infections (Anand and Panigrahi 2021; Sellappan et al. 2022). Due to the use of nanomaterials with outstanding chemical and physical properties, it is possible to transform and modify conventional molecular tests into modern and high-performance diagnostic tools that can be directly used in agricultural fields and outside laboratories (Li et al. 2020). Studies on applications of metal nanoparticles and carbon nanomaterials to plant pathogen biosensors have been presented in Table 1. Two types of nanomaterials are increasingly being considered for use in biosensors, namely gold nanoparticles and carbon nanotubes. Gold nanoparticles (AuNPs) demonstrate a variety of electrical, optical, and catalytical properties as well as the ability to bind molecules, such as nucleic acids, peptides, proteins, and polymers. These make them ideal for application in biosensing devices (Yadav et al. 2020). Thus, Zhan and coworkers (2018) have developed AuNPs-based biosensor for the detection of *Phytophthora infestans* with a detection threshold of 0.1 pg μL^{-1} of pathogen gDNA. In another study, AuNPs were used by Lei et al. (2021) to produce a dynamic microcantilever biosensor for the rapid detection of *Leptosphaeria maculans* responsible for severe rapeseed yield losses. Moreover, Yang and coworkers (2015) summarized the advantages of a carbon nanotube-based biosensors, pointing out the high sensitivity and fast reaction rate, the ability to immobilize enzymes without the loss of their biological activity, the low effect of contamination, and long-term stability. The high potential of carbon nanotubes (CNTs) for use in biosensors is attributed to their properties, including large surface area ratio and hollow tube or capacity to mediate rapid electron transfer kinetics. For example, semiconducting single-walled carbon nanotubes with anti-SDE1 have been used in a chemoreceptive biosensor for the early detection of Huanglongbing (HLB) in citrus trees. The device demonstrated improved sensitivity compared to the standard ELISA test, the minimum required concentration for assessment was in a range from 3 nM to 2.6 μM, while the detection limit for ELISA ranged between 1.4 nM to 140 nM (Tran et al. 2020).

Nanomaterials for Controlling Plant Diseases

In addition, the antimicrobial activity of nanomaterials has been widely studied against important plant pathogens, indicating their use for pest and disease control, as shown in Table 2. In the number of nanomaterials antimicrobial activity of carbon nanomaterials (Lipsa et al. 2020; El-Abeid et al. 2020), polymeric nanostructures (Oh et al. 2019; Vanti et al. 2020; Ahmed et al. 2021a) and

Table 1. Nanomaterials used for the detection of plant pathogens.

Type of Nanomaterial	Biosensor Format	Plant	Target	References
AuNPs	Lateral flow biosensor	Potato (*Solanum tuberosum*)	DNA of *Phytophthora infestans, Alternaria solani,* and *Rhizoctonia solani*	Zhan et al. 2018
AuNPs	Dynamic microcantilever biosensor	Oilseed rape (*Brassica oleracea*)	DNA of *Leptosphaeria maculans*	Lei et al., 2021
AuNPs	Integrated RPA and an AuNP probe	Tomato and genus *Solanum*	DNA of tomato yellow leaf curl virus	Wang and Yang 2019
CNPs	Fluorometric-based nanobiosensor	Citrus	Citrus tristeza virus	Shojaei et al. 2016
rGO and ZnONPs	Electrochemical biosensor	Oil palm	Chemical markers for early detection of Basal stem rot disease (induced by *Ganoderma boninense*)	Rahmat et al. 2020
MWCNTs and CuNPs	Electrochemical biosensor	Cotton	DNA viruses that belong to the genera *Begomovirus* of the family *Geminiviridae*	Tahir et al. 2018
MWCNTs	Chemical sensors based on CNTs	Strawberry (*Fragaria x ananassa*)	Volatile organic compounds (VOC) of *Aspergillus* sp. *Rhizopus* sp.	Greenshields et al. 2016
SWNTs	Electrical gas sensor with SWNTs functionalized with ssDNA	Citrus trees	Biomarkers of citrus huanglongbing disease caused by *Candidatus Liberibacter* (ethyl hexanol, linalool, tetradecene, and phenylacetaldehyde)	Wang et al. 2019
SWNTs	SWNT-based chemiresistive biosensor	Citrus trees	Label-free detection and quantification of protein-based biomarker SDE1 for citrus greening	Tran et al. 2020

AuNPs, gold nanoparticles; CNPs, carbon nanoparticles; rGO, reduced graphene oxide; ZnONPs, zinc oxide nanoparticles; SWCNTs, single-walled carbon nanotubes; MWCNTs, multi-walled carbon nanotubes.

nanoparticles based on silver, magnesium, zinc, and copper (Cai et al. 2018; Pham et al. 2019; Win et al. 2020; El-Batal et al. 2020; Irshad et al. 2021) were studied. Khan et al. (2021) reported a comparative investigation of the antiparasitic and antimicrobial activity of silver nanoparticles (AgNPs) on nematode *Meloidogyne incognita*, bacterium *Ralstonia solanacearum*, and fungus *Fusarium oxysporum*. Their results proved that biologically synthesized rectangular AgNPs with sizes ranging between 55–70 nm at a concentration of 100 µg/mL exhibited antinematode, antifungal, and antibacterial activity. These findings imply the potential of bio-AgNPs for application for controlling plant pathogens (Khan et al. 2021). Furthermore, El-Abeid et al. (2020) have identified a potential mechanism of action for the reduced graphene oxide-copper nanoparticle (rGO-CuONP) nanocomposite against *Fusarium oxysporum,* a causal agent of wilt in tomato and pepper. Microscopic observation illustrated strong damage and the appearance of numerous cavities in the cell wall surface in hyphae, macro- and microconidia, and chlamydospores. This action may be due to the non-specific interaction of rGO with the cell wall and/or the effect of CuONPs on biomolecules present on the cell wall surface including phosphorus or sulfur in their structure (El-Abeid et al. 2020).

Interestingly, several reports also provide insight into the simultaneous antimicrobial and pathogen resistance-enhancing effects in plants of nanomaterials based on iron oxide, copper, magnesium, and zinc (Bilesky-Jose et al. 2021; Haggag and Eid 2022; Abdelkhalek and Al-Askar 2020; Shende et al. 2021). Therefore, chemically prepared sulfur nanoparticles (SNPs) were evaluated for enhancement of the immune response of *Fusarium oxysporum*-infected tomato.

Table 2. Biological activity of nanomaterials in plant protection against pathogens.

Nanomaterial	Synthesis Method	Average Size/ Zeta Potential	Activity	References
α-Fe_2O_3 nanoparticles	Biological from *Trichoderma harzianum*	207 nm/–13 mV	Enhancement of biological activity of *Trichoderma* against *Sclerotinia sclerotiorum*	Bilesky-Jose et al. 2021
AgNPs	Biological from strawberry waste	55 nm	Inhibitory effect on nematode, *Meloidogyne incognita*, bacterium, *Ralstonia solanacearum* and fungus, *Fusarium oxysporum*	Khan et al. 2021
SiO_2-NPs	Chemical	76.7 nm	Enhancement of immune response by activation of salicylic acid-dependent defense pathway in *Arabidopsis thaliana* against *Pseudomonas syringae pv.* tomato.	El-Shetehy et al. 2021
Sulfur nanoparticles (SNPs)	Chemical	30 nm/–25.7 mV	Inhibition of *Fusarium oxysporum* f. sp. *Lycopersici* growth and activation of systemic acquired resistance (SAR) in tomatoes	Cao et al. 2021
CuNPs	Biological from *Aspergillus flavus*	8 nm/–26 mV	Antifungal activity against *Aspergillus niger*, *Fusarium oxysporum,* and *Alternaria alternata*	Shende et al. 2021
ZnONPs	Biological from leaf extract of *Mentha spicata*	74.68 nm	Induction of SAR after foliar treatment of tomato during Tobacco mosaic virus (TMV) infection	Abdelkhalek and Al-Askar 2020
Ag@FeO-NPs@Chitosan composite	Biological from *Streptomyces aureofaciens*	< 50 nm	Inhibition of the growth and spores germination of soilborne pathogens	Haggag and Eid 2022
CuONPs	Biological from *Penicilium chrysogenum*	9.70 nm	Antimicrobial activity against *Fusarium oxysporum* and *Ralstonia solanacearum*	El-Batal et al. 2020
MgONPs	Biological from strawberry	100 nm	Antinematode activity against *Meloidogyne incognita*	Khan et al. 2022
Chitosan guar nanoparticle (CGNP)	Ionic gelation method	122 nm/–30 mV	Inhibition of rice pathogens *Pyricularia grisea* and *Xanthomonas oryzae*	Sathiyabama and Muthukumar 2020

Foliar spraying resulted in 1.43-fold higher disease suppression than commercial fungicide hymexazol; after SNPs treatment activation of the stress response (increased content and activity of disease-related enzymes and antioxidants) was observed (Cao et al. 2021).

How do Nanomaterials Interact With Plants?

In fact, nanomaterials are able to overcome physiological barriers and penetrate plant tissues, negatively affecting plant functions by inducing oxidative stress, damaging cell walls, membranes, and organelles, or interfering with biomolecules crucial to metabolic processes. However, the defense mechanisms of plants against various biotic and abiotic stresses depend considerably on the plant species, growth stage, and other factors. However, the exact mechanism of plant response to nanomaterials is not fully understood (Dev et al. 2018). Nanomaterials might induce oxidative stress and impair the synthesis of molecules essential for plant growth and development. Accordingly, studies mainly focus on the antioxidant system, gene expression, and synthesis of proteins or hormones responsible for alleviating the effects of stress (Ghafari et al. 2020).

Antioxidative System Activity in Response to Oxidative Stress Generated by NMs

Nanomaterials might induce a strong increase in the amount of reactive oxygen species (ROS) as a byproduct of the plant detoxification mechanism. Production of ROS in response to nanomaterials and antioxidant activity is affected by the exposure time of NMs, their type and concentration, as well as the plant species (Dev et al. 2018). As is well known, defense mechanisms based on ROS scavenging in plant systems follow diverse enzymatic and non-enzymatic pathways and are necessary to protect plants from stress factors (Ma et al. 2015). There are three types of superoxide dismutase (SOD) in plants based on the type of catalytic ion, including Fe-SOD, Mn-SOD, and Cu-Zn-SOD. These enzymes participate in the detoxification process by converting $O_2^{\bullet-}$ to the less toxic H_2O_2 and further induction of antioxidant pathways, for instance, catalase (CAT) converts H_2O_2 to H_2O and O_2. In some cases, H_2O_2 can be involved in a Fenton reaction of metal ions (Fe^{2+}, Cu^{2+}) and result in the formation of the hydroxyl radical HO^{-}, highly reactive ROS (hROS), that can cause irreversible changes in biomolecules, such as lipids, proteins, and nucleic acids (Ma et al. 2015). Another issue is the ascorbate-glutathione (Asada-Halliwell) pathway, where a reaction is mediated by ascorbate peroxidase (APX), which converts H_2O_2 to H_2O by oxidizing ascorbate to two products, monodehydroascorbate (MDHA) and dehydroascorbate (DHA). Finally, glutathione peroxidase (GPX), which is responsible for the production of oxidized disulfide glutathione form (GSSG) with direct conversion of H_2O_2 to H_2O, and glutathione reductase, which reduces the GSSG to monomeric glutathione (GSH) (Dev et al. 2018; Hasanuzzaman et al. 2019). Moreover, non-enzymatic oxidative stress response includes biomolecules, such as anthocyanin, glutathione, ascorbic acid, carotenoids, phenolic compounds, or proline (Ahmad et al. 2010). The activity of antioxidant enzymes is a parameter that represents the oxidative stress defense mechanisms induced by the exposure of plants to nanomaterials. Significantly higher activity of antioxidants enzymes was observed in *Salvia verticillata* after foliar treatment with multiwalled-carbon nanotubes (MWCNTs) at a concentration > 1,000 mg mL^{-1}. Results displayed two times the increased activity of SOD, 2.1-fold higher activity of peroxidase, and 3.9-fold enhancement in catalase activity compared to control samples. In addition, increased content of malondialdehyde (MDA) and proline were also detected (Rahmani et al. 2020). The activity of ROS-scavenging enzymes indicates defense mechanisms that remove H_2O_2 to protect cells from nanomaterial-induced damage (Fan et al. 2018). In another study, the content of anthocyanin, a pigment that scavenges free radicals and chelates metal ions significantly increased in plants, such as *Arabidopsis, Solanum tuberosum*, and *Brassica rapa* ssp. *rapa* after treatment with metal nanoparticles (Qian et al. 2013; Bagherzadeh Homaee and Ehsanpour 2015; Thiruvengadam et al. 2015).

Adaptation to Nanomaterials and Detoxification

The plant responses at the phenotypic and physiological levels are altered by gene expression and protein synthesis. A number of studies were conducted on plants exposed to nanomaterials and the main results are summarized in Table 3. Proteomic analysis of *Triticum aestivum* after AgNPs treatment displayed important changes in the expression of proteins depending on targeted plant tissue. It implicated various responses to AgNPs-stress in leaves and root cells. Increased content of α-amylases, a fructose-bisphosphate aldolase, and aconitate hydratases accumulation in roots and leaves were observed, respectively. Authors suggest that by altering the levels of enzymes involved in energy metabolism, cells can produce more reducing substances to facilitate the AgNPs-stress response. Moreover, the results revealed higher production of enzymes, namely methionine synthase and S-adenosylmethionine synthetase, which are committed to sulfur amino acid biosynthesis (Vannini et al. 2014). While in another study, in both ZnO-NPs and Ag-NPs stressed soybean (*Glycine max* L.) roots more than two-fold increase in the content of methionine gamma-lyase was observed (Hossain et al. 2016). The product of the reaction catalyzed by these enzymes, S-adenosylmethionine, is employed in processes, including the synthesis of the plant hormone ethylene, cell wall, chlorophylls, secondary metabolites, DNA replication, and methylation

Table 3. Plant responses at different levels to various types of nanomaterials.

Tested Plant	Type of Nanomaterial	Concentration	Effects of NMs on Plants	Biochemical and Molecular Mechanisms for the Adverse Effects of NMs on Plants	References
Tomato (*Lycopersicon esculentum)*	AgNPs	10 mg L^{-1}, 20 mg L^{-1}, and 30 mg L^{-1}	Accumulation of Ag in plant tissues reduced plant biomass caused morphological changes in xylem cells and shifted the balance of water and nutrient dynamics	Upregulation by 23.50%, 52.09%, and 7.6% of genes related to membrane transporters H+-ATPase, potassium transporter, and sulfate transporter	Noori et al. 2020
Wheat (*Triticum aestivum*)	AgNPs-PVP coated	10 mg L^{-1}	Adversely affected seedling growth and induced morphological modifications in root tip cells	Altered expression of several proteins mainly involved in primary metabolism and cell defense	Vannini et al. 2014
Tobacco *Nicotiana tabacum*	AgNPs	100 µM	n.a.	Accumulation of pathogenesis-related (PR) proteins involved in modifications of cell wall	Peharec Štefanić 2019
Arabidopsis (*Arabidopsis thaliana)*	AgNPs	1.0 mg L^{-1}; 2.5 mg L^{-1}	Decreased plant fresh weight, inhibited photosynthesis, and delayed flowering	Stimulation of activity of molecules associated with the tricarboxylic acid cycle and in sugar metabolism, reduction of transcription by 25–40% of flowering key genes including AP1, LFY, FT, and SOC1,	Ke et al. 2018
Broad bean (*Vicia faba*)	ZnONPs	10 mg L^{-1}, 25 mg L^{-1}, 100 mg L^{-1}, and 200 mg L^{-1}	Seed germination and seedling growth were enhanced at lower concentrations (10 mg/mL and 25 mg/mL) and inhibited at higher concentrations (100 mg/mL and 200 mg/mL)	Altered expression of peroxidase isoenzymes and α- and β-esterase isoenzymes, induction of chromosomal aberration, and formation of micronuclei and vacuolated nuclei	Youssef and Elamawi 2020
Soyabean (*Glycine max* cultivar Enrei)	ZnONPs	10 ppm	Improved root and hypocotyl growth, higher biomass production	Increased biosynthesis of proteins (273) related to metabolism, stress, photosynthesis, transport, and amino acid metabolism, decreased level of proteins (198) associated with the cell wall, RNA metabolism, and lipid metabolism	Komatsu et al. 2022
Cucumber (*Cucumis sativus*)	CuNPs	50 mg L^{-1}, 100 mg L^{-1}, and 200 mg L^{-1}	Adverse phenotypic alterations, reduced biomass, and decreased levels of the photosynthetic pigments in a concentration-dependent manner	Induction of copper-zinc superoxide dismutase (Cu-Zn SOD) gene expression, CuNP at all tested concentrations caused genomic alterations confirmed by RAPD analysis	Mosa et al. 2018
Mustard *(Brassica rapa)*	CuO NPs	50 mg L^{-1}, 250 mg L^{-1}, and 500 mg L^{-1}	Decrease of root and shoot length, significantly reduced after treatment of 250 and 500 mg L^{-1}	Decreased chlorophyll, carotenoid, and sugar content and increased proline, anthocyanins, and malondialdehyde. Upregulation of genes related to oxidative stress enzymes, glucosinolate, and phenolic compounds	Chung et al. 2019

Coriander (*Coriandrum sativum*)	CuNPs	200 mg L^{-1}, 400 mg L^{-1} and 800 mg L^{-1}	Decreased biomass and root length	Induced oxidative stress (higher H_2O_2 and MDA content) and genotoxicity in genomic DNA confirmed by RAPD technique analysis	Al Quraidi et al. 2019
Lilac sage (*Salvia erticillate*)	MWCNT	50 mg L^{-1}, 100 mg L^{-1}, 250 mg L^{-1}, 500 mg L^{-1}, and 1,000 mg L^{-1}	After foliar application of MWCNT at a concentration > 100 mg mL^{-1} decreased content of photosynthetic pigments	> 100 mg mL^{-1} MWCNT caused increased antioxidant enzymes (SOD, CAT, and POD) activities, overproduction of proline, two-fold higher protein content as well as higher expression of rosmarinic acid synthase and RA accumulation	Rahmani et al. 2020
Arabidopsis (*Arabidopsis thaliana*)	MWCNT	1,500 mg L^{-1}, 2,500 mg L^{-1}, or 3,500 mg L^{-1}	Dose-depended inhibition of root growth and leaf development	Increased H_2O_2 and malondialdehyde (MDA) content, alternated SOD, CAT, POD activity, hypermethylation of genes associated with stilbenoid, diarylheptanoid, and gingerol biosynthesis, tyrosine metabolism, phosphatidylinositol signaling system, and inositol phosphate metabolism and hypomethylation of genes related to ABC transporters, starch, and sucrose metabolism, and plant hormone signal transduction	Yang et al. 2021

(Hossain et al. 2016). Moreover, S-adenosylmethionine is essential for polyamine and glutathione (GSH) synthesis. GSH is one of the major molecules behind the sequestration of metals from inside the cell (Hossain et al. 2012). Interestingly, some studies indicate the upregulation of membrane transporters genes (Noori et al. 2020) and enhanced synthesis of defense compounds, protecting against pests and infections, such as rosmaric acid after exposure to AgNPs and MWCNT (Peharec Štefanić 2019; Rahmani et al. 2020).

Furthermore, the uptake of nanomaterials might be limited by exudates and mucilage (highly hydrated components from molecules including polysaccharides, proteins, and phenolic acids), promoting stabilization of nanomaterials in the rhizosphere solution (Lin and Xing 2008). Avellan et al. (2017) have observed that positively charged AuNPs stimulated the border cells on the root cap of *Arabidopsis thaliana* to release high-density mucus. The mucilage suppressed the translocation of AuNPs into the root by entrapment and immobilization of NPs. Interestingly, no similar effect was observed after treatment with negatively charged AuNPs, which were mostly observed in line with the cell wall, indicating apoplastic transport inside root tissue. In contrast, metabolomic analysis of root exudates of cucumber exposed to the CuNPs (at concentrations of 10 mg mL^{-1} and 20 mg mL^{-1}) revealed stimulation in the synthesis of amino acids, phenolic compounds, and ascorbic acid. Enhanced production and release of these low-molecular-weight substances have been implicated as a defense against metal stress by participating in the sequestration or exclusion of CuNPs or Cu ions, as well as improving antioxidant efficiency (Zhao et al. 2016). Additionally, plant growth-promoting bacteria may play a supporting role in preventing nanomaterials from entering plant tissues. As reported by Ahmed et al. (2021b) overproduction of EPS by *Azotobacter salinestris* significantly reduced the penetration of metal oxide (ZnO, CuO, Al_2O_3, and TiO_2) nanoparticles into tomato (*Solanum lycopersicum* L.).

The mechanisms of metal detoxification in plants include transport to storage parts, compartmentalization in subcellular parts, chelate formation, and elimination from the plant body (Rajput et al. 2019c). The transport and accumulation of ZnONPs in *Phaseolus vulgaris* were studied by Cruz et al. (2017, 2019). There was a decreasing Zn content from root to shoot after ZnONPs application, indicating that Zn in nano-form is stored, in lower tissues, contrary to the application of aqueous $ZnSO_4$ solution, where increased content was noted in higher tissues. In addition, the transcriptional analysis indicated increased expression levels of metal transporters located in the tonoplasts, implying that the mechanism for the tendency to accumulate Zn in lower tissues may be related to increased compartmentalization of Zn in vacuoles (Cruz et al. 2017, 2019). Furthermore, the high metal tolerance and absorption capacity of some plant species make them useful for environmental remediation. The main phytoremediation strategies include stabilization, degradation, extraction, and volatilization of contaminants and are based on processes naturally occurring in plants, such as uptake and sorption, translocation, metabolism, and evapotranspiration (da Conceição Gomes et al. 2016). Zhang and coworkers (2015) showed limited transport and potential to root accumulation of ZnONPs in *Schoenoplectus tabernaemontani*. The Zn nanoparticles and their aggregates were observed in cells of the root epidermis and intercellular space. A similar accumulation of nanoparticles was observed in the roots of wheat, rice, oat, and cucumber (Zhao et al. 2017a; Cai et al. 2017; Asgari et al. 2018; Alsuwayyid et al. 2022). Nowadays, with the expanding prevalence of NMs in soil or water, research efforts increasingly focus on the potential of plants for the phytoremediation of environments contaminated with nanomaterials (Ebrahimbabaie et al. 2020).

Techniques for Evaluation of Toxicity to Plants

As mentioned in the previous paragraph, nanomaterials influence plants in multiple ways, affecting individual cells and tissues, thereby altering their growth and development (Parsons et al. 2010; Ma et al. 2011; Dev et al. 2018; Wang et al. 2019). Mostly, the phytotoxicity of nanomaterials was tested using well-studied model plants, including onion (*Allium cepa*), thale cress (*Arabidopsis thaliana*),

cucumber (*Cucumis sativus*), corn (*Zea mays*) rice (*Oryza sativa*), tobacco (*Nicotiana tabacum*), oilseed rape (*Brassica oleracea*), and lettuce (*Lactuca sativa*). The assays involve both evaluations of physiological and morphological parameters, as well as assessment of the implications for cell cycle or DNA damage after treatment with nanomaterials at specified periods and doses (Wang et al. 2012; Zhu et al. 2012; Ke et al. 2018; Peharec Štefanić 2019; Mosa et al. 2018; Zhang et al. 2021).

Techniques for Nanoparticle Detection

Various types of electron microscopy (such as transmission electron microscopy/scanning electron microscopy, and scanning transmission electron microscopy) have been applied to the investigation of nanomaterial uptake and localization in plants (Miralles et al. 2012; Ye et al. 2021). For instance, transmission electron microscopy (TEM) was used for the detection of TiO_2NPs in the cytoplasm of wheat roots cortex cells (Du et al. 2011), while scanning electron microscopy (SEM) coupled with energy dispersive X-ray (EDX) was employed for investigating nanoscale zero-valent iron (nZVI) uptake in *Leonurus cardiaca* leaves (Jafari and Hatami 2022). The inductively coupled plasma (ICP)-based techniques (such as ICP-optical emission spectrometry, ICP-mass spectrometry, and single-particle-ICP-mass spectrometry) are also used to determine the accumulation of nanomaterials in plant tissues, and the main advantage of this type of analysis is low detection threshold. Hence, sp-ICP-MS were used to obtain details on the concentration and particle size distribution of CuONPs accumulated in leaves of kale, lettuce, and collard green (Keller et al. 2018). Other techniques frequently used for the analysis of the morphology, chemical composition, and distribution of NMs in plants are the synchrotron-based X-ray approaches (Zhu et al. 2014; Castillo-Michel et al. 2017). Zhang et al. (2019) used TEM and synchrotron-based X-ray absorption near edge spectroscopy (XANES) for the detection of cerium nanoparticles in four plant species: monocots (corn and wheat) and dicots (soybean and cabbage). In another study reported by Larue et al. (2014), results from SEM and micro-X-ray fluorescence (μXRF) revealed that foliar-applied AgNPs penetrated leave cells of *Lactuca sativa*, attached to the cell wall and formed agglomerates with size 2 μm. In addition, ICP-MS analysis showed that the total content of AgNPs after 7 days of exposure was 240 μg per seedling. Recently, ICP-MS and X-ray fluorescence imaging (XFI) were used for the evaluation of biodistribution and real-time tracking of AuNPs in *Matricaria chamomilla*. The authors pointed out that XFI mapping by deep tissue imaging can be successfully exploited to assess the fate and interactions of NPs in plants, avoiding tissue destruction (Liu et al. 2022).

Approaches to Elucidate the Molecular Mechanism of Plant Response to Nanomaterials

The genotoxicity and cytotoxicity of nanomaterials are assessed by a wide range of approaches, including genomic, proteomic, and metabolomic methods. Currently, microscopic observation, electrophoresis-based methods, molecular markers, and polymerase chain reaction-based techniques are used to identify plant responses to nanomaterials at the molecular level (Barabadi et al. 2019; Rico et al. 2020). A number of studies on the genotoxic effect of nanomaterials focus on chromosomal aberrations, micronucleus formation, genomic (gDNA damage), mutational events, and copy number variation (Marmiroli et al. 2022). In a study reported by Banerjee et al. (2021) increase in micronuclei formation, a decrease in mitotic index, chromosomal abbreviation (chromosome breaks, anaphase-telophase bridges or multipolar anaphase-telophase cells), and DNA damage (four-fold increase in tail DNA detected in comet assay) were observed in *Allium cepa* root tip cells treated with CdSe quantum dots (QDs) at a concentration of 50 nM. Nevertheless, the authors suggest that the genotoxic effect is related to ROS generation, as evidenced by an increased antioxidant defense response. Moreover, in order to better understand the mechanism of toxicity of nanomaterials high-throughput methods, such as quantitative real-time PCR (qRT-PCR) or cDNA microarrays, are used to analyze changes in gene expression (Marmiroli et al. 2022). Results from global gene expression analysis of *Nicotiana tabacum* L. cv. Bright Yellow-2 (BY-2) cells exposed

to 12 mg mL^{-1} of CuNPs demonstrated altered expression of 2692 genes. Performing gene ontology (GO) and Kyoto Encyclopedia of Genes and Genomes (KEGG) analysis specified that the genes were associated with oxidative stress (Dai et al. 2018). The phytotoxic effect of CuNPs on cucumber (*Cucumis sativus*) was evaluated by Mosa and coworkers (2018). The high accumulation level of CuNPs in plant roots was confirmed by X-ray fluorescence (XRF), atomic absorption spectroscopy (AAS), and SEM analysis. Results from the random amplified polymorphic DNA (RAPD) technique showed that treatment with CuNPs at a concentration of 200 mg L^{-1} induced genomic alterations in *C. sativus* and enhanced expression of copper-zinc superoxide dismutase (Cu-Zn SOD) gene (qRT-PCR analysis). In addition, changes in membrane permeability, an increase in H_2O_2 and MDA content, and a decrease in chlorophyll content (a and b) were recorded. All of these shifts resulted in the inhibition of seedling growth and a decrease in their biomass (Mosa et al. 2018). Considering that changes in gene expression and molecule biosynthesis can be induced by very negligible doses of contaminants, the above techniques are important in assessing toxicity associated with chronic exposure to nanomaterials. In addition, toxicological results enable the development of screening methods based on specific gene mutations and biomarkers for detecting alleged nanomaterial toxicity and associated risks (Jha and Pudake 2016).

Translocation of Nanomaterials in Plants

Uptake of Nanomaterials

In fact, there are two basic pathways of plant exposure to nanoparticles: foliar and root. The bioavailability of nanomaterials to plants and further translocation or accumulation is affected by factors, including the physicochemical properties of NMs, plant physiology, and environmental conditions (Lv et al. 2019). However, with regard to the various factors affecting the interaction of nanomaterials with plants, there is still a need for research to better understand such nanostructures. A number of studies showed that the uptake of NMs by plants and further transport to other plant tissues depends on their shape, size, and chemical composition as well as the anatomy of the exposed plants (Zhao et al. 2017b; Lyu et al. 2022; Zong et al. 2022).

Roots

Adsorption or uptake by the root surface is the initial stage of NMs translocation by plants from the soil. The efficiency of these processes highly depends on the size and surface charge of the nanomaterial, as indicated by several reports (Xia et al. 2013; Taylor et al. 2014; Hu et al. 2018; Lyu et al. 2022). Observations by TEM of wheat roots showed the penetration of smaller TiO_2 NPs with a size of 20 nm into the cortex cells, while larger ones with a diameter of 50 nm could not penetrate but adhered to the wall of the periderm cells (Du et al. 2011). Recently, Zong et al. (2022) reported higher translocation of nanosized (43 nm) CuONPs to cucumber roots, compared with copper oxide particles with a size of 510 nm. Nevertheless, NMs may undergo a wide range of biotransformation in the soil environment, affecting their bioavailability to plant roots. Several reports showed that after exposure to positively charged NPs root cap border cells are stimulated to increase mucilage production, which immobilizes positively charged NPs and acts as a barrier to root cells (Li et al. 2016; Avellan et al. 2017). According to Zhu et al. (2012), negatively charged (–24 mV) AuNPs were taken up with higher efficiency at 43–86% than similarly sized, positively charged (+ 24 mV) AuNPs at 13–25% uptake efficiency. The results from the above studies indicated also species-dependent uptake of NPs with the lowest uptake by rice, followed by pumpkin, radish, and ryegrass seedlings.

Leaves

It should be noted that the cuticle acts as a protective layer of plant tissues and plays a key role in the translocation of NMs from the leaf surface to the interior of the plant. According to the literature,

small hydrophilic structures can be translocated through the aqueous pores present in the cuticle and stomatal apparatus. In the case of hydrophobic molecules, the translocation occurs by diffusion through the hydrophobic cuticle (Eichert et al. 2008). For instance, 60 nm AgNPs were immobilized on the surface of the cuticle and not observed on its inner side. Further analysis displayed that the adsorption of AgNPs was mainly facilitated by cutin (specifically with aliphatic hydroxy acids groups) and prevented by epicuticular waxes and pectin (Marciano et al. 2008). Furthermore, nanoparticles may enter plant organisms through stomata, hydathodes, and trichomes (Zhao et al. 2017a; Bombo et al. 2019; Spielman-Sun et al. 2020). Spielman-Sun et al. (2020) identified that the surface properties of AuNPs affected their distribution on the leaves. Citrate-reduced AuNPs were randomly distributed on leaves surface, while AuNPs coated with LM6M-antibody (specific for α-1,5-arabinan in stomata) and bovine serum albumin (BSA) were observed around stomata and trichomes, respectively. The results indicated that appropriate surface modification of the nanoparticles contributes to their targeted accumulation in areas particularly vulnerable to pathogen attacks and leads to an improvement in their anti-pathogenic efficacy (Spielman-Sun et al. 2020).

Translocation of Nanomaterials in Plants

After entering the plant, the transport of NMs through tissues is conducted through the apoplast and symplast pathways. Symplastic transport is based on transfer between the cytoplasm of cells across plasmodesmata or sieve plates. In contrast, apoplastic transport is defined as the movement beyond the plasma membrane in intercellular spaces through the cell walls of adjacent individual cells as well as xylem vessels (Pérez-de-Luque 2017). Indeed, some mechanisms have been identified to enable NPs to penetrate plant cells, including endocytosis-like or non-endocytic permeation, association with carrier proteins via aquaporins, or induction of new and large pore assembly (Palocci et al. 2017; Dai et al. 2018; Akdemir 2021; Dong et al. 2022). For instance, clathrin-independent endocytosis was identified as the main pathway for poly(lactic-co-glycolic) acid (PLGA) NPs internalization by grapevine cells. It has also been shown that the cell wall acts predominantly as a size-exclusion filter for the nanoparticle's uptake (Palocci et al. 2017). Gold nanoparticles with a size of 3.5 nm penetrated the tobacco root cells, while 18 nm AuNPs formed aggregates on the root surface. It is suggested that the transport of smaller particles occurred through pores (3.3–5.2 nm in size) in the cell walls (Carpita et al. 1979; Sabo-Attwood et al. 2012; Milewska-Hendel et al. 2017). It has been studied that small NMs after entering the cortex cells may form aggregates ~ 2 μm and their further transport is limited (Zhang et al. 2017; Dong et al. 2022). Size-dependent influx into plant cells was observed for SeNPs in wheat; exposure to 40 nm NPs resulted in 1.8-fold and 2.2-fold higher accumulation compared to SeNPs with diameter at 140 and 240 nm, respectively (Hu et al. 2018). However, certain nanomaterials can interact and modify the cell wall, thereby supporting their entry into the cell (Molnár et al. 2020). Hence, AuNPs affect the arrangement of specific pectin and arabinogalactan protein (AGP) epitopes in root cell walls, changing the chemical composition of the cell wall (Mielewska-Hendel et al. 2021). Whereas, Ag ions released from silver nanoparticles may bind to hydroxyl groups and change the cellulose structure in the cell wall, enabling their transport into the cytoplasm (Paiva Pinheiro et al. 2021).

Long-Distance Transport

The vascular tissues of plants play a significant role in the long-distance transport of NMs (Deepa et al. 2015; Hasaneen et al. 2016; Ma et al. 2017). In maize (*Zea mays* L.) CuNPs were translocated from the root to the shoot via the xylem and relocated back to the root via the phloem. In addition, microscopic observation indicated an apoplastic way through epidermal cortical cells by endocytosis up to the endodermis and the xylem (Wang et al. 2012). Nevertheless, the translocation of NPs from endodermis may be limited by the Casparian stripe. The crossing of this tissue has not been fully evaluated; however, it is suggested that in seedlings the incomplete development of this stripe at the top of the root facilitates penetration of NPs into the xylem (Wang et al. 2012). In turn, after

foliar spraying, the chitosan nanoparticles were detected in sieve tubes of French bean phloem tissue (Hasaneen et al. 2016). In another study, Dong and coworkers (2022) observed graphene in the cytoplasm of the cortex, xylem, and mesophyll cells of *Triticum aestivum*. The results also displayed symplastic transport of graphene particles through plasmodesmata of adjacent, as well as further xylem and phloem-mediated transport. The long-distance transport of nanomaterials in plants is significantly influenced by the type of nanomaterials and application form but also by plant species and stage of development (Hasaneen et al. 2016; Ma et al. 2017).

Adverse Effect of NPs on Crop Yield and Quality

The increasing use of various nanomaterials (NMs) in medicine, agriculture, and industry, increases the threat to the environment, including agricultural areas. NMs can be absorbed from soils through plant roots or under foliar exposure and can reach all plant organs, including fruits and grains (El-Moneim et al. 2021). The interaction of nanomaterials with plants highly depends on the magnitude of their concentration, shape, and chemical nature of the NMs, as well as environmental conditions and plant species. Due to their unique properties and high reactivity nanomaterials might negatively affect basic cellular processes (including proliferation and metabolism) by interfering with transport across cell membranes, inducing oxidative stress, or altering gene regulation (de la Rosa et al. 2021). Furthermore, some studies indicated the negative effects of NMs, paying particular attention to the yield of economically important crops. In addition, the presence of nanomaterials in plant-origin foods poses a risk to human and animal health. The study of the interaction between NMs and plants, and their content in plant organs, as well as the associated risks to humans, is essential for the food production and medicine sectors (El-Moneim et al. 2021).

Effect of Concentrations

Seed germination is the first stage and most important phase for the growth of crop plants and yield quality (Rifna et al. 2019). Carbon nanotubes at low concentrations were recognized to stimulate seed germination and plant growth by improving water adsorption and transport such as by activation of water channels (Villagarcia et al. 2012; Hatami et al. 2017). Seedlings of wheat, maize, peanut, and garlic were stimulated by multiwalled-carbon nanotubes in a dose-dependent manner until the maximum tested concentration was at 50 μg mL^{-1} (Srivastava and Rao 2014). However, in another study, a tenfold increase in the concentration of single and multi-walled carbon nanotubes (from 0.1% to 1%) caused necrosis, disorders in root formation, and loss of turgor in plants (Basiuk et al. 2019). Similar results were also presented by Gohari et al. (2020). They observed that MWCNT functionalized with carboxylic acid groups at a concentration of 50 μg mL^{-1}, under optimal conditions, promoted the growth of *Ocimum basilicum* seedlings. Additionally, under salinity stress, they act as protective factors and stimulated seedlings to synthesize chlorophyll, carotenoids, and also activity of the antioxidant system. However, treatments with higher concentrations (100 μg mL^{-1}) displayed toxic effects and lead to lowered photosynthetic efficiency or decreased membrane stability (Gohari et al. 2020). A toxic effect was observed in seeds of *Lupinus termis* treated with AgNPs at concentrations 400 ppm, 600 ppm, 800 ppm, and 900 ppm, where relative germination (RG) compared to control samples decreased by 22%, 33.4%, 44%, and 67%, respectively (Al-Huqail et al. 2018). Salehi et al. (2021) evaluated the effect of foliar-applied cerium oxide nanoparticles (CeO_2NPs) on bean plants (*Phaseolus vulgaris* L.) at a concentration range between 250–2000 mg L^{-1}. The findings pointed out that seeds from treated plants accumulated 45 μg Ce per 1 gram of dry mass while produced pollen grains sustained severe structural chromosome injuries under exposure to the maximum tested concentration and led to pollen abortion thereby consequently yield loss (Salehi et al. 2021).

Effect of Size and Agglomeration

There was a size-dependent toxic effect on the growth and development of *Salvinia minima* after treating AgNPs with an average size of 10 nm and 40 nm. Smaller AgNPs (10 nm) tended to form agglomerates more often than larger ones, but these structures were dynamic and not stable over long periods; this did not affect their dissolution ability. Higher relative growth inhibition was observed in seedlings treated with 10 nm AgNPs, than with 40 nm AgNPs. Chlorophyll content was differently modulated by these two sized NPs depending on the medium used. In moderately hard water (MHW) both AgNPs reduced the synthesis of chlorophyll while in natural organic matter (NOM) larger AgNPs inhibited and smaller ones stimulated the synthesis of chlorophyll compared to control samples (Thwala et al. 2021). Application of copper oxide nanoparticles (CuONPs) with an average size of 25 nm to soybeans significantly lowered the amount of seed yield compared to CuONPs with sizes of 50 nm and 250 nm and controls. With the use of the smallest CuONPs at a concentration of 500 mg mL^{-1}, increased hydrogen peroxide and malondialdehyde content, and improved activity of antioxidant system enzymes, namely SOD, catalase, peroxidase was observed (Yusefi-Tanha et al. 2020). It is suggested that the smaller size of CuONPs facilitates overcoming cellular barriers and enables them to move into the cell, thereby triggering higher oxidative stress. In contrast, larger-size CuONPs tend to be less surface reactive due to their smaller surface-to-volume ratio. As a result, they become potentially incapable of crossing cell barriers, displaying lower toxicity and not affecting crop plant productivity (Wang et al. 2012; Hong et al. 2015; Yusefi-Tanha et al. 2020).

Effect of Shapes

Another consideration in the uptake, translocation, and toxicity of nanomaterials is their shape, which determines chemical reactivity or possible biotransformation pathways in crop plants (Siddiqi et al. 2016). Zhang et al. (2017) reported shape-depended accumulation of CeO_2NPs in cucumber. Rod-like NPs were strongly accumulated in shoots and rapidly transformed Ce^{3+} ions when compared to octahedral, cubic, or irregularly shaped particles. Syu et al. (2014) demonstrated the shape-dependent effects of AgNPs on *Arabidopsis thaliana* seedlings. The results showed that AgNPs with triangular and decidual shapes mostly had a positive effect on seedling development, but treatment with spherical AgNPs led to reduced cotyledon growth. Moreover, increased anthocyanin content and SOD 2 activity suggested induction of oxidative stress by spherical AgNPs (Syu et al. 2014).

Effect of Surface Properties

Two-dimensional graphene oxide (GO) and reduced graphene oxide (rGO) nanosheets with negative and positive charges, respectively, demonstrated a contrasting impact on rice seedling growth. GO significantly inhibited shoot and root growth at concentrations of 100 mg L^{-1} and 250 mg L^{-1} while at the same dosage, rGO did not affect these parameters. The surface oxygen content was pointed as the main factor affecting their phytotoxicity (Zhang et al. 2020). Besides, noticeably more severe adverse effects on germination and growth of tobacco (*Nicotiana tabacum* L.) seedlings occurred after implementation of AgNPs coated with cetyltrimethylammonium bromide (CTAB) than polyvinylpyrrolidone (PVP). The research indicated that the toxic potency of AgNP-PVP was predominantly related to the release of Ag^{+} ions, whereas the phytotoxicity of AgNP-CTAB was attributed to the surface coverage itself (Biba et al. 2020). Distinct levels of phytotoxicity on lettuce were also identified for graphene quantum dots (GQDs) subjected to various functionalizations, i.e., amination, carboxylation, and hydroxylation. The results confirmed the superior phytotoxicity of hydroxylated GQDs compared to the remaining two functionalizations, noting that aminated GQDs showed the lowest phytotoxicity. The surface property-dependent toxicity was observed by changes in growth parameters (reduced seedling length and amount of biomass) and by physiological responses, including disruption of photosynthesis and activation of antioxidant protection mechanism

as well as regulation of phytohormone synthesis. In addition, GQDs affected mineral content in nutrient profiles at different levels, where hydroxylated GQDs showed the strongest effect (increase in Ca content and decrease in Mg, K, P, Mn, and Zn content) (Zhang et al. 2021).

Are Nanoparticles Transferred From One Generation to Another?

The comprehensive overview of NMs, i.e., transfer to subsequent generations of plants and NMs-induced transgenerational changes is lacking. Studies in this area are quite limited. Lin et al. (2009) showed that treatment of rice seedlings with carbon-based nanomaterials [fullerene C_{70} and multiwalled-carbon nanotubes (MWCNTs)] resulted in the accumulation of CNMs in seeds harvested from mature plants. Furthermore, C70 aggregates were observed in the leaf tissues of the next generation. In another study, Liu and coworkers (2018, 2019a, b) showed that CuONPs treatment in the previous generation of rice caused their accumulation in seeds but had no effect on Cu content in plants in the next generation. However, several studies suggested that nanomaterials translocated and accumulated in seeds may affect plant development in the next generation (Wang et al. 2013; Hernandez-Viezcas et al. 2013). For instance, irrigation of *Raphanus sativus* seedlings with ZnONPs and CuNPs suspension at a concentration of 1,000 mg mL^{-1} resulted in increased content of Zn (0.12 mg g^{-1}) and Cu (0.11 mg g^{-1}) obtained seeds comparing to untreated ones (Cu and Zn content, 0.03 and 0.04 mg g^{-1}, respectively). In a subsequent generation, reduced biomass, shoot, and root lengths were observed (Singh and Kumar 2018). Recently, Khan and coworkers (2022) investigated the impact of TiO_2NPs at a concentration range between 25–200 μg mL^{-1} on growth, yield quality, biochemical parameters, and heritable transgenerational alterations in the second generation of lentils (*Lens culinaris* Medik.) seedlings. Exposure of seeds in the first generation to NPs concentrations higher than 25 μg ml^{-1} led to reduced growth and development (number of branches and seeds), as well as lowered protein content in F2 generation seedlings in a dose-dependent manner. In addition, there was an increase in antioxidant enzyme activity (SOD and CAT), H_2O_2, and MDA content compared to control seedlings. However, subsequent generations displayed lower stress levels and relatively greater tolerance than in treated populations. In contrast, results presented by Medina-Velo (2018) showed that the parent plant's treatment with ZnONP not affected the yield, sugar, and protein content or nutrient profile of the second generation of bean (*Phaseolus vulgaris*) seeds. There was only a slightly lower Ni and increased Ca content in seeds from the second generation of plants. Indeed, finding this marginal effect highlights the feasibility of using ZnONPs in agricultural soils to improve crop quality. However, further studies at the molecular and genetic levels are required to provide the necessary insight into understanding the transgenerational effects of residual NPs (Medina-Velo et al. 2018).

Conclusions

Plants are exposed to nanomaterials that are introduced into the environment either intentionally (e.g., agricultural applications) or unintentionally (e.g., residues from industry). The growing interest in the use of nanomaterials in agriculture is due to their superior biological activities against plant pathogens but also as fertilizers. Despite the many positive aspects of the use of nanoformulations in agriculture, it has been observed, especially at higher doses, that NMs may bring negative consequences for plant organisms. Research indicates that the effects of NMs on plants depend on their properties but also the plant species and environmental conditions. Overall, in response to NMs toxicity, plants intensify the synthesis of biomolecules related to the stress and antioxidant systems. Uptake and biotransformation of NMs by plants are also limited by natural barriers, such as cuticle or mucilage. Nevertheless, the not fully understood mechanisms of NMS interactions with plants should be clarified by future research, especially on the effects on plant development and crop quality. Importantly for consumers, the risk of NMs accumulation in crop plants should be also assessed, as it poses a threat to animal and human health. In addition, non-standardized tests for properly assessing the safety of nanomaterials are another challenge.

Acknowledgement

J.T.W. acknowledges grant No. 2022/45/N/NZ9/01483 from National Science Centre, Poland.

References

Abdelkhalek, A. and Al-Askar, A.A. 2020. Green synthesized ZnO nanoparticles mediated by Mentha spicata extract induce plant systemic resistance against Tobacco mosaic virus. App. Sci. 10: 5054.

Ahmad, P., Jaleel, C.A., Salem, M.A., Nabi, G. and Sharma, S. 2010. Roles of enzymatic and nonenzymatic antioxidants in plants during abiotic stress. Crit. Rev. Biotechnol. 30: 161–175.

Ahmed, B., Syed, A., Rizvi, A., Shahid, M., Bahkali, A.H., Khan, M.S. and Musarrat, J. 2021b. Impact of metal-oxide nanoparticles on growth, physiology and yield of tomato (*Solanum lycopersicum* L.) modulated by *Azotobacter salinestris* strain ASM. Environ. Pollut. 269: 116218.

Ahmed, T., Noman, M., Luo, J., Muhammad, S., Shahid, M., Ali, M.A. and Li, B. 2021a. Bioengineered chitosan-magnesium nanocomposite: A novel agricultural antimicrobial agent against *Acidovorax oryzae* and *Rhizoctonia solani* for sustainable rice production. Int. J. Biol. Macromol. 168: 834–845.

Akdemir, H. 2021. Evaluation of transcription factor and aquaporin gene expressions in response to Al_2O_3 and ZnO nanoparticles during barley germination. Plant Physiol. Biochem. 166: 466–476.

Al-Huqail, A.A., Hatata, M.M., Al-Huqail, A.A. and Ibrahim, M.M. 2018. Preparation, characterization of silver phyto nanoparticles and their impact on growth potential of *Lupinus termis* L. seedlings. Saudi J. Biol. Sci. 25: 313–319.

AlQuraidi, A.O., Mosa, K.A. and Ramamoorthy, K. 2019. Phytotoxic and genotoxic effects of copper nanoparticles in coriander (*Coriandrum sativum*—Apiaceae). Plants 8: 19.

Alsuwayyid, A.A., Alslimah, A.S., Perveen, K., Bukhari, N.A. and Al-Humaid, L.A. 2022. Effect of zinc oxide nanoparticles on *Triticum aestivum* L. and bioaccumulation assessment using ICP-MS and SEM analysis. J. King Saud Univ. Sci. 34: 101944.

Anand, K. and Panigrahi, B. 2021. Green synthesized nanoparticles: a way to produce novel nano-biosensor for agricultural application. pp. 175–190. In Nanotechnology in Sustainable Agriculture, CRC Press.

Asgari, F., Majd, A., Jonoubi, P. and Najafi, F. 2018. Effects of silicon nanoparticles on molecular, chemical, structural and ultrastructural characteristics of oat (*Avena sativa* L.). Plant Physiol. Biochem. 127: 152–160.

Avellan, A., Schwab, F., Masion, A., Chaurand, P., Borschneck, D., Vidal, V. and Levard, C. 2017. Nanoparticle uptake in plants: gold nanomaterial localized in roots of *Arabidopsis thaliana* by X-ray computed nanotomography and hyperspectral imaging. Environ. Sci. Technol. 51: 8682–8691.

Babu, S., Singh, R., Yadav, D., Rathore, S.S., Raj, R., Avasthe, R. and Singh, V.K. 2022. Nanofertilizers for agricultural and environmental sustainability. Chemosphere 292: 133451.

Bagherzadeh Homaee, M. and Ehsanpour, A.A. 2015. Physiological and biochemical responses of potato (*Solanum tuberosum*) to silver nanoparticles and silver nitrate treatments under *in vitro* conditions. Indian J. Plant Physiol. 20: 353–359.

Banerjee, R., Goswami, P., Chakrabarti, M., Chakraborty, D., Mukherjee, A. and Mukherjee, A. 2021. Cadmium selenide (CdSe) quantum dots cause genotoxicity and oxidative stress in *Allium cepa* plants. Mutat. Res. Genet. Toxicol. Environ. Mutagen. 865: 503338.

Barabadi, H., Najafi, M., Samadian, H., Azarnezhad, A., Vahidi, H., Mahjoub, M.A. and Ahmadi, A. 2019 A systematic review of the genotoxicity and antigenotoxicity of biologically synthesized metallic nanomaterials: are green nanoparticles safe enough for clinical marketing? Medicina 55: 439.

Basiuk, V.A., Terrazas, T., Luna-Martínez, N. and Basiuk, E.V. 2019. Phytotoxicity of carbon nanotubes and nanodiamond in long-term assays with Cactaceae plant seedlings. Fullerenes, Nanotubes and Carbon Nanostructures 27: 141–149.

Biba, R., Matić, D., Lyons, D.M., Štefanić, P.P., Cvjetko, P., Tkalec, M. and Balen, B. 2020. Coating-dependent effects of silver nanoparticles on tobacco seed germination and early growth. Int. J. Mol. Sci. 21: 3441.

Bilesky-Jose, N., Maruyama, C., Germano-Costa, T., Campos, E., Carvalho, L., Grillo, R. and De Lima, R. 2021. Biogenic α-Fe_2O_3 nanoparticles enhance the biological activity of *Trichoderma* against the plant pathogen *Sclerotinia sclerotiorum*. ACS Sustain. Chem. Eng. 9: 1669–1683.

Bombo, A.B., Pereira, A.E.S., Lusa, M.G., de Medeiros Oliveira, E., de Oliveira, J.L., Campos, E.V.R. and Mayer, J.L.S. 2019. A mechanistic view of interactions of a nanoherbicide with target organism. J. Agric. Food Chem. 67: 4453–4462.

Cai, F., Wu, X., Zhang, H., Shen, X., Zhang, M., Chen, W. and Wang, X. 2017. Impact of TiO_2 nanoparticles on lead uptake and bioaccumulation in rice (*Oryza sativa* L.). NanoImpact 5: 101–108.

Cai, L., Chen, J., Liu, Z., Wang, H., Yang, H. and Ding, W. 2018. Magnesium oxide nanoparticles: effective agricultural antibacterial agent against *Ralstonia solanacearum*. Front. Microbiol. 9: 790.

Cao, X., Wang, C., Luo, X., Yue, L., White, J.C., Elmer, W. and Xing, B. 2021. Elemental sulfur nanoparticles enhance disease resistance in tomatoes. ACS Nano 15: 11817–11827.

Carpita, N., Sabularse, D., Montezinos, D. and Delmer, D.P. 1979. Determination of the pore size of cell walls of living plant cells. Science 205: 1144–1147.

Castillo-Michel, H.A., Larue, C., Del Real, A.E.P., Cotte, M. and Sarret, G. 2017. Practical review on the use of synchrotron based micro-and nano-X-ray fluorescence mapping and X-ray absorption spectroscopy to investigate the interactions between plants and engineered nanomaterials. Plant Physiol. Biochem. 110: 13–32.

Chung, I.M., Rekha, K., Venkidasamy, B. and Thiruvengadam, M. 2019. Effect of copper oxide nanoparticles on the physiology, bioactive molecules, and transcriptional changes in *Brassica rapa* ssp. *rapa* seedlings. Wat. Air Soil Poll. 230: 1–14.

da Conceição Gomes, M.A., Hauser-Davis, R.A., de Souza, A.N. and Vitória, A.P. 2016. Metal phytoremediation: General strategies, genetically modified plants and applications in metal nanoparticle contamination. Ecotoxicol. Environ. Saf. 134: 133–147.

da Cruz, T.N., Savassa, S.M., Gomes, M.H., Rodrigues, E.S., Duran, N.M., de Almeida, E. and de Carvalho, H.W. 2017. Shedding light on the mechanisms of absorption and transport of ZnO nanoparticles by plants via *in vivo* X-ray spectroscopy. Environ. Sci.: Nano 4: 2367–2376.

da Cruz, T.N., Savassa, S.M., Montanha, G.S., Ishida, J.K., de Almeida, E., Tsai, S.M. and Pereira de Carvalho, H.W. 2019. A new glance on root-to-shoot in vivo zinc transport and time-dependent physiological effects of $ZnSO_4$ and ZnO nanoparticles on plants. Sci. Rep. 9: 1–12.

Dai, Y., Wang, Z., Zhao, J., Xu, L., Xu, L., Yu, X. and Xing, B. 2018. Interaction of CuO nanoparticles with plant cells: internalization, oxidative stress, electron transport chain disruption, and toxicogenomic responses. Environ. Sci.: Nano 5: 2269–2281.

de la Rosa, G., Vázquez-Núñez, E., Molina-Guerrero, C., Serafín-Muñoz, A.H. and Vera-Reyes, I. 2021. Interactions of nanomaterials and plants at the cellular level: current knowledge and relevant gaps. Nanotechnol. Environ. Eng. 6: 1–19.

de Paiva Pinheiro, S.K., Miguel, T.B.A.R., de Medeiros Chaves, M., de Freitas Barros, F.C., Farias, C.P., de Moura, T.A. and Wu, H. 2021. Silver nanoparticles (AgNPs) internalization and passage through the *Lactuca sativa* (Asteraceae) outer cell wall. Funct. Plant Biol. 48: 1113–1123.

Deepa, M., Sudhakar, P., Nagamadhuri, K.V., Balakrishna Reddy, K., Giridhara Krishna, T. and Prasad, V. 2015. First evidence on phloem transport of nanoscale calcium oxide in groundnut using solution culture technique. Appl. Nanosci. 5: 545–551.

Dev, A., Srivastava, A.K. and Karmakar, S. 2018. Nanomaterial toxicity for plants. Environ. Chem. Lett. 16: 85–100.

Dhyani, K., Meenu, M., Bezbaruah, A.N., Kar, K.K. and Chamoli, P. 2022. Current prospective of nanomaterials in agriculture and farming. pp. 173–194. In Nanomaterials for Advanced Technologies, Springer.

Dong, S., Jing, X., Lin, S., Lu, K., Li, W., Lu, J. and Mao, L. 2022. Root hair apex is the key site for symplastic delivery of graphene into plants. Environ. Sci. Technol. 56: 12179–12189.

Du, W., Sun, Y., Ji, R., Zhu, J., Wu, J. and Guo, H. 2011. TiO_2 and ZnO nanoparticles negatively affect wheat growth and soil enzyme activities in agricultural soil. J. Environmen. Monitoring 13: 822–828.

Ebrahimbabaie, P., Meeinkuirt, W. and Pichtel, J. 2020. Phytoremediation of engineered nanoparticles using aquatic plants: Mechanisms and practical feasibility. J. Environ. Sci. 93: 151–163.

Eichert, T., Kurtz, A., Steiner, U. and Goldbach, H.E. 2008. Size exclusion limits and lateral heterogeneity of the stomatal foliar uptake pathway for aqueous solutes and water-suspended nanoparticles. Physiologia plantarum, 134: 151–160.

El-Abeid, S.E., Ahmed, Y., Daròs, J.A. and Mohamed, M.A. 2020. Reduced graphene oxide nanosheet-decorated copper oxide nanoparticles: A potent antifungal nanocomposite against fusarium root rot and wilt diseases of tomato and pepper plants. Nanomaterials 10: 1001.

El-Batal, A.I., El-Sayyad, G.S., Mosallam, F.M. and Fathy, R.M. 2020. *Penicillium chrysogenum*-mediated mycogenic synthesis of copper oxide nanoparticles using gamma rays for in vitro antimicrobial activity against some plant pathogens. J. Clust. Sci. 31: 79–90.

El-Moneim, D.A., Dawood, M.F., Moursi, Y.S., Farghaly, A.A., Afifi, M. and Sallam, A. 2021. Positive and negative effects of nanoparticles on agricultural crops. Nanotechnol. Environ. Eng. 6: 1–11.

El-Shetehy, M., Moradi, A., Maceroni, M., Reinhardt, D., Petri-Fink, A., Rothen-Rutishauser, B. and Schwab, F. 2021. Silica nanoparticles enhance disease resistance in *Arabidopsis plants*. Nature Nanotechnol. 16: 344–353.

Fan, X., Xu, J., Lavoie, M., Peijnenburg, W.J.G.M., Zhu, Y., Lu, T. and Qian, H. 2018. Multiwall carbon nanotubes modulate paraquat toxicity in *Arabidopsis thaliana*. Environ. Poll. 233: 633–641.

Fen, L.B., Rashid, A.H.A., Nordin, N.I., Hossain, M.M., Uddin, S.M.K., Johan, M.R. and Thangadurai, D. 2022. Applications of nanomaterials in agriculture and their safety aspect. pp. 243–299. In Biogenic Nanomaterials, Apple Academic Press.

Ghafari, J., Moghadasi, N. and Shekaftik, S.O. 2020. Oxidative stress induced by occupational exposure to nanomaterials: a systematic review. Industrial Health 58: 492–502.

Greenshields, M.W., Cunha, B.B., Coville, N.J., Pimentel, I.C., Zawadneak, M.A., Dobrovolski, S. and Hümmelgen, I.A. 2016. Fungi active microbial metabolism detection of *Rhizopus* sp. and *Aspergillus* sp. section nigri on strawberry using a set of chemical sensors based on carbon nanostructures. Chemosensors 4: 19.

Haggag, W.M. and Eid, M.M. 2022. Antifungal and antioxidant activities of Ag@ FeO-NPs@ Chitosan preparation by endophyte *Streptomyces aureofaciens* Int. J. Agric. Technol. 18: 535–548.

Hasaneen, M.N.A.G., Abdel-Aziz, H.M.M. and Omer, A.M. 2016. Effect of foliar application of engineered nanomaterials: carbon nanotubes NPK and chitosan nanoparticles NPK fertilizer on the growth of French bean plant. Biochem. Biotechnol. Res. 4: 68–76.

Hasanuzzaman, M., Bhuyan, M.B., Anee, T.I., Parvin, K., Nahar, K., Mahmud, J.A. and Fujita, M. 2019. Regulation of ascorbate-glutathione pathway in mitigating oxidative damage in plants under abiotic stress. Antioxidants 8: 384.

Hatami, M., Hadian, J. and Ghorbanpour, M. 2017. Mechanisms underlying toxicity and stimulatory role of single-walled carbon nanotubes in *Hyoscyamus niger* during drought stress simulated by polyethylene glycol. J. Hazard. Mater. 324: 306–320.

Hernandez-Viezcas, J.A., Castillo-Michel, H., Andrews, J.C., Cotte, M., Rico, C., Peralta-Videa, J.R. and Gardea-Torresdey, J.L. 2013. *In situ* synchrotron X-ray fluorescence mapping and speciation of CeO_2 and ZnO nanoparticles in soil cultivated soybean (*Glycine max*). ACS Nano 7: 1415–1423.

Hong, J., Rico, C.M., Zhao, L., Adeleye, A.S., Keller, A.A., Peralta-Videa, J.R. and Gardea-Torresdey, J.L. 2015. Toxic effects of copper-based nanoparticles or compounds to lettuce (*Lactuca sativa*) and alfalfa (*Medicago sativa*). Environ. Sci.: Process. Impacts 17: 177–185.

Hossain, M.A., Piyatida, P., da Silva, J.A.T. and Fujita, M. 2012. Molecular mechanism of heavy metal toxicity and tolerance in plants: central role of glutathione in detoxification of reactive oxygen species and methylglyoxal and in heavy metal chelation. J. Botany 2012: 872875.

Hossain, Z., Mustafa, G., Sakata, K. and Komatsu, S. 2016. Insights into the proteomic response of soybean towards Al_2O_3, ZnO, and Ag nanoparticles stress. J. Hazard. Mater. 304: 291–305.

Hu, T., Li, H., Li, J., Zhao, G., Wu, W., Liu, L. and Guo, Y. 2018. Absorption and bio-transformation of selenium nanoparticles by wheat seedlings (*Triticum aestivum* L.). Front. Plant Sci. 9: 597.

Irshad, M.A., Nawaz, R., Rehman, M.Z., Imran, M., Ahmad, J., Ahmad, S. and Ali, S. 2020. Synthesis and characterization of titanium dioxide nanoparticles by chemical and green methods and their antifungal activities against wheat rust. Chemosphere 258: 127352.

Jafari, A. and Hatami, M. 2022. Foliar-applied nanoscale zero-valent iron (nZVI) and iron oxide (Fe_3O_4) induce differential responses in growth, physiology, antioxidative defense and biochemical indices in *Leonurus cardiaca* L. Environ. Res. 215: 114254.

Jha, S. and Pudake, R.N. 2016. Molecular mechanism of plant–nanoparticle interactions. Plant Nanotechnol. 155–181.

Ke, M., Qu, Q., Peijnenburg, W.J.G.M., Li, X., Zhang, M., Zhang, Z. and Qian, H. 2018. Phytotoxic effects of silver nanoparticles and silver ions to *Arabidopsis thaliana* as revealed by analysis of molecular responses and of metabolic pathways. Sci. Total Environ. 644: 1070–1079.

Keller, A.A., Huang, Y. and Nelson, J. 2018. Detection of nanoparticles in edible plant tissues exposed to nano-copper using single-particle ICP-MS. J. Nanopart. Res. 20: 1–13.

Khan, A.U., Khan, M., Khan, A.A., Parveen, A., Ansari, S. and Alam, M. 2022. Effect of phyto-assisted synthesis of magnesium oxide nanoparticles (MgO-NPs) on bacteria and the root-knot nematode. Bioinorg. Chem. Appl. 2022: 3973841.

Khan, M., Khan, A.U., Bogdanchikova, N. and Garibo, D. 2021. Antibacterial and antifungal studies of biosynthesized silver nanoparticles against plant parasitic nematode *Meloidogyne incognita*, plant pathogens *Ralstonia solanacearum* and *Fusarium oxysporum*. Molecules 26: 2462.

Komatsu, S., Murata, K., Yakeishi, S., Shimada, K., Yamaguchi, H., Hitachi, K. and Fukuda, R. 2022. Morphological and proteomic analyses of soybean seedling interaction mechanism affected by fiber crosslinked with zinc-oxide nanoparticles. Int. J. Mol. Sci. 23: 7415.

Larue, C., Castillo-Michel, H., Sobanska, S., Cécillon, L., Bureau, S., Barthès, V. and Sarret, G. 2014. Foliar exposure of the crop *Lactuca sativa* to silver nanoparticles: evidence for internalization and changes in Ag speciation. J. Hazard. Mater. 264: 98–106.

Lei, R., Wu, P., Li, L., Huang, Q., Wang, J., Zhang, D. and Wang, X. 2021. Ultrasensitive isothermal detection of a plant pathogen by using a gold nanoparticle-enhanced microcantilever sensor. Sens. Actuators B: Chem. 338: 129874.

Li, H., Ye, X., Guo, X., Geng, Z. and Wang, G. 2016. Effects of surface ligands on the uptake and transport of gold nanoparticles in rice and tomato. J. Hazard. Mater. 314: 188–196.

Li, Z., Yu, T., Paul, R., Fan, J., Yang, Y. and Wei, Q. 2020. Agricultural nanodiagnostics for plant diseases: recent advances and challenges. Nanoscale Advances 2: 3083–3094.

Lin, D. and Xing, B. 2008. Root uptake and phytotoxicity of ZnO nanoparticles. Environ. Sci. Technol. 42: 5580–5585.

Lin, S., Reppert, J., Hu, Q., Hudson, J.S., Reid, M.L., Ratnikova, T.A. and Ke, P.C. 2009. Uptake, translocation, and transmission of carbon nanomaterials in rice plants. Small 5: 1128–1132.

Lipșa, F.D., Ursu, E.L., Ursu, C., Ulea, E. and Cazacu, A. 2020. Evaluation of the antifungal activity of gold–chitosan and carbon nanoparticles on *Fusarium oxysporum.* Agronomy 10: 1143.

Liu, J., Dhungana, B. and Cobb, G.P. 2018. Environmental behavior, potential phytotoxicity, and accumulation of copper oxide nanoparticles and arsenic in rice plants. Environ. Toxicol. Chem. 37: 11–20.

Liu, J., Wolfe, K. and Cobb, G.P. 2019a. Exposure to copper oxide nanoparticles and arsenic causes intergenerational effects on Rice (*Oryza sativa* japonica Koshihikari) seed germination and seedling growth. Environmental Toxicology and Chemistry 38: 1978–1987.

Liu, J., Wolfe, K., Potter, P.M. and Cobb, G.P. 2019b. Distribution and speciation of copper and arsenic in rice plants (*Oryza sativa* japonica 'Koshihikari') treated with copper oxide nanoparticles and arsenic during a life cycle. Environ. Sci. Technol. 53: 4988–4996.

Liu, Y., Kornig, C., Qi, B., Schmutzler, O., Staufer, T., Sanchez-Cano, C. and Parak, W.J. 2022. Size- and ligand-dependent transport of nanoparticles in *Matricaria chamomilla* as demonstrated by mass spectroscopy and X-ray fluorescence imaging. ACS Nano 16: 12941–12951.

Lv, J., Christie, P. and Zhang, S. 2019. Uptake, translocation, and transformation of metal-based nanoparticles in plants: recent advances and methodological challenges. Environmental Science: Nano 6: 41–59.

Lyu, L., Wang, H., Liu, R., Xing, W., Li, J., Man, Y.B. and Wu, F. 2022. Size-dependent transformation, uptake, and transportation of SeNPs in a wheat–soil system. J. Hazard. Mater. 424: 127323.

Ma, C., White, J.C., Dhankher, O.P. and Xing, B. 2015. Metal-based nanotoxicity and detoxification pathways in higher plants. Environ. Sci. Technol. 49: 7109–7122.

Ma, Y., He, X., Zhang, P., Zhang, Z., Guo, Z., Tai, R. and Chai, Z. 2011. Phytotoxicity and biotransformation of La_2O_3 nanoparticles in a terrestrial plant cucumber (*Cucumis sativus*). Nanotoxicology 5: 743–753.

Ma, Y., He, X., Zhang, P., Zhang, Z., Ding, Y., Zhang, J. and Yang, K. 2017. Xylem and phloem based transport of CeO_2 nanoparticles in hydroponic cucumber plants. Environ. Sci. Technol. 51: 5215–5221.

Marciano, A., Chefetz, B. and Gedanken, A. 2008. Differential adsorption of silver nanoparticles to the inner and outer surfaces of the agave americana cuticle. J. Phys. Chem. C 112: 18082–18086.

Marmiroli, M., Marmiroli, N. and Pagano, L. 2022. Nanomaterials Induced Genotoxicity in Plant: Methods and Strategies. Nanomaterials 12: 1658.

Medina-Velo, I.A., Zuverza-Mena, N., Tamez, C., Ye, Y., Hernandez-Viezcas, J.A., White, J.C. and Gardea-Torresdey, J.L. 2018. Minimal transgenerational effect of ZnO nanomaterials on the physiology and nutrient profile of *Phaseolus vulgaris*. ACS Sustain. Chem. Eng. 6: 7924–7930.

Milewska-Hendel, A., Sala, K., Gepfert, W. and Kurczyńska, E. 2021. Gold nanoparticles-induced modifications in cell wall composition in barley roots. Cells 10: 1965.

Miralles, P., Church, T.L. and Harris, A.T. 2012. Toxicity, uptake, and translocation of engineered nanomaterials in vascular plants. Environ. Sci. Technol. 46: 9224–9239.

Molnár, Á., Rónavári, A., Bélteky, P., Szőllősi, R., Valyon, E., Oláh, D. and Kolbert, Z. 2020. ZnO nanoparticles induce cell wall remodeling and modify ROS/RNS signalling in roots of *Brassica* seedlings. Ecotoxicol. Environ. Saf. 206: 111158.

Montes, A., Bisson, M.A., Gardella Jr, J.A. and Aga, D.S. 2017. Uptake and transformations of engineered nanomaterials: critical responses observed in terrestrial plants and the model plant *Arabidopsis thaliana*. Sci. Total Environ. 607: 1497–1516.

Mosa, K.A., El-Naggar, M., Ramamoorthy, K., Alawadhi, H., Elnaggar, A., Wartanian, S. and Hani, H. 2018. Copper nanoparticles induced genotoxicty, oxidative stress, and changes in superoxide dismutase (SOD) gene expression in cucumber (*Cucumis sativus*) plants. Front. Plant Sci. 9: 872.

Noori, A., Ngo, A., Gutierrez, P., Theberge, S. and White, J.C. 2020. Silver nanoparticle detection and accumulation in tomato (*Lycopersicon esculentum*). J. Nanopart. Res. 22: 1–16.

Oh, J.W., Chun, S.C. and Chandrasekaran, M. 2019. Preparation and *in vitro* characterization of chitosan nanoparticles and their broad-spectrum antifungal action compared to antibacterial activities against phytopathogens of tomato. Agronomy 9: 21.

Palocci, C., Valletta, A., Chronopoulou, L., Donati, L., Bramosanti, M., Brasili, E. and Pasqua, G. 2017. Endocytic pathways involved in PLGA nanoparticle uptake by grapevine cells and role of cell wall and membrane in size selection. Plant Cell Rep. 36: 1917–1928.

Parsons, J.G., Lopez, M.L., Gonzalez, C.M., Peralta-Videa, J.R. and Gardea-Torresdey, J.L. 2010. Toxicity and biotransformation of uncoated and coated nickel hydroxide nanoparticles on mesquite plants. Environ. Toxicol. Chem. 29: 1146–1154.

Peharec Štefanić, P., Jarnević, M., Cvjetko, P., Biba, R., Šikić, S., Tkalec, M. and Balen, B. 2019. Comparative proteomic study of phytotoxic effects of silver nanoparticles and silver ions on tobacco plants. Environ. Sci. Pollut. Res. 26: 22529–22550.

Pérez-de-Luque, A. 2017. Interaction of nanomaterials with plants: what do we need for real applications in agriculture? Front. Environ. Sci. 5: 12.

Pham, N.D., Duong, M.M., Le, M.V. and Hoang, H.A. 2019. Preparation and characterization of antifungal colloidal copper nanoparticles and their antifungal activity against *Fusarium oxysporum* and *Phytophthora capsici.* Comptes Rendus Chimie, 22: 786–793.

Qian, H., Peng, X., Han, X., Ren, J., Sun, L. and Fu, Z. 2013. Comparison of the toxicity of silver nanoparticles and silver ions on the growth of terrestrial plant model *Arabidopsis thaliana*. J. Environ. Sci. 25: 1947–1956.

Rahmani, N., Radjabian, T. and Soltani, B.M. 2020. Impacts of foliar exposure to multi-walled carbon nanotubes on physiological and molecular traits of *Salvia verticillata* L., as a medicinal plant. Plant Physiol. Biochem. 150: 27–38.

Rahmat, N., Yusof, N.A., Isha, A., Mui-Yun, W., Hushiarian, R. and Akanbi, F.S. 2020. Detection of stress induced by ganoderma boninense infection in oil palm leaves using reduced graphene oxide and zinc oxide nanoparticles screen-printed carbon electrode. IEEE Sensors Journal 20: 13253–13261.

Rajput, V.D., Minkina, T., Sushkova, S., Chokheli, V. and Soldatov, M. 2019. Toxicity assessment of metal oxide nanoparticles on terrestrial plants. Compr. Anal. Chem. 87: 189–207.

Rico, C.M., Wagner, D., Abolade, O., Lottes, B. and Coates, K. 2020. Metabolomics of wheat grains generationally-exposed to cerium oxide nanoparticles. Sci. Total Environ. 712: 136487.

Rifna, E.J., Ramanan, K.R. and Mahendran, R. 2019. Emerging technology applications for improving seed germination. Trends Food Sci. Technol. 86: 95–108.

Ruttkay-Nedecky, B., Krystofova, O., Nejdl, L. and Adam, V. 2017. Nanoparticles based on essential metals and their phytotoxicity. J. Nanobiotechnol. 15: 1–19.

Sabo-Attwood, T., Unrine, J.M., Stone, J.W., Murphy, C.J., Ghoshroy, S., Blom, D. and Newman, L.A. 2012. Uptake, distribution and toxicity of gold nanoparticles in tobacco (*Nicotiana xanthi*) seedlings. Nanotoxicology 6: 353–360.

Salehi, H., Chehregani Rad, A., Raza, A. and Chen, J.T. 2021. Foliar application of CeO_2 nanoparticles alters generative components fitness and seed productivity in Bean crop (*Phaseolus vulgaris* L.). Nanomaterials 11: 862.

Sathiyabama, M. and Muthukumar, S. 2020. Chitosan guar nanoparticle preparation and its *in vitro* antimicrobial activity towards phytopathogens of rice. Int. J. Biol. Macromol. 153: 297–304.

Sellappan, L., Manoharan, S., Sanmugam, A. and Anh, N.T. 2022. Role of nanobiosensors and biosensors for plant virus detection. pp. 493–506. In Nanosensors for Smart Agriculture Elsevier.

Shende, S., Bhagat, R., Raut, R., Rai, M. and Gade, A. 2021. Myco-fabrication of copper nanoparticles and its effect on crop pathogenic fungi. IEEE Trans. Nanobioscience 20: 146–153.

Shojaei, T.R., Salleh, M.A.M., Sijam, K., Rahim, R.A., Mohsenifar, A., Safarnejad, R. and Tabatabaei, M. 2016. Fluorometric immunoassay for detecting the plant virus *Citrus tristeza* using carbon nanoparticles acting as quenchers and antibodies labeled with CdTe quantum dots. Microchimica Acta 183: 2277–2287.

Siddiqi, K.S. and Husen, A. 2016. Engineered gold nanoparticles and plant adaptation potential. Nanoscale Res. Lett. 11: 1–10.

Singh, D. and Kumar, A. 2018. Investigating long-term effect of nanoparticles on growth of Raphanus sativus plants: a trans-generational study. Ecotoxicology 27: 23–31.

Spielman-Sun, E., Avellan, A., Bland, G.D., Clement, E.T., Tappero, R.V., Acerbo, A.S. and Lowry, G.V. 2020. Protein coating composition targets nanoparticles to leaf stomata and trichomes. Nanoscale 12: 3630–3636.

Srivastava, A. and Rao, D.P. 2014. Enhancement of seed germination and plant growth of wheat, maize, peanut and garlic using multiwalled carbon nanotubes. European Chemical Bulletin 3: 502–504.

Syu, Y.Y., Hung, J.H., Chen, J.C. and Chuang, H.W. 2014. Impacts of size and shape of silver nanoparticles on *Arabidopsis* plant growth and gene expression. Plant Physiol. Biochem. 83: 57–64.

Tahir, M.A., Bajwa, S.Z., Mansoor, S., Briddon, R.W., Khan, W.S., Scheffler, B.E. and Amin, I. 2018. Evaluation of carbon nanotube-based copper nanoparticle composite for the efficient detection of agroviruses. J. Hazard. Mater. 346: 27–35.

Taylor, A.F., Rylott, E.L., Anderson, C.W. and Bruce, N.C. 2014. Investigating the toxicity, uptake, nanoparticle formation and genetic response of plants to gold. PLOS One 9: e93793.

Thiruvengadam, M., Gurunathan, S. and Chung, I.M. 2015. Physiological, metabolic, and transcriptional effects of biologically-synthesized silver nanoparticles in turnip (*Brassica rapa* ssp. *rapa* L.). Protoplasma 252: 1031–1046.

Thwala, M., Klaine, S. and Musee, N. 2021. Exposure media and nanoparticle size influence on the fate, bioaccumulation, and toxicity of silver nanoparticles to higher plant salvinia minima. Molecules 26: 2305.

Tran, T.T., Clark, K., Ma, W. and Mulchandani, A. 2020. Detection of a secreted protein biomarker for citrus Huanglongbing using a single-walled carbon nanotubes-based chemiresistive biosensor. Biosens. Bioelectron. 147: 111766.

Vannini, C., Domingo, G., Onelli, E., De Mattia, F., Bruni, I., Marsoni, M. and Bracale, M. 2014. Phytotoxic and genotoxic effects of silver nanoparticles exposure on germinating wheat seedlings. J. Plant Physiol. 171: 1142–1148.

Vanti, G.L., Masaphy, S., Kurjogi, M., Chakrasali, S. and Nargund, V.B. 2020. Synthesis and application of chitosan-copper nanoparticles on damping off causing plant pathogenic fungi. Int. J. Biol. Macromol. 156: 1387–1395.

Villagarcia, H., Dervishi, E., de Silva, K., Biris, A.S. and Khodakovskaya, M.V. 2012. Surface chemistry of carbon nanotubes impacts the growth and expression of water channel protein in tomato plants. Small 8: 2328–2334.

Wang, H., Ramnani, P., Pham, T., Villarreal, C.C., Yu, X., Liu, G. and Mulchandani, A. 2019. Gas biosensor arrays based on single-stranded DNA-functionalized single-walled carbon nanotubes for the detection of volatile organic compound biomarkers released by huanglongbing disease-infected citrus trees. Sensors 19: 4795.

Wang, Q., Ebbs, S.D., Chen, Y. and Ma, X. 2013. Trans-generational impact of cerium oxide nanoparticles on tomato plants. Metallomics 5: 753–759.

Wang, Z., Xie, X., Zhao, J., Liu, X., Feng, W., White, J.C. and Xing, B. 2012. Xylem-and phloem-based transport of CuO nanoparticles in maize (*Zea mays* L.). Environ. Sci. Technol. 46: 4434–4441.

Win, T.T., Khan, S. and Fu, P. 2020. Fungus-(*Alternaria* sp.) mediated silver nanoparticles synthesis, characterization, and screening of antifungal activity against some phytopathogens. J. Nanotechnol. 2020: 8828878.

Xia, B., Dong, C., Zhang, W., Lu, Y., Chen, J. and Shi, J. 2013. Highly efficient uptake of ultrafine mesoporous silica nanoparticles with excellent biocompatibility by *Liriodendron* hybrid suspension cells. Sci. China Life Sci. 56: 82–89.

Yadav, N., Chhillar, A.K. and Rana, J.S. 2020. Detection of pathogenic bacteria with special emphasis to biosensors integrated with AuNPs. Sensors Int. 1: 100028.

Yang, Z., Deng, C., Wu, Y., Dai, Z., Tang, Q., Cheng, C. and Yan, A. 2021. Insights into the mechanism of multi-walled carbon nanotubes phytotoxicity in *Arabidopsis* through transcriptome and m6A methylome analysis. Sci. Total Environ. 787: 147510.

Ye, Y., Cota-Ruiz, K., Cantu, J.M., Valdes, C. and Gardea-Torresdey, J.L. 2021. Engineered nanomaterials' fate assessment in biological matrices: recent milestones in electron microscopy. ACS Sustain. Chem. Eng. 9: 4341–4356.

Youssef, M.S. and Elamawi, R.M. 2020. Evaluation of phytotoxicity, cytotoxicity, and genotoxicity of ZnO nanoparticles in *Vicia faba*. Environ. Sci. Pollut. Res. 27: 18972–18984.

Yusefi-Tanha, E., Fallah, S., Rostamnejadi, A. and Pokhrel, L.R. 2020. Particle size and concentration dependent toxicity of copper oxide nanoparticles (CuONPs) on seed yield and antioxidant defense system in soil grown soybean (*Glycine max* cv. Kowsar). Sci. Total Environ. 715: 136994.

Zhan, F., Wang, T., Iradukunda, L. and Zhan, J. 2018. A gold nanoparticle-based lateral flow biosensor for sensitive visual detection of the potato late blight pathogen, *Phytophthora infestans.* Anal. Chim. Acta 1036: 153–161.

Zhang, D., Hua, T., Xiao, F., Chen, C., Gersberg, R.M., Liu, Y. and Tan, S.K. 2015. Phytotoxicity and bioaccumulation of ZnO nanoparticles in *Schoenoplectus tabernaemontani.* Chemosphere 120: 211–219.

Zhang, P., Xie, C., Ma, Y., He, X., Zhang, Z., Ding, Y. and Zhang, J. 2017. Shape-dependent transformation and translocation of ceria nanoparticles in cucumber plants. Environ. Sci. Technol. Lett. 4: 380–385.

Zhang, P., Ma, Y., Xie, C., Guo, Z., He, X., Valsami-Jones, E. and Zhang, Z. 2019. Plant species-dependent transformation and translocation of ceria nanoparticles. Environ. Sci. Nano 6: 60–67.

Zhang, P., Guo, Z., Luo, W., Monikh, F.A., Xie, C., Valsami-Jones, E. and Zhang, Z. 2020. Graphene oxide-induced pH alteration, iron overload, and subsequent oxidative damage in rice (*Oryza sativa* L.): A new mechanism of nanomaterial phytotoxicity. Environ. Sci. Technol. 54: 3181–3190.

Zhang, P., Wu, X., Guo, Z., Yang, X., Hu, X. and Lynch, I. 2021. Stress response and nutrient homeostasis in lettuce (*Lactuca sativa*) exposed to graphene quantum dots are modulated by particle surface functionalization. Adv. Biol. 5: 2000778.

Zhao, J., Ren, W., Dai, Y., Liu, L., Wang, Z., Yu, X. and Xing, B. 2017a. Uptake, distribution, and transformation of CuO NPs in a floating plant *Eichhornia crassipes* and related stomatal responses. Environ. Sci. Technol. 51: 7686–7695.

Zhao, L., Huang, Y., Adeleye, A.S. and Keller, A.A. 2017b. Metabolomics reveals Cu $(OH)_2$ nanopesticide-activated anti-oxidative pathways and decreased beneficial antioxidants in spinach leaves. Environ. Sci. Technol. 51: 10184–10194.

Zhao, L., Huang, Y., Hu, J., Zhou, H., Adeleye, A.S. and Keller, A.A. 2016. 1H NMR and GC-MS based metabolomics reveal defense and detoxification mechanism of cucumber plant under nano-Cu stress. Environ. Sci. Technol. 50: 2000–2010.

Zhu, Y., Cai, X., Li, J., Zhong, Z., Huang, Q. and Fan, C. 2014. Synchrotron-based X-ray microscopic studies for bioeffects of nanomaterials. Nanomedicine: Nanotechnol. Biol. Med. 10: 515–524.

Zhu, Z.J., Wang, H., Yan, B., Zheng, H., Jiang, Y., Miranda, O.R. and Vachet, R.W. 2012. Effect of surface charge on the uptake and distribution of gold nanoparticles in four plant species. Environ. Sci. Technol. 46: 12391–12398.

Zong, X., Wu, D., Zhang, J., Tong, X., Yin, Y., Sun, Y. and Guo, H. 2022. Size-dependent biological effect of copper oxide nanoparticles exposure on cucumber (*Cucumis sativus*). Environ. Sci. Technol. Poll. Res. 1–10.

frontiers | Frontiers in Microbiology

TYPE Original Research
PUBLISHED 20 February 2023
DOI 10.3389/fmicb.2023.1125685

P3

OPEN ACCESS

EDITED BY
Amr Fouda,
Al-Azhar University,
Egypt

REVIEWED BY
Salem S. Salem,
Al-Azhar University,
Egypt
Samy Selim,
Al Jouf University,
Saudi Arabia

*CORRESPONDENCE
Joanna Trzcińska-Wencel
✉ trzcinska@doktorant.umk.pl
Magdalena Wypij
✉ mwypij@umk.pl

SPECIALTY SECTION
This article was submitted to Microbiotechnology, a section of the journal Frontiers in Microbiology

RECEIVED 16 December 2022
ACCEPTED 30 January 2023
PUBLISHED 20 February 2023

CITATION
Trzcińska-Wencel J, Wypij M, Rai M and Golińska P (2023) Biogenic nanosilver bearing antimicrobial and antibiofilm activities and its potential for application in agriculture and industry.
Front. Microbiol. 14:1125685.
doi: 10.3389/fmicb.2023.1125685

Biogenic nanosilver bearing antimicrobial and antibiofilm activities and its potential for application in agriculture and industry

Joanna Trzcińska-Wencel[1]*, Magdalena Wypij[1]*, Mahendra Rai[1,2] and Patrycja Golińska[1]

[1]Department of Microbiology, Nicolaus Copernicus University in Toruń, Toruń, Poland, [2]Nanobiotechnology Laboratory, Department of Biotechnology, SGB Amravati University, Amravati, Maharashtra, India

Introduction: Due to the increasing resistance of bacteria and fungi to antimicrobials, it is necessary to search for effective alternatives to prevent and treat pathogens causing diseases in humans, animals, and plants. In this context, the mycosynthesized silver nanoparticles (AgNPs) are considered as a potential tool to combat such pathogenic microorganisms.

Methods: AgNPs were synthesized from *Fusarium culmorum* strain JTW1 and characterized by Transmission Electron Microscopy (TEM), X-ray diffraction (XRD), Fourier Transform Infrared (FTIR) spectroscopy, Nanoparticle Tracking Analysis (NTA), Dynamic Light Scattering (DLS) and Zeta potential measurement. The minimum inhibitory (MIC) and biocidal concentrations (MBC) were determined against 13 bacterial strains. Moreover, the combined effect of AgNPs with antibiotics (streptomycin, kanamycin, ampicillin, tetracycline) was also studied by determining the Fractional Inhibitory Concentration (FIC) index. The anti-biofilm activity was examined by crystal violet and fluorescein diacetate (FDA) assays. Furthermore, antifungal activity of AgNPs was evaluated against a panel of phytopathogenic fungi *viz.*, *Botrytis*, *Colletotrichum*, *Fusarium*, *Phoma*, *Sclerotinia*, and an oomycete pathogen *Phytophthora* by agar well-diffusion and micro-broth dilution method to evaluate the minimal AgNPs concentrations that inhibit fungal spore germination.

Results: Fungi-mediated synthesis resulted in the formation of small (15.56±9.22nm), spherical and stable (zeta potential of – 38.43 mV) AgNPs with good crystallinity. The results of FTIR spectroscopy indicated the presence of various functional groups, namely hydroxyl, amino, and carboxyl ones, from the biomolecules on the surface of AgNPs. The AgNPs showed antimicrobial and antibiofilm formation activities against Gram-positive and Gram-negative bacteria. The values of MIC and MBC ranged between 16–64 and 32–512 μgmL^{-1}, respectively. The enhanced effect of AgNPs in combination with antibiotics was confirmed against human pathogens. The highest synergistic effect (FIC=0.0625) was demonstrated by the combination of AgNPs with streptomycin against two strains of *Escherichia coli* (ATCC 25922 and ATCC 8739), followed by *Klebsiella pneumoniae* and *Pseudomonas aeruginosa* (FIC=0.125). Enhanced effects of AgNPs with ampicillin were also shown against *Staphylococcus aureus* ATCC 25923 (FIC=0.125) and *P. aeruginosa* (FIC=0.25), as well as kanamycin against *S. aureus* ATCC 6538 (FIC=0.25). The crystal violet assay revealed that the lowest

concentration of AgNPs (0.125 μgmL^{-1}) reduced the development of biofilms of *Listeria monocytogenes* and *Salmonella enterica*, while the maximum resistance was shown by *Salmonella infantis*, its biofilm was reduced after exposure to a concentration of 512 μgmL^{-1}. A high inhibitory effect on the activity of bacterial hydrolases was observed by the FDA assay. AgNPs at a concentration of 0.125μgmL^{-1} reduced the hydrolytic activity of all biofilms formed by the tested pathogens, except *E. coli* ATCC 25922, *P. aeruginosa*, and *Pectobacterium carotovorum* (efficient concentration was 2-fold higher, at 0.25 μgmL^{-1}), while the hydrolytic activity of *E. coli* ATCC 8739, *Salmonella infantis* and *S. aureus* ATCC 6538 was suppressed after treatment with AgNPs at concentrations of 0.5, 2 and 8 μgmL^{-1}, respectively. Moreover, AgNPs inhibited fungal growth and spore germination of *Botrytis cinerea*, *Phoma lingam,* and *Sclerotinia sclerotiorum*. MIC and MFC values of AgNPs against spores of these fungal strains were determined at 64, 256, and 32 μgmL^{-1}, and zones of growth inhibition were 4.93, 9.54, and 3.41 mm, respectively.

Discussion: *Fusarium culmorum* strain JTW1 was found to be an eco-friendly biological system for an easy, efficient and inexpensive synthesis of AgNPs. In our study, the mycosynthesised AgNPs demonstrated remarkable antimicrobial (antibacterial and antifungal) and antibiofilm activities against a wide range of human and plant pathogenic bacteria and fungi singly and in combination with antibiotics. These AgNPs could be applied in medicine, agriculture, and food industry to control such pathogens that cause numerous human diseases and crop losses. However, before using them extensive animal studies are required to evaluate the toxicity, if any.

KEYWORDS

AgNPs, biofilm, food-borne pathogens, human pathogens, mycosynthesis, plant pathogens

1. Introduction

Modern medicine, veterinary, food, and agriculture sectors are struggling with microbial diseases due to the increasing resistance of microorganisms to available antimicrobials agents (Food and Agriculture Organization of the United Nations (FAO), 2017; Xie et al., 2018; Hashempour-Baltork et al., 2019). Antibiotic resistance results from the excessive and reckless use of antibiotics in agricultural food production, healthcare, and environmental protection sectors (Xie et al., 2018; Caniça et al., 2019; Dadgostar, 2019; Larsson and Flach, 2022). A wide range of pathogenic bacteria cause chronic infections by forming complex multicellular structures known as biofilms. Moreover, some studies indicate that conventional antibiotics may induce phenotypic changes in bacterial cells which subsequently trigger biofilm formation (Olivares et al., 2020). Biofilms provide a stable protective environment for the dissemination of microorganisms due to a self-synthesized structure which is an organic and highly hydrated matrix composed of exopolysaccharides, proteins, and nucleic acids (Hall-Stoodley and Stoodley, 2005; Olivares et al., 2020). There are several hypotheses of biofilm recalcitrant to antibiotics, including persistent cells, adaptive responses, and lower penetration of antimicrobial agents (Sahoo et al., 2021). In response to the growing threat of bacterial pathogens, it is necessary to develop approaches that are wide-ranging and effective in controlling bacterial outbreaks. An alternative to conventional chemicals is the formulation of agents that may prevent biofilm formation and also act on individual bacterial cells.

The growing population and increasing demand for food, require solutions to increase crop yields and ensure safety in food production, distribution, and storage (Fung et al., 2018; Wypij et al., 2023). Nowadays, microbial diseases of plants are becoming an increasing problem as they reduce crop yields and significantly affect the food industry on both a global and regional scale (Charkowski, 2018; Charkowski et al., 2020). Among the most notable bacterial pathogens of plants are *Pseudomonas syringae*, *Ralstonia solanacearum, Agrobacterium tumefaciens, Xanthomonas* spp., *Erwinia amylovora,* and *Pectobacterium carotovorum* (Mansfield et al., 2012; Iwu and Okoh, 2019). The bacterial diseases of crop plants including black rot (Schaad et al., 1980; Maji and Nath, 2015), soft rot (Pérombelon and Kelman, 1980; Pérombelon, 2002), bacterial speck (Shenge et al., 2007; Butsenko et al., 2020), and fire blight (Johnson and Stockwell, 1998; Vanneste, 2000; Peil et al., 2021). While, fungal pathogens, for example, *Fusarium oxysporum, Botrytis cinerea, Colletotrichum acutatum, Puccinia* sp., *Sclerotinia sclerotiorum,* etc., have a broad host range and cause pre-and post-harvest diseases. Among them, causal agents of grey and white mold as well as black leg and dry rot are worthy of note (Amselem et al., 2011; Dean et al., 2012; Gabal et al., 2019). Plant pathogens spread rapidly and are increasingly aggressive and harmful leading to yield losses in cereals (maize, wheat, rice), vegetables (potatoes, tomatoes, brassicas), and fruits (Sundin et al., 2016; Nawaz et al., 2020; Hampf et al., 2021). Indeed, foodborne illnesses caused by bacteria, are another concern with ensuring human food security (Gandhi and Chikindas, 2007; Scallan Walter et al., 2021).

Bacterial pathogens such as *Listeria* sp., or the the members of *Enterobacteriaceae* family are proliferated *via* the fecal-oral routes by ingestion of contaminated water or food. Virulent strains of these bacteria cause a broad-spectrum of disorders like nausea, watery or bloody diarrhea, vomiting, and inflammatory changes (Allocati et al., 2013). Thus, intracellular pathogen *Listeria monocytogenes* is responsible for listeriosis, a very severe and deadly illness (Chlebicz and Śliżewska, 2018). Symptoms of the infection in healthy adult patients may include lack of appetite, stomachache, nausea, or diarrhea. Nonetheless, the infection is particularly dangerous for newborns, the elderly, immunocompromised patients, and poses a risk of miscarriage for pregnant women (Zhu et al., 2017).

Silver nanoparticles (AgNPs) have pronounced antimicrobial activity, even at low concentrations (Salleh et al., 2020). Some studies indicate, that AgNPs reveal long-term antibiofilm activities by multi-site action due to their unique properties, which include nano-size and high surface area (Martinez-Gutierrez et al., 2013; Ali et al., 2015; Soliman et al., 2022). Basically, biological methods of nanoparticle synthesis have been recognized as a substitute for physical and chemical ones (Rai et al., 2021b; Al-Rajhi et al., 2022). In addition, biologically synthesized AgNPs are capped with molecules of natural origin, which enables them to interact easily with bactericides along with bacterial cells and therefore, improves their antimicrobial efficiency (Wypij et al., 2020). Among the biological synthesis methods of nanoparticles (NPs) are those mediated by plants, algae, bacteria or fungi (Wypij et al., 2021; Al-Rajhi et al., 2022; Salem et al., 2022, 2023). Among microorganisms, fungi reveal the strong potential to secrete metabolites involved in the synthesis of metallic nanoparticles (MNPs) (Rai et al., 2021a; Shaheen et al., 2021). Mycosynthesis is an environmentally friendly, inexpensive, and simple method, which can be used for the efficient production of AgNPs (Lahiri et al., 2021; Salem et al., 2023). Current research efforts focus on the optimization of mycosynthesis of AgNPs with desired physio-chemical and biological properties, which may be used to eradicate bacterial pathogens (Zhao et al., 2018).

Hence, the present study was designed to synthesize AgNPs from *Fusarium culmorum* strain JTW1 in an easy, eco-friendly, efficient, and inexpensive way and to estimate the potential use of AgNPs in the biomedicine, agriculture, and food production industry. The mycosynthesized AgNPs were characterized using UV–vis spectrophotometry (UV–Vis), Transmission Electron Microscopy (TEM), X-ray diffraction (XRD) spectroscopy, Energy-dispersive X-ray spectroscopy (EDX), Fourier-Transform Infrared Spectroscopy (FTIR), Nanoparticle Tracking Analysis (NTA), Dynamic Light Scattering (DLS) and Zeta potential measurement. The comprehensive antibacterial activity of AgNPs, including estimation of minimal inhibitory and biocidal concentrations (MIC and MBC, respectively), efficacy of combined antibiotics and AgNPs as well as antibiofilm activity against a wide range of Gram-positive and Gram-negative pathogenic bacteria of humans and plants were investigated. Mycosynthesized AgNPs were tested against a set of fungal and oomycete plant pathogens, including *Alternaria alternata* IOR 1783, *Botrytis cinerea* IOR 1873, *Colletotrichum acutatum* IOR 2153, *Fusarium oxysporum* IOR 342, *Fusarium solani* IOR 825, *Phoma lingam* IOR 2284, *Sclerotinia sclerotiorum* IOR 2242, *Phytophthora cactorum* IOR 1925, *Phytophthora cryptogea* IOR 2080, *Phytophthora megasperma* IOR 404 and *Phytophthora plurivora* IOR 2303.

2. Materials and methods

2.1. Isolation and identification

Fusarium culmorum strain JTW1 was isolated using ten-fold dilution procedure on Potato Dextrose Agar (PDA, A&A Biotechnology) from soil samples collected in Różankowo near Toruń, Poland. The Petri plates were incubated at 26°C for 7 days. Initially, the morphological and cultural characteristics of isolate *F. culmorum* strain JTW1 were studied after 7 days at 26°C on PDA. The isolate was identified by internal transcribed spacer (ITS) sequence. The genomic DNA of the isolate was extracted using Genomic Mini AX Yeast Spin Kit (A&A Biotechnology) according to the manufacturer's instructions by A&A Biotechnology (Gdańsk, Poland) while amplification of ITS region and sequencing were carried out by Genomed S.A. (Warsaw, Poland). The ITS region of the ribosomal DNA of the isolate was amplified using the ITS1 and ITS2 primers (White et al., 1990). The Basic Local Alignment Search Tool (BLAST) at the National Centre of Biological Information (NCBI) was used to find the closest similarity between the isolate sequence and corresponding sequences available in the database. *F. culmorum* isolate JTW1 was deposited in the Deutsche Sammlung von Mikroorganismen und Zellkulturen (DSMZ) in Brunschweig, Germany under accession number DSM 114849.

2.2. Synthesis and characterization of mycosynthesized nanoparticles

Fusarium culmorum strain JTW1 was cultured in 250 ml Potato Dextrose Broth (PDB, A&A Biotechnology) for 7 days at 26°C in shaking conditions (120 revolutions per minute; rpm) and then the biomass was centrifugated at 6,500×*g* (Thermo Scientific, USA), washed three times with sterile distilled water, and re-suspended in sterile water for 4 days for cell autolysis. Thereafter, the cell filtrate was obtained by centrifugation of autolysate at 4000×*g* for 5 min and passing it through sterile Whatman filter paper No. 1. For mycosynthesis of AgNPs, the fungal extract obtained from *F. culmorum* strain JTW1 was treated with a 100 mM aqueous solution of silver nitrate ($AgNO_3$; 1 mM final concentration). A biosynthesis reaction was induced on sunlight for 1 h and then the reaction mixture was incubated at room temperature in the dark. AgNPs were collected by centrifugation at 13,000×*g* (Thermo Scientific, USA) for 1 h and dried at 37°C (Thermo Scientific, USA; Wypij et al., 2022).

The physico-chemical analyses were performed as previously described by Wypij et al. (2018, 2022).

The primary detection of AgNPs was carried out by visual observation of color change after treatment of fungal extract with $AgNO_3$ and sunlight induction. The UV–Visible (UV–Vis) spectrophotometer (NanoDrop 2000, Thermo Scientific, USA) was used for scanning the absorbance spectra in a range of wavelengths from 200 to 800 nm, at the resolution of 1 nm.

Transmission Electron Microscopy (TEM) and Energy Dispersive X-Ray (EDX) analyses were performed to determine the size, morphology, and elemental composition of AgNPs from *F. culmorum* strain JTW1. Prior to analysis, AgNPs solution was deposited on a carbon-coated copper grid (400 µm mesh size) and dried at room temperature. Analysis was performed using a transmission electron

microscope (FEI Tecnai F20 X-Twintool, Fei, Hillsboro, OR, USA) operating at an acceleration voltage of 100 kV.

The crystalline nature of AgNPs was confirmed by X-ray diffraction analysis using Philips X'Pert diffractometer (X'Pert Pro, Analytical Philips, Lelyweg, Netherlands) equipped with Cu Kα ($\lambda = 1.54056$ Å) radiation source and using Ni as a filter in range 5°–120°. The collected peaks were compared to the standard database of the International Centre for Diffraction Data (ICDD).

The functional groups present on the surface of AgNPs were identified using Fourier-Transform Infrared (FTIR) spectroscopy. Briefly, a sample for analysis was prepared by combining dry AgNPs with KBr powder in a ratio of 1:100. The AgNPs were characterized by FTIR spectrophotometer (Perkin-Elmer FTIR-2000, USA) in the range 400–4,000 cm^{-1} at a resolution of 4 cm^{-1}.

The size of synthesized nanoparticles was measured using Nanosight (NanoSight NS300, Malvern, UK). The solution of AgNPs in MilliQ water was sonicated at 20 Hz for 15 min (Sonic Ruptor 250, Omni Int., Kennesaw, GA, USA), 1000-fold diluted with the MilliQ water, and filtered through a 0.22-µm filter (Millipore) prior to analysis. During measurement, five 1-min videos were captured at the cell temperature of 25°C and syringe speed of 50 µl/s. The size distribution of AgNPs was analyzed using NanoSight Software NTA version 3.4 Build 3.4.4.

To determine the size distribution and zeta potential of AgNPs the Zetasizer Nano Instrument (Malvern Instruments Ltd., Malvern, United Kingdom) was used. The AgNPs size and dispersity were measured by dynamic light scattering (DLS) to obtain information about volume [%] as a function of particle size [nm]. Zeta potential measurement and nanoparticle size distribution analysis were carried out on AgNPs sample suspended in MilliQ water, sonicated for 15 min at 20 Hz (Sonic Ruptor 250, Omni Int., Kennesaw, GA, USA) to obtain a homogenous suspension, 1000-fold diluted, and filtered through a 0.22 µm Millipore filter prior to analyses. Zetasizer software was used to analyze the data of AgNPs sample.

2.3. Evaluation of antibacterial activity of AgNPs and antibiotics

2.3.1. Bacterial strains

The antibacterial activity of mycosynthesized AgNPs and antibiotics was evaluated against Gram-negative bacterial strains, namely *Escherichia coli* ATCC 25922, *E. coli* ATCC 8739, *Klebsiella pneumoniae* ATCC 700603, *Pseudomonas aeruginosa* ATCC 10145, *Salmonella enterica* PCM 2565, *Salmonella infantis* (strain from Sanitary-Epidemiology Station in Toruń, Poland), *Agrobacterium tumefaciens* IOR 911, *Pectobacterium carotovorum* PCM 2056, *Pseudomonas syringae* IOR 2188 and *Xanthomonas campestris* IOR 512 and Gram-positive bacteria including *Staphylococcus aureus* ATCC 6538, *S. aureus* ATCC 25923 and *Listeria monocytogenes* PCM 2191.

2.3.2. Minimum inhibitory concentration and minimum biocidal concentration determination for AgNPs and antibiotics

The micro-dilution method was used for estimation of the minimum inhibitory concentration (MIC) of antibiotics and AgNPs according to the Clinical Laboratory Standards Institute standard [Clinical and Laboratory Standards Institute (CLSI), 2012]. Briefly, to estimate the MIC of AgNPs and antibiotics, bacteria were grown in Tryptic Soy Broth (TSB, Becton Dickinson) for 24 h at 37°C and 28°C for human and phytopathogens, respectively. Then, the density of bacterial suspension in sterile distilled water was established at 0.5 McFarland unit (approx. 1.5×10^8 colony forming units per mL; CFU mL^{-1}) and ten-fold dilution. Antimicrobials were tested, in triplicate, using sterile 96-well plates (Nest) in the concentration range 0.125–2048 for AgNPs and 0.016–2048 µg mL^{-1} for antibiotics. The TSB medium was used as a diluent for AgNPs and growth medium. The final volume and bacterial concentration in each well were 150 µl and 1.5×10^5 CFU mL^{-1}, respectively. Inoculated plates were incubated for 24 h at 37 or 28°C, respectively. The MIC value of AgNPs and antibiotics was defined as the lowest concentration of the antimicrobial agent showing no visible bacterial growth after incubation time. To determine the minimum biocidal concentration (MBC) of AgNPs and antibiotics, samples from all wells without visible bacterial growth were spread onto Trypticase Soy Agar (TSA, Becton Dickinson) in Petri plates and incubated for 24 h at 37 or 28°C, respectively. The MBC values were read as the lowest concentration of antimicrobial agent that inhibited bacterial growth ≥99.9% (Wypij et al., 2021).

2.3.3. Fractional inhibitory concentration index determination

This assay was performed, in triplicate, using sterile 96-well plates (Nest) and TSB medium for bacterial growth. Combined antimicrobial agents (AgNPs and antibiotic) were tested in the concentration range from 1/32 to 2x MIC. The final concentration of bacteria in each well was as for the MIC assay described above. The combined antibacterial effect of AgNPs and antibiotics, as FIC index, was calculated using the formula:

$$\text{FIC index} = \frac{\text{MIC}\left(\begin{array}{c}\text{°AgNPs in}\\ \text{combination}\\ \text{with antibiotic}\end{array}\right)}{\text{MIC}\left(\text{AgNPs alone}\right)} + \frac{\text{MIC}\left(\begin{array}{c}\text{°AgNPs in}\\ \text{combination}\\ \text{with antibiotic}\end{array}\right)}{\text{MIC}\left(\text{antibiotic alone}\right)}$$

Values of the FIC index were interpreted as follows: >2.0 denote antagonistic activity, from 0.5 to 2.0 signify an additive effect, while values <0.5 specify a synergistic effect of antimicrobials (Ruden et al., 2009).

2.4. Antibiofilm activity of AgNPs

2.4.1. Inhibition of biofilm formation

The ability to biofilm formation by tested bacteria in presence of AgNPs was evaluated, in triplicate, in 96-well flat-bottom plates using crystal violet staining assay (Feoktistova et al., 2016). Each well contained 150 µl of TSB, desired concentration of AgNPs in the range 0.125–512 µg mL^{-1} (2-fold dilutions of AgNPs were maintained from 0.125 to 512 µg mL^{-1}), and tested bacteria (final concentration approx. 1.5×10^5 CFU mL^{-1}). The plates were incubated for 24 h at 37 or 28°C, respectively. The positive (inoculated TSB without nanoparticles) and negative (sterile TSB) controls as well as background (nanoparticles in TSB) were maintained during the test. After incubation, the suspension was gently removed and wells were washed with sterile

distilled water to eliminate planktonic cells. Adherent cells were fixed by drying at room temperature for 1 h and stained with 1% water solution of crystal violet (BTL) for 15 min. Crystal violet was removed and biofilm was washed thrice with sterile distilled water. The aliquots (200 µl) of 99.9% ethanol (Avantor) were added to each well to release absorbed crystal violet from biofilm and absorbance at the wavelength of 595 nm was read using a plate reader (SpectraMax iD3 Multi-Mode Microplate Reader, Molecular Devices, USA). The data were averaged, and the standard deviation was also calculated. Results are presented as percent of biofilm formation in the presence of AgNPs compared to control and calculated using the following formula:

$$\text{Biofilm formation}\,[\%] = \frac{A_{595}\ \text{after AgNPs treatment}}{A_{595}\text{without AgNPs treatment}} \times 100\%$$

2.4.2. Evaluation of hydrolytic activity of biofilm

Hydrolytic activity of biofilms developed in presence of different concentrations (mentioned above) of AgNPs from *F. culmorum* strain JTW1 were assessed using fluoresceine diacetate (FDA; Sigma-Aldrich) assay (Peeters et al., 2008). Bacterial biofilm was developed in the presence of AgNPs in sterile 96-well flat bottom plates dedicated for fluorescence assays (Thermo Fisher Scientific, USA), as described above. The positive and negative controls as well as background samples were also maintained. Plates were incubated as described previously. After incubation, the suspension was gently removed and wells were washed thrice with 3-(Morpholin-4-yl)propane-1-sulfonic acid (MOPS) buffer (Sigma-Aldrich), pH 7. Subsequently, working solution (0.02%, w/v) of FDA in acetone was prepared, which was then diluted 1:100 (v/v) with MOPS buffer. The aliquots (200 µl) of the FDA solution in MOPS were added to each well and plates were incubated for 4 h at 37°C or 28°C, respectively in the darkness. Fluorescence measurements were performed using plate reader (SpectraMax iD3 Multi-Mode Microplate Reader, Molecular Devices, USA) at an excitation wavelength 494 nm and an emission wavelength 518 nm. Results were shown as percence of released fluorescein compared to the control sample which is directly proportional to the activity of hydrolases produced by developed biofilms. Hydrolytic activity was calculated using the following formula:

$$\text{Hydrolytic activity}\,[\%] = \frac{\text{Fluorescence after AgNPs treatment}}{\text{Fluorescence without AgNPs treatment}} \times 100\%$$

2.5. Antifungal activity

2.5.1. Antifungal assay using agar-well diffusion method

Preliminary screening assay was performed to estimate inhibitory effect of AgNPs against 12 phytopathohenic fungi, namely *Alternaria alternata* IOR 1783 (isolated from kohlrabi), *Botrytis cinerea* IOR 1873 (isolated from tomato), *Colletotrichum acutatum* IOR 2153 (isolated from blueberry), *Fusarium oxysporum* IOR 342 (isolated from pine), *Fusarium solani* IOR 825 (isolated from parsley), *Phoma lingam* IOR 2284 (isolated from rape), *Sclerotinia sclerotiorum* IOR 2242 (isolated from broccoli), and oomycetes, such as *Phytophthora cactorum* IOR 1925 (isolated from strawberry), *Phytophthora cryptogea* IOR 2080 (isolated from Lawson cypress), *Phytophthora megasperma* IOR 404 (isolated from raspberry), *Phytophthora plurivora* IOR 2303 (isolated from *Quercus petraea*) using agar well-diffusion method (Magaldi et al., 2004), with some modifications. Briefly, fungal colonies grown on potato dextrose agar (PDA, Becton Dickinson) in Petri plates for 14 days at 26°C were washed with 10 ml of sterile distilled water to release fungal spores/sclerotia. Their suspensions were collected and filtered through a sterile cotton wool syringe filter to remove mycelia. The concentration of fungal spores/sclerotia were estimated using cell counting chamber (Brand, Germany) and diluted to adjust concentration of 10^6 spores mL^{-1}. One milliliter of such suspension was added into 6 ml of sterile melted PDA and spread on the surface of sterile medium in Petri plates, as a second layer. Subsequently, the wells (Ø =5 mm) were cut in the inoculated plates using sterile cork borer and filled with 50 µl of AgNPs solution at concentration of 3 mg mL^{-1}. Then, inoculated plates were incubated for 7 days at 26°C and zones of inhibition of fungal growth around wells were measured in mm.

2.5.2. Determination of minimum inhibitory concentration and minimum fungicidal concentration of AgNPs against fungal spores

Two-fold broth microdilution method [Clinical and Laboratory Standards Institute (CLSI), 2012] adopted for fungal spores, in potato dextrose broth (PDB, A&A Biotechnology), was used to evaluate inhibition of spore germination of the fungal strains, namely *Botrytis cinerea* IOR 1873, *Phoma lingam* IOR 2284 and *Sclerotinia sclerotiorum* IOR 2242 that were selected in agar-well diffusion assay described above. Assay was performed, in triplicate, in sterile 96-well plates (Nest). The AgNPs concentration range was 2–2048 µg mL^{-1}. Each well was inoculated with spore/sclerotia suspension (final concentration 10^5 spores mL^{-1}). Negative (sterile broth) and positive (inoculated broth without AgNPs) controls were also maintained. Plates were incubated at 26°C and examined after 7 days for MIC determination. For minimal fungicidal concentration (MFC) the 100 µl from wells without visible fungal growth were spread on the surface of sterile PDA in Petri plates and incubated at 26°C for 7 days.

2.6. Statistical analyses

The data were presented as mean ± standard deviation (SD). For results from antibiofilm assays the differences between means were statistically tested by One-way ANOVA followed by Tukey's test and considered statistically significant if $p < 0.05$. The data were analyzed by Statistica Software (StatSoft Inc., Tulsa, OK, United States).

3. Results

3.1. Isolation and identification

The ITS sequence of isolate JTW1 showed 100% similarity to corresponding sequence of *Fusarium culmorum* isolate F52 (ITS sequence accession number: MH681149). Strain morphology and growth on potato dextrose agar are shown in Supplementary Figure S1.

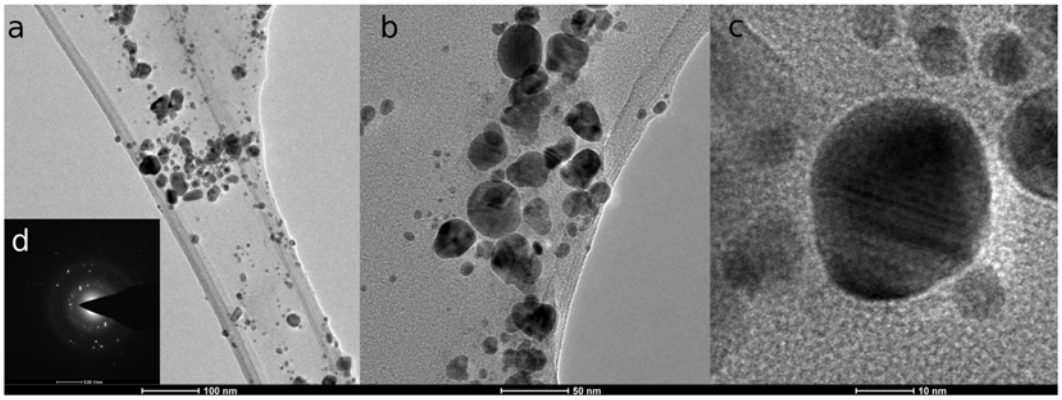

FIGURE 1
TEM micrographs of silver nanoparticles from *F. culmorum* strain JTW1 **(A–C)** and SAED.

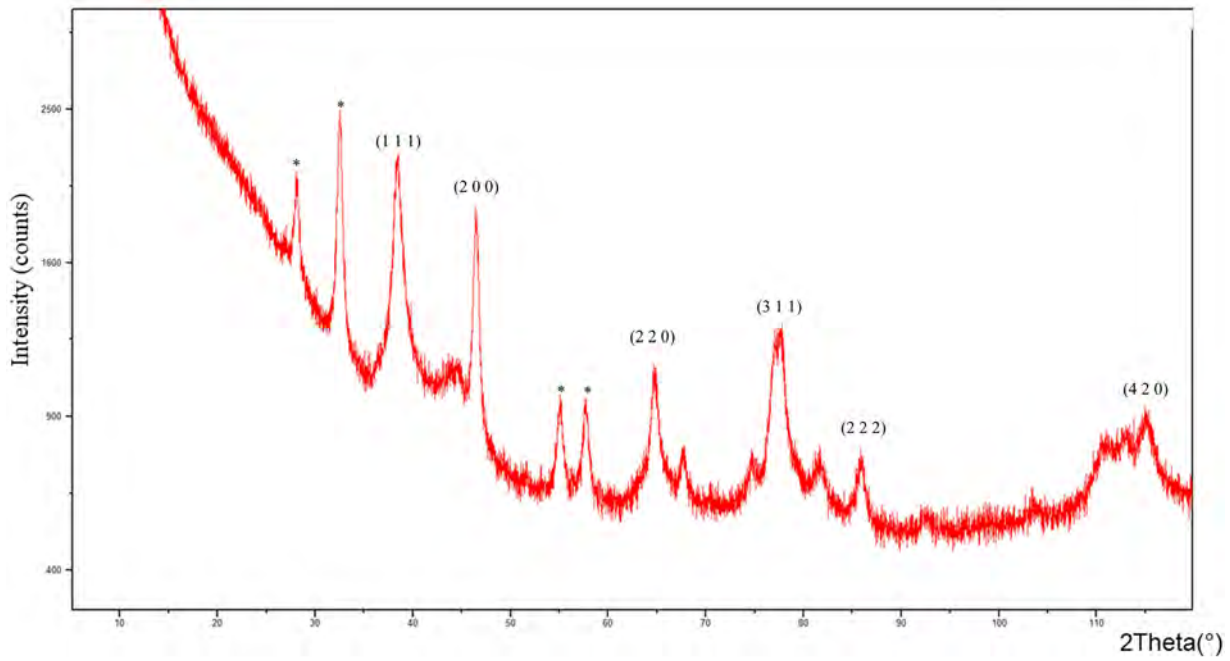

FIGURE 2
X-ray diffraction (XRD) pattern of AgNPs from *F. culmorum* strain JTW1.

3.2. Synthesis and characterization of mycosynthesized silver nanoparticles

The color change of the reaction mixture (cell filtrate with silver nitrate) from yellow to dark-brown indicated the formation of AgNPs. The UV–Vis spectroscopy of AgNPs showed the maximum absorption peak at 430 nm (Supplementary Figure S2) which confirmed reduction of Ag^{+} to Ag^{0} and AgNPs formation.

TEM micrographs (Figure 1) revealed that mycosynthesized AgNPs were polydisperse, spherical, with the size range from 3.58 to 58.63 nm. The average size was determined at 15.56 ± 9.22 nm. Energy dispersive X-ray (EDX) spectrum of AgNPs confirmed the presence of silver metal, as shown in Supplementary Figure S3. The elemental analysis data obtained from EDX displayed a 53.00 W% mass of Ag, followed by 44.49 W% of C, and 2.00 W% of O. The EDX pattern showed silver peaks at 3, 22, and 24 keV.

The XRD patterns of AgNPs showed diffraction peaks at: 38.412°, 46.565°, 64.752°, 77.645°, 85.929° and 115.118° corresponding to (1 1 1), (2 0 0), (2 2 0), (3 1 1) (2 2 2), and (4 2 0) planes of the face-centered cubic (fcc) silver crystal, respectively (Figure 2).

FTIR analyses of AgNPs, shown in Figure 3, revealed peaks at 3448.75, 2923.34, 2852.38, 1632.52, 1384.60, 1352.28 and 1085.60 cm^{-1}.

Particle size distribution provided by NTA is presented in Figure 4. This analysis revealed that average size and concentration of AgNPs were 188.4 nm and 1.46×10^{12} particles mL^{-1}, respectively. The zeta potential analysis demonstrated that nanoparticles were negatively charged (−38.43 mV), as shown in Supplementary Figure S4. The dynamic light scattering (DLS)

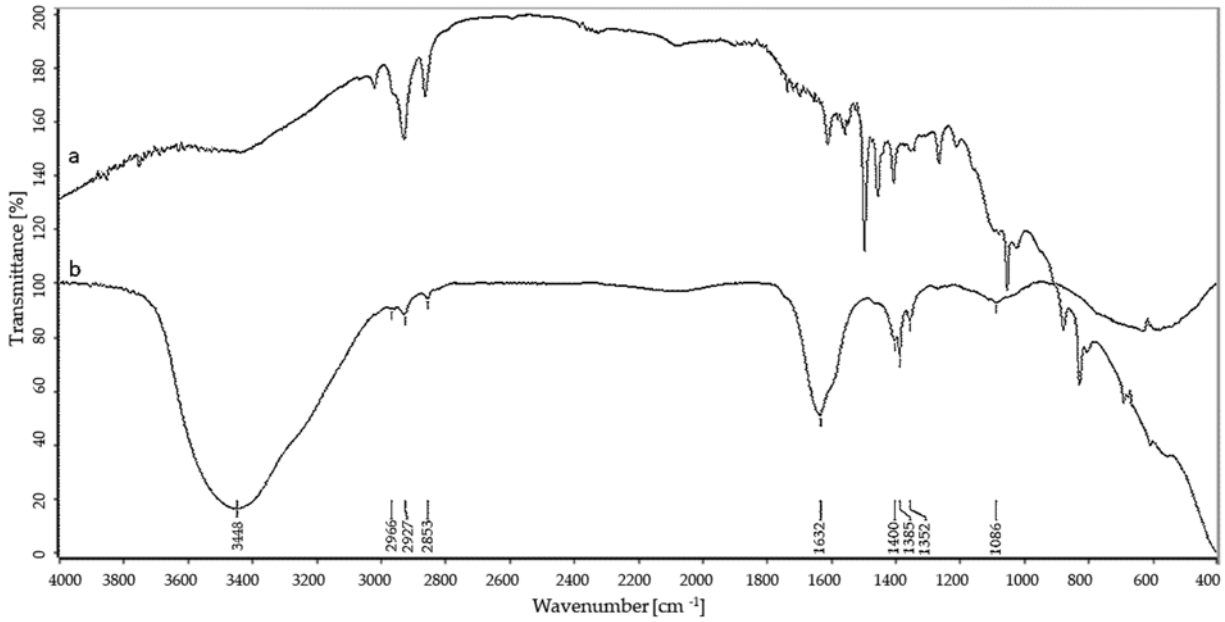

FIGURE 3
FTIR spectra of control (a) and silver nanoparticles (b).

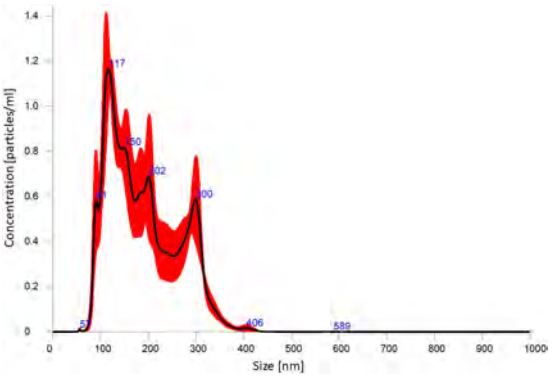

FIGURE 4
Silver nanoparticle size distribution from nanoparticle tracking analysis.

presented that the most frequent were AgNPs with a dimension of 169.9 nm (Supplementary Figure S5).

3.3. Antimicrobial activity

3.3.1. Minimal inhibitory concentration and minimal biocidal concentration of silver nanoparticles against bacterial strains

The MIC and MBC values of the AgNPs are shown in Table 1. AgNPs synthesized from *F. culmorum* strain JTW1 exhibited strong antibacterial activity against Gram-negative and Gram-positive bacteria. The findings presented here indicate that the activities of AgNPs against different pathogenic microbes were dose-dependent. MIC and MBC of AgNPs against human and food-borne pathogens were in the range of 16–64 and 32–512 $\mu g\,mL^{-1}$, respectively.

The AgNPs from *F. culmorum* strain JTW1 showed the maximum antibacterial activity against phytopathogens as follows: *P. syringae* (MIC = 8 $\mu g\,mL^{-1}$ and MBC = 128 $\mu g\,mL^{-1}$), *A. tumefaciens* (MIC = 8 $\mu g\,mL^{-1}$ and MBC = 256 $\mu g\,mL^{-1}$), *X. campestris* (MIC = 32 $\mu g\,mL^{-1}$ and MBC = 64 $\mu g\,mL^{-1}$) and *P. carotovorum* (MIC = 128 $\mu g\,mL^{-1}$ and MBC = 512 $\mu g\,mL^{-1}$).

3.3.2. MICs and MBCs of antibiotics against bacteria

The MIC and MBC values of the antibiotics are shown in Table 2. All microorganisms were sensitive to antibiotics in a dose-dependent manner. Minimum inhibitory concentration (MIC) values ranged from 0.016–16, 4–64, 4–128, and 0.064–2048 $\mu g\,mL^{-1}$ for tetracycline, streptomycin, kanamycin, and ampicillin, respectively. Overall, Gram-negative bacteria showed lower susceptibility to tested antibiotics than Gram-positive ones. *K. pneumoniae* and *P. aeruginosa* strains were most resistant to tested antibiotics. All of the antibiotics were most efficient (MIC and MBC values in the range 0.016–16 $\mu g\,mL^{-1}$) against both *S. aureus* strains. The only exception was tetracycline, for which the MBC was not determined up to the test concentration of 2048 $\mu g\,mL^{-1}$.

3.3.3. Effects of AgNPs combinations with different antibiotics against human pathogens – FIC index determination

The combined effects of AgNPs from *F. culmorum* strain JTW1 and conventional antibiotics against bacterial strains were demonstrated by using a checkboard method and determination of the FIC index (Table 3). Synergistic effects were found for AgNPs and streptomycin against both *E. coli* strains (FIC = 0.0625), *K. pneumoniae* (FIC = 0.125), and *P. aeruginosa* (FIC = 0.125). MIC values of AgNPs and streptomycin, in combination, were decreased 16-fold against

E. coli, and 8-fold against *K. pneumoniae* and *P. aeruginosa* when compared to antimicrobials used separately. The combination of AgNPs with ampicillin significantly enhanced the antibacterial activity of antimicrobials against *S. aureus* ATCC 25923 (FIC index = 0.125) and *P. aeruginosa* (FIC index = 0.25). The implemented dose of AgNPs and ampicillin were 8 and 4 times lower, respectively, than MIC values of antimicrobials used alone. Synergistic effects of AgNPs in combination with kanamycin was observed only against *S. aureus* ATCC 6538 (FIC index = 0.25); concentration of AgNPs and antibiotic were reduced four times. In turn, a combination of AgNPs and tetracycline revealed an additive effect against test bacteria (FIC index values were 0.5 or 1).

3.4. Antibiofilm formation activity of AgNPs

Bacterial biofilm formation was assessed using crystal violet assay while the hydrolytic activity of the formed biofilms was determined by FDA assay (Figures 5-7). Percentages of biofilm formation and hydrolytic activity of biofilms after AgNPs treatment was estimated compared to control samples (without AgNPs). Metabolic activity and formation of biofilms were inhibited by AgNPs at a concentration range of 0.125–512 $\mu g\,mL^{-1}$, in a dose-dependent manner, for all tested microorganisms.

The most effective inhibition of biofilm formation was observed for *Pseudomonas aeruginosa*. In this case, significant inhibition (by 37%) of biofilm formation was found in the presence of 0.25 $\mu g\,mL^{-1}$ AgNPs. The AgNPs at a concentration of 0.5 $\mu g\,mL^{-1}$ inhibited formation of biofilm by *E. coli* ATCC 25922, by nearly 30%, while at concentration of 64 $\mu g\,mL^{-1}$ by >80%. Similarly, AgNPs at concentration of 64 $\mu g\,mL^{-1}$ reduced by >60% formation of biofilm by *E. coli* ATCC 8739. In turn, the biofilm formation by *P. aeruginosa* and *K. pneumoniae* was strongly (by 91%) inhibited after treatment with 16 and 64 $\mu g\,mL^{-1}$ of AgNPs, respectively. The maximum tested concentration (512 $\mu g\,mL^{-1}$) prevented the formation of *S. aureus* ATCC 6538 and *S. aureus* ATCC 25923 biofilms by 50 and 88%, respectively.

AgNPs significantly inhibited the metabolic activity of biofilms formed by strains of *E. coli, K. pneumoniae, P. aeruginosa* and *S. aureus* (Figure 5). Analyses of hydrolases activity in biofilm formed by *P. aeruginosa* in the presence of AgNPs at concentration of 0.25 $\mu g\,mL^{-1}$ showed significant decrease in enzyme activity (by 56.6%) while at concentrations ≥16 $\mu g\,mL^{-1}$ complete inhibition of activity. The latter is in line with the results of biofilm formation which was strongly prevented. The AgNPs concentrations of 32, 64, and 256 $\mu g\,mL^{-1}$ completely inactivated the hydrolytic enzymes of *E. coli* ATCC 8739, *K. pneumoniae,* and *S. aureus* ATCC 25923 biofilms, respectively. The highest tested concentration (512 $\mu g\,mL^{-1}$) of AgNPs clearly reduced (by 97.02%) the hydrolytic activity of *E. coli* ATCC 25922 biofilm. The hydrolytic activity of the *S. aureus* ATCC 6538 biofilm remained high until the AgNPs concentration of 16 $\mu g\,mL^{-1}$, while higher concentrations caused a decrease in enzyme activity ranging from 23 to 11.7% (32–512 $\mu g\,mL^{-1}$).

Metabolic activity of biofilms of *Listeria monocytogenes* and *Salmonella enterica* were notably inhibited with AgNPs at a concentration of 0.125 $\mu g\,mL^{-1}$ while the biofilm formation was completely inhibited after treatment of the bacteria with AgNPs at a concentration of 64 $\mu g\,mL^{-1}$ or higher (Figure 6). Biofilm of *S. infantis* was extensively formed up to a concentration of 256 $\mu g\,mL^{-1}$ of AgNPs and exhibited hydrolytic activity (> 82%) up to AgNPs concentration

TABLE 1 Minimal inhibitory (MIC) and minimal biocidal (MBC) concentration values [μgmL^{-1}] of AgNPs against bacterial strains.

Tested microorganisms	AgNPs	
	MIC	MBC
Escherichia coli ATCC 8739	32	64
Escherichia coli ATCC 25922	32	32
Klebsiella pneumoniae ATCC 700603	64	128
Pseudomonas aeruginosa ATCC 10145	16	32
Staphylococcus aureus ATCC 6538	16	64
Staphylococcus aureus ATCC 25923	16	128
Listeria monocytogenes PCM 2191	64	512
Salmonella enterica PCM 2565	32	32
Salmonella infantis	64	64
Agrobacterium tumefaciens IOR 911	8	256
Pectobacterium carotovorum PCM 2056	128	512
Pseudomonas syringae IOR 2188	8	128
Xanthomonas campestris IOR 512	32	64

TABLE 2 MIC and MBC values [μgmL^{-1}] of antibiotics: streptomycin, kanamycin, ampicillin, and tetracycline against human pathogenic bacteria.

	Ampicillin		Kanamycin		Streptomycin		Tetracycline	
Tested microorganisms	MIC	MIC	MBC	MBC	MIC	MBC	MIC	MBC
Escherichia coli ATCC 8739	4	4	16	16	16	64	0.5	>2048
Escherichia coli ATCC 25922	4	4	16	16	16	16	0.25	0.5
Klebsiella pneumoniae ATCC 700603	2048	>2048	128	>2048	4	4	16	512
Pseudomonas aeruginosa ATCC 10145	512	512	128	128	64	64	8	32
Staphylococcus aureus ATCC 6538	0.064	0.064	4	4	4	4	0.016	>2048
Staphylococcus aureus ATCC 25923	0.064	0.125	4	4	16	16	0.064	>2048
Listeria monocytogenes PCM 2191	0.25	16	4	16	16	128	0.25	64
Salmonella enterica PCM 2565	0.25	0.5	8	8	32	2048	0.25	32
Salmonella infantis	1	2	16	16	32	1,024	0.5	128

TABLE 3 FIC index values of AgNPs in combination with antibiotics: ampicillin (AM), kanamycin (K); streptomycin (S), and tetracycline (TE) against bacteria.

Test microorganisms	FIC index			
	AgNPs+AM	AgNPs+K	AgNPs+S	AgNPs+ TE
Escherichia coli ATCC 8739	1	1	0.0625	1
Escherichia coli ATCC 25922	1	1	0.0652	1
Klebsiella pneumoniae ATCC 700603	1	1	0.125	1
Pseudomonas aeruginosa ATCC 10145	0.25	1	0.125	1
Staphylococcus aureus ATCC 6538	1	0.25	1	1
Staphylococcus aureus ATCC 25923	0.125	1	1	1
Listeria monocytogenes PCM 2191	1	0.5	0.5	0.5
Salmonella enterica PCM 2565	1	0.5	1	0.5
Salmonella infantis	1	0.5	1	0.5

FIC values > 2.0 denote antagonistic activity, from 0.5 to 2.0 signify an additive effect, while values < 0.5 specify a synergistic effect of antimicrobials (Ruden et al., 2009).

of 2 μg mL^{-1}, while higher AgNPs concentrations resulted in enzyme inactivation (Figure 6).

AgNPs significantly inhibited the enzymatic activity of hydrolases and the formation of biofilm by bacterial plant pathogens (Figure 7). Among them, the most susceptible was *A. tumefaciens* which after exposure to the lowest tested concentration (0.125 μg mL^{-1}) of AgNPs caused a decrease in hydrolytic activity to 8% and biofilm formation to 63%. An increase in the dose of AgNPs to 1 μg mL^{-1} completely inhibited hydrolase activity and reduced biofilm formation by 83%. Biofilm formation of *P. syringae, X. campestris,* and *P. carotovorum* was reduced by 80, 73, and 56%, and hydrolytic activity remained below 10% in the presence of 0.5 μg mL^{-1} of AgNPs.

3.5. Antifungal activity

Three out of 11 fungal phytopathogens were susceptible to AgNPs from *F. culmorum* strain JTW1 tested using agar well diffusion method. The highest efficiency was observed against *Botrytis cinerea* IOR 1873, followed by *Phoma lingam* IOR 2284 and *Sclerotinia sclerotiorum* IOR 2242. The zones of growth inhibition were found to be 9.54, 4.93, and 3.41 mm, respectively (Table 4; Supplementary Figure S5). AgNPs exhibited strong inhibitory effects against fungal spore germination (Table 4). MIC and MFC values of AgNPs against spore germination of three tested fungal strains were in the range of 32–256 μg mL^{-1}. Among them, sclerotia of *Sclerotinia sclerotiorum* displayed the highest susceptibility (MIC and MFC at 32 μg mL^{-1}), followed by spores of *Botrytis cinerea* (MIC and MFC at 64 μg mL^{-1}) and *Phoma lingam* (MIC and MFC at 256 μg mL^{-1}).

4. Discussion

We synthesized AgNPs by mycelial extract of *Fusarium culmorum* isolate JTW1 after treatment with 1 mM aqueous solution of silver nitrate, and visually characterized by the color change, from light-yellow to dark-brown. The color change provides evidence of the formation of AgNPs due to the surface plasmon resonance (SPR) exhibited by the synthesized AgNPs (Smitha et al., 2008). Synthesis of myco-AgNPs was confirmed spectroscopically by observation of a characteristic absorbance peak at 430 nm, which is characteristic of AgNPs. According to the literature, the absorption peaks between 380–450 nm are related to the surface plasmon resonance (SPR) of silver nanoparticles (Desai et al., 2012; Mistry et al., 2021). Our UV–Vis results corroborate with those presented by Huang et al. (2018) and Osorio-Echavarría et al. (2021) who showed that AgNPs synthesized from fungi releveled strong peaks at 430 nm.

Mycosynthesized silver nanoparticles are well known for their bioactivities including antimicrobial activity against both Gram-positive and Gram-negative bacteria (Majeed et al., 2018). The bioactivity of AgNPs is highly dependent on the size, shape, stability, and capping molecules of nanoparticles as well as target cells (e.g., bacterial strain; Li et al., 2012). Therefore, comprehensive characterization of the physical and chemical properties of mycosynthesized AgNPs is important for their potential application.

In the present study, various analytical techniques were used to characterize silver nanoparticles, namely TEM, EDX, XRD, FTIR, DLS, NTA, and Zeta potential measurement. TEM analysis showed small (average size 16 nm) and spherical nanoparticles from *F. culmorum*. Similarly, Bawaskar et al. (2010) reported the synthesis of spherical and small (average size 11 nm) AgNPs by *F. culmorum* extract after challenging with 1 mM $AgNO_3$ at ambient temperature. Our results are also in accordance with the findings of Azmath et al. (2016), who reported the fabrication of AgNPs from *Colletotrichum* sp. ALF2-6 with a size ranging from 5 to 60 nm, but with highly variable shapes. However, TEM micrographs showed a clearly smaller size of AgNPs from *F. culmorum* strain JTW1 than NTA and DLS analyses (188.4 and 169.9 nm, respectively) used for further characterization. In the case of the latter analyses the larger size of nanoparticles is due to the presence of capping molecules from fungal extract on the surface of AgNPs (Joshi et al., 2013). Moreover, smaller nanoparticles may not be detected in the DLS technique, as they can be covered by bigger ones (Tomaszewska et al., 2013). In turn, EDX spectrum confirmed elemental composition of AgNPs and the peaks observed at 3, 22, and 24 keV were typical for the absorption of AgNPs due to surface plasmon resonance (Soliman et al., 2022). The X-ray diffraction pattern confirmed the reduction of Ag^+ ions and the formation of AgNPs with a face-centered cubic (fcc) structure. However, several unassigned peaks were also recorded in the XRD analysis. It is suggested that these additional peaks arise due to the crystallization of the bioorganic phase

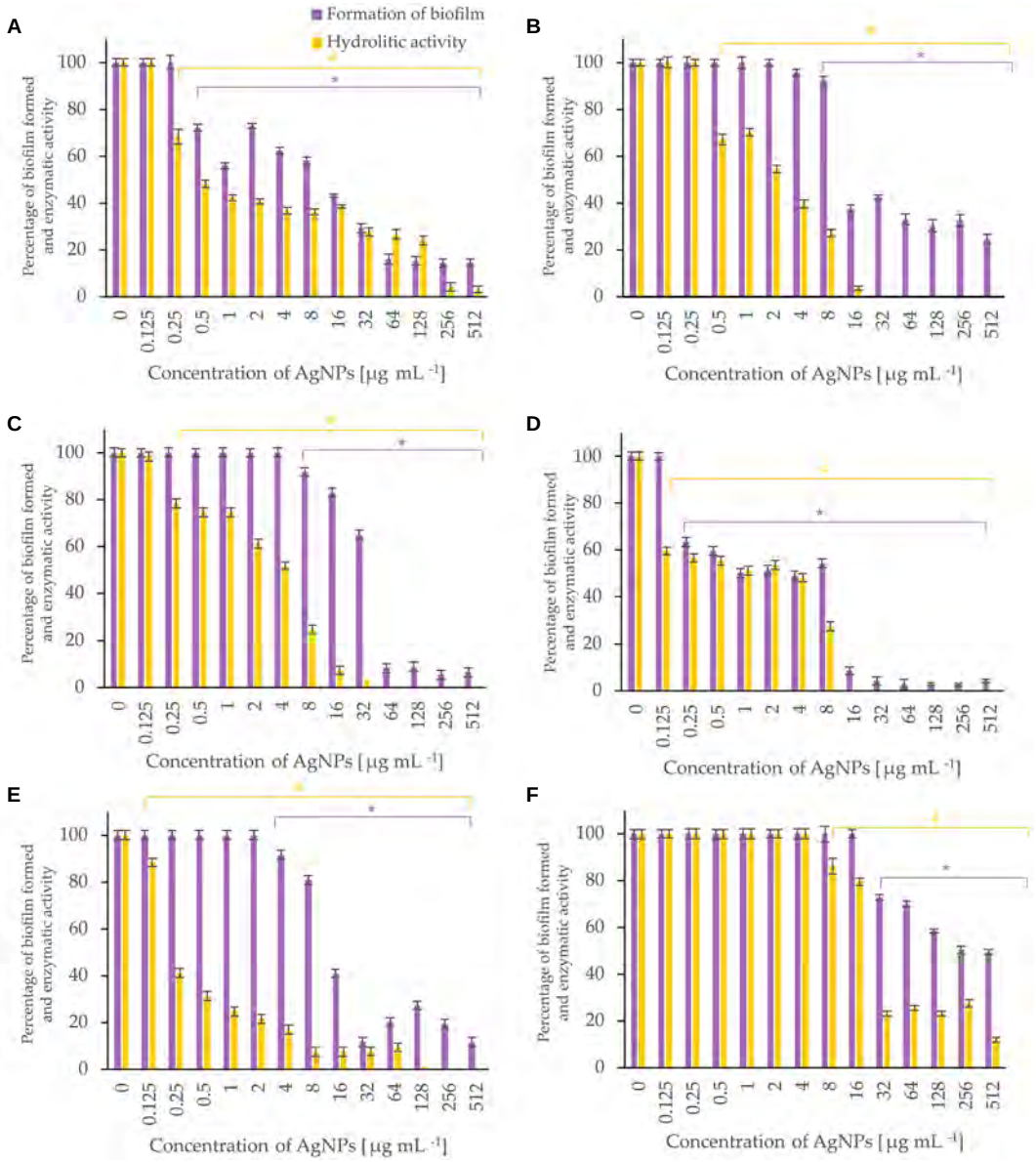

FIGURE 5
Percent of bacterial biofilm formation and hydrolase activity in biofilms after treatment with various concentrations of AgNPs from *F. culmorum* strain JTW1. *E. coli* ATCC 25922 **(A)**, *E. coli* ATCC 8739 **(B)**, *K. pneumoniae* ATCC 700603 **(C)**, *P. aeruginosa* ATCC 10145 **(D)**, *S. aureus* ATCC 25923 **(E)**, *S. aureus* ATCC 6538 **(F)**. The statistical significance (value of $p<0.05$) of tested variants (different concentrations of AgNPs) compared with untreated control were indicated by * and # signs for biofilm formation and hydrolytic activity tests, respectively.

on the surface of the AgNPs (Elumalai et al., 2017; Wypij et al., 2022). The presence of biomolecules on the surface of synthesized AgNPs was confirmed by FT-IR measurements which revealed characteristic peaks. The band recorded at 3448.75 cm^{-1} was assigned to the stretching vibrations of primary and secondary amines and indicated the presence of free OH and NH groups. The peaks at 2923.34 and 2852.38 cm^{-1} showed the presence of CH stretching (Ghaseminezhad et al., 2012; Wypij et al., 2021). A band at 1632.52 cm^{-1} corresponded to the bending vibrations of the amide I and amide II bands of proteins (Elamawi et al., 2018). The bands observed at 1384.60 and 1352.28 cm^{-1} can be assigned to the C–N stretching vibrations of aromatic amines (Jain et al., 2011; Salem, 2022) while the peak at 1085.60 cm^{-1} can be associated with the C–N stretching vibrations of the aliphatic amines (Vigneshwaran et al., 2007). The presence of different functional groups associated with amines, alkanes, and a carboxylic acid, on the surface of AgNPs suggest that various biomolecules from fungal extracts can be involved in nanoparticle formation and stabilization (Ammar and El-Desouky, 2016; Akther et al., 2019). Besides, the biological capping of AgNPs prevent their aggregation and may affect their biological activity, including antimicrobial activity (Hamouda et al., 2019). The high negative value of zeta potential (−38.43 mV) confirmed the repulsion among the particles and indicates their high stability. Elamawi et al. (2018) reported negatively charged (−19.7 mV) and well-dispersed silver nanoparticles synthesized from *Trichoderma longibrachiatum*. However, their zeta potential was much lower suggesting lower stability.

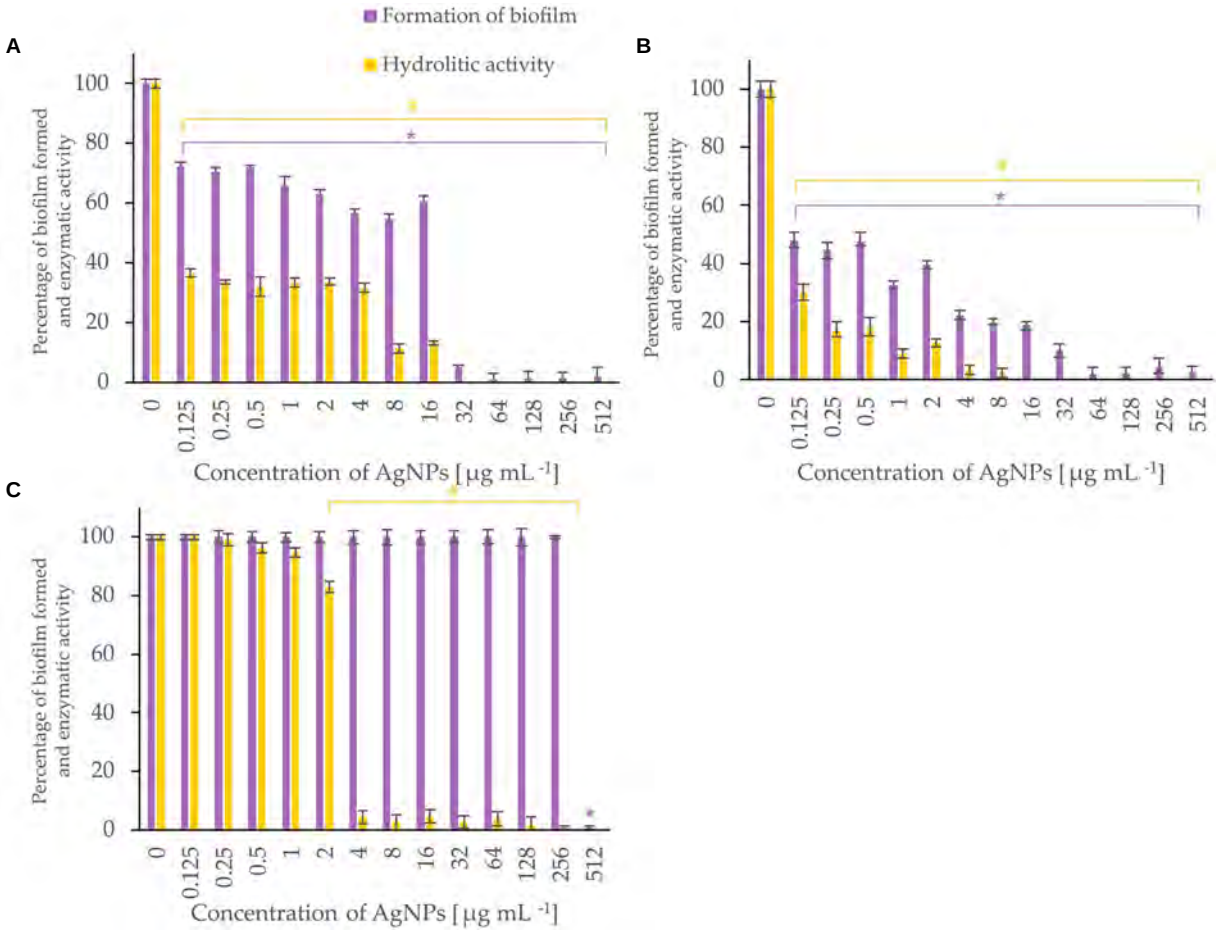

FIGURE 6
Percent of bacterial biofilm formation and hydrolase activity in biofilms after treatment with various concentrations of AgNPs from *F. culmorum* strain JTW1. *Listeria monocytogenes* **(A)**, *Salmonella enterica* **(B)**, *S. infantis* **(C)**. The statistical significance (value of $p<0.05$) of tested variants (different concentrations of AgNPs) compared with untreated control were indicated by * and # signs for biofilm formation and hydrolytic activity tests, respectively.

AgNPs synthesized from *F. culmorum* strain JTW1 demonstrated remarkable antimicrobial activity against human pathogens (*Escherichia coli, Klebsiella pneumoniae, Pseudomonas aeruginosa,* and *Staphylococcus aureus*), food-borne pathogens (*Listeria monocytogenes, Salmonella enterica, Salmonella infantis*) and plant pathogens (*Agrobacterium tumefaciens, Pectobacterium carotovorum, Pseudomonas syringae,* and *Xanthomonas campestris*). Interestingly, among human pathogens, the most sensitive to mycosynthesized AgNPs was *P. aeruginosa*, followed by *E. coli, K. pneumoniae,* and food-borne pathogens, including Gram-positive *L. monocytogenes*. It is particularly significant that AgNPs from *F. culmorum* JTW1 inhibited the growth of members of Gram-negative bacteria that are on the list of multidrug-resistant taxa highlighted by the World Health Organization (WHO) (2021).

AgNPs have been found to be effective in the management of plant diseases caused by bacteria, such as *Xanthomonas oryzae, X. phaseoli, Ralstonia solanacearum, Clavibacter michiganensis* and many more (Tariq et al., 2022). In the present study, *P. carotovorum* was found to be the least sensitive to mycosynthesized AgNPs (MIC and MBC values were 128 and 512 μg mL^{-1}, respectively) when compared to *P. syringae, X. campestris,* and *A. tumefaciens.*

It is suggested that effective action of silver nanoparticles against bacteria may be through the progressive release of lipopolysaccharides and proteins as well as the further formation of irregularly shaped pits at the outer membrane of Gram-negative bacteria (Amro et al., 2000; Fayaz et al., 2010). Salvioni et al. (2017) demonstrated that antimicrobial activity of negatively charged AgNPs depended on the concentration and was associated with their incorporation into the membrane of Gram-negative bacteria (*E. coli*) and penetration into the cells. In addition, intracellular leakage and coagulation of nanoparticles on the bacterial surface were also observed. In turn, treatment of Gram-positive *S. aureus* with AgNPs resulted in the appearance of blisters on the surface of cells and cell lysis (Salvioni et al., 2017). Other studies indicated that AgNPs or released Ag^+ ions after penetration into a cell may generate free radicals (Qing et al., 2018; Tian et al., 2018) and interact with biomolecules and intracellular structures (Li et al., 2010; Adeyemi et al., 2020; Gul et al., 2021). Yuan et al. (2017) reported that AgNPs caused lower lactate dehydrogenase activity (LDH) and decreased levels of adenosine triphosphate (ATP) in *P. aeruginosa* and *S. aureus*. Moreover, ROS generated after AgNPs treatment led to inhibition of metabolic activity and the growth of bacterial cells. It is claimed that due to the different mechanisms of

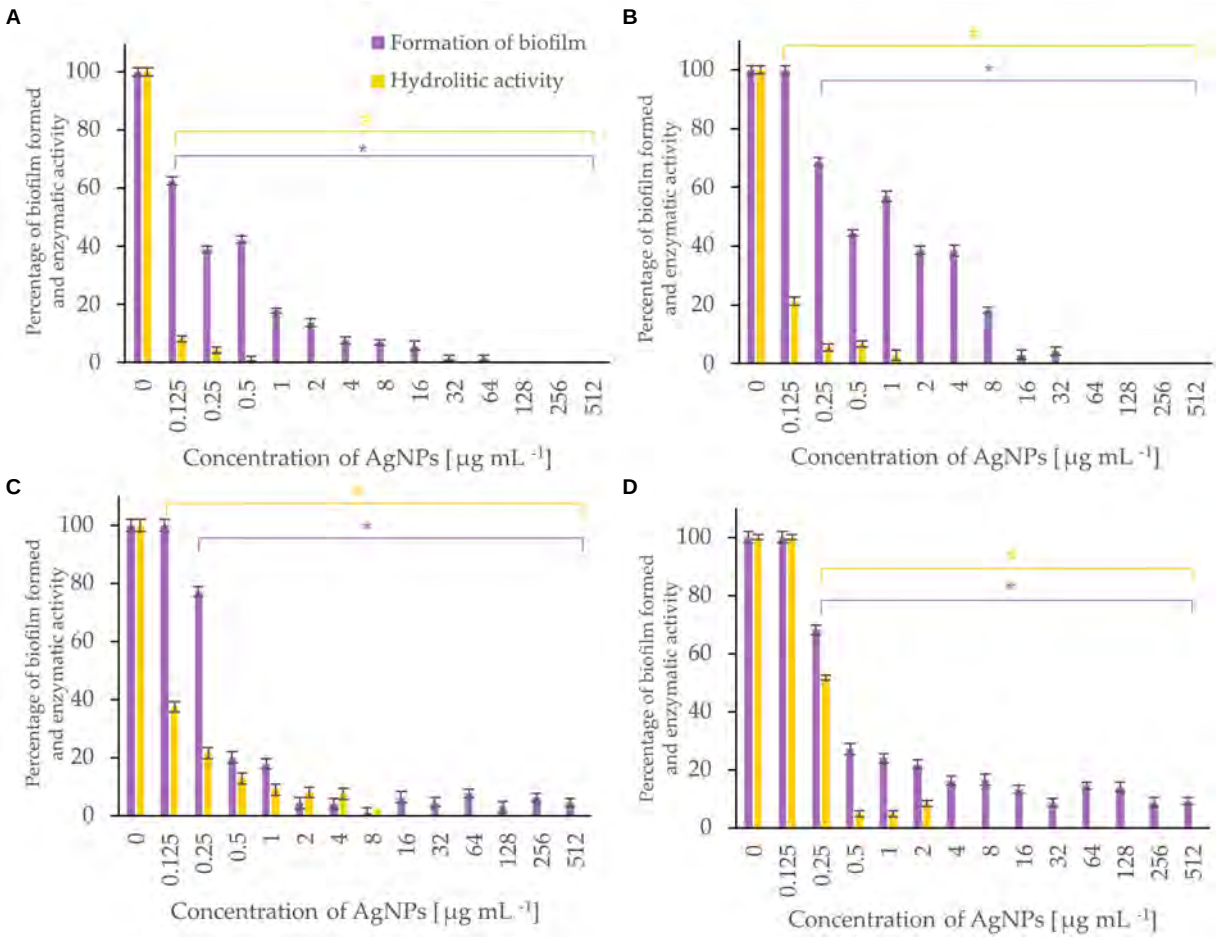

FIGURE 7
Percent of bacterial biofilm formation and hydrolase activity in biofilms after treatment with various concentrations of AgNPs from *F. culmorum* strain JTW1. *A. tumefaciens* **(A)**, *P. carotovorum* **(B)**, *P. syringae* **(C)**, *X. campestris* **(D)**. The statistical significance (value of $p<0.05$) of tested variants (different concentrations of AgNPs) compared with untreated control were indicated by * and # signs for biofilm formation and hydrolytic activity tests, respectively.

TABLE 4 Antifungal activity of AgNPs form *Fusarium culmorum* strain JTW1 against plant pathogens.

Tested strains	Zone of growth inhibition [mm]	MIC [μgmL^{-1}]	MFC [μgmL^{-1}]
Botrytis cinerea IOR 1873	4.93	64	64
Phoma lingam IOR 2284	9.54	256	256
Sclerotinia sclerotiorum IOR 2242	3.41	32	32

AgNPs action, which affect various aspects of bacterial growth and metabolism, the development of microbial resistance to nanoparticles is limited (Wang L. et al., 2017).

In the present study, tested antibiotics demonstrated antibacterial activity against Gram-negative and Gram-positive bacteria which was increased in combination with AgNPs from *F. culmorum* strain JTW1. The enhanced antimicrobial activity against *E. coli*, *K. pneumoniae,* and *P. aeruginosa* was observed for a combination of AgNPs and streptomycin and against *P. aeruginosa* with ampicillin. In the case of *S. aureus,* increased activity of ampicillin and kanamycin was observed when combined with AgNPs. The increased antimicrobial effect may be due to the binding of antibiotics to AgNPs. The molecules of antibiotics react easily with nanoparticles due to many active groups such as hydroxyl and amido groups (Wypij et al., 2022). Hence, AgNPs may be covalently bound to streptomycin due to the presence of four-terminal $-NH_2$ groups in antibiotic structure. In addition, this association might be enhanced by the electrostatic interactions between negatively charged AgNPs and positively charged streptomycin molecules (Wang C. et al., 2017). Moreover, biologically synthesized nanoparticles showed more stable adsorption of ampicillin when compared to chemically synthesized ones due to the presence of an organic layer on their surface, which acts as a stabilizer (Rogowska et al., 2017). It is claimed that AgNPs in combination with antibiotics can promote cell wall disruption and damage, and facilitate the transport of antibiotics into the cell by increasing membrane permeability. Other mechanisms of AgNPs action include inhibition of enzymes responsible for the hydrolysis of antibiotics due to the disruption of their structure and release of Ag^+ ions (Panáček et al., 2016).

Therefore, it is assumed that the combination of AgNPs and antibiotics enhanced their inhibitory activity against pathogenic bacteria. This allows the use of lower doses of antibacterial agents and reduces the risk of resistance to antimicrobial agents (Hemeg, 2017).

AgNPs are reported to hinder the biofilm formation in many bacteria (Markowska et al., 2013; Ansari et al., 2021; Hetta et al., 2021). Crystal violet staining and fluorescein diacetate assay was used for the visualization of adherent biofilm bacteria and measurement of biofilm activity, respectively. Interestingly, AgNPs from *Fusarium culmorum* strain JTW1, at low concentration (0.25 μg mL^{-1}), efficiently inhibited the formation and hydrolytic activity of *P. aeruginosa* biofilm. Similar results were reported by Akther et al. (2020) who studied the efficiency of AgNPs synthesized from *Rhizopus arrhizus* BRS-07 in reducing biofilm formation by *P. aeruginosa* and found that the formation of this structure was inhibited by 7–93% in a dose-dependent manner (5–25 μg mL^{-1}). Furthermore, AgNPs synthesized from *F. culmorum* strain JTW1 at a higher concentration of 64 μg mL^{-1} also efficiently (by 67–96%) reduced the formation of biofilms in *E. coli* strains, *P. aeruginosa,* and *K. pneumoniae.* These nanoparticles were found to be more active against biofilm than those reported by Ramachandran and Sangeetha (2017) which completely inhibited the formation of *Escherichia coli* (ETEC12), *Klebsiella pneumoniae* (SKP7) and *Pseudomonas aeruginosa* (ETPS11) biofilms after treatment with AgNPs at a concentration of 100 μg mL^{-1}. Ansari et al. (2014) found the highest antibiofilm efficiency of commercially available water-soluble AgNPs (5–10 nm) against *Escherichia coli* and *Klebsiella* spp. at the concentration of 50 μg mL^{-1}. The inhibition of biofilm formation by AgNPs is a consequence of bacterial growth arrest, prevention of exopolysaccharide formation (Ansari et al., 2014), and disruption of bacterial quorum sensing signaling (Akther et al., 2020). In our study, although AgNPs at the lower concentrations had no impact on biofilm formation by *E. coli* ATCC 8739, *K. pneumoniae,* and *S. aureus* ATCC 25923, they significantly decreased the activity of hydrolases.

Food-borne pathogens, such as *Listeria monocytogenes* and *Salmonella enterica* are known to form biofilms, which ultimately leads to serious problems in the food industry (Harrell et al., 2021; Muthulakshmi et al., 2022). Our findings confirmed that both the aforementioned bacteria showed sensitivity to mycofabricated AgNPs. However, the development of biofilm in *L. monocytogenes* was more prevented than *S. infantis*. Our results are in line with those reported by Chlumsky et al. (2020) who showed higher activity of AgNPs in reducing biofilm formation and a decrease in metabolic activity against *L. monocytogenes, S. aureus* than *S. infantis* S59. The *in vitro* studies on the AgNPs from *Terminalia catappa* leaf extract against *L. monocytogenes* revealed the inhibition of biofilm formation and reduction in the virulence factors such as protease production, at concentrations of 50 and 100 μg mL^{-1} (Muthulakshmi et al., 2022). Similarly, AgNPs from *F. culmorum* strain JTW1 remarkably prevented biofilm formation ability in bacterial plant pathogens, especially in *A. tumefaciens* and *P. carotovorum.* Moreover, a significant reduction in the hydrolase enzymatic activity of these bacteria was recorded. Recently, Olfati et al. (2021) also reported the inhibitory effect of AgNPs synthesized from *Calendula officinalis* extract against the biofilm formation of *P. carotovorum*. Consequently, the obtained results clearly reveal that mycosynthesized AgNPs not only effectively inhibited the activity of enzymes but also the growth of the bacteria. Therefore, it can be hypothesized that the ability to inhibit the hydrolytic enzyme activity of bacteria may occur due to an interaction of AgNPs with proteins, causing an alteration in structure and interfering with enzymatic functions (Wigginton et al., 2010).

Silver nanoparticles from *F. culmorum* strain JTW1 showed strong inhibitory activity against the growth and spore germination of *Botrytis cinerea, Sclerotinia sclerotiorum,* and *Phoma lingam,* but not against remaining fungal strains. Similarly, antifungal activity of AgNPs obtained from strains of the genus *Trichoderma* to plant pathogens was shown in other studies reported by Guilger et al. (2017) and Tomah et al. (2020). For instance, AgNPs synthesized from *Trichoderma* sp. at a concentration of 200 μg mL^{-1} reduced the growth of mycelia of *Sclerotinia sclerotiorum*, formation of new sclerotia and their germination (Tomah et al., 2020). The authors further reported the changes in fungal cells by induction of pore formation in the cell wall and further accumulation of AgNPs inside the fungal cells (Tomah et al., 2020). Similarly, Guilger et al. (2017) found that AgNPs at a concentration of 0.31×10^{12} NPs/mL inhibited mycelial growth and the formation of new sclerotia of *Sclerotinia sclerotiorum*. However, in our study, inhibition of sclerotia germination was achieved at a much lower concentration of myco-AgNPs (32 μg mL^{-1}) showing their higher effectiveness in elimination of *S. sclerotiorum*. In another study, Malandrakis et al. (2019) tested the sensitivity of a number of fungal pathogens to commercially available silver nanoparticles (size <100 nm) and reported the highest susceptibility of *Botrytis cinerea,* followed by *Verticillium dahliae, Colletotrichum gloeosporioides, Monilia fructicola, Alternaria alternata, Fusarium oxysporum* f. sp. *Radicis-Lycopersici* and *Fusarium solani* (the latter was unaffected in tested concentration range). The higher inhibitory effect of AgNPs was observed against spores germination (EC_{50} values in the range 5.08–390.20 μg mL^{-1}) than mycelial growth (EC_{50} value were > 306 μg mL^{-1}) of tested pathogens (Malandrakis et al., 2019). Our findings provide evidence of the differential response of fungal pathogens to AgNPs. The highest inhibition of mycelial growth was recorded in *P. lingam* (9.54 mm), followed by *B. cinerea* (4.93 mm) and *S. sclerotiorum* (3.41 mm) whereas, in the case of spore germination, maximum inhibition was found in *S. sclerotiorum* (32 μg mL^{-1}), followed by *B. cinerea* (64 μg mL^{-1}) and *P. lingam* (256 μg mL^{-1}). Nevertheless, our findings of antimicrobial potential of AgNPs against a wide range of fungal crop pathogens indicate their potential for use in agricultural crop management to protect against diseases such as gray or white mold, blackleg, canker, and dry rot.

5. Conclusion

In this study, AgNPs were effectively synthesized from *Fusarium culmorum* strain JTW1. They were comprehensively characterized using UV–vis, TEM, XRD, NTA, Zeta potential measurements, and FTIR which revealed small size, spherical shape, stability, crystalline nature of AgNPs, and that mycosynthesized AgNPs were capped with biomolecules. Moreover, AgNPs were found to have strong antimicrobial potential against bacterial pathogens of humans and plants. AgNPs also enhanced antibacterial activity of streptomycin against Gram-negative bacteria, namely *E. coli* strains ATCC 8739 and ATCC 25922, *K. pneumoniae* ATCC 700603, *P. aeruginosa* ATCC 10145, ampicillin against *P. aeruginosa*, and ampicillin and kanamycin against Gram-positive *S. aureus* ATCC 25923 and *S. aureus* ATCC 6538, respectively. Furthermore, AgNPs significantly reduced bacterial biofilm formation and inhibited activity of hydrolytic enzymes synthesized by biofilm cells. In addition, AgNPs showed great

potential to inhibit fungal spore germination, which is crucial in the fungal spread in the environment, and growth of fungal mycelia. Therefore, these mycosynthesized silver nanoparticles in view of their unique properties, have a high potential as an antimicrobial agent in medicine and promising solution to control or reduce pathogens in agriculture and the food industry.

Data availability statement

The original contributions presented in the study are included in the article/Supplementary material, further inquiries can be directed to the corresponding authors.

Author contributions

PG and MR conceived research and edited and reviewed it. PG and JT-W designed research. JT-W and MW conducted experiments and acquired the funds. JT-W analyzed data and wrote the manuscript. All authors have read and agreed to the published version of the manuscript.

Funding

This research was funded by Excellence Initiative – Research University, Nicolaus Copernicus University in Torun, Grant4NCUStudents (38/2021/Grants4NCUStudents and 02/2021/Grants4NCUStudents). The ACP was funded from EF-IDUB of Nicolaus Copernicus University.

Acknowledgments

MR and PG would like to thank Polish National Agency for Academic Exchange Programme, for financial support under the grant PPN/ULM/2019/1/00117/DEC/1 2019-10-02. JT-W acknowledges grant No. 2022/45/N/NZ9/01483 from National Science Centre, Poland.

Conflict of interest

The authors declare that the research was conducted in the absence of any commercial or financial relationships that could be construed as a potential conflict of interest.

Publisher's note

All claims expressed in this article are solely those of the authors and do not necessarily represent those of their affiliated organizations, or those of the publisher, the editors and the reviewers. Any product that may be evaluated in this article, or claim that may be made by its manufacturer, is not guaranteed or endorsed by the publisher.

Supplementary material

The Supplementary material for this article can be found online at: https://www.frontiersin.org/articles/10.3389/fmicb.2023.1125685/full#supplementary-material

References

Adeyemi, O. S., Shittu, E. O., Akpor, O. B., Rotimi, D., and Batiha, G. E. S. (2020). Silver nanoparticles restrict microbial growth by promoting oxidative stress and DNA damage. *EXCLI J.* 19, 492–500. doi: 10.17179/excli2020-1244

Akther, T., Khan, M. S., and Hemalatha, S. (2020). Biosynthesis of silver nanoparticles via fungal cell filtrate and their anti-quorum sensing against *Pseudomonas aeruginosa*. *J. Environ. Chem. Eng.* 8:104365. doi: 10.1016/j.jece.2020.104365

Akther, T., Mathipi, V., Kumar, N. S., Davoodbasha, M., and Srinivasan, H. (2019). Fungal-mediated synthesis of pharmaceutically active silver nanoparticles and anticancer property against A549 cells through apoptosis. *Environ. Sci. Pollut. Res.* 26, 13649–13657. doi: 10.1007/s11356-019-04718-w

Ali, K., Ahmed, B., Dwivedi, S., Saquib, Q., Al-Khedhairy, A. A., and Musarrat, J. (2015). Microwave accelerated green synthesis of stable silver nanoparticles with Eucalyptus globulus leaf extract and their antibacterial and antibiofilm activity on clinical isolates. *PLoS One* 10:e0131178. doi: 10.1371/journal.pone.0131178

Allocati, N., Masulli, M., Alexeyev, M. F., and Di Ilio, C. (2013). *Escherichia coli* in Europe: an overview. *Int. J. Environ. Res. Public Health* 10, 6235–6254. doi: 10.3390/ijerph10126235

Al-Rajhi, A. M., Salem, S. S., Alharbi, A. A., and Abdelghany, T. M. (2022). Ecofriendly synthesis of silver nanoparticles using Kei-apple (*Dovyalis caffra*) fruit and their efficacy against cancer cells and clinical pathogenic microorganisms. *Arab. J. Chem.* 15:103927. doi: 10.1016/j.arabjc.2022.103927

Ammar, H. A. M., and El-Desouky, T. A. (2016). Green synthesis of nanosilver particles by *Aspergillus terreus* HA 1N and *Penicillium expansum* HA 2N and its antifungal activity against mycotoxigenic fungi. *J. Appl. Microbiol.* 121, 89–100. doi: 10.1111/jam.13140

Amro, N. A., Kotra, L. P., Wadu-Mesthrige, K., Bulychev, A., Mobashery, S., and Liu, G. Y. (2000). High-resolution atomic force microscopy studies of the *Escherichia coli* outer membrane: structural basis for permeability. *Langmuir* 16, 2789–2796. doi: 10.1021/la991013x

Amselem, J., Cuomo, C. A., van Kan, J. A., Viaud, M., Benito, E. P., Couloux, A., et al. (2011). Genomic analysis of the necrotrophic fungal pathogens *Sclerotinia sclerotiorum and Botrytis cinerea*. *PLoS Genet.* 7:e1002230. doi: 10.1371/journal.pgen.1002230

Ansari, M. A., Asiri, S. M. M., Alzohairy, M. A., Alomary, M. N., Almatroudi, A., and Khan, F. A. (2021). Biofabricated fatty acids-capped silver nanoparticles as potential antibacterial, antifungal, antibiofilm and anticancer agents. *Pharmaceuticals* 14:139. doi: 10.3390/ph14020139

Ansari, M. A., Khan, H. M., Khan, A. A., Cameotra, S. S., and Pal, R. (2014). Antibiofilm efficacy of silver nanoparticles against biofilm of extended spectrum β-lactamase isolates of *Escherichia coli* and *Klebsiella pneumoniae*. *Appl. Nanosci.* 4, 859–868. doi: 10.1007/s13204-013-0266-1

Azmath, P., Baker, S., Rakshith, D., and Satish, S. (2016). Mycosynthesis of silver nanoparticles bearing antibacterial activity. *Saudi Pharm. J.* 24, 140–146. doi: 10.1016/j.jsps.2015.01.008

Bawaskar, M., Gaikwad, S., Ingle, A., Rathod, D., Gade, A., Duran, N., et al. (2010). A new report on mycosynthesis of silver nanoparticles by *Fusarium culmorum*. *Curr. Nanosci.* 6, 376–380. doi: 10.2174/157341310791658919

Butsenko, L., Pasichnyk, L., Kolomiiets, Y., and Kalinichenko, A. (2020). The effect of pesticides on the tomato bacterial speck disease pathogen *Pseudomonas syringae* pv. *tomato*. *Appl. Sci.* 10:3263. doi: 10.3390/app10093263

Caniça, M., Manageiro, V., Abriouel, H., Moran-Gilad, J., and Franz, C. M. (2019). Antibiotic resistance in foodborne bacteria. *Trends Food Sci. Technol.* 84, 41–44. doi: 10.1128/AEM.00973-07

Charkowski, A. O. (2018). The changing face of bacterial soft-rot diseases. *Annu. Rev. Phytopathol.* 56, 269–288. doi: 10.1146/annurev-phyto-080417-045906

Charkowski, A., Sharma, K., Parker, M. L., Secor, G. A., and Elphinstone, J. (2020). "Bacterial diseases of potato," in *The Potato Crop: Its Agricultural, Nutritional and Social Contribution to Humankind*. eds. H. Campos and O. Ortiz (Cham: Springer), 351–388.

Chlebicz, A., and Śliżewska, K. (2018). Campylobacteriosis, salmonellosis, yersiniosis, and listeriosis as zoonotic foodborne diseases: a review. *Int. J. Environ. Res. Public Health* 15:863. doi: 10.3390/ijerph15050863

Chlumsky, O., Purkrtova, S., Michova, H., Svarcova, V., Slepicka, P., Fajstavr, D., et al. (2020). The effect of gold and silver nanoparticles, chitosan and their combinations on bacterial biofilms of food-borne pathogens. *Biofouling* 36, 222–233. doi: 10.1080/08927014.2020.1751132

Clinical and Laboratory Standards Institute (CLSI) (2012). *Methods for Dilution Antimicrobial Susceptibility Tests for Bacteria that Grow Aerobically; Approved Standard 9th*. Document M07-A9, CLSI Wayne, USA.

Dadgostar, P. (2019). Antimicrobial resistance: implications and costs. *Infect. Drug Resist.* 12, 3903–3910. doi: 10.2147/IDR.S234610

Dean, R., Van Kan, J. A., Pretorius, Z. A., Hammond-Kosack, K. E., Di Pietro, A., Spanu, P. D., et al. (2012). The top 10 fungal pathogens in molecular plant pathology. *Physiol. Mol. Plant Pathol.* 13, 414–430. doi: 10.1111/j.1364-3703.2011.00783.x

Desai, R., Mankad, V., Gupta, S. K., and Jha, P. K. (2012). Size distribution of silver nanoparticles: UV-visible spectroscopic assessment. *Nanosci. Nanotechnol. Lett.* 4, 30–34. doi: 10.1166/nnl.2012.1278

Elamawi, R. M., Al-Harbi, R. E., and Hendi, A. A. (2018). Biosynthesis and characterization of silver nanoparticles using *Trichoderma longibrachiatum* and their effect on phytopathogenic fungi. *Egypt. J. Biol. Pest Control* 28, 1–11. doi: 10.1186/s41938-018-0028-1

Elumalai, D., Hemavathi, M., Deepaa, C. V., and Kaleena, P. K. (2017). Evaluation of phytosynthesised silver nanoparticles from leaf extracts of *Leucas aspera* and *Hyptis suaveolens* and their larvicidal activity against malaria, dengue and filariasis vectors. *Parasite Epidemiol. Control* 2, 15–26. doi: 10.1016/j.parepi.2017.09.001

Fayaz, A. M., Balaji, K., Girilal, M., Yadav, R., Kalaichelvan, P. T., and Venketesan, R. (2010). Biogenic synthesis of silver nanoparticles and their synergistic effect with antibiotics: a study against gram-positive and gram-negative bacteria. *Nanomed. Nanotechnol. Biol. Med.* 6, 103–109. doi: 10.1016/j.nano.2009.04.006

Feoktistova, M., Geserick, P., and Leverkus, M. (2016). Crystal violet assay for determining viability of cultured cells. *Cold Spring Harb. Protoc.* 2016:pdb.prot087379. doi: 10.1101/pdb.prot087379

Food and Agriculture Organization of the United Nations (FAO). (2017). The Future of Food and Agriculture – Trends and Challenges. Available at: https://www.fao.org/3/i6583e/i6583e.pdf (Accessed May 5, 2022).

Fung, F., Wang, H. S., and Menon, S. (2018). Food safety in the 21st century. *Biom. J.* 41, 88–95. doi: 10.1016/j.bj.2018.03.003

Gabal, E., Amal-Asran, M., Mohamed, M. A., and Abd-Elsalam, K. A. (2019). "*Botrytis* gray Mold Nano-or biocontrol: present status and future prospects" in *Nanobiotechnology Applications in Plant Protection: Volume 2*. eds. K. Abd-Elsalam and R. Prasad (Cham: Springer), 85–118.

Gandhi, M., and Chikindas, M. L. (2007). *Listeria*: a foodborne pathogen that knows how to survive. *Int. J. Food Microbiol.* 113, 1–15. doi: 10.1016/j.ijfoodmicro.2006.07.008

Ghaseminezhad, S. M., Hamedi, S., and Shojaosadati, S. A. (2012). Green synthesis of silver nanoparticles by a novel method: comparative study of their properties. *Carbohydr. Polym.* 89, 467–472. doi: 10.1016/j.carbpol.2012.03.030

Guilger, M., Pasquoto-Stigliani, T., Bilesky-Jose, N., Grillo, R., Abhilash, P. C., Fraceto, L. F., et al. (2017). Biogenic silver nanoparticles based on *Trichoderma harzianum*: synthesis, characterization, toxicity evaluation and biological activity. *Sci. Rep.* 7, 1–13. doi: 10.1038/srep44421

Gul, A., Shaheen, A., Ahmad, I., Khattak, B., Ahmad, M., Ullah, R., et al. (2021). Green synthesis, characterization, enzyme inhibition, antimicrobial potential, and cytotoxic activity of plant mediated silver nanoparticle using *Ricinus communis* leaf and root extracts. *Biomol. Ther.* 11:206. doi: 10.3390/biom11020206

Hall-Stoodley, L., and Stoodley, P. (2005). Biofilm formation and dispersal and the transmission of human pathogens. *Trends Microbiol.* 13, 7–10. doi: 10.1016/j.tim.2004.11.004

Hamouda, R. A., Yousuf, W. E., Abdeen, E. E., and Mohamed, A. (2019). Biological and chemical synthesis of silver nanoparticles: characterization, MIC and antibacterial activity against pathogenic bacteria. *J. Chem. Pharm. Res.* 11, 1–12.

Hampf, A. C., Nendel, C., Strey, S., and Strey, R. (2021). Biotic yield losses in the southern Amazon, Brazil: making use of smartphone-assisted plant disease diagnosis data. *Front. Plant Sci.* 12:548. doi: 10.3389/fpls.2021.621168

Harrell, J. E., Hahn, M. M., D'Souza, S. J., Vasicek, E. M., Sandala, J. L., Gunn, J. S., et al. (2021). Salmonella biofilm formation, chronic infection, and immunity within the intestine and hepatobiliary tract. *Front. Cell. Infect. Microbiol.* 10:624622. doi: 10.3389/fcimb.2020.624622

Hashempour-Baltork, F., Hosseini, H., Shojaee-Aliabadi, S., Torbati, M., Alizadeh, A. M., and Alizadeh, M. (2019). Drug resistance and the prevention strategies in food borne bacteria: an update review. *Adv. Pharm. Bull.* 9, 335–347. doi: 10.15171/apb.2019.041

Hemeg, H. A. (2017). Nanomaterials for alternative antibacterial therapy. *Int. J. Nanomed.* 12, 8211–8225. doi: 10.2147/IJN.S132163

Hetta, H. F., Al-Kadmy, I., Khazaal, S. S., Abbas, S., Suhail, A., El-Mokhtar, M. A., et al. (2021). Antibiofilm and antivirulence potential of silver nanoparticles against multidrug-resistant *Acinetobacter baumannii*. *Sci. Rep.* 11, 10751–10711. doi: 10.1038/s41598-021-90208-4

Huang, W., Fang, X., Wang, H., Chen, F., Duan, H., Bi, Y., et al. (2018). Biosynthesis of AgNPs by *B. maydis* and its antifungal effect against *Exserohilum turcicum*. *IET Nanobiotechnol.* 12, 585–590. doi: 10.1049/iet-nbt.2017.0263

Iwu, C. D., and Okoh, A. I. (2019). Preharvest transmission routes of fresh produce associated bacterial pathogens with outbreak potentials: a review. *Int. J. Environ. Res. Public Health* 16:4407. doi: 10.3390/ijerph16224407

Jain, N., Bhargava, A., Majumdar, S., Tarafdar, J. C., and Panwar, J. (2011). Extracellular biosynthesis and characterization of silver nanoparticles using *Aspergillus flavus* NJP08: a mechanism perspective. *Nanoscale* 3, 635–641. doi: 10.1039/C0NR00656D

Johnson, K. B., and Stockwell, V. O. (1998). Management of fire blight: a case study in microbial ecology. *Annu. Rev. Phytopathol.* 36, 227–248. doi: 10.1146/annurev.phyto.36.1.227

Joshi, P. A., Bonde, S. R., Gaikwad, S. C., Gade, A. K., Abd-Elsalam, K., and Rai, M. K. (2013). Comparative studies on synthesis of silver nanoparticles by *Fusarium oxysporum* and *Macrophomina phaseolina* and its efficacy against bacteria and *Malassezia furfur*. *J. Bionanosci.* 7, 378–385. doi: 10.1166/jbns.2013.1148

Lahiri, D., Nag, M., and Ray, R. R. (2021). "Mycosynthesis of silver nanoparticles: mechanism and applications" in *Nanobiotechnology—Microbes and Plant Assisted Synthesis of Nanoparticles, Mechanisms and Applications*. eds. S. Ghosh and T. Webster (Netherlands: Elsevier), 91–104.

Larsson, D. G. J., and Flach, C. F. (2022). Antibiotic resistance in the environment. *Nat. Rev. Microbiol.* 20, 257–269. doi: 10.1038/s41579-021-00649-x

Li, G., He, D., Qian, Y., Guan, B., Gao, S., Cui, Y., et al. (2012). Fungus-mediated green synthesis of silver nanoparticles using *Aspergillus terreus*. *Int. J. Mol. Sci.* 13, 466–476. doi: 10.3390/ijms13010466

Li, W. R., Xie, X. B., Shi, Q. S., Zeng, H. Y., Ou-Yang, Y. S., and Chen, Y. B. (2010). Antibacterial activity and mechanism of silver nanoparticles on *Escherichia coli*. *Appl. Microbiol. Biotechnol.* 85, 1115–1122. doi: 10.1007/s00253-009-2159-5

Magaldi, S., Mata-Essayag, S., Hartung de Capriles, C., Perez, C., Colella, M. T., Olaizola, C., et al. (2004). Well diffusion for antifungal susceptibility testing. *Int. J. Infect. Dis.* 8, 39–45. doi: 10.1016/j.ijid.2003.03.002

Majeed, S., Danish, M., Zahrudin, A. H. B., and Dash, G. K. (2018). Biosynthesis and characterization of silver nanoparticles from fungal species and its antibacterial and anticancer effect. *Karbala Int. J. Mod. Sci.* 4, 86–92. doi: 10.1016/j.kijoms.2017.11.002

Maji, A., and Nath, R. (2015). Pathogenecity test by using different inoculation methods on *Xanthomonas campestris* pv. *campestris* caused of black rot of cabbage. *Int. J. Appl. Res. Nat. Prod.* 3, 53–58.

Malandrakis, A. A., Kavroulakis, N., and Chrysikopoulos, C. V. (2019). Use of copper, silver and zinc nanoparticles against foliar and soil-borne plant pathogens. *Sci. Total Environ.* 670, 292–299. doi: 10.1016/j.scitotenv.2019.03.210

Mansfield, J., Genin, S., Magori, S., Citovsky, V., Sriariyanum, M., Ronald, P., et al. (2012). Top 10 plant pathogenic bacteria in molecular plant pathology. *Mol. Plant Pathol.* 13, 614–629. doi: 10.1111/j.1364-3703.2012.00804.x

Markowska, K., Grudniak, A. M., and Wolska, K. I. (2013). Silver nanoparticles as an alternative strategy against bacterial biofilms. *Acta Biochim. Pol.* 60, 523–530. doi: 10.18388/abp.2013_2016

Martinez-Gutierrez, F., Boegli, L., Agostinho, A., Sánchez, E. M., Bach, H., Ruiz, F., et al. (2013). Anti-biofilm activity of silver nanoparticles against different microorganisms. *Biofouling* 29, 651–660. doi: 10.1080/08927014.2013.794225

Mistry, H., Thakor, R., Patil, C., Trivedi, J., and Bariya, H. (2021). Biogenically proficient synthesis and characterization of silver nanoparticles employing marine procured fungi *Aspergillus brunneoviolaceus* along with their antibacterial and antioxidative potency. *Biotechnol. Lett.* 43, 307–316. doi: 10.1080/08927014.2013.794225

Muthulakshmi, L., Suganya, K., Murugan, M., Annaraj, J., Duraipandiyan, V., Al Farraj, D. A., et al. (2022). Antibiofilm efficacy of novel biogenic silver nanoparticles from *Terminalia catappa* against food-borne *Listeria monocytogenes* ATCC 15,313 and mechanisms investigation *in-vivo* and *in-vitro*. *J. King Saud Univ. Sci.* 34:102083. doi: 10.1016/j.jksus.2022.102083

Nawaz, A., Tariq, J. A., Lodhi, A. M., and Memon, R. M. (2020). Studies on characteristics of *Xanthomonas oryzae* isolates associated with Rice crop. *J. App. Res. Plant Sci.* 1, 30–35. doi: 10.38211/joarps.2020.1.1.5

Olfati, A., Kahrizi, D., Balaky, S. T. J., Sharifi, R., Tahir, M. B., and Darvishi, E. (2021). Green synthesis of nanoparticles using *Calendula officinalis* extract from silver sulfate and their antibacterial effects on *Pectobacterium caratovorum*. *Inorg. Chem. Commun.* 125:108439. doi: 10.1016/j.inoche.2020.108439

Olivares, E., Badel-Berchoux, S., Provot, C., Prévost, G., Bernardi, T., and Jehl, F. (2020). Clinical impact of antibiotics for the treatment of *Pseudomonas aeruginosa* biofilm infections. *Front. Microbiol.* 10:2894. doi: 10.3389/fmicb.2019.02894

Osorio-Echavarría, J., Osorio-Echavarría, J., Ossa-Orozco, C. P., and Gómez-Vanegas, N. A. (2021). Synthesis of silver nanoparticles using white-rot fungus Anamorphous *Bjerkandera* sp. R1: influence of silver nitrate concentration and fungus growth time. *Sci. Rep.* 11, 1–14. doi: 10.1038/s41598-021-82514-8

Panáček, A., Smékalová, M., Kilianová, M., Prucek, R., Bogdanová, K., Večeřová, R., et al. (2016). Strong and nonspecific synergistic antibacterial efficiency of antibiotics combined with silver nanoparticles at very low concentrations showing no cytotoxic effect. *Molecules* 21:26. doi: 10.3390/molecules21010026

Peeters, E., Nelis, H. J., and Coenye, T. (2008). Comparison of multiple methods for quantification of microbial biofilms grown in microtiter plates. *J. Microbiol. Methods* 72, 157–165. doi: 10.1016/j.mimet.2007.11.010

Peil, A., Emeriewen, O. F., Khan, A., Kostick, S., and Malnoy, M. (2021). Status of fire blight resistance breeding in Malus. *J. Plant Pathol.* 103, 3–12. doi: 10.1007/s42161-020-00581-8

Pérombelon, M. C. M. (2002). Potato diseases caused by soft rot erwinias: an overview of pathogenesis. *Plant Pathol.* 51, 1–12. doi: 10.1046/j.0032-0862.2001.Shorttitle.doc.x

Pérombelon, M. C. M., and Kelman, A. (1980). Ecology of the soft rot erwinias. *Annu. Rev. Phytopathol.* 18, 361–387. doi: 10.1146/annurev.py.18.090180.002045

Qing, Y., Cheng, L., Li, R., Liu, G., Zhang, Y., Tang, X., et al. (2018). Potential antibacterial mechanism of silver nanoparticles and the optimization of orthopedic implants by advanced modification technologies. *Int. J. Nanomedicine* 13, 3311–3327. doi: 10.2147/IJN.S165125

Rai, M., Bonde, S., Golinska, P., Trzcińska-Wencel, J., Gade, A., Abd-Elsalam, K. A., et al. (2021a). *Fusarium* as a novel fungus for the synthesis of nanoparticles: mechanism and applications. *J. Fungi* 7:139. doi: 10.3390/jof7020139

Rai, M., Ingle, A. P., Trzcińska-Wencel, J., Wypij, M., Bonde, S., Yadav, A., et al. (2021b). Biogenic silver nanoparticles: what we know and what do we need to know? *Nano* 11:2901. doi: 10.3390/nano11112901

Ramachandran, R., and Sangeetha, D. (2017). Antibiofilm efficacy of silver nanoparticles against biofilm forming multidrug resistant clinical isolates. *J. Pharm. Innov.* 6:36.

Rogowska, A., Rafińska, K., Pomastowski, P., Walczak, J., Railean-Plugaru, V., Buszewska-Forajta, M., et al. (2017). Silver nanoparticles functionalized with ampicillin. *Electrophoresis* 38, 2757–2764. doi: 10.1002/elps.201700093

Ruden, S., Hilpert, K., Berditsch, M., Wadhwani, P., and Ulrich, A. S. (2009). Synergistic interaction between silver nanoparticles and membrane-permeabilizing antimicrobial peptides. *Antimicrob. Agents Chemother.* 53, 3538–3540. doi: 10.1128/AAC.01106-08

Sahoo, J. P., Mishra, A. P., Samal, K. C., and Dash, A. K. (2021). Insights into the antibiotic resistance in biofilms–a review. *Environ. Conserv. J.* 22, 59–67. doi: 10.36953/ECJ.2021.22307

Salem, S. S. (2022). Baker's yeast-mediated silver nanoparticles: characterisation and antimicrobial biogenic tool for suppressing pathogenic microbes. *BioNanoScience* 12, 1220–1229. doi: 10.1007/s12668-022-01026-5

Salem, S. S., Ali, O. M., Reyad, A. M., Abd-Elsalam, K. A., and Hashem, A. H. (2022). Pseudomonas indica-mediated silver nanoparticles: antifungal and antioxidant biogenic tool for suppressing mucormycosis fungi. *J. Fungi* 8:126. doi: 10.3390/jof8020126

Salem, S. S., Hammad, E. N., Mohamed, A. A., and El-Dougdoug, W. (2023). A comprehensive review of nanomaterials: types, synthesis, characterization, and applications. *Biointerface Res. Appl. Chem.* 13:41. doi: 10.33263/BRIAC131.041

Salleh, A., Naomi, R., Utami, N. D., Mohammad, A. W., Mahmoudi, E., Mustafa, N., et al. (2020). The potential of silver nanoparticles for antiviral and antibacterial applications: a mechanism of action. *Nano* 10:1566. doi: 10.3390/nano10081566

Salvioni, L., Galbiati, E., Collico, V., Alessio, G., Avvakumova, S., Corsi, F., et al. (2017). Negatively charged silver nanoparticles with potent antibacterial activity and reduced toxicity for pharmaceutical preparations. *Int. J. Nanomedicine* 12, 2517–2530. doi: 10.2147/IJN.S127799

Scallan Walter, E. J., Griffin, P. M., Bruce, B. B., and Hoekstra, R. M. (2021). Estimating the number of illnesses caused by agents transmitted commonly through food: a scoping review. *Foodborne Pathog. Dis.* 18, 841–858. doi: 10.1089/fpd.2021.0038

Schaad, N. W., Sitterly, W. R., and Humaydan, H. (1980). Relationship of incidence of seedborne *Xanthomonas campestris* to black rot of crucifers. *Plant Dis.* 64, 91–92. doi: 10.1094/PD-64-91

Shaheen, T. I., Salem, S. S., and Fouda, A. (2021). "Current advances in fungal nanobiotechnology: Mycofabrication and applications" in *Microbial Nanobiotechnology: Principles and Applications*. eds. A. Lateef, E. B. Gueguim-Kana, N. Dasgupta and S. Ranjan (Singapore: Springer)

Shenge, K. C., Mabagala, R. B., Mortensen, C. N., Stephan, D., and Wydra, K. (2007). First report of bacterial speck of tomato caused by *Pseudomonas syringae* pv. tomato in Tanzania. *Plant Dis.* 91:462. doi: 10.1094/PDIS-91-4-0462C

Smitha, S. L., Nissamudeen, K. M., Philip, D., and Gopchandran, K. G. (2008). Studies on surface plasmon resonance and photoluminescence of silver nanoparticles. *Spectrochim. Acta A Mol. Biomol. Spectrosc.* 71, 186–190. doi: 10.1016/j.saa.2007.12.002

Soliman, M. K., Salem, S. S., Abu-Elghait, M., and Azab, M. S. (2022). Biosynthesis of silver and gold nanoparticles and their efficacy towards antibacterial, antibiofilm, cytotoxicity, and antioxidant activities. *Appl. Biochem. Biotechnol.* 195, 1158–1183. doi: 10.1007/s12010-022-04199-7

Sundin, G. W., Castiblanco, L. F., Yuan, X., Zeng, Q., and Yang, C. H. (2016). Bacterial disease management: challenges, experience, innovation and future prospects: challenges in bacterial molecular plant pathology. *Mol. Plant Pathol.* 17, 1506–1518. doi: 10.1111/mpp.12436

Tariq, M., Mohammad, K. N., Ahmed, B., Siddiqui, M. A., and Lee, J. (2022). Biological synthesis of silver nanoparticles and prospects in plant disease management. *Molecules* 27:4754. doi: 10.3390/molecules27154754

Tian, X., Jiang, X., Welch, C., Croley, T. R., Wong, T. Y., Chen, C., et al. (2018). Bactericidal effects of silver nanoparticles on lactobacilli and the underlying mechanism. *ACS Appl. Mater. Interfaces* 10, 8443–8450 doi: 10.1021/acsami.7b17274

Tomah, A. A., Alamer, I. S. A., Li, B., and Zhang, J. Z. (2020). Mycosynthesis of silver nanoparticles using screened *Trichoderma* isolates and their antifungal activity against *Sclerotinia sclerotiorum*. *Nano* 10:1955. doi: 10.3390/nano10101955

Tomaszewska, E., Soliwoda, K., Kadziola, K., Tkacz-Szczesna, B., Celichowski, G., Cichomski, M., et al. (2013). Detection limits of DLS and UV-Vis spectroscopy in characterization of polydisperse nanoparticles colloids. *J. Nanomat.* 2013, 1–10. doi: 10.1155/2013/313081

Vanneste, J. (2000). *Fire Blight: The Disease and Its Causative Agent, Erwinia Amylovora*. New York, USA: CABI

Vigneshwaran, N., Ashtaputre, N. M., Varadarajan, P. V., Nachane, R. P., Paralikar, K. M., and Balasubramanya, R. H. (2007). Biological synthesis of silver nanoparticles using the fungus *Aspergillus flavus*. *Mater. Lett.* 61, 1413–1418. doi: 10.1016/j.matlet.2006.07.042

Wang, L., Hu, C., and Shao, L. (2017). The antimicrobial activity of nanoparticles: present situation and prospects for the future. *Int. J. Nanomedicine* 12, 1227–1249. doi: 10.2147/IJN.S121956

Wang, C., Xu, S., Zhang, K., Li, M., Li, Q., Xiao, R., et al. (2017). Streptomycin-modified Fe3O4–Au@ Ag core–satellite magnetic nanoparticles as an effective antibacterial agent. *J. Mater. Sci.* 52, 1357–1368. doi: 10.1007/s10853-016-0430-6

White, T. J., Bruns, T., Lee, S. J. W. T., and Taylor, J. (1990). Amplification and direct sequencing of fungal ribosomal RNA genes for phylogenetics. *PCR Protocols* 18, 315–322. doi: 10.1016/B978-0-12-372180-8.50042-1

Wigginton, N. S., Titta, A. D., Piccapietra, F., Dobias, J. A. N., Nesatyy, V. J., Suter, M. J., et al. (2010). Binding of silver nanoparticles to bacterial proteins depends on surface modifications and inhibits enzymatic activity. *Environ. Sci. Technol.* 44, 2163–2168. doi: 10.1021/es903187s

World Health Organization (WHO). (2021). *Antimicrobial Resistance*. Available at: https://www.who.int/news-room/fact-sheets/detail/antimicrobial-resistance (Accessed May 15, 2022).

Wypij, M., Czarnecka, J., Świecimska, M., Dahm, H., Rai, M., and Golinska, P. (2018). Synthesis, characterization and evaluation of antimicrobial and cytotoxic activities of biogenic silver nanoparticles synthesized from *Streptomyces xinghaiensis* OF1 strain. *World J. Microbiol. Biotechnol.* 34, 23–13. doi: 10.1007/s11274-017-2406-3

Wypij, M., Jędrzejewski, T., Ostrowski, M., Trzcińska, J., Rai, M., and Golińska, P. (2020). Biogenic silver nanoparticles: assessment of their cytotoxicity, genotoxicity and study of capping proteins. *Molecules* 25:3022. doi: 10.3390/molecules25133022

Wypij, M., Jędrzejewski, T., Trzcińska-Wencel, J., Ostrowski, M., Rai, M., and Golińska, P. (2021). Green synthesized silver nanoparticles: antibacterial and anticancer activities, biocompatibility, and analyses of surface-attached proteins. *Front. Microbiol.* 12:632505. doi: 10.3389/fmicb.2021.632505

Wypij, M., Ostrowski, M., Piska, K., Wójcik-Pszczoła, K., Pękala, E., Rai, M., et al. (2022). Novel antibacterial, cytotoxic and catalytic activities of silver nanoparticles synthesized from acidophilic actinobacterial SL19 with evidence for protein as coating biomolecule. *J. Microbiol. Biotechnol.* 32, 1195–1208. doi: 10.4014/jmb.2205.05006

Wypij, M., Trzcińska-Wencel, J., Golińska, P., Avila-Quezada, G. D., Ingle, A. P., and Rai, M. (2023). The strategic applications of natural polymer nanocomposites in food packaging and agriculture: chances, challenges, and consumers' perception. *Front. Chem.* 10:1106230. doi: 10.3389/fchem.2022.1106230

Xie, W. Y., Shen, Q., and Zhao, F. J. (2018). Antibiotics and antibiotic resistance from animal manures to soil: a review. *Eur. J. Soil Sci.* 69, 181–195. doi: 10.1111/ejss.12494

Yuan, Y. G., Peng, Q. L., and Gurunathan, S. (2017). Effects of silver nanoparticles on multiple drug-resistant strains of *Staphylococcus aureus* and *Pseudomonas aeruginosa* from mastitis-infected goats: an alternative approach for antimicrobial therapy. *Int. J. Mol. Sci.* 18:569. doi: 10.3390/ijms18030569

Zhao, X., Zhou, L., Riaz Rajoka, M. S., Yan, L., Jiang, C., Shao, D., et al. (2018). Fungal silver nanoparticles: synthesis, application and challenges. *Crit. Rev. Biotechnol.* 38, 817–835. doi: 10.1080/07388551.2017.1414141

Zhu, Q., Gooneratne, R., and Hussain, M. A. (2017). *Listeria monocytogenes* in fresh produce: outbreaks, prevalence and contamination levels. *Foods* 6:21. doi: 10.3390/foods6030021

Supplementary Material

Biogenic nanosilver bearing antimicrobial and antibiofilm activities and its potential for application in agriculture and industry

Joanna Trzcińska-Wencel [1*], Magdalena Wypij [1*], Mahendra Rai [1,2], Patrycja Golińska[1]

[1]Department of Microbiology, Nicolaus Copernicus University in Toruń, Toruń, Poland;

[2]Nanobiotechnology Laboratory, Department of Biotechnology, SGB Amravati University, Amravati, India

*** Correspondence:**
Joanna Trzcińska-Wencel and Magdalena Wypij
trzcinska@doktorant.umk.pl and mwypij@umk.pl

Supplementary figures:

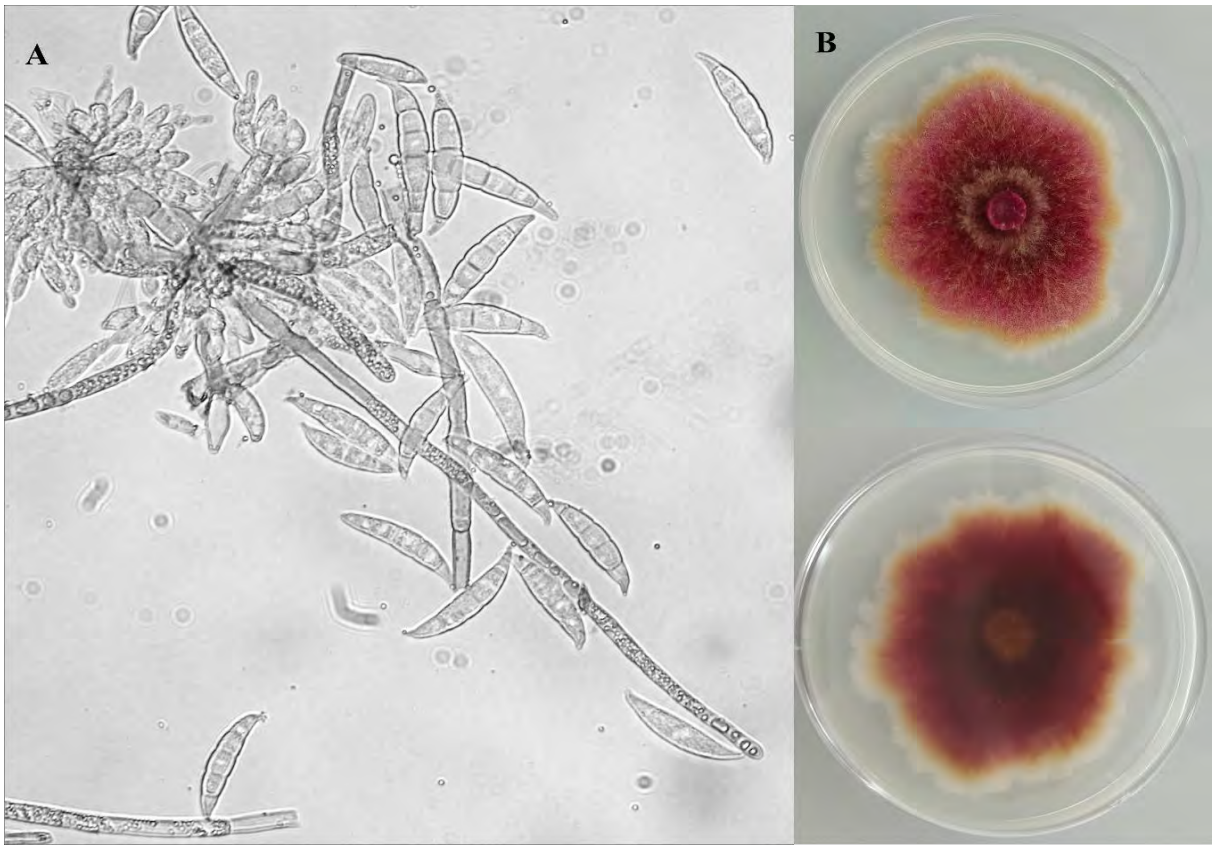

Supplementary Figure S1. Fungal strain *Fusarium culmorum* strain JTW1: light microscopic observation (A), growth on the potato dextrose agar (B).

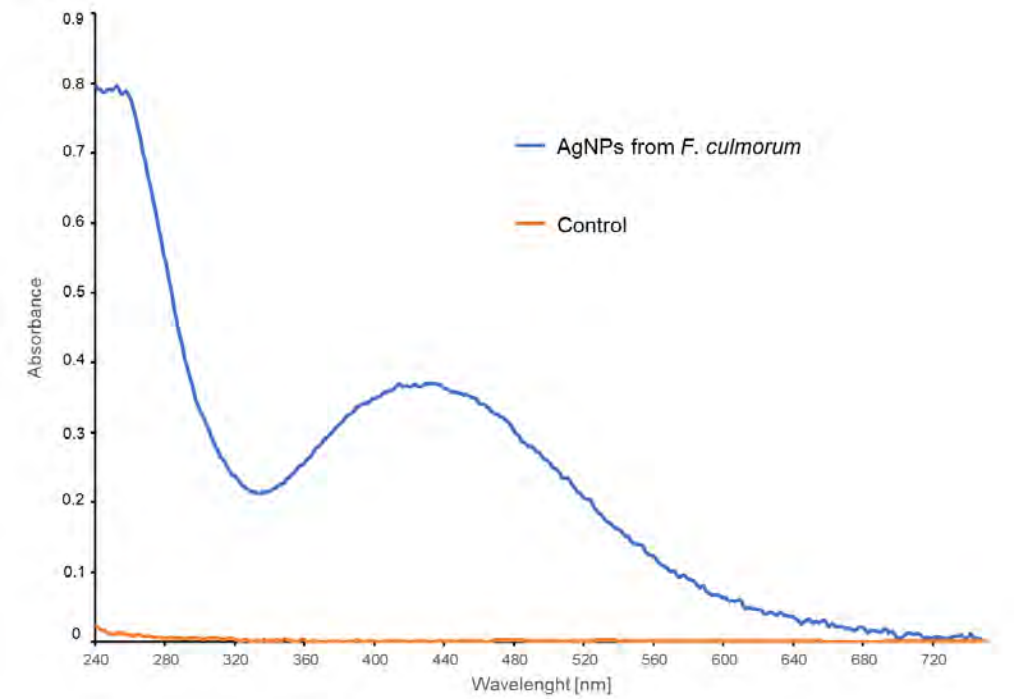

Supplementary Figure S2. The UV-Visible spectra of AgNPs from *Fusarium culmorum* strain JTW1 with the maximum absorbance peak at 430 nm.

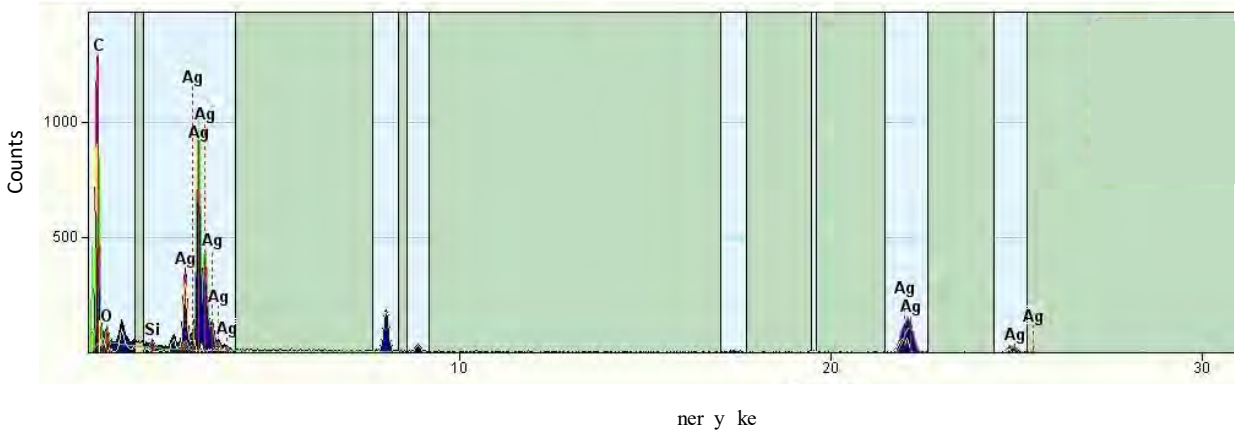

Supplementary Figure S3. Energy dispersive X-ray (EDX) spectrum of AgNPs from *Fusarium culmorum* strain JTW1.

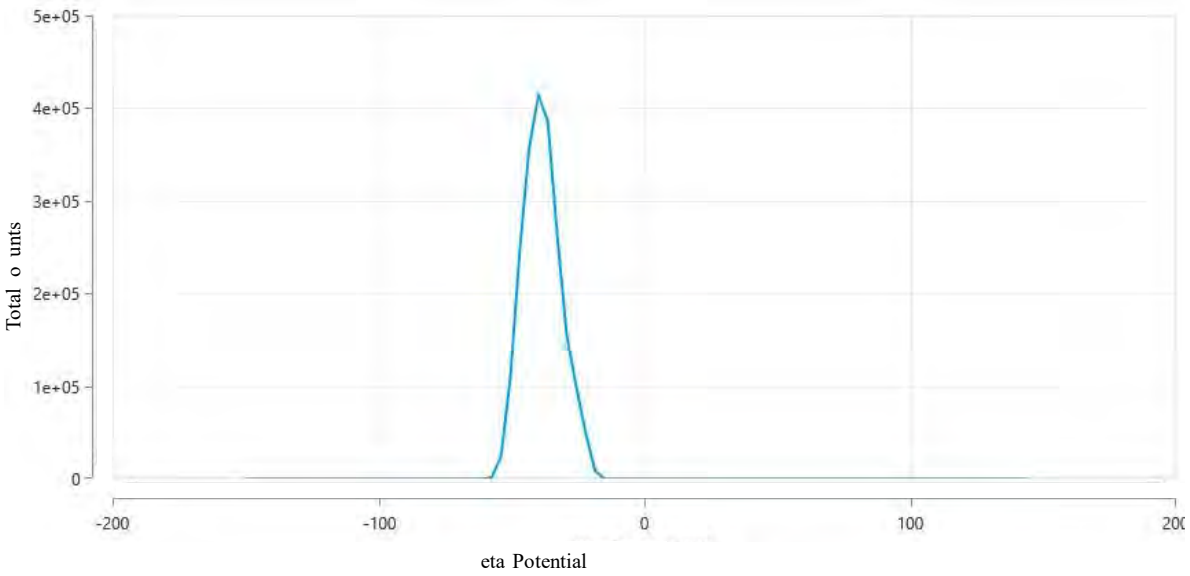

Supplementary Figure S4. The zeta potential of AgNPs from *Fusarium culmorum* strain JTW1.

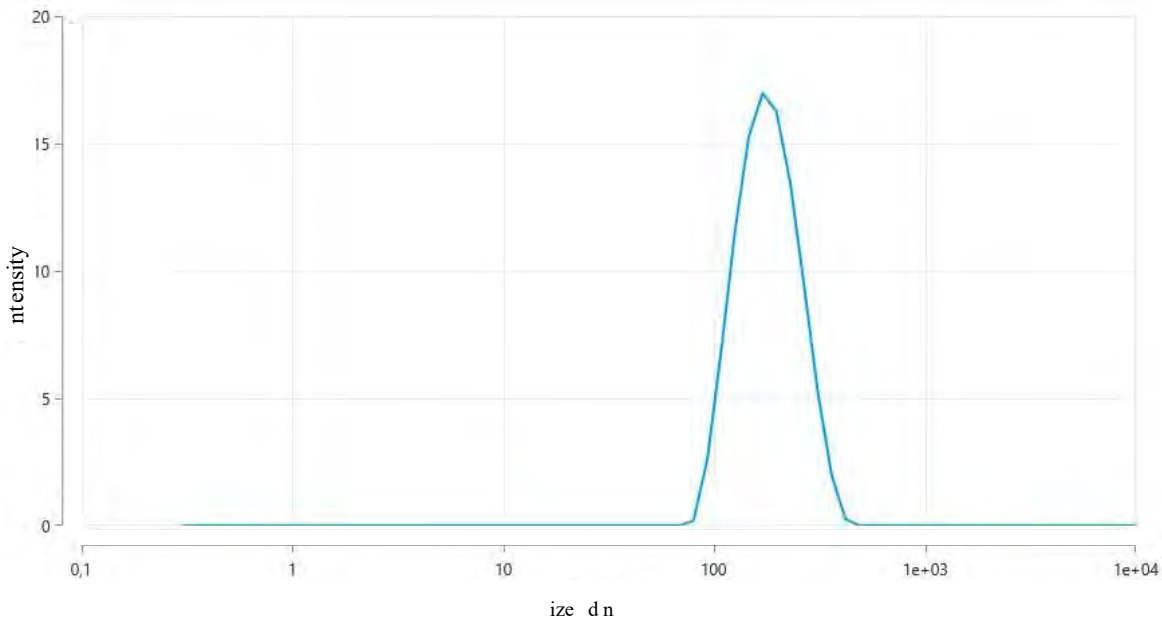

Supplementary Figure S5. Particle size distribution of AgNPs from *Fusarium culmorum* strain JTW1 estimated using dynamic light scattering (DLS).

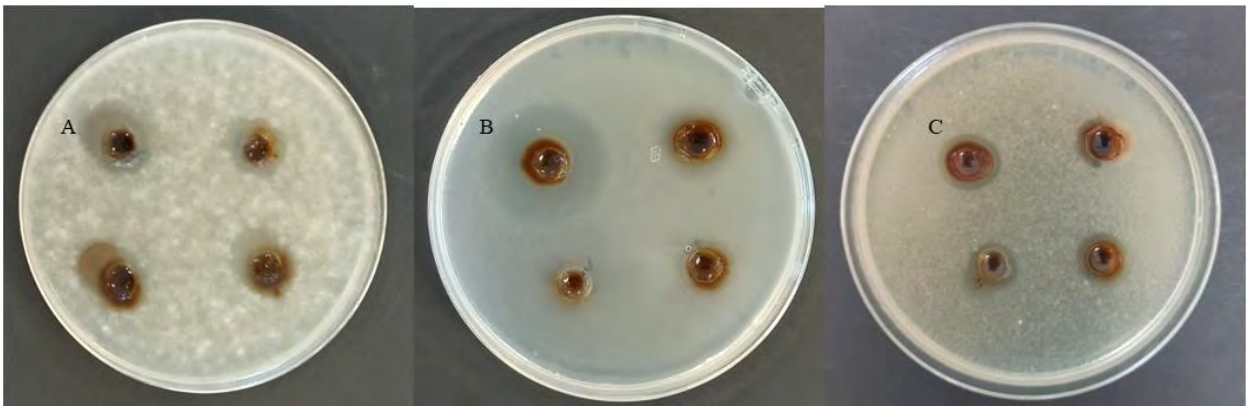

Supplementary Figure S6. Antifungal activity of AgNPs from *Fusarium culmorum* strain JTW1 against *Botrytis cinerea* IOR 1873 (A), *Phoma lingam* IOR 2284 (B) and *Sclerotinia sclerotiorum* IOR 2242 (C).

frontiers | Frontiers in Chemistry

P4

TYPE Original Research
PUBLISHED 04 August 2023
DOI 10.3389/fchem.2023.1235437

OPEN ACCESS

EDITED BY
Sirikanjana Thongmee,
Kasetsart University, Thailand

REVIEWED BY
Lakshmi Narayanan Mosur Saravana Murthy,
Intel, United States
Devendra Jain,
Maharana Pratap University of Agriculture and Technology, India

*CORRESPONDENCE
Joanna Trzcińska-Wencel,
trzcinska@doktorant.umk.pl
Patrycja Golińska,
golinska@umk.pl

RECEIVED 06 June 2023
ACCEPTED 20 July 2023
PUBLISHED 04 August 2023

CITATION
Trzcińska-Wencel J, Wypij M, Terzyk AP, Rai M and Golińska P (2023), Biofabrication of novel silver and zinc oxide nanoparticles from *Fusarium solani* IOR 825 and their potential application in agriculture as biocontrol agents of phytopathogens, and seed germination and seedling growth promoters. *Front. Chem.* 11:1235437. doi: 10.3389/fchem.2023.1235437

Biofabrication of novel silver and zinc oxide nanoparticles from *Fusarium solani* IOR 825 and their potential application in agriculture as biocontrol agents of phytopathogens, and seed germination and seedling growth promoters

Joanna Trzcińska-Wencel[1]*, Magdalena Wypij[1], Artur P. Terzyk[2], Mahendra Rai[1,3] and Patrycja Golińska[1]*

[1]Department of Microbiology, Faculty of Biological and Veterinary Sciences, Nicolaus Copernicus University in Toruń, Toruń, Poland, [2]Physicochemistry of Carbon Materials Research Group, Department of Chemistry of Materials, Adsorption and Catalysis, Faculty of Chemistry, Nicolaus Copernicus University in Toruń, Toruń, Poland, [3]Nanobiotechnology Laboratory, Department of Biotechnology, SGB Amravati University, Amravati, India

Introduction: Plant pathogenic microorganisms adversely affect the growth and yield of crops, which consequently leads to losses in food production. Metal-based nanoparticles (MNPs) can be a remedy to solve this problem.

Methods: Novel silver nanoparticles (AgNPs) and zinc oxide nanoparticles (ZnONPs) were biosynthesized from *Fusarium solani* IOR 825 and characterized using Dynamic Light Scattering (DLS), Fourier Transform Infrared (FTIR) spectroscopy, Transmission Electron Microscopy (TEM), X-ray diffraction (XRD) and measurement of Zeta potential. Antibacterial activity of NPs was evaluated against four plant pathogenic strains by determination of the minimum inhibitory (MIC) and biocidal concentrations (MBC). Micro-broth dilution method and poisoned food technique were used to assess antifungal activity of NPs against a set of plant pathogens. Effect of nanopriming with both types of MNPs on maize seed germination and seedlings growth was evaluated at a concentration range of 1–256 μg mL^{-1}.

Results: Mycosynthesis of MNPs provided small (8.27 nm), spherical and stable (zeta potential of −17.08 mV) AgNPs with good crystallinity. Similarly, ZnONPs synthesized by using two different methods (ZnONPs(1) and ZnONPs(2)) were larger in size (117.79 and 175.12 nm, respectively) with Zeta potential at −9.39 and −21.81 mV, respectively. The FTIR spectra showed the functional groups (hydroxyl, amino, and carboxyl) of the capping molecules on the surface of MNPs. The values of MIC and MBC of AgNPs against bacteria ranged from 8 to 256 μg mL^{-1} and from 512 to 1024 μg mL^{-1}, respectively. Both types of ZnONPs displayed antibacterial activity at 256–1024 μg mL^{-1} (MIC) and 512–2048 μg mL^{-1} (MBC), but in the concentration range tested, they revealed no activity against *Pectobacterium carotovorum*. Moreover, AgNPs and ZnONPs inhibited the

mycelial growth of *Alternaria alternata, Fusarium culmorum, Fusarium oxysporum, Phoma lingam,* and *Sclerotinia sclerotiorum*. MIC and MFC values of AgNPs ranged from 16–128 and 16–2048 μg mL $^{-1}$, respectively. ZnONPs showed antifungal activity with MIC and MFC values of 128–2048 μg mL^{-1} and 256–2048 μg mL^{-1}, respectively. The AgNPs at a concentration of ≥32 μg mL^{-1} revealed sterilization effect on maize seeds while ZnONPs demonstrated stimulatory effect on seedlings growth at concentrations of ≥16 μg mL^{-1} by improving the fresh and dry biomass production by 24% and 18%–19%, respectively.

Discussion: AgNPs and ZnONPs mycosynthesized from *F. solani* IOR 825 could be applied in agriculture to prevent the spread of pathogens. However, further toxicity assays should be performed before field evaluation. In view of the potential of ZnONPs to stimulate plant growth, they could be crucial in increasing crop production from the perspective of current food assurance problems.

KEYWORDS

applied microbiology, biocontrol, biofabrication, biogenic nanoparticles, bionanotechnology, crop protection, mycosynthesis, plant pathogens

1 Introduction

Plant diseases caused by pathogenic microorganisms adversely affect the growth and yield of crops, which consequently leads to losses in food production (Peng et al., 2021). Recently, Van Dijk et al. (2021) presented a set of projections on the growth of food demand between 2010 and 2050 and the risks of food shortage and hunger. The majority of food safety research focuses on common denominators such as climate change, resistant pathogens, and the need for sustainable agriculture while addressing human health and environmental concerns (Zakirov et al., 2021). The use of technological advances, including mechanization, pesticides or fertilizers, allowed to achieve higher productivity of crop plants (Jacquet et al., 2022). It is estimated that 70%–80% of plant diseases are caused by fungal pathogens particularly by secretion of toxins that cause various physiological disorders, growth inhibition, chlorosis, wilting, etc. (Peng et al., 2021). Maize belongs to the most frequent crop plants worldwide, including Poland (Król et al., 2018), and is particularly vulnerable to pathogenic fungi, e.g., *Fusarium* spp. (Czembor et al., 2015). In addition, microbial diseases lead to yield losses, while mycotoxins produced by fungi contaminate and reduce the quality of maize grains (Czembor et al., 2015). A number of synthetic chemical pesticides are required to prevent crop diseases. However, some negative aspects of pesticides on the environment and human health have been unequivocally documented, therefore limiting their use is of high priority (Jacquet et al., 2022). A number of studies have been conducted to design the remedy for addressing this excessive and seemingly irreplaceable application of traditional chemicals which showed that a prospective solution may be the use of products at the nanoscale (Pestovsky and Martinez-Antonio, 2017). Metal-based nanoparticles (MNPs) show promising potential for use in agriculture field as they demonstrate broad range of antibacterial and antifungal activities (Singh et al., 2021). The use of bio-nanoparticles (bio-NPs) as antimicrobial agents might empower a significant reduction in the dose used while maintaining antimicrobial efficacy compared to conventional materials. From an agro-ecological point of view, the application of nanoparticles (NPs) obtained from biological sources may mitigate the negative consequences of agriculture procedures imposed on the environment (Hazarika et al., 2022).

To date, various studies on the potential use of MNPs as fungicides have been reported (Malandrakis et al., 2022). Silver and zinc oxide nanoparticles (AgNPS and ZnONPs, respectively) display antimicrobial activity depending, in particular, on their physicochemical properties and the targeted pathogen (Gudkov et al., 2021). Some reports showed antimicrobial activity of biosynthesized AgNPs and ZnONPs against, e.g., *Escherichia coli, Pseudomonas aeruginosa*, *Staphylococcus aureus, Xanthomonas oryzae* pv. *oryzae, Alternaria alternata, Pyricularia oryzae, Sclerotinia sclerotiorum,* and many more (Consolo et al., 2020; El Sayed and El-Sayed, 2020; Ogunyemi et al., 2020; Pillai et al., 2020). It is suggested that the high ability of biosynthesized NPs to control microbial pathogens is due to their large surface area, small size, and high concentration of released ions or capping agents on the surface of the metallic core (Gudkov et al., 2021). In addition, zinc plays an important role in cell function and proliferation (membrane stability, metabolic processes, enzymatic activity, photosynthesis) and consequently in plant physiology (Cakmak et al., 2010; Faizan et al., 2020). It has been reported that the foliar and soil use of ZnONPs for maize biofortification resulted in higher Zn availability and uptake and affected Zn content in edible crop organs than the commonly used zinc sulfate ($ZnSO_4$). The higher bioavailability of zinc in nano form is attributed to its lower solubility than that of $ZnSO_4$ salts (Umar et al., 2021). In another study, maize and wheat supplementation with ZnONPs in lower doses (100 mg L^{-1}) improved seedling length and biomass production, and enzyme activity (α-amlyase, antioxidative system enzymes), which suggests potential application of ZnONPs as stimulators of crop plant growth (Srivastav et al., 2021). However, some phytotoxic effects of MNPs to plant development has been summarized by Abedi et al. (2022). This aspect is important before the evaluation of plant growth protection and/or promotion with the use of nanoparticles in the field. The diverse properties (small sizes, variable shapes, chemical nature) of MNPs determine their high reactivity and subsequently their uptake, translocation, and interactions in plants (de la Rosa et al., 2021). Some studies reported, that MNPs affect basic cellular processes by inducing oxidative stress, disrupting cell membrane transport or altering gene expression (Lee et al., 2013; Akhtar et al., 2022). Recently, Wan and coworkers (2019) found that ZnONPs (at

concentration >100 mg L^{-1}) caused endocytosis and led to the rearrangement of microfilament in the epidermal cells of elongation zones of *Arabidopsis* seedlings. However, above changes were temporary, and plants after NPs-related stress recovered faster than those treated with Zn^{2+} ions. In addition, MNPs introduced into the soil environment may cause changes in soil fertility, as well as affect microorganisms and invertebrates. Wei and coworkers (2021) reported diversified effects of ZnO, Cu, and γ-Fe_2O_3 NPs on plant (*Salvia miltiorrhiza*) growth and soil environment. For instance, the effect of NPs on seedling aboveground biomass depended on the type of NPs and dose applied (100 and 700 mg kg^{-1}). CuNPs showed no effect on plant biomass production at tested concentrations. In the case of ZnONPs, their lower concentrations (100 mg kg^{-1}) promoted growth, while higher concentrations (700 mg kg^{-1}) reduced it. In turn, γ-Fe_2O_3 NPs at both tested concentrations promoted plant growth. Moreover, the increase in the relative abundance of *S. miltiorrhiza* rhizosphere microorganisms, namely, the plant growth-promoting bacteria (*Sphingomonas*), superoxide dismutase producers (*Aminobacter*), and the metal-tolerant bacteria (*Thiobacillus* and *Metarhizium*) after MNPs-treatment was observed (Wei et al., 2021). The above findings indicate that various nanomaterials introduced into the environment might have undesirable effects, thus there is an urgent need to properly identify and study the effects of plant exposure to nanoparticles.

The synthesis of nanoparticles covers a variety of approaches, which include physical, chemical, biological, and their combination (Rai et al., 2021). The formation and structural parameters of nanoparticles depend on the reaction conditions and type of the stabilizing agent used in the synthesis (Lallo da Silva et al., 2019). Numerous studies have shown that the ability to form nanoparticles is demonstrated by plants (Balachandar et al., 2019; Verma and Bharadvaja, 2022), bacteria (Quinteros et al., 2019; Saeed et al., 2020), actinomycetes (Wypij et al., 2021, 2022), fungi (Feroze et al., 2020), and viruses (Le et al., 2017) by using their live cultures, biomass, extracts, and metabolites. Mycosynthesis of various nanoparticles is intensively studied by many researchers (Ingle et al., 2009; Abd El-Aziz et al., 2015; Clarance et al., 2020). The benefits of fungal-mediated synthesis of nanoparticles include the simplicity of preparation and the relatively undemanding stages of the synthesis process (Ganachari et al., 2012; Zare et al., 2017). Moreover, these microorganisms seem to possess an outstanding ability to tolerate metals, and fungal metabolites are involved in the reduction of metal salts as well as the further formation of metallic nanoparticles (Kobashigawa et al., 2019; Rai et al., 2021). Further research needs to focus on optimizing the synthesis process to obtain efficient scale production and nanoproducts with the sought-after bioactivity important for their potential application (Sasani et al., 2023). The adaptation of environmental conditions to the growth of microorganisms as well as synthesis conditions assists in the efficient production of nanoparticles with well-defined morphology and biological activity (Paul and Roychoudhury, 2021; Murillo-Rábago et al., 2022).

The aim of the study was to evaluate the ability of fungal extract from *F. solani* IOR 825 to synthesize AgNPs and ZnONPs and to optimize the reaction parameters for high production yields and biological activity of generated nanoproducts. It is the first report on the synthesis of silver and zinc oxide nanoparticles from *Fusarium solani* IOR 825 strain. The novel nanoparticles were assessed for antimicrobial activities against a wide set of phytopathogenic bacteria, fungi, and oomycetes. Moreover, the potential of these AgNPs and ZnONPs for sterilization of maize (*Zea mays*) seeds and the effect of seeds nanopriming on their germination and seedling growth (shoot and root elongation, fresh and dry mass production) was also evaluated. This is also the first report on the potential use of nanoparticles from *F. solani* species in agriculture for the protection and promotion of maize growth.

2 Material and methods

2.1 Biosynthesis and determination of physical and chemical properties of metal-based nanoparticles

2.1.1 Optimization of fungal growth

For the synthesis of AgNPs and ZnONPs fungal extracts obtained from *F. solani* IOR 825 isolated from parsley was used. The fungal strain was purchased from the bank of plant pathogens of the Institute of Plant Protection (IOR), the National Research Institute of Poland. In order to optimize efficient production of fungal biomass, each strain was cultured in three kinds of media, namely, potato dextrose broth (PDB, A&A Biotechnology), Sabouraud dextrose broth (SDB, Becton Dickinson) and Czapek dox (CDB, Oxoid). Broths (200 mL) were inoculated with the disc (Ø 5 mm) of fungal strain grown for 7 days at 26°C on potato dextrose agar (PDA, Becton Dickinson) cut with a sterile cork borer. Inoculated broth was incubated for 10 days at 26°C in shaking conditions at 150 rpm. Next, fungal biomass was harvested at 6000 rpm for 10 min and washed three times with sterile distilled water to remove medium components. Obtained biomass was weighed and the fungal culture medium that promoted the most efficient biomass production was selected for further studies on mycosynthesis of nanoparticles.

2.1.2 Preparation of fungal extract and mycosynthesis of nanoparticles

The fungal extract used for the synthesis of silver and zinc oxide nanoparticles was prepared from the fungal biomass, as described previously by Wypij et al. (2022) and Trzcińska-Wencel et al. (2023).

Synthesis of AgNPs was carried out as described previously by Trzcińska-Wencel et al. (2023).

Zinc oxide nanoparticles were synthesized after challenging the fungal extract with the aqueous solution of $ZnSO_4$ (100 mM), as a precursor. Two methods were developed for sufficient synthesis of nanoparticles. The first synthesis method (1) involved the combination of the fungal extract, $ZnSO_4$, and NaOH in a ratio of 1:1:1 (v/v/v) with a final volume of 150 mL and heating for 15 min at 40°C. In the second method (2), the pH of the mixture of fungal extract and $ZnSO_4$ (1:1, v/v) was adjusted at pH 11 with NaOH (0.4 M). Finally, biosynthesized ZnONPs were centrifugated at 6000 x g for 10 min (Thermo Scientific, United States), washed three times with sterile distilled water to remove unwanted components, and obtained pellet was dried at 37°C.

2.1.3 Detection and characterization of NPs

Confirmation of the NPs synthesis and evaluation of the physico-chemical properties of the nanoparticles were carried out as previously described by Wypij et al. (2021). The formation of NPs was verified using UV-Vis spectrometry (NanoDrop One, Thermo Fisher Scientific, United States) in the wavelength range from 200 to 700 nm at the resolution of 1 nm.

Transmission Electron Microscopy (TEM) and Energy Dispersive X-ray Spectroscopy (EDX) The morphology, size, and elemental composition of the NPs were specified by TEM and EDX analysis using a transmission electron microscope coupled with energy dispersive X-ray spectrometer (FEI Tecnai F20 X-Twintool, Fei, Hillsboro, OR, United States). Sample preparation involved the suspension of NPs in deionized water and deposition of the solution (2 µL) on a carbon-coated copper grid (mesh size 400 µm). Samples were dried at room temperature for 24 h prior to measurements.

X-ray diffraction (XRD) The powder of NPs was deposited on the sample holder acquiring a smooth surface and used for XRD studies. Analysis was performed with X' Pert PRO Analytical X6 diffractometer (PANalytical, Netherlands) with Ni filter and CuKα (λ = 1.54056 Å) radiation source. The diffraction was recorded over a 2θ range of 5°–120° and compared with the standard database.

Fourier Transform Infrared Spectroscopy (FT-IR) For FTIR analysis, the potassium bromide (KBr) method was used, briefly dried NPs were ground with KBr (1:1, w/w) and used for measurements. The spectrum was recorded in the range of 4,000–400 cm^{-1} using a spectrometer (Spectrum 2000; Perkin-Elmer, Waltham, Massachusetts, United States) running at the resolution of 4 cm^{-1}.

Dynamic light scattering (DLS) Dynamic light scattering and zeta potential measurement were used for the determination of size distribution (hydrodynamic diameter) and stability (zeta potential value) of biosynthesized NPs. Dried NPs were suspended in ultrapure Milli-Q water and sonicated for 15 min at 30 kHz prior to measurements. The analysis was performed using Particulate Systems, NanoPlus HD (Micromeritics, Particulate Systems, Norcross, GA, United States).

2.2 Antimicrobial activity studies

2.2.1 Antibacterial activity

The antibacterial activity of synthesized MNPs was assessed against plant pathogenic bacterial strains, namely, *Agrobacterium tumefaciens* IOR 911, *Pectobacterium carotovorum* PCM 2056, *Pseudomonas syringae* IOR 2188 and *Xanthomonas campestris* IOR 512 according to Clinical Laboratory Standard Institute (CLSI, 2012). Strains were grown in 20 mL of trypticase soy broth (TSB, Becton Dickinson) for 24 h at 26°C under shaking conditions (120 rpm) and used for the preparation of inocula in distilled water at an optical density of 0.5 McFarland scale (1.5×10^8 CFU mL^{-1}). Minimal inhibitory concentrations (MICs) of nanoparticles were determined, in triplicate, by the 2-fold microdilution method in 96-well plates at the concentration range 1–2048 µg mL^{-1}. The final concentration of bacteria in each well was 1.5×10^{-6} CFU mL^{-1} while the final volume of sample in the wells was 150 µL. Both a negative control (sterile medium) and a positive control (inoculated medium) were performed. The MICs of NPs were defined as the concentrations for which no visible growth was noted after 24 h of incubation at 26°C.

After the determination of MICs of NPs, an aliquot (100 µL) of samples from wells with no visible bacterial growth was spread on tryptic soy agar (TSA, Becton Dickinson) in Petri plates and incubated for 24 h at 26°C. The lowest concentration of NPs which resulted in the elimination of 99.9% of bacteria was identified as minimal biocidal concentration (MBC).

2.3 Antifungal activity

2.3.1 Tested microorganisms

Antifungal activity of MNPs was evaluated against: *Alternaria alternata*, *Alternaria alternata* IOR 1783, *Aspergillus niger*, *Botrytis cinerea* IOR 1873, *Colletotrichum acutatum* IOR 2153, *Fusarium culmorum*, *Fusarium culmorum* IOR 2333, *Fusarium culmorum* DSM 114849, *Fusarium graminearum* A, *Fusarium graminearum* D, *Fusarium oxysporum*, *Fusarium oxysporum* IOR 342, *Fusarium oxysporum* D, *Fusarium poae* A, *Fusarium tricinctum*, *Penicillium* sp., *Penicillium spinulosum*, *Phoma lingam* IOR 2284, *Sclerotinia sclerotiorum* IOR 2242 and oomycetes *Phytophthora megasperma* IOR 404, *Phytophthora cryptogea* IOR 2080 and *Phytophthora plurivora* IOR 2303.

2.3.2 Inhibition of fungal mycelia growth

Antifungal activity of nanoparticles was evaluated, in triplicate, using poisoned food technique. The final NPs concentrations in the PDA medium were 100 and 200 µg mL^{-1} for AgNPs, and 100 and 1000 µg mL^{-1} for ZnONPs. The aqueous stock solution of nanoparticles was used to prepare the final concentration of NPs in the agar medium. The required stock solution of nanoparticles was added into cooled molten PDA (45°C) followed by manual rotation in a sterile Erlenmeyer flask to disperse the NPs in the medium. The medium (20 mL) was dispensed into sterile Petri dishes (9 cm in diameter) with a sterile serological pipette to avoid bubbles. The medium was allowed to solidify at room temperature (23°C ± 2°C) for 1 hour. Agar discs with fungal mycelia (6 mm in diameter), grown on PDA medium for 7 days, were cut using a sterile cork borer and aseptically inoculated at the center of the Petri plates. Control plates were PDA media without the nanoparticles inoculated following the same procedure. The plates were incubated at 28°C. The fungal colony diameter was recorded after 7 days of incubation. The percentage inhibition of the mycelial growth of the test fungi by the nanoparticles was calculated using the formula by Philippe et al. (2012).

$$\text{Inhibition of mycelial growth (MGI) (\%)} = \frac{dc - dct}{dc} \text{x100}$$

where dc is the mean diameter of the colony in the control sample, and dct is the mean diameter of the colony in the treated sample.

2.3.3 Inhibition of spore germination

To assess the ability of NPs to inhibit spore germination, minimum inhibitory and minimum fungicidal concentrations (MICs and MFCs) were determined according to the Clinical Laboratory Standard Institute (CLSI, 2012) protocol with slight

modifications. Spore suspensions were prepared by washing fungal colonies grown on PDA medium for 14 days at 26°C with 5 mL sterile distilled water. The spore suspensions were then filtered through a sterile cotton wool filter to remove any residual mycelia. The density of spores in the suspension was set at approx. 1×10^6 spores per mL by using a cell counting chamber (Brand, Germany), 10-fold diluted and used for assays. Assay was performed as earlier described for bacteria, albeit in potato dextrose broth (PDB). The final concentration of spores in each well was 1×10^3 spores per mL. Sterile broth provided negative control while inoculated with spores was positive control. Inoculated plates were incubated for 2 days at 26°C and recorded for MIC. Finally, aliquots (100 µL) from wells without visible microbial growth were spread on the PDA surface and incubated under the same conditions for 7 days for MFC determination. MFC was defined as the lowest concentration at which no fungal growth was observed.

2.4 Influence of NPs on maize (*Zea* mays) seed germination and seedling growth

2.4.1 Seeds sterilization and priming with NPs

For germination assays, seeds of maize were purchased from Torseed S.A (Toruń, Poland). Seeds were surface sterilized for 30 min with 30% H_2O_2 and 70% ethanol (1:1, v:v), followed by 5 times washing with sterile distilled water and placed on ½ Murashige and Skoog (MS) agar medium in sterile culture boxes for 10 days at 22°C ± 2°C for germination. In order to analyze sterilization efficiency, 100 µl of post-wash water from each variant was spread on sterile PDA and Reasoner's 2A agar (R2A) media and incubated for 7 days for the detection of microbial contaminations.

Two varieties of experiments were performed. In the first one, the sterilization potential of both types of NPs to seed surface was evaluated. The 15 non-sterile seeds were soaked for 30 min with 25 mL of AgNPs or ZnONPs solution in water at concentrations of 1, 8, 32, 64, 128, and 256 µg mL^{-1}, washed 5 times with sterile distilled water. Seed sterilized by the standard method and soaked with sterile distilled water served as the control. All seeds were placed on ½ Murashige and Skoog (MS) agar medium in sterile Petri plates for 3 days at 22°C ± 2°C for germination. The germinated seeds were transferred into culture boxes with ½ MS and grown for another 7 days for seedling growth.

As treatment with ZnONPs did not result in seed sterilization, in the second variant of the experiment, seeds treatment with ZnONPs at a concentration range of 1–256 µg mL^{-1} was preceded by standard sterilization method to determine effect of nanoparticles on seed germination and seedling growth. In both experiments seeds treated with sterile distilled water were implemented as a control, and all experiments were performed in triplicate.

2.4.2 Estimation of germination and growth parameters

The root and shoot length were measured with the ruler in centimeters [cm]. Fresh and dry weight mass were also determined in miligrams [mg]. Various parameters of germination and seedlings growth were calculated using the following formulas:

$$Germination\ percentage\ (\%) = \left(\sum n/N\right) x\ 100$$

where ∑n–the total number of seeds germinated after 10 days; N is the total number of seeds used for analysis. Scott et al. (1984)

$$Mean\ germination\ time\ (MGT) = \Sigma\ f^{*}x/\Sigma n$$

where f –number of germinated seeds at day x; x - number of day from sowing; Σn–total number of germinated seeds. Orchard (1997)

$$Germination\ Rate\ Index\ (GRI) = G1/1 + G2/2 + \ldots + Gx/x$$

where G1, G2 . . . Gx–germination percentage in the subsequent days after sowing. Esechie (1994)

$$Vigour\ index\ I = Germination\ \% \times SL$$

where SL - Seedling length (Root + Shoot). Abdul-Baki and Anderson (1973)

$$Vigour\ index\ II = Germination\ \% \times SDW$$

where SDW - Seedling dry weight (Root + Shoot)

2.5 Statistical analyses

Statistica software (StatSoft Inc., Tulsa, OK, United States States) was used for data analysis. Results were shown as mean ± standard error (SE). The means were then compared to determine statistical significance (if $p < 0.05$) by One-way ANOVA followed by Tukey's test.

3 Results

3.1 Biosynthesis and determination of physical and chemical properties of metal-based nanoparticles

3.1.1 Optimization of fungal growth

The most efficient growth of *Fusarium solani* IOR 825 was observed in SDB medium (42.75 ± 1.58 g L^{-1}), followed by CDB (34.22 ± 1.21 g L^{-1}) and PDB (20.44 ± 1.03 g L^{-1}). For further studies, SDB was selected for *F. solani* IOR 825 biomass production.

3.1.2 Mycosynthesis, visual detection, and characterization of NPs

The UV-visible spectrometry of fungal extract from *F. solani* IOR 825 combined with $AgNO_3$ showed a maximum absorbance peak at 420 nm and indicated the formation of AgNPs (Supplementary Figure S1). Synthesis efficiency was estimated at 26.35 mg of AgNPs per 100 mL of fungal extract as presented in Supplementary Table S1. Fungal-mediated synthesis resulted in the formation of spherical and oval-shaped small AgNPs with an average size of 8.27 ± 3.07 and sizes ranging from 2.99 to 21.53 nm (Figures 1A, B). The EDX studies of AgNPs displayed silver and carbon contents at 55.43% and 44.56%, respectively (Supplementary Table S2). X-ray pattern of AgNPs demonstrated peaks at 38.20, 46.31, 64.59, and 77.58 corresponding to reflections of the crystallographic planes (111), (200), (220), and (311), respectively, and revealed the formation of AgNPs (Figure 1C). AgNPs showed Zeta potential of −17.08 mV, while hydrodynamic

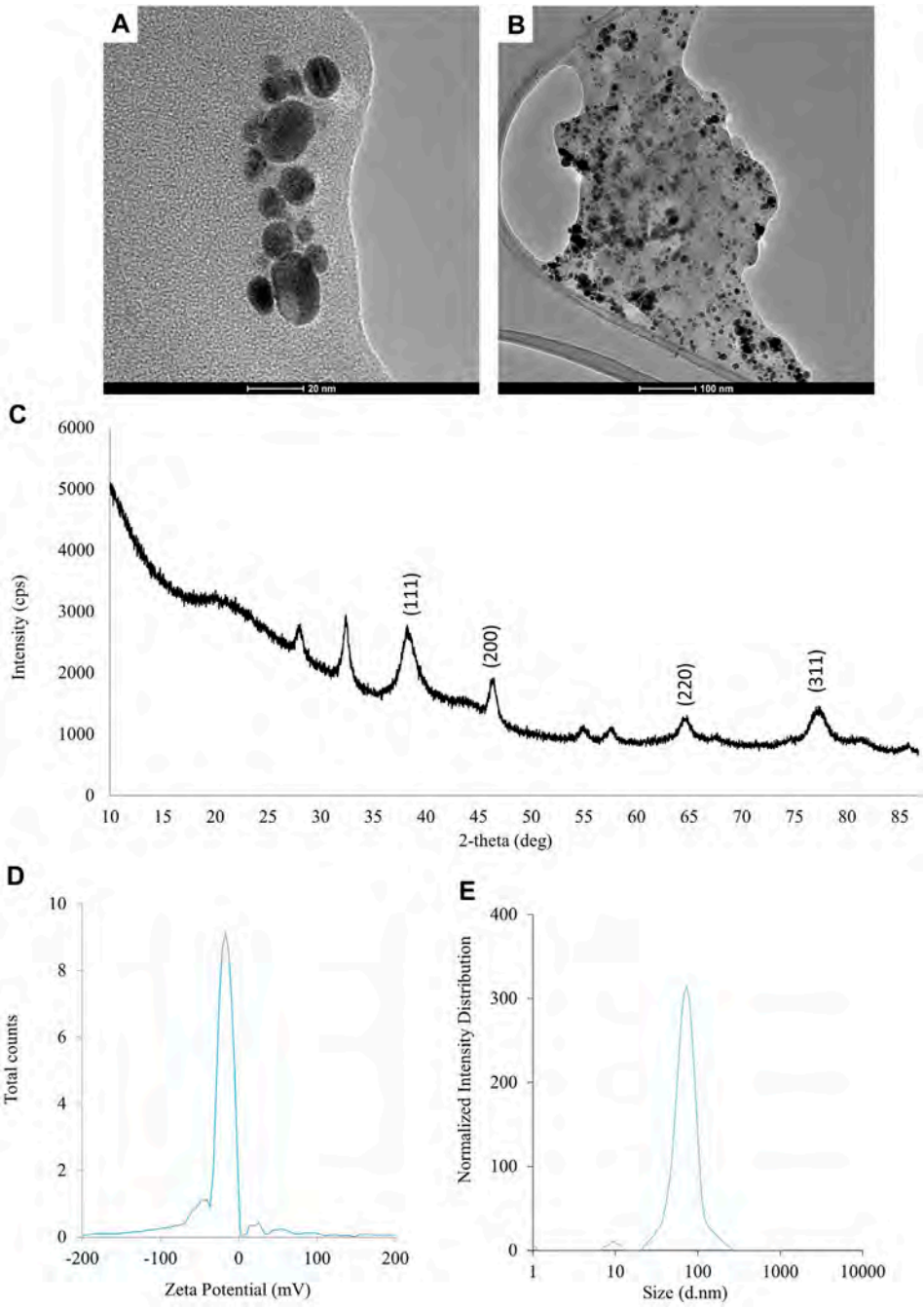

FIGURE 1
The results of the evaluation of physico-chemical properties of AgNPs synthesized from *Fusarium solani* IOR 825: TEM micrographs **(A, B)**, X-ray diffractogram **(C)**, Zeta potential **(D)** and particle diameter from DLS analysis **(E)**.

diameter ranged from 20.6 to 260.5 nm with the highest frequency in the size of 68.3 ± 1.23 nm (Figures 1D, E). FTIR spectra of synthesized AgNPs showed adsorption bands at 3429.39, 2923.83, 2852.66, 1743.48, 1631.79, 1384.43, 1353.79, 1082.81 and 607.31 cm^{-1} (Figure 2).

The synthesis of ZnONPs (1) was observed as a white precipitate in the reaction mixture and confirmed by the presence of maximum absorbance peak at wavelength 375 nm (Supplementary Figure S1). The synthesis yield of ZnONPs (1) was found to be 435.56 mg per 100 mL of fungal extract (Supplementary Table S1). TEM micrographs of ZnONPs (1) showed irregularly shaped structures with an average size of 117.79 ± 4.71 and a size ranging from 54.44 to 209.69 nm (Figures 3A, B). ZnONPs (1) consisted of 70.94% of zinc, 18.76% of oxygen and 10.03% of other minor elements (Mo, Al, Si) (Supplementary Table S2). The diffractogram of ZnONPs (1) showed peaks at 32.10, 34.80, 36.60, 48.10, 57.00, 63.00, 68.40 corresponding to (100), (002), (101), (102), (110), (103), (200), (112), (201) lattice plane values, respectively, and was recognized as hexagonal wurtzite phase of ZnO (Figure 3C). ZnONPs (1) were found

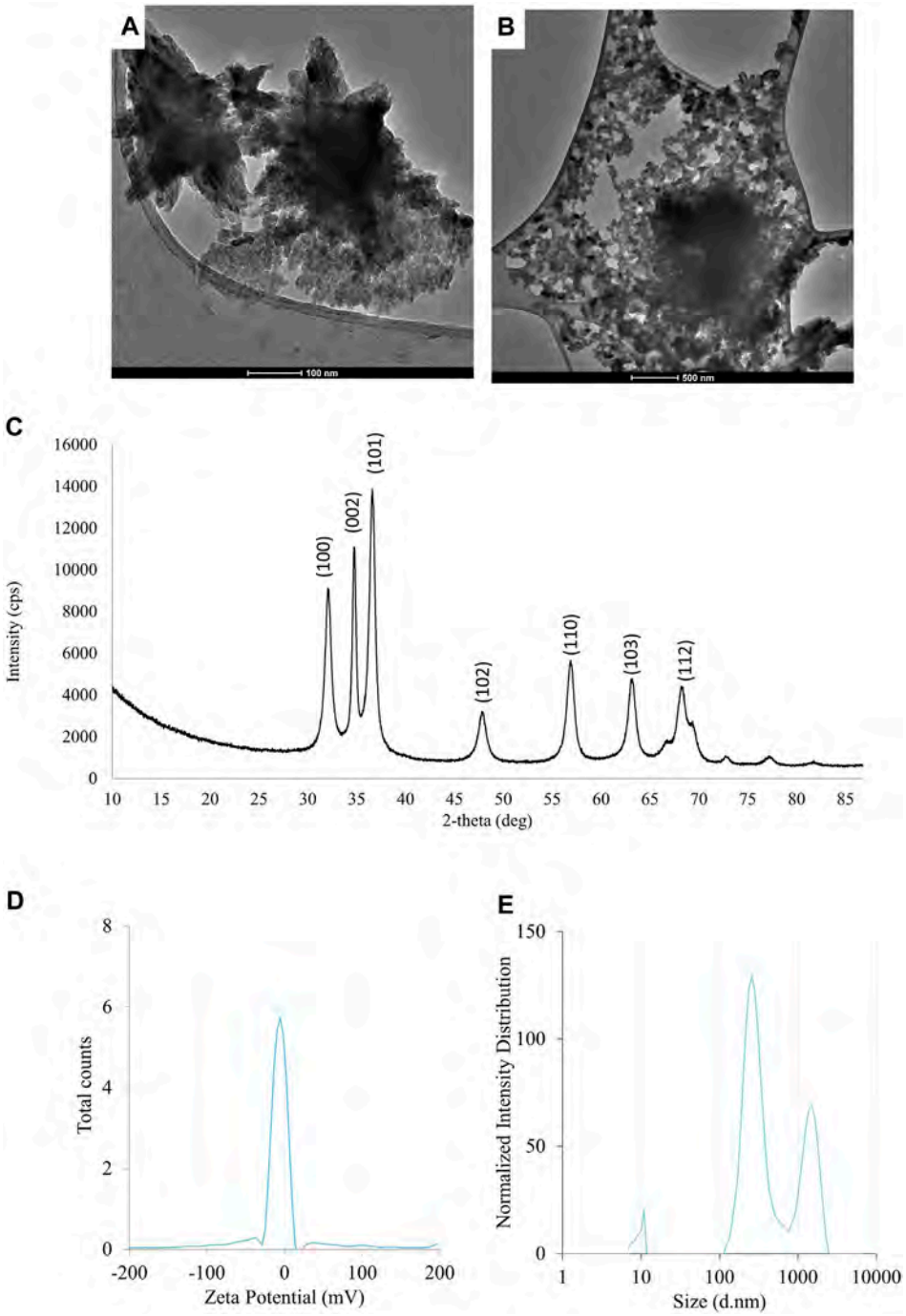

FIGURE 2
The results of the evaluation of physico-chemical properties of ZnONPs (1) synthesized from *Fusarium solani* IOR 825: TEM micrographs **(A,B)**, X-ray diffractogram **(C)**, Zeta potential **(D)** and particle diameter from DLS analysis **(E)**. (1); first method of ZnONP synthesis.

to be negatively charged (−9.39 mV), with hydrodynamic diameters from 112.9 to 2495.9 nm and the largest fraction of size of 261.23 ± 53.5 (Figures 3D, E). The FTIR spectrum showed peaks at 3393.27, 2961.51, 2926.43, 1589.56, 1553.60, 1512.21, 1388.66, 1352.63, 1329.21, 1119.10, 1045.11, 940.98, 830.97, 738.83, 694.20, 608.67 and 480.24 cm^{-1} (Figure 2).

The UV-vis spectrum of ZnONPs (2) demonstrated an adsorption peak at the wavelength of 375 nm (Supplementary Figure S1). The synthesis efficiency reached 525.8 mg of NPs per 100 mL of fungal extract (Supplementary Table S1). TEM analysis displayed nanorods-like NPs with an average length 175.12 ± 7.96 and size ranging from 64.84 to 443.02 nm (Figures 4A, B). The elemental composition from the EDX analysis demonstrated 78.67% of zinc, 19.35% of oxygen and 1.98% of carbon and aluminum (Supplementary Table S2). The XRD peaks at 32.10, 34.80, 36.60, 48.10, 57.00, 63.00, 66.00, 68.40, 69.55 were assigned to

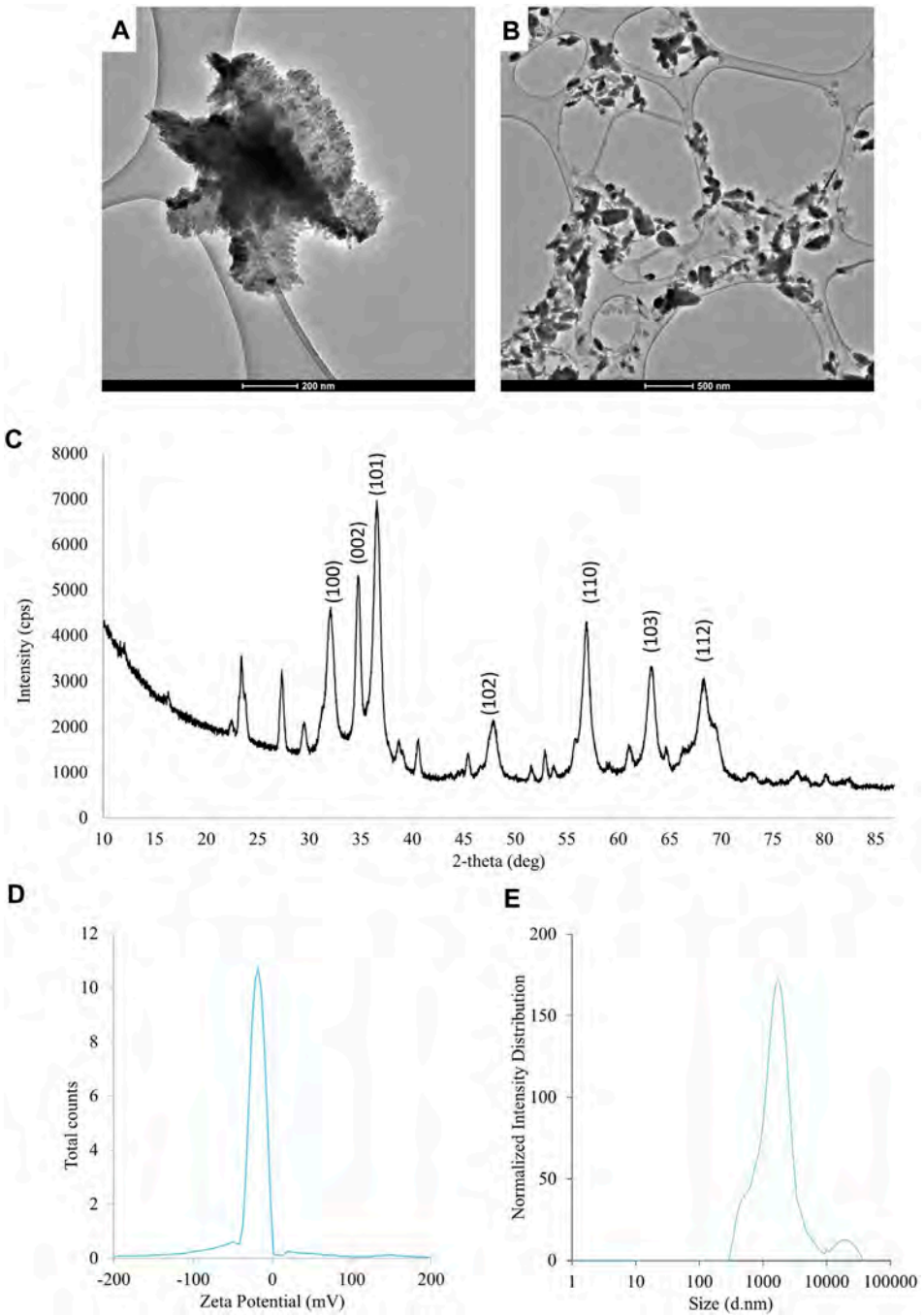

FIGURE 3
The results of the evaluation of physico-chemical properties of ZnONPs (2) synthesized from *Fusarium solani* IOR 825: TEM micrographs **(A,B)**, X-ray diffractogram **(C)**, Zeta potential **(D)** and particle diameter from DLS analysis **(E)**. (2); second method of ZnONP synthesis.

(100), (002), (101), (102), (110), (103), (200), (112), (201) lattice plane of hexagonal wurtzite phase of ZnO (Figure 4C). DLS analyses revealed NPs size between 292.9–9264.2 nm, with the maximum amount of NPs in the size of 1711.82 ± 123.59 nm while Zeta potential measurements showed negatively charged (−21.81 mV) ZnONPs (2) (Figures 4D, E). As shown in Figure 2, FTIR analysis revealed peaks at 3398.02, 2925.85, 2855.49, 1631.63, 1503.82, 1400.67, 1385.79, 1042.27, 912.62, 705.43, 640.79 and 536.84 cm^{-1}. Results from FTIR spectroscopy, summarized in Table 1, indicate the presence of various functional groups on the surface of NPs.

3.2 Antimicrobial activity

Antibacterial activity of NPs from *F. solani* IOR 825 against plant pathogens was determined based on minimal inhibitory (MIC) and biocidal (MBC) concentrations, as presented in Table 2.

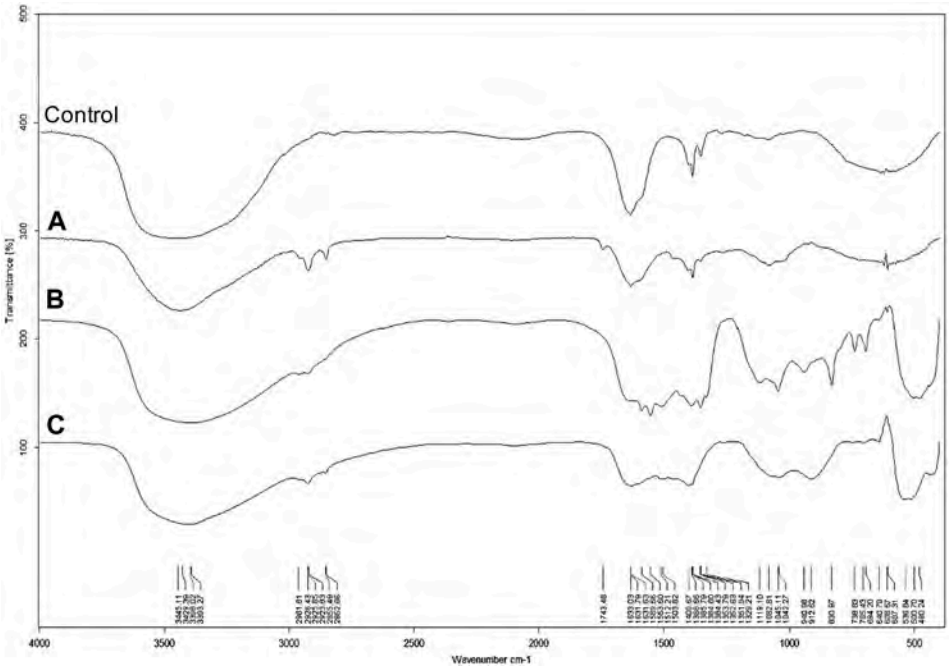

FIGURE 4
FTIR spectra of AgNPs **(A)**, ZnONPs (1) **(B)**, ZnONPs (2) **(C)** synthesized from *Fusarium solani* IOR 825. (1); first method of ZnONP synthesis, (2); second method of ZnONP synthesis.

TABLE 1 An overview of functional groups identified on the surface of AgNPs and ZnONPs from *Fusarium solani* IOR 825 based on FTIR analysis.

Band position [cm^{-1}], assigned functional groups	AgNPs	ZnONPs (1)	ZnONPs (2)
3393–3445 cm^{-1} (N–H stretching, primary amine)	+	+	+
2960–2925 (C-H stretching, aromatic compound)	+	+	+
2855 (O-H stretching, intramolecular bonded)	+	+	+
1740 (C-H bending, aromatic compound)	+	–	–
1632 (C=C stretching, alkene)	+	+	+
1590–1510 (C=O carbonyl group)	–	+	+
1450 (C-H bending, alkane, methyl group)	+	–	–
1400–1350 (C-H bending, aldehyde, alkane)	+	+	+
1120–1040 (C-N stretching, aromatic and aliphatic amine)	+	+	+
940–700 (C=C bending, alkene)	–	+	+
610–480 (metal)	+	+	+

+; – peak determined in an analyzed sample, –; peak not recorded in the analyzed sample.
ZnONP (1); first method of nanoparticle synthesis, ZnONP (2); second method of nanoparticle synthesis.

The highest antibacterial activity of AgNPs was observed against *Pseudomonas syringae,* followed by *Xanthomonas campestris, Agrobacterium tumefaciens* and *Pectobacterium carotovorum*; the MIC and MBC values ranged from 8 to 256 μg mL^{-1} and from 512 to 1024 μg mL^{-1}, respectively.

The MIC values for ZnONPs (1) were determined at a concentration of 256 μg mL^{-1} against *A. tumefaciens* and *X. campestris*, and 1024 μg mL^{-1} against *P. syringae*. In turn, the corresponding MBC values of these nanoparticles were found to be 512, 2048 and 2048 μg mL^{-1}, respectively.

The ZnONPs (2) showed inhibitory effect against *P. syringae* and *X. campestris* at a concentration of 512 μg mL^{-1} while the corresponding biocidal activity of NPs was not determined at the tested concentration range. The inhibitory and biocidal activities against *A. tumefaciens* were recorded at a concentration of 1024 μg mL^{-1}.

None of the ZnONPs were found to be active against *P. carotovorum* at the tested concentration range.

The results of antifungal activity of AgNPs and ZnONPs are shown in Table 3. The food poisoned method revealed that *S. sclerotiorum* was most susceptible to AgNPs, followed by *Phoma lingam, Botrytis*

TABLE 2 Antibacterial activity against phytopathogens of NPs synthesized from *Fusarium solani* IOR 825 presented as minimal inhibitory and biocidal concentrations (MICs and MBCs) [μg mL^{-1}].

Bacterial phytopathogens	AgNPs		ZnONPs (1)		ZnONPs (2)	
	MIC	MBC	MIC	MBC	MIC	MBC
Agrobacterium tumefaciens IOR 911	128	1024	256	512	1024	1024
Pectobacterium carotovorum PCM 2056	256	1024	>2048	>2048	>2048	>2048
Pseudomonas syringae IOR 2188	8	512	1024	2048	512	>2048
Xanthomonas camperstris IOR 512	256	512	256	2048	512	>2048

ZnONP (1); first method of nanoparticle synthesis, ZnONP (2); second method of nanoparticle synthesis.

TABLE 3 Antifungal activity of NPs synthesized from *Fusarium solani* IOR 825 against phytopathogens presented as minimal inhibitory and minimal fungicidal concentrations (MICs and MFCs) [μg mL^{-1}] and mycelial growth inhibition (MGI) [%].

	AgNPs				ZnONPs (1)				ZnONPs (2)			
	% MGI		MIC	MBC	% MGI		MIC	MBC	% MGI		MIC	MBC
NPs contentrations [μg mL^{-1}]	100	200			100	1000			100	1000		
Alternaria alternata	-	57	32	32	-	52	1024	>2048	-	57	1024	>2048
Alternaria alternata IOR 1783	-	48	32	32	-	52	512	512	-	57	256	512
Aspergillus niger	-	-	32	64	-	19	512	2048	-	35	512	2048
Botrytis cinerea IOR 1873	45	58	32	32	-	-	1024	2048	-	-	1024	1024
Colletotrichum acutatum IOR 2153	-	-	64	64	-	-	1024	2048	-	-	1024	2048
Fusarium culmorum	-	-	64	2048	-	-	2048	2048	-	-	2048	2048
Fusarium culmorum IOR 2333	-	-	64	256	-	-	2048	2048	-	-	1024	1024
Fusarium culmorum DMS 114849	-	19	64	2048	-	25	2048	2048	-	23	2048	2048
Fusarium graminearum A	-	-	64	256		47	2048	2048	-	53	1024	1024
Fusarium graminearum D	-	-	32	32	-	-	2048	2048	-	-	1024	>2048
Fusarium oxysporum	-	-	64	64	-	-	2048	2048	-	-	1024	2048
Fusarium oxysporum IOR 342	-	-	128	>2048	40	100	128	512	62	100	256	256
Fusarium oxysporum D	14	20	32	32	-	31	2048	2048	22	34	2048	2048
Fusarium poae A	-	-	32	32	-	38	1024	2048	-	37	2048	2048
Fusarium tricinctum	-	-	64	64	-	-	2048	2048	-	-	>2048	>2048
Penicillium sp.	-	-	64	1024	-	-	2048	>2048	-	-	2048	>2048
Penicillum spinulosum	-	-	64	1024	-	-	2048	>2048	-	-	512	>2048
Phoma lingam IOR 2284	49	61	64	64	39	63	2048	1024	29	60	1024	1024
Sclerotinia sclerotiorum IOR 2242	52	100	16	16	-	72	512	512	-	72	1024	1024
Phytophthora megasperma IOR 404	-	-	32	32	-	-	>2048	>2048	-	-	>2048	>2048
Phytophthora cryptogea IOR 2080	-	-	32	32	-	-	>2048	>2048	-	-	>2048	>2048
Phytophthora plurivora IOR 2303	-	-	32	32	-	-	>2048	>2048	-	-	>2048	>2048

ZnONP (1); first method of nanoparticle synthesis, ZnONP (2); second method of nanoparticle synthesis.
(–); no antifungal activity.

cinerea, and both *Alternaria alternata* strains. The remaining strains were found to be less or not susceptible to AgNPs at the tested concentration range. Determination of MIC and MFC of AgNPs against fungal spores showed their highest activity against *S. sclerotiorum* (MIC and MBC values at 16 μg mL^{-1}). The slightly lower antifungal activity (MIC and MBC = 32 μg mL^{-1}) of AgNPs was noted for both *A. alternata* strains, *B.*

TABLE 4 Germination parameters of maize seeds after sterilization with various concentrations of AgNPs and pretreatment with ZnONPs (1) and ZnONPs (2).

	Treatment [μg mL^{-1}]	% germination	MGT [day]	GRI [%/day]	Vigour index I	Vigour index II
AgNPs	0	90.00	3.78	28.01	2206.16	3957.62
	32	82.50	3.61	29.14	2304.39	4326.20
	64	82.50	3.64	28.89	2436.06	4363.58
	128	87.50	3.66	29.00	2427.12	4347.94
	256	87.50	3.57	29.52	2335.58	3884.63
ZnONPs (1)	0	90	3.78	28.01	2209.35	3957.62
	1	92.5	3.78	27.93	2240.51	3806.82
	8	97.5	3.64	29.19	2324.32	4168.38
	16	90	3.86	27.18	2584.22	4711.75
	32	92.5	3.81	27.48	2854.74	5316.10
	64	90	3.69	28.52	2754.78	4910.63
	128	90	3.75	28.15	2803.71	4932.74
	256	95	3.72	28.38	3036.71	5247.18
ZnONPs (2)	0	90	3.78	28.01	2209.35	3957.62
	1	90	3.76	28.07	2416.50	4234.28
	8	90	3.53	29.95	2498.03	3994.16
	16	100	3.83	27.38	2996.54	5199.35
	32	90	3.83	27.31	2653.71	4602.11
	64	90	3.69	28.52	2792.48	4710.99
	128	92.5	3.73	28.29	3038.07	5111.09
	256	95	3.74	28.20	3093.61	5150.36

ZnONP (1); first method of nanoparticle synthesis, ZnONP (2); second method of nanoparticle synthesis.
MGT; mean germination time, GRI; germination rate index.

cinerea, Fusarium graminearum D, *Fusarium oxysporum* D, *Fusarium poae* A and three *Phytophthora* strains. The AgNPs inhibited spore germination of *Aspergillus niger* at a concentration of 32 μg mL^{-1} while their biocidal effect was achieved at a concentration of 64 μg mL^{-1}. Similarly, MIC and MFC of AgNPs against *P. lingam* spores were noted at 64 μg mL^{-1}. The higher MIC and MBC values of AgNPs, from 64 to 2048 μg mL^{-1}, were determined against the other tested microorganisms, with the exception of *F. oxysporum* IOR 342 for which the MBC values were not determined in the tested concentration range.

The highest mycelial growth inhibition, determined by food poisoned technique, was found for *F. oxysporum* IOR 342, followed by *S. sclerotiorum, P. lingam* and both *A. alternata* strains, when treated with ZnONPs (1). MIC and MFC of ZnONPs (1) against fungal spores were found in the range of 128–2048 μg mL^{-1}. The most sensitive to ZnONPs (1) were spores of *F. oxysporum* IOR 342; the inhibitory and biocidal effects were observed at a concentration of 128 and 512 μg mL^{-1}, respectively. The high susceptibility to ZnONPs (1) was also observed for *A. alternata* IOR 1783 and *S. sclerotiorum* IOR 2242 (MIC and MBC of 512 μg mL^{-1}).

In the case of ZnONPs (2) similar pattern was observed, as described for ZnONPs (1), with exception for MIC and MBC values against *S. sclerotiorum* which were found to be two times higher (Table 3).

None of ZnONPs showed spore inhibition activity, within the concentration ranges tested, against oomycete strains from the genus *Phytophthora* (Table 3).

3.3 Effect of NPs on germination and growth of maize (*Zea* mays) seedlings

The pretreatment of maize seeds with AgNPs at concentrations equal to or higher than 32 μg mL $^{-1}$ was found to be an effective method of seed surface sterilization. However, priming of seeds with ZnONPs within tested concentration range (1–256 μg mL $^{-1}$) showed no sterilization effect. The sterilization of seeds with AgNPs and seeds priming with ZnONPs had no significant effect on maize seed germination, when compared to the control (Table 4).

Values of both vigor indexes (I and II) (Table 4) showed an acceleration of seedling growth after treatment with AgNPs at concentrations of 32, 64 and 128 μg ml $^{-1}$, as indicated by significantly longer shoots and higher seedling dry weight (Figures 5A, C). However, application of the maximum tested concentration of AgNPs (256 μg ml $^{-1}$) resulted in significantly lower fresh biomass of seedlings (507.11 mg) when compared to

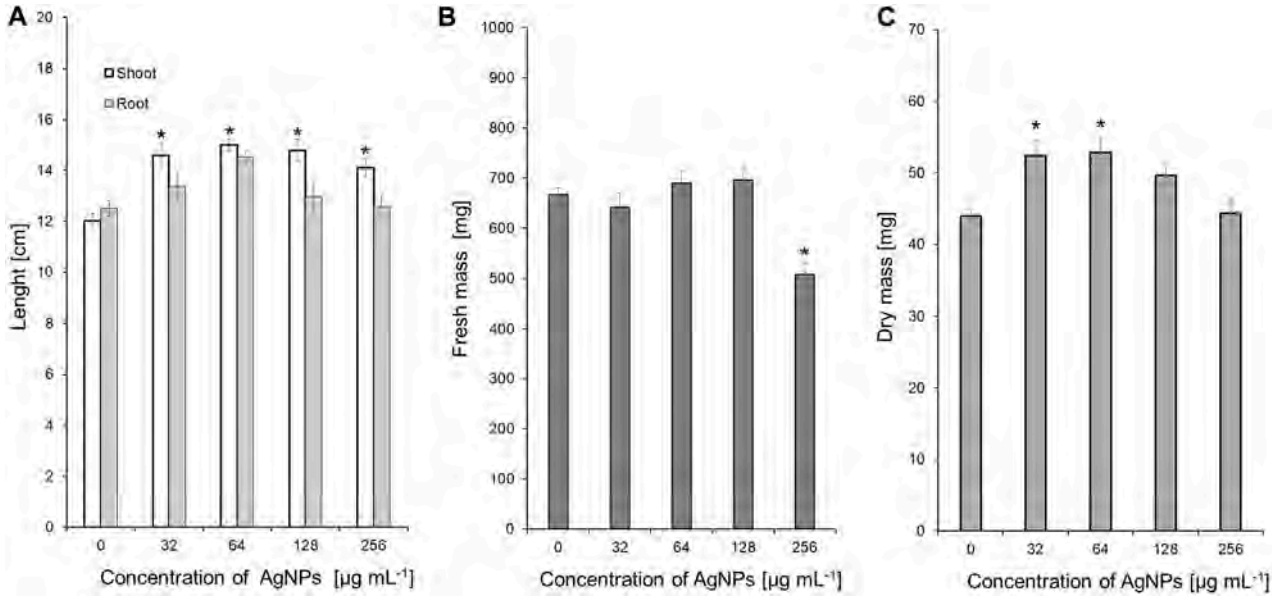

FIGURE 5
The length of shoots and roots **(A)**, as well as fresh **(B)** and dry weight **(C)** of 10-day-old maize seedlings after sterilization of seeds with AgNPs. Data presented as mean and standard error (SE), * denote statistical significance (p-value <0.05) between AgNPs treatment and control.

TABLE 5 Variation in the growth parameters of maize seedlings after treatment of seeds with various concentrations of NPs compared to the control expressed as %.

Treatment [µg mL^{-1}]	Seedling length			Fresh mass			Dry mass		
	AgNPs	ZnONPs (1)	ZnONPs (2)	AgNPs	ZnONPs (1)	ZnONPs (2)	AgNPs	ZnONPs (1)	ZnONPs (2)
1		−1.3	9.4		−6.1	−1.4		−6.4	7.0
8		−2.9	13.1*		−4.9	−5.2		−2.8	0.9
16		17.0	22.1*		24.2*	23.8*		19.1*	18.2*
32	13.9*	25.7*	20.1*	−3.7	32.1*	24.9*	19.3*	30.7*	16.3*
64	20.5*	24.7*	26.4*	3.5	25.7*	27.6*	20.3*	24.1*	19.0*
128	13.2*	26.9*	33.8*	4.3	29.5*	40.5*	13.0	24.6*	25.7*
256	8.9	30.2*	32.7*	−24.0*	30.0*	34.0*	1.0	25.6*	23.3*

*Denote statistical significance (p-value <0.05) between NPs, treatment and control.
ZnONP (1); first method of nanoparticle synthesis, ZnONP (2); second method of nanoparticle synthesis.

control (666.85 mg) (Figure 5B). Although AgNPs were used for sterilization purpose, their lowest effective concentrations (32 and 64 µg mL^{-1}) significantly improved parameters of seedlings, especially seedling length (13.9%–20.5%) and dry mass (19.3%–20.3%), as summarized in Table 5.

The vigour indexes of seedlings were found to be higher after treatment with ZnONPs (1) at concentrations above 16 µg ml $^{-1}$. Seedling vigour index I increased after treatment with ZnONPs (1) at concentrations of 16–256 µg ml $^{-1}$ from 2209 in control to 2584–3037 in tested samples. The highest vigour index II (5316) was found at concentrations of 32 µg ml $^{-1}$ (Table 4). Growth of seedlings roots and shoots was improved by ZnONPs (1) at concentrations of ≥16 and ≥32 µg ml $^{-1}$, respectively (Figures 6A, B). ZnONPs (1) stimulated the growth of maize seedlings as indicated by higher plant fresh and dry weight. A statistically significant increase in maize biomass production was noted for ZnONPs (1) at concentrations of ≥16 µg ml $^{-1}$, when compared to the control (Figures 6C, D). Overall, the growth parameters of maize seedlings were increased after seeds pretreatment with ZnONPs (1) at concentration ranges between 32 and 256 µg mL^{-1}, namely, length (by 26%–30%), fresh weight (by 24%–30%), dry weight (by 19%–30%) (Table 5).

Seedling vigour index I after treatment with ZnONPs (2) at concentrations of 8–256 µg ml $^{-1}$ increased to 2498–3094 in tested seedlings when compared to control (2209). The strongest effect on improving seedling condition was observed after treatment of maize seeds with ZnONPs (2) at a concentration of 16 µg ml $^{-1}$, as proved

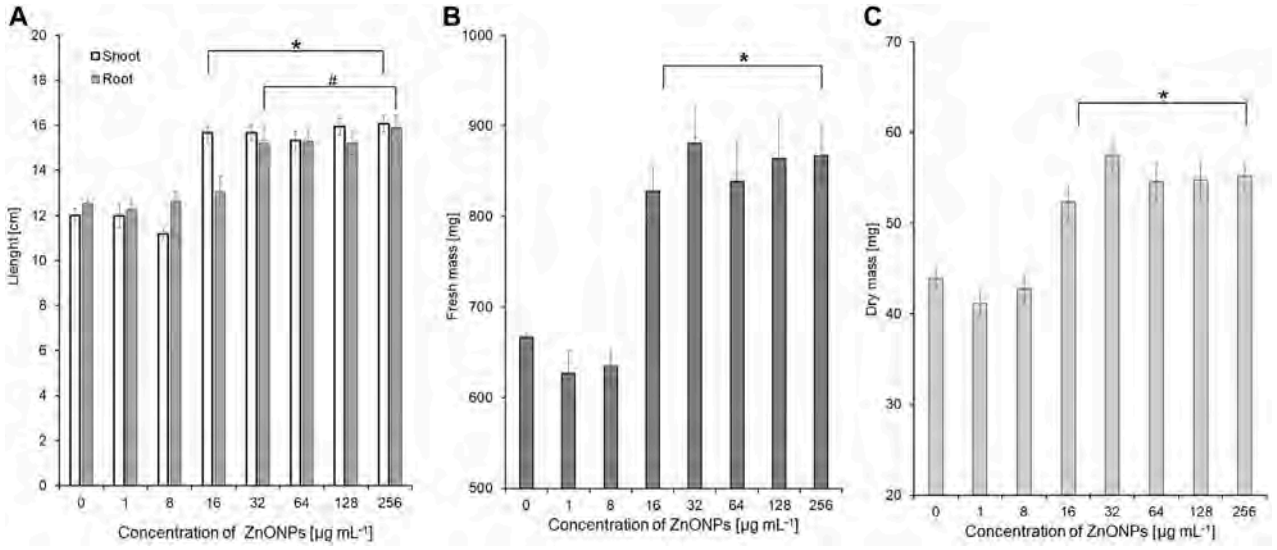

FIGURE 6
The length of shoots and roots **(A)**, as well as fresh **(B)** and dry weight **(C)** of 10-day-old maize seedlings after seed pretreatment with ZnONPs (1) at different concentrations. Data presented as mean and standard error (SE), * and # denote statistical significance (p-value <0.05) between ZnONPs treatment and control. (1); first method of ZnONP synthesis

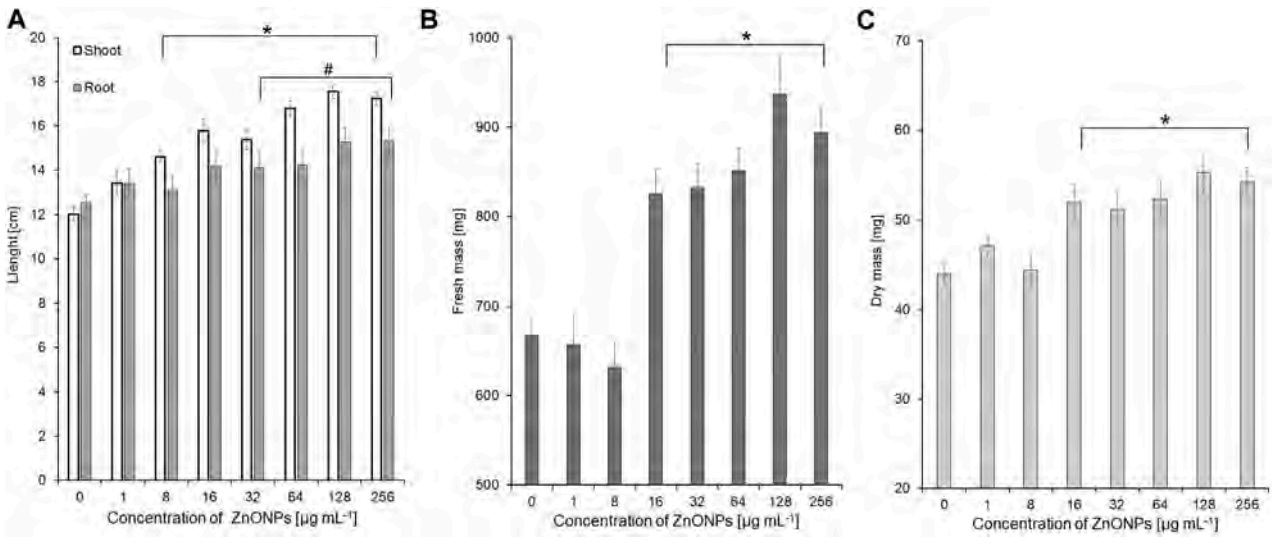

FIGURE 7
The length of shoots and roots **(A)**, as well as fresh **(B)** and dry weight **(C)** of 10-day-old maize seedlings after seed pretreatment with ZnONPs (2) at different concentrations. Data presented as mean and standard error (SE), * and # denote statistical significance (p-value <0.05) between ZnONPs treatment and control. (2); second method of ZnONP synthesis.

by seedling vigour indexes (5199) when compared to untreated control (3958) (Table 4). ZnONPs (2) concentrations ≥8 and 128 µg ml $^{-1}$ stimulated elongation of shoots and roots, respectively (Figure 7A). The fresh and dry weight of seedlings increased after seeds priming with ZnONPs (2); a statistically significant difference was noted for concentrations of ≥16 µg ml $^{-1}$, when compared to the control (Figures 7B, C). To sum up, parameters of maize seedlings were increased after seed pretreatment with ZnONPs (2) at concentration ranges between 32 and 256 µg mL^{-1}. The length of seedlings was improved by 13%–34%, their fresh weight by 24%–40% and dry weight by 16%–26%, as presented in Table 5.

4 Discussion

Fungi play a pivotal role in synthesis of different kinds of nanoparticles. Among these, various *Fusarium* species have

garnered attention by the researchers (Rai et al., 2021). Several researchers successfully synthesized variety of nanoparticles including silver, gold, copper, and zinc oxide NPs synthesis from different strains of *F. solani* (Ingle et al., 2009; Abd El-Aziz et al., 2015; Vijayan et al., 2016; Clarance et al., 2020; El Sayed and El-Sayed, 2020; Sasani et al., 2023). Nevertheless, there is no standard synthesis protocol, as there are many factors that affect the synthesis yields of final product sizes, shapes, and other physicochemical characteristics (Sonawane et al., 2022). Therefore, the present work focuses on optimization of *F. solani* IOR 825 growth, high-throughput synthesis process, and fabrication of biologically active nanoparticles. The main requirements for the biosynthesis of NPs are solutions of metal ions as well as reducing and coating agents (fungal origin), the initial aim was to optimize the growth of the fungus in order to acquire a large portion of biomass, with a view to its subsequent use in preparing a cell-free extract after autolysis. The SDB medium was selected and used for further culture of *F. solani* IOR 825, as the highest fungal growth rate was recorded when compared with PDB or CDB, which may be due to the medium content consisting of dextrose, digested animal tissues (amino acids source) and casein, which provide carbon and nitrogen sources for growth. Similarly, Merlin et al. (2013) pointed out dextrose as the preferred carbon source, and the supplementation of amino acids to the growth medium that resulted in increased growth of *F. solani* strain LCPANF01.

The fungal extract obtained after cell autolysis, which contains variable biomolecules, is preferably used for the synthesis of NPs along with metal precursors. This extracellular process allows for more efficient synthesis of NPs and reduction of post-production steps, such as purification (Michael et al., 2022). Similarly, El Sayed and El-Sayed (2020) used cell-free extracts from *F. solani* KJ 623702 and silver nitrate ($AgNO_3$; final concentration of 0.5 mM) or zinc sulfate ($ZnSO_4$; 0.005 mM), as precursors, for green synthesis of corresponding nanoparticles. A basic visual observation of changes in the color of the mixture to dark brown (AgNPs) or white (ZnONPs) indicated that the synthesis reaction had been initiated. The reduction of metal ions and nanoparticles formation were confirmed by UV-visible spectroscopy and the detection of maximum absorbance peaks at wavelengths 422 nm and 375 nm for AgNPs and ZnONPs, respectively (El Sayed and El-Sayed, 2020), which is in line with our observations. It is well known, that the maximum absorption for AgNPs and ZnONPs ranges from 420 to 450 nm and 330–380 nm, respectively (Musa et al., 2017; Anjum et al., 2023). However, the slight shifts in the UV-vis spectra are due to differences in particle size or the presence of molecules from the biological extracts used for the synthesis (Saion et al., 2013; Ballotin et al., 2016; Musa et al., 2017; Guilger-Casagrande et al., 2019; Urnukhsaikhan et al., 2021). A number of studies on the synthesis of ZnONPs by precipitation method using fungal extracts have been reported (Ghorbani et al., 2015). In our study, two factors, namely, temperature, and pH, were considered for ZnONPs synthesis, as these factors are of great importance for the morphology and size of formed NPs (Moezzi et al., 2011). The heating of the reaction mixture (fungal extract and salt precursor) improves the kinetics of the reaction and affect NPs properties (Moezzi et al., 2011). Authors reported that an increase in the temperature of the reaction from 25°C to 90 °C between addition of $ZnSO_4$ and NaOH led to the lower solubility of the final product, which is important for further applications. In another study, Abdullah et al. (2020) indicated that strong alkaline (pH > 10) reaction environment favors the formation of ZnONPs. It is consistent with observation from this study, the ZnONPs were formed after a temperature rise to 40°C or at room temperature after adjusting the pH to 11.

TEM analysis showed the formation of small and spherical AgNPs from extract of *F. solani* IOR 835 which is in line with recently published reports on the fungal synthesis of such nanoparticles (Lofty et al., 2021; Sasani et al., 2023). These authors synthesized spherical and small (7–23 and 27.5–58.3 nm) AgNPs from *Aspergillus terreus* and *F. solani*, respectively. In contrast, ZnONPs synthesized from *F. solani* IOR 825 were irregularly shaped and bigger (54.44–209.69 nm and 64.84–443.02 nm) than those synthesized from *Trichoderma asperellum* (44–78 nm), it may be related to the use of another salt precursor ($Zn(NO_3)_2$ (Shobha et al., 2023). Whereas, Elrefaey et al., 2022 synthesized rectangular ZnONPs with size between 23 and 140 nm using extract of marine alga *Cystoseira crinite,* $ZnSO_4$ (0.05 M aqueous solution), as a precursor, and 1 M NaOH and heating the reaction mixture up to 45°C for 30 min. Apart from the reaction parameters (precursor, temperature, pH), the physicochemical properties of the bio-NPs are determined by the composition of the fungal extract (Lofty et al., 2021). Similar results, confirming the fungal-mediated formation of AgNPs and ZnONPs with crystalline structures were reported by other researchers (Talam et al., 2012; Nallal et al., 2021; Shobha et al., 2023). Furthermore, Singh D. et al. (2014) revealed that low concentration of precursor (1 mM $AgNO_3$) as well as room temperature (below 25°C) allowed for efficient mycosynthesis of small AgNPs (average size 18 nm) with good stability (Zeta potential–33.4 mV) which prevented their agglomeration. Jain et al. (2020) used zinc sulfate for microbial-mediated synthesis of ZnONPs and suggested that a larger hydrodynamic diameter of biologically synthesized ZnONPs might result from aggregation of particles. The zeta potential is an indicator of surface charge potential which is an important parameter for understanding the stability of nanoparticles in aqueous suspensions. In our studies, a low value of Zeta potential (−9.39 mV) indicated lower stability of ZnONPs (2) and the tendency to aggregate therefore larger particles diameter were observed in DLS analysis. It has been stated in the literature that nanoparticles with a Zeta potential higher than +30 mV or lower than −30 mV are considered to be very stable in the dispersion medium by pushing the same charges (Rai et al., 2018). In another study, Singh K. et al. (2014) pointed out that the DLS results encompass the layer of solvent at the interface and capping biomolecules on the nanoparticles' surface. This was also indicated by the results of FTIR analysis, where bands identified suggest the presence of functional groups from biomolecules such as proteins (N–C-and C–C), aromatic compounds (C-H), amines (C-N), hydrocarbons (C-H, C=C) from the fungal extract which are employed in the synthesis and take part in the reduction of metal ions and subsequent stabilization of the nanoparticles (Abdullah et al., 2020; Wypij et al., 2022). The bands detected between 400 cm^{-1}–600 cm^{-1} imply the formation of bonding between metal and biomolecules present in fungal extract. Our results agree with the findings reported by Salem (2022) and Shobha et al. (2023) where bands for biosynthesized nanoparticles were found at 609.3 and 414.6 cm^{-1} for AgNPs and 534 cm^{-1} for ZnONPs, respectively.

Mycosynthesized NPs from *F. solani* IOR 825 showed antimicrobial activity against a wide range of bacterial and fungal pathogens of plants in a dose-dependent manner, highly depending on the targeted strain. In a similar study by Namburi and coworkers (2021), antibacterial activity of biosynthesized AgNPs was found against *Xanthomonas oryzae* pv. *oryzae* at concentration of 2.5 μg mL^{-1} while another report indicated effectiveness of AgNPs synthesized from *Ulva fasciata* extract against *X. campestris* pv. *malvacearum* at higher concentration of 40 μg mL^{-1} (Rajesh et al., 2012). In a study conducted by Manosalva et al. (2019) AgNPs showed activity against *E. coli*, *P. syringae,* and *Staphylococcus aureus*. The activity of AgNPs was affected by both the bacterial strain and the size of the NPs (23, 92, and 220 nm); the highest sensitivity to AgNPs was detected for *Escherichia coli* (MIC 5–30 μg mL^{-1} and MBC 10–50 μg mL^{-1}), followed by *P. syringae* (MIC 10–40 μg mL^{-1} and MBC 30–60 μg mL^{-1}) and *S. aureus* (MIC 50–80 μg mL^{-1} and MBC 60–80 μg mL^{-1}). In addition, the growth of bacterial strains, namely, *Ralstonia solanacearum*, *P. syringae*, *X. campestris,* and *X. oryzae* was inhibited by ZnONPs synthesized from *C. tomentosa* leaf extract at various concentrations of 125, 500, 250 and 250 μg mL^{-1}, respectively. A similar trend was found in our study, where *P. syringae* showed lower sensitivity to ZnONPs than *X. campestris*. The growth of *P. syringae* was inhibited by ZnONPs (1) and ZnONPs (2) at concentrations of 1024 and 512 μg mL^{-1}, respectively, while *X. campestris* at concentrations of 256 and 512 μg mL^{-1}, respectively. Several studies indicated that antibacterial mechanisms of metal nanoparticles include the destruction of membrane integrity, cell morphology changes, the release of metal ions, and the generation of reactive oxygen species generation (Reddy et al., 2007; Jiang et al., 2016; Gallón et al., 2019). To date, the antifungal activity of biosynthesized AgNPs and ZnONPs were tested against plant pathogens, e.g., *Alternaria brassicae* (Dhiman et al., 2021), *F. oxysporum* (González-Merino et al., 2021; Macías Sánchez et al., 2023) and *F. graminearum* (Ibrahim et al., 2020). For example, Talie et al. (2020) showed lower antifungal activity of AgNPs biosynthesized from *Helvella leucopus* which at a concentration of 20 mg mL^{-1} inhibited spore germination of *Penicillium chrysogenum, A. niger,* and *A. alternata* by 83.21, 77.32% and 69.10%, respectively. The dose-dependent antifungal activity of AgNPs biosynthesized from *Trichoderma viride* against *F. oxysporum* and *Alternaria brassicicola* was reported by Kumari et al. (2019). These results corroborate our studies. Inhibition of mycelial growth was observed at AgNPs concentration of 5%, while complete suppression was determined at a nanoparticle concentration of 25%. In addition, they suggested that the action of AgNPs against *A. brassicicola* led to the generation of superoxide radicals, as well as the disruption of the mycelial structure (Kumari et al., 2019). Jain et al. (2020) evaluated antimicrobial activity of bio-ZnONPs against *X. oryzae* and *Alternaria* sp. with the maximum effect at concentration of 100 and 250 μg ml^{-1}, respectively. Similary to the results of the present work, Jamdagni et al. (2018) found that ZnONPs synthesized from *Nyctanthes arbor-tristis* flower extract showed MIC values of 16 μg mL^{-1} against *A. niger*, 64 μg mL^{-1} against *A. alternata* and *F. oxysporum*, and 128 μg mL^{-1} against *B. cinerea* and *Penicillium expansum*. Whereas, Zhu et al. (2021) reported inhibitory effect of ZnONPs synthesized from *Cinnamomum camphora* (L.) leaf extract on mycelial growth and spore germination of *A. alternata* at concentrations of 20–160 mg mL^{-1}. The proposed mechanisms of antifungal activity of ZnONPs included excessive synthesis and accumulation of malondialdehyde in *A. alternata* cells and damage to the cell membrane, leading to leakage of proteins and nucleic acids (Zhu et al., 2021). In turn, Nandhini et al. (2019) observed the plasmolysis of spores of *Sclerospora graminicola* after treatment with ZnONPs at a concentration of 50 ppm. The differences in antimicrobial activity of both types of ZnONPs biosynthesized from *F. solani* IOR 825 may result from different protocols used for their biofabrication. There are several important factors that affect the synthesis of nanoparticles, including pH of the reaction solution, temperature, pressure and time of the reaction, the concentration of the extracts and precursors, and above all the protocols that are followed for the synthesis process (Patra and Baek, 2014; Wypij et al., 2019). Consequently, nanoparticles of different sizes, shapes, structures and properties are formed which affect their biological activity, including antimicrobial activity (Patra and Baek, 2014; Wypij et al., 2019), as discussed above.

A notable antimicrobial activity of mycosynthesized AgNPs was further confirmed in seeds sterilization tests. The minimum concentration of AgNPs that effectively sterilized maize seeds (32 μg mL^{-1}) was equal to or twice lower than the majority of MICs determined against the tested bacterial and fungal plant pathogens. It is noteworthy that at this concentration no negative effects of AgNPs on seed germination or seedling growth were observed, as mentioned previously. Previously, Morsy et al. (2014) used bioAgNPs form cyanobacteria for sterilization of maize, sorghum, soybean and sesame seeds. Although the authors used 2.5 higher AgNPs dose than in the present study, they noted incomplete sterilization of seeds indicated by the presence of fungi from genera *Fusarium* and *Alternaria* sp. *Aspergillus* spp. or *Pencillium* spp. The results of the present study showed that overall AgNPs at tested concentration range did not negatively affected seedling parameters, except of fresh biomass production at concentration of 256 μg mL^{-1}. It may suggest phytotoxicity of AgNPs at higher doses. Similarly, dose-dependent plant responses to AgNPs priming of seeds were reported by other authors. In the study by Labeeb et al. (2020), AgNPs at concentrations of 20 and 40 mg L^{-1} increased germination of seeds and root length of green pea (*Pisum sativum* L.), while higher concentrations (80 and 160 mg L^{-1}) decreased seed germination and reduced seedling growth. It has been suggested that the phytotoxicity of AgNPs, especially at higher doses, may be related to their small size which facilitates their transport. Once penetrating into plant tissues and cells, they display cytotoxic and genotoxic effects (Scherer et al., 2019).

Although ZnONPs from *F. solani* IOR 825 were found to display non-sterilizing properties, they significantly improved seedling growth by stimulating shoot and root elongation, and fresh and dry matter production. A number of reports have proven the importance of Zn for plant growth and development as well as their resistance to biotic or abiotic stresses, that result from its involvement in physiological processes (Camp, 1945; Rudani et al., 2018). Zn content is essential for plants as a component of the cytochrome complex, for membrane integrity or as a cofactor or complexing ion for enzyme activity (Hacisalihoglu, 2020). Some other reports highlight a significant role of Zn in cell elongation and synthesis of tryptophan, a precursor of indole-3-acetic acid (Mašev and Kutáček, 1966; Sharifi et al., 2016; Sharma et al., 2021). The beneficial effects of ZnONPs on seeds germination and early seedling growth were reported by other authors who showed enhanced wheat grains germination and seedlings growth after priming the seeds with ZnONPs at a

concentration of 10 mg L^{-1} (Rai-Kalal and Jajoo, 2021). Recently, the mechanisms of ZnONPs action as a nanobiofeltilizer for plant growth promotion were studied by Sun et al. (2020), Khan et al. (2021) and El-Badri et al. (2021). They found that these NPs increased zinc uptake by plants, maximized plant production and improved plant resistance to biotic and abiotic stresses. In turn, Itroutwar and coworkers (2020a) identified the accumulation of ZnONPs in maize seeds endosperm leading to improved germination. It has been suggested that ZnONPs facilitate water uptake and increase α-amylase activity during germination (Itroutwar et al., 2020b; Rai-Kalal and Jajoo, 2021; Sharma et al., 2021). Moreover, study conducted by El-Badri and coworkers (2021) showed that ZnONPs activity as plant growth promoter was associated with increasing metabolic activity and modulating the expression of hormone genes (abscisic acid (ABA) and gibberellic acid (GA)) during seed germination. In another study, Rawashdeh et al. (2020) showed improved germination and enhanced biomass production under salt stress after nanopriming seeds with ZnONPs. The mechanism of action of ZnONPs was attributed to stimulation of enzyme biosynthesis, induction of carbohydrate decomposition and increased activity of the antioxidant system.

Both positive and negative effects of ZnONPs on seed germination and plant growth have been reported, but many studies have shown that bio-synthesized ZnONPs are more stable and biocompatible (due to capping and stabilizing agents of natural origin on their surface) compared to chemical ones (Singh et al., 2018). The use of bio-ZnONPs in the preparation of seeds of agronomically important crops can contribute to increased crop productivity and quality. Although there is still limited information on the interaction of nanoparticles with plants, further efforts should be made to clarify them (Tondey et al., 2021).

5 Conclusion

In this study, AgNPs and ZnONPs were effectively synthesized from *F. solani* IOR 825. They were comprehensively characterized using UV–vis, TEM, XRD, DLS, Zeta potential measurements, and FTIR which revealed the small size and spherical shape of AgNPs, the larger size of ZnONPs, and for both stability, crystalline nature, and that mycosynthesized nanoparticles were capped with biomolecules. The AgNPs were found to have strong antimicrobial potential against bacterial pathogens of plants. The lower sensitivity of pathogenic bacteria was demonstrated to ZnONPs. In addition, both types of NPs showed the potential to inhibit fungal spore germination, which is crucial in the fungal spread in the environment, and growth of fungal mycelia. The AgNPs revealed sterilization effect on maize seeds while ZnONPs demonstrated stimulatory effect on seedlings growth by improving fresh and dry biomass production. The present work highlights that mycosynthesized silver and zinc oxide nanoparticles in view of their unique properties, have a high potential as a promising agent to control or prevent the growth of pathogens in agriculture and enhance crop productivity. Nevertheless, continued investigations into their effects on plant development, growth and long-term toxicity are required.

Data availability statement

The original contributions presented in the study are included in the article/Supplementary Material, further inquiries can be directed to the corresponding authors.

Author contributions

PG, MR, and MW conceived research, PG and JT-W designed research, JT-W carried out experiments, APT performed Zeta-potential and DLS analyses, JT-W analyzed data and wrote the manuscript, PG and MR edited and reviewed it. JT-W acquired the funds. All authors contributed to the article and approved the submitted version.

Funding

This research was funded by grant No. 2022/45/N/NZ9/01483 from National Science Centre, Poland. The ACP was funded from IDUB of Nicolaus Copernicus University in Toruń, Poland.

Acknowledgments

MR and PG would like to thank Polish National Agency for Academic Exchange Programme, for financial support under the grant PPN/ULM/2019/1/00117/U/00001.

Conflict of interest

The authors declare that the research was conducted in the absence of any commercial or financial relationships that could be construed as a potential conflict of interest.

Publisher's note

Supplementary material

The Supplementary Material for this article can be found online at: https://www.frontiersin.org/articles/10.3389/fchem.2023.1235437/full#supplementary-material

References

Abd El-Aziz, A. R. M., Al-Othman, M. R., Mahmoud, M. A., and Metwaly, H. A. (2015). Biosynthesis of silver nanoparticles using *Fusarium solani* and its impact on grain borne fungi. *Dig. J. Nanomater. Biostructures* 10, 655–662.

Abdullah, F. H., Bakar, N. A., and Bakar, M. A. (2020). Low temperature biosynthesis of crystalline zinc oxide nanoparticles from *Musa acuminata* peel extract for visible-light degradation of methylene blue. *Optik* 206, 164279. doi:10.1016/j.ijleo.2020.164279

Abdul-Baki, A. A., and Anderson, J. D. (1973). Vigor determination in soybean seed by multiple criteria 1. *Crop Sci.* 13, 630–633. doi:10.2135/cropsci1973.0011183X001300060013x

Abedi, T., Gavanji, S., and Mojiri, A. (2022). Lead and zinc uptake and toxicity in maize and their management. *Plants* 11, 1922. doi:10.3390/plants11151922

Akhtar, N., Khan, S., Jamil, M., Rehman, S. U., Rehman, Z. U., and Rha, E. S. (2022). Combine effect of ZnO NPs and bacteria on protein and gene's expression profile of rice (*Oryza sativa* L) plant. *Toxics* 10, 305. doi:10.3390/toxics10060305

Anjum, S., Vyas, A., and Sofi, T. A. (2023). Fungi-mediated synthesis of nanoparticles: Characterization process and agricultural applications. *J. Sci. Food Agric.* 103, 4727–4741. doi:10.1002/jsfa.12496

Balachandar, R., Gurumoorthy, P., Karmegam, N., Barabadi, H., Subbaiya, R., Anand, K., et al. (2019). Plant-mediated synthesis, characterization and bactericidal potential of emerging silver nanoparticles using stem extract of *Phyllanthus pinnatus*: A recent advance in phytonanotechnology. *J. Clust. Sci.* 30, 1481–1488. doi:10.1007/s10876-019-01591-y

Ballottin, D., Fulaz, S., Souza, M. L., Corio, P., Rodrigues, A. G., Souza, A. O., et al. (2016). Elucidating protein involvement in the stabilization of the biogenic silver nanoparticles. *Nanoscale Res. Lett.* 11, 313–319. doi:10.1186/s11671-016-1538-y

Cakmak, I., Kalayci, M., Kaya, Y., Torun, A. A., Aydin, N., Wang, Y., et al. (2010). Biofortification and localization of zinc in wheat grain. *J. Agri. Food Chem.* 58, 9092–9102. doi:10.1021/jf101197h

Camp, A. F. (1945). Zinc as a nutrient in plant growth. *Soil Sci.* 60, 157–164. doi:10.1097/00010694-194508000-00009

Clarance, P., Luvankar, B., Sales, J., Khusro, A., Agastian, P., Tack, J. C., et al. (2020). Green synthesis and characterization of gold nanoparticles using endophytic fungi *Fusarium solani* and its *in-vitro* anticancer and biomedical applications. *Saudi. J. Biol. Sci.* 27, 706–712. doi:10.1016/j.sjbs.2019.12.026

Clinical and Laboratory Standards Institute (CLSI) (2004). Method for antifungal disk diffusion susceptibility Testing of Yeasts, approved guideline. *Document M44-A*. USA: CLSI Wayne.

Clinical and Laboratory Standards Institute (CLSI) (2012). Methods for dilution antimicrobial susceptibility Tests for Bacteria that grow aerobically; approved standard 9th. *Document M07-A9*. USA: CLSI Wayne.

Consolo, V. F., Torres-Nicolini, A., and Alvarez, V. A. (2020). Mycosinthetized Ag, CuO and ZnO nanoparticles from a promising *Trichoderma harzianum* strain and their antifungal potential against important phytopathogens. *Sci. Rep.* 10, 20499–9. doi:10.1038/s41598-020-77294-6

Czembor, E., Stępień, Ł., and Waśkiewicz, A. (2015). Effect of environmental factors on *Fusarium* species and associated mycotoxins in maize grain grown in Poland. *PloS one* 10, e0133644. doi:10.1371/journal.pone.0133644

de la Rosa, G., Vázquez-Núñez, E., Molina-Guerrero, C., Serafín-Muñoz, A. H., and Vera-Reyes, I. (2021). Interactions of nanomaterials and plants at the cellular level: Current knowledge and relevant gaps. *Nanotechnol. Environ. Eng.* 6, 7–19. doi:10.1007/s41204-020-00100-1

Dhiman, S., Singh, S., Varma, A., and Goel, A. (2021). Phytofabricated zinc oxide nanoparticles as a nanofungicide for management of *Alternaria* blight of Brassica. *Biometals* 34, 1275–1293. doi:10.1007/s10534-021-00342-9

El Sayed, M. T., and El-Sayed, A. S. (2020). Biocidal activity of metal nanoparticles synthesized by *Fusarium solani* against multidrug-resistant bacteria and mycotoxigenic fungi. *J. Microbiol. Biotechnol.* 30, 226–236. doi:10.4014/jmb.1906.06070

El-Badri, A. M., Batool, M., Wang, C., Hashem, A. M., Tabl, K. M., Nishawy, E., et al. (2021). Selenium and zinc oxide nanoparticles modulate the molecular and morpho-physiological processes during seed germination of *Brassica napus* under salt stress. *Ecotoxicol. Environ. Saf.* 225, 112695. doi:10.1016/j.ecoenv.2021.112695

Elrefaey, A. A. K., El-Gamal, A. D., Hamed, S. M., and El-Belely, E. F. (2022). Algae-mediated biosynthesis of zinc oxide nanoparticles from *Cystoseira crinite* (Fucales; Sargassaceae) and it's antimicrobial and antioxidant activities. *Egypt. J. Chem.* 65, 0–240. doi:10.21608/EJCHEM.2021.87722.4231

Esechie, H. (1994). Interaction of salinity and temperature on the germination of sorghum. *J. Agron. Crop Sci.* 172, 194–199. doi:10.1111/j.1439-037X.1994.tb00166.x

Faizan, M., Hayat, S., and Pichtel, J. (2020). "Effects of zinc oxide nanoparticles on crop plants: A perspective analysis," in *Sustainable agriculture Reviews 41. Sustainable agriculture Reviews*. Editors S. Hayat, J. Pichtel, M. Faizan, and Q. Fariduddin (Cham: Springer), 83–99. doi:10.1007/978-3-030-33996-8_4

Feroze, N., Arshad, B., Younas, M., Afridi, M. I., Saqib, S., and Ayaz, A. (2020). Fungal mediated synthesis of silver nanoparticles and evaluation of antibacterial activity. *Microsc. Res. Tech.* 83, 72–80. doi:10.1002/jemt.23390

Gallón, S. M. N., Alpaslan, E., Wang, M., Larese-Casanova, P., Londoño, M. E., Atehortúa, L., et al. (2019). Characterization and study of the antibacterial mechanisms of silver nanoparticles prepared with microalgal exopolysaccharides. *Mater. Sci. Eng. C* 99, 685–695. doi:10.1016/j.msec.2019.01.134

Ganachari, S. V., Bhat, R., Deshpande, R., and Venkataraman, A. (2012). Extracellular biosynthesis of silver nanoparticles using fungi *Penicillium diversum* and their antimicrobial activity studies. *BioNanoScience* 2, 316–321. doi:10.1007/s12668-012-0046-5

Ghorbani, H. R., Mehr, F. P., Pazoki, H., and Rahmani, B. M. (2015). Synthesis of ZnO nanoparticles by precipitation method. *Orient. J. Chem.* 31, 1219–1221. doi:10.13005/ojc/310281

González-Merino, A. M., Hernández-Juárez, A., Betancourt-Galindo, R., Ochoa-Fuentes, Y. M., Valdez-Aguilar, L. A., and Limón-Corona, M. L. (2021). Antifungal activity of zinc oxide nanoparticles in *Fusarium oxysporum - Solanum lycopersicum* pathosystem under controlled conditions. *J. Phytopathol.* 169, 533–544. doi:10.1111/jph.13023

Gudkov, S. V., Burmistrov, D. E., Serov, D. A., Rebezov, M. B., Semenova, A. A., and Lisitsyn, A. B. (2021). A mini review of antibacterial properties of ZnO nanoparticles. *Front. Phys.* 9, 641481. doi:10.3389/fphy.2021.641481

Guilger-Casagrande, M., Germano-Costa, T., Pasquoto-Stigliani, T., Fraceto, L. F., and Lima, R. D. (2019). Biosynthesis of silver nanoparticles employing *Trichoderma harzianum* with enzymatic stimulation for the control of *Sclerotinia sclerotiorum*. *Sci. Rep.* 9, 14351. doi:10.1038/s41598-019-50871-0

Hacisalihoglu, G. (2020). Zinc (Zn): The last nutrient in the alphabet and shedding light on Zn efficiency for the future of crop production under suboptimal Zn. *Plants* 9, 1471. doi:10.3390/plants9111471

Hazarika, A., Yadav, M., Yadav, D. K., and Yadav, H. S. (2022). An overview of the role of nanoparticles in sustainable agriculture. *Biocatal. Agric. Biotechnol.* 43, 102399. doi:10.1016/j.bcab.2022.102399

Ibrahim, E., Zhang, M., Zhang, Y., Hossain, A., Qiu, W., Chen, Y., et al. (2020). Green-synthesization of silver nanoparticles using endophytic bacteria isolated from garlic and its antifungal activity against wheat *Fusarium* head blight pathogen *Fusarium graminearum*. *Nanomaterials* 10, 219. doi:10.3390/nano10020219

Ingle, A., Rai, M., Gade, A., and Bawaskar, M. (2009). *Fusarium solani*: A novel biological agent for the extracellular synthesis of silver nanoparticles. *J. Nanopart. Res.* 11, 2079–2085. doi:10.1007/s11051-008-9573-y

Itroutwar, P. D., Govindaraju, K., Tamilselvan, S., Kannan, M., Raja, K., and Subramanian, K. S. (2020b). Seaweed-based biogenic ZnO nanoparticles for improving agro-morphological characteristics of rice (*Oryza sativa* L). *J. Plant. Growth Regul.* 39, 717–728. doi:10.1007/s00344-019-10012-3

Itroutwar, P. D., Kasivelu, G., Raguraman, V., Malaichamy, K., and Sevathapandian, S. K. (2020a). Effects of biogenic zinc oxide nanoparticles on seed germination and seedling vigor of maize *(Zea mays*). *Biocatal. Agric. Biotechnol.* 29, 101778. doi:10.1016/j.bcab.2020.101778

Jacquet, F., Jeuffroy, M. H., Jouan, J., Le Cadre, E., Litrico, I., Malausa, T., et al. (2022). Pesticide-free agriculture as a new paradigm for research. *Agron. Sustain. Dev.* 42, 8–24. doi:10.1007/s13593-021-00742-8

Jain, D., Bhojiya, A. A., Singh, H., Daima, H. K., Singh, M., Mohanty, S. R., et al. (2020). Microbial fabrication of zinc oxide nanoparticles and evaluation of their antimicrobial and photocatalytic properties. *Front. Chem.* 8, 778. doi:10.3389/fchem.2020.00778

Jamdagni, P., Khatri, P., and Rana, J. S. (2018). Green synthesis of zinc oxide nanoparticles using flower extract of Nyctanthes arbor-tristis and their antifungal activity. *J. King. Saud. Univ. Sci.* 30, 168–175. doi:10.1016/j.jksus.2016.10.002

Jiang, Y., Zhang, L., Wen, D., and Ding, Y. (2016). Role of physical and chemical interactions in the antibacterial behavior of ZnO nanoparticles against *E. coli*. *Mater. Sci. Eng. C* 69, 1361–1366. doi:10.1016/j.msec.2016.08.044

Khan, M. I., Fatima, N., Shakil, M., Tahir, M. B., Riaz, K. N., Rafique, M., et al. (2021). Investigation of *in-vitro* antibacterial and seed germination properties of green synthesized pure and nickel doped ZnO nanoparticles. *Phys. B Condens. Matter* 601, 412563. doi:10.1016/j.physb.2020.412563

Kobashigawa, J. M., Robles, C. A., Ricci, M. L. M., and Carmarán, C. C. (2019). Influence of strong bases on the synthesis of silver nanoparticles (AgNPs) using the ligninolytic fungi *Trametes trogii*. *Saudi J. Biol. Sci.* 26, 1331–1337. doi:10.1016/j.sjbs.2018.09.006

Król, A., Księżak, J., Kubińska, E., and Rozakis, S. (2018). Evaluation of sustainability of maize cultivation in Poland. A Prospect theory—PROMETHEE approach. *Sustainability* 10, 4263. doi:10.3390/su10114263

Kumari, M., Giri, V. P., Pandey, S., Kumar, M., Katiyar, R., Nautiyal, C. S., et al. (2019). An insight into the mechanism of antifungal activity of biogenic nanoparticles than their chemical counterparts. *Pestic. Biochem. Physiol.* 157, 45–52. doi:10.1016/j.pestbp.2019.03.005

Labeeb, M., Badr, A., Haroun, S. A., Mattar, M. Z., El-Kholy, A. S., and El-Mehasseb, I. M. (2020). Ecofriendly synthesis of silver nanoparticles and their effects on early growth and cell division in roots of green pea (*Pisum sativum* L). *Gesunde Pflanz.* 72, 113–127. doi:10.1007/s10343-019-00491-5

Lallo da Silva, B., Abuçafy, M. P., Berbel Manaia, E., Oshiro Junior, J. A., Chiari-Andréo, B. G., Pietro, R. C. R., et al. (2019). <p>Relationship between structure and antimicrobial activity of zinc oxide nanoparticles: An Overview</p>. *Int. J. Nanomedicine* 14, 9395–9410. doi:10.2147/IJN.S216204

Le, D. H., Lee, K. L., Shukla, S., Commandeur, U., and Steinmetz, N. F. (2017). Potato virus X, a filamentous plant viral nanoparticle for doxorubicin delivery in cancer therapy. *Nanoscale* 9, 2348–2357. doi:10.1039/C6NR09099K

Lee, S., Kim, S., Kim, S., and Lee, I. (2013). Assessment of phytotoxicity of ZnO NPs on a medicinal plant, *Fagopyrum esculentum*. *Environ. Sci. Pollut. Res.* 20, 848–854. doi:10.1007/s11356-012-1069-8

Lotfy, W. A., Alkersh, B. M., Sabry, S. A., and Ghozlan, H. A. (2021). Biosynthesis of silver nanoparticles by Aspergillus terreus: Characterization, optimization, and biological activities. *Front. Bioeng. Biotechnol.* 9, 633468. doi:10.3389/fbioe.2021.633468

Macías Sánchez, K. L., González Martínez, H. D. R., Carrera Cerritos, R., and Martínez Espinosa, J. C. (2023). *In vitro* evaluation of the antifungal effect of AgNPs on Fusarium oxysporum f. sp. lycopersici. Nanomater. *(Basel)* 13, 1274. doi:10.3390/nano13071274

Malandrakis, A. A., Kavroulakis, N., and Chrysikopoulos, C. V. (2022). Metal nanoparticles against fungicide resistance: Alternatives or partners? *Pest Manag. Sci.* 78, 3953–3956. doi:10.1002/ps.7014

Manosalva, N., Tortella, G., Cristina Diez, M., Schalchli, H., Seabra, A. B., Durán, N., et al. (2019). Green synthesis of silver nanoparticles: Effect of synthesis reaction parameters on antimicrobial activity. *World J. Microbiol. Biotechnol.* 35, 88–89. doi:10.1007/s11274-019-2664-3

Mašev, N., and Kutáček, M. (1966). The effect of zinc on the biosynthesis of tryptophan, andol auxins and gibberellins in barley. *Biol. Plant.* 8, 142–151. doi:10.1007/BF02930623

Merlin, J. N., Christhudas, I. V. S. N., Kumar, P. P., and Agastian, P. (2013). Optimization of growth and bioactive metabolite production. *Fusarium solani Asian J. Pharm. Clin. Res.* 6, 98–103.

Michael, A., Singh, A., Roy, A., and Islam, M. (2022). Fungal-and algal-derived synthesis of various nanoparticles and their applications. *Bioinorg. Chem. Appl.* 2022, 1–14. doi:10.1155/2022/3142674

Moezzi, A., Cortie, M., and McDonagh, A. (2011). Aqueous pathways for the formation of zinc oxide nanoparticles. *Dalton Trans.* 40, 4871–4878. doi:10.1039/C0DT01748E

Morsy, F. M., Nafady, N. A., Abd-Alla, M. H., and Elhady, D. A. (2014). Green synthesis of silver nanoparticles by water soluble fraction of the extracellular polysaccharides/matrix of the cyanobacterium Nostoc commune and its application as a potent fungal surface sterilizing agent of seed crops. *Univ. J. Microbiol. Res.* 2, 36–43. doi:10.13189/ujmr.2014.020303

Murillo-Rábago, E. I., Vilchis-Nestor, A. R., Juarez-Moreno, K., Garcia-Marin, L. E., Quester, K., and Castro-Longoria, E. (2022). Optimized synthesis of small and stable silver nanoparticles using intracellular and extracellular components of fungi: An alternative for bacterial inhibition. *Antibiotics* 11, 800. doi:10.3390/antibiotics11060800

Musa, I., Qamhieh, N., and Mahmoud, S. T. (2017). Synthesis and length dependent photoluminescence property of zinc oxide nanorods. *Results Phys.* 7, 3552–3556. doi:10.1016/j.rinp.2017.09.035

Nallal, V. U. M., Prabha, K., VethaPotheher, I., Ravindran, B., Baazeem, A., Chang, S. W., et al. (2021). Sunlight-driven rapid and facile synthesis of Silver nanoparticles using *Allium ampeloprasum* extract with enhanced antioxidant and antifungal activity. *Saudi J. Biol. Sci.* 28, 3660–3668. doi:10.1016/j.sjbs.2021.05.001

Namburi, K. R., Kora, A. J., Chetukuri, A., and Kota, V. S. M. K. (2021). Biogenic silver nanoparticles as an antibacterial agent against bacterial leaf blight causing rice phytopathogen *Xanthomonas oryzae* pv. *Oryzae. Bioprocess Biosyst. Eng.* 44, 1975–1988. doi:10.1007/s00449-021-02579-7

Nandhini, M., Rajini, S. B., Udayashankar, A. C., Niranjana, S. R., Lund, O. S., Shetty, H. S., et al. (2019). Biofabricated zinc oxide nanoparticles as an eco-friendly alternative for growth promotion and management of downy mildew of pearl millet. *Crop Prot.* 121, 103–112. doi:10.1016/j.cropro.2019.03.015

Ogunyemi, S. O., Zhang, M., Abdallah, Y., Ahmed, T., Qiu, W., Ali, M. A., et al. (2020). The bio-synthesis of three metal oxide nanoparticles (ZnO, MnO2, and MgO) and their antibacterial activity against the bacterial leaf blight pathogen. *Front. Microbiol.* 11, 588326. doi:10.3389/fmicb.2020.588326

Orchard, T. (1977). Estimating the parameters of plant seedling emergence. *Seed Sci. Technol.* 5, 61–69.

Patra, J. K., and Baek, K. H. (2014). Green nanobiotechnology: Factors affecting synthesis and characterization techniques. *J. Nanomat.* 2014, 1–12. doi:10.1155/2014/417305

Paul, A., and Roychoudhury, A. (2021). Go green to protect plants: Repurposing the antimicrobial activity of biosynthesized silver nanoparticles to combat phytopathogens. *Nanotechnol. Environ. Eng.* 6, 10. doi:10.1007/s41204-021-00103-6

Peng, Y., Li, S. J., Yan, J., Tang, Y., Cheng, J. P., Gao, A. J., et al. (2021). Research progress on phytopathogenic fungi and their role as biocontrol agents. *Front. Microbiol.* 12, 670135. doi:10.3389/fmicb.2021.670135

Pestovsky, Y. S., and Martínez-Antonio, A. (2017). The use of nanoparticles and nanoformulations in agriculture. *J. Nanosci. Nanotechnol.* 17, 8699–8730. doi:10.1166/jnn.2017.15041

Philippe, S., Souaïbou, F., Guy, A., Sébastien, D. T., Boniface, Y., Paulin, A., et al. (2012). Chemical Composition and Antifungal activity of Essential oil of Fresh leaves of *Ocimum gratissimum* from Benin against six Mycotoxigenic Fungi isolated from traditional cheese wagashi. *Int. Res. J. Biol. Sci.* 1, 22–27.

Pillai, A. M., Sivasankarapillai, V. S., Rahdar, A., Joseph, J., Sadeghfar, F., Rajesh, K., et al. (2020). Green synthesis and characterization of zinc oxide nanoparticles with antibacterial and antifungal activity. *J. Mol. Struct.* 1211, 128107. doi:10.1016/j.molstruc.2020.128107

Quinteros, M. A., Bonilla, J. O., Alborés, S. V., Villegas, L. B., and Páez, P. L. (2019). Biogenic nanoparticles: Synthesis, stability and biocompatibility mediated by proteins of *Pseudomonas aeruginosa*. *Colloids Surf. B* 184, 110517. doi:10.1016/j.colsurfb.2019.110517

Rai, M., Gupta, I., Ingle, A. P., Biswas, J. K., and Sinitsyna, O. V. (2018). "Nanomaterials, what are they, why they cause ecotoxicity, and how this can be dealt with?," in *Nanomaterials, Ecotoxicity, safety, and public Perception* Editors M. Rai and J. K. Biswas 1st ed. (Switzerland: Springer Cham), 3–18. doi:10.1007/978-3-030-05144-0_1

Rai, M., Ingle, A. P., Trzcińska-Wencel, J., Wypij, M., Bonde, S., Yadav, A., et al. (2021). Biogenic silver nanoparticles: What we know and what do we need to know? *Nanomaterials* 11, 2901. doi:10.3390/nano11112901

Rai-Kalal, P., and Jajoo, A. (2021). Priming with zinc oxide nanoparticles improve germination and photosynthetic performance in wheat. *Plant Physiol. biochem.* 160, 341–351. doi:10.1016/j.plaphy.2021.01.032

Rajesh, S., Raja, D. P., Rathi, J. M., and Sahayaraj, K. (2012). Biosynthesis of silver nanoparticles using Ulva fasciata (Delile) ethyl acetate extract and its activity against *Xanthomonas campestris* pv. *Malvacearum. J. Biopestic.* 5, 119.

Rawashdeh, R. Y., Harb, A. M., and AlHasan, A. M. (2020). Biological interaction levels of zinc oxide nanoparticles; lettuce seeds as case study. *Heliyon* 6, e03983. doi:10.1016/j.heliyon.2020.e03983

Reddy, K. M., Feris, K., Bell, J., Wingett, D. G., Hanley, C., and Punnoose, A. (2007). Selective toxicity of zinc oxide nanoparticles to prokaryotic and eukaryotic systems. *Appl. Phys. Lett.* 90, 2139021–2139023. doi:10.1063/1.2742324

Rudani, L., Vishal, P., and Kalavati, P. (2018). The importance of zinc in plant growth-A review. *Int. Res. J. Nat. Appl.* 5, 38–48.

Saeed, S., Iqbal, A., and Ashraf, M. A. (2020). Bacterial-mediated synthesis of silver nanoparticles and their significant effect against pathogens. *Environ. Sci. Pollut. Res.* 27, 37347–37356. doi:10.1007/s11356-020-07610-0

Saion, E., Gharibshahi, E., and Naghavi, K. (2013). Size-controlled and optical properties of monodispersed silver nanoparticles synthesized by the radiolytic reduction method. *Int. J. Mol. Sci.* 14, 7880–7896. doi:10.3390/ijms14047880

Salem, S. S. (2022). Baker's yeast-mediated silver nanoparticles: Characterisation and antimicrobial biogenic tool for suppressing pathogenic microbes. *BioNanoScience* 12, 1220–1229. doi:10.1007/s12668-022-01026-5

Sasani, M., Fataei, E., Safari, R., Nasehi, F., and Mosayyebi, M. (2023). Antimicrobial potentials of Iron oxide and silver nanoparticles green-synthesized in *Fusarium solani*. *J. Chem. Health Risks* 13, 95–104. doi:10.22034/JCHR.2021.1928198.1293

Scherer, M. D., Sposito, J. C., Falco, W. F., Grisolia, A. B., Andrade, L. H., Lima, S. M., et al. (2019). Cytotoxic and genotoxic effects of silver nanoparticles on meristematic cells of *Allium cepa* roots: A close analysis of particle size dependence. *Sci. Total Environ.* 660, 459–467. doi:10.1016/j.scitotenv.2018.12.444

Scott, S. J., Jones, R. A., and Williams, W. (1984). Review of data analysis methods for seed germination 1. *Crop Sci.* 24, 1192–1199. doi:10.2135/cropsci1984.0011183X002400060043x

Sharifi, R., Mohammadi, K., and Rokhzadi, A. (2016). Effect of seed priming and foliar application with micronutrients on quality of forage corn (*Zea mays*). *Environ. Exp. Bot.* 14, 151–156. doi:10.22364/eeb.14.21

Sharma, D., Afzal, S., and Singh, N. K. (2021). Nanopriming with phytosynthesized zinc oxide nanoparticles for promoting germination and starch metabolism in rice seeds. *J. Biotechnol.* 336, 64–75. doi:10.1016/j.jbiotec.2021.06.014

Shobha, B., Ashwini, B. S., Ghazwani, M., Hani, U., Atwah, B., Alhumaidi, M. S., et al. (2023). Trichoderma-mediated ZnO nanoparticles and their antibiofilm and antibacterial activities. *J. Fungi* 9, 133. doi:10.3390/jof9020133

Singh, A., Singh, N. Á., Afzal, S., Singh, T., and Hussain, I. (2018). Zinc oxide nanoparticles: A review of their biological synthesis, antimicrobial activity, uptake, translocation and biotransformation in plants. *J. Mat. Sci.* 53, 185–201. doi:10.1007/s10853-017-1544-1

Singh, D., Rathod, V., Ninganagouda, S., Hiremath, J., Singh, A. K., and Mathew, J. (2014). Optimization and characterization of silver nanoparticle by endophytic fungi *Penicillium* sp. isolated from *Curcuma longa* (turmeric) and application studies against MDR *E. coli* and *S. aureus*. *Bioinorg. Chem. Appl.* 2014, 1–8. doi:10.1155/2014/408021

Singh, K., Panghal, M., Kadyan, S., Chaudhary, U., and Yadav, J. P. (2014). Green silver nanoparticles of Phyllanthus amarus: As an antibacterial agent against multi drug resistant clinical isolates of *Pseudomonas aeruginosa*. *J. Nanobiotechnol.* 12, 40–49. doi:10.1186/s12951-014-0040-x

Singh, R. P., Handa, R., and Manchanda, G. (2021). Nanoparticles in sustainable agriculture: An emerging opportunity. *J. Control. Release* 329, 1234–1248. doi:10.1016/j.jconrel.2020.10.051

Sonawane, H., Shelke, D., Chambhare, M., Dixit, N., Math, S., Sen, S., et al. (2022). Fungi-derived agriculturally important nanoparticles and their application in crop

stress management–Prospects and environmental risks. *Environ. Res.* 212, 113543. doi:10.1016/j.envres.2022.113543

Srivastav, A., Ganjewala, D., Singhal, R. K., Rajput, V. D., Minkina, T., Voloshina, M., et al. (2021). Effect of ZnO nanoparticles on growth and biochemical responses of wheat and maize. *Plants* 10, 2556. doi:10.3390/plants10122556

Sun, H., Du, W., Peng, Q., Lv, Z., Mao, H., and Kopittke, P. M. (2020). Development of ZnO nanoparticles as an efficient Zn fertilizer: Using synchrotron-based techniques and laser ablation to examine elemental distribution in wheat grain. *J. Agric. Food Chem.* 68, 5068–5075. doi:10.1021/acs.jafc.0c00084

Talam, S., Karumuri, S. R., and Gunnam, N. (2012). Synthesis, characterization, and spectroscopic properties of ZnO nanoparticles. *Int. Sch. Res. Not.* 2012, 1–6. doi:10.5402/2012/372505

Talie, M. D., Wani, A. H., Ahmad, N. U. S. R. A. T., Bhat, M. Y., and War, J. M. (2020). Green synthesis of silver nanoparticles (AgNPs) using *Helvella leucopus* Pers. and their antimycotic activity against fungi causing fungal rot of Apple. *Asian J. Pharm. Clin. Res.* 13, 161–165. doi:10.22159/ajpcr.2020.v13i4.37024

Tondey, M., Kalia, A., Singh, A., Dheri, G. S., Taggar, M. S., Nepovimova, E., et al. (2021). Seed priming and coating by nano-scale zinc oxide particles improved vegetative growth, yield and quality of fodder maize (*Zea mays*). *Agronomy* 11, 729. doi:10.3390/agronomy11040729

Trzcińska-Wencel, J., Wypij, M., Rai, M., and Golińska, P. (2023). Biogenic nanosilver bearing antimicrobial and antibiofilm activities and its potential for application in agriculture and industry. *Front. Microbiol.* 14, 1125685. doi:10.3389/fmicb.2023.1125685

Umar, W., Hameed, M. K., Aziz, T., Maqsood, M. A., Bilal, H. M., and Rasheed, N. (2021). Synthesis, characterization and application of ZnO nanoparticles for improved growth and Zn biofortification in maize. *Arch. Agron. Soil Sci.* 67, 1164–1176. doi:10.1080/03650340.2020.1782893

Urnukhsaikhan, E., Bold, B. E., Gunbileg, A., Sukhbaatar, N., and Mishig-Ochir, T. (2021). Antibacterial activity and characteristics of silver nanoparticles biosynthesized from *Carduus crispus*. *Sci. Rep.* 11, 21047. doi:10.1038/s41598-021-00520-2

van Dijk, M., Morley, T., Rau, M. L., and Saghai, Y. (2021). A meta-analysis of projected global food demand and population at risk of hunger for the period 2010–2050. *Nat. Food* 2, 494–501. doi:10.1038/s43016-021-00322-9

Verma, A., and Bharadvaja, N. (2022). Plant-mediated synthesis and characterization of silver and copper oxide nanoparticles: Antibacterial and heavy metal removal activity. *J. Clust. Sci.* 33, 1697–1712. doi:10.1007/s10876-021-02091-8

Vijayan, S., Koilaparambil, D., George, T. K., and Manakulam Shaikmoideen, J. (2016). Antibacterial and cytotoxicity studies of silver nanoparticles synthesized by endophytic *Fusarium solani* isolated from *Withania somnifera* (L). *J. Water Environ. Nanotechnol.* 1, 91–103. doi:10.7508/JWENT.2016.02.003

Wan, J., Wang, R., Wang, R., Ju, Q., Wang, Y., and Xu, J. (2019). Comparative physiological and transcriptomic analyses reveal the toxic effects of ZnO nanoparticles on plant growth. *Environ. Sci. Technol. Lett.* 53, 4235–4244. doi:10.1021/acs.est.8b06641

Wei, X., Cao, P., Wang, G., Liu, Y., Song, J., and Han, J. (2021). CuO, ZnO, and γ-Fe2O3 nanoparticles modified the underground biomass and rhizosphere microbial community of *Salvia miltiorrhiza* (Bge) after 165-day exposure. *Ecotoxicol. Environ. Saf.* 217, 112232. doi:10.1016/j.ecoenv.2021.112232

Wypij, M., Jędrzejewski, T., Trzcińska-Wencel, J., Ostrowski, M., Rai, M., and Golińska, P. (2021). Green synthesized silver nanoparticles: Antibacterial and anticancer activities, biocompatibility, and analyses of surface-attached proteins. *Front. Microbiol.* 12, 632505. doi:10.3389/fmicb.2021.632505

Wypij, M., Ostrowski, M., Piska, K., Wójcik-Pszczoła, K., Pękala, E., Rai, M., et al. (2022). Novel antibacterial, cytotoxic and catalytic activities of silver nanoparticles synthesized from acidophilic actinobacterial SL19 with Evidence for protein as coating biomolecule. *J. Microbiol. Biotechnol.* 32, 1195–1208. doi:10.4014/jmb.2205.05006

Wypij, M., Świecimska, M., Dahm, H., Rai, M., and Golinska, P. (2019). Controllable biosynthesis of silver nanoparticles using actinobacterial strains. *Green process. Synth.* 8, 207–214. doi:10.1515/gps-2018-0070

Zakirov, I. V., Khamadeeva, Z. A., and Aleshkina, O. V. (2021). Problems and prospects of ensuring food security in conditions of economic instability: Regional aspect. *IOP Conf. Ser. Earth Environ. Sci.* 666, 042053. doi:10.1088/1755-1315/666/4/042053

Zare, E., Pourseyedi, S., Khatami, M., and Darezereshki, E. (2017). Simple biosynthesis of zinc oxide nanoparticles using nature's source, and it's *in vitro* bioactivity. *J. Mol. Struct.* 1146, 96–103. doi:10.1016/j.molstruc.2017.05.118

Zhu, W., Hu, C., Ren, Y., Lu, Y., Song, Y., Ji, Y., et al. (2021). Green synthesis of zinc oxide nanoparticles using *Cinnamomum camphora* (L) Presl leaf extracts and its antifungal activity. *J. Environ. Chem. Eng.* 9, 106659. doi:10.1016/j.jece.2021.106659

Supplementary Material

Biofabrication of novel silver and zinc oxide nanoparticles from *Fusarium solani* IOR 825 and their potential application in agriculture as biocontrol agents of phytopathogens, and seed germination and seedling growth promoters

Joanna Trzcińska-Wencel [1*], Magdalena Wypij [1], Artur P. Terzyk[2], Mahendra Rai [1,3], Patrycja Golińska[1*]

[1] Department of Microbiology, Faculty of Biological and Veterinary Sciences, Nicolaus Copernicus University in Toruń, Toruń, Poland

[2] Physicochemistry of Carbon Materials Research Group, Department of Chemistry of Materials, Adsorption and Catalysis, Faculty of Chemistry, Nicolaus Copernicus University in Toruń, Toruń, Poland

[2]Nanobiotechnology Laboratory, Department of Biotechnology, SGB Amravati University, Amravati, India;

*** Correspondence:**
Joanna Trzcińska-Wencel
trzcinska@doktorant.umk.pl
Patrycja Golińska
golinska@umk.pl

Supplementary Table 1. Maximum adsorption peaks of mycosynthesized AgNPs and ZnONPs from UV-vis analysis and synthesis efficiency expressed as mg of NPs per 100 mL of *F. solani* IOR 825 extract.

	AgNPs	ZnONPs (1)	ZnONPs (2)
A_{max} wavelength [nm]	420	357	357
Synthesis yield [mg/100 ml]	26.35	435.56	525.8

ZnONP (1); first method of nanoparticle synthesis, ZnONP (2); second method of nanoparticle synthesis

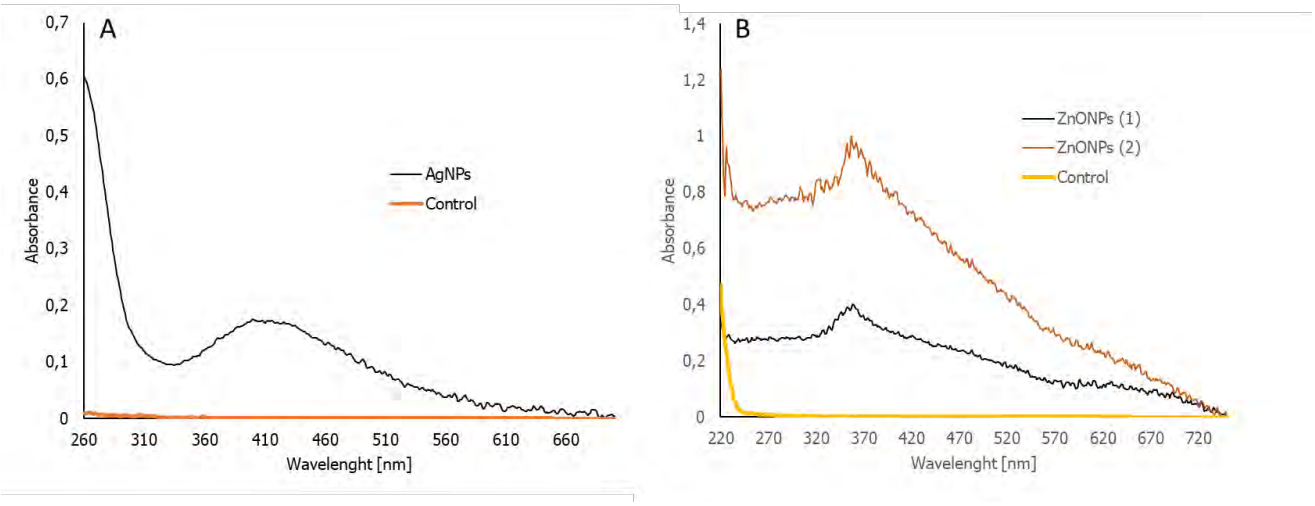

Supplementary Figure 1. UV-vis spectra of AgNPs (A) and ZnONPs (B) synthesized from *Fusarium solani* IOR 825.
ZnONP (1); first method of nanoparticle synthesis, ZnONP (2); second method of nanoparticle synthesis

Supplementary Table 2. Elemental composition of nanoparticles from *Fusarium solani* IOR 825 based on EDX analysis [weight %].

Element	AgNPs	ZnONPs (1)	ZnONPs (2)
Ag	55.43	-	-
Zn	-	70.94	78.67
O	-	18.76	19.35
other	44.56 (C)	10.03 (Mo, Al, Si)	1.98 (C, Al)

ZnONP (1); first method of nanoparticle synthesis, ZnONP (2); second method of nanoparticle synthesis

Wyjaśnienia od autora
W publikacji 4 (P4) w sekcji Results, w tekście błędnie wskazano niektóre odnośniki do wykresów/obrazów,
odnośnik Figure 2 powinien być jako Figure 4
odnośnik Figure 3 powinien być jako Figure 2
odnośnik Figure 4 powinien być jako Figure 3

Pre-sowing treatment with bio-AgNPs as a grain sterilization technique triggers an organspecific and dose-dependent response of the antioxidant system of maize

Joanna Trzcińska-Wencel[1*], Natalia Mucha[1], Mahendra Rai[2], Jarosław Tyburski[1], Patrycja Golinska[1*]

[1]Nicolaus Copernicus University in Toruń, Poland, [2]Sant Gadge Baba Amravati University, India

Submitted to Journal:
Frontiers in Plant Science

Specialty Section:
Technical Advances in Plant Science

Article type:
Original Research Article

Manuscript ID:
1494741

Received on:
11 Sep 2024

Revised on:
22 Feb 2025

Journal website link:
www.frontiersin.org

Pre-sowing treatment with bio-AgNPs as a grain sterilization technique triggers an organ-specific and dose-dependent response of the antioxidant system of maize

Trzcińska-Wencel Joanna[1*], Mucha Natalia[2], Rai Mahendra[3,4] Tyburski Jarosław[2], Golińska Patrycja[1*]

[1] Department of Microbiology, Faculty of Biological and Veterinary Sciences, Nicolaus Copernicus University in Toruń, Toruń, Poland,

[2] Department of Plant Physiology and Biotechnology, Faculty of Biological and Veterinary Sciences, Nicolaus Copernicus University in Toruń, Toruń, Poland

[3] Nanobiotechnology Laboratory, Department of Biotechnology, SGB Amravati University, Amravati, India

[4]Department of Chemistry, Federal University of Piaui (UFPI), University Campus Ministro Petrônio Portella, Ininga, Teresina, Piauí, 64049-550, Brazil

*** Correspondence:**
Trzcińska-Wencel Joanna
trzcinska@doktorant.umk.pl

Golińska Patrycja
golinska@umk.pl

Keywords: biogenic nanoparticles; seed priming; crop protection; plant growth stimulators; *Zea mays*

Abstract

Introduction: In the context of sustainable development, nanotechnology provides effective solutions for enhancing agricultural productivity. Nanomaterials (NMs) can be effective in increasing plant abiotic and biotic stress tolerance or plant pathogens and pest control. Understanding the nanoparticles (NPs)-plant interaction is essential to identify the potential of NPs for growth stimulation. However, the risk of NPs phytotoxicity needs to be estimated. Therefore, this study aimed to evaluate the effects of biologically synthesized silver nanoparticles (AgNPs) from *Fusarium solani* IOR 825 on the growth of *Zea mays*. Furthermore, the effect of AgNPs on oxidative stress and the antioxidant response was assessed.

Methods: In this study, bio-AgNPs were efficiently synthesized from *Fusarium solani* IOR 825 and characterized for physicochemical properties using Transmission Electron Microscopy (TEM), Nanoparticle Tracking Analysis (NTA), Dynamic Light Scattering (DLS), X-ray diffraction (XRD), Fourier Transform Infrared (FTIR) spectroscopy and measurement of Zeta potential. AgNPs were used for the pre-sowing treatment of maize grains to inhibit microbial pathogens present on the seed surface and therefore, to promote germination. The maize grains were sterilized with bio-AgNPs solutions at concentrations of 32 µg mL^{-1}, 128 µg $mL^{-1,}$ and 512 µg mL^{-1} and cultivated for 14 days for plantlet development. Then, germination percentage (%G), mean germination time (MGT), germination rate index (GRI), fresh and dry weight (FW, DW), and the Ag and total chlorophyll content were analyzed. Hydrogen peroxide (H_2O_2) and malondialdehyde (MDA) were determined in leaves, roots, stems, and caryopses to assess the oxidative stress. The antioxidative system response to the AgNPs treatment was studied by determining total glutathione (GSH+GSSG) and ascorbate (ASC) contents as

well as catalase (CAT), superoxide dismutase (SOD), peroxidase (POX) and ascorbate peroxidase (APX) activities.

Results: AgNPs were spherical and small (TEM average diameter of 22.97 ± 9.4 nm; NTA average size of 43 ± 36 nm and DLS average hydrodynamic diameters of 27.44 nm (14 %) and 108.4 nm (86 %). Zeta potential revealed that NPs were negatively charged (-19.5 mV (61.3 %) and -2.93 mV (38.6 %)). The diffractogram of AgNPs confirmed the presence of a face-centered cubic structure of crystalline AgNPs while FTIR spectra showed the presence of biomolecules on their surface. Results showed a dose-dependent effect on maize growth. The increase in length and fresh weight of plants treated with AgNPs concentration of 512 μg mL^{-1} was noted. The treatment with all tested concentrations of AgNPs (32 μg mL^{-1}, 128 μg mL^{-1}, and 512 μg mL^{-1}) resulted in increased dry weight of leaves. Reduced chlorophyll content was observed in plants treated with the highest tested concentration of AgNPs (512 μg mL^{-1}). The treatment of grains with AgNPs decreased H_2O_2 levels in all organs, except the stem where the oxidant's level increased. MDA levels were unaffected except for the highest concentration of AgNPs (512 μg mL^{-1}) which raised the MDA content in leaves. ASC and total glutathione levels were increased in roots and caryopsis, respectively. The highest impact of AgNPs treatment was determined for SOD activity which decreased in leaves, stem, and caryopsis and increased in roots. CAT activity was decreased in leaves, stems, and roots. There was minor effect on POX and APX activity.

Conclusion: Treating *Z. mays* grains with low concentrations of AgNPs (32 μg mL^{-1}) efficiently inhibits maize pathogens, without any negative effect on plant growth and chlorophyll content. Furthermore, it does not provoke oxidative stress. However, AgNPs may affect cellular redox systems if higher concentrations (128 μg mL^{-1} and 512 μg mL^{-1}) are used. The results indicate the potential use of biogenically synthesized AgNPs in agriculture through a crop-safe approach to eliminate pathogens and increase maize production efficiency.

1 Introduction

Maize (*Zea mays*), which belongs to the grass tribe *Andropogoneae* of the Gramineae (Poaceae) family, is one of the most important cereal crop plants, alongside wheat (*Triticum* spp.), and rice (*Oryza sativa*) (FAO, 2022). The main purposes of maize cultivation are grain acquisition (production of groats, flour, starch), silage production (livestock feed), and the use of maize by-products for other purposes, such as biofuel or ethanol production (Rouf Shah et al., 2016). Maize-based food products play a crucial role as a source of nutrients (carbohydrates, proteins, fat, micro- and macroelements) and a wide range of beneficial health substances such as vitamins (riboflavin, thiamine, vitamin C, E) or xanthophylls (lutein and zeaxanthin) (Rouf Shah et al., 2016; Revilla et al., 2022). However, the crop yield of maize is affected by abiotic (water and nutrient availability or climate factors including low temperature) and biotic factors that can highly limit maize growth. Among the abiotic factors, low-temperature inhibits the germination and growth of maize seeds. For example, in spring maize, seedling development is inhibited due to low-temperature stress at germination and the initial stage of seedling development (Zhang et al. 2020). The biotic factors are represented by a wide range of microbial pathogens e.g. *Aspergillus flavus*, *Aspergillus parasiticus*, *Colletotrichum graminicola*, *Fusarium graminearum, Fusarium moniliforme, Penicillium citrinum,* and *Rhizopus stolonifera,* etc. (Goko et al., 2021; Oldenburg & Ellner, 2015). It should be emphasized that germination and early stages of seedling growth are highly sensitive to the presence of pathogenic microbes (Lamichhane et al., 2018).

To overcome the problems caused by the above-mentioned abiotic and biotic factors in order to enhance maize production efficiency, techniques such as fertilization, pesticide application, intercropping, seed treatment and GMO cultivation are commonly used (FAO, 2024; Goodman, 2024). However, these techniques are not entirely effective or safe. For example, fertilization requires a high degree of precision, otherwise, it is ineffective, and excess fertilizer leaks into the environment causing its pollution (Srivastav et al., 2024). Moreover, chemical

fertilizers cause soil degradation (e.g. acidification) which reduces nutrient availability and disrupts the soil microbial ecosystem, ultimately reducing soil productivity (Cao et al., 2025). In turn, the use of pesticides (e.g. organophosphates and carbamates) has significant negative impacts on human and animal health as pesticide residues are detected in feed and food (EFSA, 2024) and on the environment by reducing the population of beneficial soil microorganisms, weakening soil structure and fertility (Tripathi et al., 2020; Brunelle et al., 2024; Cao et al., 2025). Meanwhile, GMO crops are associated with limited human population trust and legal regulations (Goodman, 2024). Therefore, the development of agriculture is directed toward the search for new solutions and sustainable agricultural technologies, including the implementation of innovative methods for pre-sowing seed treatment to enhance germination efficiency and early development of plants (Biswas et al., 2023), thus to improve crop yields.

Nanotechnology, particularly the use of nanoparticles (NPs), has the potential to contribute to the development of modern agriculture. NPs exhibit unique physical and chemical properties, including a high surface-to-volume ratio, and the ability to cross biological membranes and interact effectively with biological systems. In agriculture, NPs have the potential to be used as nano-pesticides, nano-fungicides, nano-herbicides, and nanofertilizers offering significant benefits. They can enhance nutrient uptake, improve stress resistance, and increase photosynthetic efficiency, resulting in improved growth and yield even under challenging conditions. Moreover, their use can reduce the environmental hazards of conventional agricultural chemicals (Singh et al., 2024; Wahab et al., 2024). NPs are effective even at low concentrations and can be delivered through various methods, including seed treatment, foliar spraying, and hydroponic delivery (Mawale et al., 2024; Nile et al., 2022). Unlike traditional fertilizers that often leach into groundwater and water reservoirs causing their pollution, NPs provide control over time and efficient nutrient release for plants (Easwaran et al., 2024; Haydar et al., 2024). Nano-priming is a novel approach for seed pre-sowing treatment with NPs for improving germination speed, promoting seedlings' vigor, and enhancing plant tolerance to stress conditions (Cao et al., 2025; Zhao et al., 2024). Its effectiveness depends on the dose and physicochemical properties of the NPs used, the time and temperature of priming, seed viability, and many other factors (Abbasi Khalaki et al., 2021). Some studies have reported that nanomaterials can penetrate the seed coat, resulting in increased water absorption. This, in turn, stimulates the enzyme system, which leads to rapid germination and seedling development.(Shang et al. 2019). Moreover, nano-enabled seed treatment can increase the disease resistance of crops by boosting immunity, which will reduce the use of pesticides. This unsophisticated, farmer-available, cost-effective, and environment-friendly seed treatment approach may help crop plants fight climate change challenges (Cao et al., 2025; Zhao et al., 2024). Although the application of NPs in agriculture is still in its developmental stages, it holds promise for increasing crop production and resilience against various stressors (Su et al., 2019; Haydar et al., 2024). A wide range of techniques are used to synthesize NPs and each of them has advantages and limitations. Chemical and physical methods of NP synthesis include techniques such as co-precipitation, the sol-gel method, and laser ablation. These procedures allow for the synthesis of uniform products with high efficiency, but require the use of hazardous chemicals that pose health and environmental risks, high temperature, pressure, and energy, as well as additional post-processing steps such as purification or stabilization (Abid et al., 2022). The growing emphasis on environmental protection prompts scientists to invent eco-friendly methods of NPs synthesis that would reduce toxic pollutant formation and minimize harmful environmental impacts (Borehalli Mayegowda et al., 2023). When compared to physical and chemical methods, the use of plants or microorganisms for the biosynthesis of NPs is simple, inexpensive, time-efficient, friendly for environment, and yields stable. Moreover, molecules from biological sources play a dual role as reducing and capping agents; the latter agent prevents NPs from agglomeration and makes them more bioavailable (Sidhu et al., 2022; Trzcińska-Wencel et al., 2023a). Moreover, bio-NPs are believed to be more biocompatible than those synthesized chemically (Dowlath et al., 2021; Xiong et al. 2022). To date, green synthesis methods include plants (Bernardo-Mazariegos et al., 2019; Masum et al., 2019), bacteria (Abdelgadir et al., 2024), fungi

(Golinska et al., 2017; Trzcińska-Wencel et al., 2023b) or algae (Waqif et al., 2024) systems. Several studies showed the great potential of fungi-mediated synthesis to provide high-yield, stable, and biologically active NPs. Due to rapid growth, significant biomass production, secretion of enzymes and adaptability to new conditions, fungal systems seem remarkably capable of synthesizing NPs, both intracellularly or extracellularly. The fungal-mediated synthesis of a wide range of NPs, including silver (AgNPs), gold (AuNPs), copper (CuNPs), zinc (ZnONPs), etc., of various shapes and sizes has been explored among different genera such as *Aspergillus*, *Colletotrichum*, *Fusarium*, *Penicillium* or *Trichoderma* (Rai & Golińska, 2023; Anjum et al., 2023). Key factors affecting the properties of mycosynthesized NPs are fungal strain, condition of growth, preparation of fungal extract, as well reaction condition e.g., type and concentration of precursor, time, pH or temperature (Brady et al., 2023). Several studies pointed out the biologically synthesized AgNPs as antimicrobials or plant growth stimulators (Mahakham et al., 2017; Acharya et al., 2020; Sencan et al., 2024). It has been shown that NPs-plant interactions depend on many variables, including the type, shape and size of the NPs, their dose and application method, as well as the plant species (Syu et al., 2014; Krishnasamy et al., 2024). AgNPs can activate expression of genes related to cell proliferation, metabolism, and hormone signaling pathways (Syu et al., 2014). Recently, Koley et al. (2023) reported that AgNPs improve germination and increase plant biomass by affecting hydrolytic enzyme activity and modulating ROS generation in seeds of chickpeas, peas and mung beans. Other studies demonstrated dose-dependent effects of AgNPs treatment on seedling growth, biochemical parameters and antioxidant system activity, highlighting the adverse effects of higher concentrations, implying a potential toxic effect (Karim et al., 2023). Since the results of studies on the effects of AgNPs on plants are limited and inconclusive, in terms of positive or negative effects on seed germination and subsequent seedling growth, there is still a need for further research (Li et al., 2017; Guilger-Casagrande et al., 2022).

The present work is a continuation of our study on efficient biosynthesis of AgNPs using *Fusarium solani* IOR 825 and their antimicrobial activity against bacterial and fungal plant pathogens, including sterilization of maize grains (Trzcińska-Wencel et al., 2023b). Those preliminary studies also determined the positive effect of bio-AgNPs on germination and basic growth parameters of seven-day-old maize seedlings. It was the first time when *Fusarium solani* IOR 825 was used as an efficient, economical, harmless, eco-friendly, and acceptable method for the synthesis of small-sized, negatively charged and stable (bio-capped) AgNPs. These NPs showed antibacterial and antifungal activity against a set of plant pathogens and effectively sterilized maize grains at low concentrations preventing the development of grain-born microorganisms. Based on these excellent outcomes we aimed to develop AgNPs through the green chemistry route with the ambition that these particles contribute some beneficial effects to industrial agriculture in the future to protect and improve maize growth without posing toxic effects or accumulation in plants. Therefore, this study aims to evaluate the effect of three selected concentrations of bio-AgNPs on the germination of maize grains and plantlet vigor, as well as on the oxidative stress parameters and the antioxidant response within individual plant organs, such as leaves, stem, roots and caryopses of 14-day-old maize plantlets.

2 Material and methods

2.1 Biosynthesis and physicochemical characteristics of AgNPs from *Fusarium solani* IOR 825

The biosynthesis and characteristics of AgNPs synthesized from *Fusarium solani* IOR 825 were performed as described previously by Trzcińska-Wencel et al. (2023b). Briefly, AgNPs were synthesized using fungal autolysate in water. For this purpose fungal strain was grown in Potato Dextrose Broth (PDB, A&A Biotechnology) at 26 °C for 7 days, followed by centrifugation (6500 × g, 10 min), biomass washing with sterile distilled water and resuspending in water (100 mL of water for 10 g of biomass) for 3 days for autolysis.

Autolysate was centrifugated (4000 × *g*, 5 min) and filtrated by sterile filter paper and used for challenging with 100 mM silver nitrate ($AgNO_3$; final concentration of 1 mM). The reaction mixture was sunlight-treated and incubated for 7 days in darkness. After this incubation period, AgNPs were centrifuged (13000 × g, 1 h) and dried at 37 °C. The mass of AgNPs was determined in mg and the powder was used to prepare the stock solution of 2048 μg mL^{-1} for further analyses. For maize grain treatment, the AgNPs stock solution was used to prepare final (32 μg mL^{-1}, 128 μg mL^{-1} and 512 μg mL^{-1}) concentrations Trzcińska-Wencel et al. (2023b). The biosynthesis of AgNPs was confirmed by using UV-Vis spectroscopy (NanoDrop One, Thermo Fisher Scientific, United States) at the wavelength range 200-700 nm with a resolution of 1 nm. The size and shape of AgNPs were determined using Transmission Electron Microscopy (TEM) (FEI, Tecnai 12 Netherland) after applying AgNPs solution on a carbon-coated copper grid with 400 μm mesh size and drying at room temperature for 24 hours. The size of AgNPs was measured based on TEM micrographs using Image J software. X-ray powder diffraction (XRD) (X' Pert PRO Analytical X6 diffractometer, PANalytical, Netherlands) with Cu Kα (λ = 1.54056 Å) radiation source and Ni as a filter in the 2θ range of 5°–120°. The functional groups on the surface of AgNPs were determined by Fourier Transform Infrared Spectroscopy (FTIR) (Spectrum 2000, Perkin-Elmer, Waltham, Massachusetts, USA). Before analysis AgNPs powder was combined with KBr (1:100 ratio; w/w) and analyzed in the range 400–4 000 cm^{-1} at a resolution of 4 cm^{-1}. Size distribution and surface potential of AgNPs in MilliQ water solution were evaluated by Nanoparticle Tracking Analysis (NTA LM20, Nanosight Limited, Amesbury, UK) and dynamic light scattering (DLS), and Zeta potential measurement (Zetasizer Nano-ZS 90, Malvern, UK). Software provided by the equipment manufacturer was used to analyze the obtained results, namely NTA, version 2.3 Build 0033 and Zetasizer Software, version 6.32.

2.2 Grains preparation, growth conditions and plant material

Maize (*Zea mays*) grains (Torseed S.A, Toruń, Poland) were sterilized in previously selected concentrations (32 μg mL^{-1} and 128 μg mL^{-1}) of AgNPs as described by Trzcińska-Wencel et al. (2023b) while a concentration of 512 μg mL^{-1} was added to this study to expand significantly the concentration range of AgNPs used for treatment of grains. Briefly, for each variant, 25 grains were selected and sterilized at room temperature for 30 min with 25 mL of 30 % H_2O_2 and 70 % ethanol, (1:1, v:v) or with 25 mL of AgNPs solutions at the concentrations of 32 μg mL^{-1}, 128 μg mL^{-1} and 512 μg mL^{-1}, and five times washed with sterile distilled water. Grains were placed on ½ Murashige and Skoog (MS) agar and germinated at 22 °C ± 2 °C for 14 days. The 14-day-old plantlets at the V2 growth stage were harvested, their length, fresh and dry weight were measured, and the plant material for biochemical analysis was frozen in liquid nitrogen immediately after harvesting and stored at -80 °C. All these parameters were estimated for root, leaves, stem and caryopsis separately (Supplementary Figure S1).

2.3 Grain germination and plantlet parameters

The parameters of grain germination were calculated, as follows:

$$G\%\ (\%) = (\sum n / N) \times 100$$

where: G% - germination percentage; $\sum n$ – the total number of grains germinated after 14 days; N - total number of grains sown (Scott et al., 1984).

$$MGT = \Sigma f^{*}x / \Sigma n$$

where: MGT- mean germination time; f –number of germinated grains at day x; x - number of days from sowing; Σn – total number of germinated grains (Orchard, 1977).

$$GRI = G1/1+G2/2+\ldots+Gx/x$$

where: GRI – germination rate index; G1, G2 … Gx – germination percentage in the subsequent days after sowing (Esechie, 1994).

Vigour index I = G % × PL

where: G% - germination percentage; PL –length of plantlets

Vigour index II = G % × PDW

where: G% - germination percentage; PDW - dry weight of plantlets (Abdul-Baki & Anderson, 1973)

The length of the shoot was measured using a ruler and expressed in cm, the fresh and dry weight of the leaves, stems, roots and caryopsis were determined in mg.

2.4 Detection of AgNPs in maize

The plant material was washed and dried at 50 ºC for 48 hours, then finely powdered and used for energy dispersive spectroscopy (EDS) analysis to assess elemental composition using a scanning electron microscope (LEO Electron Microscopy model 1430 VP Ltd, UK) coupled with an energy dispersive X-ray spectrometer (Quantax 200 with XFlash 4010 detector, Bruker AXS, Germany) (Kumari et al., 2024).

2.5 Leaf chlorophyll content

The total chlorophyll content in maize leaves was assayed according to the method described by Witham et al. (1971). Shortly, the powdered leaf tissue (0.5 g) was extracted with 1.5 ml of 80 % cooled acetone, then centrifuged at 5 000 × *g* for 5 min (Thermo Scientific, USA). The supernatant was drained into a 15 mL test tube, and the extraction of the remaining pellet was repeated 5 times (until the green color disappeared). Supernatants were combined and the absorbance of the samples was read at $\lambda_{645\ nm}$ and $\lambda_{663\ nm}$ using U-1800 spectrophotometer (Hitachi, Tokyo, Japan). The amount of total chlorophyll was calculated based on the formula:

$$\text{Total chlorophyll (mg per g FW)} = 20.2 \times (\text{Abs}\ \lambda_{645\ nm}) + 8.02 \times (\text{Abs}\ \lambda_{663\ nm}) \times (V/1000 \times FW)$$

where: V - final volume of the extract (mL); FW - fresh weight of the leaf (g)

2.6 Oxidative stress parameters and the antioxidant system activity

2.6.1 Hydrogen peroxide (H_2O_2) content

H_2O_2 content was determined according to the method described by Veljovic-Jovanovic et al. (2002) with their own modifications. The plant material (0.5 g) was ground in liquid nitrogen with a mortar and pestle, and extracted with 5 ml of 0.1 % trichloroacetic acid (TCA). After centrifugation at 10 000 × *g* at 4 °C for 10 min (Thermo Scientific, USA), the 750 µL of supernatant was taken for assay. The reaction mixture contained 125 µL of 19.8 mM 3-(dimethylamino)benzoic acid (DMAB) (Sigma) in 0.1 M phosphate buffer (pH 6.5), 115 µL of 0.456 mM 3-methyl-2-benzothiazolinone hydrazone hydrochloride (MBTH) and 10 µL of horseradish peroxidase (HRP) (Sigma) (25 U in the final volume of 1 mL). After incubation at 25 °C for 20 min the absorbance was measured at $\lambda_{590\ nm}$ using a U-1800 spectrophotometer (Hitachi, Tokyo, Japan), and H_2O_2 concentration (µmol per 1 g of fresh weight) was calculated from the standard curve.

2.6.2 Lipid peroxidation by malondialdehyde (MDA) level determination

Lipid peroxidation was determined by assessing MDA level after MDA-thiobarbituric acid (TBA) complex formation, under acidic conditions (Hodges et al., 1999). The 0.5 g of each plant organ was homogenized in liquid nitrogen and extracted with 5 mL of 80 % ethanol supplemented with 0.01 % butylated hydroxytoluene (BHT). The extract was centrifuged at 3000 × *g* for 10 min at 4 °C (Thermo Scientific, USA). The supernatant

was mixed with 20 % trichloroacetic acid (TCA) containing 0.5 % TBA and heated at 95 °C for 20 min in a water bath, and then cooled immediately on ice. The sample was centrifuged at 3000 × *g* and 4 °C for 10 min. The absorbance of the supernatant was measured at wavelengths 600 nm, 532 nm and 440 nm (U-1800 spectrophotometer, Hitachi, Tokyo, Japan). MDA level was calculated by using the equations:

$$[(Abs532_{+TBA} - Abs600_{+TBA}) - (Abs532_{-TBA} - Abs600_{-TBA})] = A \quad (1)$$

$$[(Abs440_{+TBA} - Abs600_{+TBA}) \times 0.0571] = B \quad (2)$$

$$\text{MDA equiv (nmol mL}^{-1}) = ((A - B)/\varepsilon) \times 10^3 \quad (3)$$

where: ε is corrected extinction coefficient of MDA (157 mM^{-1} cm^{-1}); $Abs532_{+TBA} - Abs600_{+TBA}$= absorbance of TBA-MDA complexes at 532 nm corrected for non-specific absorbance at 600 nm; and $Abs532_{-TBA} - Abs600_{-TBA}$ = absorbance of compounds in extract-solution without TBA at 532 nm corrected for non-specific absorbance at 600 nm; $[(Abs440_{+TBA} - Abs600_{+TBA}) \times 0.0571]$ = correction for nonspecific TBA-sugar complexes according to Hodges et al. (1999).

2.6.3 Total glutathione (GSH+GSSG) content

The 1 mL of 5 % 5-sulfosalicylic acid (SSA) was used for deproteinization of 0.1 g of homogenized plant material. After 10 min incubation on ice, the samples were centrifuged at 10 000 × *g* for 10 min. Then, the supernatant was 20-fold diluted and used for analysis. Total glutathione level was determined by assessing the reduction rate of 5,5'-dithiobis (2-nitrobenzoic acid) (DTNB) to yellow 5-thio-2-nitrobenzoic acid (TNB) by GSH with Glutathione Assay Kit (Catalog Number CS0260, Sigma-Aldrich, USA), according to manufacturer's instruction. In the reaction mixture, the glutathione reductase reduced the glutathione disulfide (GSSG) to GSH at the expense of NADPH oxidation. TNB formation rate was measured spectrophotometrically at λ_{412nm} for 5 min using a plate reader (SpectraMax iD3 Multi-Mode Microplate Reader, Molecular Devices, USA). The results were calculated by comparison to a standard curve based on a series of GSH concentrations and expressed as the nmol of total glutathione (GSH+GSSG) per 1 gram of FW.

2.6.4 Estimation of reduced and total (reduced and oxidized) ascorbate contents and ascorbate redox ratio

The plant material (0.5 g) was ground in liquid nitrogen and mixed with 5 mL 5 % trichloroacetic acid (TCA). After 10 min of incubation on ice, the samples were centrifuged at 14 000 × *g*, at 4 °C for 10 min (Thermo Scientific, USA) and the supernatant was used for analyses. The level of reduced ascorbate (ASC) in the extract was estimated by colorimetric determination of the α,α'-bipyridyl complex formed with ferrous ions (Fe^{2+}), which were reduced from ferric ions (Fe^{3+}) by ascorbate from plant extract. To determine ASC in samples, a reaction mixture was prepared by adding, in a sequential order: 135 µL of supernatant, 33.6 µL of deionized water, 40 µL of 85 % H_3PO_4, 685 µL of 0.5 % α,α'-bipyridyl and 140 µL of 1 % $FeCl_3$. To determine the total pool of ascorbate, i.e. the ASC and dehydroascorbate (DHA), the 16.8 µL of 10 mM DTT and 16.8 µL of 80 mM K_2HPO_4 were added to 135 µL of extract and incubated 5 minutes at room temperature to ensure reduction of DHA to ASC. Then, extract was mixed with 40 µL of 85 % H_3PO_4, 685 µL of 0.5 % α,α'-bipyridyl and 140 µL of 1 % $FeCl_3$. After 30 min incubation at room temperature, all samples were centrifuged at 14 000 × *g* for 5 min and the absorbance of the supernatant was measured at wavelength $\lambda_{525\ nm}$ and compared to the standard curve of ASC in the range of 0-50 µg mL^{-1} (U-1800 spectrophotometer, Hitachi, Tokyo, Japan). Based on the measurement results the ASC level and the total pool of ASC and DHA were calculated and presented as mg g FW^{-1}. To determine the redox status, the proportion of the reduced form in the total pool was calculated and presented as ASC/ASC+DHA ratio.

2.7 Antioxidant enzyme activities

2.7.1 Protein extraction

Frozen samples (0.5 g) were ground in liquid nitrogen and extracted with 2.25 mL of homogenization buffer composed of 50 mM phosphate buffer, pH 7.5, 2 mM EDTA, 8 mM $MgCl_2$, 0.1 % Triton X-100, 4 mM dithiothreitol (DTT) and centrifuged at 14 000 × *g* at 4°C for 15 min (Thermo Scientific, USA). The extract for ascorbate peroxidase (APX) activity assay was prepared with 50 mM phosphate buffer, pH 7.5, 5 mM ascorbate and 1 mM EDTA. Total protein was assayed according to Bradford (1976) with bovine serum albumin (BSA) in the concentrations range of 50-400 µg mL as standards.

2.7.2 Activity of catalase (CAT)

The activity of catalase was assayed by continuously measuring the decrease of H_2O_2 concentration in the sample (Rao et al., 1996). The reaction mixture consisted of 1.5 µL of H_2O_2 (30 %), 40-100 µL of plant extract (depending on the plant organ) and 100 mM phosphate buffer, pH 7.0, in a final volume of 1000 µL. The assay mixture was thoroughly mixed in a spectrophotometric quartz cuvette (1.5 mL volume). Then, the decrease in the $\lambda_{240\ nm}$ was measured for 90 s with U-1800 spectrophotometer (Hitachi, Tokyo, Japan). The results were processed to calculate the activity of catalase and presented as U per mg of protein.

2.7.3 Activity of superoxide dismutase (SOD)

Superoxide dismutase activity was assessed by measuring inhibition of nitroblue tetrazolium (NBT) to formazan reduction by superoxide radical, as described by Beauchamp & Fridovich (1971). To perform the assay, 25 µL of enzyme extract was mixed with 75 µL of extraction buffer, and 1.5 mL of reaction mixture (50 mM phosphate buffer, pH 7.8, 0.67 mM NBT, 1 mM L-methionine, 0.33 mM EDTA, 0.0033 mM riboflavin). For the control assay, the enzyme extract was substituted by extraction buffer, and for negative control, H_2O was used instead of the reaction mixture. Samples were incubated for 10 min in light. After that, the absorbance at $\lambda_{560\ nm}$ was measured with U-1800 spectrophotometer (Hitachi, Tokyo, Japan). The unit (U) of SOD activity was defined as the amount of enzyme which caused 50 % inhibition of the photochemical reduction of NBT to formazan constitutes, and results were demonstrated as U of enzyme per mg of protein.

2.7.4 Peroxidase (POX) activity

Peroxidase activity was assessed by determining the rate of pyrogallol oxidation to purpurogallin, in the presence of H_2O_2, as described previously by Tyburski & Mucha (2023). The increase in absorbance at $\lambda_{420\ nm}$ was followed in the reaction mixture composed of 100 mM phosphate buffer, pH 6.0, 60 mM pyrogallol, 0.66 mM H_2O_2 and 5-80 µL of plant extract (depending on plant organ) for 90 s with U-1800 spectrophotometer (Hitachi, Tokyo, Japan). To correct the results for non-enzymatic oxidation of pyrogallol, enzyme-free assays were performed. Peroxidase activity was calculated using the millimolar extinction coefficient of purpurogallin: ε = 12 mM^{-1} cm^{-1} and expressed as µmol pyrogallol min^{-1} mg^{-1} total protein.

2.7.5 Ascorbate peroxidase (APX) activity

The activity of ascorbate peroxidase was evaluated by measuring the rate of H_2O_2 decomposition in the reaction mixture composed of 970 µL of reaction buffer (50 mM phosphate buffer, pH 7.5, 1 mM EDTA), 10 µL of 50 mM ascorbate and 10 µL of enzyme extract. The reaction was initiated by adding 10 µL of 0.2 mM H_2O_2 and the decrease in absorbance at $\lambda_{290\ nm}$ was performed over 90 s (Chen & Asada, 1989; Rao et al., 1996). APX activity was calculated using the molar extinction coefficient of 2.8 mM^{-1} cm^{-1} for ascorbate and presented as µmol ascorbate min^{-1} mg^{-1} total protein.

2.8 Statistical analysis

The data analysis was performed by using GraphPad Prism version 10.0.0 (GraphPad Software, Boston, Massachusetts USA). Results were shown as a mean ± standard error (SE). The means were then compared to determine statistical significance (if $p < 0.05$) by One-way ANOVA, and post-hoc Tukey's test. The growth parameters, oxidative and antioxidant parameters quantified in the organs of plantlets developed from AgNPs-treated grains were used to perform principal component analysis (PCA) and hierarchical cluster analysis (HCA) with R 4.4.2 (R Foundation for Statistical Computing, Vienna, Austria) using factoextra, ggplot2 and dendextend R packages(Galili, 2015; Kassambara & Mundt, 2020; Wickham, 2016).

3 Results

3.1 Biosynthesis and physicochemical characteristics of AgNPs from *Fusarium solani* IOR 825

TEM analysis confirmed the formation of spherical AgNPs with sizes ranging from 8.9 to 47.9 nm and an average diameter of 22.97 ± 9.4 nm (Figure 1A). UV-visible absorption spectroscopic analysis of the mycosynthesized AgNPs showed a characteristic peak at 419 nm (Figure 1B). Results of nanoparticle tracking analysis (NTA) confirmed that the AgNPs exhibited an average size of 43 ± 36 nm and most frequently a diameter of 23 nm (Figure 1C). Results from DLS indicated that average hydrodynamic diameters of AgNPs were found to be 27.44 nm (14 %) and 108.4 nm (86 %), as shown in Figure 1D, while Zeta potential values were found to be -19.5 mV (61.3 %) and -2.93 mV (38.6 %) (Figure 1E). The diffractogram of AgNPs showed peaks at 38.63, 46.41, 65.10 and 77.09 corresponding to (1 1 1), (2 0 0), (2 2 0) and (3 1 1) planes of the face-centered cubic (fcc) silver crystal, respectively (Figure 1F). FTIR spectra showed absorption bands at 3429.21 cm^{-1} (N-H stretching, amines), 2924.03 cm^{-1} (C-H stretching, alkane), 2852.77 cm^{-1} (C-H stretching, alkane), 1743.8 cm^{-1} (C-H bending, aromatic compound), 1631.89 cm^{-1} (C=C stretching, alkene), 1384.44 cm^{-1} (C-H bending, alkane) (Figure 1G).

3.2 Germination and growth parameters

The surface sterilization of maize grains with AgNPs from *Fusarium solani* IOR 825 at the concentration range tested did not affect the germination percentage (% G), mean germination time (MGT) and germination rate index (GRI), as shown in Table 1. The gradual improvement in plant growth was observed after treatment with increasing AgNPs concentrations, when compared to control, and reflected in the increase in shoot length, fresh weight of leaves and stem of plants developed from AgNPs-treated grains (Figure 2, Supplementary Table S1). The strongest effect was observed for AgNPs treatment at a concentration of 512 µg mL^{-1}, with improvements in shoot (13.3 %) and root (11%) lengths, as well as fresh weight of leaves (22.3 %) and stem (39.2 %), and dry weight of leaves (37.8 %) and stem (43.1 %). This was also demonstrated in the vigour indexes I and II, which increased to 4334.3 (I) and 8096.1 (II), compared to the controls, which were 3980.6 and 6259.7, respectively (Table 1). On the other hand, approximately 20 % reduction in caryopsis weight was observed. Nevertheless, the stimulatory effect of the AgNPs treatment on root development was observed, the difference with the untreated control did not pass the significance test.

3.3 Analysis of AgNPs accumulation in maize

The analysis of elemental composition of plants developed from AgNPs-treated grains showed no significant difference in Ag content between tested and control samples, as shown in Supplementary Table S2.

3.4 Total chlorophyll content

AgNPs-treatments at concentrations of 32 μg mL^{-1} and 128 μg mL^{-1} showed negligible effect on total chlorophyll content in the leaves of plantlets. The application of AgNPs at a concentration of 512 μg mL^{-1} resulted in a decrease in chlorophyll content by 11.8 % (0.05 mg g FW^{-1}) (Figure 3, Supplementary Table S1).

3.5 Oxidative stress parameters

Changes in the activity of individual components of the antioxidant system for the tested plants, concerning non-treated plantlets given as percentages [%], are shown in Supplementary Table 1.

3.5.1 Hydrogen peroxide (H_2O_2) content

The accumulation of hydrogen peroxide (H_2O_2) varied depending on AgNPs concentration used and the plant organ (Figure 4A). In general, its level decreased after grain sterilization with AgNPs, and statistically lower concentrations of H_2O_2 were noted in caryopsis by 26-31 % and in leaves by 16-24 %. In roots, the concentration of H_2O_2 was reduced by 17.7 % (32 μg mL^{-1} AgNPs), 51.2 % (128 μg mL^{-1} AgNPs), and 19.5 % (512 μg mL^{-1} AgNPs). Simultaneously, in stems of maize plantlets treated with 128 μg mL^{-1} and 512 μg mL^{-1} of AgNPs the concentration of H_2O_2 increased by 21.7 % and 32.7 %, respectively.

3.5.2 Lipid peroxidation

The level of malondialdehyde (MDA) in all control plant organs and AgNPs-treated plantlets was comparable (Figure 4B). The MDA content increased slightly in roots (by 21-26%) after seed treatment with 128 μg mL^{-1} and 512 μg mL^{-1} of AgNPs but the effect was not statistically significant. Whereas, a significant increase in MDA level by 3.96 nmol g FW^{-1} (22 %) was detected in leaves of plants developed from grains treated with 512 μg mL^{-1}AgNPs-, when compared to control plants.

3.5.3 Total glutathione (GSH+GSSG) content

The total glutathione content in leaves, stems and roots was comparable between all tested variants, with no effect of the AgNPs treatment observed (Figure 4C). However, total glutathione levels gradually increased by 19.4 %, 69.4 % and 73% in caryopsis of plants treated with AgNPs at concentrations of 32 μg mL^{-1}, 128 μg mL^{-1} and 512 μg mL^{-1}, respectively.

3.5.4 Reduced and total (reduced and oxidized) ascorbate contents and ascorbate redox ratio

All AgNPs treatments increased leaf total ascorbate (ASC and DHA) content (by 21.5-48.1%) and showed no significant impact on the ascorbate redox state (Figure 5). The increase in ASC content (by 45.5-62.1%) and subsequently approx. 1.5-fold higher ASC/DHA ratios were observed in stems of plants treated with all AgNPs concentrations.

AgNPs at concentrations of 32 μg mL^{-1} and 128 μg mL^{-1} showed a minor effect on the total ascorbate pool in caryopses, while at a concentration of 512 μg mL^{-1} the parameter was reduced by 36.3 %. However, treating grains with AgNPs at concentrations of 32 μg mL^{-1}, 128 μg mL^{-1} and 512 μg mL^{-1} increased the ascorbic acid concentration by 3, 3.4 and 2.1 times, respectively. Consequently, a 3.5, 3.8 and 3.2-fold increase in ASC/DHA+ASC ratio in caryopses was observed under 32 μg mL^{-1}, 128 μg mL^{-1} and 512 μg mL^{-1} AgNPs-treatments, respectively.

Different concentration-dependent effects of AgNPs treatment on the overall ASC and DHA pool and redox status in roots were observed. Both, total ascorbate and ascorbic acid contents were not altered after treatment with the lowest concentration of AgNPs (32 μg mL^{-1}). However, the treatment of grains with AgNPs at a concentration of 128 μg mL^{-1} increased the total ascorbate pool and the content of its reduced form (ASC) by 83.8 % and 94.4 %, respectively. The ascorbate redox status was at the same level as in the control. In contrast, the treatment with the highest tested concentration of AgNPs (512 μg mL^{-1}) increased the total ascorbate by 74.2

% and the ASC content by 42.7 %. The ascorbate redox status decreased, under the highest AgNPs concentration, by 18.3 % when compared to the control (Figure 5).

3.5.5 Catalase (CAT) activity

The treatment of grains with AgNPs resulted in the reduction of catalase (CAT) activity in all variants when compared to control plantlets (Figure 6A). Significantly lower CAT activity was revealed in leaves of plants treated with 32 μg mL^{-1} and 128 μg mL^{-1} of AgNPs, with enzyme activity decreased by 38.1 % and 22. 6%, respectively. In stems of plantlets treated with 32 μg mL^{-1} and 128 μg mL^{-1} of AgNPs the activity of CAT was reduced by 38.1 % and 22.6 %, respectively. The reduction of CAT activity by 40.3 % was observed in the roots of plants developed from grains treated with the highest tested concentration of AgNPs. The CAT activity in caryopses did not differ between the control and the AgNPs-treated plants (Figure 6A).

3.5.6 Superoxide dismutase (SOD) activity

SOD activity varied substantially between the control and the AgNPs-treated variants, decreasing, in an AgNPs-dose-dependent manner, in aboveground organs and caryopses, and increasing in plant roots (Figure 6B). In leaves, SOD activity decreased by 41.2 %, 42.4 % and 25.6%, under treatments with 32 μg mL^{-1}, 128 μg mL^{-1} and 512 μg mL^{-1} of AgNPs, respectively. In stems of plants, developed from grains treated with AgNPs at concentrations of 32 μg mL^{-1}, 128 μg mL^{-1} and 512 μg mL^{-1}, SOD activity decreased by 24.2 %, 22.8 % and 60.3%, respectively. Reduced SOD activity by approximately 30-32% was recorded in caryopses of plants treated with all tested concentrations of AgNPs. The SOD activity in roots increased by 16.6-49.2%, with increasing AgNPs concentration.

3.5.7 Peroxidases (POX) activity

The surface sterilization of maize grains with AgNPs had a minor impact on peroxidase activity in developed plantlet organs (Figure 6C). Significantly lower POX activity, by 46.6 %, was observed in leaves after the use of AgNPs at a concentration of 512 μg mL^{-1}. The activity of POX was slightly reduced in stems (by 16.8 % and 14.9 % after treatment with AgNPs at concentrations of 32 μg mL^{-1} and 128 μg mL^{-1}, respectively). The AgNPs at a concentration of 512 μg mL^{-1} increased POX activity in caryopsis by 18.5 %, but the differences did not pass the significance test.

3.5.8 Ascorbate peroxidase (APX) activity

APX activity was unaffected by AgNPs treatment in leaves, stems, and roots (Figure 6D). The reduction in enzymatic activity of APX by 17 % was found in caryopsis after treatment with 128 μg mL^{-1} and 512 μg mL^{-1} of AgNPs whereas a 30.7 % reduction occurred if grains were subjected to treatment with 32 μg mL^{-1} of AgNPs (Figure 7D).

3.5.9 Principal component analysis (PCA) and hierarchical cluster analysis (HCA)

The results of PCA and HCA showing general alterations and correlations of growth and individual biochemical parameters among organs of plantlets developed from grains treated with AgNPs are demonstrated in Figure 7. The first two components PC1 and PC2 allow us to represent high values of the initial variability of the data (44.8 % and 27.8 %, respectively). The results showed that APX activity, MDA and CAT activity showed the highest contribution to PC1 (14.0 %, 12.6 % and 12.3 %, respectively) while the contribution of variables to PC2 was explained by SOD activity (16.8 %), FW (12.9 %) and GSH content (12.2 %) (Supplementary Table 3). The highest positive correlation was found for ASC and total ASC, along with POX and APX (Figure 7A-B). The effect of the individual concentrations of AgNPs (32 μg mL^{-1}, 128 μg mL^{-1} and 512 μg mL^{-1}) among plantlets organs (leaves, caryopsis, stems and roots) based on biochemical and growth parameters was assayed by HCA (Figure 7C). All organs were classified as separate groups, including untreated samples. In both leaves

and stems changes in biochemical and growth parameters under AgNPs-treatments at concentrations of 32 μg mL^{-1} and 128 μg mL^{-1} were nearest to each other, followed by concentrations of 512 μg mL^{-1} and controls. The caryopses showed dose-dependent alteration, where the two highest concentrations (128 μg mL^{-1} and 512 μg mL^{-1}) caused a similar response pattern, followed by concentration of 32 μg mL^{-1} and controls. In roots the effects of AgNPs treatment at the concentration of 32 μg mL^{-1} were found to be similar to controls, followed by concentrations of 128 and 512 μg mL^{-1}.

4 Discussion

Biological synthesis of NPs addresses the need to develop environmentally friendly, efficient and safe methods of producing NPs. Many studies showed that fungi display potential for the biosynthesis of NPs, as they efficiently produce the biomass along with a variety of chemical compounds responsible for the reduction of silver ions to silver NPs, and possess a high tolerance to metals (Borehalli Mayegowda et al., 2023). It was reported that fungal enzymes are involved in the synthesis of AgNPs (Ahmad et al., 2003; Hamedi et al., 2017). In a study conducted by El-Sayed & El-Sayed (2020), the protein-rich cell-free filtrate of *Fusarium solani* KJ 623702 was successfully used for the synthesis of AgNPs, CuNPs, and ZnONPs.

The physicochemical properties and consequently biological interactions or reactivity of biosynthesized AgNPs are highly dependent on synthesis conditions including biological source of reducing and stabilizing agents, concentration, and type of precursor salt, as well as the temperature and pH of the reaction (Sidhu et al., 2022; Trzcińska-Wencel et al., 2023a). The results of our study confirmed that the fungal strain *F. solani* IOR 825 is a system for the efficient synthesis of AgNPs with small size (10-50 nm) and the presence of natural origin capping biomolecules on their surface. This capping can be involved in the reduction of silver ions (Ag^{+}) and the formation of AgNPs, and affects their stability and antimicrobial activity. Moreover, the coating modulates the interaction between nanoparticles and biological surfaces which affects the potential uptake of nanoparticles (Huang et al., 2022; Wypij et al., 2022). In accordance with our results, El-Sayed & El-Sayed (2020) found that FTIR analysis of AgNPs from *F. solani* KJ 623702 showed peaks attributed to N-H bending, C-H stretching vibrations of protein methylene groups and O-H stretching of carboxylic acids. Authors, based on SDS-PAGE electrophoresis and FTIR results, suggested that the process of biogenic synthesis of NPs is related to the presence of various fungal-origin compounds (containing sulfur, nitrogen and phosphorus), proteins with β-sheet and a carbonyl group of amino acid residues and glycoprotein-containing polysaccharides with α-glycosidic bond (El-Sayed & El-Sayed, 2020). The nanoparticle surface properties such as surface charge and hydrophobicity/hydrophilicity are responsible for electrostatic repulsion between individual nanoparticles that prevent aggregation. This makes nanoparticles more mobile and more available for plants than bare nanoparticles. In contrast to chemically synthesized NPs, which are most frequently coated with polyvinylpyrrolidone (PVP), Arabic gum (AG), citrate and cetyltrimethylammonium bromide (CTAB), the biological NPs are coated with molecules of natural origin (plants or microbial extracts). Consequently, the biological coating is considered as less toxic than the chemical one (Sidhu et al., 2022; Wypij et al., 2022). Similar findings were described in our previous studies by Trzcińska-Wencel et al. (2023b, 2023c) who showed the potential of using the fungi of the genus *Fusarium* for the efficient, low-cost, simple and environmentally friendly synthesis of metal nanoparticles with desirable physical and chemical properties to provide biocompatibility and biological activity as well as their potential for use in multiple applications, including agriculture.

Although silver is not an essential element for plant growth as compared to other micronutrients such as copper, zinc, iron or magnesium, its high antimicrobial activity is an advantage in many applications (Duffy et al., 2018; Kakian et al., 2024). The nanoscale form can provide their slow and controlled release over time, thus prolonged antimicrobial protection and availability for plants (Bernardo-Mazariegos et al., 2019; Cao et al., 2025). Therefore, bio-AgNPs, which possess lower toxicity than chemical NPs and high antimicrobial activity, are

excellent alternatives to conventional fungicides which are based on copper compounds (Ding et al., 2019; Yen et al., 2019; Khan et al., 2021; Trzcińska-Wencel et al., 2024). Overall, bio-AgNPs show higher antimicrobial activity than biogenic CuNPs, ZnNPs and FeNPs, and the use of a lower effective dose can reduce the toxicity of nanoproducts introduced into the environment (Asghar et al., 2018; Trzcińska-Wencel et al., 2023b). This finding implies AgNPs potential for effective use at reduced doses with lower toxicity However, due to the numerous studies that suggest adverse effects of NPs (especially in high concentrations), there is a need for extensive research on the interactions that occur between NPs and organisms (Ding et al., 2019; Khan et al., 2021; Trzcińska-Wencel et al., 2024).

The germination of seeds and early growth of seedlings are identified as critical stages in the development and establishment of plants (Rajjou et al., 2012). A high threat of microbial contamination of seeds used for sowing provides a risk of fungal pathogens growth and infection of germinating seeds or developing seedlings (Magan et al., 2004). Seed priming is an effective method to prepare seeds for sowing to increase germination efficiency and achieve improved seedling growth (Abbasi Khalaki et al., 2021). As previously reported by Trzcińska-Wencel et al. (2023b), the use of AgNPs for grain pretreatment eliminated grain-borne pathogens at the lowest effective AgNPs concentration of 32 μg mL^{-1} with no impact on grain germination efficiency. In the present paper, we decided to broaden the study on the effect of AgNPs on grain germination and plantlets growth, using the effective concentration (32 μg mL^{-1}) and its 4-fold higher concentrations (128 and 512 μg mL^{-1}) and prolonged (14 days) plant growth period. Simultaneously, the disinfecting effect of the used AgNPs concentrations on grains was confirmed, as no microbial growth was visually detected on the surface of the germinating grains or plant growth medium (Supplementary Figure S2). The results showed no impact on grain germination when compared with control. Nonetheless, the treatment accelerated plantlet development as manifested by improved growth of shoot and reduction of grain weight in comparison with the control, indicating a stimulatory effect of the AgNPs on maize development. Similarly, seed pre-sowing treatments with bio-AgNPs improved the growth of licorice (*Glycyrrhiza glabra*) (Kim et al., 2023), maize (*Z. mays*) (Karim et al., 2023) onion (*Allium cepa* L.) (Acharya et al., 2019), watermelons (*Citrullus lanatus*) (Acharya et al., 2020), winged bean (*Psophocarpus tetragonolobus*) (Kamal Kumar et al., 2020), wheat (*Triticum aestivum*) (Mondéjar-López et al., 2023) and lack Gram (*Vigna mungo* (L.) Hepper) (Krishnasamy et al., 2024). In the study reported by Soliman et al. (2020) seed priming with increasing bio-AgNPs concentrations gradually improved the germination of seeds and growth of maize (*Z. mays* L.), fenugreek (*Trigonella foenum-graecum* L.), and onion (*A. cepa* L.). Moreover, stimulatory effects on the growth and development of seedlings after seed nanopriming with the AgNPs synthesized using chemical and physical methods were reported for common beans (*Phaseolus vulgaris*) (Savassa et al., 2021) and beans (Pražak et al., 2020). However, in the other experimental system, namely medium supplementation with chemically synthesized nanoparticles at a concentration of 100 ppm, the phytotoxic effects were observed on *Bacopa monnieri* (Krishnaraj et al., 2012). The higher phytotoxicity was observed under foliar application of AgNPs than root exposure in soybean and rice (Li et al., 2017) while the application of PVP-coated AgNPs resulted in limited germination and a decrease in the growth of *Triticum aestivum* L. (Vannini et al., 2014).

The bioaccumulation and translocation of AgNPs in the treated plants depends on plant (e.g., species, stage of growth), method of application, time of exposure or the dose used. The biological activity of AgNPs is determined by their physicochemical features, mainly by size, chemical composition and surface properties. These parameters influence the uptake and transport of NPs within plant organs, their interactions with cellular components (e.g. cell wall penetration) and the release of silver ions, subsequently contributing to their effect on plant growth (Nandini et al., 2023; Trzcińska-Wencel et al., 2024). AgNPs in the environment undergo various biotransformations such as aggregation, ion release, sulfidation or complexation with organic matter that determine their bioavailability to plants or toxicity. It has been noticed that AgNPs transport throughout the plant tissues via both apoplastic and symplastic pathways (Ali et al., 2021; Cao et al., 2025). However, our study

showed that the content of Ag was undetected in any of the plantlet organs even after 14 days of grain sowing. In contrast, in a study conducted by Savassa et al. (2021), the seed treatments with 1 mg L^{-1}, 10 mg L^{-1} and 100 mg L^{-1} of chemically synthesized AgNPs, Ag_2SNPs, and $AgNO_3$ (control) resulted in silver accumulation and biotransformation in *P. vulgaris* seeds. Ag was detected in the seed coat depending on Ag source and concentration used, namely 5 days after sowing the Ag from $AgNO_3$ was detected in epidermis of seeds while Ag from AgNPs and Ag_2SNPs were mainly located in the internal layer (parenchyma cells). The research of Koley and collaborators (2023) implies that seed treatment with AgNPs allows for their accumulation at a low dose, and then enables the gradual release of Ag^+ ions and stimulation of the antioxidant system with accelerated germination and growth. In a study carried out by Yan et al. (2023) the AgNPs stimulated the germination process of rice seeds due to the AgNPs uptake during imbibition process. AgNPs were accumulated in decreasing concentration in the seed coat, embryo and endosperm. The metabolomic and transcriptomic analyses revealed that AgNPs increased in stress signaling molecule synthesis, showing their potential as nanobiostimulators to ensure long-term stress memory.

According to literature, AgNPs may induce ROS generation and strengthen antioxidative system response by the enzymatic and/or non-enzymatic pathways involving both, a wide range of enzymes (e.g. superoxide dismutase, catalase, peroxidases) as well as low-molecular compounds (e.g. ascorbic acid, glutathione, proline, tocopherols) (Sharma et al., 2019). The present study was conducted to evaluate the response of the oxidative stress system and changes in photosynthetic pigment content as indicators of plantlet condition and to assess the risk of potential phytotoxicity of AgNPs to maize. To provide detailed results, the above parameters were determined separately for all organs, including leaves, stems, roots, and caryopses.

Treating maize grains with AgNPs specifically affected cellular redox agents in plant organs subjected to analysis. Symptomatically, as revealed by the lipid peroxidation assay, the treatments did not cause severe oxidative stress in any organ. On the other hand, the slight but significant increase in the rate of MDA formation occurred in leaves, but solely in plants challenged with the highest AgNPs concentration. This finding shows that standard AgNPs treatments do not increase the risk of oxidative damage. However, our results found that grain treatment with the highest concentration of AgNPs resulted in lower total chlorophyll content. Similarly, the decrease in photosynthetic pigments was reported in *Brassica* sp. seedlings exposed to AgNPs synthesized from *Aloe vera* extract (Vishwakarma et al., 2017) and in *Lupinus termis* after 10-days exposure to AgNPs synthesized from leaves extract of *Coriandrum sativum* (Al-Huqail et al., 2018). In our study, the photosynthetic rate and the maximum efficiency of photosystem II were not analyzed in AgNPs-treated corn plants. Therefore, it remains to be determined to what extent the decrease in chlorophyll content affects photosynthetic efficiency. However, this issue will be addressed in our forthcoming study. Other authors have shown that a decrease in chlorophyll content adversely affects photosynthesis. Under decreased chlorophyll levels, excess electron flow may result in an imbalance between the donor and acceptor sites of the photosystem I. This results in molecular oxygen reduction generating harmful ROS and photosystem damage (photoinhibition) (Bhattacharjee, 2019). The increase in lipid peroxidation and decrease in chlorophyll content in leaves of plants exposed to the highest AgNPs concentration might be related to increased photoinhibition occurring at excessive nanoparticle concentration. Although further experiments are required to assess if corn leaves become more susceptible to photooxidation under nonoptimal AgNPs concentrations, these findings stress the necessity of optimizing the treatment procedure thoroughly, since treating seeds with excessive AgNPs concentrations may bring about some detrimental consequences.

Although no significant oxidative damage was detected in AgNPs-treated plants, several components of the cellular redox systems were affected by treatments. Usually, the parameters were altered in an organ-specific manner. In leaves, the H_2O_2 levels were moderately reduced in the AgNPs-treated plants. The decrease in the oxidant content might be partly due to a substantial reduction in the activity of SOD, which is an H_2O_2 - producing enzyme. The stable total glutathione levels and a small increase in the ASC content might also

contribute to reducing H_2O_2 level in leaves. Therefore, the ascorbate is supposed to scavenge H_2O_2 in a non-enzymatic manner, since no increase in the APX activity can be observed (Kunert & Foyer, 2023). Gupta et al. (2018) evaluated the stimulatory effects of AgNPs on rice seedlings and suggested that growth promotion was related to efficient ROS scavenging mechanisms, including changes in glutathione-ascorbate cycle and activities of involved enzymes (ascorbate peroxidase, glutathione reductase) in leaves. In contrary to our results, authors suggested low alterations of SOD activity in response to AgNPs treatment. While, Soliman et al. (2020) reported an increase in ascorbate and glutathione content in leaves of *Z. mays*, *A. cepa* and *T. foenum-graecum*, as well as an increase in catalase and peroxidase, and ascorbate peroxidase (but the decrease of APX activity in *T. foenum-graecum* at a concentration of 25 mg L^{-1}) and upregulated expression levels of antioxidant enzymes in AgNPs-treated seedlings. In turn, our results indicate that the H_2O_2-scavenging enzymes, namely the POX and CAT, differentially reacted to AgNPs treatment. A negligible increase in POX activity and a substantial decrease in CAT activity was observed. When compared to APX and other H_2O_2-scavenging enzymes, CAT has a low affinity to its substrate. Therefore, the enzyme is involved in H_2O_2 scavenging when oxidant is accumulated to high levels (Heck et al., 2010; Černý et al., 2018). Since the H_2O_2 content decreased under the AgNPs treatment, the amount of the enzyme might be adjusted accordingly by decreasing its abundance. Earlier studies demonstrated that CAT activity is dependent on high availability of H_2O_2 (Scandalios et al., 1984; Rodríguez-Ruiz et al., 2019).

Our study shows that the activities of certain enzymes decreased at AgNPs treatment. Studies on plants overexpressing CAT, APX or SOD showed that these enzymes act synergistically to keep the homeostasis of cellular redox state, being increased or decreased in an orchestrated manner (Scandalios et al., 1984; Faize et al., 2011; Wang et al., 2017; Che et al., 2020). We suspect that the decrease in the enzyme activities might reflect their synchronized response to a decrease in H_2O_2 resulting from the AgNPs treatment and observed in all organs except coleoptile. Conversely, in coleoptile, H_2O_2 increased, but we assume that it may be a growth-related process, involving rather an apoplast H_2O_2, whereas CAT is a cytosolic enzyme and might not directly respond to changing apoplast H_2O_2 levels.

Growth of the AgNPs-treated plant roots was maintained at the control level. The H_2O_2 content was decreased in roots. This may be linked to the rise in the level of the H_2O_2-scavenging agent, namely ascorbate. Furthermore, increased ascorbate content was accompanied by high activities of the H_2O_2-consuming enzymes, namely POX and APX. At this stage of plant development, significant root growth is observed that is correlated with a wide range of physiological processes, such as auxin metabolism, cross-linking of cell wall components or cell elongation, in which peroxidases are involved (Passardi et al., 2005; Majda & Robert, 2018). POX are prevalently the apoplast-targeted enzymes. On the other hand, the majority of ascorbate is located in the cytosol, where APX isoforms are present. Therefore, we believe that the increasing ASC levels in the roots of the AgNPs-treated plants may contribute to maintaining high APX activity, which in turn, prevents excessive H_2O_2 accumulation. These mechanisms might be responsible for the reduction in H_2O_2 content in the roots of the AgNPs-treated plants. On the other hand, decreased CAT activity and increased SOD activity might favor H_2O_2 accumulation (Kumari et al., 2021). Acting simultaneously, the aforementioned factors might contribute to H_2O_2 homeostasis in roots, under the AgNPs treatment. In turn, Kim et al. (2023) observed improvements in shoot and root elongation of mung bean (*Vigna radiata*) after 12-hour seed treatment with biosynthesized AgNPs (at concentrations of 12.5, 25 and 50 ppm). Contrastingly to our findings, other authors suggest inhibition in root development after direct exposure of roots to AgNPs in soil or medium (Cvjetko et al., 2017). In the study reported by Guilger-Casagrande et al. (2022), the effect of soil exposure of soybean seedlings to bio-AgNPs resulted in a reduction in dry weight. In addition, the increase in H_2O_2 and lipid peroxidation (higher MDA content) in seedling roots was observed. Considering the inconclusive results, further research is still required

to understand the effects of AgNPs on root development in plants in view of different species and the conditions of NPs application.

The stimulatory effect of bio-AgNPs treatments on maize was observed as the reduction in biomass of the caryopsis. This was accompanied by a consistent decrease in H_2O_2 content, APX, CAT and SOD activity. Simultaneously, the redox balance of ascorbate turned to the more reduced and the content of total glutathione substantially increased. The latter effect was more pronounced under treatments with higher AgNPs concentrations. The increase in total glutathione concentration significantly distinguished the caryopsis from other organs. Glutathione is a versatile molecule, with many functions which go beyond common antioxidant roles. Glutathione is a source of sulfur for protein biosynthesis, plays a crucial role as an antioxidant and represents the potential as a highly reducing chemical barrier to prevent over-oxidation of cellular components through its direct interaction with peroxides or as a substrate for ROS-neutralizing enzymes (Noctor et al., 2012). Since ASC levels were relatively low in caryopsis, GSH is supposed to be a major low molecular weight antioxidant in this organ. Consequently, the reduction in H_2O_2 level in caryopses may be a consequence of AgNPs-dependent accumulation of GSH in this organ. It is suggested that the detoxification of Ag in plant cells is related to the direct bonding of Ag with GSH through the -SH group, or utilization of GSH for increased production of phytochelatins involved in metal detoxification (Kaur et al., 2021; Larue et al., 2014). Enhanced antioxidant protection in the caryopsis, due to AgNPs-stimulated GSH accumulation, might be important for mitigating the relatively high oxidative damage in this organ as exemplified by high lipid peroxidation. However, the latter not being related to AgNPs treatment. It should be kept in mind that at this developmental stage plant growth is still important and supported by seed reserves (Kennedy et al., 2004). Therefore, a complete analysis of the metabolic status of caryopsis in a two-week-old maize plant would be required to interpret the behavior of redox agents analyzed in this study.

The stem was the sole organ that reacted to the AgNPs-treatment with the increase in the H_2O_2 content. Since H_2O_2 may promote cell expansion growth by promoting cell wall flexibility (Majda & Robert, 2018; Marzol et al., 2022), the increase in the H_2O_2 content is in line with the enhanced stem biomass gain and stem lengthening, resulting from AgNPs administration. The H_2O_2 homeostasis, under AgNPs treatment, might be regulated by the ascorbate pool, which turned towards more reduced, when challenged with AgNPs. Whereas, the H_2O_2 levels rose in response to AgNPs treatment, no increase in lipid peroxidation was observed in the stems of the NP-treated plants. This suggests that the treatments did not increase oxidative damage in stems, but the increasing H_2O_2 content might be rather growth-related.

To sum up, the possible mechanisms of AgNPs action in plantlets that are responsible for alterations in cellular redox metabolism during the AgNPs-dependent maize growth stimulation are presented in Figure 8. The overall decrease in H_2O_2 accumulation in all organs (except stem) suggests that the efficiency of redox reactions has increased after grain treatments with AgNPs. The results indicate that specific plantlet organs showed a varying response and the induced effect depended on the applied dose. The alterations of the determined oxidative stress parameters were stronger with the application of higher AgNPs concentrations to grains. However, our results show no evidence for induction of severe oxidative stress by AgNPs in maize plantlets, as overproduction of ROS and its consequences due to the incapability of an antioxidative defense system for efficient ROS-scavenging were not detected.

5 Conclusions

To summarize, AgNPs synthesized from *Fusarium solani* IOR 825 were applied for the pretreatment of maize grains to sterilize and improve plant development. Biogenic AgNPs showed potential for application in seed priming, which is linked to its remarkable antimicrobial activity even at low concentrations against grain-borne pathogens that cause infections during germination and seedling development. The positive effect of AgNPs on

shoot elongation and enhanced biomass of maize plantlets, without any negative impact on oxidative stress or the chlorophyll content, confirmed their crop-safe biostimulatory potential. Furthermore, the biosynthesis process and pre-sowing grain technique are simple, cost-effective and environmentally friendly, indicating that they are affordable and implementable for practical use.

6 Conflict of Interest

The authors declare that the research was conducted in the absence of any commercial or financial relationships that could be construed as a potential conflict of interest.

7 Author Contributions

PG, JT, JT-W conceptualization, JT-W and NM investigation, JT-W data curation, visualisation, JT-W, JT methodology, JT-W writing original draft, PG, JT, MR writing review and editing, JT-W funding acquisition, PG supervision

8 Funding

This research was funded by grant No. 2022/45/N/NZ9/01483 from National Science Centre, Poland. The ACP was funded from IDUB of Nicolaus Copernicus University in Toruń, Poland and grant No. 2022/45/N/NZ9/01483 from National Science Centre, Poland.

9 Supplementary Material

The Supplementary Material for this article can be found online at:

10 Data Availability Statement

The original contributions presented in the study are included in the article/Supplementary Material, further inquiries can be directed to the corresponding authors.

11 Acknowledgments

We would like to acknowledge the Centre for Statistical Analysis of the Nicolaus Copernicus University in Toruń for the support in performing Principal Component Analysis (PCA) and Hierarchical Cluster Analysis (HCA).

12 References

Abbasi Khalaki, M., Moameri, M., Asgari Lajayer, B. and Astatkie, T. (2021). Influence of nano-priming on seed germination and plant growth of forage and medicinal plants. *Plant Growth Regul.* 93, 13-28. https://doi.org/10.1007/s10725-020-00670-9

Abdelgadir, A., Adnan, M., Patel, M., Saxena, J., Alam, M. J., Alshahrani, M. M., Singh, R., Sachidanandan, M., Badraoui R. and Siddiqui, A. J. (2024). Probiotic *Lactobacillus salivarius* mediated synthesis of silver nanoparticles (AgNPs-LS): A sustainable approach and multifaceted biomedical application. *Heliyon* 10. https://doi.org/10.1016/j.heliyon.2024.e37987

Abdul-Baki, A. A. and Anderson, J. D. (1973). Vigor determination in soybean seed by multiple criteria 1. *Crop Sci.* 13, 630–633. http://dx.doi.org/10.2135/cropsci1973.0011183X001300060013x

Abid, N., Khan, A. M., Shujait, S., Chaudhary, K., Ikram, M., Imran, M. Haider, J., Khan, M., Khan, Q. and Maqbool, M. (2022). Synthesis of nanomaterials using various top-down and bottom-up approaches,

717 influencing factors, advantages, and disadvantages: A review. *Adv. Colloid Interface Sci.* 300: 102597.
718 https://doi.org/10.1016/j.cis.2021.102597
719 Acharya, P., Jayaprakasha, G. K., Crosby, K. M., Jifon, J. L. and Patil, B. S. (2019). Green-synthesized
720 nanoparticles enhanced seedling growth, yield, and quality of onion (*Allium cepa* L.). *ACS Sustain.*
721 *Chem. Eng*. 7, 14580-14590. https://doi.org/10.1021/acssuschemeng.9b02180
722 Acharya, P., Jayaprakasha, G. K., Crosby, K. M., Jifon, J. L. and Patil, B. S. (2020). Nanoparticle-mediated seed
723 priming improves germination, growth, yield, and quality of watermelons (*Citrullus lanatus*) at multi-
724 locations in Texas. *Sci. Rep.* 10: 5037. https://doi.org/10.1038/s41598-020-61696-7
725 Ahmad, A., Mukherjee, P., Senapati, S., Mandal, D., Khan, M. I., Kumar, R. and Sastry, M. (2003). Extracellular
726 biosynthesis of silver nanoparticles using the fungus *Fusarium oxysporum*. *Colloids Surf. B:*
727 *Biointerfaces* 28, 313-318. https://doi.org/10.1016/S0927-7765(02)00174-1
728 Al-Huqail, A. A., Hatata, M. M., Al-Huqail, A. A. and Ibrahim, M. M. (2018). Preparation, characterization of
729 silver phyto nanoparticles and their impact on growth potential of *Lupinus termis* L. seedlings. *Saudi J.*
730 *Biol. Sci.* 25, 313-319. https://doi.org/10.1016/j.sjbs.2017.08.013
731 Ali, S., Mehmood, A., and Khan, N. (2021). Uptake, Translocation, and Consequences of Nanomaterials on
732 Plant Growth and Stress Adaptation. J. Nanomat. 2021: 6677616. https://doi.org/10.1155/2021/6677616
733 Almutairi, Z. M. and Alharbi, A. (2015). Effect of silver nanoparticles on seed germination of crop plants. *Int.*
734 *J. Nuclear Quantum Eng.* 9, 689-693. https://doi.org/10.24297/jaa.v4i1.4295
735 Anjum, S., Vyas, A., and Sofi, T. (2023). Fungi-mediated synthesis of nanoparticles: Characterization process
736 and agricultural applications. *J. Sci. Food Agric.* 103, 4727-4741. https://doi.org/10.1002/jsfa.12496
737 Asghar, M. A., Zahir, E., Shahid, S. M., Khan, M. N., Asghar, M. A., Iqbal, J., and Walker, G. (2018). Iron,
738 copper and silver nanoparticles: Green synthesis using green and black tea leaves extracts and evaluation
739 of antibacterial, antifungal and aflatoxin B1 adsorption activity. *Lwt*, *90*, 98-107.
740 https://doi.org/10.1016/j.lwt.2017.12.009
741 Beauchamp, C. and Fridovich, I. (1971). Superoxide dismutase: improved assays and an assay applicable to
742 acrylamide gels. *Anal. Biochem.* 44, 276-287. https://doi.org/10.1016/0003-2697(71)90370-8
743 Bernardo-Mazariegos, E., Valdez-Salas, B., González-Mendoza, D., Abdelmoteleb, A., Tzintzun Camacho, O.,
744 Ceceña Duran, C., and Gutiérrez-Miceli, F. (2019). Silver nanoparticles from *Justicia spicigera* and
745 their antimicrobial potentialities in the biocontrol of foodborne bacteria and phytopathogenic fungi.
746 *Revista Argentina de Microbiología,* 51, 103–109. https://doi.org/10.1016/j.ram.2018.05.002
747 Bhattacharjee, S. (2019). ROS and Regulation of Photosynthesis. In: Bhattacharjee, S. (ed) Reactive oxygen
748 species in plant biology New Delhi, India: Springer India, pp. 107-125.
749 Biswas, S., Seal, P., Majumder, B., and Biswas, A. K. (2023). Efficacy of seed priming strategies for enhancing
750 salinity tolerance in plants: An overview of the progress and achievements. *Plant Stress* 9: 100186.
751 https://doi.org/10.1016/j.stress.2023.100186
752 Borehalli Mayegowda, S.B., Roy, A., Manjula, N.G., Pandit, S., Alghamdi, S., Almehmadi, M., Allahyani, M.,
753 Awwad, N.S. and Sharma, R. (2023). Eco-friendly synthesized nanoparticles as antimicrobial agents:
754 an updated review. *Front. Cell. Infect. Microbiol.* 13: 1224778.
755 https://doi.org/10.3389/fcimb.2023.1224778
756 Bradford, M. (1976). A rapid and sensitive method for the quantitation of microgram quantities of protein
757 utilizing the principle of protein-dye binding. *Anal. Biochem.* 72, 248-254.
758 https://doi.org/10.1016/0003-2697(76)90527-3
759 Brady, N. G., O'Leary, S. L., Moormann, G. C., Singh, M. K., Watt, J. and Bachand, G. D. (2023).
760 Mycosynthesis of zinc oxide nanoparticles exhibits fungal species dependent morphological
761 preference. *Small* 19: 2205799. https://doi.org/10.1002/smll.202205799
762 Broders, K. D., Lipps, P. E., Paul, P. A. and Dorrance, A. E. (2007). Evaluation of *Fusarium graminearum*
763 associated with corn and soybean seed and seedling disease in Ohio. *Plant disease* 91, 1155-1160.
764 https://doi.org/10.1094/PDIS-91-9-1155
765 Brunelle, T., Chakir, R., Carpentier, A., Dorin, B., Goll, D., Guilpart, N., Maggi, F., Makowski, D., Nesme, T.,
766 Roosen, J., and Tang, F. H. M. (2024). Reducing chemical inputs in agriculture requires a system
767 change. *Commun. Earth Environ*. 5, 1–9. https://doi.org/10.1038/s43247-024-01533-1

Cao, Y., Turk, K., Bibi, N., Ghafoor, A., Ahmed, N., Azmat, M., Ahmed, R., Ghani, M. I., and Ahanger, M. A. (2025). Nanoparticles as catalysts of agricultural revolution: Enhancing crop tolerance to abiotic stress: A review. *Front. Plant Sci.* 15. https://doi.org/10.3389/fpls.2024.1510482

Černý, M., Habánová, H., Berka, M., Luklová, M. and Brzobohatý, B. (2018) Hydrogen Peroxide: Its role in plant biology and crosstalk with signalling networks. *Int. J. Mol. Sci*. 19: 2812. https://doi.org/10.3390/ijms19092812

Che, Y., Zhang, N., Zhu, X., Li, S., Wang, S., and Si, H. (2020). Enhanced tolerance of the transgenic potato plants overexpressing Cu/Zn superoxide dismutase to low temperature. *Sci. Hortic.*, 261: 108949. https://doi.org/10.1016/j.scienta.2019.108949

Chen, G-X. and Asada, K. (1989). Ascorbate peroxidase in tea leaves: occurrence of two isozymes and the differences in their enzymatic and molecular properties. *Plant Cell Physiol.* 30, 987–998. https://doi.org/10.1093/oxfordjournals.pcp.a077844

Cvjetko, P., Milošić, A., Domijan, A. M., Vrček, I. V., Tolić, S., Štefanić, P. P., Letofsky-Papst, I., Tkalec, M. and Balen, B. (2017). Toxicity of silver ions and differently coated silver nanoparticles in *Allium cepa* roots. *Ecotoxicol. Environ. Saf.* 137, 18-28. https://doi.org/10.1016/j.ecoenv.2016.11.009

Ding, Y., Bai, X., Ye, Z., Gong, D., Cao, J., and Hua, Z. (2019). Humic acid regulation of the environmental behavior and phytotoxicity of silver nanoparticles to *Lemna minor. Environ. Sci: Nano 6*, 3712–3722. https://doi.org/10.1039/C9EN00980A

Dowlath, M. J. H., Musthafa, S. A., Mohamed Khalith, S. B., Varjani, S., Karuppannan, S. K., Ramanujam, G. M., Arunachalam, A. M., Arunachalam, K. D., Chandrasekaran, M., Chang, S. W., Chung, W. J., and Ravindran, B. (2021). Comparison of characteristics and biocompatibility of green synthesized iron oxide nanoparticles with chemical synthesized nanoparticles. *Environ. Res.* 201, 111585. https://doi.org/10.1016/j.envres.2021.111585

Duffy, L. L., Osmond-McLeod, M. J., Judy, J., and King, T. (2018). Investigation into the antibacterial activity of silver, zinc oxide and copper oxide nanoparticles against poultry-relevant isolates of *Salmonella* and *Campylobacter*. *Food Control* 92, 293–300. https://doi.org/10.1016/j.foodcont.2018.05.008

Easwaran, C., Christopher, S. R., Moorthy, G., Mohan, P., Marimuthu, R., Koothan, V., and Nallusamy, S. (2024). Nano hybrid fertilizers: A review on the state of the art in sustainable agriculture. *Sci. Total Environ.* 929: 172533. https://doi.org/10.1016/j.scitotenv.2024.172533

El-Sayed, M. T. and El-Sayed, A. S. (2020). Biocidal activity of metal nanoparticles synthesized by *Fusarium solani* against multidrug-resistant bacteria and mycotoxigenic fungi. *J. Microbiol. Biotechnol.* 30: 226. https://doi.org/10.4014/jmb.1906.06070

Esechie, H. (1994). Interaction of salinity and temperature on the germination of sorghum. *J. Agron. Crop Sci*. 172, 194–199. https://doi.org/10.1111/j.1439-037X.1994.tb00166.x

European Food Safety Authority (EFSA). (2024). Cabrera, L. C., Di Piazza, G., Dujardin, B., Marchese, E. and Pastor, P. M. The 2022 European Union report on pesticide residues in food. *Efsa Journal* 22. https://doi.org/10.2903/j.efsa.2024.8753

Faize, M., Burgos, L., Faize, L., Piqueras, A., Nicolas, E., Barba-Espín, G., Clementeoreno, M. J., Alcobendas, R., Artlip, T. and Hernández, J. A. (2011). Involvement of cytosolic ascorbate peroxidase and Cu/Zn-superoxide dismutase for improved tolerance against drought stress. *J. Exp Bot*. 62, 2599-2613. https://doi.org/10.1093/jxb/erq432

Food and Agriculture Organization of the United Nations (FAO). (2024). Pesticides use and trade, 1990–2022. Analytical Brief Series No. 89. Rome. https://openknowledge.fao.org/handle/20.500.14283/cd1486en

Food and Agriculture Organization of the United Nations (FAO). 2022. Agricultural production statistics. 2000–2021. FAOSTAT Analytical Brief Series No. 60. Rome. https://doi.org/10.4060/cc3751en

Galili, T. (2015). dendextend: an R package for visualizing, adjusting, and comparing trees of hierarchical clustering. *Bioinformatics* 31, 3718-3720. https://doi.org/10.1093/bioinformatics/btv428

Goko, M. L., Murimwa, J. C., Gasura, E., Rugare, J. T., and Ngadze, E. (2021). Identification and characterisation of seed-borne fungal pathogens associated with maize (*Zea mays* L.). *Int. J. Microbiol.* 2021: 6702856. https://doi.org/10.1155/2021/6702856

Golinska, P., Rathod, D., Wypij, M., Gupta, I., Składanowski, M., Paralikar, P. and Rai, M. (2017). Mycoendophytes as efficient synthesizers of bionanoparticles: nanoantimicrobials, mechanism, and cytotoxicity. *Crit. Rev. Biotechnol.* 37, 765-778. https://doi.org/10.1080/07388551.2016.1235011

Goodman, R. E. (2024). Twenty-eight years of GM Food and feed without harm: why not accept them?. *GM Crops & Food*, 15*:* 40-50. https://doi.org/10.1080/21645698.2024.2305944

Guilger-Casagrande, M., Bilesky-José, N., Sousa, B. T., Oliveira, H. C., Fraceto, L. F., and Lima, R. (2022). Effects of biogenic silver and iron nanoparticles on soybean seedlings (*Glycine max*). *BMC Plant Biol.* 22, 255. https://doi.org/10.1186/s12870-022-03638-1

Gupta, S. D., Agarwal, A. and Pradhan, S. (2018). Phytostimulatory effect of silver nanoparticles (AgNPs) on rice seedling growth: An insight from antioxidative enzyme activities and gene expression patterns. *Ecotoxicol. Environ. Saf.* 161, 624-633. https://doi.org/10.1016/j.ecoenv.2018.06.023

Hamedi, S., Ghaseminezhad, M., Shokrollahzadeh, S., and Shojaosadati, S. A. (2017). Controlled biosynthesis of silver nanoparticles using nitrate reductase enzyme induction of filamentous fungus and their antibacterial evaluation. *Artif. Cells Nanomed. Biotechnol.* 45, 1588-1596. https://doi.org/10.1080/21691401.2016.1267011

Haydar, M. S., Ghosh, D., and Roy, S. (2024). Slow and controlled release nanofertilizers as an efficient tool for sustainable agriculture: Recent understanding and concerns. *Plant Nano Biol.,* 7: 100058. https://doi.org/10.1016/j.plana.2024.100058

Heck, D.E., Shakarjian, M., Kim, H.D., Laskin, J.D. and Vetrano, A.M. (2010) Mechanisms of oxidant generation by catalase. *Ann. New York Acad. Sci*. 1203, 120-5. https://doi.org/10.1111/j.1749-6632.2010.05603.x

Hodges, D.M., Delong, J.M., Forney, C.F., Prange, R.K. and Delong, J.M. 1999. Improving the thiobarbituric anthocyanin for estimating lipid peroxidation in plant tissues containing and other interfering. *Planta* 207, 604–611. https://doi.org/10.1007/s004250050524

Huang, D., Dang, F., Huang, Y., Chen, N. and Zhou, D. (2022). Uptake, translocation, and transformation of silver nanoparticles in plants. *Environ. Sci. Nano*, 9: 12-39. https://doi.org/10.1039/d1en00870f

Kakian, F., Mirzaei, E., Moattari, A., Takallu, S., and Bazargani, A. (2024). Determining the cytotoxicity of the minimum inhibitory concentration (MIC) of silver and zinc oxide nanoparticles in ESBL and carbapenemase producing *Proteus mirabilis* isolated from clinical samples in Shiraz, Southwest Iran. *BMC Research Notes* 17: 40. https://doi.org/10.1186/s13104-023-06402-2

Kamal Kumar, V., Muthukrishnan, S. and Rajalakshmi, R. (2020). Phytostimulatory effect of phytochemical fabricated nanosilver (AgNPs) on *Psophocarpus tetragonolobus* (L.) DC. seed germination: An insight from antioxidative enzyme activities and genetic similarity studies. *Curr. Plant Biol.* 23: 100158. https://doi.org/10.1016/j.cpb.2020.100158

Karim, S., Kayani, S., Akhtar, W., Fatima, I., Nazir, M. and Zaman, W. (2023). Biogenic synthesis of silver nanoparticles using *Funaria hygrometrica* Hedw. and their effects on the growth of *Zea mays* seedlings. *Microsc. Res. Tech.* 86, 686-693. https://doi.org/10.1002/jemt.24309

Kassambara A. and Mundt F (2020). Factoextra: Extract and Visualize the Results of Multivariate Data Analyses. R package version 1.0.7 https://CRAN.R-project.org/package=factoextra

Kaur, P., Gadhave, K., Garg, N., Deb, D. and Choudhury, D. (2021). Probing the interaction of glutathione with different shape of silver-nanoparticles by optical spectroscopy. *Mater. Today Commun.* 26: 102137. https://doi.org/10.1016/j.mtcomm.2021.102137

Kennedy, P. G., Hausmann, N. J., Wenk, E. H., and Dawson, T. E. (2004). The importance of seed reserves for seedling performance: an integrated approach using morphological, physiological, and stable isotope techniques. *Oecologia* 141, 547-554. https://doi.org/10.1007/s00442-004-1686-0

Khan, M., Khan, M. S. A., Borah, K. K., Goswami, Y., Hakeem, K. R., & Chakrabartty, I. (2021). The potential exposure and hazards of metal-based nanoparticles on plants and environment, with special emphasis on ZnO NPs, TiO_2 NPs, and AgNPs: a review. *Environ. Adv. 6*, 100128. https://doi.org/10.1016/j.envadv.2021.100128

Kim, M., Sung, J-S., Atchudan, R., Syed, A., Nadda, A. K., Kim, D-Y. and Ghodake, G. S. (2023). A rapid, high-yield and bioinspired synthesis of colloidal silver nanoparticles using *Glycyrrhiza glabra* root extract and assessment of antibacterial and phytostimulatory activity. *Microsc. Res. Tech.* 86, 1154-1168. https://doi.org/10.1002/jemt.24389

Koley, R., Mondal, A. and Mondal, N. K. (2023). Green synthesized silver nanoparticles mediated regulation on hydrolytic enzymes and ROS homeostasis promote growth of three pulses (*Cicer arietinum* L., *Pisum*

sativum L., and *Vigna radiata* L.). *Energ, Ecol. Environ.* 8, 537-555. https://doi.org/10.1007/s40974-023-00293-6

Krishnaraj, C., Jagan, E. G., Ramachandran, R., Abirami, S. M., Mohan, N., and Kalaichelvan, P. T. (2012). Effect of biologically synthesized silver nanoparticles on *Bacopa monnieri* (Linn.) Wettst. plant growth metabolism. *Process biochem.* 47, 651-658. https://doi.org/10.1016/j.procbio.2012.01.006

Krishnasamy, R., Natesh, R. and Obbineni, J. M. (2024). Efficient ROS scavenging improves the growth and yield in black gram (*Vigna mungo* (L.) Hepper) after seed priming and treatment using biosynthesized silver nanoparticles with P*ongamia pinnata* (L.) pierre leaf extract. *J. Plant Growth Regul.* 43, 1-17. https://doi.org/10.1007/s00344-024-11276-0

Kumari, A., Bhinda, M. S., Sharma, S., Chitara, M. K., Debnath, A., Maharana, C. and Sharma, B. (2021). ROS regulation mechanism for mitigation of abiotic stress in plants. In: Ahmad R. (ed) Reactive oxygen species, IntechOpen, London, UK, pp. 197-238. https://doi.org/10.5772/intechopen.99845

Kumari, K., Rani, N. and Hooda, V. (2024). Silver nanoparticles and silver/silica nanocomposites: Impacts on *Z. mays* L. growth, nutrient uptake and soil health. *Plant Nano Biol. 7*: 100064. https://doi.org/10.1016/j.plana.2024.100064

Kunert, K. J., and Foyer, C. H. (2023). The ascorbate/glutathione cycle. In Mittler R. and Breusegem F. V. (eds.), Advances in Botanical Research Academic Press pp. 77–112 https://doi.org/10.1016/bs.abr.2022.11.004

Lamichhane, J. R., Debaeke, P., Steinberg, C., You, M. P., Barbetti, M. J. and Aubertot, J. N. (2018). Abiotic and biotic factors affecting crop seed germination and seedling emergence: a conceptual framework. *Plant Soil* 432, 1-28. https://doi.org/10.1007/s11104-018-3780-9

Larue, C., Castillo-Michel, H., Sobanska, S., Cécillon, L., Bureau, S., Barthès, V. and Sarret, G. (2014). Foliar exposure of the crop *Lactuca sativa* to silver nanoparticles: evidence for internalization and changes in Ag speciation. *J. Hazard. Mater.* 264, 98-106. https://doi.org/10.1016/j.jhazmat.2013.10.053

Li, C. C., Dang, F., Li, M., Zhu, M., Zhong, H., Hintelmann, H., and Zhou, D. M. (2017). Effects of exposure pathways on the accumulation and phytotoxicity of silver nanoparticles in soybean and rice. *Nanotoxicology* 11, 699-709. https://doi.org/10.1080/17435390.2017.1344740

Magan, N., Sanchis, V. and Aldred, D. (2004) The role of spoilage fungi in seed deterioration. In: Aurora, D.K. (ed) Fungal Biotechnology in Agricultural, Food and Environmental Applications, Marcel Dekker, New York, USA, pp. 311-323. https://doi.org/10.1201/9780203913369

Mahakham, W., Sarmah, A. K., Maensiri, S. and Theerakulpisut, P. (2017). Nanopriming technology for enhancing germination and starch metabolism of aged rice seeds using phytosynthesized silver nanoparticles. *Sci. Rep.* 7: 8263. https://doi.org/10.1038/s41598-017-08669-5

Majda, M. and Robert, S. (2018) The role of auxin in cell wall expansion. *Int. J. Mol. Sci.* 19: 951. https://doi.org/10.3390/ijms19040951

Marzol, E., Borassi, C., Carignani Sardoy, M., Ranocha, P., Aptekmann, A. A., Bringas, M., Pennington, J., Paez-Valencia, J., Martínez Pacheco, J., Rodríguez-Garcia, D.R. Estevez, J. M. et al. (2022). Class III peroxidases PRX01, PRX44, and PRX73 control root hair growth in *Arabidopsis thaliana*. *Int. J. Mol. Sci. 23*: 5375. https://doi.org/10.3390/ijms23105375

Masum, M.M., Siddiqa, M.M., Ali, K.A., Zhang, Y., Abdallah, Y., Ibrahim, E., Qiu, W., Yan, C. and Li, B. (2019). Biogenic synthesis of silver nanoparticles using *Phyllanthus emblica* fruit extract and its inhibitory action against the pathogen *Acidovorax oryzae* strain RS-2 of rice bacterial brown stripe. *Front. Microbiol.* 10: 820. https://doi.org/10.3389/fmicb.2019.00820

Mawale, K. S., Nandini, B., and Giridhar, P. (2024). Copper and silver nanoparticle seed priming and foliar spray modulate plant growth and thrips infestation in *Capsicum* spp. *ACS Omega* 9, 3430–3444. https://doi.org/10.1021/acsomega.3c06961

Mondéjar-López, M., López-Jimenez, A. J., Ahrazem, O., Gómez-Gómez, L. and Niza, E. (2023). Chitosan coated-biogenic silver nanoparticles from wheat residues as green antifungal and nanoprimig in wheat seeds. *Int. J. Biol. Macromol.* 225, 964-973. https://doi.org/10.1016/j.ijbiomac.2022.11.159

Nandini, B., Mawale, K. S. and Giridhar, P. (2023). Nanomaterials in agriculture for plant health and food safety: a comprehensive review on the current state of agro-nanoscience. *3 Biotech* 13: 73. https://doi.org/10.1007/s13205-023-03470-w

Nile, S. H., Thiruvengadam, M., Wang, Y., Samynathan, R., Shariati, M. A., Rebezov, M., Nile, A., Sun, M., Venkidasamy, B., Xiao, J., and Kai, G. (2022). Nano-priming as emerging seed priming technology for sustainable agriculture—Recent developments and future perspectives. *J. Nanobiotechnology* 20: 254. https://doi.org/10.1186/s12951-022-01423-8

Noctor, G., Mhamdi, A., Chaouch, S., Han, Y. I., Neukermans, J., Marquez-Garcia, B. and Foyer, C. H. (2012). Glutathione in plants: an integrated overview. *Plant Cell Environ.* 35, 454-484. https://doi.org/10.1111/j.1365-3040.2011.02400.x

Oldenburg, E., and Ellner, F. (2015). Distribution of disease symptoms and mycotoxins in maize ears infected by *Fusarium culmorum* and *Fusarium graminearum. Mycotoxin Res.* 31, 117–126. https://doi.org/10.1007/s12550-015-0222-x

Orchard, T. (1977). Estimating the parameters of plant seedling emergence. *Seed Sci. Technol.* 5, 61–69.

Passardi, F., Cosio, C., Penel, C. and Dunand, C. (2005). Peroxidases have more functions than a Swiss army knife. *Plant Cell Rep.* 24, 255-265. https://doi.org/10.1007/s00299-005-0972-6

Prażak, R., Święciło, A., Krzepiłko, A., Michałek, S. and Arczewska, M. (2020). Impact of Ag nanoparticles on seed germination and seedling growth of green beans in normal and chill temperatures. *Agriculture* 10: 312. https://doi.org/10.3390/agriculture10080312

Rai, M. and Golińska, P. (Eds.). (2023). Mycosynthesis of Nanomaterials: Perspectives and Challenges. CRC Press, USA. https://doi.org/10.1201/9781003327387

Rajjou, L., Duval, M., Gallardo, K., Catusse, J., Bally, J., Job, C. and Job, D. (2012). Seed germination and vigor. *Annu. Rev. Plant Biol.* 63, 507-533. https://doi.org/10.1146/annurev-arplant-042811-105550

Rao, M.V., Paliyath, G. and Ormrod, D.P. (1996). Ultraviolet-B- and ozone-induced biochemical changes in antioxidant enzymes of *Arabidopsis thaliana*. *Plant Physiol.* 110, 125–136. https://doi.org/10.1104/pp.110.1.125

Revilla, P., Alves, M. L., Andelković, V., Balconi, C., Dinis, I., Mendes-Moreira, P., and Malvar, R. A. (2022). Traditional foods from maize (*Zea mays* L.) in Europe. *Front. Nutrition* 8: 683399. https://doi.org/10.3389/fnut.2021.683399

Rodríguez-Ruiz, M., González-Gordo, S., Cañas, A., Campos, M. J., Paradela, A., Corpas, F. J., and Palma, J. M. (2019). Sweet pepper (*Capsicum annuum* L.) fruits contain an atypical peroxisomal catalase that is modulated by reactive oxygen and nitrogen species. *Antioxidants* 8*:* 374. https://doi.org/10.3390/antiox8090374

Rouf Shah, T., Prasad, K. and Kumar, P. (2016). Maize - A potential source of human nutrition and health: A review. *Cogent Food Agric.* 2: 1166995. https://doi.org/10.1080/23311932.2016.1166995

Savassa, S. M., Castillo-Michel, H., del Real, A. E., Reyes-Herrera, J., Marques, J. P. and de Carvalho, H. W. (2021). Ag nanoparticles enhancing *Phaseolus vulgaris* seedling development: understanding nanoparticle migration and chemical transformation across the seed coat. *Env Sci Nano*, 8, 493-501. https://doi.org/10.1039/D0EN00959H

Scandalios, J. G., Tsaftaris, A. S., Chandlee, J. M., and Skadsen, R. W. (1983). Expression of the developmentally regulated catalase (Cat) genes in maize. *Dev. Gen.* 4, 281-293. https://doi.org/10.1002/dvg.1020040406

Scott, S. J., Jones, R. A. and Williams,W. (1984). Review of data analysis methods for seed germination 1. *Crop Sci.* 24, 1192–1199. https://doi.org/10.2135/cropsci1984.0011183X002400060043x

Sencan, A., Kilic, S. and Kaya, H. (2024). Stimulating effect of biogenic nanoparticles on the germination of basil (*Ocimum basilicum* L.) seeds. *Sci. Rep.* 14: 1715. https://doi.org/10.1038/s41598-023-50654-8

Sharma, S., Singh, V. K., Kumar, A. and Mallubhotla, S. (2019). Effect of nanoparticles on oxidative damage and antioxidant defense system in plants. In: Banerjee, A., Roychoudhury, A. (eds) Molecular Plant Abiotic Stress: Biology and Biotechnology, Apple Academic Press, USA pp. 315-333. ISBN: 978-1-119-46369-6 https://doi.org/10.1002/9781119463665.ch17

Sidhu, A. K., Verma, N. and Kaushal, P. (2022). Role of biogenic capping agents in the synthesis of metallic nanoparticles and evaluation of their therapeutic potential. *Front. Nanotechnol.* 3: 801620. https://doi.org/10.3389/fnano.2021.801620

Shang, Y., Hasan, M. K., Ahammed, G. J., Li, M., Yin, H., and Zhou, J. (2019). Applications of nanotechnology in plant growth and crop protection: a review. *Molecules (Basel, Switzerland)*, *24*(14), 2558. https://doi.org/10.3390/molecules24142558

Singh, A., Sharma, A., Singh, O., Rajput, V. D., Movsesyan, H., Minkina, T., Alexiou, A., Papadakis, M., Singh, R. K., Singh, S., Sousa, J. R., El-Ramady, H. R., Zulfiqar, F., Kumar, R., Al-Ghamdi, A. A., and Ghazaryan, K. (2024). In-depth exploration of nanoparticles for enhanced nutrient use efficiency and abiotic stresses management: Present insights and future horizons. *Plant Stress* 14: 100576. https://doi.org/10.1016/j.stress.2024.100576

Soliman, M., Qari, S. H., Abu-Elsaoud, A., El-Esawi, M., Alhaithloul, H. and Elkelish, A. (2020). Rapid green synthesis of silver nanoparticles from blue gum augment growth and performance of maize, fenugreek, and onion by modulating plants cellular antioxidant machinery and genes expression. *Acta Physiologiae Plantarum* 42, 1-16. https://doi.org/10.1007/s11738-020-03131-y

Srivastav, A. L., Patel, N., Rani, L., Kumar, P., Dutt, I., Maddodi, B. S. and Chaudhary, V. K. (2024). Sustainable options for fertilizer management in agriculture to prevent water contamination: a review. *Environ Dev Sustain* 26, 8303-8327. https://doi.org/10.1007/s10668-023-03117-z

Su, Y., Ashworth, V., Kim, C., Adeleye, A. S., Rolshausen, P., Roper, C., White, J., and Jassby, D. (2019). Delivery, uptake, fate, and transport of engineered nanoparticles in plants: A critical review and data analysis. *Environ. Sci: Nano*, 6, 2311–2331. https://doi.org/10.1039/C9EN00461K

Syu, Y-Y., Hung, J-H., Chen, J-C. and Chuang, H-W. (2014). Impacts of size and shape of silver nanoparticles on Arabidopsis plant growth and gene expression. *Plant Physiol. Biochem.* 83, 57-64. https://doi.org/10.1016/j.plaphy.2014.07.010

Tripathi, S., Srivastava, P., Devi, R. S., and Bhadouria, R. (2020). Influence of synthetic fertilizers and pesticides on soil health and soil microbiology. In Prasad M. N. (ed.) Agrochemicals Detection, Treatment and Remediation Butterworth-Heinemann, UK pp. 25–54. https://doi.org/10.1016/B978-0-08-103017-2.00002-7

Trzcińska-Wencel, J., Golińska, P. and Rai, M. 2024. Toxicity of nanomaterials to plants. In: Rai, M., Avila-Quezada, G. D. (eds) Nanotechnology in Plant Health, CRC Press, USA, pp. 369-389. https://doi.org/10.1201/9781003375104

Trzcińska-Wencel, J., Wypij, M., and Golińska, P. (2023a). Mycogenic synthesis of silver nanoparticles and its optimization. In Rai, M., Golińska, P. (eds) Mycosynthesis of Nanomaterials, CRC Press, USA, pp. 126-145. https://doi.org/10.1201/9781003327387

Trzcińska-Wencel, J., Wypij, M., Rai, M. and Golińska, P. (2023c). Biogenic nanosilver bearing antimicrobial and antibiofilm activities and its potential for application in agriculture and industry. *Front. Microbiol.* 14: 1125685. https://doi.org/10.3389/fmicb.2023.1125685

Trzcińska-Wencel, J., Wypij, M., Terzyk, A. P., Rai, M. and Golińska, P. (2023b). Biofabrication of novel silver and zinc oxide nanoparticles from *Fusarium solani* IOR 825 and their potential application in agriculture as biocontrol agents of phytopathogens, and seed germination and seedling growth promoters. *Front. Chem.* 11: 1235437. https://doi.org/10.3389/fchem.2023.1235437

Tyburski, J. and Mucha, N. (2023). Antioxidant response in the salt-acclimated red beet (*Beta vulgaris)* callus. *Agronomy* 13: 2284. https://doi.org/10.3390/agronomy13092284

Vannini, C., Domingo, G., Onelli, E., De Mattia, F., Bruni, I., Marsoni, M. and Bracale, M. (2014). Phytotoxic and genotoxic effects of silver nanoparticles exposure on germinating wheat seedlings. *J. Plant Physiol.* 171, 1142-1148. https://doi.org/10.1016/j.jplph.2014.05.002

Veljovic-Jovanovic, S., Noctor, G. and Foyer, C.H. (2002) Are leaf hydrogen peroxide concentrations commonly overestimated? The potential influence of artefactual interference by tissue phenolics and ascorbate. *Plant Physiol. Biochem*. 40, 501–507. https://doi.org/10.1016/S0981-9428(02)01417-1

Vishwakarma, K., Shweta, Upadhyay, N., Singh, J., Liu, S., Singh, V. P., Prasad, S.M., Chauhan, D.K., Tripathi, D.K. and Sharma, S. (2017). Differential phytotoxic impact of plant mediated silver nanoparticles (AgNPs) and silver nitrate (AgNO3) on *Brassica* sp. *Front. Plant Sci.* 8: 1501. https://doi.org/10.3389/fpls.2017.01501

Wahab, A., Muhammad, M., Ullah, S., Abdi, G., Shah, G. M., Zaman, W., and Ayaz, A. (2024). Agriculture and environmental management through nanotechnology: Eco-friendly nanomaterial synthesis for soil-plant systems, food safety, and sustainability. *Sci. Total. Environ.* 926: 171862. https://doi.org/10.1016/j.scitotenv.2024.171862

Wang, J., Wu, B., Yin, H., Fan, Z., Li, X., Ni, S. He, L. and Li, J. (2017). Overexpression of CaAPX induces orchestrated reactive oxygen scavenging and enhances cold and heat tolerances in tobacco. *BioMed Res. Int.* 2017: 4049534. https://doi.org/10.1155/2017/4049534

Waqif, H., Munir, N., Farrukh, M. A., Hasnain, M., Sohail, M. and Abideen, Z. (2024). Algal macromolecular mediated synthesis of nanoparticles for their application against citrus canker for food security. *Int. J. Biol. Macromol.* 263: 130259. https://doi.org/10.1016/j.ijbiomac.2024.130259

Wickham, H. (2016). Data Analysis. In: ggplot2. Use R!. Springer, Cham. https://doi.org/10.1007/978-3-319-24277-4_9

Witham, F.H., Blaydes, D.F. and Devlin, R.M. (1971). Experiments in Plant Physiology, Van Nostrand, New York.

Wypij, M., Ostrowski, M., Piska, K., Wójcik-Pszczoła, K., Pękala, E., Rai, M. and Golińska, P. (2022). Novel antibacterial, cytotoxic and catalytic activities of silver nanoparticles synthesized from acidophilic actinobacterial SL19 with evidence for protein as coating biomolecule. *J. Microbiol. Biotechnol.* 32, 1195-1208. https://doi.org/10.4014/jmb.2205.05006

Xiong, Z., Liu, L., Zhang, Z., Cao, L., Cao, D., Du, Z., and Tang, Y. (2022). Unravelling the role of surface modification in the dermocompatibility of silver nanoparticles in vitro and in vivo. *Chemosphere* 291: 133111. https://doi.org/10.1016/j.chemosphere.2021.133111

Yan, X., Chen, S., Pan, Z., Zhao, W., Rui, Y., and Zhao, L. (2023). AgNPs-Triggered Seed Metabolic and Transcriptional Reprogramming Enhanced Rice Salt Tolerance and Blast Resistance. *ACS Nano* 17, 492–504. https://doi.org/10.1021/acsnano.2c09181

Yen, H.J., Horng, J.L., Yu, C.H., Fang, C.Y., Yeh, Y.H., and Lin, L.Y. (2019). Toxic effects of silver and copper nanoparticles on lateral-line hair cells of zebrafish embryos. Aquatic Toxicology, 215: 105273. https://doi.org/10.1016/j.aquatox.2019.105273

Zhang, H., Zhang, J., Xu, Q., Wang, D., Di, H., Huang, J., et al. (2020). Identification of candidate tolerance genes to low-temperature during maize germination by GWAS and RNA-seq approaches. *BMC Plant Biol.* 20, 1–17. https://doi.org/10.1186/s12870-020-02543-9

Zhao, L., Zhou, X., Kang, Z., Peralta-Videa, J. R., and Zhu, Y.G. (2024). Nano-enabled seed treatment: A new and sustainable approach to engineering climate-resilient crops. *Sci. Total. Environ.* 910: 168640. https://doi.org/10.1016/j.scitotenv.2023.168640

Figure 1. Detection and physicochemical characteristics of AgNPs synthesized from *Fusarium solani* IOR 825: TEM micrographs (A), UV-vis spectrum (B), size distribution from Nanoparticle Tracking Analysis (NTA) (C), size distribution from Dynamic Light Scattering (DLS) analysis (D), Zeta potential (E), diffractogram from X-ray diffraction analysis (F), FTIR-spectrum (G).

Figure 2. The length of shoots and roots (a), fresh (b) and dry weight (c) of 14-day-old maize plantlets after sterilization of grains with AgNPs. Data presented as mean and standard error (SE) and statistical significance (*p*-value* $p \leq 0.05$, ** $p \leq 0.01$, *** $p \leq 0.001$).

Figure 3. Influence of maize grain sterilization with AgNPs on the chlorophyll content in leaves of 14-day-old maize plantlets. Data presented as mean and standard error (±SE), and statistical significance (*p*-value* $p \leq 0.05$).

Figure 4. Influence of maize grains sterilization with AgNPs on levels of hydrogen peroxide (H_2O_2) (A) malondialdehyde (MDA) (B), and total glutathione (GSH+GSSG) (C) in 14-day-old maize plantlets. Data presented as mean and standard error (±SE), and statistical significance (*p*-value* $p \leq 0.05$, ** $p \leq 0.01$, *** $p \leq 0.001$).

Figure 5. Influence of maize grains sterilization with AgNPs on the ASC+DHA content (A), ASC level (B) and ascorbate redox state [ASC/(ASC+DHA) ratio] (C) of 14-day-old maize plantlets. Data presented as mean and standard error (±SE), and statistical significance (*p*-value* $p \leq 0.05$, ** $p \leq 0.01$, *** $p \leq 0.001$).

Figure 6. Influence of maize grains sterilization with AgNPs on the activity of CAT (A), SOD (B), POX (C) and APX in 14-day-old maize plantlets. Data presented as mean and standard error (±SE), and statistical significance (*p*-value* $p \leq 0.05$, ** $p \leq 0.01$, *** $p \leq 0.001$).

Figure 7. Analysis of general alterations and correlations of growth and individual biochemical parameters among organs of plantlets developed from grains treated with AgNPs. (PCA)-biplot (A), where arrows indicate the strength of the trait influence on the first two PCs; correlation analysis between all the studied parameters, where red and blue colors represent positive and negative correlations, respectively (B); dendrogram from hierarchical cluster analysis (HCA) showing associations in changes of biochemical parameters among various AgNPs treatments and maize plantlets organs (C).
APX: ascorbate peroxidase; ASC: ascorbate; ASCr: reduced ascorbate; DW: dry weight; FW: fresh weight; GSH: glutathione; H2O2: hydrogen peroxide; MDA: malondialdehyde; POX: peroxidase; SOD: superoxide dismutase; tASC: total ascorbate; Ctrl: untreated control; 32: treatment with AgNPs at concentration of 32 µg mL^{-1}; 128: treatment with AgNPs at concentration of 128 µg mL^{-1}; 512: treatment with AgNPs at concentration of 512 µg mL^{-1}; L: leaves; S: stem; R: roots; C: caryopsis.

Figure 8. The summarized effects of AgNPs on maize growth and redox metabolism in maize plantlet organs. Upright and downward pointing arrows denote stimulatory and inhibitory effects of AgNPs treatments, respectively, (for details, see text). APX: ascorbate peroxidase; ASC: ascorbate; CAT: catalase; GSH: total glutathione; H_2O_2: hydrogen peroxide; POX: peroxidase; SOD: superoxide dismutase;

Table 1. Germination parameters of maize grains after pretreatment with AgNPs from *Fusarium solani* IOR 825.

AgNPs concentration [µg mL^{-1}]	% germination	Vigour index I	Vigour index II	MGT [day]	GRI [%/day]
0	94.3	3980.6	6259.7	3.2	31.0
32	95.7	4384.7	7759.7	3.2	31.4
128	92.9	4185.3	7660.5	3.2	31.0
512	91.4	4334.3*	8096.1*	3.2	30.5

MGT; mean germination time, GRI; germination rate index; * denote statistical significance (p-value < 0.05) between AgNPs treatment and control.

Figure 1.JPEG

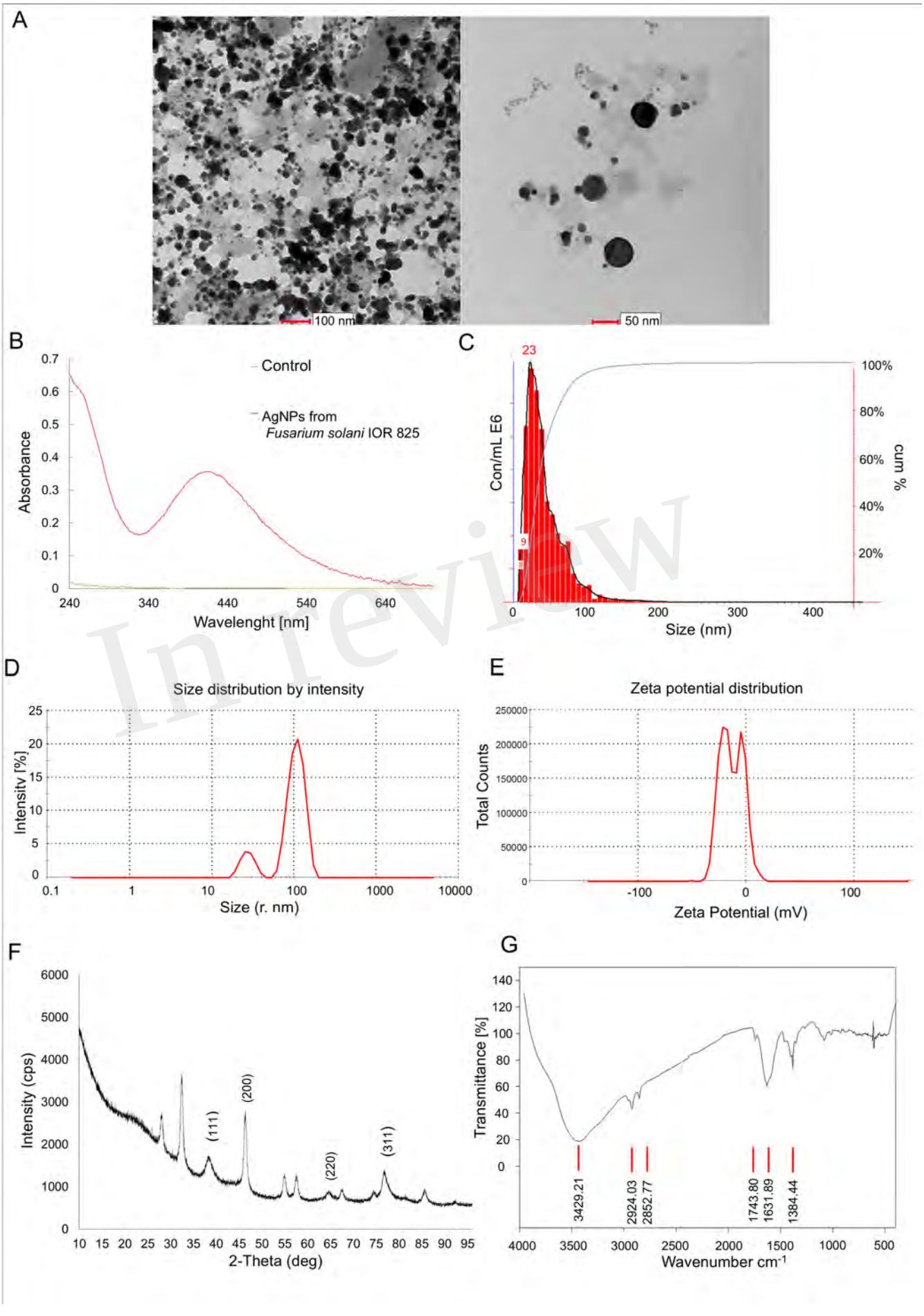

Figure 2.JPEG

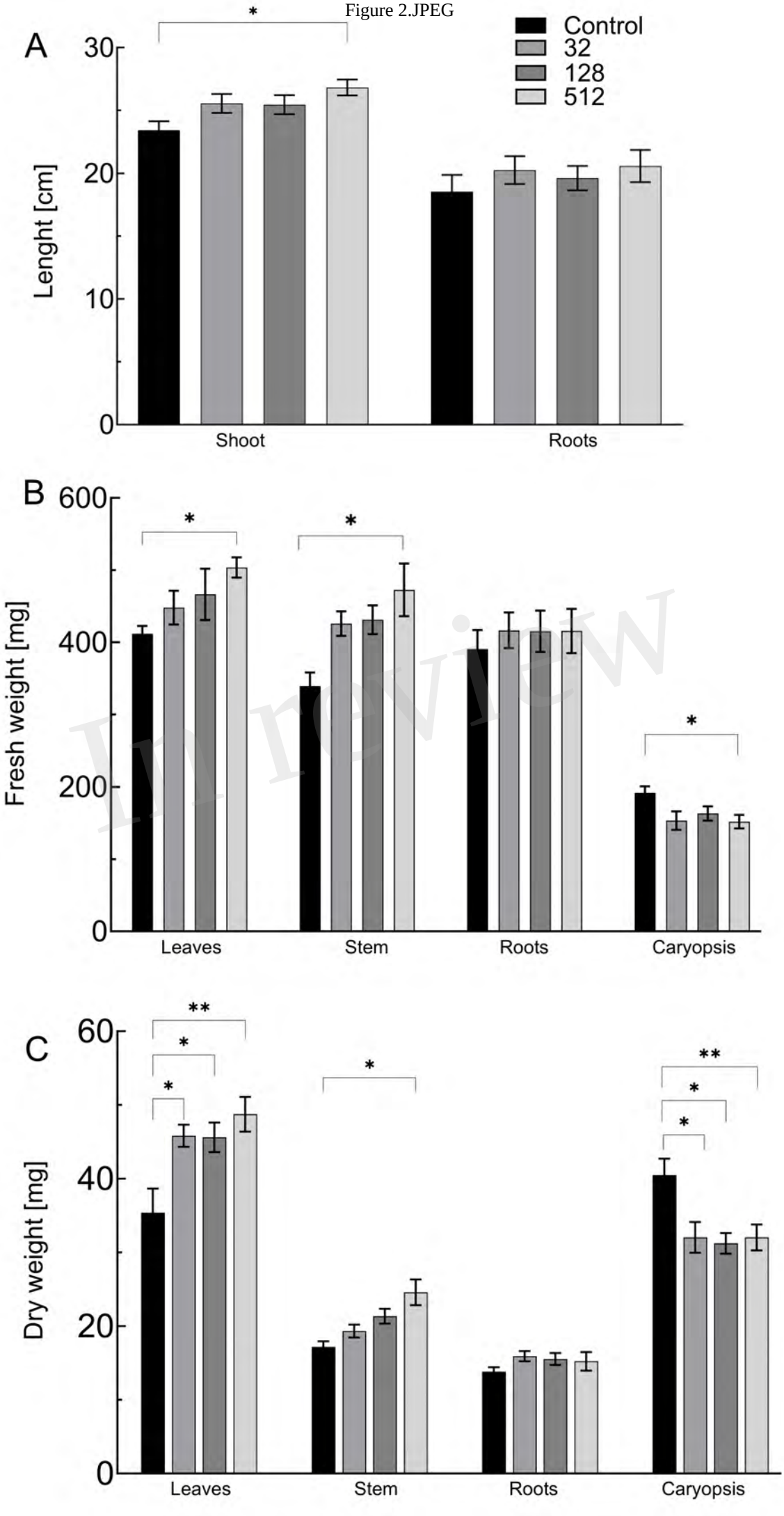

Figure 3.JPEG

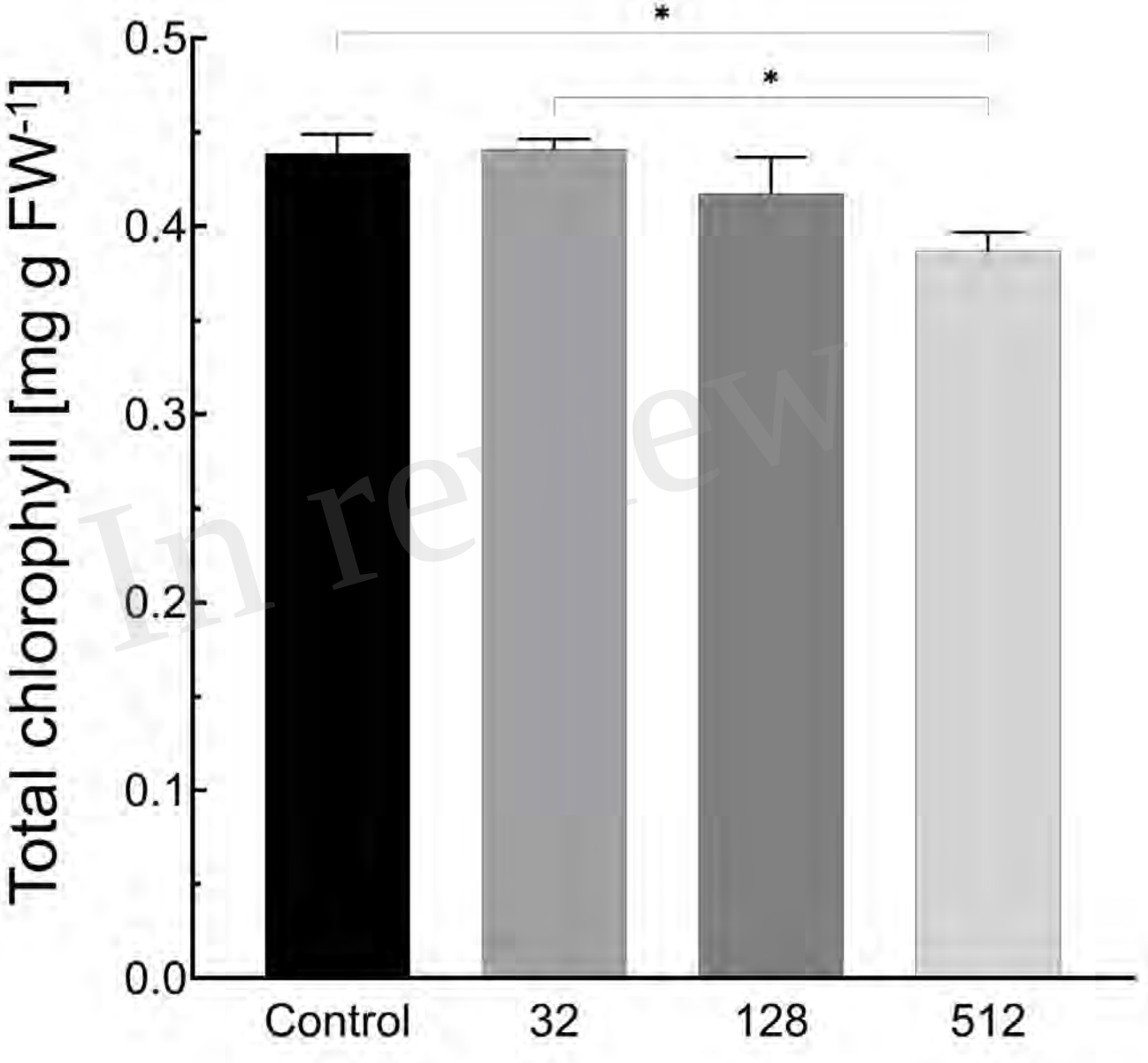

Figure 4.JPEG

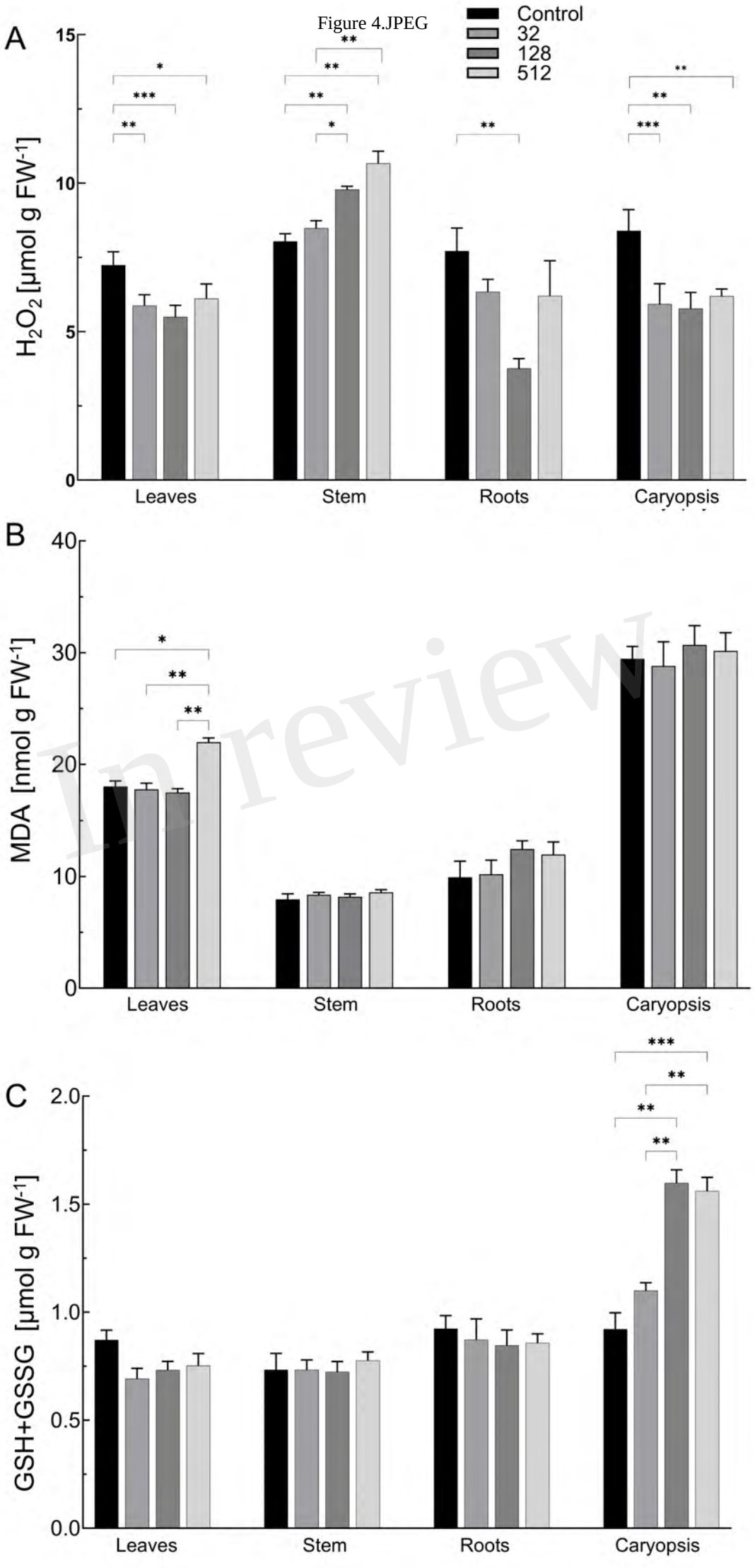

Figure 5.JPEG

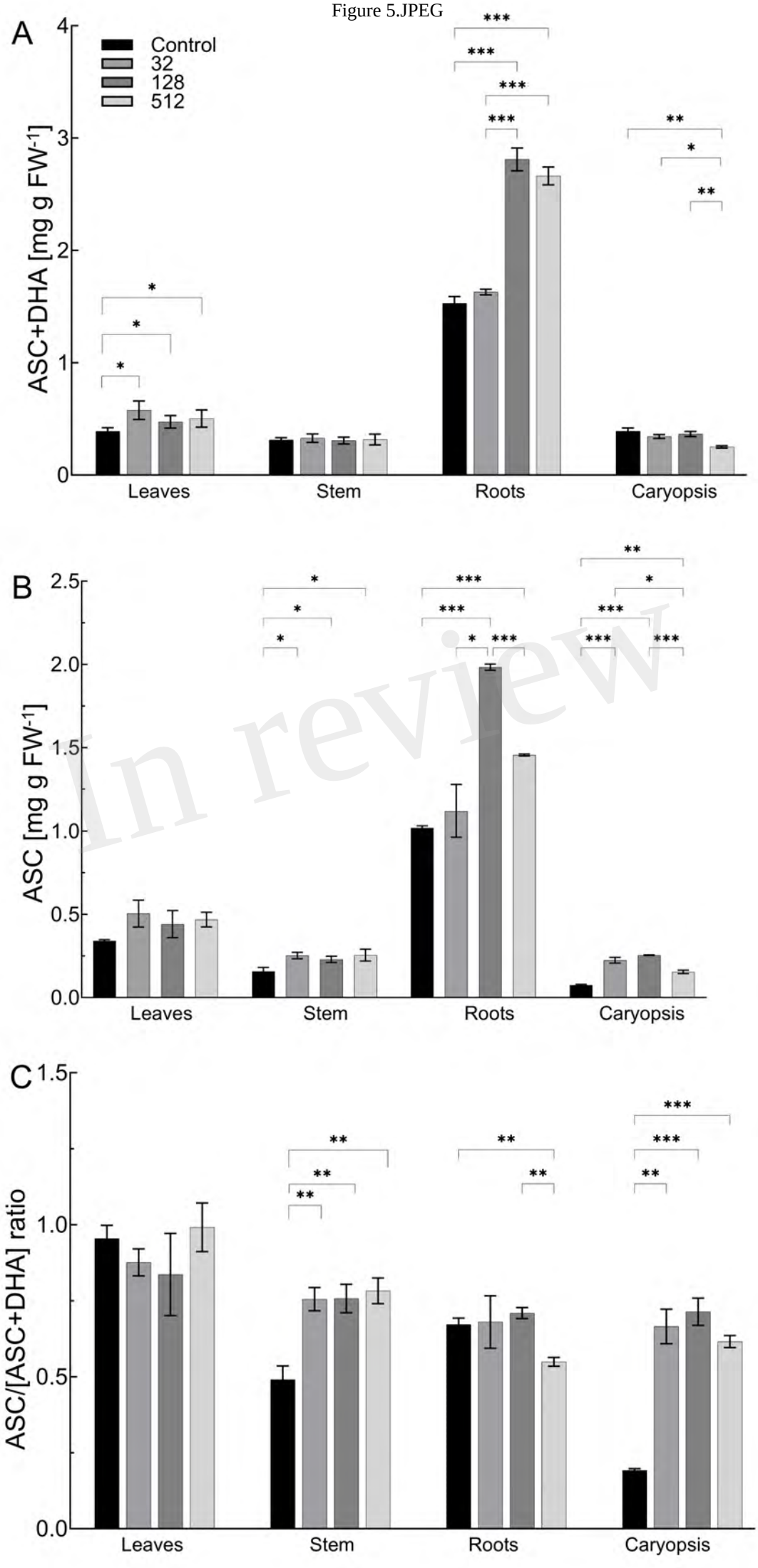

Figure 6.JPEG

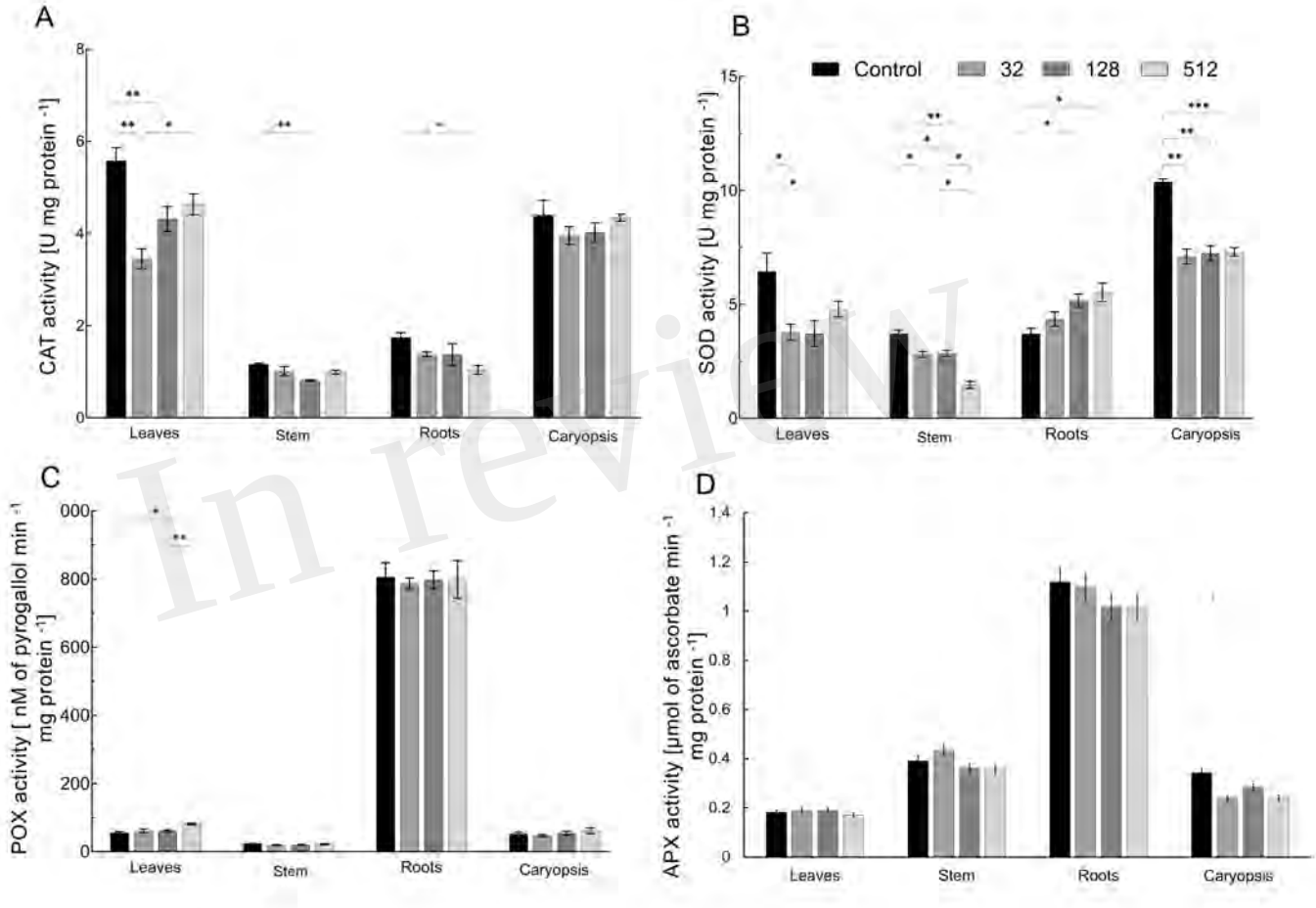

Figure 7.JPEG

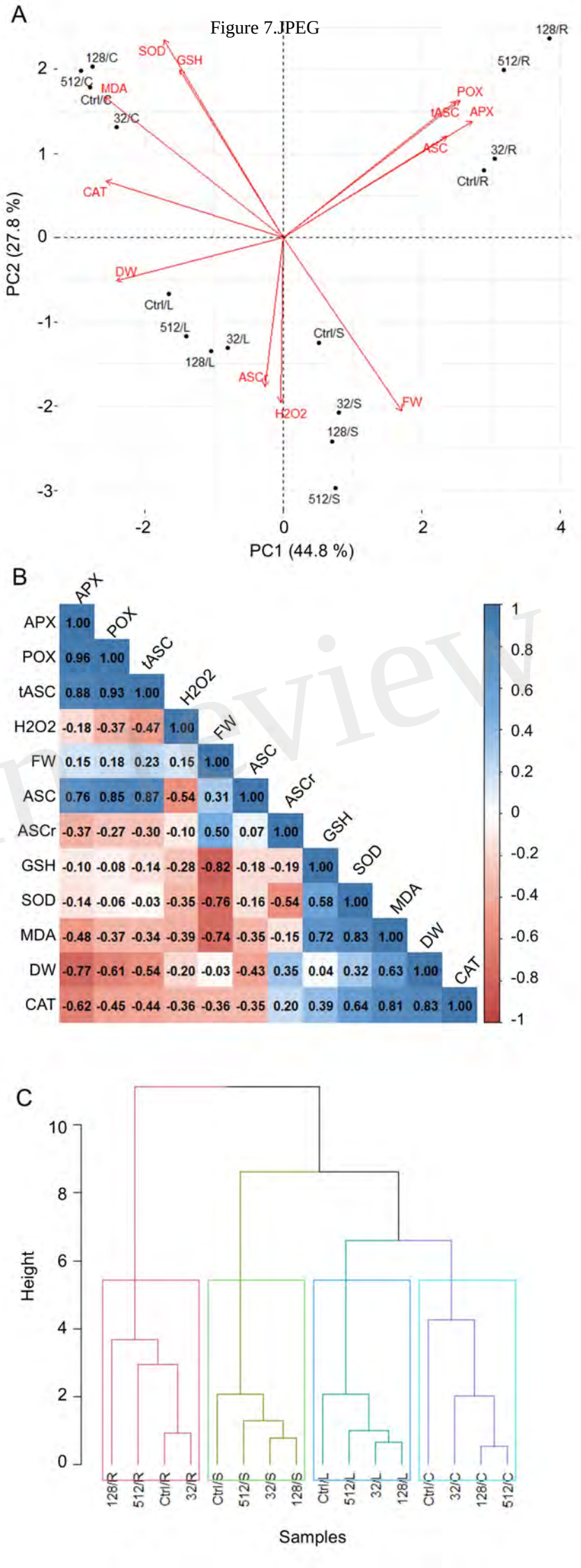

Figure 8.TIF

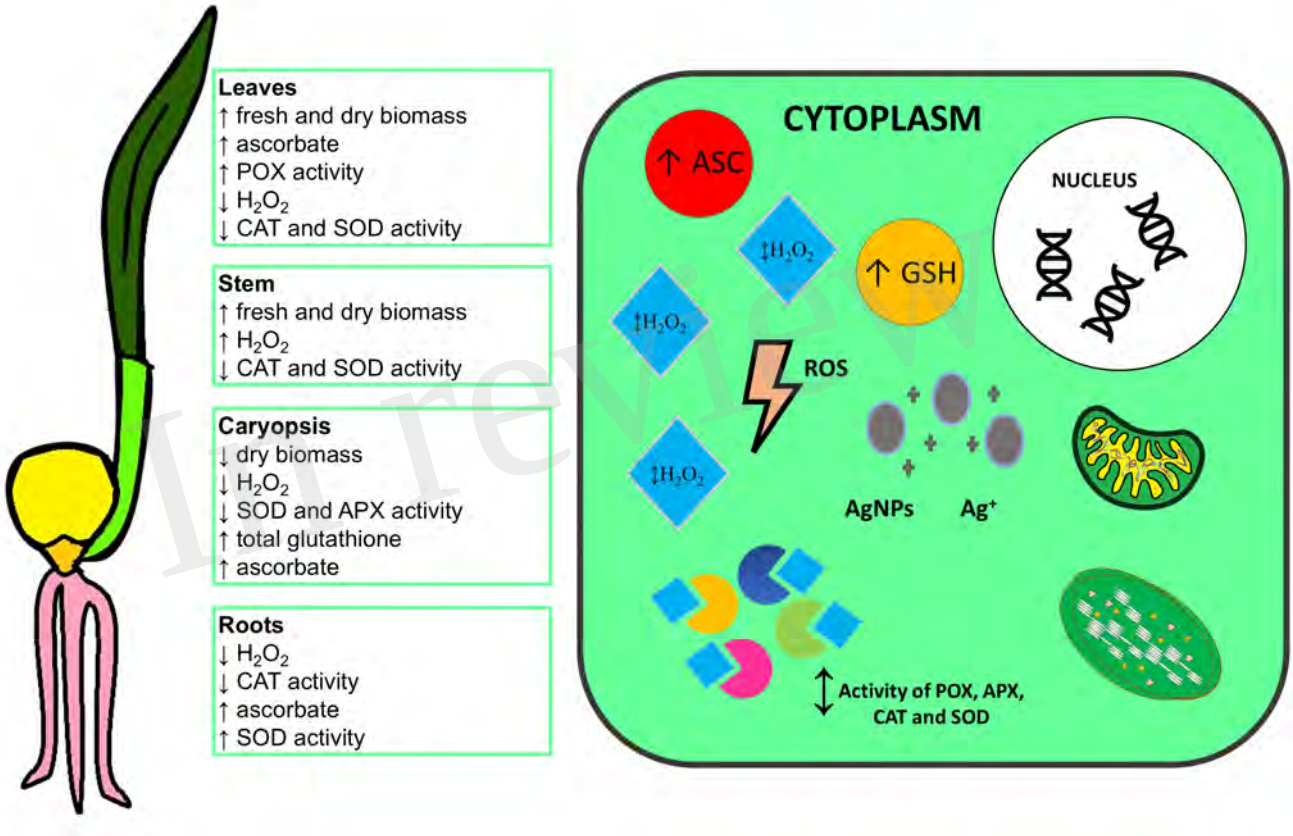
Leaves
↑ fresh and dry biomass
↑ ascorbate
↑ POX activity
↓ H_2O_2
↓ CAT and SOD activity
Stem
↑ fresh and dry biomass
↑ H_2O_2
↓ CAT and SOD activity
Caryopsis
↓ dry biomass
↓ H_2O_2
↓ SOD and APX activity
↑ total glutathione
↑ ascorbate
Roots
↓ H_2O_2
↓ CAT activity
↑ ascorbate
↑ SOD activity
CYTOPLASM
↑ ASC
↕H_2O_2
↕H_2O_2
↕H_2O_2
↑ GSH
ROS
NUCLEUS
AgNPs
Ag+
Activity of POX, APX, CAT and SOD

frontiers

Supplementary Material

Pre-sowing treatment with bio-AgNPs as a grain sterilization technique triggers an organ-specific and dose-dependent response of the antioxidant system of maize

Trzcińska-Wencel Joanna[1*], Mucha Natalia[2], Rai Mahendra[3,4] Tyburski Jarosław[2], Golińska Patrycja[1*]

[1] Department of Microbiology, Faculty of Biological and Veterinary Sciences, Nicolaus Copernicus University in Toruń, Toruń, Poland,

[2] Department of Plant Physiology and Biotechnology, Faculty of Biological and Veterinary Sciences, Nicolaus Copernicus University in Toruń, Toruń, Poland

[3] Nanobiotechnology Laboratory, Department of Biotechnology, SGB Amravati University, Amravati, India

[4]Department of Chemistry, Federal University of Piaui (UFPI), University Campus Ministro Petrônio Portella, Ininga, Teresina, Piauí, 64049-550, Brazil

*** Correspondence:**
Trzcińska-Wencel Joanna
trzcinska@doktorant.umk.pl

Golińska Patrycja
golinska@umk.pl

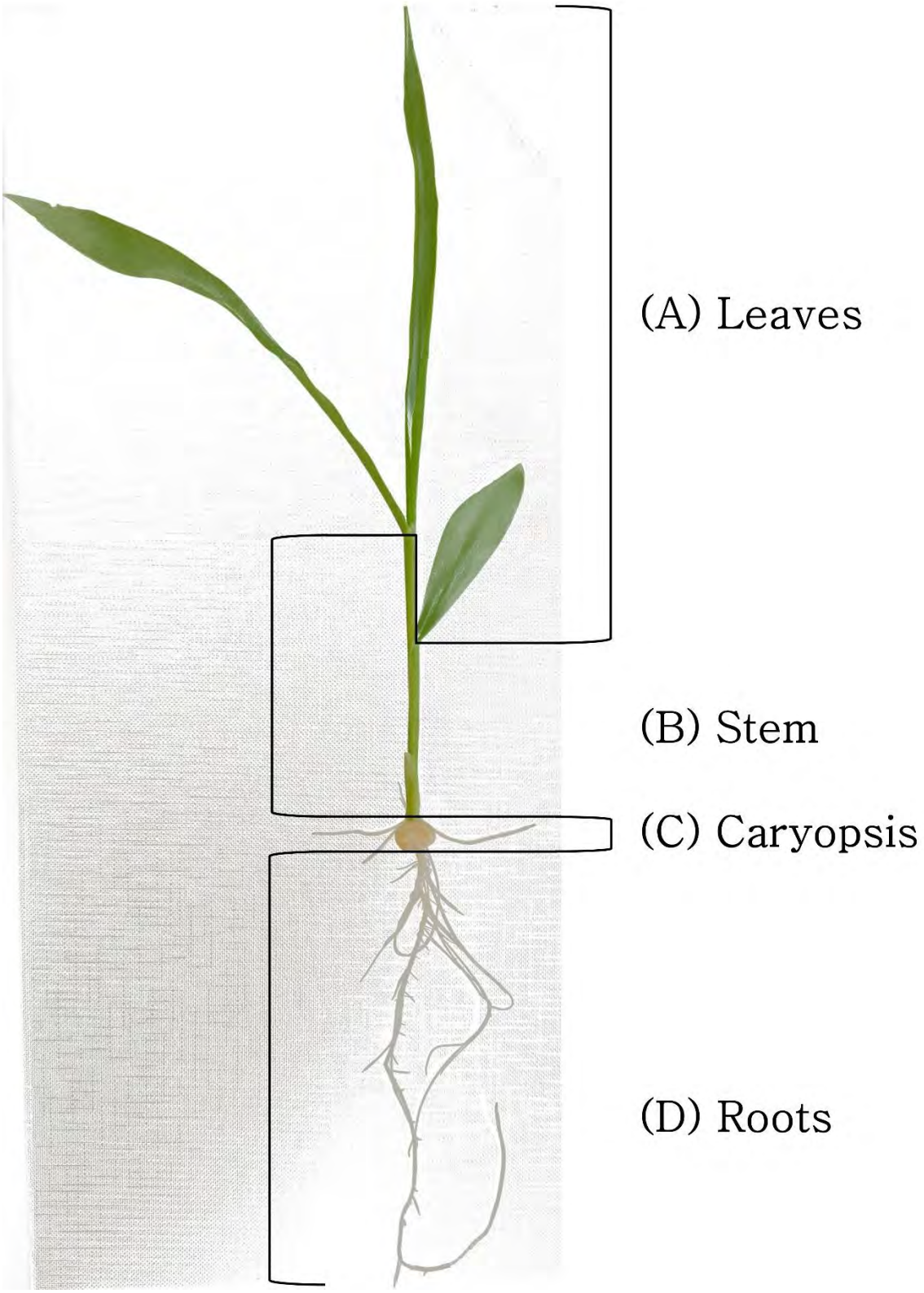

Supplementary Figure S1. Schematic diagram of a 14-day-old maize showing the individual organs (leaves, stem, caryopsis and roots) used to assess the activity of the antioxidant system.

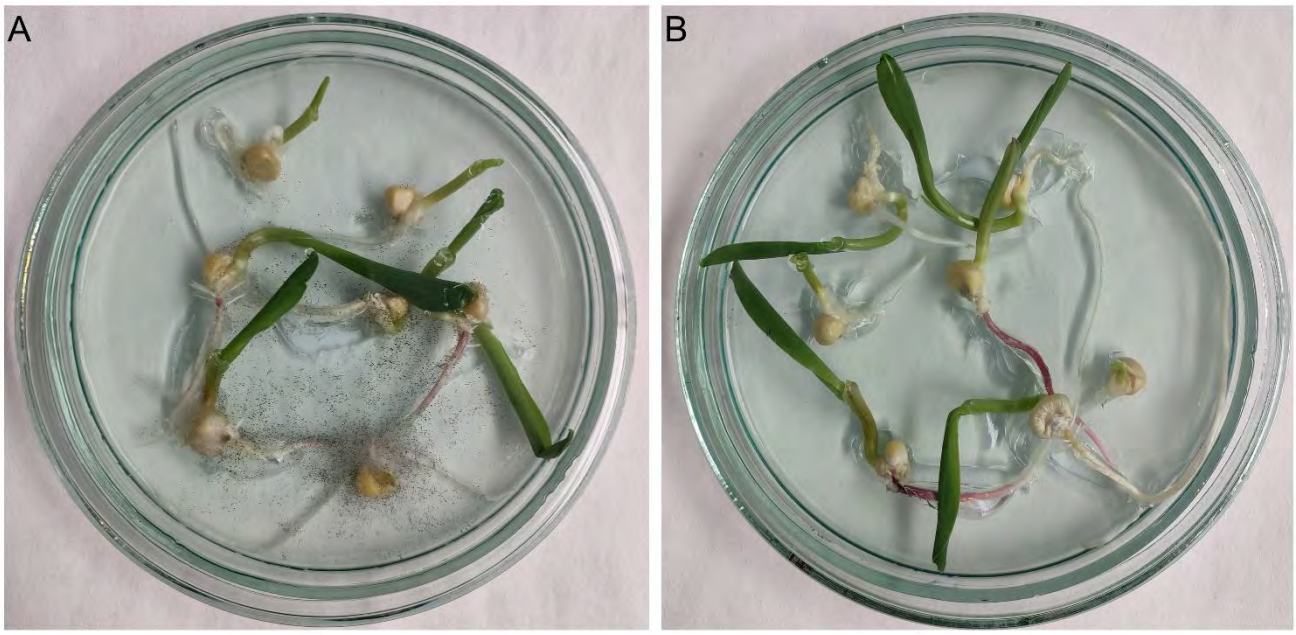

Supplementary Figure S2. The sterilization effect of AgNPs from *Fusarium solani* IOR825 on maize grains. The germinated unsterilized grains treated with sterile distilled water (without AgNPs) with visible microbial growth (A) and grains treated with AgNPs solution at the concentration of 32 µg mL^{-1} (B).

Supplementary Table 1. The summarized alterations [%] in growth parameters, accumulation of H_2O_2, malondialdehyde (MDA), total glutathione, total ascorbate and reduced ascorbate and enzymatic activity in individual organs of maize plantlets treated with bio-AgNPs in comparison with the control.

	AgNPs concentration [µg mL^{-1}]		
	32	**128**	**512**
Lenght			
Shoot	7.9	7.5	13.3*
Root	9.2	5.8	11.0
Fresh weight			
leaves	8.8	13.3	22.3*
stem	25.5	27.1	39.2*
roots	15.9	11.8	15.6
caryopsis	-20.0	-14.9	-20.8*
Dry weight			
leaves	29.5*	28.9*	37.8*
stem	12.4	24.2	43.1*
roots	15.2	12.4	10.1
caryopsis	-20.9*	-22.9*	-20.9*
Chlorophyll content			
Leaves	0.4	-4.9	-11.8*
H_2O_2 concentration			
leaves	-18.8*	-24.1*	-15.5*
stem	5.5	21.7*	32.7*
roots	-17.7	-51.2*	-19.5
caryopsis	-29.4*	-31.2*	-26.2*
MDA concentration			
leaves	-1.4	-3.0	22.0*
stem	5.3	3.0	7.9
roots	2.7	25.5	20.5
caryopsis	-2.2	4.2	2.4
Total glutathione			
leaves	-20.7	-16.0	-13.8
stem	0.0	-1.3	5.9
roots	-5.5	-8.4	-7.1
caryopsis	19.4	73.5*	69.4*
Total ascorbate			
leaves	48.1*	21.5*	29.1*
stem	4.7	-2.0	0.8
roots	6.6	83.8*	74.2*
caryopsis	-12.5	-6.7	-36.3*
Reduced ASC			
leaves	47.9*	29.3*	37.3*
stem	60.5	45.9	62.1
roots	9.9	94.4*	42.7*
caryopsis	201.2*	241.7*	107.3*
CAT activity			
leaves	-38.1*	-22.6*	-17.0
stem	-13.0	-30.5*	-15.0

roots	-21.1	-21.1	-40.3*
caryopsis	-10.1	-8.4	-1.3
SOD activity			
leaves	-41.4*	-42.4*	-25.6
stem	-24.2*	-22.8*	-60.3*
roots	17.6	39.6*	49.2*
caryopsis	-31.6*	-30.2*	-29.6*
POX activity			
leaves	9.2	9.2	46.4*
stem	-16.8	-14.9	-5.4
roots	-2.4	-1.1	-0.9
caryopsis	-9.6	3.3	18.5
APX activity			
leaves	3.3	4.4	-6.6
stem	11.4	-7.9	-9.1
roots	-1.9	-9.0	-2.7
caryopsis	-30.7*	-17.2	-17.8

Supplementary Table S2. The content of elements in the organs of 14-day-old maize treated with AgNPs determined by EDS analysis, data presented in mass %.

AgNPs concentration [µg mL^{-1}] / organ		C	N	O	Na	Mg	Al	Si	P	S	Cl	K	Ag
512 L	Mean	12.1	5.57	73.53	0.00	0.19	0.69	0.03	1.02	0.39	1.06	5.28	0.13
	SD	1.89	0.8	1.34	0.00	0.09	0.26	0.05	0.51	0.2	0.46	1.65	0.1
	SE	0.95	0.4	0.67	0.00	0.04	0.13	0.03	0.25	0.1	0.23	0.83	0.05
512 S	Mean	9.37	6.66	72.96	0.19	0.47	0.34	0.000	0.76	0.28	1.45	6.78	0.09
	SD	1.65	1.14	1.91	0.44	0.33	0.32	0.010	0.24	0.15	0.4	1.16	0.1
	SE	0.74	0.51	0.85	0.19	0.15	0.14	0.000	0.11	0.07	0.18	0.52	0.04
512 R	Mean	6.87	6.61	68.74	1.51	0.5	0.55	0.21	0.83	1.81	1.1	10	0.27
	SD	1.96	0.67	3.14	0.62	0.33	0.22	0.17	0.37	0.88	0.36	5.7	0.15
	SE	0.74	0.25	1.19	0.23	0.12	0.08	0.07	0.14	0.33	0.14	2.16	0.06
512 C	Mean	14.78	4.8	77.97	0.63	0.3	0.41	0.00	0.17	0.14	0.16	0.6	0.06
	SD	0.49	0.17	0.36	0.04	0.05	0.08	0.00	0.05	0.04	0.05	0.07	0.03
	SE	0.24	0.09	0.18	0.02	0.03	0.04	0.00	0.02	0.02	0.03	0.04	0.01
32 C	Mean	15.62	3.37	76.99	0.53	0.41	0.62	0.07	0.43	0.18	0.28	1.08	0.07
	SD	2.54	2.41	2.53	0.62	0.46	0.33	0.15	0.38	0.18	0.28	0.55	0.09
	SE	1.27	1.21	1.26	0.31	0.23	0.17	0.07	0.19	0.09	0.14	0.27	0.04
128 C	Mean	14.8	3.63	77.6	0.79	0.35	0.89	0.04	0.24	0.25	0.25	1.02	0.06
	SD	1.6	1.51	1.2	0.36	0.22	0.66	0.07	0.11	0.12	0.06	0.12	0.05
	SE	0.8	0.75	0.6	0.18	0.11	0.33	0.04	0.06	0.06	0.03	0.06	0.03
0 C	Mean	17.8	2.95	75.2	0.5	0.29	1.00	0.6	0.22	0.17	0.16	0.69	0.03
	SD	2.68	2.17	2.63	0.28	0.15	1.25	1.17	0.08	0.05	0.06	0.13	0.04
	SE	1.2	0.97	1.18	0.12	0.07	0.56	0.52	0.04	0.02	0.02	0.06	0.02

L-leaves; S- stem; R- roots, C- caryopsis

Supplementary Table 3. The contribution of individual biochemical and growth parameters to PC1 and PC2 [%]

	Contribution [%]	
Biochemical or growth parameters	PC1	PC2
CAT	12.34514	1.375484
SOD	5.614616	16.82229
POX	12.26855	8.055341
APX	14.03461	5.854754
H_2O_2	0.002599	11.65415
MDA	12.5625	8.478893
GSH	4.203117	12.1508
tASC	11.75398	8.023095
ASC	10.53573	4.39781
ASCr	0.135178	9.516119
FW	5.559772	12.88525
DW	10.98421	0.78602

APX: ascorbate peroxidase; ASC: ascorbate; ASCr: reduced ascorbate; DW: dry weight; FW: fresh weight; GSH: glutathione; H_2O_2: hydrogen peroxide; MDA: malondialdehyde; POX: peroxidase; SOD: superoxide dismutase; tASC: total ascorbate.

ZnONPs biosynthesized from *Fusarium solani* IOR 825: unveiling their growth stimulating effects in maize (*Zea mays* L.)

Trzcińska-Wencel Joanna[1*], Mucha Natalia[2], Nadrowska Julia[1], Gade Anikiet[1], Rai Mahendra[3,4], Tyburski Jarosław[2], Golińska Patrycja[1]

[1] Department of Microbiology, Faculty of Biological and Veterinary Sciences, Nicolaus Copernicus University in Toruń, Toruń, Poland,

[2] Department of Plant Physiology and Biotechnology, Faculty of Biological and Veterinary Sciences, Nicolaus Copernicus University in Toruń, Toruń, Poland

[3] Nanobiotechnology Laboratory, Department of Biotechnology, SGB Amravati University, Amravati, India

[4]Department of Chemistry, Federal University of Piaui (UFPI), Teresina, Brazil

*** Correspondence:**

Trzcińska-Wencel Joanna

trzcinska@doktorant.umk.pl

Abstract

Maize is economically and globally important crops, but its efficient production depends on germination and primary stage of seedling establishment. This study aimed to evaluate the stimulatory effect of ZnONPs synthesized from *Fusarium solani* IOR 825 on maize seed germination and growth. The antioxidant activity was evaluated in 14-day old plantlets developed from grains treated with ZnONPs. The ZnONPs were small in size (48 nm) with hexagonal wurtzite structure, negative charge (-7.5mV), and functional groups on their surface. The ZnONPs at concentrations of 32 and 128 µg mL^{-1} enhanced fresh (10-32%) and dry (19-40%) weight of plantlets. The increased activity of catalase (CAT) by 19-32%, ascorbate peroxidase (APX) by 16-33%, and higher total ascorbate by 18-47% and reduced ascorbate content by 122-123% were found in leaves, roots, and stems, respectively, along with higher H_2O_2 content. The positive correlations of fresh weight and H_2O_2 (0.82) and dry weight with ascorbate redox ratio (0.73) were indicated.

The growth stimulation was associated with the modulation of H_2O_2 levels in roots, leaves and stems. accompanied by enhanced activity of APX, CAT, and non-enzymatic antioxidants. These findings suggest that ZnONPs can serve as safe and effective growth promoters for maize in agricultural applications.

Keywords: agricultural nanotechnology; crop enhancement; biogenic nanoparticles; zinc oxide nanoparticles; growth promoters; maize

Introduction

The continuous growth of the global human population, along with problems of food insecurity, malnutrition, and hunger in developing countries have garnered the attention of the scientific community. Crop production has become insufficient and ineffective due to several challenges such as climate change, contamination of the environment, loss of genetic diversity, resistance of pathogens and pests to agrochemicals [1]. Maize is one of the most economically and globally important crops with high demand in food and livestock feed production [2-3]. Maize-based products primarily contain carbohydrates, proteins and fat. Moreover, maize serves as a source of various phytochemicals and functional ingredients such as phenolic compounds, phytosterols, carotenoids and vitamins [4]. In common with other crops, corn is vulnerable to climate changes, attacks of pests and pathogens or inappropriate management (fertilization and agrotechnical treatments, unsuitable yield storage) [5].

In this regard, a wide range of agrotechnical practices, biostimulants, and fertilizers are currently being developed and used for sustainable crop improvement. However, it is important to advance the strategies to increase crop production and maintain low ecological impact, addressing emerging adversities by optimizing germination and growth conditions [6]. Among various techniques proposed to improve nutrient use efficiency and mitigation of the harmful effects of biotic and abiotic stresses are precision fertilization and irrigation methodologies, use of biostimulants, development of genomic engineering, innovation in strategies of diseases, and pest and weeds detection and elimination [7-9]. These also include seed priming techniques (biopriming, hydropriming, osmopriming, etc.) applied before sowing to promote germination and seedling establishment, as well as implicate the morpho-physiological response of developing plants to various unexpected environmental factors [10]. Moreover, seed priming techniques are considered environmentally sustainable and cost-effective, making them safe and affordable for farmers [10].

Recently, growing attention has been paid to nano-priming, which depends on the use of nanomaterials (NMs), including metal nanoparticles, metal-oxide nanoparticles, carbon-based, and polymeric nanomaterials. Since nanoparticles (NPs) represent products with unique properties determined by their extremely small size (less than 100 nm) and associated high surface-to-volume ratio, the availability and absorption of active ingredients, nutrients or micro- and macroelements by plants is highly facilitated [11]. Research has focused on seed nanopriming and evaluation of their effect on germination, seedling establishment, plant growth, and development [12]. A diverse impact of NMs on plants' germination and growth has been identified, including modulation of gene expression, changes in nutrient uptake, chlorophyll content or variation of antioxidant defense, depending on NMs type and properties, application protocol, as well as plant species [13-14].

Some reports indicate a high potential of zinc oxide nanoparticles (ZnONPs) for pre-sowing treatments of seeds e.g. rice (*Oryza sativa* L.), pepper (*Capsicum annuum* L.) or wheat (*Triticum aestivum* L.) to enhance their germination, growth and productivity [15-18]. Zinc plays a dual role as a

structural/catalytic component in plants being essential for gene expression, biosynthesis of proteins, enzymatic activity, ion transport, cellular metabolism, proliferation, production of growth hormones, and chlorophyll [19]. The crucial role of Zn has been proven in the regulation of psychological and molecular mechanisms of response to various stresses [20-21]. However, Zn in excessive concentrations is toxic to plants and leads to inefficient biomass production associated with lower photosynthetic efficiency, inhibition of cell elongation and division, and disruption of membrane integrity [19, 22]. Moreover, there are some reports indicating the adverse effect of ZnONPs on plants, nevertheless, their effect depends upon environmental conditions, plant species or stage of growth [23-24]. In addition, the biological activity of ZnONPs highly rests on their physicochemical properties. The methods and conditions of the synthesis process for manufacturing ZnONPs are crucial for the properties of the final products [25-28].

A number of methods have been applied to synthesize ZnONPs, involving chemical, and physical processes or their combinations, such as sol-gel, co-precipitation, microemulsion, laser ablation, hydrothermal, high-energy ball milling, etc. [29]. Interestingly, ZnONPs can be synthesized by biological systems such as plants, bacteria or fungi [30-31]. The process of fungal-mediated synthesis is recognized for its high yields, easy handling, as well as low toxicity of the residues. The use of fungi in the biogenic synthesis of ZnONPs provides a wide range of natural metabolites that act as reducing and stabilizing agents [32]. The biological synthesis of NPs reduces the excessive use of chemicals or the high energy and pressure required in physical or chemical processes [30-31, 33-34].

In the present study, which is a continuation of the previous study [35], ZnONPs were biosynthesized from *Fusarium solani* IOR 825, analyzed for physicochemical properties by various techniques and used at different concentrations of (32, 128 and 512 μg mL^{-1}) for pre-sowing treatment of maize grains. The effect of this treatment was evaluated on the germination, growth, and vigour of 14-day old plantlets. To gain a more comprehensive understanding of the ZnONPs-plant interactions, the chlorophyll content and antioxidative system components were determined in leaves, stems, roots and germinated grains.

Results

Biosynthesis and physicochemical properties of ZnONPs from *Fusarium solani* IOR 825

The biosynthesis of ZnONPs was observed as a white precipitate on the bottom of the flask after challenging the fungal extract of *Fusarium solani* IOR 825 with precursor salt ($ZnSO_4$) and NaOH, followed by heating to 40 ºC and verified by UV-vis spectroscopy which revealed a maximum absorbance peak at a wavelength of 361 nm (**Figure 1a**). XRD analysis of ZnONPs showed peak positions at 31.8, 34.5, 36.3, 47.6, 56.7, 62.9, 67.8 (**Figure 1b**) indexed with the diffraction planes (100), (002), (101), (102), (110), (103) and (112) which confirmed the hexagonal wurtzite structure of ZnONPs. TEM microphotographs showed nanostructures with an irregular shape and an average size of 48 nm (**Figure 1c**). DLS and NTA analysis results of ZnONPs confirmed an average size of 273.5 nm

and 59 nm, respectively (**Figure 1d and 1e**). The ZnONPs were negatively charged (-7.5 mV) (**Figure 1f**). FTIR spectrum of ZnONPs showed absorption bands at 3393, 2961, 2361, 1632, 1589, 1553, 1512, 1119, 1045, 940, 830, 738, 694, 608, 500, 480 cm^{-1}, as shown in **Figure 1G**.

The influence of ZnONPs treatments on maize organs – germination, biomass accumulation, and biochemical parameters

The pre-sowing treatment of grains with all tested concentrations (32, 128, and 512 µg mL^{-1}) of biosynthesized ZnONPs showed no effect on germination efficiency as indicated by germination percentage, mean germination time and germination rate index (**Table 1**). The stimulation of plant growth was observed by increased fresh and dry weight of plantlets developed from ZnONPs-treated seeds, however, no significant results (p-value > 0.05) were reported for plantlets length in comparison to controls (**Figure 2, Table 1**). The application of ZnONPs at concentrations of 32 and 128 µg mL^{-1} showed substantially higher values of vigour index II, namely 5851.2 and 5734.4, respectively, compared to controls (4601.1).

To evaluate the effect of ZnONPs used as pre-sowing treatments on maize growth and development, the chlorophyll content (**Figure 3**), H_2O_2, malondialdehyde (MDA), and total glutathione (GSH+GSSG) levels (**Figure 4**), the concentration of reduced (ASC) and total (reduced and oxidized; ASC+DHA) ascorbate and ascorbate redox ratio (**Figure 5**), as well as activity of antioxidant enzymes (**Figure 6**) were estimated in organs (leaves, stems, caryopses and roots) of 14-day-old plantlets. All variations in parameters were determined as a percentage [%], when compared to control samples, as presented in **Supplementary Table 1.**

Leaves

The application of ZnONPs at concentrations of 32 and 128 µg mL^{-1} resulted in significantly (p-value ≤ 0.05) higher fresh and dry weight of leaves by 27.8-31.6 and 21.9-22.7 %, respectively when compared to control plantlets. However, there was no significant difference (p-value >0.05) between fresh and dry weights of leaves of control plantlets and these developed from grains after ZnONPs treatment at a concentration of 512 µg mL^{-1} (**Figures 2b and 2c, Table S1**). The chlorophyll content in maize plantlets was unaffected after pre-sowing treatment with ZnONPs at the lowest concentration (32 µg mL^{-1}) and reduced by 13 % when higher (128 and 512 µg mL^{-1}) concentrations were applied (**Figure 3, Table S1**). After application of ZnONPs at the concentration of 32 µg mL^{-1} the decrease in the H_2O_2 level by 10 % and activity of APX by 30 % was observed, while application of ZnONPs at a concentration of 512 µg mL^{-1} resulted in accumulation of H_2O_2 of 31 % higher content than in controls. Similar to the H_2O_2 concentration, MDA and total glutathione contents increased, under the treatment with the highest ZnONPs dose, by 70 and 67 %, respectively, in comparison to controls or plantlets treated with lower ZnONPs concentrations (**Figures 4 and 6d, Table S1**). There was a slight shift in ascorbate redox status, as increase in reduced ascorbate by 11 % and a higher ASC/ASC+DHA redox ratio of 0.37 were

identified for this treatment when compared to ratio of 0.33 in controls (**Figure 5c, Table S1**). In the leaves of plantlets developed from maize grains treated with ZnONPs at concentrations of 128 and 512 µg mL^{-1}, the activity of CAT was enhanced by 19-32 %, while POX and APX activities were reduced by 13-26 and 15-26 %, respectively (**Figures 6a, 6c, 6d, Table S1**).

Stems

The application of ZnONPs at concentrations of 32 and 128 µg mL^{-1} resulted in significantly higher (*p*-value ≤ 0.05) fresh (by 23 %) and dry (by 19-21 %) weights of stems as compared to controls. However, there was no increase in the mass of stems detected in plantlets developed from grains treated with ZnONPs at a concentration of 512 µg mL^{-1} (**Figures 2b and 2c, Table S1**). Application of all tested nanoparticle concentrations increased the level of H_2O_2 in stems by 43-50 %. The ZnONPs at concentration of 32 µg mL^{-1} showed no substantial effect on MDA, total glutathione, ascorbate content or antioxidant enzyme activity in stems (**Figures 4, 5, 6, Table S1**). While 30-32 % reduction in MDA content was found in stems of plantlets developed from grains treated with ZnONPs at concentration of 128 and 512 µg mL^{-1} in comparison to controls. Under ZnONPs treatments at concentration of 128 µg mL^{-1} the levels of ASC and ASC+DHA increased by 122 and 18 %, respectively, and the redox ratio (0.38) remained comparable to controls (0.4). The pre-sowing grain treatment with the highest tested concentration of ZnONPs (512 µg mL^{-1}) resulted in increase of ASC and ASC+DHA by 123 and 48 %, as compared to controls, respectively and ascorbate redox status was found to be 1.85-fold higher (0.74) in comparison to controls (0.4) (**Figure 5, Table S1**). The ZnONPs pre-sowing treatments showed no statistically significant (*p*-value > 0.05) influence on activity of tested antioxidant enzymes (CAT, SOD, POX, APX) in stems of maize plantlets (**Figure 6, Table S1**).

Roots

All of the ZnONPs at concentrations of 32, 128 and 512 µg mL^{-1} treatments resulted in improved fresh weights (FW) of roots by 10.3, 22.9 and 27.3 % (**Figure 2b, Table S1**). The plantlets developed from grains after treatment with ZnONPs at concentrations of 32 and 128 µg mL^{-1} showed increased dry weight (DW) of roots by 41.6 and 24.7%, respectively, when compared to controls (**Figure 2c, Table S1**). No substantial changes in H_2O_2, MDA, total glutathione, ascorbate, CAT, POX, SOD activities were observed in roots of plantlets developed from grains after treatment with ZnONPs at concentration of 32 µg mL^{-1}, except 25 % increase in APX activity (**Figures 4, 5 and 6, Table S1**). In roots of plantlets developed from grains treated with ZnONPs at concentrations of 128 and 512 µg mL^{-1} results revealed an increase in H_2O_2 content by 57-71 %, APX activity by 16-33 % and a decrease in CAT activity by 42-43 % (**Figures 6a and 6d**). The MDA levels and SOD activity were comparable to controls (**Figures 4b and 6b, Table S1**).

Caryopsis

Results showed no statistically significant differences (p-value > 0.05) in fresh and dry weights of treated and untreated grains after 14 days from sowing (**Figure 2b and 2c, Table S1**). In the maize grains treated with ZnONPs at all tested concentrations (32, 128 and 512 μg mL^{-1}) the level of H_2O_2 increased by approx. 50 % while the MDA was higher by 35-89 % when compared to control (**Figures 4a and 4b, Table S1**). The ZnONPs-treatment at the highest tested concentration (512 μg mL^{-1}) increased the level of total glutathione by 71 % when compared to the control (**Figure 4c, Table S1**).

In caryopses treated with ZnONPs at concentrations of 128 and 512 μg mL^{-1}, there was an increase in the contribution of the reduced form of ASC by 41.5 and 45.7 %, respectively and higher ascorbate redox ratio (0.96-0.98, respectively) in comparison to controls (ascorbate redox ratio of 0.55) (**Figure 5, Table S1**). Application of ZnONPs at concentrations of 128 and 512 μg mL^{-1} increased SOD and CAT activities by 47 and 96 %, and 68 and 38 %, respectively, and decreased APX activity by 24 and 27 %, respectively (**Figure 6a, 6b, and 6d, Table S1**). The activity of POX was found to be higher by 19 % in plantlets developed from grains soaked with ZnONPs at concentration of 512 μg mL^{-1} (**Figure 6c, Table S1**)

Relationship between biochemical and growth parameters of maize plantlets developed from grains treated with ZnONPs

The results of principal component analysis (PCA) and hierarchical clustering analysis (HCA) of biochemical and growth parameters of maize plantlets developed from grains treated with ZnONPs from *F. solani* IOR 825 are presented in **Figure 7** and **Supplementary Table 2.** The results showed that the first two components represent 44.4 % (PC1) and 34.5 % (PC2) of variables, respectively. The PC1 was explained by H_2O_2 (14.5 %), APX activity (13.9 %), and POX activity (12.9 %) while the highest contribution to PC2 was attributed to ascorbate redox ratio (ASCr, 18.8 %), dry weight (DW) of plantlets (16.9 %) and total glutathione (GSH, 15.0 %) (**Figure 7a and 7b, Table S2**). The strongest positive correlation was observed for the fresh weight (FW) and H_2O_2 (0.82) and between FW and total ascorbate pool (0.78) while dry weight (DW) was positively correlated with ascorbate redox ratio (0.73) and CAT activity (0.68), and negatively correlated with activities of POX, APX and SOD (-0.56, -0.65 and -0.66, respectively) (**Figure 7c**). The hierarchical clustering dendrogram (**Figure 7d**) shows the similarities and differences in the application of particular concentrations of ZnONPs between the effects induced in different organs of maize. In the leaves the alterations in the biochemical and growth parameters under ZnONPs treatments at concentrations of 32 and 128 μg mL^{-1} were classified as the most similar, followed by control plantlets and plantlets developed from grains treated with ZnONPs at concentration of 512 μg mL^{-1}. In the caryopsis and stems, a similar pattern of the dose-depended response to ZnONPs treatment was observed (controls were classified close to concentration of 32 μg mL^{-1}, while concentration of 128 with concentration of 512 μg mL^{-1}). In the roots, treated with ZnONPs at 512 μg

211 mL^{-1} a response similar to that of untreated plantlets occurred, whereas treatments with ZnONPs at 32
212 µg mL^{-1} and 128 µg mL^{-1} produced comparable effects on the physio-morphological features of maize.

213 **Discussion**

214 Nanomaterials used as nanopriming agents play a crucial role in sustainable agriculture [36] These
215 nanomaterials can be synthesized by biological methods and is reported as an eco-friendly and
216 constitutes an alternative to physical and chemical procedures [37]. A wide range of systems, such as
217 plants or microorganisms (bacteria, fungi, yeast) are used in the synthesis of NPs, considering the
218 contribution of phytochemicals, enzymes, proteins, carbohydrates or amino acids in the formation and
219 stabilization of NPs [37-38]. Most recently, the biosynthesis of ZnONPs from plants (*Ficus carica* latex,
220 *Phyllanthus niruri* plant extract), bacteria (*Bacillus paramycoides*) or fungi (*Aspergillus* sp.) were
221 reported along with numerous biological activities (antimicrobial, anticancer, photocatalytic,
222 antioxidant) [30-31, 40]. Interestingly, fungi represent a natural and high-throughput system for the
223 synthesis of NPs as they display high metal tolerance and simplicity in cultivation linked to the
224 production of biomolecules involved in biosynthesis [32]. The present study is a continuation of the
225 research on biosynthesized ZnONPs from *Fusarium solani* IOR 825 with antimicrobial properties
226 against bacterial and fungal plant pathogens, as well as stimulators of maize growth. These ZnONPs
227 inhibited the growth of mycelia and spore germination of *Alternaria alternata, Aspergillus niger,*
228 *Fusarium culmorum, Fusarium oxysporum, Fusarium poae, Phoma lingam* and *Sclerotinia sclerotiorum*
229 while stimulatory effect of ZnONPs on maize growth were observed at concentration range of 16-256
230 µg mL^{-1} [35]. The characterization of this batch of ZnONPs from *F. solani* IOR 825 pointed out their
231 small size of 48 nm, 59 nm and 259 nm by TEM, NTA , DLS, respectively, and the hexagonal wurtzite
232 structure. Our results from FTIR analysis confirmed the formation of ZnONPs and presence of
233 functional groups on the NPs surface as band at 480 and 570 cm^{-1} corresponds to Zn–O stretching mode
234 while other bands were assigned to C-H bending (694, 783, 830 and 940 cm^{-1}), C-O stretching (1045,
235 1119, cm^{-1}), C=C stretching (1512 cm^{-1}), N-H bending (1553 cm^{-1}), C-H stretching (2961 cm^{-1}) and O-
236 H stretching (3393 cm^{-1}). Similarly, in the study reported by Mohamed et al. [41], *Fusarium*
237 *keratoplasticum* and *Aspergillus niger* were used for the synthesis of ZnONPs with sizes ranging
238 between 10 and 42 nm (hexagonal) and 8 and 38 nm (nanorod-shaped), respectively. In addition, the
239 XRD analysis confirmed the crystalline nature of both ZnONPs while the FTIR spectra showed a
240 number of peaks indicating the presence of phenolic groups and amino and carboxyl groups of proteins
241 on ZnONPs surface. Similar findings were reported by Sharma et al. [42], who performed the fungal-
242 mediated synthesis of ZnONPs by using cell-free extract from *Phanerochaete chrysosporium*. Their
243 TEM observations revealed the ZnONPs with size ranging from 5 to 200 nm and both the XRD and the
244 FTIR results pointed toward ZnONPs formation. Additionally, the FTIR spectra showed peaks at 3848–
245 3618 cm^{-1} and 531 cm^{-1} attributed to hydroxyl (O–H) groups and Zn-O stretching, respectively [42].

The ZnONPs synthesized via the green route demonstrate a range of biological activities favored by their small size, crystalline nature or coating of biological origin which reinforces their potential for various applications, including enhancing agricultural crop production [37-38]. To date, the positive effects of application of biosynthesized ZnONPs were shown for *Vigna radiata* (mung bean), *Cajanus cajan* (red gram), *Solanum lycopersicum* L. (tomato), *Capsicum annuum* L. (red pepper) [33, 43]. Furthermore, stimulation of growth and seed germination at low concentrations of ZnO particles (nano- and micro-particles), as well as toxic effects at higher doses were presented for *Ocimum basilicum* L., *Lactuca sativa* L., and *Lepidium sativum* L. [44]. Since, the research indicates positive and negative effects caused by ZnONPs on the crop plants, based on the results from our previous report [35], the selected concentrations of ZnONPs (32, 128 and 512 μg mL^{-1}) were used to comprehensively evaluate the effect of pre-sowing ZnONPs treatment on the germination, growth and condition of developed maize plantlets to explore safe concentrations for stimulation of seedling development. The effects of ZnONPs on plants, in general, are not fully understood, and plant response to ZnONPs is mainly dependent on plant species, type and dose of NPs, as well as treatment and growth conditions [45]. Our study showed that the germination of maize grains was found unaffected by ZnONPs-treatments, however, the increased biomass production and higher vigour indexes were observed at lower concentrations (32 and 128 μg mL^{-1}), but unchanged when compared to control after application of ZnONPs at higher (512 μg mL^{-1}) concentration. A similar effect was described by Pandya et al. [46], where the application of ZnONPs for seed priming resulted in improved growth of wheat (*Triticum aestivum* L.), but the effect was gradual up to the concentration of ZnONPs equal to 250 ppm and diminished by 500 ppm. In turn, in the study conducted by Sharma and coworkers [42], the ZnONPs synthesized by using extract from leaf of *Eucalyptus lanceolata* were applied for seed priming and foliar spraying on maize (*Zea mays* L. var. PG2458). Their results indicated a dose-dependent effect for both methods of NPs application. ZnONPs at low concentration (200 ppm) improved morphological and physiological attributes of maize seedlings while 2-fold increase in the dose showed phytotoxic effect on shoot length and fresh biomass. This contrasts with our findings, where a 4-fold increase in ZnONPs concentration showed neither stimulatory nor adverse effects on biomass production. Thus, these studies, similar to our findings emphasize the importance of optimizing the pre-sowing seed treatment process as the concentration of ZnONPs is an important determinant of the effect of ZnONPs application on plant growth and development [42,44].

It is well known, that in plants ROS and antioxidative systems play a crucial role in response to various stresses, and just as importantly, are involved in different processes of plant growth and development [47-48]. The antioxidant system, including enzymatic and non-enzymatic components, establishes the ROS balance between the harmful consequences of oxidative stress which suppresses germination and seedling growth, as well as participates in signaling that is essential for stimulating plant growth [47]. Therefore, in our study the condition of maize plantlets developed from grains pre-sowing treated with different concentrations of ZnONPs, was evaluated by determination of chlorophyll content, assessment

of H_2O_2 level, alterations in lipid peroxidation, antioxidative enzymes activity and non-enzymatic antioxidants content; aforementioned parameters were estimated in all organs of plantlets.

Analysis of the growth performance and biochemical response of maize organs revealed that applications of optimal concentrations of ZnONPs (32 and 128 μg mL^{-1}) caused comparable effects towards each other in leaves and roots however, the patterns of response differed between organs. For instance, there was a higher yield of fresh biomass in leaves and more efficient dry matter production in roots after application of optimal concentrations of ZnONPs (32 and 128 μg mL^{-1}). In all maize plantlets levels of H_2O_2 were generally higher in the leaves than in the roots. Moreover, in maize plantlets developed from ZnONPs-treated grains, the H_2O_2 content increased in the roots and was maintained at a control level in the leaves. In addition, these ZnONPs treatments resulted in increased APX and CAT activity in roots and leaves, respectively. Taken together, these shifts in the levels of enzyme activity may be associated with a lower affinity of CAT for the substrate than the affinity of APX [49]. Furthermore, different effect was shown after applying the highest tested concentration of ZnONPs, namely in the leaves more pronounced decrease in activity POX and APX and increase in glutathione and ascorbate content and CAT activity were observed. Nevertheless, these responses were insufficient to trigger growth stimulation, as fresh and dry biomass of leaves did not change. In addition, reduced chlorophyll content and increased lipid peroxidation were reported. In turn, the same ZnONPs-treatment showed slight stimulation of root growth expressed by the increase of fresh weight which can be related to lower APX activity resulting in a higher increase in H_2O_2 content in comparison to optimal stimulatory ZnONPs-treatments. Similar observations were reported by Salam et al. [50] for root growth of maize, developed from grains treated with ZnONPs at concentration of 500 mg L^{-1}. A number of studies showed H_2O_2 as a particularly important signaling molecule involved in plant development, including root elongation, by modulation of cell production, mainly its rate and spatial profiles of cells [48, 51-52]. Our results indicate that the improved growth of maize plantlets, as a result of ZnONPs grains treatment is associated with maintaining adequate enzymes activity in leaves and roots. Similarly, Abdel Latef, et al. [53] found that the soaking of the seeds of lupine (*Lupinus termis*) with ZnONPs at the effective concentration range of 20-80 mg L^{-1} stimulated plant growth. Contrary to our findings they reported that in seedlings developed from seeds treated with ZnONPs at concentration of 20 mg L^{-1} the activity of CAT, SOD, and POX were unaffected, but an APX activity was 2-fold higher in the leaves. Moreover, ZnONPs at the most stimulatory concentrations of 60 mg L^{-1} increased the activity of all analyzed enzymes (SOD, POX, CAT, APX) in the leaves and positively affected chlorophyll content, but reduced MDA content [53]. Similar to our results, the pre-sowing treatment of seeds with ZnNPs and FeNPs altered the changes in the antioxidant system's performance and contributed to the efficient promotion of spinach (*Basella alba*) growth under normal conditions and also the neutralization of the negative consequences of Pb stress. The increased SOD, CAT, and POX activity were observed in 20-day-old *B. alba* seedlings developed from seeds primed with ZnNPs and FeNPs at concentrations of 200 mg L^{-1} under normal and Pb-stress conditions. While analysis of other biochemical parameters confirmed

decrease in H_2O_2 and MDA contents and increase in proline level [54]. Recently, Ashwini et al. [55] reported that the soaking of the groundnut seeds with ZnONPs at concentration of 1000 ppm resulted in stimulation of seedling development determined concurrently with increased activity of CAT, SOD, APX, guaiacol peroxidase (GPX) and polyphenol oxidase (PPO) in leaves, as well as higher chlorophyll content. However, our study showed that treatments with the 512 μg mL^{-1} ZnONPs triggered oxidative stress, especially in leaves. This was indicated by simultaneous raise in H_2O_2 and MDA content and might cause a slight, but considerable reduction in leaf chlorophyll content. In turn, different effects on chlorophyll content were observed in leaves of okra, depending on the applied ZnONPs dose, treatment time and crop variety. Namely, reduced content of chlorophyll *a* and *b* were noted in hybrid variety developed from grains treated with ZnONPs at concentration of 20 and 40 mg L^{-1} for 18 h, but higher chlorophyll content were estimated in hybrid variety treated with these ZnONPs for 24 h. For the Desi variety, an increase in chlorophyll content was recorded in both time treatments (18 and 24 h), but a higher level appeared after treatment with the lower concentration [56]. Positive effect on the chlorophyll content were most frequently reported for foliar application of ZnONPs in wheat [57], mung bean [58], sorghum [59] or saffron [60]. However, the seed priming with ZnONPs positively affected the efficiency of photosynthesis in wheat, as increased chlorophyll content and improved chlorophyll *a* fluorescence parameters were observed in 5- days old seedlings [16].

Furthermore, caryopses and stems showed a dose-dependent pattern of response to ZnONPs pre-sowing treatments, where application of ZnONPs at 32 μg mL^{-1} did not substantially affect biochemical parameters compared to controls, and concentrations of 128 and 512 μg mL^{-1} induced similar impacts, however, the pattern of changes varied between both organs. More precisely, the treatment of grains with ZnONPs at concentration of 32 μg mL^{-1} enhanced fresh and dry weight of stems and accumulation of H_2O_2, while other parameters were comparable to controls. Similar stimulation of growth was observed in stems of plantlets developed from grains treated with ZnONPs at concentration of 128 μg mL^{-1} while NPs at concentration of 512 μg mL^{-1} showed no stimulatory effect. In the last two cases, the H_2O_2 increased and MDA level decreased in stems, but the treatment of grains with the highest concentration of ZnONPs (512 μg mL^{-1}) resulted in a higher increase in the total pool of ascorbate and accumulation of glutathione. To date, various functions of ascorbic acid and its redox state in plant physiology have been described, including the regulation of ROS, modulation of gene expression, signal transduction pathways, phytohormone-related plant responses to various factors, or acting as an enzyme cofactor, as discussed in [61]. Other studies reported the role of ascorbic acid in cell proliferation and differentiation [62-63]. Our results showed that the growth of roots and leaves was associated with changes in enzyme activity (APX and CAT, respectively), thus it can be suggested that extensive synthesis of non-enzymatic antioxidants, such as ascorbate and glutathione, was involved in the mechanism of growth stimulation by modulating H_2O_2 in the stems of seedlings developed from grains soaked in ZnONPs. Likewise, in a study described by Ahmad et al. [64], treatment of soybeans with ZnONPs positively affected ascorbic acid and glutathione synthesis in control and arsenic-stressed

plants. Our study showed that ascorbate and glutathione high throughput biosynthesis and maintenance of a higher ratio of reduced ASC to total pool of ASC and DHA allowed not only for an increase in stem biomass, but also for a reduction in lipid peroxidation. While Ahmad and coauthors [64] reported improved growth of soybean shoot, increased H_2O_2 along with higher MDA levels as a result of ZnONPs application. In addition, they found that the ZnONPs treatment increased activities of dehydroascorbate reductase (DHAR), monodehydroascorbate reductase (MDHAR) and SOD, however, the activities of CAT, APX and glutathione reductase (GR) maintained at control level at normal conditions and increased after ZnONPs-treatment only under arsenic stress [64]. Similarly, the ZnONPs biosynthesized from *Salvadora persica* leaves extract showed a stimulatory dose-dependent effect after seed nanopriming on hybrid and Desi varieties of okra crop, as improved length, fresh and dry weight of shoot and root were noted. Nanoprimig with ZnONPs at concentration of 40 mg L^{-1} increased the H_2O_2 and non-enzymatic antioxidants (ascorbate, proline and flavonoid) content [56].

Consistent with the pattern observed in the stems, in the residue of the germinated grains ZnONPs-treatment at the lowest concentration (32 µg mL^{-1}) resulted in higher H_2O_2 accumulation and unchanged other components of the antioxidant system compared to the control. While application of ZnONPs at higher concentrations of 128 and 512 µg mL^{-1} raised the fraction of reduced ascorbate and altered enzyme activity, namely increased CAT, and SOD activity and decreased APX activity. The highest tested concentration of ZnONPs (512 µg mL^{-1}) induced higher glutathione synthesis and POX activity. However, all tested concentrations of ZnONPs triggered higher lipid peroxidation. Indeed, an essential difference between the germinated seed and other organs is the simultaneously increased activity of the enzymes CAT, POX, and, interestingly, SOD. To date, post-germination studies on caryopsis regarding antioxidant enzyme activity or biochemical parameters are not available, therefore, the above data are important in understanding the significant role of ZnONPs in seed germination and growth promotion of maize.

Overall, these results suggests that the maize plantlet organs are under oxidative challenge and the antioxidant accumulation is required to maintain the redox balance under treatment with the highest nanoparticle concentration. Regarding the risk assessment, our findings, mentioned above, suggest that leaf functions might be adversely affected by highest ZnONPs concentration as manifested by a decrease in chlorophyll content and substantial lipid peroxidation in leaf tissues. Contrastingly, both root and stem tissues are capable to mitigate the oxidative stress due to the treatment with the high ZnONPs concentration. However, the mechanisms seem to be different, namely a concerted total ASC and total glutathione accumulation in stems and a constitutively high POX and APX activity in roots.

Conclusions

In this study, we compared the effect of different ZnONPs concentrations (32, 128, and 512 µg mL^{-1}) on pre-sowing treatment on maize by evaluation of growth parameters (fresh and dry weight, length), total chlorophyll content, and changes in various biochemical parameters. The pre-sowing priming of maize

grains with biologically synthesized ZnONPs from *Fusarium solani* IOR 825 showed the stimulatory effects on plants at optimized concentrations and contributed to the moderation of levels and activity of various biochemical parameters in 14-day old plantlets. Our results indicate that the improved growth, as a result of ZnONPs grains treatment, may be due to increased H_2O_2 content, which is modulated through distinct mechanisms: CAT-dependent in leaves, APX-dependent in roots, and ASC-dependent in stems. Pre-sowing treatment with ZnONPs at optimal concentrations resulted in adequately maintained levels of these antioxidants to ensure balance for growth stimulation without causing oxidative stress. In addition, since maize growth was not impaired even after a 4-fold increase in the effective dose, it can be concluded that the ZnONPs are biocompatible and safe as maize growth stimulators.

Materials and methods

Biological synthesis and determination of properties of ZnONPs

The biosynthesis conditions and determination of physicochemical properties of ZnONPs were described previously by Trzcińska-Wencel et al. [35]. Briefly, the fungal strain, *Fusarium solani* IOR 825 (purchased from the Institute of Plant Protection (IOR), National Research Institute of Poland) was grown on Sabouraud dextrose broth (SDB, Becton Dickinson) for 7 days at 26 ºC. Fungal biomass was harvested (6,000 × *g*, 10 min), washed three times and resuspended in sterile distilled water (10 g of biomass per 100 mL of water), and allowed to autolyze for 4 days at room temperature. After incubation the autolyzed biomass was centrifuged (4,000 × *g*, 5 min) and supernatant was used for the biosynthesis of ZnONPs. The NPs were synthetized by challenging fungal autolysate with salt precursor (100 mM $ZnSO_4$) and NaOH (100 mM) in a ratio of 1:1:1 (v/v/v) under continuous stirring on magnetic stirrer, followed by heating of the reaction mixture at 40 ºC for 15 min. After the white precipitate appeared, the ZnONPs were centrifuged (5,000 × *g*, 5 min), washed three times with sterile distilled water and dried at 37 ºC. The mass of ZnONPs was determined in mg and powder was used for further analyses.
The determination of physicochemical characteristics of ZnONPs was performed as described in [35]. The synthesis of ZnONPs was confirmed by UV-Vis spectroscopy (NanoDrop One, Thermo Scientific, USA) in the wavelength range from 200 to 700 nm at the resolution of 1 nm. The X-ray powder diffraction (XRD) was applied to verify the crystalline structure of ZnONPs and carried out by using X' Pert PRO Analytical X6 diffractometer (PANalytical, Netherlands) with Ni filter and CuKα radiation source. To determine shape and size, an aqueous solution of ZnONPs (1 µl) was deposited on a carbon-coated copper grid (400 µm grid), left overnight at room temperature for drying and observed using a transmission electron microscope (TEM) (FEI, Tecnai 12, The Netherlands). The hydrodynamic diameter, size distribution and Zeta potential of ZnONPs were determined by performing Nanoparticle Tracking Analysis (NTA LM20, Nanosight Limited, Amesbury, UK) and Dynamic Light Scattering (DLS) with Zeta potential measurement (Zetasizer Nano-ZS 90, Malvern, UK). Before analyses

ZnONPs powder was suspended in MilliQ water and sonicated for 15 min at 30 kHz (Sonic Ruptor 250, Omni Int., USA). Analysis of the functional groups on the surface of ZnONPs was performed by Fourier Transform Infrared Spectroscopy (FTIR) (Spectrum 2000; Perkin- Elmer, Waltham, USA) after mixing with KBr in the ratio 1:100. The spectrum was analyzed in a range from 4,000 to 400 cm^{-1} with the resolution of 4 cm^{-1}.

Effect of ZnONPs on maize seed germination and development – treatments, measurements, and plant material

Maize (*Zea mays* L.) grains (Torseed S.A., Torun, Poland) were used to evaluate the effect of biosynthesized ZnONPs on their germination, plant growth and antioxidant system as previously described by Trzcińska-Wencel et al.[35] with slight modifications. The 25 grains were sterilized with 25 mL of a solution consisting of 30 % H_2O_2 and 70 % ethanol (1:1, v/v) for 30 minutes and washed 5 times with sterile distilled water. The grains were then treated with 25 mL of ZnONPs water solutions at concentrations of 32, 128 and 512 µg mL^{-1} or water (control) for 30 minutes and placed on ½ Murashige and Skoog (MS) agar medium in culture boxes and cultured for 14 days at 22 ± 2 °C. The germination efficiency was evaluated based on the following parameters, germination percentage (G %) [65], mean germination time (MGT) [66] and germination rate index (GRI) [67]. The length of shoot and roots in centimeters [cm], as well as weight of leaves, stems, roots and caryopses in milligrams [mg] were recorded for 14-days old plantlet (V2 growth stage). Furthermore, the vigour indexes were calculated according to [68] on the basis of G % and length of plantlets (vigour index I) and G % and dry weight of plantlets (vigour index II). The plant material for biochemical analysis was frozen in liquid nitrogen immediately after harvesting and stored at -80°C.

Total chlorophyll content

To assess the chlorophyll content in leaves of maize plantlets the leaf tissue (0.5 g) grounded in liquid nitrogen was extracted with cooled acetone (80 %, 1.5 mL) and centrifuged at 5,000 × *g* for 5 min (model 5810R, Eppendorf, Germany). To ensure total extraction, the process was repeated five times and the absorbance of the supernatant was measured using spectrophotometer (model U-1800, Hitachi, Tokyo, Japan) at $\lambda_{645\ nm}$ and $\lambda_{663\ nm}$ [69]. The total chlorophyll (mg g FW^{-1}) was calculated as follows:

$$\text{Total chlorophyll (mg g FW}^{-1}) = 20.2 \times (\text{Abs } \lambda_{645\ nm}) + 8.02 \times (\text{Abs } \lambda_{663\ nm}) \times (V/1000 \times FW)$$

where: V is the final volume of the extract (mL); FW is a fresh weight used for extract preparation (g)

Hydrogen peroxide (H_2O_2) level

The concentration of H_2O_2 was determined using the method with 3-(dimethylamino)benzoic acid (DMAB), 3-methyl-2-benzothiazolinone hydrazone hydrochloride (MBTH) and horseradish peroxidase

(HRP) [70]. The plant material (0.5 g) was grounded in liquid nitrogen, mixed with trichloroacetic acid (TCA) (0.1 %, 5 mL) and centrifuged for 10 min at 10,000 × *g*, 4°C (model 5810R, Eppendorf, Germany). The supernatant was diluted with water (1:1, v/v) and used for analyses. The reaction mixture included 750 µL of supernatant, 125 µL of 19.8 mM DMAB, 115 µL of 0.456 mM MBHT and 10 µL of HRP (0.25 U). The sample was incubated for 20 min at 25 °C and absorbance at $\lambda_{590\ nm}$ was measured using spectrophotometer (model U-1800, Hitachi, Tokyo, Japan). H_2O_2 content was calculated from the standard curve and presented as µmol of H_2O_2 per 1 g of fresh weight.

Lipid peroxidation based on malondialdehyde (MDA) content

Lipid peroxidation was estimated by measurement of malondialdehyde (MDA) content according to the method described by Hodges et al. [71]. For this assay, 0.5 g of plant sample from each variant was powdered in liquid nitrogen, extracted with 80 % ethyl alcohol with 0.01 % butylated hydroxytoluene (BHT) and centrifuged for 10 min at 3,000 x *g* and at 4 ºC (model 5810R, Eppendorf, Germany). The reaction mixture, with a final volume of 1.8 mL, was made by mixing supernatant and 20 % TCA with 0.5 % thiobarbituric acid (TBA) at a ratio of 1:1 (v/v). The sample after heating for 20 min at 95 ºC was cooled on ice and centrifuged for 10 min at 3,000 x *g* at 4 ºC. Absorbance readings at wavelengths 400, 532 and 600 nm were performed for supernatant using spectrophotometer (model U-1800, Hitachi, Tokyo, Japan). The corrected extinction coefficient of MDA (157 mM^{-1} cm^{-1}) was used to calculate the MDA concentration in plant organs and presented as nmol g FW^{-1} [71].

Level of total glutathione

Total glutathione content was assessed by using the Glutathione Assay Kit (Catalog Number CS0260, Sigma-Aldrich, USA), according to the manufacturer's instructions. Briefly, 0.1 g of plant material was deproteinized with 5 % 5-sulfosalicicylic acid (SSA), centrifuged (10 min at 10,000 × *g*) and 20-fold diluted. The formation of 5-thio-2-nitrobenzoic acid (TNB) in a reaction mixture composed of plant extract, 5,5'-dithiobis(2-nitrobenzoic acid) (DTNB), glutathione reductase and NADPH in potassium phosphate buffer (100 mM, pH 7.0 with 1 mM EDTA) was continuously measured spectrophotometrically for 5 min at $\lambda_{412\ nm}$ using a plate reader (SpectraMax iD3 Multi-Mode Microplate Reader, Molecular Devices, USA). The results were compared with standard curve and presented as nmol of GSH per 1 gram of FW.

Estimation of ascorbic acid (ASC) and dehydroascorbic acid (DHA) content

The plant sample (0.5 g) was extracted in TCA (5 mL, 5%) and centrifuged for 10 min at 14,000 × *g* at 4 °C (model 5810R, Eppendorf, Germany). A 33.6 µL of H_2O was added to 135 µL of supernatant to determine the reduced ascorbate (ASC) in the reaction where ferrous ions (Fe^{2+}) form a complex with α,α'-bipyridyl [72]. Then16.8 µL of 10 mM DTT and 16.8 µL of 80 mM K_2HPO_4 were added to 135 µL

of supernatant to estimate the total pool of ascorbic acid which enabled the reduction of dehydroascorbate (DHA) to ascorbate (ASC). To all tested samples 40 µL of 85 % H_3PO_4, 685 µL of 0.5 % α,α'-bipyridyl, and 140 µL of 1 % $FeCl_3$ were added in the order listed. Samples were well mixed, incubated for 30 minutes at room temperature and centrifuged for 5 min at 14,000 × *g*. The supernatants were analyzed using spectrophotometer (model U-1800 Hitachi, Tokyo, Japan). The absorbance of the supernatant at $\lambda_{525\ nm}$ was compared to the standard curve (0-50 µg of ASC mL^{-1}) and the level of ASC and total contents of ASC and DHA were calculated. Based on these results the ratio of ASC to pool of ASC and DHA in each sample was calculated.

Preparation of enzyme extract

The extracts for analyses of enzyme activities (catalase, superoxide dismutase and peroxidase) were prepared by homogenization of 0.5 g sample with phosphate buffer (50 mM, pH 7.5) which contained 2 mM EDTA, 8 mM $MgCl_2$, 0.1 % Triton X-100 and 4 mM dithiothreitol (DTT). For ascorbate peroxidase extraction 50 mM phosphate buffer (pH 7.5) was supplemented with 1 mM EDTA and 5 mM ascorbate. Samples were centrifuged for 15 min at 14,000 × *g* at 4 °C (model 5810R, Eppendorf, Germany) and supernatants were used for analyses. The protein content in plant extracts was assessed using the method described by Bradford [73]. The bovine serum albumin (50-400 µg) was used as a standard.

Enzymatic activity of catalase (CAT)

Assay for determination of CAT activity was carried out according to [74]. Briefly, the extract (40-100 µL) was diluted in phosphate buffer (100 mM, pH 7.0) to a total volume of 998.5 µL, and 1.5 µL of H_2O_2 (30 %) was added and mixed thoroughly before measurement. The decrease in absorbance at the $\lambda_{240\ nm}$ was recorded for 90 s with spectrophotometer (model U-1800, Hitachi, Tokyo, Japan). The controls (without H_2O_2 or without extract) were also maintained. The activity of CAT was calculated based on the decomposition of H_2O_2 in the reaction mixture with the use of extinction coefficient of H_2O_2 (43.6 M^{-1} cm^{-1}) and presented as U of enzyme per mg of protein.

Enzymatic activity of superoxide dismutase (SOD)

SOD activity was estimated based on inhibition in the reduction of nitroblue tetrazolium (NBT) to formazan [75]. Briefly, 100 µL of enzyme extract was added to the 1.5 mL of reaction mixture containing phosphate buffer (50 mM, pH 7.8), NBT (0.67 mM), riboflavin (0.0033 mM), L-methionine (1 mM), and EDTA (0.33 mM) and incubated for 10 min in the light. Two types of control were prepared, namely (1) the extract was replaced with extraction buffer and (2) the reaction mixture was substituted with water. The NBT reduction was measured spectroscopically at $\lambda_{560\ nm}$ (model U-1800, Hitachi, Tokyo, Japan). The unit (U) of SOD activity was defined as the amount of enzyme which causes 50 % inhibition

of NBT reduction in the presence of riboflavin in the light. Results were presented as U per mg of protein.

Enzymatic activity of peroxidase (POX)

The activity of POX was examined as described previously in [72], by recording the increase in the absorbance at $\lambda_{420\,nm}$ due to the pyrogallol oxidation to purpurogallin in the presence of H_2O_2 and enzyme extract. For this purpose, 5-80 µL of extract was added to phosphate buffer (100 mM, pH 6.0) with pyrogallol (60 mM) to the final volume (990 µL). Prior to measurements, a 10 µL of 66 mM H_2O_2 was added to the reaction mixture and the absorbance was measured for 90 s using spectrophotometer (model U-1800, Hitachi, Tokyo, Japan). The millimolar extinction coefficient of purpurogalin: $\varepsilon = 12\ mM^{-1}\ cm^{-1}$ was used for the calculation of the POX activity which was reported as µmol pyrogallol min^{-1} mg^{-1} total protein.

Enzymatic activity of ascorbate peroxidase (APX)

To determine the activity of APX the rate of H_2O_2 decomposition was measured [74, 76]. Briefly, 10 µL of plant extract was mixed with 980 µL of reaction solution containing phosphate buffer (50 mM, pH 7.5), EDTA (1 mM), ascorbic acid (0.5 mM), and 10 µL of H_2O_2 (0.2 mM). The decrease in the absorbance at $\lambda_{290\,nm}$ for the 90s was recorded using spectrophotometer (model U-1800, Hitachi, Tokyo, Japan). The extinction coefficient of 2.8 $mM^{-1}\ cm^{-1}$ of ascorbate was used for the calculation of APX activity and results were presented as µmol of ascorbate min^{-1} mg^{-1} protein.

Statistical analysis

The data analyses were performed by using Statistica software (StatSoft Inc., Tulsa, OK, USA). Results were shown as a mean ± standard error (SE). The means were then compared to determine statistical significance (if p-value* $p \leq 0.05$, ** $p \leq 0.01$, *** $p \leq 0.001$) by One-way ANOVA, and post-hoc Tukey's test. The principal component analysis (PCA) and hierarchical cluster analysis (HCA) were performed to assess the relationship between ZnONPs treatments and changes in growth parameters, oxidative and antioxidative system components in maize organs. The R packages (factoextra, ggplot2 and dendextend) were used to analyze average values of all parameters in R 4.4.2 (R Foundation for Statistical Computing, Vienna, Austria) [77-79].

Data availability

All data generated or analysed during this study are included in this published article (and its Supplementary Information files), further inquiries can be directed to the corresponding authors.

References

1. Alaimo, K., Chilton, M. & Jones, S. J. Food insecurity, hunger, and malnutrition. in *Present Knowledge in Nutrition* 311–326 (Elsevier, 2020).
2. Ai, Y. & Jane, J. Macronutrients in Corn and Human Nutrition. *Compr. Rev. Food Sci. Food Saf.* **15**, 581–598 (2016).
3. Loy, D. D. & Lundy, E. L. Nutritional Properties and Feeding Value of Corn and Its Coproducts. in *Corn* 633–659 (Elsevier, 2019).
4. Rouf Shah, T., Prasad, K. & Kumar, P. Maize—A potential source of human nutrition and health: A review. *Cogent Food Agric.* **2**,1166995; https://doi.org/10.1080/23311932.2016.1166995 (2016).
5. Wilson, A. B., Avila-Diaz, A., Oliveira, L. F., Zuluaga, C. F. & Mark, B. Climate extremes and their impacts on agriculture across the Eastern Corn Belt Region of the U.S. *Weather Clim. Extrem.* **37**, 100467; 10.1016/j.wace.2022.100467 (2022).
6. Arora, P. K. et al. Next-generation fertilizers: the impact of bionanofertilizers on sustainable agriculture. *Microb. Cell Fact.* **23**, 254; 10.1186/s12934-024-02528-5 (2024).
7. Chen, C., Pan, J. & Lam, S. K. A review of precision fertilization research. *Environ. Earth Sci.* **71**, 4073–4080 (2014).
8. Meena, S. D., Susank, M., Guttula, T., Chandana, S. H. & Sheela, J. Crop Yield Improvement with Weeds, Pest and Disease Detection. *Procedia Comput. Sci.* **218**, 2369–2382 (2023).
9. Yahaya, S. M., Mahmud, A. A., Abdullahi, M. & Haruna, A. Recent advances in the chemistry of nitrogen, phosphorus and potassium as fertilizers in soil: A review. *Pedosphere* **33**, 385–406 (2023).
10. Zulfiqar, F. Effect of seed priming on horticultural crops. *Sci. Hortic. (Amsterdam)*. **286**, 110197; 10.1016/j.scienta.2021.110197 (2021).
11. Nile, S. H. et al. Nano-priming as emerging seed priming technology for sustainable agriculture—recent developments and future perspectives. *J. Nanobiotechnology* **20**, 254; 10.1186/s12951-022-01423-8 (2022).
12. Kandhol, N. et al. Nano-priming: Impression on the beginner of plant life. *Plant Stress* **5**, 100091; 10.1016/j.stress.2022.100091 (2022).
13. Szőllősi, R., Molnár, Á., Kondak, S., & Kolbert, Z. Dual effect of nanomaterials on germination and seedling growth: Stimulation vs. phytotoxicity. *Plants* **9**, 1745 (2020).
14. Yang, L. et al. Nanopriming boost seed vigor: Deeper insights into the effect mechanism. *Plant Physiol. Biochem.* **214**, 108895 (2024).
15. Hoang, S. A. et al. Metal nanoparticles as effective promotors for Maize production. *Sci. Rep.* **9**, 13925; 10.3390/plants9121745 (2019).
16. Rai-Kalal, P. & Jajoo, A. Priming with zinc oxide nanoparticles improve germination and photosynthetic performance in wheat. *Plant Physiol. Biochem.* **160**, 341–351 (2021).
17. Waqas Mazhar, M. et al. Seed nano-priming with Zinc Oxide nanoparticles in rice mitigates drought and enhances agronomic profile. *PLoS One* **17**, e0264967; 10.1371/journal.pone.0264967 (2022).

18. Olkhovskaya, I. P., Krokhmal, I. I. & Glushchenko, N. N. Improvement of the Morphophysiological Parameters of Pepper after the Presowing Treatment of Seeds with Zinc Nanoparticles. *Russ. J. Phys. Chem. B* **18**, 527–532 (2024).
19. Kaur, H. & Garg, N. Zinc toxicity in plants: a review. *Planta* **253**, 129; 10.1007/s00425-021-03642-z (2021).
20. Umair Hassan, M. et al. The Critical Role of Zinc in Plants Facing the Drought Stress. *Agriculture* **10**, 396; 10.3390/agriculture10090396 (2020).
21. Donia, D. T. & Carbone, M. Seed Priming with Zinc Oxide Nanoparticles to Enhance Crop Tolerance to Environmental Stresses. *Int. J. Mol. Sci.* **24**, 17612; 10.3390/ijms242417612 (2023).
22. Tsonev, T. & Cebola Lidon, F. J. Zinc in plants - An overview. *Emirates J. Food Agric.* **24**, 322–333 (2012).
23. Youssef, M. S. & Elamawi, R. M. Evaluation of phytotoxicity, cytotoxicity, and genotoxicity of ZnO nanoparticles in *Vicia faba*. *Environ. Sci. Pollut. Res.* **27**, 18972–18984 (2020).
24. Shen, M. et al. Bioaccumulation and phytotoxicity of ZnO nanoparticles in soil-grown *Brassica chinensis* L. and potential risks. *J. Environ. Manage.* **306**, 114454; 10.1016/j.jenvman.2022.114454 (2022).
25. Lee, S., Kim, S., Kim, S. & Lee, I. Assessment of phytotoxicity of ZnO NPs on a medicinal plant, *Fagopyrum esculentum*. *Environ. Sci. Pollut. Res.* **20**, 848–854 (2013).
26. Chen, J. et al. Phytotoxicity and bioaccumulation of zinc oxide nanoparticles in rice (*Oryza sativa* L.). *Plant Physiol. Biochem.* **130**, 604–612 (2018).
27. Zafar, H., Abbasi, B. H. & Zia, M. Physiological and antioxidative response of *Brassica nigra* (L.) to ZnO nanoparticles grown in culture media and soil. *Toxicol. Environ. Chem.* **101**, 281–299 (2019).
28. Li, Z. et al. Particle Size Determines the Phytotoxicity of ZnO Nanoparticles in Rice (*Oryza sativa* L.) Revealed by Spatial Imaging Techniques. *Environ. Sci. Technol.* **57**, 13356–13365 (2023).
29. Ali, A., Phull, A.-R. & Zia, M. Elemental zinc to zinc nanoparticles: is ZnO NPs crucial for life? Synthesis, toxicological, and environmental concerns. *Nanotechnol. Rev.* **7**, 413–441 (2018).
30. El-Refai, H. A. et al. Biosynthesis of Zinc Oxide Nanoparticles Using *Bacillus paramycoides* for In Vitro Biological Activities and In Vivo Assessment Against Hepatorenal Injury Induced by CCl4 in Rats. *Appl. Biochem. Biotechnol.* **196**, 5953–5973 (2024).
31. Ramesh, P., Rajendran, A. & Ashokkumar, M. Biosynthesis of zinc oxide nanoparticles from *Phyllanthus Niruri* plant extract for photocatalytic and antioxidant activities. *Int. J. Environ. Anal. Chem.* **104**, 1561–1572 (2024).
32. Ravi, P. et al. Biogenic Nano Zinc Oxide Particle Production and Their Antimicrobial Potentials: A Review. *J. Clust. Sci.* **36**, 8; 10.1007/s10876-024-02733-7 (2025).
33. Rani, P., Kaur, G., Rao, K. V., Singh, J. & Rawat, M. Impact of Green Synthesized Metal Oxide Nanoparticles on Seed Germination and Seedling Growth of *Vigna radiata* (Mung Bean) and *Cajanus cajan* (Red Gram). *J. Inorg. Organomet. Polym. Mater.* **30**, 4053–4062 (2020).

631 34. Sharma, P. et al. Green synthesis of zinc oxide nanoparticles using Eucalyptus lanceolata leaf litter:
632 characterization, antimicrobial and agricultural efficacy in maize. *Physiol. Mol. Biol. Plants* **28**, 363–
633 381 (2022).
634 35. Trzcińska-Wencel, J., Wypij, M., Terzyk, A. P., Rai, M. & Golińska, P. Biofabrication of novel silver
635 and zinc oxide nanoparticles from Fusarium solani IOR 825 and their potential application in
636 agriculture as biocontrol agents of phytopathogens, and seed germination and seedling growth
637 promoters. *Front. Chem.* **11**, 1235437; 10.3389/fchem.2023.1235437 (2023).
638 36. Shelar, A. et al. Nanoprimers in sustainable seed treatment: Molecular insights into abiotic-biotic
639 stress tolerance mechanisms for enhancing germination and improved crop productivity. *Sci. Total*
640 *Environ.* **951**, 175118; 10.1016/j.scitotenv.2024.175118 (2024).
641 37. Ahmed, S., Annu, Chaudhry, S. A. & Ikram, S. A review on biogenic synthesis of ZnO nanoparticles
642 using plant extracts and microbes: A prospect towards green chemistry. *J. Photochem. Photobiol. B*
643 *Biol.* **166**, 272–284 (2017).
644 38. Youssef, F., Ismail, S., Fouad, O. & Mohamed, G. Green synthesis and Biomedical Applications of
645 Zinc Oxide Nanoparticles. Review. *Egypt. J. Vet. Sci.* **55**, 287–311 (2024).
646 39. Al-darwesh, M. Y., Ibrahim, S. S. & Hamid, L. L. *Ficus carica* latex mediated biosynthesis of zinc
647 oxide nanoparticles and assessment of their antibacterial activity and biological safety. *Nano-*
648 *Structures & Nano-Objects* **38**, 101163; 10.1016/j.rechem.2024.101724 (2024).
649 40. Abdelrahman, S. E. S. A. H. et al. Bio-fabricated zinc oxide nanoparticles mediated by endophytic
650 fungus Aspergillus sp. SA17 with antimicrobial and anticancer activities: in vitro supported by in
651 silico studies. *Front. Microbiol.* **15**, 1366614; 10.3389/fmicb.2024.1366614 (2024).
652 41. Mohamed, A. A. et al. Fungal strain impacts the shape, bioactivity and multifunctional properties of
653 green synthesized zinc oxide nanoparticles. *Biocatal. Agric. Biotechnol.* **19**, 101103;
654 10.1016/j.bcab.2019.101103 (2019).
655 42. Sharma, J. L., Dhayal, V. & Sharma, R. K. White-rot fungus mediated green synthesis of zinc oxide
656 nanoparticles and their impregnation on cellulose to develop environmental friendly antimicrobial
657 fibers. *3 Biotech* **11**, 269; 10.1007/s13205-021-02840-6 (2021).
658 43. Singh, N., Singh, M. K., Yadav, R. K., Azim, Z. & Raghuvansi, J. Green synthesis and
659 characterization of nano zinc oxide and comparative study of its impact on germination and metabolic
660 activities of *Solanum lycopersicum* L. and *Capsicum annuum* L. *Vegetos,* 10.1007/s42535-024-
661 00838-y (2024).
662 44. Caser, M., Percivalle, N. M. & Cauda, V. The Application of Micro- and Nano-Sized Zinc Oxide
663 Particles Differently Triggers Seed Germination in Ocimum basilicum L., Lactuca sativa L., and
664 Lepidium sativum L. under Controlled Conditions. *Horticulturae* **10**, 575;
665 10.3390/horticulturae10060575 (2024).

45. Kumar, A. et al. The Role of Zinc Oxide Nanoparticles in Plants: A Critical Appraisal. in *Nanomaterial Biointeractions at the Cellular, Organismal and System Levels* 249–267 (Springer, Cham, 2021).
46. Pandya, P., Kumar, S., Patil, G., Mankad, M. & Shah, Z. Impact of ZnO nanopriming on physiological and biochemical traits of wheat (*Triticum aestivum* L.) seedling. *CABI Agric. Biosci.* **5**, 27; 10.1186/s43170-024-00228-z (2024).
47. Choudhary, A., Kumar, A. & Kaur, N. ROS and oxidative burst: Roots in plant development. *Plant Divers.* **42**, 33–43 (2020).
48. Voothuluru, P. et al. Apoplastic Hydrogen Peroxide in the Growth Zone of the Maize Primary Root. Increased Levels Differentially Modulate Root Elongation Under Well-Watered and Water-Stressed Conditions. *Front. Plant Sci.* **11**, 392; 10.3389/fpls.2020.00392 (2020).
49. De Gara, L., Paciolla, C., De Tullio, M. C., Motto, M. & Arrigoni, O. Ascorbate-dependent hydrogen peroxide detoxification and ascorbate regeneration during germination of a highly productive maize hybrid: Evidence of an improved detoxification mechanism against reactive oxygen species. *Physiol. Plant.* **109**, 7–13 (2000).
50. Salam, A. et al. Seed priming with zinc oxide nanoparticles downplayed ultrastructural damage and improved photosynthetic apparatus in maize under cobalt stress. *J. Hazard. Mater.* **423**, 127021; 10.1016/j.jhazmat.2021.127021 (2022).
51. Zhang, J. et al. Ascorbate peroxidase 1 confers resistance to southern corn leaf blight in maize. *J. Integr. Plant Biol.* **64**, 1196–1211 (2022).
52. Mukherjee, S. & Corpas, F. J. H2O2, NO, and H2S networks during root development and signalling under physiological and challenging environments: Beneficial or toxic? *Plant. Cell Environ.* **46**, 688–717 (2023).
53. Abdel Latef, A. A. H., Abu Alhmad, M. F. & Abdelfattah, K. E. The Possible Roles of Priming with ZnO Nanoparticles in Mitigation of Salinity Stress in Lupine (*Lupinus termis*) Plants. *J. Plant Growth Regul.* **36**, 60–70 (2017).
54. Gupta, N. et al. Seed Priming with ZnO and Fe3O4 Nanoparticles Alleviate the Lead Toxicity in Basella alba L. through Reduced Lead Uptake and Regulation of ROS. *Plants* **11**, 2227; 10.3390/plants11172227 (2022).
55. Ashwini, M. N., Gajera, H. P., Hirpara, D. G., Savaliya, D. D. & Kandoliya, U. K. Comparative impact of seed priming with zinc oxide nanoparticles and zinc sulphate on biocompatibility, zinc uptake, germination, seedling vitality, and antioxidant modulation in groundnut. *J. Nanoparticle Res.* **26**, 235; 10.1007/s11051-024-06141-w (2024).
56. Ramzan, M. et al. Enhancing physio-biochemical characteristics in okra genotypes through seed priming with biogenic zinc oxide nanoparticles synthesized from halophytic plant extracts. *Sci. Rep.* **14**, 23753; 10.1038/s41598-024-74129-6 (2024).

57. Hussain, A. et al. Zinc oxide nanoparticles alter the wheat physiological response and reduce the cadmium uptake by plants. *Environ. Pollut.* **242**, 1518–1526 (2018).
58. Raliya, R., Tarafdar, J. C. & Biswas, P. Enhancing the Mobilization of Native Phosphorus in the Mung Bean Rhizosphere Using ZnO Nanoparticles Synthesized by Soil Fungi. *J. Agric. Food Chem.* **64**, 3111–3118 (2016).
59. Dimkpa, C. O., White, J. C., Elmer, W. H. & Gardea-Torresdey, J. Nanoparticle and Ionic Zn Promote Nutrient Loading of Sorghum Grain under Low NPK Fertilization. *J. Agric. Food Chem.* **65**, 8552–8559 (2017).
60. Rostami, M., Talarposhti, R. M., Mohammadi, H. & Demyan, M. S. Morpho-physiological Response of Saffron (*Crocus Sativus* L.) to Particle Size and Rates of Zinc Fertilizer. *Commun. Soil Sci. Plant Anal.* **50**, 1250–1257 (2019).
61. Akram, N. A., Shafiq, F. & Ashraf, M. Ascorbic Acid-A Potential Oxidant Scavenger and Its Role in Plant Development and Abiotic Stress Tolerance. *Front. Plant Sci.* **8**, 613; 10.3389/fpls.2017.00613 (2017).
62. Tsukagoshi, H., Busch, W. & Benfey, P. N. Transcriptional Regulation of ROS Controls Transition from Proliferation to Differentiation in the Root. *Cell* **143**, 606–616 (2010).
63. Wu, S.-Y. et al. Ascorbic acid-mediated reactive oxygen species homeostasis modulates the switch from tapetal cell division to cell differentiation in Arabidopsis. *Plant Cell* **35**, 1474–1495 (2023).
64. Ahmad, P. et al. Zinc Oxide Nanoparticles Application Alleviates Arsenic (As) Toxicity in Soybean Plants by Restricting the Uptake of as and Modulating Key Biochemical Attributes, Antioxidant Enzymes, Ascorbate-Glutathione Cycle and Glyoxalase System. *Plants* **9**, 825; 10.3390/plants9070825 (2020).
65. Scott, S. J., Jones, R. A. & Williams, W. A. Review of Data Analysis Methods for Seed Germination. *Crop Sci.* **24**, 1192–1199 (1984).
66. Orchard, T. J. Estimating the parameters of plant seedling emergence. *Seed Sci. Technol.* **5**, 61–69 (1977).
67. Esechie, H. A. Interaction of Salinity and Temperature on the Germination of Sorghum. *J. Agron. Crop Sci.* **172**, 194–199 (1994).
68. Abdul-Baki, A. A. & Anderson, J. D. Vigor Determination in Soybean Seed by Multiple Criteria. *Crop Sci.* **13**, 630–633 (1973).
69. Witham, F. H., Blaydes, D. F. & Devlin, R. M. *Experiments in Plant Physiology.* (Van Nostrand, New York, 1971).
70. Veljovic-Jovanovic, S., Noctor, G. & Foyer, C. H. Are leaf hydrogen peroxide concentrations commonly overestimated? The potential influence of artefactual interference by tissue phenolics and ascorbate. *Plant Physiol. Biochem.* **40**, 501–507 (2002).

71. Hodges, D. M., DeLong, J. M., Forney, C. F. & Prange, R. K. Improving the thiobarbituric acid-reactive-substances assay for estimating lipid peroxidation in plant tissues containing anthocyanin and other interfering compounds. *Planta* **207**, 604–611 (1999).
72. Tyburski, J. & Mucha, N. Antioxidant Response in the Salt-Acclimated Red Beet (Beta vulgaris) Callus. *Agronomy* **13**, 2284; 10.3390/agronomy13092284 (2023).
73. Bradford, M. M. A rapid and sensitive method for the quantitation of microgram quantities of protein utilizing the principle of protein-dye binding. *Anal. Biochem.* **72**, 248–254 (1976).
74. Rao, M. V., Paliyath, G. & Ormrod, D. P. Ultraviolet-B- and Ozone-Induced Biochemical Changes in Antioxidant Enzymes of Arabidopsis thaliana. *Plant Physiol.* **110**, 125–136 (1996).
75. Beauchamp, C. & Fridovich, I. Superoxide dismutase: Improved assays and an assay applicable to acrylamide gels. *Anal. Biochem.* **44**, 276–287 (1971).
76. Chen, G.-X. & Asada, K. Ascorbate Peroxidase in Tea Leaves: Occurrence of Two Isozymes and the Differences in Their Enzymatic and Molecular Properties. *Plant Cell Physiol.* **30**, 987–998 (1989).
77. Galili, T. dendextend: an R package for visualizing, adjusting and comparing trees of hierarchical clustering. *Bioinformatics* **31**, 3718–3720 (2015).
78. Wickham, H. Data Analysis. in *ggplot2. Use R!* 189–201 (Springer, Cham, 2016). 10.1007/978-3-319-24277-4_9
79. Kassambara, A. & Mundt, F. factoextra: Extract and Visualize the Results of Multivariate Data Analyses. 10.32614/CRAN.package.factoextra (2020).

Acknowledgements

This research was funded by grant No. 2022/45/N/NZ9/01483 from the National Science Centre, Poland and is part of project No. 2022/45/P/NZ9/01571 co-funded by the National Science Centre and the European Union's Horizon 2020 research and innovation programme under the Marie Skłodowska-Curie grant agreement no. 945339.

Author Contributions

PG, JT, JT-W conceptualization, JT-W performed all experiments, curated and visualized data, wrote original draft, acquired funding, JN assisted in plant material collection, NM assisted in plant toxicity analyses, AG co-analyzed physicochemical properties of ZnONPs, JT-W, JT methodology, JT-W, PG, JT, MR writing review and editing, PG supervision.

Competing interests

The authors declare no competing interests.

Figure legends

Figure 1. Detection and physicochemical characteristics of ZnONPs from *Fusarium solani* IOR 825: UV-vis spectrum (a), diffractogram from X-ray diffraction analysis (b), TEM micrographs (c), size distribution from Dynamic Light Scattering (DLS) analysis (d), size distribution from Nanoparticle Tracking Analysis (NTA) (e), Zeta potential (f), FTIR-spectrum (g).

Figure 2. The length of shoots and roots (a), fresh (b) and dry weight (c) of 14-day-old maize plantlets after ZnONPs pre-sowing treatments. Data presented as mean and standard error (±SE) and statistical significance *(p*-value* $p \leq 0.05$, ** $p \leq 0.01$, *** $p \leq 0.001$).

Figure 3. Influence of maize grain pre-sowing treatments with ZnONPs on the chlorophyll content in leaves of 14-day-old maize plantlets. Data presented as mean and standard error (±SE), and statistical significance (*p*-value* $p \leq 0.05$).

Figure 4. Influence of maize grain pre-sowing treatments with ZnONPs on levels of hydrogen peroxide (H_2O_2) (a) malondialdehyde (MDA) (b), and total glutathione (GSH+GSSG) (c) in 14-day-old maize plantlets. Data presented as mean and standard error (±SE), and statistical significance (*p*-value* $p \leq 0.05$, ** $p \leq 0.01$, *** $p \leq 0.001$).

Figure 5. Influence of maize grains pre-sowing treatments with ZnONPs on the ASC+DHA content (a), ASC level (b) and ascorbate redox state [ASC/(ASC+DHA) ratio] (c) of 14-day-old maize plantlets. Data presented as mean and standard error (±SE), and statistical significance (*p*-value* $p \leq 0.05$, ** $p \leq 0.01$, *** $p \leq 0.001$).

Figure 6. Influence of maize grains pre-sowing treatments with ZnONPs on the activity of CAT (a), SOD (b), POX (c) and APX (d) in 14-day-old maize plantlets. Data presented as mean and standard error (±SE), and statistical significance (*p*-value* $p \leq 0.05$, ** $p \leq 0.01$, *** $p \leq 0.001$).

Figure 7. Analysis of general alterations and correlations of growth and individual biochemical parameters among organs of plantlets developed from grains treated with ZnONPs. Variables plot (a), where color arrows indicate the contribution of the trait on the first two PCs; (PCA)-biplot (b), correlation analysis between all the studied parameters, where red and blue colors represent positive and negative correlations, respectively (c); dendrogram from hierarchical cluster analysis (HCA) showing associations in changes of biochemical parameters among various ZnONPs treatments and maize plantlets organs (d).

APX: ascorbate peroxidase; ASC: ascorbate; ASCr: reduced ascorbate; DW: dry weight; FW: fresh weight; GSH: glutathione; H_2O_2: hydrogen peroxide; MDA: malondialdehyde; POX: peroxidase; SOD: superoxide dismutase; tASC: total ascorbate; Ctrl: untreated control; 32: treatment with ZnONPs at concentration of 32 µg mL^{-1}; 128: treatment with ZnONPs at concentration of 128 µg mL^{-1}; 512: treatment with ZnONPs at concentration of 512 µg mL^{-1}; L: leaves; S: stems; R: roots; C: caryopsis.

802 **Table 1.** The effect of ZnONPs pre-sowing treatment on germination parameters and vigour of 14-days
803 old maize plantlets.
804

ZnONPs [μg mL^{-1}]	**% germination**	**MGT [day]**	**GRI [%/day]**	**Vigour index I**	**Vigour index II**
0 (Control)	87.2	3.3	28.3	2946.8	4991.0
32	88.7	3.3	28.4	3290.3*	5851.2*
128	86.5	3.2	28.2	2880.4	5734.4*
512	85.4	3.3	27.6	2799.5	4601.1

805 MGT; mean germination time, GRI; germination rate index; * denote statistical significance (*p*-value
806 < 0.05) between ZnONPs treatment and control.
807

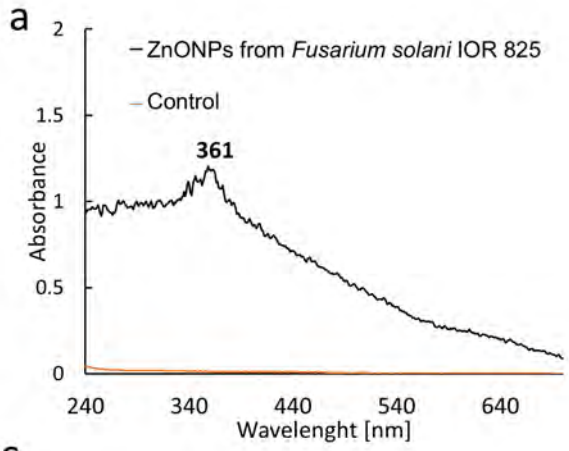
a
ZnONPs from Fusarium solani IOR 825
Control
361
Absorbance
Wavelenght [nm]

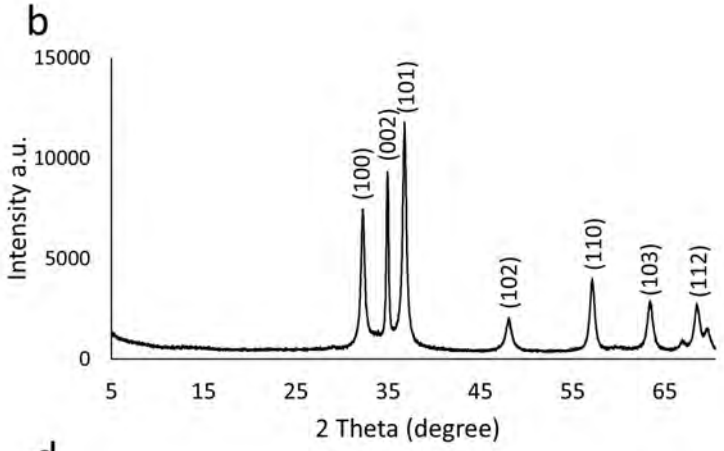
b
Intensity a.u.
(100)
(002)
(101)
(102)
(110)
(103)
(112)
2 Theta (degree)

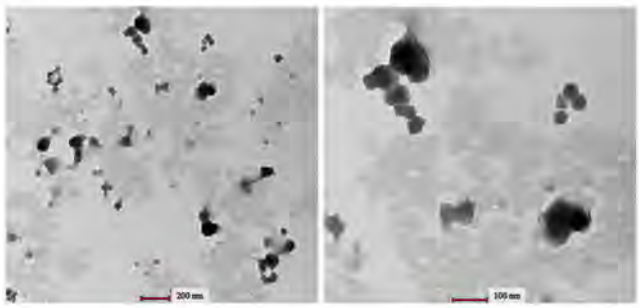
c

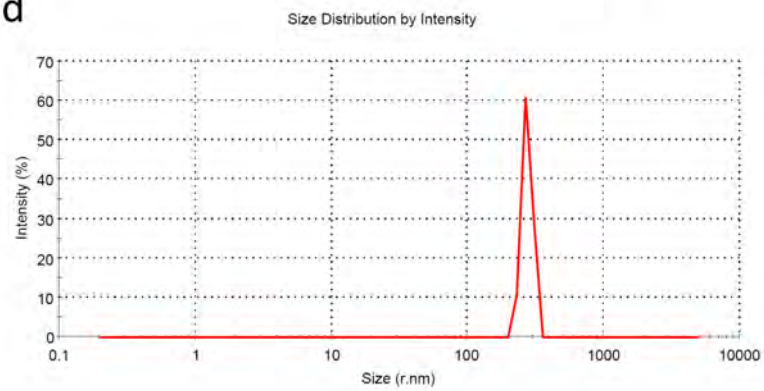
d
Size Distribution by Intensity
Intensity (%)
Size (r.nm)

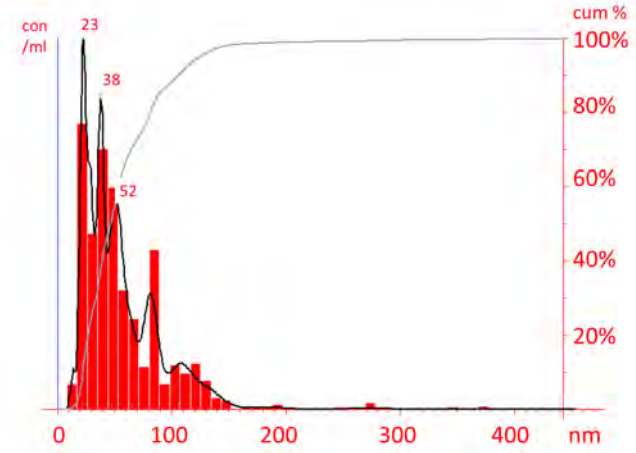
e
con /ml
cum %
23
38
52
nm

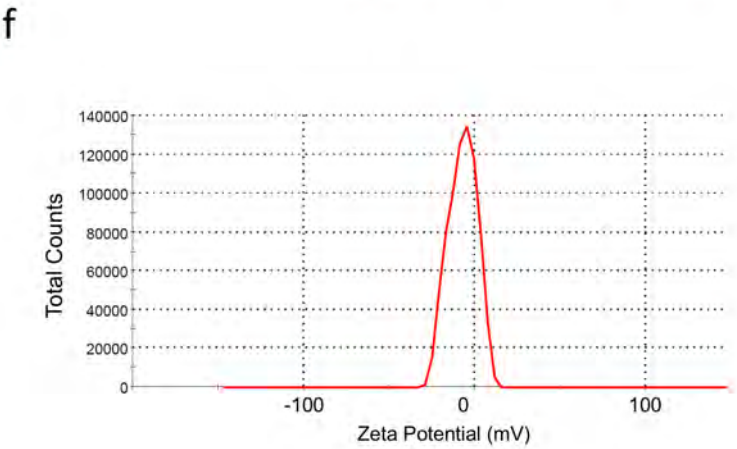
f
Total Counts
Zeta Potential (mV)

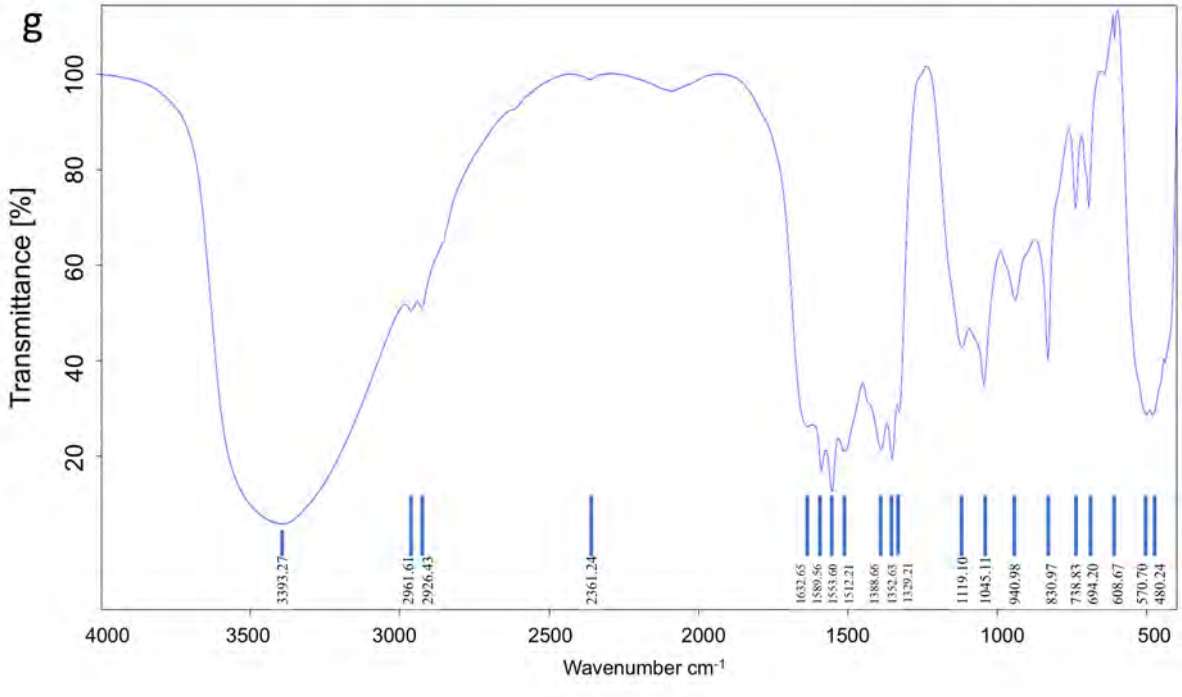
g
Transmittance [%]
3393.27
2961.61
2926.43
2361.24
1632.65
1589.56
1553.60
1512.21
1388.66
1352.63
1329.21
1119.10
1045.11
940.98
830.97
758.83
694.20
608.67
570.70
480.24
Wavenumber cm-1

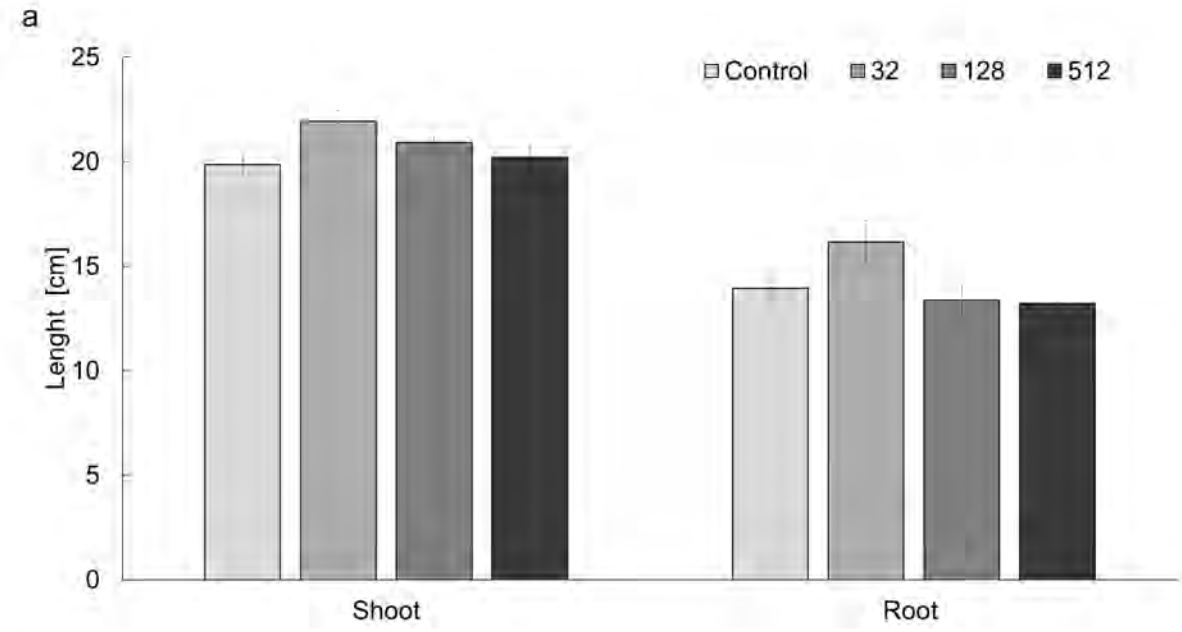
a
Control
32
128
512
Lenght [cm]
25
20
15
10
5
0
Shoot
Root

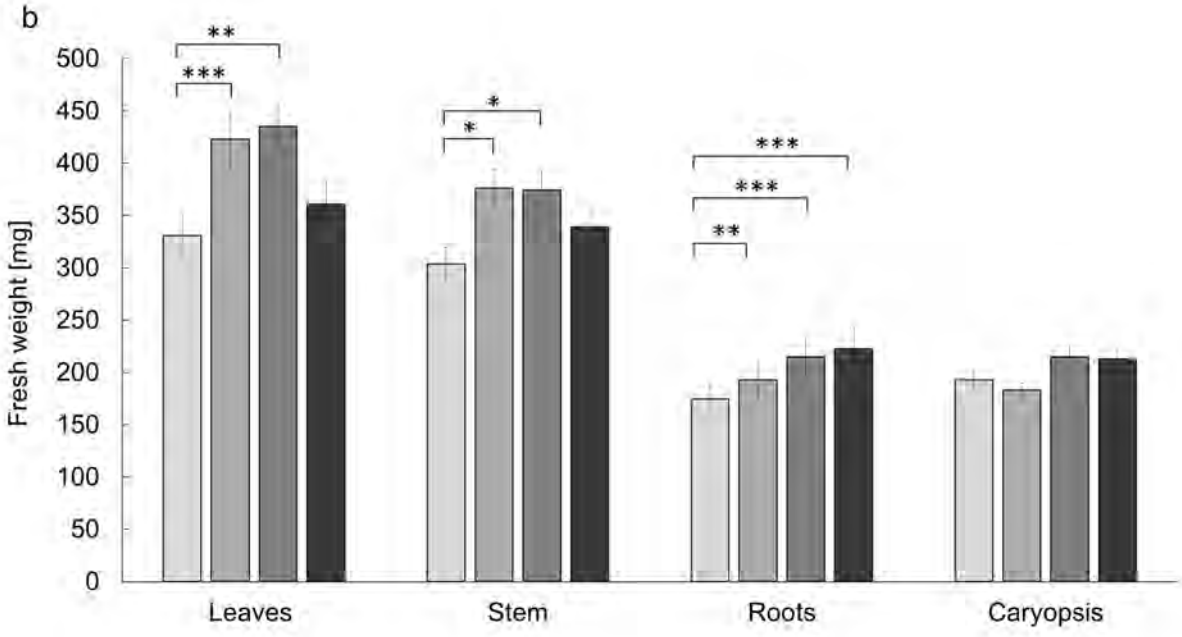
b
Fresh weight [mg]
500
450
400
350
300
250
200
150
100
50
0
**
***
*
*
***
***
**
Leaves
Stem
Roots
Caryopsis

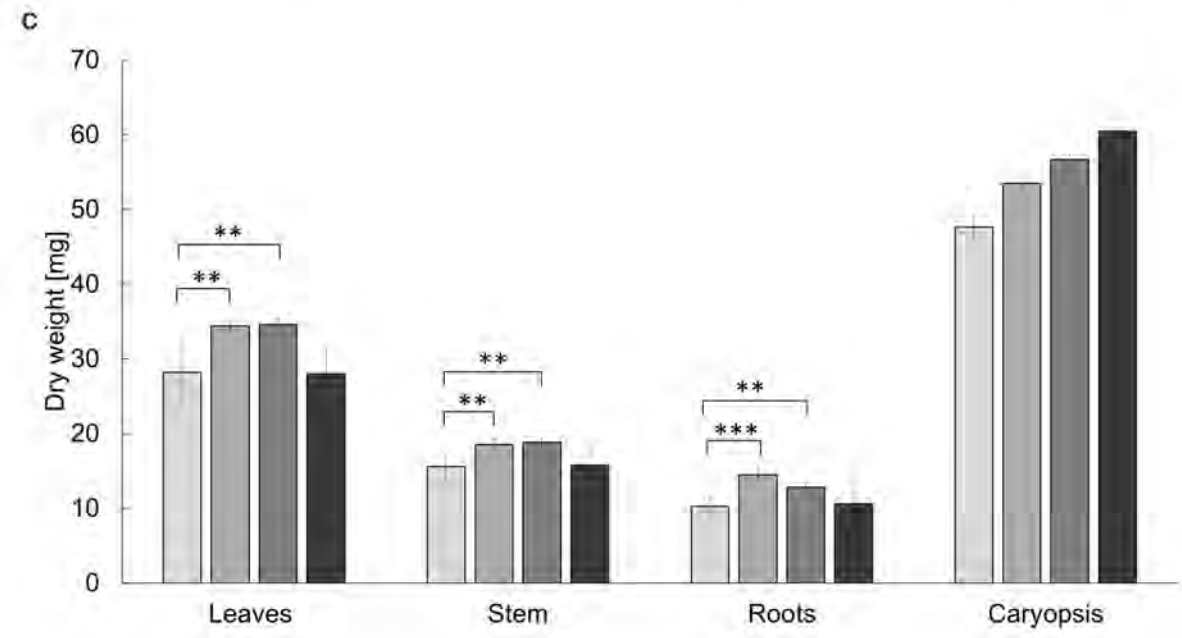
c
Dry weight [mg]
70
60
50
40
30
20
10
0
**
**
**
**
**
***
Leaves
Stem
Roots
Caryopsis

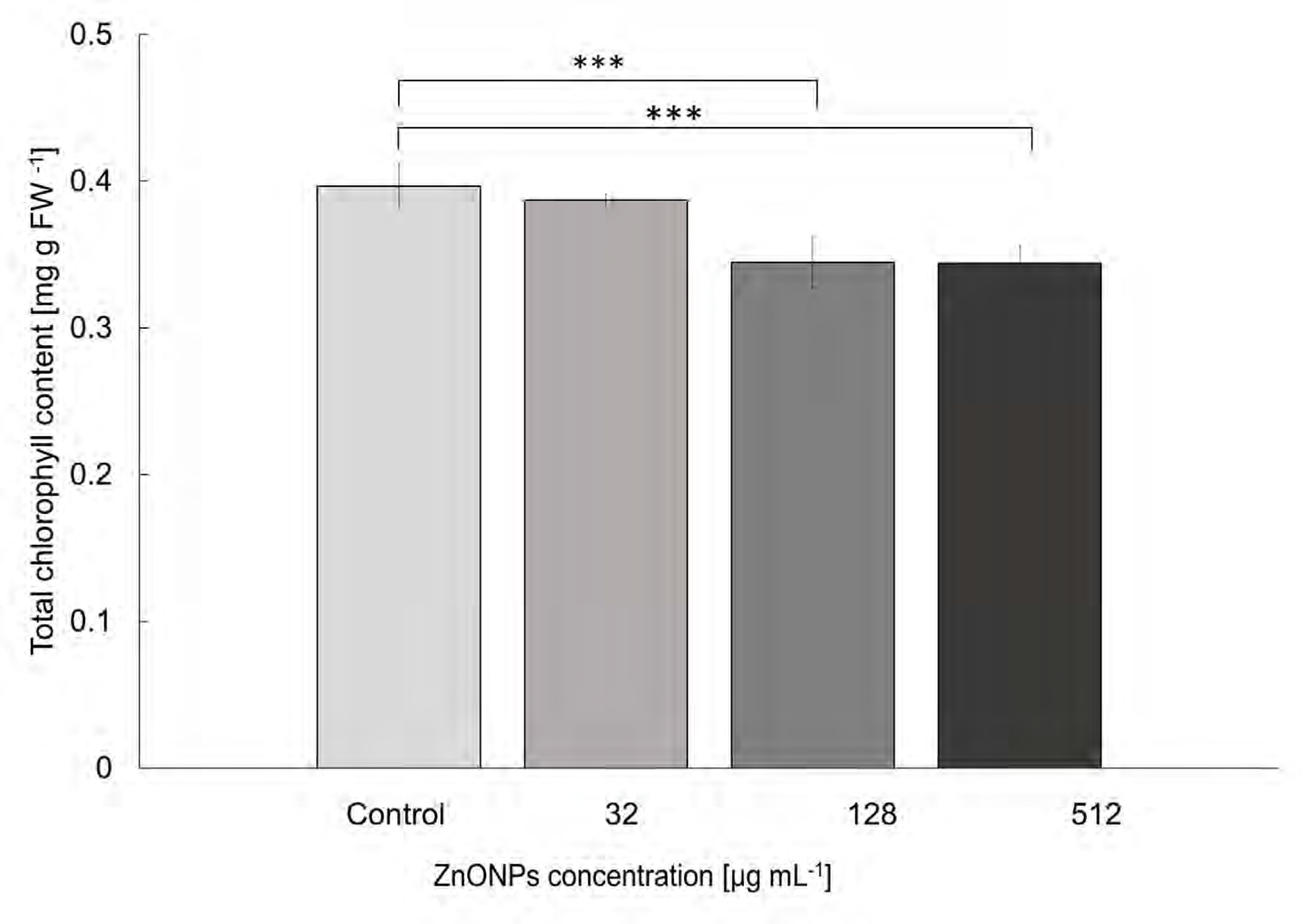
0.5
0.4
0.3
0.2
0.1
0
***
***
Total chlorophyll content [mg g FW -1]
Control
32
128
512
ZnONPs concentration [µg mL-1]

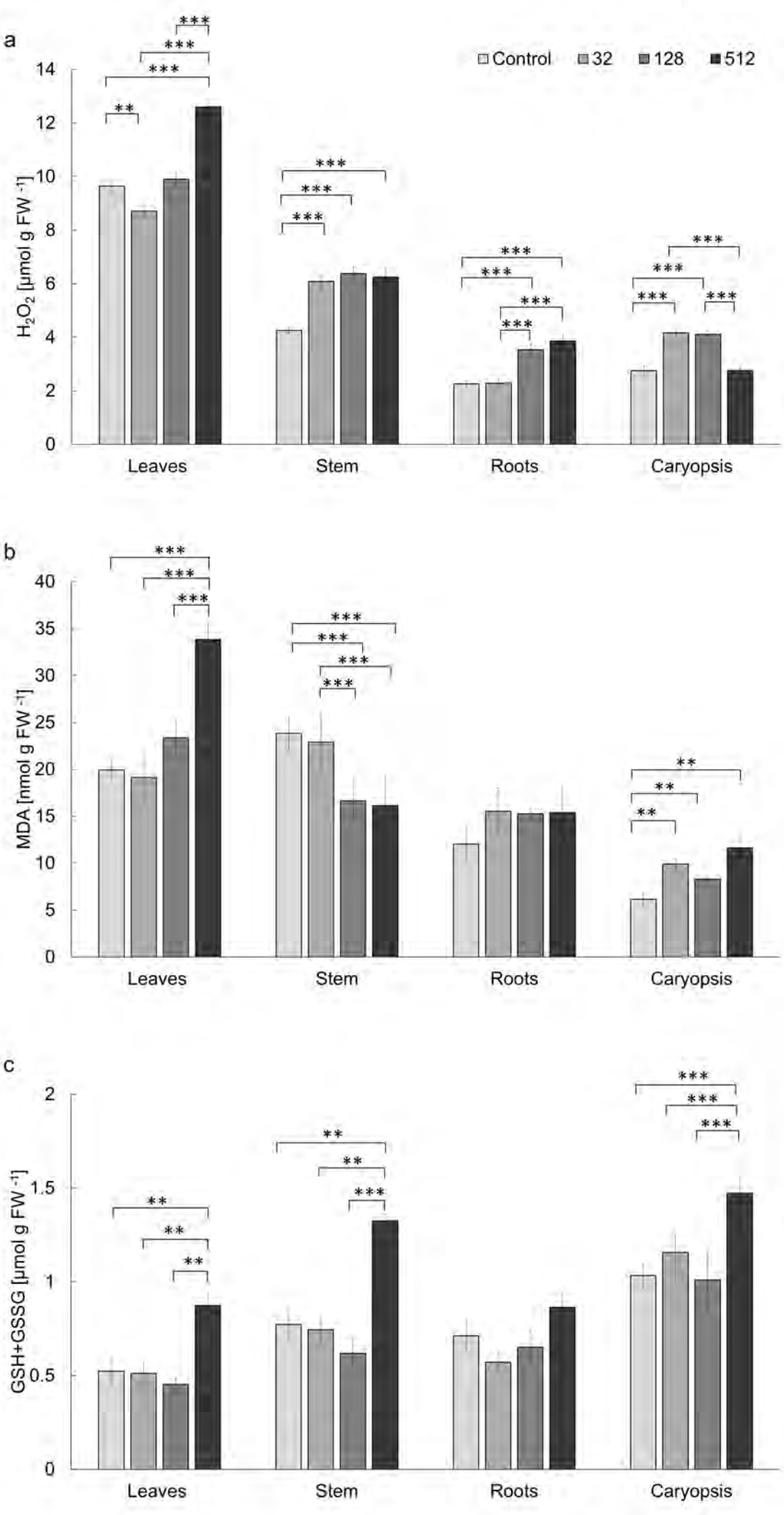
a
Control
32
128
512
H_2O_2 [µmol g FW $^{-1}$]
0
2
4
6
8
10
12
14
Leaves
Stem
Roots
Caryopsis
b
MDA [nmol g FW $^{-1}$]
0
5
10
15
20
25
30
35
40
Leaves
Stem
Roots
Caryopsis
c
GSH+GSSG [µmol g FW $^{-1}$]
0
0.5
1
1.5
2
Leaves
Stem
Roots
Caryopsis

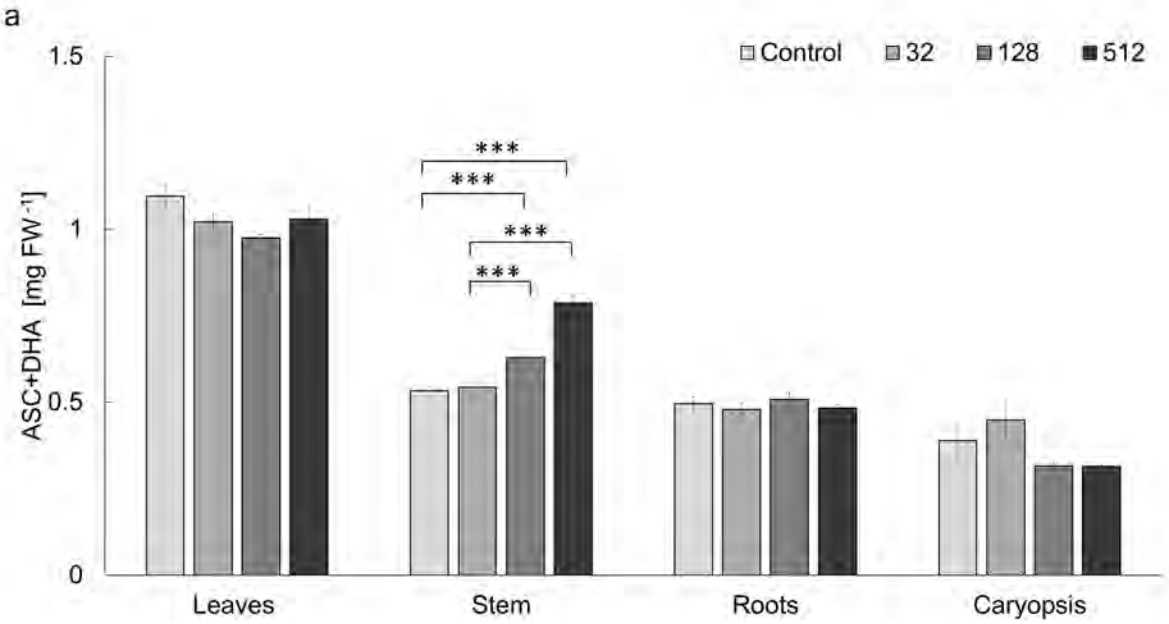
a
Control
32
128
512
ASC+DHA [mg FW-1]
1.5
1
0.5
0
***
***
***
***
Leaves
Stem
Roots
Caryopsis

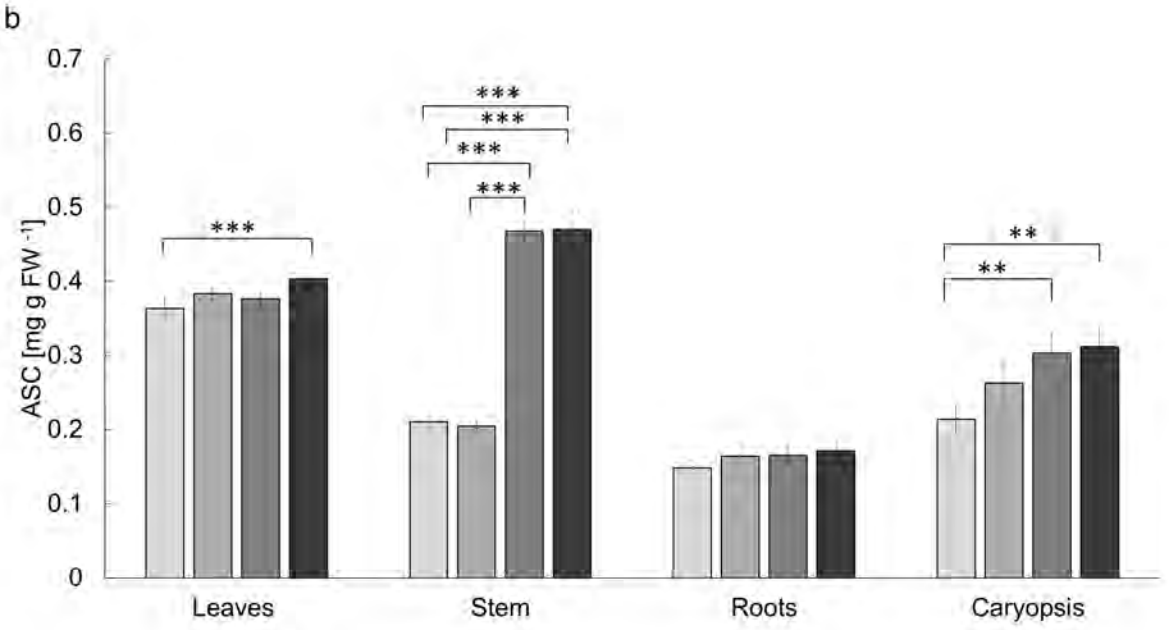
b
ASC [mg g FW-1]
0.7
0.6
0.5
0.4
0.3
0.2
0.1
0
***
***
***
***
***
**
**
Leaves
Stem
Roots
Caryopsis

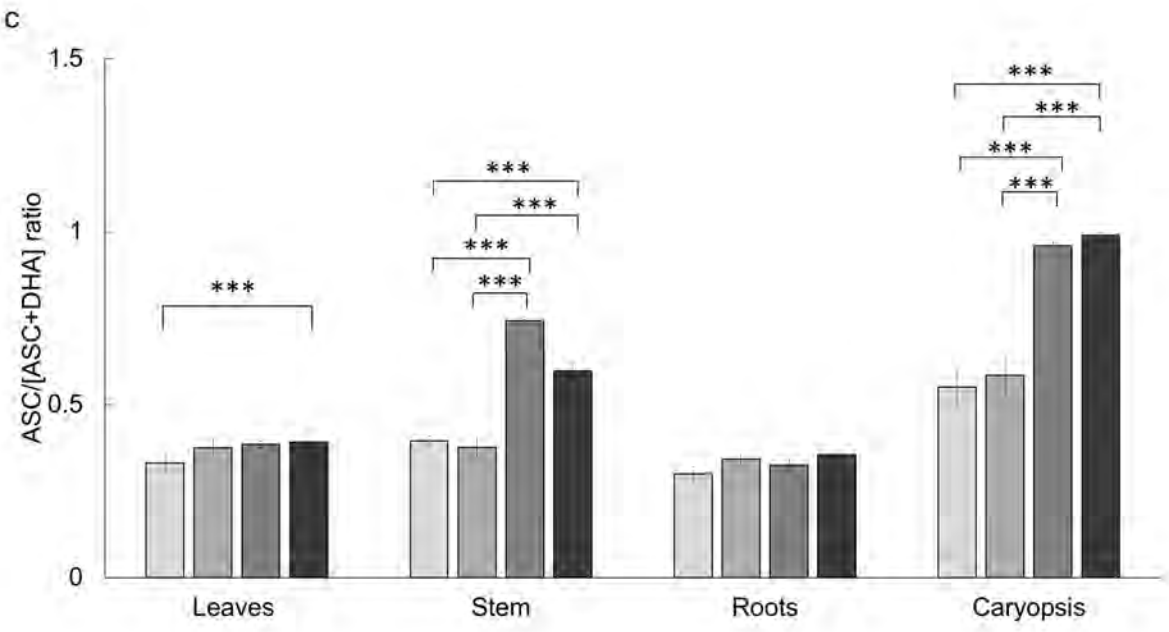
c
ASC/[ASC+DHA] ratio
1.5
1
0.5
0
***
***
***
***
***
***
***
***
Leaves
Stem
Roots
Caryopsis

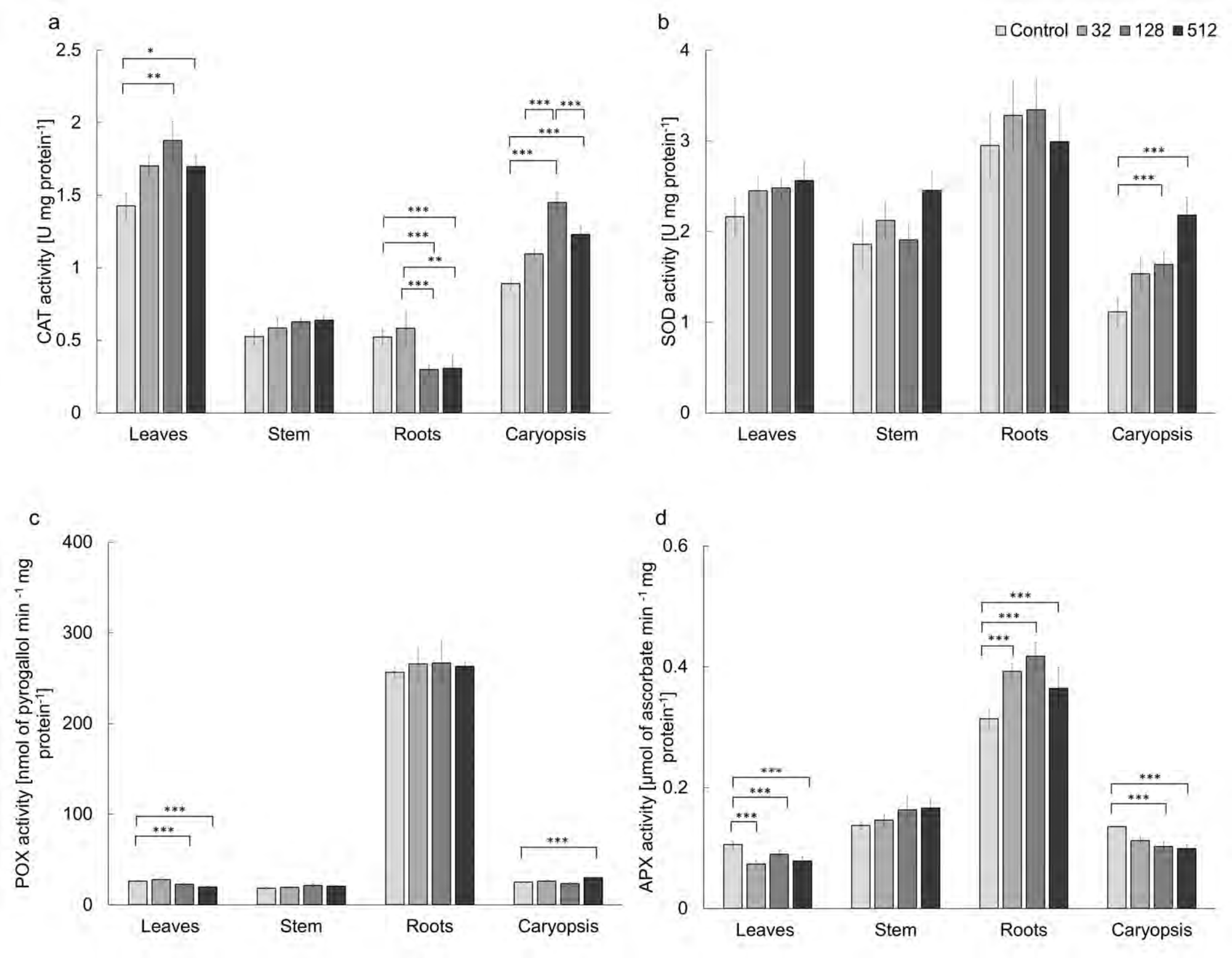
a
b
c
d
Control
32
128
512
CAT activity [U mg protein-1]
SOD activity [U mg protein-1]
POX activity [nmol of pyrogallol min -1 mg protein-1]
APX activity [µmol of ascorbate min -1 mg protein-1]
Leaves
Stem
Roots
Caryopsis

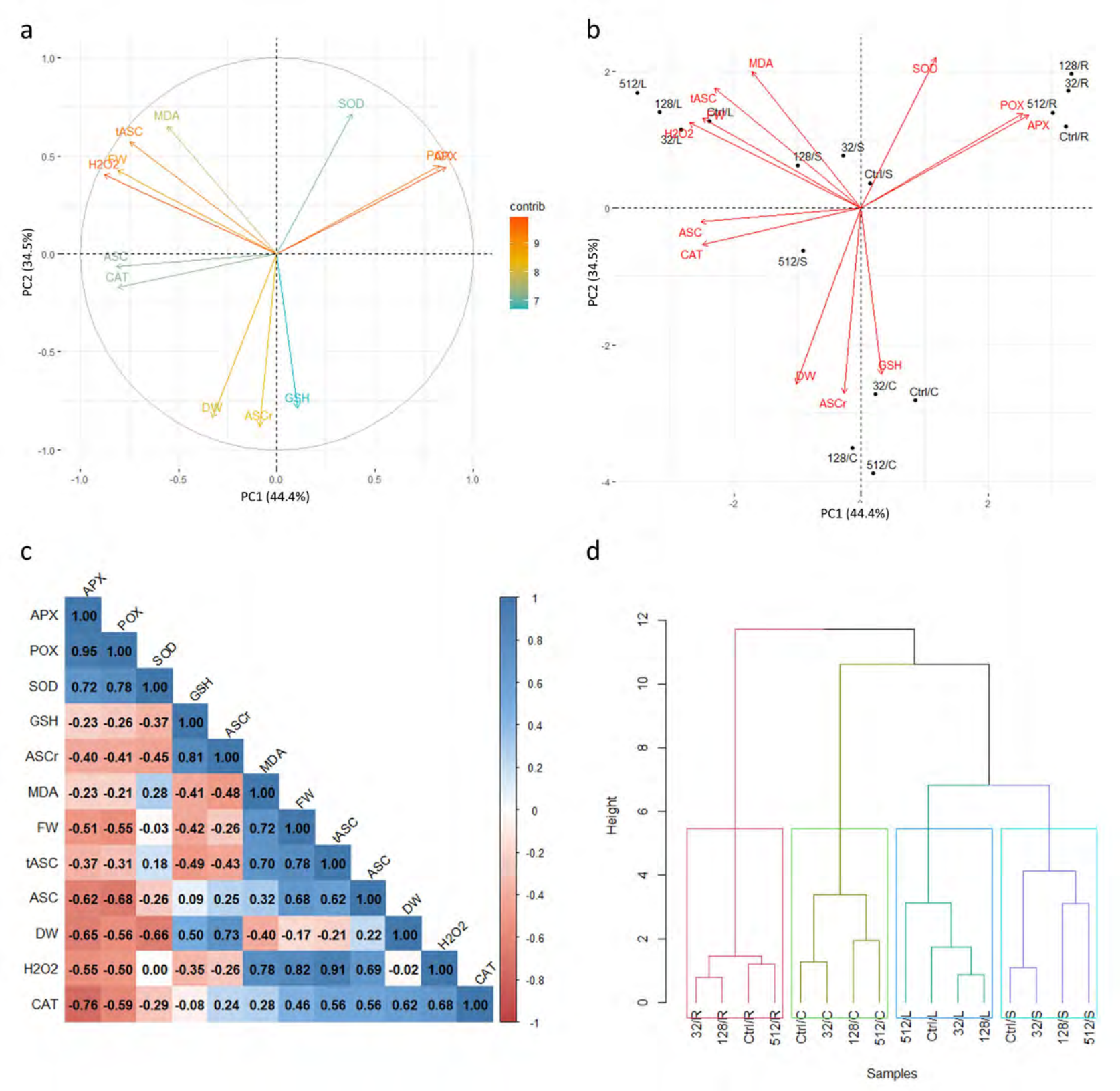
a
MDA
tASC
FW
H2O2
SOD
APX
ASC
CAT
DW
ASCr
GSH
contrib
PC1 (44.4%)
PC2 (34.5%)
b
MDA
SOD
128/R
32/R
512/L
128/L
tASC
Ctrl/L
POX
512/R
APX
Ctrl/R
H2O2
32/L
32/S
128/S
Ctrl/S
ASC
CAT
512/S
DW
GSH
32/C
Ctrl/C
ASCr
128/C
512/C
PC1 (44.4%)
PC2 (34.5%)
c
APX
POX
SOD
GSH
ASCr
MDA
FW
tASC
ASC
DW
H2O2
CAT
d
Height
Samples
32/R
128/R
Ctrl/R
512/R
Ctrl/C
32/C
128/C
512/C
512/L
Ctrl/L
32/L
128/L
Ctrl/S
32/S
128/S
512/S

Supplementary Material

ZnONPs biosynthesized from *Fusarium solani* IOR 825: unveiling their growth stimulating effects in maize (*Zea mays* L.)

Trzcińska-Wencel Joanna[1*], Mucha Natalia[2], Nadrowska Julia[1], Gade Anikiet[1], Rai Mahendra[3], Tyburski Jarosław[2], Golińska Patrycja[1]

[1] Department of Microbiology, Faculty of Biological and Veterinary Sciences, Nicolaus Copernicus University in Toruń, Toruń, Poland,

[2] Department of Plant Physiology and Biotechnology, Faculty of Biological and Veterinary Sciences, Nicolaus Copernicus University in Toruń, Toruń, Poland

[3] Nanobiotechnology Laboratory, Department of Biotechnology, SGB Amravati University, Amravati, India

[4]Department of Chemistry, Federal University of Piaui (UFPI), Teresina, Brazil

*** Correspondence:**
Trzcińska-Wencel Joanna
trzcinska@doktorant.umk.pl

Supplementary Table 1. The summarized alterations [%] in growth parameters, accumulation of H_2O_2, malondialdehyde (MDA), total glutathione, total ascorbate and reduced ascorbate and enzymatic activity in individual organs of maize plantlets treated with bio-ZnONPs in comparison with the control.

	ZnONPs concentration [µg mL^{-1}]		
	32	**128**	**512**
Lenght			
Shoot	0.0	10.5	5.4
Root	0.0	15.8	-4.1
Fresh weight			
leaves	27.8*	31.6*	9.1
stem	23.9*	23.2*	11.6
roots	10.3*	22.9*	27.3*
caryopsis	-5.1	11.3	10.2
Dry weight			
leaves	21.9*	22.7*	-0.7
stem	18.9*	20.6*	0.8
roots	41.6*	24.7*	3.4
caryopsis	12.3	19.0	27.0
Chlorophyll content			
Leaves	-2.4	-13.1*	-13.2*
H_2O_2 concentration			
leaves	-9.6*	2.7	30.7*
stem	42.7*	50.0*	46.9*
roots	1.1	57.0*	71.3*
caryopsis	51.3*	49.3*	0.0
MDA concentration			
leaves	-4.0	17.0	69.6*
stem	-4.0	-30.2*	-32.4*
roots	29.0	26.8	27.9
caryopsis	60.2*	34.6*	88.5*
Total glutathione			
leaves	-2.1	-13.5	66.7*
stem	-3.7	-19.7	71.4*
roots	-19.9	-8.7	21.1
caryopsis	11.9	-2.5	42.3*
Total ascorbate			
leaves	-6.8	-11.0	-6.1
stem	1.9	18.1*	47.6*
roots	-3.3	2.7	-2.6
caryopsis	15.6	-18.8	-18.9

Reduced ASC			
leaves	5.5	3.5	11.0*
stem	-2.9	122.0*	123.2*
roots	10.4	11.4	15.4
caryopsis	22.7	41.5*	45.7*
CAT activity			
leaves	19.4	31.6*	19.1*
stem	11.6	19.6	21.6
roots	11.2	-42.9*	-41.5*
caryopsis	22.9	62.6*	38.0*
SOD activity			
leaves	13.2	14.6	18.4
stem	14.1	2.6	31.9
roots	11.3	13.4	1.5
caryopsis	38.0	47.2*	95.9*
POX activity			
leaves	6.4	-12.9*	-25.5*
stem	7.3	18.5	13.2
roots	3.6	4.0	2.6
caryopsis	4.6	-7.2	19.3*
APX activity			
leaves	-30.3*	-14.8*	-25.5*
stem	6.5	18.7	21.0
roots	25.0*	33.0*	16.1*
caryopsis	-16.8	-24.2*	-26.7*

* denote statistical significance (p-value < 0.05) between ZnONPs treatment and control.

Supplementary Table 3. The contribution of individual biochemical and growth parameters to PC1 and PC2 [%]

	PC1	**PC2**
CAT	12.3	0.7
SOD	2.8	12.4
POX	12.9	4.9
APX	13.9	4.7
H_2O_2	14.5	3.9
MDA	5.8	10.2
GSH	0.2	15.0
tASC	10.5	7.9
ASC	12.6	0.1
ASCr	0.1	18.8
FW	12.3	4.4
DW	2.0	16.9

APX: ascorbate peroxidase; ASC: ascorbate; ASCr: reduced ascorbate; DW: dry weight; FW: fresh weight; GSH: glutathione; H_2O_2: hydrogen peroxide; MDA: malondialdehyde; POX: peroxidase; SOD: superoxide dismutase; tASC: total ascorbate.

VI Podsumowanie i wnioski

Wyniki badań nad biosyntezą AgNPs oraz ZnONPs z wykorzystaniem szczepów grzybowych z rodzaju *Fusarium* oraz ich aktywnością przeciwdrobnoustrojową i potencjałem do stymulowania wzrostu kukurydzy pozwoliły ma sformułowanie następujących wniosków:

1) Grzyby z rodzaju *Fusarium* są wydajnym systemem do syntezy nanocząstek AgNPs i ZnONPs o różnych właściwościach fizyko-chemicznych oraz aktywności biologicznej, w zależności od wykorzystanego szczepu i metody syntezy.
2) AgNPs 1 z *Fusarium culmorum* JTW1 wykazywały najsilniejszą aktywność przeciwbakteryjną, synergistyczne działanie z antybiotykami, hamowały formowanie i aktywność hydrolityczną biofilmów.
3) AgNPs 2 z *Fusarium solani* IOR 825 wykazywały wysoką aktywności wobec grzybów fitopatogennych, dezynfekującą powierzchnię ziarniaków kukurydzy i stymulującą jej wzrost.
4) AgNPs 2 w najniższym stężeniu dezynfekującym powierzchnię ziarniaków (32 µg mL^{-1}) stymulują produkcję suchej masy liści i powodują niewielkie zmiany u 14-dniowych roślin, w tym:
    a) spadek zawartości H_2O_2, wyższą zawartość całkowitego askorbinianu oraz niższą aktywność katalazy i dysmutazy ponadtlenkowej w liściach
    b) brak istotnych zmian badanych parametrów w korzeniach
    c) większy udział formy zredukowanej ASC, niższą aktywność dysmutazy ponadtlenkowej w łodygach,
    d) spadek zawartości H_2O_2, większy udział formy zredukowanej ASC, niższą aktywność dysmutazy ponadtlenkowej w skiełkowanych ziarniakach,
5) ZnONPs 1 z *Fusarium solani* IOR 825 w stężeniach 32 µg mL^{-1} stymulowały wzrost kukurydzy nie powodując efektu toksycznego.
6) ZnONPs 1 w najniższym stężeniu (32 µg mL^{-1}) stymulującym wzrost kukurydzy powodują spadek zawartości H_2O_2 i niższą aktywność peroksydazy askorbinianowej w liściach, wyższą aktywność peroksydazy askorbinianowej w korzeniach, wzrost zawartości H_2O_2 w łodygach oraz wzrost zawartości H_2O_2 i MDA w skiełkowanych ziarniakach.

7) Zastosowanie wyższych stężeń AgNPs i ZnONPs skutkowało zróżnicowanym wpływem na aktywność enzymów i syntezę przeciwutleniaczy nieenzymatycznych.
8) Najwyższe testowane stężenie (512 µg mL^{-1}) nanocząstek powodowało m.in. peroksydację lipidów i zmniejszenie zawartości chlorofilu.

Podsumowując, badania przeprowadzone w niniejszej pracy wskazują, że AgNPs i ZnONPs syntezowane z wykorzystaniem *Fusarium solani* IOR 825, w stężeniu 32 µg mL^{-1} wykazują potencjał do bezpiecznego stosowania w rolnictwie, który wynika z ich wysokiej aktywności przeciwdrobnoustrojowej i stymulującej wzrost kukurydzy, bez wywoływania stresu oksydacyjnego, czy negatywnego wpływu na zawartość chlorofilu. Warto podkreślić, że biosynteza nanocząstek i technika traktowania ziarniaków są proste, opłacalne i przyjazne dla środowiska, co jest kolejnym atutem do zastosowania takich nanocząstek w praktyce.

Pozostaje jednak wiele pytań w którym kierunku powinny zmierzać dalsze badania nad zastosowaniem bionanocząstek w uprawie roślin, w tym jakie gatunki roślin powinny być badanie priorytetowo i na jakim etapie swojego rozwoju, aby lepiej zrozumieć mechanizmy stymulacji wzrostu czy toksyczności nanocząstek u tych organizmów? W jaki sposób mechanizmy te zmieniają się w różnych fazach wzrostu? Jak ustandaryzować metodykę tych badań? Jak prowadzić współpracę w zakresie nanotechnologii pomiędzy naukowcami, ekspertami ds. danych i agronomami, aby sprostać wyzwaniom związanym praktycznym wykorzystaniem nanoproduktów? Pytanie, jakie regulacje prawne i strategie można wprowadzić, aby rozwiązania nanotechnologiczne mogły być bezpiecznie stosowane w rolnictwie? również pozostaje otwarte.

VII Literatura

1. Abbasi Khalaki, M., Moameri, M., Asgari Lajayer, B., & Astatkie, T. (2021). Influence of nano-priming on seed germination and plant growth of forage and medicinal plants. Plant Growth Regulation, 93, 13–28. https://doi.org/10.1007/s10725-020-00670-9
2. Abbaszadegan, A., Ghahramani, Y., Gholami, A., Hemmateenejad, B., Dorostkar, S., Nabavizadeh, M., & Sharghi, H. (2015). The effect of charge at the surface of silver nanoparticles on antimicrobial activity against Gram-positive and Gram-negative bacteria: A preliminary study. Journal of Nanomaterials, 2015: 720654. https://doi.org/10.1155/2015/720654
3. Abdelgadir, A., Adnan, M., Patel, M., Saxena, J., Alam, M. J., Alshahrani, M. M., Singh, R., Sachidanandan, M., Badraoui, R., & Siddiqui, A. J. (2024). Probiotic *Lactobacillus salivarius* mediated synthesis of silver nanoparticles (AgNPs-LS): A sustainable approach and multifaceted biomedical application. Heliyon, 10: e37987. https://doi.org/10.1016/j.heliyon.2024.e37987
4. Abid, N., Khan, A. M., Shujait, S., Chaudhary, K., Ikram, M., Imran, M., Haider, J., Khan, M., Khan, Q., & Maqbool, M. (2022). Synthesis of nanomaterials using various top-down and bottom-up approaches, influencing factors, advantages, and disadvantages: A review. Advances in Colloid and Interface Science, 300: 102597. https://doi.org/10.1016/j.cis.2021.102597
5. Acharya, P., Jayaprakasha, G. K., Crosby, K. M., Jifon, J. L., & Patil, B. S. (2020). Nanoparticle-mediated seed priming improves germination, growth, yield, and quality of watermelons (*Citrullus lanatus)* at multi-locations in Texas. Scientific Reports, 10: 5037. https://doi.org/10.1038/s41598-020-61696-7
6. Ahmad, A., Mukherjee, P., Senapati, S., Mandal, D., Khan, M. I., Kumar, R., & Sastry, M. (2003). Extracellular biosynthesis of silver nanoparticles using the fungus *Fusarium oxysporum*. Colloids and Surfaces B: Biointerfaces, 28, 313–318. https://doi.org/10.1016/S0927-7765(02)00174-1
7. Akhtar, J., & Kumar, P. (2024). Seed-borne fungi: Challenges in seed health testing for biosecurity and agricultural sustainability. Indian Phytopathology, 77, 257–269. https://doi.org/10.1007/s42360-024-00723-3
8. Alabdallah, N. M., Hasan, M. M., Hammami, I., Alghamdi, A. I., Alshehri, D., & Alatawi, H. A. (2021). Green synthesized metal oxide nanoparticles mediate growth regulation and physiology of crop plants under drought stress. Plants, 10: 8. https://doi.org/10.3390/plants10081730
9. Alavi, M., & Ashengroph, M. (2023). Mycosynthesis of AgNPs: Mechanisms of nanoparticle formation and antimicrobial activities. Expert Review of Anti-Infective Therapy, 21, 355–363. https://doi.org/10.1080/14787210.2023.2179988
10. Ali, A., Phull, A.-R., & Zia, M. (2018). Elemental zinc to zinc nanoparticles: Is ZnO NPs crucial for life? Synthesis, toxicological, and environmental concerns. Nanotechnology Reviews, 7, 413–441. https://doi.org/10.1515/ntrev-2018-0067
11. Amin, Z., Ullah, M., Wahab, A., Naeem, M., Khan, S. U., & Hasan, N. (2024). Fundamentals of nanotechnology. W: Shahzad, R., Fiaz, S., Qayyum, A., Ul Islam, M., & Lee I.J. (Red.), Revolutionizing agriculture: A comprehensive exploration of

agri-nanotechnology (s. 1–16). Springer Nature Switzerland. https://doi.org/10.1007/978-3-031-76000-6_1
12. Ashour, M. A., & Abd-Elhalim, B. T. (2024). Biosynthesis and biocompatibility evaluation of zinc oxide nanoparticles prepared using *Priestia megaterium* bacteria. Scientific Reports, 14: 4147. https://doi.org/10.1038/s41598-024-54460-8
13. Ashwini, M. N., Gajera, H. P., Hirpara, D. G., Savaliya, D. D., & Kandoliya, U. K. (2024). Comparative impact of seed priming with zinc oxide nanoparticles and zinc sulphate on biocompatibility, zinc uptake, germination, seedling vitality, and antioxidant modulation in groundnut. Journal of Nanoparticle Research, 26: 235. https://doi.org/10.1007/s11051-024-06141-w
14. Asif, N., Fatima, S., Aziz, Md. N., Shehzadi, Zaki, A., & Fatma, T. (2021). Biofabrication and characterization of cyanobacteria derived ZnO NPs for their bioactivity comparison with commercial chemically synthesized nanoparticles. Bioorganic Chemistry, 113: 104999. https://doi.org/10.1016/j.bioorg.2021.104999
15. Begam, A., Pramanick, M., Dutta, S., Paramanik, B., Dutta, G., Patra, P. S., Kundu, A., & Biswas, A. (2024). Inter-cropping patterns and nutrient management effects on maize growth, yield and quality. Field Crops Research, 310: 109363. https://doi.org/10.1016/j.fcr.2024.109363
16. Bhattacharjee, S. (2019). ROS and regulation of photosynthesis. W: Bhattacharjee S. (Red.), Reactive oxygen species in plant biology (s. 107–125). Springer India. https://doi.org/10.1007/978-81-322-3941-3_5
17. Bhushan, B. (2017). Introduction to nanotechnology. W: Bhushan B. (Red.), Springer handbook of nanotechnology (s. 1–19). Springer. https://doi.org/10.1007/978-3-662-54357-3_1
18. Borehalli Mayegowda, S., Roy, A., N. G., M., Pandit, S., Alghamdi, S., Almehmadi, M., Allahyani, M., Awwad, N. S., & Sharma, R. (2023). Eco-friendly synthesized nanoparticles as antimicrobial agents: An updated review. Frontiers in Cellular and Infection Microbiology, 13: 1224778. https://doi.org/10.3389/fcimb.2023.1224778
19. Brown, H. E., Esher, S. K., & Alspaugh, J. A. (2020). Chitin: A “Hidden Figure” in the fungal cell wall. W: Latgé J. P. (Red.), The fungal cell wall: An armour and a weapon for human fungal pathogens (s. 83–111). Springer International Publishing. https://doi.org/10.1007/82_2019_184
20. Burlakoti, S., Devkota, A. R., Poudyal, S., & Kaundal, A. (2024). Beneficial plant–microbe interactions and stress tolerance in maize. Applied Microbiology, 4: 3. https://doi.org/10.3390/applmicrobiol4030068
21. Camp, A. F. (1945). Zinc as a nutrient in plant growth. Soil Science, 60, 157-164.
22. Cao, Y., Turk, K., Bibi, N., Ghafoor, A., Ahmed, N., Azmat, M., Ahmed, R., Ghani, M. I., & Ahanger, M. A. (2025). Nanoparticles as catalysts of agricultural revolution: Enhancing crop tolerance to abiotic stress: a review. Frontiers in Plant Science, 15: 1510482. https://doi.org/10.3389/fpls.2024.1510482
23. Caser, M., Percivalle, N. M., & Cauda, V. (2024). The application of micro- and nano-sized zinc oxide particles differently triggers seed germination in *Ocimum basilicum* L., *Lactuca sativa* L., and *Lepidium sativum* L. under Controlled Conditions. Horticulturae, 10: 575. https://doi.org/10.3390/horticulturae10060575

24. Chan, Y. S., & Mat Don, M. (2013). Biosynthesis and structural characterization of Ag nanoparticles from white rot fungi. Materials Science and Engineering: C, 33, 282–288. https://doi.org/10.1016/j.msec.2012.08.041
25. Chen, J., Dou, R., Yang, Z., You, T., Gao, X., & Wang, L. (2018). Phytotoxicity and bioaccumulation of zinc oxide nanoparticles in rice (*Oryza sativa* L.). Plant Physiology and Biochemistry, 130, 604–612. https://doi.org/10.1016/j.plaphy.2018.08.019
26. Cheng, H., Chen, L., McClements, D. J., Xu, H., Long, J., Zhao, J., Xu, Z., Meng, M., & Jin, Z. (2024). Recent advances in the application of nanotechnology to create antioxidant active food packaging materials. Critical Reviews in Food Science and Nutrition, 64, 2890–2905. https://doi.org/10.1080/10408398.2022.2128035
27. Choudhary, A., Kumar, A., & Kaur, N. (2020). ROS and oxidative burst: roots in plant development. Plant Diversity, 42, 33–43. https://doi.org/10.1016/j.pld.2019.10.002
28. Dakos, V., Matthews, B., Hendry, A. P., Levine, J., Loeuille, N., Norberg, J., Nosil, P., Scheffer, M., & De Meester, L. (2019). Ecosystem tipping points in an evolving world. Nature Ecology & Evolution, 3, 355–362. https://doi.org/10.1038/s41559-019-0797-2
29. Deng, H., McShan, D., Zhang, Y., Sinha, S. S., Arslan, Z., Ray, P. C., & Yu, H. (2016). Mechanistic study of the synergistic antibacterial activity of combined silver nanoparticles and common antibiotics. Environmental Science & Technology, 50, 8840–8848. https://doi.org/10.1021/acs.est.6b00998
30. Dhiman, S., Singh, S., Varma, A., & Goel, A. (2021). Phytofabricated zinc oxide nanoparticles as a nanofungicide for management of *Alternaria* blight of *Brassica*. BioMetals, 34, 1275–1293. https://doi.org/10.1007/s10534-021-00342-9
31. Donia, D. T., & Carbone, M. (2023). Seed priming with zinc oxide nanoparticles to enhance crop tolerance to environmental stresses. International Journal of Molecular Sciences, 24: 17612. https://doi.org/10.3390/ijms242417612
32. Dowlath, M. J. H., Musthafa, S. A., Mohamed Khalith, S. B., Varjani, S., Karuppannan, S. K., Ramanujam, G. M., Arunachalam, A. M., Arunachalam, K. D., Chandrasekaran, M., Chang, S. W., Chung, W. J., & Ravindran, B. (2021). Comparison of characteristics and biocompatibility of green synthesized iron oxide nanoparticles with chemical synthesized nanoparticles. Environmental Research, 201: 111585. https://doi.org/10.1016/j.envres.2021.111585
33. du Jardin, P. (2015). Plant biostimulants: Definition, concept, main categories and regulation. Scientia Horticulturae, 196, 3–14. https://doi.org/10.1016/j.scienta.2015.09.021
34. Durán, N., Marcato, P. D., Alves, O. L., De Souza, G. I., & Esposito, E. (2005). Mechanistic aspects of biosynthesis of silver nanoparticles by several *Fusarium oxysporum* strains. Journal of Nanobiotechnology, 3: 8. https://doi.org/10.1186/1477-3155-3-8
35. El Badawy, A. M., Silva, R. G., Morris, B., Scheckel, K. G., Suidan, M. T., & Tolaymat, T. M. (2011). Surface charge-dependent toxicity of silver nanoparticles. Environmental Science & Technology, 45, 283–287. https://doi.org/10.1021/es1034188

36. El-Badri, A. M., Batool, M., Wang, C., Hashem, A. M., Tabl, K. M., Nishawy, E., Kuai, J., Zhou, G., & Wang, B. (2021). Selenium and zinc oxide nanoparticles modulate the molecular and morpho-physiological processes during seed germination of *Brassica napus* under salt stress. Ecotoxicology and Environmental Safety, 225: 112695. https://doi.org/10.1016/j.ecoenv.2021.112695
37. El-Moneim, D. A., Dawood, M. F. A., Moursi, Y. S., Farghaly, A. A., Afifi, M., & Sallam, A. (2021). Positive and negative effects of nanoparticles on agricultural crops. Nanotechnology for Environmental Engineering, 6: 21. https://doi.org/10.1007/s41204-021-00117-0
38. Es-haghi, A., Taghavizadeh Yazdi, M. E., Sharifalhoseini, M., Baghani, M., Yousefi, E., Rahdar, A., & Baino, F. (2021). Application of response surface methodology for optimizing the therapeutic activity of ZnO nanoparticles biosynthesized from *Aspergillus niger*. Biomimetics, 6: 34. https://doi.org/10.3390/biomimetics6020034
39. Essawy, A. A., Hussein, M. F., Hasanin, T. H. A., El Agammy, E. F., Alsaykhan, H. S., Alanazyi, R. F., & Essawy, A. I. (2024). Insights for precursors influence on the solar-assisted photocatalysis of greenly synthesizing zinc oxide NPs towards fast and durable wastewater detoxification. Ceramics, 7, 1100-1121. https://doi.org/10.3390/ceramics7030072
40. Faizan, M., Sharma, P., Sultan, H., Alam, P., Sehar, S., Rajput, V. D., & Hayat, S. (2024). Nano-priming: Improving plant nutrition to support the establishment of sustainable agriculture under heavy metal stress. Plant Nano Biology, 10: 100096. https://doi.org/10.1016/j.plana.2024.100096
41. Fayaz, A. M., Balaji, K., Girilal, M., Yadav, R., Kalaichelvan, P. T., & Venketesan, R. (2010). Biogenic synthesis of silver nanoparticles and their synergistic effect with antibiotics: A study against Gram-positive and Gram-negative bacteria. Nanomedicine: Nanotechnology, Biology and Medicine, 6, 103–109. https://doi.org/10.1016/j.nano.2009.04.006
42. Food and Agriculture Organization (FAO). (2022). Agricultural production statistics 2000–2021. FAOSTAT Analytical Briefs, 60. https://openknowledge.fao.org/handle/20.500.14283/cc3751en
43. Food and Agriculture Organization FAO. (2024). Pesticides use and trade, 1990–2022. FAOSTAT Analytical Briefs, 89. https://openknowledge.fao.org/handle/20.500.14283/cd1486en
44. Gaber, S. E., Hashem, A. H., El-Sayyad, G. S., & Attia, M. S. (2024). Antifungal activity of myco-synthesized bimetallic ZnO-CuO nanoparticles against fungal plant pathogen *Fusarium oxysporum*. Biomass Conversion and Biorefinery, 14, 25395–25409. https://doi.org/10.1007/s13399-023-04550-w
45. Gallo, M. B., Bader, A. N., Torres-Nicolini, A., Alvarez, V. A., & Consolo, V. F. (2025). Proteomic analysis of *Trichoderma harzianum* secretome and their role in the biosynthesis of zinc/iron oxide nanoparticles. Scientific Reports, 15: 3252. https://doi.org/10.1038/s41598-025-87581-9
46. Gao, Y., Arokia Vijaya Anand, M., Ramachandran, V., Karthikkumar, V., Shalini, V., Vijayalakshmi, S., & Ernest, D. (2019). Biofabrication of zinc oxide nanoparticles

from *Aspergillus niger,* their antioxidant, antimicrobial and anticancer activity. Journal of Cluster Science, 30, 937–946. https://doi.org/10.1007/s10876-019-01551-6

47. Garcidueñas-Piña, C., Tirado-Fuentes, C., Ruiz-Pérez, J., Valerio-García, R. C., & Morales-Domínguez, J. F. (2023). Silver nanoparticles synthesized with extracts of leaves of *Raphanus sativus* L, *Beta vulgaris* L, and *Ocimum basilicum* and its application in seed disinfection. Nanomaterials and Nanotechnology, 2023: 9874979. https://doi.org/10.1155/2023/9874979
48. Ghetas, H. A., Abdel-Razek, N., Shakweer, M. S., Abotaleb, M. M., Ahamad Paray, B., Ali, S., Eldessouki, E. A., Dawood, M. A., & Khalil, R. H. (2022). Antimicrobial activity of chemically and biologically synthesized silver nanoparticles against some fish pathogens. Saudi Journal of Biological Sciences, 29, 1298–1305. https://doi.org/10.1016/j.sjbs.2021.11.015
49. González-Merino, A. M., Hernández-Juárez, A., Betancourt-Galindo, R., Ochoa-Fuentes, Y. M., Valdez-Aguilar, L. A., & Limón-Corona, M. L. (2021). Antifungal activity of zinc oxide nanoparticles in *Fusarium oxysporum-Solanum lycopersicum* pathosystem under controlled conditions. Journal of Phytopathology, 169, 533–544. https://doi.org/10.1111/jph.13023
50. Guilger, M., Pasquoto-Stigliani, T., Bilesky-Jose, N., Grillo, R., Abhilash, P. C., Fraceto, L. F., & Lima, R. (2017). Biogenic silver nanoparticles based on *Trichoderma harzianum*: Synthesis, characterization, toxicity evaluation and biological activity. Scientific Reports, 7: 44421. https://doi.org/10.1038/srep44421
51. Gupta, K., & Chundawat, T. S. (2020). Zinc oxide nanoparticles synthesized using *Fusarium oxysporum* to enhance bioethanol production from rice-straw. Biomass and Bioenergy, 143: 105840. https://doi.org/10.1016/j.biombioe.2020.105840
52. Gupta, S. D., Agarwal, A., & Pradhan, S. (2018). Phytostimulatory effect of silver nanoparticles (AgNPs) on rice seedling growth: An insight from antioxidative enzyme activities and gene expression patterns. Ecotoxicology and Environmental Safety, 161, 624–633. https://doi.org/10.1016/j.ecoenv.2018.06.023
53. Gurgur, E., Oluyamo, S. S., Adetuyi, A. O., Omotunde, O. I., & Okoronkwo, A. E. (2020). Green synthesis of zinc oxide nanoparticles and zinc oxide–silver, zinc oxide–copper nanocomposites using *Bridelia ferruginea* as biotemplate. SN Applied Sciences, 2: 911. https://doi.org/10.1007/s42452-020-2269-3
54. Hacisalihoglu, G. (2020). Zinc (Zn): The last nutrient in the alphabet and shedding light on Zn efficiency for the future of crop production under suboptimal Zn. Plants, 9: 1471. https://doi.org/10.3390/plants9111471
55. Hamouda, R. A., Abd El-Mongy, M., & Eid, K. F. (2019). Comparative study between two red algae for biosynthesis silver nanoparticles capping by SDS: Insights of characterization and antibacterial activity. Microbial Pathogenesis, 129, 224–232. https://doi.org/10.1016/j.micpath.2019.02.016
56. Herrera Pérez, G. M., Castellano, L. E., & Ramírez Valdespino, C. A. (2024). *Trichoderma* and mycosynthesis of metal nanoparticles: Role of their secondary metabolites. Journal of Fungi, 10: 443. https://doi.org/10.3390/jof10070443
57. Hickey, L. T., Hafeez, A., Robinson, H., Jackson, S. A., Leal-Bertioli, S. C., Tester, M., Gao, C., Godwin, I. D., Hayes, B. J., & Wulff, B. B. (2019). Breeding crops to

feed 10 billion. Nature Biotechnology, 37, 744–754. https://doi.org/10.1038/s41587-019-0152-9

58. Hussain, A., Alajmi, M. F., Khan, M. A., Pervez, S. A., Ahmed, F., Amir, S., Husain, F. M., Khan, M. S., Shaik, G. M., Hassan, I., Khan, R. A., & Rehman, M. T. (2019). Biosynthesized silver nanoparticle (AgNP) from *Pandanus odorifer* leaf extract exhibits anti-metastasis and anti-biofilm potentials. Frontiers in Microbiology, 10:8. https://doi.org/10.3389/fmicb.2019.00008
59. Ingle, A., Gade, A., Pierrat, S., Sonnichsen, C., & Rai, M. (2008). Mycosynthesis of silver nanoparticles using the fungus *Fusarium acuminatum* and its activity against some human pathogenic bacteria. Current Nanoscience, 4, 141–144. https://doi.org/10.2174/157341308784340804
60. Jaramillo-López, P. F., Blas Romero, J., Sarabia, M., Fonteyne, S., Saldivia-Tejeda, A., Verhulst, N., Vestergård, M., & Larsen, J. (2024). Non-target effects of pesticide and microbial seed treatments in maize and barley on the resident soil microbiota under conservation agriculture. European Journal of Soil Biology, 122: 103653. https://doi.org/10.1016/j.ejsobi.2024.103653
61. Kadam, V. V., Ettiyappan, J. P., & Mohan Balakrishnan, R. (2019). Mechanistic insight into the endophytic fungus mediated synthesis of protein capped ZnO nanoparticles. Materials Science and Engineering: B, 243, 214–221. https://doi.org/10.1016/j.mseb.2019.04.017
62. Kaiser, K. G., Delattre, V., Frost, V. J., Buck, G. W., Phu, J. V., Fernandez, T. G., & Pavel, I. E. (2023). Nanosilver: An old antibacterial agent with great promise in the fight against antibiotic resistance. Antibiotics, 12: 1264. https://doi.org/10.3390/antibiotics12081264
63. Kamal Kumar, V., Muthukrishnan, S., & Rajalakshmi, R. (2020). Phytostimulatory effect of phytochemical fabricated nanosilver (AgNPs) on *Psophocarpus tetragonolobus* (L.) DC. seed germination: An insight from antioxidative enzyme activities and genetic similarity studies. Current Plant Biology, 23: 100158. https://doi.org/10.1016/j.cpb.2020.100158
64. Kang, M., Liu, Y., Weng, Y., Wang, H., & Bai, X. (2024). A critical review on the toxicity regulation and ecological risks of zinc oxide nanoparticles to plants. Environmental Science: Nano, 11, 14–35. https://doi.org/10.1039/D3EN00630A
65. Karim, S., Kayani, S., Akhtar, W., Fatima, I., Nazir, M., & Zaman, W. (2023). Biogenic synthesis of silver nanoparticles using *Funaria hygrometrica* Hedw. and their effects on the growth of *Zea mays* seedlings. Microscopy Research and Technique, 86, 686–693. https://doi.org/10.1002/jemt.24309
66. Kashyap, A. S., Manzar, N., Vishwakarma, S. K., Mahajan, C., & Dey, U. (2024). Tiny but mighty: Metal nanoparticles as effective antimicrobial agents for plant pathogen control. World Journal of Microbiology and Biotechnology, 40: 104. https://doi.org/10.1007/s11274-024-03911-5
67. Kaur, R., Choudhary, D., Bali, S., Bandral, S. S., Singh, V., Ahmad, M. A., Rani, N., Singh, T. G., & Chandrasekaran, B. (2024). Pesticides: An alarming detrimental to health and environment. Science of The Total Environment, 915: 170113. https://doi.org/10.1016/j.scitotenv.2024.170113

68. Khalil, M., & Alqahtany, F. Z. (2020). Comparative studies of the synthesis and physical characterization of ZnO nanoparticles using *Nerium oleander* flower extract and chemical methods. Journal of Inorganic and Organometallic Polymers and Materials, 30, 3750–3760. https://doi.org/10.1007/s10904-020-01494-w
69. Khatri, P., Kumar, P., Shakya, K. S., Kirlas, M. C., & Tiwari, K. K. (2024). Understanding the intertwined nature of rising multiple risks in modern agriculture and food system. Environment, Development and Sustainability, 26, 24107–24150. https://doi.org/10.1007/s10668-023-03638-7
70. Koley, R., Mondal, A., & Mondal, N. K. (2023). Green synthesized silver nanoparticles mediated regulation on hydrolytic enzymes and ROS homeostasis promote growth of three pulses (*Cicer arietinum* L., *Pisum sativum* L., and *Vigna radiata* L.). Energy, Ecology and Environment, 8, 537–555. https://doi.org/10.1007/s40974-023-00293-6
71. Kretschmer, M., Leroch, M., Mosbach, A., Walker, A.S., Fillinger, S., Mernke, D., Schoonbeek, H.J., Pradier, J.M., Leroux, P., Waard, M. A. D., & Hahn, M. (2009). Fungicide-driven evolution and molecular basis of multidrug resistance in field populations of the grey mould fungus *Botrytis cinerea.* PLOS Pathogens, 5: e1000696. https://doi.org/10.1371/journal.ppat.1000696
72. Kumar, A., Singh, I. K., Mishra, R., Singh, A., Ramawat, N., & Singh, A. (2021). The role of zinc oxide nanoparticles in plants: A critical appraisal. W: Sharma N. & Sahi S. (Red.), Nanomaterial biointeractions at the cellular, organismal and system levels (s. 249–267). Springer International Publishing. https://doi.org/10.1007/978-3-030-65792-5_10
73. Kumar, R., Singh, S. P., Ivanov, F., Maksimov, A. Y., Latsynnik, E., Minkina, T., & Keswani, C. (2024). *Trichoderma*-mediated synthesis of ZnONPs: Trend efficient for repressing two seed- and soil-borne phytopathogens *Phomopsis vexans* and *Colletotrichum capsici*. BioNanoScience, 14, 5363–5376. https://doi.org/10.1007/s12668-024-01495-w
74. Lavecchia, R., García-Martínez, J. B., Contreras-Ropero, J. E., Barajas-Solano, A. F., & Zuorro, A. (2024). Antibacterial and photocatalytic applications of silver nanoparticles synthesized from *Lacticaseibacillus rhamnosus*. International Journal of Molecular Sciences, 25: 11809. https://doi.org/10.3390/ijms252111809
75. Li, G., He, D., Qian, Y., Guan, B., Gao, S., Cui, Y., Yokoyama, K., & Wang, L. (2012). Fungus-mediated green synthesis of silver nanoparticles using *Aspergillus terreus*. International Journal of Molecular Sciences, 13, 466-476. https://doi.org/10.3390/ijms13010466
76. Li, J., Sang, H., Guo, H., Popko, J. T., He, L., White, J. C., Parkash Dhankher, O., Jung, G., & Xing, B. (2017). Antifungal mechanisms of ZnO and Ag nanoparticles to *Sclerotinia homoeocarpa.* Nanotechnology, 28: 155101. https://doi.org/10.1088/1361-6528/aa61f3
77. Li, L., Pan, H., Deng, L., Qian, G., Wang, Z., Li, W., & Zhong, C. (2022). The antifungal activity and mechanism of silver nanoparticles against four pathogens causing kiwifruit post-harvest rot. Frontiers in Microbiology, 13: 988633. https://doi.org/10.3389/fmicb.2022.988633

78. Li, Z., Yan, W., Li, Y., Xiao, Y., Shi, Y., Zhang, X., Lei, J., Min, K., Pan, Y., Chen, X., Liu, Q., & Jiang, G. (2023). Particle size determines the phytotoxicity of ZnO nanoparticles in rice (*Oryza sativa* L.) revealed by spatial imaging techniques. Environmental Science & Technology, 57, 13356–13365. https://doi.org/10.1021/acs.est.3c03821
79. Ma, L., Lv, S., Tang, J., Liu, J., Li, W., Deng, J., Deng, Y., Du, J., Liu, X., & Zeng, X. (2019). Study on bioactive molecules involved in extracellular biosynthesis of silver nanoparticles by *Penicillium aculeatum* Su1. Materials Experts, 475-483. https://doi.org/10.1166/mex.2019.1508
80. Magan, N., Sanchis, V., & Aldred, D. (2004). The role of spoilage fungi in seed deterioration. W: Arora D.K. (Red.) Fungal Biotechnology in Agricultural, Food, and Environmental Applications, CRC Press, (s. 311–324). ISBN: 9780429223808
81. Maniah, K., Olyan Al-Otibi, F., Mohamed, S., Said, B. A., Ragab AbdelGawwad, M., & Taha Yassin, M. (2024). Synergistic antibacterial activity of biogenic AgNPs with antibiotics against multidrug resistant bacterial strains. Journal of King Saud University - Science, 36: 103461. https://doi.org/10.1016/j.jksus.2024.103461
82. Martín, I., Gálvez, L., Guasch, L., & Palmero, D. (2022). Fungal pathogens and seed storage in the dry state. Plants, 11:3167. https://doi.org/10.3390/plants11223167
83. Mašev, N., & Kutáček, M. (1966). The effect of zinc on the biosynthesis of tryptophan, andol auxins and gibberellins in barley. Biologia Plantarum, 8, 142–151. https://doi.org/10.1007/BF02930623
84. Matras, E., Gorczyca, A., Przemieniecki, S. W., & Oćwieja, M. (2022). Surface properties-dependent antifungal activity of silver nanoparticles. Scientific Reports, 12: 18046. https://doi.org/10.1038/s41598-022-22659-2
85. Mendes, C. R., Dilarri, G., Forsan, C. F., Sapata, V. M., Lopes, P. R., de Moraes, P. B., Montagnolli, R. N., Ferreira, H., & Bidoia, E. D. (2022). Antibacterial action and target mechanisms of zinc oxide nanoparticles against bacterial pathogens. Scientific Reports, 12: 2658. https://doi.org/10.1038/s41598-022-06657-y
86. Miedaner, T., & Juroszek, P. (2021). Global warming and increasing maize cultivation demand comprehensive efforts in disease and insect resistance breeding in north-western Europe. Plant Pathology, 70, 1032–1046. https://doi.org/10.1111/ppa.13365
87. Miller, W. R., & Arias, C. A. (2024). ESKAPE pathogens: Antimicrobial resistance, epidemiology, clinical impact and therapeutics. Nature Reviews Microbiology, 22, 598–616. https://doi.org/10.1038/s41579-024-01054-w
88. Mittal, D., Kaur, G., Singh, P., Yadav, K., & Ali, S. A. (2020). Nanoparticle-based sustainable agriculture and food science: Recent advances and future outlook. Frontiers in Nanotechnology, 2: 579954. https://doi.org/10.3389/fnano.2020.579954
89. Mohamed, A. A., Abu-Elghait, M., Ahmed, N. E., & Salem, S. S. (2021). Eco-friendly mycogenic synthesis of ZnO and CuO nanoparticles for in vitro antibacterial, antibiofilm, and antifungal applications. Biological Trace Element Research, 199, 2788–2799. https://doi.org/10.1007/s12011-020-02369-4
90. Mohd Yusof, H., Abdul Rahman, N., Mohamad, R., Zaidan, U. H., & Samsudin, A. A. (2022). Optimization of biosynthesis zinc oxide nanoparticles: desirability-function based response surface methodology, physicochemical characteristics, and its

antioxidant properties. OpenNano, 8: 100106. https://doi.org/10.1016/j.onano.2022.100106

91. Mongy, Y., & Shalaby, T. (2024). Green synthesis of zinc oxide nanoparticles using *Rhus coriaria* extract and their anticancer activity against triple-negative breast cancer cells. Scientific Reports, 14: 13470. https://doi.org/10.1038/s41598-024-63258-7
92. Noman, M., Ahmed, T., Hussain, S., Niazi, M. B., Shahid, M., & Song, F. (2020a). Biogenic copper nanoparticles synthesized by using a copper-resistant strain *Shigella flexneri* SNT22 reduced the translocation of cadmium from soil to wheat plants. Journal of Hazardous Materials, 398: 123175. https://doi.org/10.1016/j.jhazmat.2020.123175
93. Noman, M., Shahid, M., Ahmed, T., Tahir, M., Naqqash, T., Muhammad, S., Song, F., Abid, H. M., & Aslam, Z. (2020b). Green copper nanoparticles from a native *Klebsiella pneumoniae* strain alleviated oxidative stress impairment of wheat plants by reducing the chromium bioavailability and increasing the growth. Ecotoxicology and Environmental Safety, 192: 110303. https://doi.org/10.1016/j.ecoenv.2020.110303
94. Pintos, B., de Diego, H., & Gomez-Garay, A. (2024). Nanopriming-induced enhancement of cucumber seedling development: Exploring biochemical and physiological effects of silver nanoparticles. Agronomy, 14: 1866. https://doi.org/10.3390/agronomy14081866
95. Prażak, R., Święciło, A., Krzepiłko, A., Michałek, S., & Arczewska, M. (2020). Impact of Ag nanoparticles on seed germination and seedling growth of green beans in normal and chill temperatures. agriculture, 10: 312. https://doi.org/10.3390/agriculture10080312
96. Qamar, S. U., & Ahmad, J. N. (2021). Nanoparticles: Mechanism of biosynthesis using plant extracts, bacteria, fungi, and their applications. Journal of Molecular Liquids, 334: 116040. https://doi.org/10.1016/j.molliq.2021.116040
97. Rai, M., & Golinska, P. (Red.). (2023). Mycosynthesis of nanomaterials: Perspectives and challenges. CRC Press. https://doi.org/10.1201/9781003327387
98. Rai, M., Bonde, S., Golinska, P., Trzcińska-Wencel, J., Gade, A., Abd-Elsalam, K. A., Shende, S., Gaikwad, S., & Ingle, A. P. (2021). *Fusarium* as a novel fungus for the synthesis of nanoparticles: Mechanism and applications. Journal of Fungi, 7: 139. https://doi.org/10.3390/jof7020139
99. Rajjou, L., Duval, M., Gallardo, K., Catusse, J., Bally, J., Job, C., & Job, D. (2012). Seed germination and vigor. Annual Review of Plant Biology, 63, 507–533. https://doi.org/10.1146/annurev-arplant-042811-105550
100. Ramzan, M., Parveen, M., Naz, G., Sharif, H. M., Nazim, M., Aslam, S., Hussain, A., Rahimi, M., & Alamer, K. H. (2024). Enhancing physio-biochemical characteristics in okra genotypes through seed priming with biogenic zinc oxide nanoparticles synthesized from halophytic plant extracts. Scientific Reports, 14: 23753. https://doi.org/10.1038/s41598-024-74129-6
101. Rani, P., Kaur, G., Rao, K. V., Singh, J., & Rawat, M. (2020). Impact of green synthesized metal oxide nanoparticles on seed germination and seedling growth of *Vigna radiata* (mung bean) and *Cajanus cajan* (red gram). Journal of Inorganic and

Organometallic Polymers and Materials, 30, 4053–4062. https://doi.org/10.1007/s10904-020-01551-4

102. Ribeiro, L. G., Roque, G. S., Conrado, R., & De Souza, A. O. (2023). Antifungal activity of mycogenic silver nanoparticles on clinical yeasts and phytopathogens. Antibiotics, 12: 91. https://doi.org/10.3390/antibiotics12010091
103. Rilda, Y., Sari, L. M., Armaini, A., Imelda, I., & Pardi, H. (2024). Characterization and evaluation of the anti-bacterial activity of facile biosynthesis zinc oxide nanorods using *Spirulina platensis*. Separation Science and Technology, 59, 686–696. https://doi.org/10.1080/01496395.2024.2332371
104. Rodrigues, A. S., Batista, J. G., Rodrigues, M. Á. V., Thipe, V. C., Minarini, L. A., Lopes, P. S., & Lugão, A. B. (2024). Advances in silver nanoparticles: A comprehensive review on their potential as antimicrobial agents and their mechanisms of action elucidated by proteomics. Frontiers in Microbiology, 15: 1440065. https://doi.org/10.3389/fmicb.2024.1440065
105. Rouf Shah, T., Prasad, K., & Kumar, P. (2016). Maize—A potential source of human nutrition and health: A review. Cogent Food & Agriculture, 2: 1166995. https://doi.org/10.1080/23311932.2016.1166995
106. Rouphael, Y., & Colla, G. (2020). Biostimulants in agriculture. Frontiers in Plant Science, 11: 40. https://doi.org/10.3389/fpls.2020.00040
107. Salih, A. M., Qahtan, A. A., Al-Qurainy, F., & Al-Munqedhi, B. M. (2022). Impact of biogenic Ag-containing nanoparticles on germination rate, growth, physiological, biochemical parameters, and antioxidants system of tomato (*Solanum tuberosum* L.) in vitro. Processes, 10: 825. https://doi.org/10.3390/pr10050825
108. Sencan, A., Kilic, S., & Kaya, H. (2024). Stimulating effect of biogenic nanoparticles on the germination of basil (*Ocimum basilicum* L.) seeds. Scientific Reports, 14: 1715. https://doi.org/10.1038/s41598-023-50654-8
109. Sharifi, R. (2016). Effect of seed priming and foliar application with micronutrients on quality of forage corn (*Zea mays*). Environmental and Experimental Biology, 14, 151–156. https://doi.org/10.22364/eeb.14.21
110. Sharma, D., Afzal, S., & Singh, N. K. (2021). Nanopriming with phytosynthesized zinc oxide nanoparticles for promoting germination and starch metabolism in rice seeds. Journal of Biotechnology, 336, 64–75. https://doi.org/10.1016/j.jbiotec.2021.06.014
111. Sharma, P., Urfan, M., Anand, R., Sangral, M., Hakla, H. R., Sharma, S., Das, R., Pal, S., & Bhagat, M. (2022). Green synthesis of zinc oxide nanoparticles using *Eucalyptus lanceolata* leaf litter: Characterization, antimicrobial and agricultural efficacy in maize. Physiology and Molecular Biology of Plants, 28, 363–381. https://doi.org/10.1007/s12298-022-01136-0
112. Shen, M., Liu, W., Zeb, A., Lian, J., Wu, J., & Lin, M. (2022). Bioaccumulation and phytotoxicity of ZnO nanoparticles in soil-grown *Brassica chinensis* L. and potential risks. Journal of Environmental Management, 306: 114454. https://doi.org/10.1016/j.jenvman.2022.114454
113. Shruthi, T. S., Meghana, M. R., Medha, M. U., Sanjana, S., Navya, P. N., & Kumar Daima, H. (2019). Streptomycin functionalization on silver nanoparticles for improved

antibacterial activity. Materials Today: Proceedings, 10, 8–15. https://doi.org/10.1016/j.matpr.2019.02.181

114. Siddique, K., Shahid, M., Shahzad, T., Mahmood, F., Nadeem, H., Saif ur Rehman, M., Hussain, S., Sadak, O., Gunasekaran, S., Kamal, T., & Ahmad, I. (2021). Comparative efficacy of biogenic zinc oxide nanoparticles synthesized by *Pseudochrobactrum* sp. C5 and chemically synthesized zinc oxide nanoparticles for catalytic degradation of dyes and wastewater treatment. Environmental Science and Pollution Research, 28, 28307–28318. https://doi.org/10.1007/s11356-021-12575-9
115. Singh, A., Rawat, S., Rajput, V. D., Minkina, T., Mandzhieva, S., Eloyan, A., Singh, R. K., Singh, O., El-Ramady, H., & Ghazaryan, K. (2024). Nanotechnology products in agriculture and environmental protection: Advances and challenges. Egyptian Journal of Soil Science, 64, 1355–1378. https://doi.org/10.21608/ejss.2024.300047.1802
116. Singh, N., Singh, M. K., Yadav, R. K., Azim, Z., & Raghuvansi, J. (2024). Green synthesis and characterization of nano zinc oxide and comparative study of its impact on germination and metabolic activities of *Solanum lycopersicum* L. and *Capsicum annuum* L. Vegetos. https://doi.org/10.1007/s42535-024-00838-y
117. Singh, P. M., Tiwari, A., Maity, D., & Saha, S. (2022). Recent progress of nanomaterials in sustainable agricultural applications. Journal of Materials Science, 57, 10836–10862. https://doi.org/10.1007/s10853-022-07259-9
118. Singh, S., Gade, J. V., Verma, D. K., Elyor, B., & Jain, B. (2024). Exploring ZnO nanoparticles: UV–visible analysis and different size estimation methods. Optical Materials, 152: 115422. https://doi.org/10.1016/j.optmat.2024.115422
119. Soliman, M., Qari, S. H., Abu-Elsaoud, A., El-Esawi, M., Alhaithloul, H., & Elkelish, A. (2020). Rapid green synthesis of silver nanoparticles from blue gum augment growth and performance of maize, fenugreek, and onion by modulating plants cellular antioxidant machinery and genes expression. Acta Physiologiae Plantarum, 42: 148. https://doi.org/10.1007/s11738-020-03131-y
120. Song, K., Zhao, D., Sun, H., Gao, J., Li, S., Hu, T., & He, X. (2022). Green nanopriming: Responses of alfalfa (*Medicago sativa* L.) seedlings to alfalfa extracts capped and light-induced silver nanoparticles. BMC Plant Biology, 22: 323. https://doi.org/10.1186/s12870-022-03692-9
121. Stearns, P. N. (2008). Western Civilization in World History. Routledge. https://doi.org/10.4324/9780203930090
122. Szerencsés, B., Igaz, N., Tóbiás, Á., Prucsi, Z., Rónavári, A., Bélteky, P., Madarász, D., Papp, C., Makra, I., Vágvölgyi, C., Kónya, Z., Pfeiffer, I., & Kiricsi, M. (2020). Size-dependent activity of silver nanoparticles on the morphological switch and biofilm formation of opportunistic pathogenic yeasts. BMC Microbiology, 20: 176. https://doi.org/10.1186/s12866-020-01858-9
123. Tomah, A. A., Alamer, I. S. A., Li, B., & Zhang, J.-Z. (2020). Mycosynthesis of silver nanoparticles using screened *Trichoderma* isolates and their antifungal activity against *Sclerotinia sclerotiorum.* Nanomaterials, 10: 1955. https://doi.org/10.3390/nano10101955

124. Tripathi, N., & Goshisht, M. K. (2022). Recent advances and mechanistic insights into antibacterial activity, antibiofilm activity, and cytotoxicity of silver nanoparticles. ACS Applied Bio Materials, 5, 1391–1463. https://doi.org/10.1021/acsabm.2c00014
125. Umair Hassan, M., Aamer, M., Umer Chattha, M., Haiying, T., Shahzad, B., Barbanti, L., Nawaz, M., Rasheed, A., Afzal, A., Liu, Y., & Guoqin, H. (2020a). The critical role of zinc in plants facing the drought stress. Agriculture, 10: 396. https://doi.org/10.3390/agriculture10090396
126. Vazquez-Muñoz, R., Meza-Villezcas, A., Fournier, P. G., Soria-Castro, E., Juarez-Moreno, K., Gallego-Hernández, A. L., Bogdanchikova, N., Vazquez-Duhalt, R., & Huerta-Saquero, A. (2019). Enhancement of antibiotics antimicrobial activity due to the silver nanoparticles impact on the cell membrane. PLOS ONE, 14: e0224904. https://doi.org/10.1371/journal.pone.0224904
127. Voothuluru, P., Mäkelä, P., Zhu, J., Yamaguchi, M., Cho, I.J., Oliver, M. J., Simmonds, J., & Sharp, R. E. (2020). Apoplastic hydrogen peroxide in the growth zone of the maize primary root. Increased levels differentially modulate root elongation under well-watered and water-stressed conditions. Frontiers in Plant Science, 11: 392. https://doi.org/10.3389/fpls.2020.00392
128. Wanarska, E., & Maliszewska, I. (2019). The possible mechanism of the formation of silver nanoparticles by *Penicillium cyclopium*. Bioorganic Chemistry, 93: 102803. https://doi.org/10.1016/j.bioorg.2019.02.028
129. Wang, X., Xie, H., Wang, P., & Yin, H. (2023). Nanoparticles in plants: Uptake, transport and physiological activity in leaf and root. Materials, 16: 3097. https://doi.org/10.3390/ma16083097
130. Waqif, H., Munir, N., Farrukh, M. A., Hasnain, M., Sohail, M., & Abideen, Z. (2024). Algal macromolecular mediated synthesis of nanoparticles for their application against citrus canker for food security. International Journal of Biological Macromolecules, 263: 130259. https://doi.org/10.1016/j.ijbiomac.2024.130259
131. Yan, X., Chen, S., Pan, Z., Zhao, W., Rui, Y., & Zhao, L. (2023). AgNPs-triggered seed metabolic and transcriptional reprogramming enhanced rice salt tolerance and blast resistance. ACS Nano, 17, 492–504. https://doi.org/10.1021/acsnano.2c09181
132. Zafar, H., Abbasi, B. H., & Zia, M. (2019). Physiological and antioxidative response of *Brassica nigra* (L.) to ZnO nanoparticles grown in culture media and soil. Toxicological & Environmental Chemistry, 101, 281–299. https://doi.org/10.1080/02772248.2019.1691555
133. Zain, M., Ma, H., Ur Rahman, S., Nuruzzaman, Md., Chaudhary, S., Azeem, I., Mehmood, F., Duan, A., & Sun, C. (2024). Nanotechnology in precision agriculture: Advancing towards sustainable crop production. Plant Physiology and Biochemistry, 206: 108244. https://doi.org/10.1016/j.plaphy.2023.108244
134. Zhang, Y., Pan, X., Liao, S., Jiang, C., Wang, L., Tang, Y., Wu, G., Dai, G., & Chen, L. (2020). Quantitative proteomics reveals the mechanism of silver nanoparticles against multidrug-resistant *Pseudomonas aeruginosa* biofilms. Journal of Proteome Research, 19, 3109–3122. https://doi.org/10.1021/acs.jproteome.0c00114

135. Zhou, W., Li, M., & Achal, V. (2025). A comprehensive review on environmental and human health impacts of chemical pesticide usage. Emerging Contaminants, 11: 100410. https://doi.org/10.1016/j.emcon.2024.100410
136. Zhu, W., Hu, C., Ren, Y., Lu, Y., Song, Y., Ji, Y., Han, C., & He, J. (2021). Green synthesis of zinc oxide nanoparticles using *Cinnamomum camphora* (L.) Presl leaf extracts and its antifungal activity. Journal of Environmental Chemical Engineering, 9: 106659. https://doi.org/10.1016/j.jece.2021.106659
137. Zulfiqar, F. (2021). Effect of seed priming on horticultural crops. Scientia Horticulturae, 286: 110197. https://doi.org/10.1016/j.scienta.2021.110197

Curriculum vitae

Joanna Trzcińska-Wencel
trzcinska@doktorant.umk.pl

ORCID ID: 0000-0001-9119-0054
https://orcid.org/0000-0001-9119-0054
https://www.scopus.com/authid/detail.uri?authorId=57222117954

Wykształcenie:

2020-2025	Szkoła Doktorska Nauk Ścisłych i Przyrodniczych *Academia Scientiarum Thoruniensis* , Uniwersytet Mikołaja Kopernika w Toruniu. Tytuł projektu: Nanocząstki srebra i tlenku cynku pochodzenia grzybowego: biosynteza, aktywność przeciwdrobnoustrojowa i stymulatory wzrostu kukurydzy.
2018-2020	Wydział Nauk Biologicznych i Weterynaryjnych, Uniwersytet Mikołaja Kopernika w Toruniu Biotechnologia, tytuł pracy magisterskiej: Biogeniczne nanocząstki srebra - analiza cytotoksyczności wobec bakterii i białek opłaszczających nanocząstki.
2015-2018	Wydział Biologii i Ochrony Środowiska Uniwersytet Mikołaja Kopernika w Toruniu Biotechnologia, tytuł pracy licencjackiej: Bakterie priobotyczne jako czynnik stymulujący układ odpornościowy.

Udział w projektach badawczych:

02.2023 - 08.2025	Mykogeniczne nanocząstki metali do stymulacji wzrostu roślin i zwiększenia produkcji roślinnej. Preludium nr. 2022/45/N/NZ9/01483 Narodowe Centrum Nauki.
12.2022 - 12.2023	Search for the antifungal activity of biogenic nanoparticles against selected plant pathogens. Grants4NCUStudents, Inicjatywa Doskonałości – Uczelnia Badawcza (IDUB), Uniwersytet Mikołaja Kopernika w Toruniu.
12.2021 - 12.2022	Biological nano-alternatives to conventional pesticides. Grants4NCUStudents, Inicjatywa Doskonałości – Uczelnia Badawcza (IDUB), Uniwersytet Mikołaja Kopernika w Toruniu.
05.2021 - 05.2022	Silver nanoparticles as an alternative strategy against bacterial biofilm formation and antibiotic-resistant bacteria. Grants4NCUStudents, Inicjatywa Doskonałości – Uczelnia Badawcza (IDUB), Uniwersytet Mikołaja Kopernika w Toruniu.
10.2024 - 09.2025	Stypendium naukowe w grancie Nanoferti: Development of innovative nanofertilizers for sustainable agriculture. POLONEZ BIS 2, współfinansowanym ze środków Narodowego Centrum Nauki, Polska nr. 2021/43/P/NZ9/02934 oraz programu ramowego Unii Europejskiej w zakresie badań naukowych i innowacji Horyzont 2020 na podstawie umowy nr 945339 w ramach działań „Marie Skłodowska-Curie”. PI: Dr. Aniketkumar Gade.

2021 – 2023	Udział w projekcie: Development of new environmentally-friendly and biologically active nanomaterials. W ramach programu im. Stanisława Ulama, Narodowej Agencji Wymiany Akademickiej (NAWA). PI: prof. Mahendra Rai
2017 – 2023	Udział w projekcie: Badanie możliwości wykorzystania nanocząstek srebra wytwarzanych przez promieniowce jako czynnika antybakteryjnego i antygrzybowego nietoksycznego dla komórek eukariotycznych. Preludium, nr 2016/23/N/NZ9/00247, NCN PI: dr Magdalena Wypij

Staże i szkolenia:

06.2022	Miesięczny staż w Laboratorium Technologii i Struktury Nanomateriałów, Centrum Nanotechnologii VSB - Uniwersytetu Technicznego w Ostrawie, Ostrawa, Republika Czeska. Tytuł projektu: The use of different techniques for analysis of physico-chemical properties of biogenic nanoparticles. Finansowany w ramach mobilności dla doktorantów, Inicjatywa Doskonałości – Uczelnia Badawcza (IDUB), Uniwersytet Mikołaja Kopernika w Toruniu.
5 - 6.11.2022	Szkolenie "Workshop on Crystal Structure Determination from Powder Diffraction", Uniwersytet Old Dominion, Wirginia, USA (online).
18 - 20.03.2024	Szkolenie „Technika MALDI w rutynowej diagnostyce klinicznej - warsztaty dotyczące identyfikacji patogenów klinicznych i wykrywania oporności na antybiotyki", ICNT UMK, Toruń, Polska.
15 - 17.09.2021	Szkolenie "Introduction to GIS Techniques with QGIS and Mapping the Species Distribution and Diversity" at the Conference on Plant Productivity and Food Safety: Soil Science, Microbiology, Agricultural Genetics, and Food Quality, UMK, Toruń, Polska.
2018/19	Kurs: Innowacyjne metody w walce z patogenami klinicznymi, UMK, Toruń, Polska.

Stypendia, nagrody i wyróżnienia:

1. 2023/2024 Zwiększone stypendium doktoranckie finansowane w ramach Emerging Fields (EF): Komórki jako platformy eksperymentalne i biofabryki (CExFact) w ramach programu Inicjatywa Doskonałości - Uczelnia Badawcza. UMK w Toruniu.
2. 2024/2025. Zwiększone stypendium doktoranckie finansowane w ramach Emerging Fields (EF): Komórki jako platformy eksperymentalne i biofabryki (CExFact) w ramach programu Inicjatywa Doskonałości - Uczelnia Badawcza. UMK w Toruniu.
3. 07.2024 Nagroda Rektora za działalność organizacyjną na rzecz Społeczności Akademickiej Uniwersytetu Mikołaja Kopernika w Toruniu za rok 2023/24.
4. 2017/2018 Stypendium Rektora dla najlepszych studentów UMK w Toruniu.
5. 2019/2020 III miejsce w Konkursie na Najlepszą Pracę Magisterską, Wydział Nauk Biologicznych i Weterynaryjnych, UMK w Toruniu
6. 10.2024. Nagroda za najlepszy poster: "Biosynthesized metal nanoparticles for pre-sowing seed treatment and growth stimulation of *Zea mays*." Trzcińska-Wencel, J., Mucha, N., Tyburski, J., & Golińska, P. Na International Conference on Plant Nanotechnology, 14-16.10.2024, Poznań, Polska.
7. 09.2022. Nagroda za najlepszą prezentację: "Mycosynthesis of metal-based nanoparticles and evaluation of their potential as antimicrobial agents for crop protection." Trzcińska-Wencel, J.,

Wypij, M., Wachnowicz, B., Rai, M., & Golińska, P. Na Second Edition of Virtual International Conference “Plant productivity and food safety: Soil science, microbiology, agricultural genetics and food quality”, 15-16.09.2022, UMK w Toruniu.

8. 09.2021. Nagroda za najlepszy poster: "Biogenic silver nanoparticles as a tool to combat bacterial and fungal plant pathogens. "Trzcińska-Wencel, J., Golińska, P., Wypij, M., & Rai, M. Na Virtual International Conference “Plant productivity and food safety: Soil science, microbiology, agricultural genetics and food quality”, 15-17.09.2021, UMK w Toruniu.
9. 05.2021. III miejsce w konkursie na najlepszy poster: "Green synthesized silver nanoparticles: Antibacterial activity, biocompatibility, and analyses of surface-attached proteins." Trzcińska-Wencel, J., Wypij, M., Rai, M., & Golińska, P. Na NanoOstrava 2021: 7th Nanomaterials and Nanotechnology Meeting, Ostrava, 17-20.05.2021, Ostrawa, Republika Czeska.

Działalnosć organizacyjna:

- **2024:** Fascynujący dzień Roślin, Noc biologów
- **2023:** Dzień Otwarty Nauk Ścisłych, Przyrodniczych i Technicznych; Noc biologów; Dzień Otwarty Wydziału Nauk Biologicznych i Weterynaryjnych
- **2022:** Noc biologów
- **2021:** Fascynujący dzień Roślin, Noc biologów, Dzień Otwarty Wydziału Nauk Biologicznych i Weterynaryjnych

Publikacje:

1. **Trzcińska-Wencel, J.,** Wypij, M., Terzyk, A. P., Rai, M., & Golińska, P. (2023). Biofabrication of novel silver and zinc oxide nanoparticles from *Fusarium solani* IOR 825 and their potential application in agriculture as biocontrol agents of phytopathogens, and seed germination and seedling growth promoters. *Front. Chem.*, 11: 1235437.
2. **Trzcińska-Wencel, J.,** Wypij, M., Rai, M., & Golińska, P. (2023). Biogenic nanosilver bearing antimicrobial and antibiofilm activities and its potential for application in agriculture and industry. *Front. Microbiol.*, 14: 888.
3. **Trzcińska-Wencel, J.,** Golińska, P., & Rai, M. (2024). Toxicity of nanomaterials to plants. W: M. Rai & G. D. Avila-Quezada (Red.) *Nanotechnology in Plant Health* (s. 369-389). CRC Press, Taylor and Francis Group.
4. **Trzcińska-Wencel, J.,** Wypij, M., & Golińska, P. (2023). Mycogenic synthesis of silver nanoparticles and its optimization. W: M. Rai & P. Golińska (Red.) *Mycosynthesis of Nanomaterials: Perspectives and Challenges* (s. 126-145). CRC Press, Taylor and Francis Group.
5. Golińska, P., Wypij, M., **Trzcińska-Wencel, J.,** & Rai, M. (2024). Applications of nanomaterials for environment management: toxicity, safety, and regulations. W: J. K. Biwas & M. Rai (Red.), *Nanotechnology for Environmental Management*. CRC Press, Taylor and Francis Group
6. Wypij, M., **Trzcińska-Wencel, J.,** Golinska, P., Avila Quezada, G. D., Ingle, A. P., & Rai, M. (2023). The strategic applications of natural polymer nanocomposites in food packaging and agriculture: Chances, challenges, and consumers’ perception. *Front. Chem.*, 10: 1633.
7. Rai, M., Ingle, A. P., Yadav, A., Golińska, P., **Trzcińska-Wencel, J.,** Rathod, S., & Bonde, S. (2023). Nanotechnology as a promising approach for detection, diagnosis and treatment of food allergens. *Curr. Nanosci.*, 19, 90-102.
8. Rai, M., Wypij, M., **Trzcińska-Wencel, J.,** Yadav, A., Ingle, A. P., Avila-Quezada, G. D., & Golińska, P. Myconanotechnology: Opportunities and challenges. W: M. Rai & P. Golińska (Red.) *Myconanotechnology Emerging Trends and Applications* (s. 3-25). CRC Press, Taylor and Francis Group.

9. Fandzloch, M., Augustyniak, A. W., **Trzcińska-Wencel, J.,** Golińska, P., & Roszek, K. (2024). A new MOF@ bioactive glass composite reinforced with silver nanoparticles–a new approach to designing antibacterial biomaterials. *Dalton Trans.* 53, 10928-10937.
10. Fandzloch, M., Bodylska, W., **Trzcińska-Wencel, J.,** Golińska, P., Roszek, K., Wiśniewska, J., Bartmański, M., Lewińska, A., & Jaromin, A. (2023). Cu-HKUST-1 and hydroxyapatite–The interface of two worlds toward the design of functional materials dedicated to bone tissue regeneration. *ACS Biomater. Sci. Eng.* 9, 4646-4653.
11. Fandzloch, M., Bodylska, W., Barszcz, B., **Trzcińska-Wencel, J.,** Roszek, K., Golińska, P., & Lukowiak, A. (2022). Effect of ZnO on sol–gel glass properties toward (bio) application. *Polyhedron*, 223: 115952.
12. Wypij, M., Jędrzejewski, T., Ostrowski, M., **Trzcińska, J.,** Rai, M., & Golińska, P. (2020). Biogenic silver nanoparticles: Assessment of their cytotoxicity, genotoxicity and study of capping proteins. *Molecules*, 25: 3022.
13. Rai, M., Bonde, S., Golinska, P., **Trzcińska-Wencel, J.,** Gade, A., Abd-Elsalam, K., & Ingle, A. (2021). *Fusarium* as a novel fungus for the synthesis of nanoparticles: mechanism and applications. *J. Fungi*, 7: 139.
14. Wypij, M., Jędrzejewski, T., **Trzcińska-Wencel, J.,** Ostrowski, M., Rai, M., & Golińska, P. (2021). Green synthesized silver nanoparticles: Antibacterial and anticancer activities, biocompatibility, and analyses of surface-attached proteins. *Front. Microbiol.*, 12: 888.
15. Rai, M., Ingle, A. P., **Trzcińska-Wencel, J.,** Wypij, M., Bonde, S., Yadav, A., Kratošová, G., & Golińska, P. (2021). Biogenic silver nanoparticles: What we know and what do we need to know? *Nanomaterials*, 11: 2901.
16. Rai, M., Wypij, M., Ingle, A. P., **Trzcińska-Wencel, J.,** & Golińska, P. (2021). Emerging trends in pullulan-based antimicrobial systems for various applications. *Int. J. Mol. Sci.*, 22: 13596.

Udział w konferencjach:

1. Trzcińska-Wencel, J., Mucha, N., Tyburski, J., & Golińska, P. (2024). Metal nanoparticles as maize growth promoters, evaluation of their antimicrobial activity and potential phytotoxicity. 14th International Conference Nanomaterials: Applications & Properties, 8-13.09.2024, Ryga, Łotwa, poster.
2. Trzcińska-Wencel, J., Mucha, N., Tyburski, J., & Golińska, P. (2024). Biosynthesized Metal Nanoparticles with Antimicrobial Activity for Stimulation of Plant Growth. 10th Nanotech & Nanomaterials Research Conference (Nano London-2024), 06-08.11.2024, Londyn, Wielka Brytania, poster.
3. Trzcińska-Wencel, J., Mucha, N., Tyburski, J., & Golińska, P. (2024). Bioinspired silver nanoparticles for effective control of fungal phytopathogens and their impact on growth and physiological condition of maize (*Zea mays*) seedlings. 9th International Weigl Conference: 27-29.06.2024, Rzeszów, Polska, poster.
4. Trzcińska-Wencel, J., Mucha, N., Tyburski, J., & Golińska, P. (2024). Biosynthesized metal nanoparticles for pre-sowing seed treatment and growth stimulation of *Zea mays*. International Conference on Plant Nanotechnology, 14-16.10. 2024, Poznań, Polska, poster.
5. Trzcińska-Wencel, J., Wypij, M., Wachnowicz, B., Rai, M., & Golińska, P. (2022). Mycosynthesis of metal-based nanoparticles and evaluation of their potential as antimicrobial agents for crop protection. Second Edition of Virtual International Conference "Plant productivity and food safety: Soil science, microbiology, agricultural genetics and food quality", 15-16.09.2022 (online), Toruń, Polska, prezentacja.

6. Trzcińska-Wencel, J., Wypij, M., Murawska, A., Rai, M., & Golińska, P. (2022). Mycosynthesized silver and zinc oxide nanoparticles: Their characteristic, antimicrobial and antibiofilm activities. 12th International Conference Nanomaterials: Applications & Properties 11-16.09.2022, Kraków, Poland, poster.
7. Trzcińska-Wencel, J., Wypij, M., Rai, M., Wachnowicz, B., & Golińska, P. (2022). Silver and zinc oxide nanoparticles from Fusarium solani: Biosynthesis, properties, and antimicrobial activity. 22nd IEEE International Conference on Nanotechnology: 4-8.07.2022 Palma de Mallorca, Hiszpania, prezentacja.
8. Trzcińska-Wencel, J., Golińska, P., Wypij, M., & Rai, M. (2021). Biogenic silver nanoparticles as a tool to combat bacterial and fungal plant pathogens. Virtual International Conference "Plant productivity and food safety: Soil science, microbiology, agricultural genetics and food quality", 15-17.09.2021 (online), Toruń, Polska, poster.
9. Trzcińska-Wencel, J., Golińska, P., & Wypij, M. (2021). Biologiczne nanocząstki srebra: Aktywność przeciwdrobnoustrojowa, cytotoksyczność i analiza biomolekuł opłaszczających. Biotechnologia: Dziś na Uniwersytecie Technologiczno-Przyrodniczym, jutro w regionie kujawsko-pomorskim. 10.06.2021, Bydgoszcz, poster.
10. Trzcińska-Wencel, J., Wypij, M., Golińska, P., & Rai, M. (2021). Can we combat plant pathogens using bio-silver nanoparticles? ICA2021: 13th International Conference on Agrophysics "Agriculture in changing climate". 14-16.09.2020 (online), Lublin, Polska, poster.
11. Trzcińska-Wencel, J., Wypij, M., Rai, M., & Golińska, P. (2021). Green synthesized silver nanoparticles: Antibacterial activity, biocompatibility, and analyses of surface-attached proteins. NanoOstrava 2021: 7th Nanomaterials and Nanotechnology Meeting, 17-20.05. 2020, Ostrawa, Czechy, poster.

Współautor:

1. Golińska, P., Nadrowska, J., Trzcińska-Wencel, J., & Gade, A. (2024). Metal bionanoparticles: optimization of mycosynthesis, characteristics and antimicrobial against crop pathogens. 10th Nanotech & Nanomaterials Research Conference (Nano London-2024), 06-08.11.2024, Londyn, Wielka Brytania.
2. Gade, A., Trzcińska-Wencel, J., Nadrowska, J., Rai, M., & Golińska, P. (2024). Bionanocomposites: A green material for sustainable future. Sympozjum Biomateriały w medycynie i kosmetologii, 28.02.2024, Toruń, Polska.
3. Gade, A., Trzcińska-Wencel, J., Nadrowska, J., Rai, M., & Golińska, P. (2024). Fungi as a sustainable source for nanoparticle synthesis. Conference on Fungal Frontiers: Biodiversity, Biomolecules and Bioengineering Applications for Sustainable Perspectives & 51st Annual Meeting of Mycological Society of India (Prof. C.V. Subramanian Birth Centenary Celebration), 27-29.11.2024 Jodhpur, Indie.
4. Gade, A., Nadrowska, J., Trzcińska-Wencel, J., Golińska, P., & Rai, M. (2024). Synthesis of nanoparticles by soil fungi: An environment-friendly approach. 9th International Weigl Conference: 27-29.06.2024, Rzeszów, Polska.
5. Nadrowska, J., Trzcińska-Wencel, J., Golińska, P., & Gade, A. (2024). Optimization of biosynthesis of metal-based nanoparticles, their characteristics and antimicrobial activities against crop pathogens. 9th International Weigl Conference: 27-29.06.2024, Rzeszów, Polska.
6. Trzcińska-Wencel, J., Nadrowska, J., Rai, M., & Golińska, P. (2024). Biosynthesis, characterization and antimicrobial efficiency of silver nanoparticles from *Fusarium oxysporum*. Sympozjum Biomateriały w medycynie i kosmetologii, 28.02.2024, Toruń, Polska.

7. Wachnowicz, B., Olszewski, J., Trzcińska-Wencel, J., Rai, M., & Golińska, P. (2023). Mycosynthesis of metal nanoparticles, their characteristics and antimicrobial activity. Sympozjum Biomateriały w medycynie i kosmetologii, 22.02.2023, Toruń, Polska.
8. Wypij, M., Trzcińska-Wencel, J., Rai, M., & Golińska, P. (2021). Bionanotechnology as a tool in biomedical and agricultural applications. 17th International Conference on Advanced Nanomaterials, 2021, Aveiro, Portugalia.
9. Bodylska, W., Barszcz, B., Trzcińska-Wencel, J., Golińska, P., Roszek, K., Łukowiak, A., & Fandzloch, M. (2021). Cu-HKUST-1@hydroxyapatite jako przykład biokompatybilnego kompozytu o właściwościach antybakteryjnych. Ogólnopolskie Forum Chemii Nieorganicznej, 7-9.09.2021, Toruń, Polska.
10. Barszcz, B., Trzcińska-Wencel, J., Golińska, P., Roszek, K., Łukowiak, A., & Fandzloch, M. (2021). Pierwszy przykład kompozytu typu MOF@bioaktywne szkło i jego bioaplikacja. Ogólnopolskie Forum Chemii Nieorganicznej, 7-9.09.2021, Toruń, Polska.
11. Fandzloch, M., Roszek, K., Trzcińska-Wencel, J., & Golińska, P. (2021). Multifunctional MOF@hydroxyapatite composites. 3rd International Workshop on Functional Nanostructured Materials, 2021, Krakow, Polska.
12. Bodylska, W., Barszcz, B., Trzcińska-Wencel, J., Golińska, P., Roszek, K., Łukowiak, A., & Fandzloch, M. (2022). Charakterystyka i aplikacja biokompatybilnego kompozytu typu MOF@hydroksyapatyt. Zjazd Zimowy Sekcji Młodych Polskiego Towarzystwa Chemicznego 2021, Poznań, Polska.
13. Barszcz, B., Bodylska, W., Trzcińska-Wencel, J., Golińska, P., Roszek, K., & Fandzloch, M. (2022). Bioaktywne szkło i jego kompozyty. Zjazd Zimowy Sekcji Młodych Polskiego Towarzystwa Chemicznego 2021, Poznań, Polska.
14. Fandzloch, M., Barszcz, B., Bodylska, W., Roszek, K., Trzcińska-Wencel, J., & Golińska, P. (2022). Functional materials based on hydroxyapatite nanoparticles and MOFs. 1st International Conference on Advanced Materials for Bio-Related Applications (AMBRA 2022), 16-19.05.2022, Wrocław, Polska.
15. Fandzloch, M., Augustyniak, A., Trzcińska-Wencel, J., Golińska, P., & Roszek, K. (2022). Design of composites based on bioglass nanoparticles and MOF for antimicrobial applications. Spanish Royal Society of Chemistry XXXVIII Biennial Meeting, 27-30.06.2022, Granada, Hiszpania.

Podsumowanie osiągnięć

- Artykuły (oryginalne, przeglądowe, rozdziały): 16
- Sumaryczny IF: 52,727
- Punkty MNiSW: 1 460
- indeks H (wg bazy Scopus): 6